



This work is protected by copyright and other intellectual property rights and duplication or sale of all or part is not permitted, except that material may be duplicated by you for research, private study, criticism/review or educational purposes. Electronic or print copies are for your own personal, non-commercial use and shall not be passed to any other individual. No quotation may be published without proper acknowledgement. For any other use, or to quote extensively from the work, permission must be obtained from the copyright holder/s.

**An evaluation of the antiparasitic activities
of a novel natural product and open-access
Pathogen Box libraries**

Hamza N. Hameed



**Thesis submitted to Keele University for the degree
of Doctor of Philosophy**

March 2019

Abstract

Using a novel library of natural products isolated from temperate zone plants, the antiparasitic activity of 643 Phytopure library compounds were determined against intraerythrocytic *P. falciparum*, the blood-stream form of *T. b brucei* and axenic amastigotes of *L. mexicana*. Twelve compounds with a 50% inhibitory effect (EC₅₀) values of less than 6 μM were detected against *P. falciparum*, 25 compounds with an EC₅₀ values of less than 2.8 μM against *T. b brucei*, and 23 compounds with an EC₅₀ values of less than 2.8 μM against *L. mexicana*. The cytotoxicity effects, and thus their selectivity of action against each parasite, of these selected compounds were determined against a human liver cell line (HepG2) to establish priorities for further work. Here, four structurally-related triterpene compounds (700022, 700107, 700136 and 700240) were shown to have activity against axenic and intramacrophage amastigote stages with reasonable selectivity when compared to the THP-1 and HepG2 human cells.

By exposing promastigote *L. mexicana* to increasing concentrations over 28 weeks, a 700022 resistant line was generated *in vitro*. Promastigotes of this resistant cell line were 7.5-fold more resistant to 700022 than compared to the parental wild type line, with axenic promastigotes having a 40-fold increase in resistance. Interestingly, the 700022 resistant promastigotes had a 25% smaller cell surface area and a 85% reduction in flagellum length. The 700022-resistant line was cross resistant to the related triterpenes 700107, 700136 and 700240 and miltefosine (11.8-fold compared to wild type strain). The potential for mutations within genes (LmMT/LmRos3) that encode subunits of the miltefosine transporter complex were investigated. No mutations were associated with LmMT, with three nonsynonymous mutations found in LmRos3.

This thesis also reports the evaluation of transgenic *L. mexicana* expressing a novel NanoLuc luciferase, and a PEST-tagged variant, as a tractable, rapid and sensitive system for antileishmanial compound screening. The validity of this approach is demonstrated by a screen of the MMV Pathogen Box. The opportunity afforded by the transgenic *L. mexicana* expressing NanoLuc-PEST in an *in vitro* infected macrophage model is also demonstrated. These transgenic *L. mexicana* offer an opportunity for high-throughput screening programmes that assess the more clinically-relevant activity against intracellular amastigote parasite without the time, specialist and post-assay processing burdens associated with current high-content imaging techniques.

Declaration:

Work presented in this thesis has been published in the following journal article:

Berry SL, Hameed H, Thomason A, Maciej-Hulme ML, Saif Abou-Akkada S, Horrocks P, Price HP. 2018. Development of NanoLuc-PEST expressing Leishmania mexicana as a new drug discovery tool for axenic- and intramacrophage-based assays. PLoS Negl Trop Dis, vol. 12(7), e0006639

LIST OF CONTENTS

ABSTRACT	I
LIST OF CONTENTS	III
LIST OF FIGURES	VIII
LIST OF TABLES	XVI
ABBREVIATIONS	XVIII
ACKNOWLEDEMENTS	XXI
CHAPTER 1: General introduction	1
1.1 The global impact of parasitic diseases	1
1.2 Malaria	3
1.2.1 Background of the Disease	3
1.2.2 Life Cycle of <i>Plasmodium falciparum</i>	6
1.2.3.1 Asexual life cycle of <i>Plasmodium falciparum</i>	7
a. Liver Stage/Pre-erythrocytic phase	7
b. Erythrocyte stage	8
c. Sexual Stage	10
1.2.3 Clinical manifestation and classification of malaria	11
1.2.3.1 Uncomplicated malaria	13
1.2.3.2 Severe <i>falciparum</i> malaria	14
1.2.4 Strategies for malaria control	17
a. Vector control	17
b. Chemoprophylaxis and chemoprevention	18
c. Vaccination	19
1.2.5 Overview of Antimalarial Drugs	20
1.2.5.1 Chloroquine (CQ)	21
1.2.5.2 Quinine (QN)	22
1.2.5.3. Mefloquine (MQ)	22
1.2.5.4. Artemisinin	24
1.3 Human African Trypanosomiasis (Sleeping Sickness)	26
1.3.1 Background of the Disease	26
1.3.2 The life cycle of <i>Trypanosoma brucei</i>	28
1.3.3 The clinical features of HAT	30
1.3.4 Pharmacological treatment of HAT	30
1.4 Leishmaniasis	34
1.4.1 Background of the Disease	34
1.4.2 Clinical forms of Leishmaniasis	35

1.4.2.1 Visceral Leishmaniasis	36
1.4.2.2 Cutaneous Leishmaniasis	38
1.4.2.3 Mucocutaneous Leishmaniasis (MCL)	40
1.4.3 The life cycle of leishmania	40
1.4.4 Control strategies for Visceral Leishmaniasis	42
1.4.5 Treatment of Leishmaniasis	44
1.4.5.1 Pentavalent antimonials [Sb(V)]	46
1.4.5.2 Amphotericin B (AmB)	48
1.4.5.3 Miltefosine	50
1.4.5.4 Paromomycin	50
1.4.5.6 Combination therapy	51
1.4.5.7 New hope for novel drugs for leishmaniasis	53
1.6 The search for new drugs includes natural products	55
1.7 The objective of this study	59
Chapter 2: Materials and methods	60
2.1 Materials (source of stocks and reagents)	60
2.2 Cell culture methods	60
2.2.1 <i>Plasmodium falciparum</i>	60
2.2.1.1 Preparation of growth medium for <i>P. falciparum</i> culture	60
2.2.1.2 Preparation of normal human erythrocytes	61
2.2.1.3 <i>In vitro</i> intraerythrocytic culture of <i>P. falciparum</i>	61
2.2.1.4 Assessment of Parasitaemia with Giemsa Staining	62
2.2.1.5 <i>P. falciparum</i> culture synchronisation using sorbitol-lysis method	62
2.2.2 <i>Trypanosoma brucei</i>	63
2.2.2.1 <i>In vitro</i> culture of <i>T. brucei</i>	63
2.2.3 <i>Leishmania mexicana</i>	63
2.2.3.1 <i>In vitro</i> culture of <i>L. mexicana</i>	63
2.2.3.2 Generation of plasmid constructs and <i>L. mexicana</i> transfection	64
2.2.3.3 Long term storage of promastigote cells culture	65
2.3 Drug assays	65
2.3.1 Drug stocks preparation	65
a. Phytopure compounds library	65
b. Pathogen Box compounds	65
2.3.2 Malaria SYBR-green (MSF) assay	66

2.3.3 Standard protocol for AlamarBlue (AlamarBlue) assay	66
2.3.4 Luciferase assay	66
2.3.5 Nano-Glo Luciferase Assay	67
2.3.6 Drug screening experiments against <i>P. falciparum</i>	67
2.3.6.1 Initial screening of intraerythrocytic <i>P. falciparum</i>	67
2.3.6.2 Determination of the 50% effect concentration (EC ₅₀)	68
2.3.6.3 Determination of the 50% lethal dose (LD ₅₀)	68
2.3.6.4 Bioluminescent Relative Rate of Kill (BRRoK) assay	69
2.3.6.5 Cytotoxicity assay	71
2.3.7 Drug screening experiments against <i>Trypanosoma brucei</i>	71
2.3.7.1 <i>In vitro</i> drug screening experiments	71
2.3.7.2 <i>In vitro</i> determination of ant-itypanosomal activity	72
2.3.8 Drug screening experiments against <i>Leishmania mexicana</i>	72
2.3.8.1 <i>In vitro</i> drug screening experiments	72
2.3.8.2 <i>In vitro</i> determination of antileishmanial activity	73
2.3.8.3 Macrophages (THP-1) cell line cytotoxicity assay	73
2.3.8.4 Infected macrophages and treatments	74
2.3.8.5 <i>In vitro</i> drug screening of MMV Pathogen Box against <i>L. mexicana</i> NanoLuc-PEST-transgenic line	75
2.4 Generating drug-resistance	76
2.5 Morphological and ultrastructural analysis of the Leishmanial parasite ...	76
2.5.1 Immunofluorescence assay	76
2.5.2 Scanning electron microscopy (SEM) of metacyclic promastigotes.....	77
2.5.3 Transmission Electron Microscopy (TEM)	78
2.6 Molecular Biology Techniques	78
2.6.1 Isolation of Genomic DNA	78
2.6.2 Amplification reactions	79
2.6.3 PCR product analysis	80
2.6.4 Ligation	80
2.6.5 Transformation of bacteria	80
2.6.6 Selecting transformed colonies	81
2.6.7 Purification of plasmid DNA	81
2.6.8 Digestion of plasmid with restriction enzyme	82
2.6.9 Genomic DNA sequencing of LmMT and LmRos3	82
2.6.10 Sequence analysis	82
2.7 Data analysis	83

2.8 Chemical laboratories	83
Chapter 3: Screening of Phytopure library compounds against <i>P. falciparum</i>, <i>T. brucei</i> and <i>L. mexicana</i>	84
3.1 Introduction	84
3.2 Results	88
3.2.1 Antiplasmodial activity	88
3.2.1.1 Initial screening of intraerythrocytic <i>P. falciparum</i>	88
3.2.1.2 Confirmation of EC ₅₀ determination in a second <i>P. falciparum</i> strain (3D7)	94
3.2.1.3 Determination of estimated 50% lethal dose (LD ₅₀) in Dd2luc using bioluminescence assay	101
3.2.1.4 <i>In vitro</i> determination of Bioluminescence Relative Rate of Kill (BRRoK)	105
3.2.1.5 <i>In vitro</i> determination of cytotoxic effects against the human HepG2 cell line	110
3.2.2 Antitrypanosomal activity	114
3.2.2.1 Optimization of the proliferation assay	114
3.2.2.2 Screening of Phytopure library against <i>T. brucei</i>	115
3.2.2.3 Determination of EC ₅₀ values of 25 hits from Phytopure library screen by using Alamar Blue viability assay	115
3.2.2.4 <i>In vitro</i> determination of cytotoxic effects against the human HepG2 cell line	119
3.2.3 Antileishmanial activity	128
3.2.3.1 Optimization of the proliferation assay	128
3.2.3.2 Screening of Phytopure library against <i>L. mexicana</i>	129
3.2.3.3 Determination of EC ₅₀ values of 23 hits from Phytopure screens by using Alamar Blue viability assay	134
3.2.3.4 <i>In vitro</i> determination of cytotoxic effects against the human THP-1 and HepG2 cell lines	137
3.2.3.5 Validation of the four <i>L. mexicana</i> hits against <i>L. donovani</i>	143
3.2.3.6 Validation of the four <i>L. mexicana</i> hits against an intracellular macrophage model	145
3.2.4 An investigation of the biophysical properties the of Phytopure compound hits	150
3.3 Discussion	153
3.3.1 Intraerythrocytic <i>P. falciparum</i>	153
3.3.2 <i>T. brucei</i> bloodstream stages	157
3.3.3 <i>L. mexicana</i> parasites	158
3.3.4 Comparison of activity across parasites tested – a cautionary note	160
Chapter 4: Initial studies exploring the action of, and resistance to, compound 700022 in <i>Leishmania mexicana</i>	165
4.1 Introduction	165
4.2 Results	170
4.2.1 Generation of 700022-resistant <i>L. mexicana</i>	170

4.2.2 Comparative morphological examination of 700022-resistant and wild-type <i>L. mexicana</i>	175
4.2.3 Investigating the molecular basis of the 700022 resistant phenotype ...	184
4.2.3.1 Sequence analysis of LmMT	190
4.2.3.2 Sequence analysis of LmRos	192
4.3 Discussion	194
Chapter 5: Validation of bioluminescence screening and intramacrophage assays using <i>L. mexicana</i> expressing a NanoLuc-PEST reporter	201
5.1 Introduction	201
5.2 Results	205
5.2.1 Evaluation of NanoLuc assay parameters	205
5.2.3 Screening of MMV Pathogen Box against <i>L. mexicana</i> NanoLuc-PEST-transgenic line	211
5.2.4 Determination of EC ₅₀ values of selected compounds	215
5.2.5 Intracellular macrophage assay	218
5.2.6 <i>In vitro</i> cell cytotoxicity assay	224
5.2.7 Evaluation the initial cytocidal effect of antileishmanial reference compounds	226
5.3 Discussion	229
Chapter 6 Perspectives	236
References list	244
Appendix 1 (chapter 3)	286
Appendix 2 (chapter 4)	302
Appendix 3 (chapter 4)	310
Appendix 4 (chapter 4)	316
Appendix 5 (chapter 4)	322
Appendix 6 (chapter 5)	324

LIST OF FIGURES

Figure 1.1: The original Neglected Tropical Diseases (from Mackey <i>et al.</i> , 2014).	1
Figure 1.2: Map shows the global distribution of malaria endemicity (source-modified from WHO, 2014).	4
Figure 1.3: Asexual and sexual life cycles of <i>Plasmodium falciparum</i> in the human host and mosquito vector (Source: MMV).	7
Figure 1.4: Diagram showing asexual blood cycle of <i>Plasmodium falciparum</i> in humans, which usually takes 48 h to complete (Bozdech <i>et al.</i> , 2003).	10
Figure 1.5: Sexual cycle of the Plasmodium parasite in gut of mosquito (Angrisano <i>et al.</i> , 2012).	11
Figure 1.6: Manifestations of severe falciparum malaria, in 6189 children in studies conducted in Africa and 2605 adults in studies conducted in South-East Asia. The left side shows the relative importance of the clinical syndrome of severe falciparum malaria by age, and Venn diagrams on the right show the mortality in children and adults associated with manifestations of cerebral, malaria renal impairment and metabolic acidosis alone or in combination (John and Sons, 2014).	13
Figure 1.7: Rate of population with access to an ITN and proportion sleeping under an ITN, sub-Saharan Africa, 2000–2013. Source: ITN coverage model from the Malaria Atlas Project.	18
Figure 1.8: Chemical structure of mefloquine, quinine and chloroquine	23
Figure 1.9: Chemical structures of (A) artemisinins (B) dihydroartemisinin, (C) artemether and (D) artesunate (Ericsson, 2014).	25
Figure 1.10: Proposed mechanism of action for artemisinin (Bray <i>et al.</i> , 2005).	26
Figure 1.11: Geographic distribution of Human African trypanosomiasis (A) <i>T. b gambiense</i> and (B) <i>T. b. rhodesiense</i> . Source- modified from WHO, available at: http://www.who.int/trypanosomiasis_african/country/en/	27
Figure 1.12: Lifecycle of the human African trypanosomiasis. Source- modified from CDC, available at: https://www.cdc.gov/parasites/sleepingsickness/biology.html	29
Figure 1.13: Antitrypanosomal drugs in clinical use.	33
Figure 1.14: Distribution and endemicity of visceral leishmaniasis (VL) worldwide according to 2015 annual country reports. The majority of VL cases occur in just six countries — Bangladesh, Brazil, Ethiopia, India, Nepal and Sudan (source: WHO Global Health Observatory Link and access date).	37
Figure 1.15: Distribution and endemicity of cutaneous leishmaniasis, (CL) worldwide according to 2015 country reports. (Source: WHO Global Health Observatory).	39
Figure 1.16: Developmental forms of promastigote and amastigote. Each form has a nucleus (n) and kinetoplast (k) in the single mitochondrion (mt). The flagellum (f) arises from the flagellar pocket (fp). Source: (Bates, 2015).	40
Figure 1.17: Life Cycle of leishmanial parasite. (CDC, 2013) https://www.cdc.gov/parasites/leishmaniasis/biology.html	42
Figure 1.18: Chemical structure of current antileishmania drugs	44

Figure 1.19: Mode of action and resistance for pentavalent antimony in leishmania amastigotes.	47
Figure 1.20: The mode of action of amphotericin B against leishmanial parasites	49
Figure 1.21: DNDi planning activities in CL	54
Figure 2.1: Schematic representation of a bioluminescence assay (to measure LD ₅₀ and RoK) and fluorescence assay (to measure EC ₅₀).	70
Figure 3.1: Screening the Phytopure library against <i>P. falciparum</i> . Dot plot graphs reporting the mean % normalized growth (n=4) obtained from intraerythrocytic trophozoite stages of <i>P. falciparum</i> exposed to 20 μM (open circle) and 2 μM (filled circle) of compounds over 48 hours. The range of compound ID reported on each dot plot is above of each chart (note that no detail on actual compound ID shown on x-axis, this is provided in table appendix 1).	90
Figure 3.2: Prioritizing compounds for EC ₅₀ determination in <i>P. falciparum</i> . The scatter plot compares the % normalized growth following exposure to 20 μM or 2 μM for 70 Phytopure library compounds (see ID starting 70xxxx). Fourteen compounds (shown in red) were selected for EC ₅₀ determination.	91
Figure 3.3: Log concentration normalized response curves for 30 Phytopure compounds used to estimate EC ₅₀ values in intraerythrocytic <i>P. falciparum</i> . (A) Reports compounds with EC ₅₀ determined < 6μM. The data show a mean ± StDev of n=9 measurements.	93
Figure 3.4: Log concentration normalized response curves for 12 Phytopure compounds in two strains of <i>P. falciparum</i> . The data show a mean ± StDev from three biological replicates. Non-linear regression curves in green are for the 3D7 strain and in black for the Dd2 strain. The EC ₅₀ with 95% CI values are shown in Table 3.2.	96
Figure 3.5: Correlation between EC ₅₀ values determined in two strains of <i>P. falciparum</i> . The mean EC ₅₀ value of 12 Phytopure compounds from 3D7 and Dd2 strains are plotted with the results of a linear regression analysis.	98
Figure 3.6: Log concentration normalized response curves comparing LD ₅₀ and EC ₅₀ values determined for 12 Phytopure compounds. The normalised 6 hour bioluminescence response is used to determine the LD ₅₀ (open circles and dotted lines) with the normalized 48 hours fluorescence curves being used to determine the EC ₅₀ (filled circles and full line). The data shown is a mean ± StDev from three independant biological replicates (n=9).	103
Figure 3.7: BRRoK assays for 12 Phytopure compounds. Each curves represent the concentration-dependant killing effects for (A) the indicated Phytopure compounds or (B) a benchmark antimalarials. The BRRoK was measured after 3 hours (red line), 6 hours (black line) and 48 hours (green line) with the mean and StDev (n=9) of normalised bioluminescence signal reported. The Phytopure compound data are plotted (top to bottom, predicted fastest to slowest) according to the ratio of LD ₅₀ /EC ₅₀ from Table 3.4.	107
Figure 3.8: Correlation of BRRoK assay data to determine the relative rates of kill for the 12 Phytopure compounds. Each chart relates the indicated correlation between 9x, 3x, 1x and 0.3x EC ₅₀ data at 6hours (e.g. top left compares 9X v. 3X EC ₅₀ data). The filled red circles represent benchmark antimalarial drugs, green circles represent the six Phytopure compounds with LD ₅₀ /EC ₅₀ ratio < 2, black circles represent the six Phytopure compounds with	109

LD ₅₀ /EC ₅₀ ratio > 2. Note all <i>p</i> values and <i>r</i> ² for a linear regression of the 16 data points are reported on each graph.	
Figure 3.9: Initial determination of cytotoxicity of the 12 Phytopure compounds against HepG2 cells. Log concentration normalized growth curves were fitted for HepG2 (green lines) and <i>P. falciparum</i> (black line) Dd2 strain. The data shown is a mean (n=9) ± StDev from at three independent biological replicates.	112
Figure 3.10: Determination of initial blood stream form <i>T. brucei</i> seeding density. The graph plots a logarithmic growth regression analysis of a 48 hours Alamar Blue assay (fluorescence at 615nm) versus the initial seeding density to optimize the selection of conditions for a 96-well multiplate growth assay. Data represents the mean ± StDev of n=3.	114
Figure 3.11: Screening the Phytopure library compounds against <i>T. brucei</i> . Each panel reports the mean ± StDev (n=4) of normalized parasite growth when exposed to 2µM of the indicated compound. The Compound ID is 700-xxx with the suffix listed for each compound on the x-axis.	116
Figure 3.12: EC ₅₀ activity of 25 Phytopure compounds against <i>T. brucei</i> and initial determination of cytotoxicity. Log concentration normalised response curves to determine EC ₅₀ activity against <i>T. brucei</i> (black curves) and CC ₅₀ against HepG2 cells (green curves) for the indicated Phytopure compounds. The data shown is a mean ± StDev of n=9. There was no CC ₅₀ assay done for compound 701156.	121
Figure 3.13: Determination of initial <i>L. mexicana</i> axenic amastigote seeding density. The graph plots a logarithmic growth regression analysis of a 72 hours Alamar Blue assay (fluorescence at 615nm) versus the initial seeding density to optimize the selection of conditions for a 96-well multiplate growth assay. Data represents the mean ± StDev of n=3.	128
Figure 3.14: Screening the Phytopure library compounds against <i>L. mexicana</i> . Each panel reports the mean ± StDev (n=4) of normalized parasite growth when exposed to 2µM of the indicated compound. The Compound ID is 700-xxx with the suffix listed for each compound on the x-axis.	130
Figure 3.15: EC ₅₀ activity of 23 Phytopure compounds against <i>L. mexicana</i> and initial determination of cytotoxicity. Log concentration normalised response curves to determine EC ₅₀ activity against <i>L. mexicana</i> (black curves) and CC ₅₀ against THP-1 cells (red curves) or HepG2 (green curves) for the indicated Phytopure compounds. The data shown is a mean ± StDev of n=9. HepG2 assays were not carried out for all compounds.	135
Figure 3.16: EC ₅₀ activity of 700022, 700107, 700136 and 700240 Phytopure compounds against <i>L. donovani</i> . Log concentration normalised response curves to determine EC ₅₀ activity against <i>L. donovani</i> (black dotted curves). To aid comparison, the EC ₅₀ activity against <i>L. mexicana</i> (black full line curve) and CC ₅₀ against THP-1 cells (red curves) or HepG2 (green curves) are also shown for the indicated Phytopure compounds. The data shown is a mean ± StDev of n=9. Note the EC ₅₀ curves for 700107 are overlapping.	144
Figure 3.17: Scoring <i>L. mexicana</i> infected THP-1. The panels represent fluorescent imaging of Sybr Green I staining of nuclear material imaged using an EVOS fluorescence imaging system. (A) Images from the uninfected differentiated THP-1 control. Images from the 0.75µM amphotericin B treatment of	147

<p>infected differentiated THP-1 where (B) intracellular <i>L. mexicana</i> amastigotes are not evident or (C) are evident (white arrows). Bar = 100µm</p>	
<p>Figure 3.18: Compounds 700022, 700107, 700136 and 700240 are effective against <i>L. mexicana</i> intramacrophage amastigotes. (A and B) illustrate the proportion of differentiated THP-1 that show evidence of intramacrophage amastigotes following exposure to the fold EC₅₀ concentration of amphotericin B (AmB) or the four Phytoquest compounds from two independent biological repeats. Each graph represents the mean mean ± range from two technical repeats. (C) Illustrates these two data sets, normalized in each case against their respective mean untreated control, combined together to show the mean ± StDev (n=4).</p>	148
<p>Figure 3.19: Distribution of <i>L. mexicana</i> parasite count in infected macrophages. Box and whisker plots of counts of intramacrophage amastigotes in infected differentiated THP-1 following exposure to the treatment shown on the x-axis. The box represents the 25-75% mean distribution with the central line as the mean. Whiskers show the total distribution of the counts of intramacrophage amastigotes. AmB; amphotericin B.</p>	150
<p>Figure 3.20: Comparison of 6 hours BRRoK data for structurally related Phytopure compounds. Comparison of mean normalized bioluminescence signals (from Figure 3.7) clustered by compound structure. Structures for the indicated compounds are shown to the right.</p>	156
<p>Figure 3.21: Phytopure compound activity across multiple species (A) A Venn diagram of the compounds identified to have an EC₅₀ < 2 µM activity in one or more of the indicated species (B) Bar chart reporting the distribution of HepG2 CC₅₀ values of compounds that target a single species or multiple (two or three species) in this study. Boxes, compounds with selectivity indices of >20. Dotted box, 700046 has a selectivity against <i>P. falciparum</i> and <i>T. brucei</i>. Significance is determined from an unpaired t-test of distribution.</p>	162
<p>Figure 4.1: Binding and uptake of miltefosine (MIL) in <i>Leishmania</i> spp. A schematic representing the uptake of MIL across a membrane by the MT/Ros3 MIL transporter. The hydrophobic MIL is typically bound to serum albumin (represented here is a tissue culture system using bovine serum albumin, BSA) which acts as a reservoir. The translocation of MIL from the outer to the inner leaflet of the plasma membrane is facilitated by the <i>Leishmania</i> miltefosine transporter (MT), a P4-ATPase subfamily flipase shown here as the α-unit, with its β-subunit termed Ros3 (Perez-Victoria <i>et al.</i>, 2003).</p>	169
<p>Figure 4.2: Selection of a 700022-resistant line in <i>L. mexicana</i>. (A) Promastigote cultures are exposed sequentially to the indicated concentration of 700022 (increasing tone of gray to show increase in concentration). These concentrations of 700022 are based on the EC₅₀ in promastigotes determined at start of week 0, 10, 15 and 25. At the indicated points (circles) the EC₅₀ of 700022 was determined in promastigotes (red, note y-axis is split with different concentration ranges indicated) or axenic amastigotes (black) prepared from the promastigote culture under selection. Log concentration normalized response graphs to determine the EC₅₀ in promastigotes (B) or axenic amastigotes (C). The key indicates the weeks of selection as well as the EC₅₀ (in µM). The mean±StDev (n=9) are reported.</p>	172

Figure 4.3: Observation of resistance stability for <i>L. mexicana</i> axenic amastigotes and promastigotes under compound pressure in stepwise concentrations after 28 weeks (black), and 60 days after removal from compound pressure (red).	173
Figure 4.4: 700022-resistant <i>L. mexicana</i> axenic amastigotes showed decreased sensitivity to related triterpenes. Log concentration-normalised response curves for the related triterpenes 700022, 700107, 700136 and 700240. Response curves for axenic parasites before exposure to 700022 (black lines) and after 8 weeks of selection (red lines). The mean \pm StDev (n=9) are reported.	174
Figure 4.5: Comparative immunofluorescence microscopy analysis wild-type and 700022 resistant <i>L. mexicana</i> . Representative images of promastigotes from wild-type (A) and 700022-resistant (B) stained for α -tubulin (green) and DNA (blue). Note the absence of flagellum in the 700022-resistant promastigotes. The same staining was applied to wild-type (C) and 700022-resistant (D) axenic amastigotes. N, nucleus; F, flagellum; K, kinetoplast. Bars = 10 μ m	177
Figure 4.6: ImageJ analysis of <i>L. mexicana</i> promastigotes stained for α -tubulin content. Using the area tool (white) the area of the promastigote cell is outlined in wild-type (A) and 700022-resistant cells. Using the length tool (red), the length of the flagellum is indicated in the same images	178
Figure 4.7: ImageJ analysis of <i>L. mexicana</i> axenic amastigotes stained for α -tubulin content. Using the area tool (white) the area of the amastigote cell is outlined in wild-type (A) and 700022-resistant cells.	178
Figure 4.8: Scatterplots of the distribution of cell body size and flagellum length in wild type and 700022-resistant <i>L. mexicana</i> . Box and whisker plots (boxes illustrate 25 to 75% distribution and median, with whiskers showing range of data. (A) Compares the distribution of flagellar length (μ m) in wild-type (WT) and 700022-resistant (r700022) promastigotes. (B) and (C) compare the surface area (μ m ²), a surrogate determination of cell size, in promastigotes and axenic amastigotes, respectively. The significance of the difference in means is shown (two-way t-test).	179
Figure 4.9: Scanning electron microscopy of <i>L. mexicana</i> promastigotes. Wild-type promastigotes that are (A) untreated or (B) exposed to 1x EC ₅₀ (11.4 μ M) of 700022. 700022-resistant promastigotes that are (C) untreated or (D) exposed to 1x EC ₅₀ (85.6 μ M) of 700022C.	181
Figure 4.10: Transmission electron microscopy of wild type <i>L. mexicana</i> promastigotes. Wild-type promastigotes that are (A) untreated or (B) exposed to 1x EC ₅₀ (11.4 μ M) of 700022 for 24 hours. N, nucleus; K, kinetoplast; M, mitochondria; FP, flagellar pocket; F, flagellar; acidocalcisomes (black arrows).	182
Figure 4.11: Transmission electron microscopy of 700022-resistant <i>L. mexicana</i> promastigotes. 700022-resistant promastigotes that are (A) untreated or (B) exposed to 1x EC ₅₀ (85.6.4 μ M) of 700022 for 24 hours. N, nucleus; K, kinetoplast; acidocalcisomes appear as vacuoles or with an electron-dense inclusion (black arrows) following exposure to 700022.	183
Figure 4.12: Exploring cross-resistance in 700022-resistant <i>L. mexicana</i> . (A) Log concentration -response curves used to estimate EC ₅₀ of the indicated compound/drug in wild type (green curve) and 700022-resistant promastigotes (black curve). (B) Log concentration -response curves used to	186

<p>estimate EC₅₀ of the indicated compound/drug in wild type (green curve) and 700022-resistant axenic amastigotes (black curve). The data shown is a mean ± StDev from at least two biological replicates. See also Table 4.3.</p>	
<p>Figure 4.13: Schematic illustrating the mapping of mutations in <i>Leishmania</i> MT gene associated with miltefosine resistance, as previously discibed (see Table 4.4). Fragments 1 to 3 were chosen to amplify from <i>L. mexicana</i> genomic DNA.</p>	189
<p>Figure 4.14: Verification of PCR amplification from (A) LmMT and (B) LmROS3 genes. Size fractionation of <i>Eco</i>RI restricted plasmid clone containing the following PCR product; 1&2 are fragment 1, 3&4 are fragment 2 and 5&6 are fragment 3 of LmMT gene; 7 and 10 are 100bp markers (Bioline); 8 and 9 are of LmROS3. R; 700022-resistant line; WT, wild type. Note that fragment sizes are larger than in Figure 4.13 as include flanking regions with restriction sites.</p>	189
<p>Figure 4.15: Schematic representing sequence analysis of LmMT gene. (A) A summary of all SNP identified in various clones after sequencing. The nucleotide position of each SNP is indicated by a bar, with the effect on amino acid sequence shown adjacent. For ease, NS SNP are shown in red throughout, with synonymous SNP in green. (B) A summary of the 12 clones for each fragment of LmMT sequenced compared LmxM.13.1530. The WT-prefix is for the pre-selection wild type and the R-prefix for 700022-selected parasites. The HH code uniquely identifies the PCR clone sequenced. Note that the synonymous G2541A SNP in all fragment 3 clones sequenced is marked only once in the schematic.</p>	191
<p>Figure 4.16: Schematic representing sequence analysis of LmROS3 gene. (A) A summary of all SNP identified in various clones after sequencing. The nucleotide position of each SNP is indicated by a bar, with the effect on amino acid sequence shown adjacent. For ease, NS SNP are shown in red throughout, with synonymous SNP in green. (B) A summary of the 9 clones for LmROS3 sequenced compared to LmxM.31.0510. The WT-prefix is for the pre-selection wild type and the R-prefix for 700022-selected parasites. The HH code uniquely identifies the PCR clone sequenced.</p>	193
<p>Figure 4.17: Comparison of the effect of parasite growth between <i>L. mexicana</i> WT and 700022 resistant line. The number of parasites were counted over a 72 hours for <i>L. mexicana</i> promastigotes, and over a 48 hours for <i>L. mexicana</i> amastigotes. The growth of resistant cells was two times more than to the <i>L. mexicana</i> wild type of both forms promastigotes and amastigotes over a 72 hours and 48 hours period respectively. The resistant cells are smaller but they growth and divided faster than WT cells after remove the drug pressure.</p>	197
<p>Figure 5.1: Optimizing assay volumes for bioluminescence assays with NanoLuc and NanoLuc-PEST transgenic <i>L. mexicana</i>. Correlating bioluminescence signal with parasite volume for (A) NanoLuc and (B) NanoLuc-PEST transgenic <i>L. mexicana</i>. Black lines represent untreated control parasites, and Red lines represent parasites exposed to 0.2 μM AmB. Data represent mean ± StDev of n=3 technical replicates. Charts C and D report the bioluminescent signal from 20 μL of NanoLuc and NanoLuc-PEST transgenic <i>L. mexicana</i> (respectively) with increasing volumes of Nano-Glo reagent. Bars show mean ± StDev of n=3 technical replicates.</p>	207

<p>Figure 5.2: Amphotericin B concentration-normalized response profiles. Graphs depicting the concentration-response to amphotericin B in the (A) parental, (B) NanoLuc and (C) NanoLuc-PEST <i>L. mexicana</i> lines. The black line on each graph represents the response as determined using the fluorescent-based AlamarBlue assay. The green and blue lines represent the bioluminescent activity in the respective (B) NanoLuc and (C) NanoLuc-PEST <i>L. mexicana</i> lines. Mean values \pm StDev (n=6) are shown. Data are reported in Table 5.3.</p>	208
<p>Figure 5.3: Miltefosine concentration-normalized response profiles. (A) Concentration-response curve of the parental <i>L. mexicana</i> cell line, measured using the fluorescence-based AlamarBlue assay. (B) Concentration-response curve of the transgenic NanoLuc-PEST expressing <i>L. mexicana</i> clone measured using both the fluorescence-based AlamarBlue assay (black) and the bioluminescence-based assay (blue). Mean values are shown (n=6) \pm StDev. EC₅₀ values for the parental and NanoLuc-PEST cell lines are reported in Table 5.4.</p>	210
<p>Figure 5.4: MMV Pathogen Box screening using the NanoLuc-PEST assay. The library is provided as five plates labelled A to E (and as shown here), each with 80 compounds – shown here on the x-axis (see also Table S2). The relative bioluminescence of the NanoLuc-PEST expressing <i>L. mexicana</i> when screened against 2 μM (filled circle) or 10 μM (open circle) is shown with the lines marking the StDev. The dashed line shows the point at which a 95% reduction in relative bioluminescence, ie a 95% kill, was achieved.</p>	213
<p>Figure 5.5: Screening the MWV Pathogen Box using the NanoLuc-PEST-based bioluminescence assay. Scatterplot correlating the mean bioluminescence following exposure to the indicated concentration of compounds. The mean (n=4) bioluminescence signal is shown, with the key illustrating the disease screen that identified the compound for inclusion in the library (www.pathogenbox.org) (A) Illustrates the full library dataset with (B) providing an inset of the most potent compounds from the MMV Pathogen Box screen.</p>	214
<p>Figure 5.6: Log-concentration response curves for MMV Pathogen Box hits. Concentration-normalised bioluminescence response curves for 22 hits against axenic <i>L. mexicana</i> amastigotes. The data shown is a mean \pm StDev from at least three biological replicates. EC₅₀ estimates are reported in Table 5.5.</p>	217
<p>Figure 5.7: Bioluminescence assays of intracellular activity of MMV Pathogen Box compounds. The concentration response curves (mean\pmStDev of n=9) for the indicated MMV Pathogen Box compound, amphotericin B (AmB) or miltefosine (MIL) against intracellular amastigotes in THP-1 (dotted lines) or axenic amastigotes (full line).</p>	220
<p>Figure 5.8: EC₅₀ responses to Amphotericin B (AmB), Miltefosine (MIL), Pentamidine and Hygromycin B in axenic <i>L. mexicana</i> amastigotes expressing NanoLuc-PEST. Mean values are shown (n=4) \pm StDev.</p>	227
<p>Figure 5.9: Time and concentration-dependent loss of bioluminescence representing a timecourse of cytotoxic activity for antileishmanial drugs. The mean normalized bioluminescent signal from <i>L. mexicana</i> NanoLuc-Pest transgenic lines exposed to increasing fold-EC₅₀ concentrations of amphotericin B (AmB), miltefosine (MIL), pentamidine and hygromycin B.</p>	228

The key indicates the time for each concentration-reponse reported on each graph. Data represent mean±StDev (n=9).	
Figure 5.10: The bioluminescent reaction catalyzed by NanoLuc luciferase.	229
Figure 5.11: Comparison of bioluminescence- and microscopy-based intramacrophage infection assays following treatment with Amphotericin B. (a) Infection of PMA-differentiated THP-1 was assessed by the NanoLuc-PEST-expressing transgenic <i>L. mexicana</i> , using the novel bioluminescence-based assay. Infected cells were exposed to 0.8 µM amphotericin B, or left untreated, for 72 hours. Relative bioluminescence is shown after each treatment, calculated against the average value for the untreated cells. Mean values are shown (n=4) ± SD. Results were analysed by Paired T Test on raw data ($p<0.001$). (b) Infection of PMA-differentiated THP-1 macrophages was assessed by the NanoLuc-PEST-expressing transgenic <i>L. mexicana</i> , using the standard microscopy-based counting assay. Infected cells were exposed to 0.8 µM amphotericin B, or left untreated, for 72 hours.	233
Figure 6.1: Comparing 700022 activity between axenic amastigotes (red) and intramacrophage amastigotes (blue). Concentration–response curves for compound 700022 against: intracellular <i>L. mexicana</i> NanoLuc-PEST-transgenic line (blue), axenic amastigotes of NanoLuc-PEST-transgenic line (red) as well as the human cell lines HepG2 (green) and THP-1 (black). Most data from chapter 5. The data for the intracellular <i>L. mexicana</i> NanoLuc-PEST-transgenic line represent one biological repeat of three technical repeats.	238
Figure 6.2. Structure of MMV690102.	241

LIST OF TABLES

Table 1.1: First reported resistance to some antimalarial drugs (Sinha <i>et al.</i> , 2014).	20
Table 1.2: Drugs used in treatment of human African trypanosomiasis. i.m., intramuscularly; i.v., intravenously. (Büscher <i>et al.</i> , 2017).	33
Table 1.3: Leishmania species and their clinical manifestation (Bates, 2007; McCall <i>et al.</i> , 2013).	35
Table 1.4: Antileishmania drugs properties. i.v. = intravenous. i.m. = intramuscular. CID = PubChem Compound Identifier	45
Table 1.5: Combination therapy of antileishmania drugs	52
Table 1.6: Antiparasitic activity of natural product sources	57
Table 2.1: Oligonucleotide sequences for cloning and integration	64
Table 2.2: List of genes and oligonucleotide sequences used for gene sequences. All the oligonucleotides were bought from Eurofins Genomics.	80
Table 2.3: EcoRI digestion reaction.	82
Table 3.1: EC ₅₀ data of 14 Phytopure compounds obtained from intraerythrocytic <i>P. falciparum</i> with an EC ₅₀ of <6µM determined from three independent biological repeats (highlighted in green). The 95% confidence intervals (95% CI) are reported for the the EC ₅₀ of these 12 compounds.	94
Table 3.2: EC ₅₀ in Dd2 and 3D7 strains of <i>P. falciparum</i> for 12 Phytopure compounds.	97
Table 3.3: A, information generated from PhytoQuest for high interest compounds against <i>P. falciparum</i> . B, the structure of each compound.	98
Table 3.4: Estimates of EC ₅₀ and LD ₅₀ of 12 Phytopure compounds in the Dd2 strain of <i>P. falciparum</i> . The data shown for benchmark antimalarial drugs1 chloroquine (CQ), quinine (QN), atovaquone (ATQ) and dihydroartemisinin(DHA) were obtained from Ullah <i>et al.</i> (2017) ¹ .	104
Table 3.5: <i>In vitro</i> antiplasmodial activity (EC ₅₀) and cytotoxicity (CC ₅₀) against HepG2 cells for the 12 Phytopure compounds. SIA, is calculated as CC ₅₀ /EC ₅₀ using Dd2 strain, whilst SIB is calculated using the 3D7 strain. (Ullah, 2017) ¹ , (Lelie`vre <i>et al.</i> , 2012) ² .	113
Table 3.6: <i>In vitro</i> antitrypanosomal activity (EC ₅₀) and cytotoxicity (CC ₅₀) against HepG2 cells of 25 Phytopure compounds. SI*, is calculated as CC ₅₀ /EC ₅₀ . (Thao <i>et al.</i> , 2014) ¹ .	122
Table 3.7: (A) Source information and (B) structure of 25 hit compounds from Phytopure library against <i>T. brucei</i> .	123
Table 3.8: <i>In vitro</i> antileishmanial activity (EC ₅₀), and cytotoxicity (CC ₅₀) against THP-1 cell line and HepG2 cell line for 23 Phytopure compounds. SI, is calculated as CC ₅₀ /EC ₅₀ . (Mehta <i>et al.</i> , 2010) ¹ ; (Escudero-Martínez <i>et al.</i> , 2017) ²	136
Table 3.9: A, information generated from PhytoQuest for high interest compounds against <i>L. mexicana</i> . B, the structure of each compound.	139
Table 3.10: <i>In vitro</i> antileishmanial activity, and cytotoxicity of compounds (700022, 700107, 700136 and 700240) against <i>L. donovani</i> amastigotes, THP-1 cells and HepG2 cells. SI, is calculated as CC ₅₀ /EC ₅₀ .	145
Table 3.11: Exploring 33 compounds properties depending on Lipinski's Rule of Five and Veber's rules.	152
Table 3.12: Table reporting most active compounds	163

Table 4.1: Cross-resistance to related triterpenes in 700022-resistant <i>L. mexicana</i> . Resistance index, RI is a ratio of the mean EC ₅₀ after 8 weeks selection compared to that in WT (unselected) parasites	175
Table 4.2: Measurements of morphological forms; cells surface area and flagellum length for <i>L. mexicana</i> WT and resistant line	179
Table 4.3: Cross resistance of 700022-resistant <i>L. mexicana</i> promastigotes and amastigotes towards other antileishmanial drugs. Resistance Index (RI) is the ratio between the EC ₅₀ of resistant line/the EC ₅₀ for the wild-type strain. 700022-r, <i>L. mexicana</i> resistant to 700022.	187
Table 4.4: Mutations identified in MT miltefosine transporter genes in Leishmania spp	188
Table 4.5 Mutations identified in miltefosine transporter genes LmROS3 and LmMT in this study. WT, wild type pre-selection; R, 700022-resistant; Syn, synonymous; Non-syn, non-synonymous; AA, amino acid.	194
Table 5.1: Studies reporting the screening of the MMV Pathogen Box and Malaria Box libraries	204
Table 5.2: Table reporting volumes used to evaluate NanoLuc assay	206
Table 5.3: Comparison of the EC ₅₀ , Z' and Signal:Background (S:B) values of amphotericin B (AmB) activity against wild-type and NanoLuc-expressing <i>L. mexicana</i> in fluorescent and bioluminescence assays.	209
Table 5.4: Comparison of the EC ₅₀ , Z' and Signal:Background (S:B) values of miltefosine (MIL) (AmB) activity against wild-type and NanoLuc-PEST expressing <i>L. mexicana</i> in fluorescence and bioluminescence assays.	210
Table 5.5: EC ₅₀ values for MMV Pathogen box hits against axenic <i>L. mexicana</i> amastigotes.	217
Table 5.6: A, activity of the most potent MMV compounds against axenic and intra-macrophage amastigotes using a bioluminescence assay. B, structure of compounds	221
Table 5.7: Human cytotoxicity data for selected MMV Pathogen Box compounds.	225
Table 5.8: Comparison the EC ₅₀ values between antileishmanial drugs	227
Table 5.9: Activity of selected kinetoplastid hits against <i>L. infantum</i> intracellular macrophage and cytotoxicity	231
Table 5.10: <i>In vitro</i> time-to-kill for current antileishmanial reference compounds. (Van den Kerkhof <i>et al.</i> , 2018) ¹ (Maes <i>et al.</i> , 2017) ²	234
Table 6.1: Activity of Phytopure compound 700022 against intracellular and extracellular <i>L. mexicana</i> amastigotes using luminescence assay. SI1, is calculated as CC ₅₀ /EC ₅₀ using axenic amastigotes whilst SI2 is calculated using intra-macrophage amastigote data.	239

ABBREVIATIONS

AAT	animal African trypanosomiasis
ACTs	artemisinin-based combination therapies
AmB:	Amphotericine B
ATQ	Atovaquone
bp	base pair
BRRoK	Bioluminescent Relative Rate of Kill
BSA	Bovine Serum Albumin
CC ₅₀	50% cytotoxicity Concentration
CI	Confidence intervals
CL	Cutaneous leishmaniasis
CNS	central nervous system
CQ	Chloroquine
DAPI	4', 6-Diamidino-2-Phenylindole
DDT	dichloro-diphenyl-trichloroethane
DHA	dihydroartemisinin
DMEM	Dulbecco's modification of Eagle medium
DMSO	Dimethyl sulfoxide
DNA	Deoxyribonucleic Acid
DNDi	Drugs for Neglected Diseases initiative
EC ₅₀	50% Effective Concentration
EDTA	Ethylene Diamine Tetra acetic acid
EPI	expanded programme on immunisation
FBS	Fetal Bovine Serum
GDP	gross domestic product
GPI	glycosylphosphatidylinositol
HAT	human African trypanosomiasis
HCT	Haematocrit
HepG2	liver hepatocellular carcinoma
HIV	The human immunodeficiency virus
HTA	Human Tissue Authority
HTS	High Throughput Screening
i.m.	intramuscular
i.v.	intravenous
IF	immunofluorescent
IPT	intermittent preventive treatment
iRBS	infected red blood cell
IRS	indoor residual spraying
ITNs	Insecticide treated nets
k	kinetoplast
L	litres
LAmB	liposomal-amphotericin B
LB	Luria-Bertani medium
LD ₅₀	the 50% lethal dose

LD ₅₀ 50%	Lethal Dose
LPG	lipophosphoglycan
LRR	leucine-rich repeat
Luc	Luciferase
M	Molar
MCL	Mucocutaneous Leishmaniasis
MCL:	Muco-cutaneous leishmaniasis
MDA	Mass drug administration
mg	milligram
MIL:	Miltefosine
ml	millilitre
mM	millimolar
MMV	Medicine for Malaria Venture
Mwt	molecular weight
MQ	Mefloquine
MSF	Malaria SYBR Green I Fluorescence
MT	miltefosine transporter
MW	Molecular weight
NECT	nifurtimox–eflornithine combination therapy
NGS	Next-generation sequencing
NMCPs	national malaria control programmes
NS	nonsynonymous
ORh+	Type-O-Rhesus Positive
PBS	Phosphate Buffer Saline
PCR	Polymerase chain reaction
PCT	parasitaemia
Pf	<i>Plasmodium falciparum</i>
PfEMP1	<i>Plasmodium falciparum</i> erythrocyte membrane protein 1
PKDL	Post Kala azar dermal
PMA	phorbol 12-myristate 13-acetate
PQ	PhytoQuest
QN	Quinine
R&D	Research and Development
RBCs	Red Blood cells
RNA	Ribonucleic acid
RO5	Lipinski's rule-of-five
RPMI	Roswell Park Memorial Institute
RT	Room Temperature
S to B	Signal-to-Background
Sb(V)	Pentavalent antimonials
SD	Standard Deviation
SEM	Scanning electron microscopy
SI	selective index
SL	Luciferase Substrate
SMC	Seasonal malaria chemoprevention

SNPs	Single nucleotide polymorphisms
TCP	Target Candidate Profiles
TEM	Transmission Electron Microscopy
THP-1	human monocytic leukemia cell
v/v	Volume/volume WHO World Health Organisation
+ve	Positive control
-ve	Negative control
VL	Visceral leishmaniasis
w/v	Weight/volume
WBCs	White Blood cells
WHO	World Health Organization
WT	Wild type
µg	Microgram
µL	Microliter
µm	Micrometre
°C	Degree Celsius

ACKNOWLEDGMENTS

I would like first to express my sincere gratitude to my supervisor Professor Paul Horrocks for his great supervision, encouragement, unstinting moral and technical support. I will never be able to repay them for their patience, guidance, advice and support throughout my PhD. I learnt so much from you, scientifically, and personally. You gave me space to grow as an independent scientist and I will be forever thankful.

Also I would like to give special thanks to my sponsor, The Higher Committee for Education Development in Iraq (HCED), for the funding and the opportunity to do a PhD.

It is also my pleasure to thank of PhytoQest Ltd (in particular prof. Robert Nash and Barbara Bartholomew) for the supply of the natural product compounds library used in this thesis.

I would also like to thank my adviser Dr Helen Price for her invaluable guidance and her helpful input on my presentations and reports over the years.

I would like to acknowledge the assistance of Dr Sarah Oates who was invaluable at the start of my project, and all other colleagues of the Keele Life Sciences department for their cooperation-it was much appreciated.

I would like to thank my family for their unconditional love and encouragement with particular thanks to my mother.

At the end, a special thanks to my lovely wife Zainab for her unwavering support and endless patience during my PhD study and you gave me your unconditional support at all times. And my kids, Zaid and Zain for their patience during my studies. You are the soul of my passionate commitment to my work.

Chapter 1: General introduction

1.1 The global impact of parasitic diseases

Malaria and the Neglected Tropical Diseases (NTDs) are major causes of global morbidity and mortality. The NTDs were originally a group of seventeen bacterial, parasitic, viral, and fungal infections defined by the World Health Organization (WHO) as communicable diseases with a diverse geographical impact affecting about 1 billion people (including an estimated 500 million children) across some of the poorest countries (Figure 1.1) (WHO, 2013). The group of diseases described as NTD increased in 2017 to include conditions such as snake bite and deep infecting mycoses – with a current list available at www.who.int/neglected_diseases/diseases. NTDs are responsible for more than 500,000 deaths every year and include conditions that cause cognitive impairment, stunted growth during childhood, anemia, blindness, and severe pain (Hotez *et al.*, 2007; Conteh *et al.*, 2010; Barry *et al.*, 2013). In 2010, according to the Global Burden of Disease Study, NTDs accounted for some 26 million disability-adjusted life years (DALYs) (Hotez *et al.*, 2014). The reasons for this neglect are poverty with sub-standard sanitation, geographical isolation, rarity of data regarding to the local and global burden, and insufficient financial and funding resources for their control (Hotez *et al.*, 2009; Allotey *et al.*, 2010).

Virus	Prokaryotic	Eukaryotic		
		Unicellular	Multicellular	
			Bilateral symmetry	Pseudocoelomate
Dengue Rabies	Buruli Ulcer Leprosy Trachoma Treponematoses	Chagas Disease Human African Trypanosomiasis Leishmaniases	Dracunculiasis Lymphatic Filariasis Onchocerciasis	Cysticercosis/Taeniasis Echinococcosis Foodborne Trematodiasis Schistosomiasis
			Soil-transmitted Helminthiases	

Figure 1.1: The original Neglected Tropical Diseases (from Mackey *et al.*, 2014).

In recent years, there has been considerable increase in efforts to reduce the burden of several NTDs, but they still contribute to suffering in many countries and recognise the potential impact of future global warming (Booth, 2018). Diagnostics are needed to detect and monitor the levels of infection and to eventually certify the elimination or eradication of NTDs in regions following intervention (Dowdle and Cochi, 2011). In NTD endemic areas, preventive chemotherapy is typically considered to be likely performed through mass drug administration (MDA) to reduce the reservoir of infection and eventually reduce mortality (Cromwell and Fullman, 2018; Keenan *et al.*, 2018) and in 2015 approximately 1 billion people were receiving preventive chemotherapy for one or more NTDs (WHO, 2017). There is however, an argument to be made for a more focussed delivery of MDA recognising that infection diseases are often twice higher in people from socioeconomically disadvantaged groups compared with their better-off compatriots (Houweling *et al.*, 2016).

In this thesis I focused to study the impact of *P. falciparum* (human malaria), *L. mexicana* (leishmania cutaneous), and *T. b. brucei*. These eukaryotic parasites are responsible for a range of diseases in humans. **Human African trypanosomiasis (HAT)**, also called sleeping sickness is caused by two subspecies of *T. brucei* - *T. brucei gambiense* and *T. brucei rhodesiense* (Büscher *et al.*, 2017). The symptoms of late stage HAT include sleep disorder and psychiatric disorders, changes of behaviour, confusion and poor coordination. HAT can be fatal if not properly diagnosed and treated, although cases of asymptomatic chronic infections have been described in West Africa (Chappuis *et al.*, 2005). **Leishmaniasis** is caused by an intracellular protozoa parasite with over 20 *Leishmania* species known to be transmitted and infective to humans. These parasites have been implicated in a range of disease conditions according to the observed clinical symptom presentations; cutaneous leishmaniasis, muco-cutaneous leishmaniasis and visceral leishmaniasis (Burza *et al.*, 2018). Parasites that cause **Malaria** are associated with the highest mortality and morbidity among

human parasitic infections (Bern *et al.*, 2008; Ashley *et al.*, 2018). About 40% of the world's population are at risk of infection by malarial parasites, with some 465,000 mortalities recorded annually (WHO, 2017a). This burden is heightened due to the development and spread of resistance to antimalarial drugs (Guantai and Chibale, 2011; Ginsburg and Deharo, 2011). Drug-resistant parasites typically usually result from indiscriminate use of antimalarial drugs (changes in drug accumulation), or reduced affinity of the drug target due to mutations in enzymes related to drug targets allowing parasites to escape from therapies (White, 1999; Kheir, 2011). The history of antimalarial drug treatment over the last 100 years is marked by the discovery of new drugs often followed by the detection and then spread of parasites resistant to this drug. Therefore, the need for new classes of antimalarial drugs that will attack novel molecular targets is a continuous issue in antimalarial drug treatment (Sinha *et al.*, 2014).

1.2 Malaria

1.2.1 Background of the Disease

Malaria is one of the most common and debilitating infectious diseases in tropical and subtropical zones. The impact of malaria can be represented both in terms of its impact on health and its socioeconomic impact in endemic countries (Orem *et al.*, 2012). An estimated 3.2 billion people live in 97 countries with malaria and 3.3 billion people at risk which amounts about 50% of the world population (Dinko *et al.*, 2016; WHO, 2016) (Figure 1.2). There is an approximately 212 million infections with malarial parasite all over the world; most of these cases (82%) were in the WHO African Regions, followed by the WHO Southeast Asia Regions (12%) and the WHO Eastern Mediterranean Regions (5%). Globally, malaria deaths were 429,000, and 90% of these deaths were in the WHO African

Regions, followed by the WHO Southeast Asia Regions (7%) and the WHO Eastern Mediterranean Regions (Belachew, 2018).

The greatest burden of this was among children aged <5 years, who have yet to acquire immunity to the disease and subsequently account for 78% of total malaria-associated deaths worldwide (WHO, 2014).

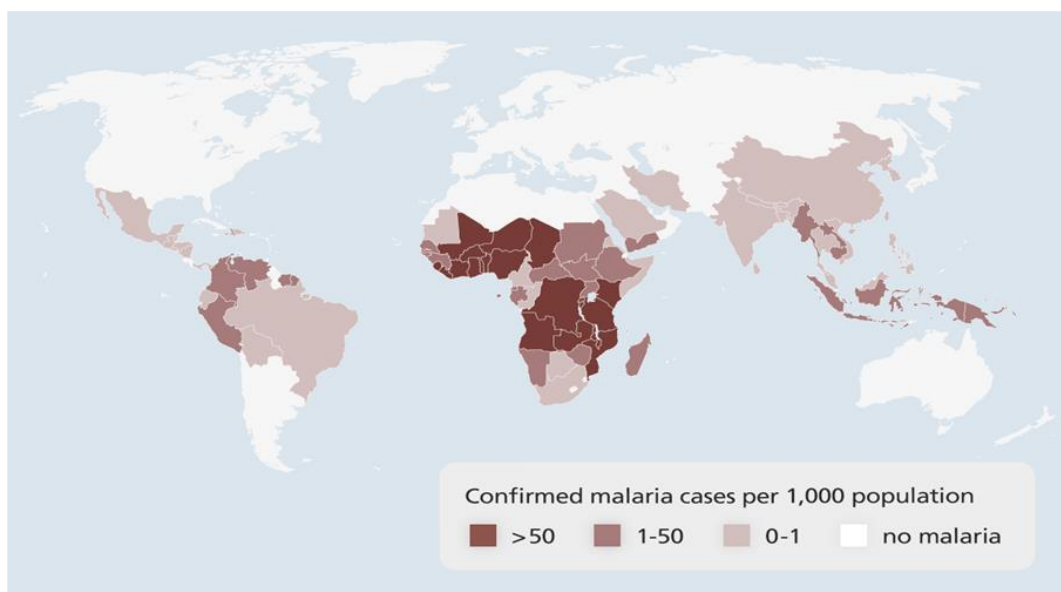


Figure 1.2: Map shows the global distribution of malaria endemicity (source- modified from WHO, 2014).

Malaria is caused by infection with parasitic protozoans belonging to the genus *Plasmodium* found in tropical and subtropical regions. The infection is transmitted through the bite of an *Anopheles* mosquito in the human host, when *Plasmodium* sporozoites infect the liver cells and then they infect red blood cells. The five species of protozoan responsible for disease malarial infections in human are; *P. vivax*, *P. falciparum*, *P. malariae*, *P. ovale* and *P. knowlesi* (circulates mainly among long-tailed and pig-tailed macaques that inhabit forested areas of South-East Asia) (Hellemond *et al.*, 2009; Cowman *et al.*, 2012). The most common are *P. vivax* and *P. falciparum*, the effects of which may be particularly severe in pregnancy which causes indirect death from abortion and intrauterine growth retardation. However, *P.*

ovale and *P. malariae* cause comparatively less severe clinical disease compared to other species (White *et al.*, 2014; Tuteja, 2007). The signs and symptoms are varied according to age, and local patterns of transmission (Guintran *et al.*, 2006). The economic burdens of malaria in stable transmission areas can be considerable, due to huge losses of income, high costs of treatment, low rates of education and agricultural production (Kiszewski and Teklehaimanot, 2004). Malaria accounts for up to 40% of public health expenditures, 30–50% of in-patient hospital admissions, and about 60% of out-patient health clinic visits in endemic countries. The impact of this on endemic countries is a decrease in gross domestic product (GDP) of 1.3% (GDP is defined here as the sum of the monetary value of all the goods and services produced by a country) (Mwamtobe *et al.*, 2014).

Over time, the risk of malaria infection in a particular region varies due to malaria epidemics, changes in travel habits and patterns of migration, and the development of drug resistance. Thus, health system strengthening, infrastructure development and poverty reduction may all aid malaria control and elimination (MacPherson *et al.*, 2009). Between the 1940s and the 1950s relentless regional and international efforts to treat malaria began, and further strategies have been developed with varied approaches over time. Between the beginning of this period and 1978, malaria was eliminated in parts of the Americas, Europe, and Asia. However, these efforts failed in many epidemic areas, particularly sub-Saharan Africa (Henry, 211). Recently there has been more attention to these areas by donor governments and multilateral institutions who have helped to decrease cases and deaths (WHO, March 2013). Between 2005 and 2013, annual funding for malaria management was increased at a rate of 22% by the Global Fund. The United Kingdom Department for International Development (DFID), The United States President's Malaria Initiative (PMI), the World Bank and other donors accounted for 49% of total disbursed funding in the year 2010, resulting in a rapid scaling up of malaria control in Africa (WHO, march 2013; WHO, 2014).

The most important strategic areas of malaria parasite control actions have been identified and include; intermittent preventive treatment (IPT) with two doses of sulfadoxine–pyrimethamine for pregnant women; and control of parasite transmission, focusing on the use of insecticide treated nets (ITNs) and indoor residual spraying (IRS) (Van Eijk *et al.*, 2013).

1.2.2 Life Cycle of *Plasmodium falciparum*

The *Plasmodium* parasites responsible for malarial disease have complex life cycles and spread between human hosts by the female mosquito vector (Figure 1.3) (Angrisano *et al.*, 2012). The parasite has a sexual and an asexual life cycle. The sexual life cycle begins in the gut and abdominal wall of the female *Anopheles* mosquito, while the asexual cycle begins in the liver of the infected human host and later when it enters the bloodstream where it invades and replicates within red blood cells. It is this intraerythrocytic part of the cycle that is responsible for the symptoms of the disease (Leera *et al.*, 2014).

The infection becomes symptomatic 10–15 days after being infected with malaria parasites. Such symptoms may include fever, chills, headaches, muscle pains, sweating and vomiting. In some cases the disease may progress to severe malaria where patients may present with additional complications such as; cerebral malaria, acute respiratory syndrome, severe anemia, kidney failure, hypoglycemia, pulmonary edema, seizures, coma and death may ensue (Betterton-Lewis, 2007; Shahinas *et al.*, 2013).

The erythrocytic stages have been studied *in vitro* culture, made possible in research by the growth of a continuous culture system that allows asexual parasite replication in erythrocyte stage. Most antimalarial chemotherapeutic agents are infections targeted at the asexual blood-stages of the parasite life cycle. By contrast, in liver stage there is a lack of *in vitro* culture (Vaughan *et al.*, 2012; Paaijmans, 2014).

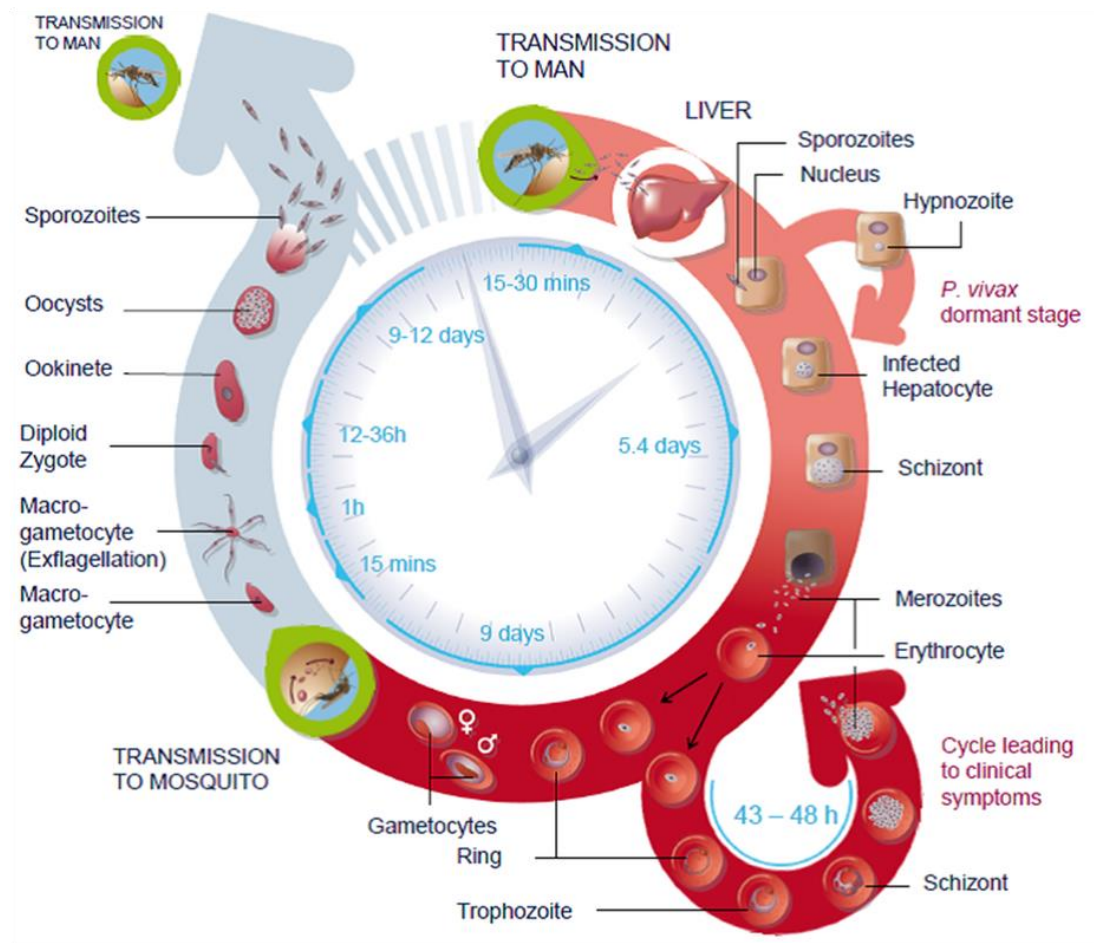


Figure 1.3: Asexual and sexual life cycles of *Plasmodium falciparum* in the human host and mosquito vector (Source: MMV).

1.2.3.1 Asexual life cycle of *Plasmodium falciparum*

a. Liver Stage/Pre-erythrocytic phase

The infection begins when the sporozoites from the salivary gland of a female mosquito are injected under the skin when the mosquito feeds on a human. The sporozoites enter the circulatory system and then travel through the blood stream to the liver where they invade hepatocytes (Prudêncio *et al.*, 2006).

The sporozoite begins asexual replication, within the pre-erythrocytic stage, taking about 10-14 days (depending on the *Plasmodium* species). The sporozoites mature and reproduce

asexually, becoming multinucleated schizonts (Figure 1.3). Over this period, the human host is asymptomatic. When the schizont matures and subsequently ruptures, it releases thousands of merozoite stage parasite into the circulatory system from the parenchymal cells of the liver (NIH, 2007; Betterton-lewis 2007). These merozoites may repeat the hepatic stages, or may enter the erythrocytic cycle (Leera *et al.* 2014). Some *Plasmodium* species, such as *P. vivax* and *P. ovale* can exist in a dormant state in the liver as hypnozoites. This stage is responsible for relapses of malaria (Prudêncio *et al.*, 2006).

b. Erythrocyte stage

The merozoites released from hepatocytes into the bloodstream invade the erythrocyte, initiating a second phase of asexual reproduction (Cox, 2010). The malarial parasite grows and divides inside the erythrocyte, completing asexual cycle approximately every 24 hours in *P. knowlesi*, 48 hours in *P. falciparum*, *vivax* and *ovale* and 72 hours in *P. malariae* to produce between 8 and 32 parasites (PHE, 2013). The parasite displays morphological changes within red blood cells during its asexual cycle. The different stages of the intra-erythrocytic cycle are shown in Figure 1.4. The merozoite develops into the ring form, is characterized by an extended central nucleus forming a ring, in which it spends between 20 and 24 hours (Shahinas *et al.*, 2013; Bannister and Mitchell, 2003). Parasites in this stage feed on hemoglobin and plasma nutrients from host erythrocytes through an endocytic process, in order to provide nutrients for growth and to synthesis molecules. This stage also extensively modifies the host RBC membrane (Van Dooren *et al.*, 2005). The ring eventually enlarges to become a mature trophozoite which appears from 24 h to 36 h (Baumeister *et al.*, 2010). During this period the parasite is at its most active in terms of metabolism, development and RBC modification. The malaria parasite undergoes digestion of hemoglobin within its food vacuole, producing toxic haem products which are polymerized

into non-toxic hemozoin (dark pigment) (Shahinas *et al.*, 2013; Van Dooren *et al.*, 2005). Asexual reproduction takes place when the parasite undergoes several cycles of cell division, resulting in the schizont stage. Schizonts undergo cell division to form about 6 to 36 new merozoites which are released and subsequently invade several uninfected red blood cells. These then progress through the asexual cycle within the red blood cell, releasing a new set of merozoites after 48 hours, thus repeating the cycle (Leera *et al.*, 2014; Cox, 2010).

Plasmodium falciparum is the most virulent species causing human malaria, during the cyclical asexual phase of its development. At this point in its life cycle, it induces modifications of its host cell by establishing new permeation pathways in order to absorb nutrients (Oberli *et al.*, 2014). This modification involves the parasite exporting more than 10% of all its proteins into the cytosol of the infected red blood cell (Mundwiler-Pachlatko and Beck, 2013). The *Plasmodium* surface anion channel (PSAC), consisting of members of the cytoadherence linked antigen (CLAG) protein family, mediates this transport (Mundwiler-Pachlatko and Beck, 2013; Nguitragool *et al.*, 2011). As a consequence, the infected erythrocyte increases its rigidity and adhesiveness resulting in alterations in microcirculatory blood flow. These alterations are responsible for many of the clinical manifestations of the pathogenesis of malaria (Oberli *et al.*, 2014; Maier *et al.*, 2008). The PfEMP1 protein (*Plasmodium falciparum* erythrocyte membrane protein 1) plays a key role in the pathology of *falciparum* malaria and displaying a variety of different binding phenotypes (Mundwiler-Pachlatko and Beck, 2013). Electron-dense protrusions appear on the surface of the host cell forming the anchor for the erythrocyte surface protein PfEMP1 (Oberli *et al.*, 2014). These unique alterations induced by *P. falciparum*, mediates cytoadherence to vascular endothelium resulting in iRBC cytoadherence and are therefore linked to disease severity.

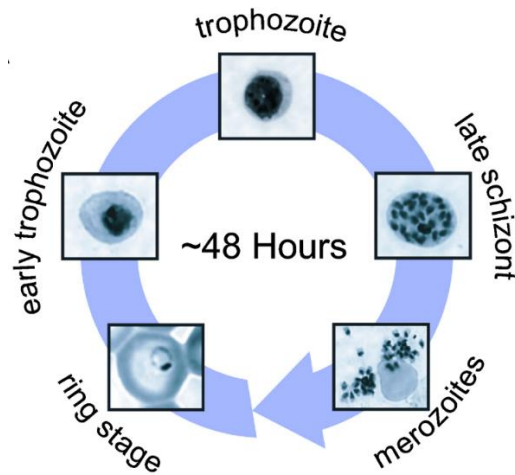


Figure 1.4: Diagram showing asexual blood cycle of *Plasmodium falciparum* in humans, which usually takes 48 h to complete (Bozdech *et al.*, 2003).

c. Sexual Stage

Within the erythrocyte, some of the merozoites undergo differentiation into male and female sexual forms known as gametocytes. The gametocytes do not cause illness but remain in the peripheral blood and exit from the host via the bite of a female *Anopheles* mosquito. The gametocytes are produced when the parasite is placed under stress factors such as antimalarial drugs or the immune system (Leera *et al.*, 2014; Cox 2010).

When a mosquito ingests infected blood, it becomes infected with male and female gametocytes which enter the gut of the mosquito. This begins a process known as sporogony, in which the gametocytes differentiate into male and female gametes and fertilization occurs generating zygotes. The zygote changes shape, converts to a retort form, finally producing a motile ookinete after 24 h in the gut lumen of the mosquito gut (Figure 1.5) (Angrisano *et al.*, 2012; Anil and Marcelo, 2009). Approximately 48 h later, the ookinetes that first penetrated the peritrophic matrix then cross the midgut epithelium. Once an ookinete has reached the basal lamina it differentiates and begins maturation, losing its elongated shape, forming a young oocyst (Angrisano *et al.*, 2012). After 10-12 days, the oocyst matures and

undergoes several rounds of nuclear division (sporogony of the parasite takes place), it releases several thousand sporozoites into the body cavity or haemocoel. Finally, these sporozoites then migrate to the mosquito's salivary glands and are injected into the human host when the mosquito feeds, beginning the asexual cycle again (Cox 2010; Anil and Marcelo, 2009).

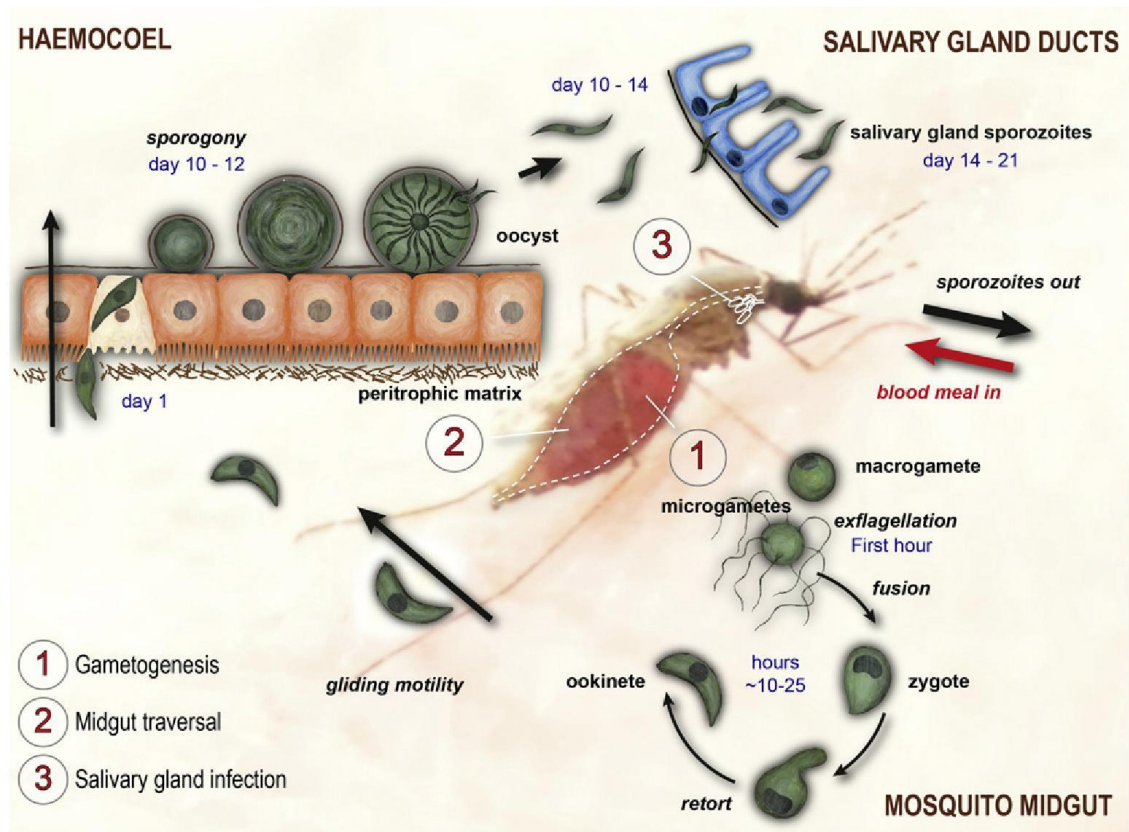


Figure 1.5: Sexual cycle of the *Plasmodium* parasite in gut of mosquito (Angrisano *et al.*, 2012).

1.2.3 Clinical manifestation and classification of malaria

The clinical manifestation of malaria infections in humans are caused by parasites in the erythrocytic stage of the life cycle. The symptoms are caused by the infection of red blood cells with the parasites and may result in a wide range of outcomes and pathologies. The severity of infection ranges from asymptomatic presentation to severe complications and ultimately death. Many factors influence the disease manifestations of the infection,

including host age, previously acquired host immunity and the species genotype of the infecting parasite. Children under five have little immunity and as a result are those most at risk of clinical malaria (Weatherall *et al.*, 2002). Malaria may be classified as either uncomplicated or severe based on clinical presentation.

Severe malaria is defined on clinical symptoms in children and adults. In younger children, the presenting symptoms associated with severe malaria include three main categories: severe anaemia, cerebral malaria and metabolic acidosis (John and Sons, 2014). Severe anaemia and hypoglycaemia are more common in children (White *et al.*, 2014). While adults may also present with cerebral malaria and acidosis, they more frequently present with acute pulmonary oedema, jaundice and renal failure. These complications are associated with increased mortality in adults (Figure 1.6) (Njuguna and Newton, 2004; Mwamtobe *et al.*, 2014). In sub-Saharan Africa, the clinical symptoms associated with increased mortality rates are cerebral malaria, hypoglycemia, lactic acidosis and jaundice. Repeated convulsions are an additional complication that may occur usually in association with one or more of the symptoms above. The complications of severe malaria can develop rapidly and progress to death within hours or days (Trampuz *et al.*, 2003; Jallow *et al.*, 2012).

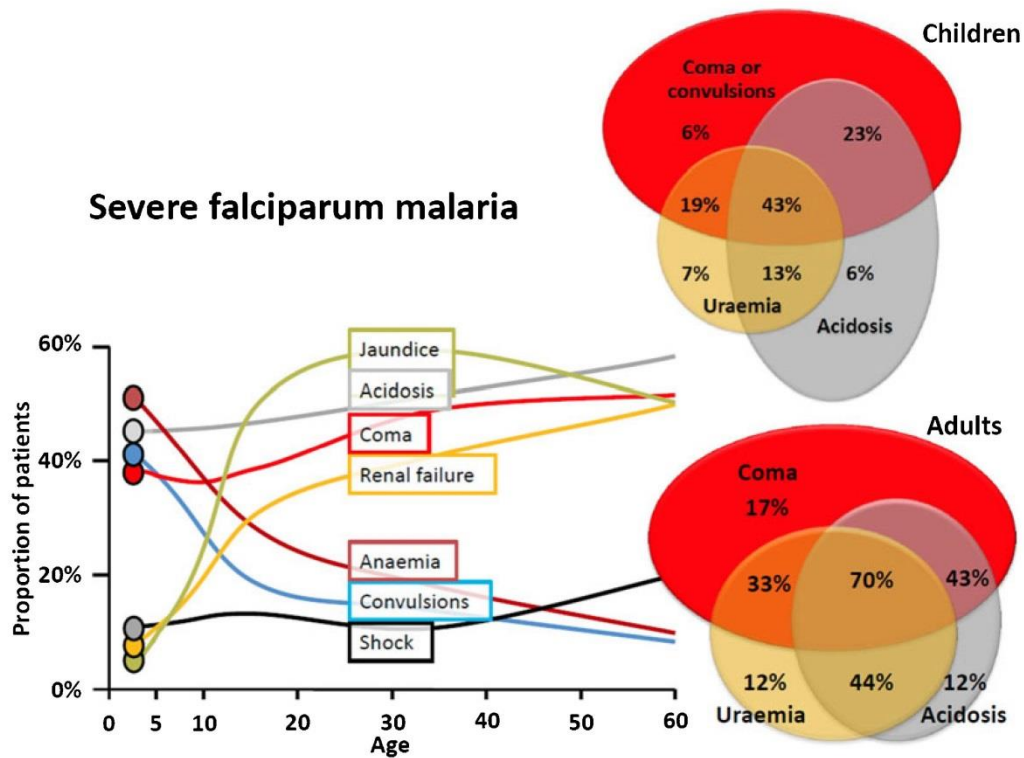


Figure 1.6: Manifestations of severe *falciparum* malaria, in 6189 children in studies conducted in Africa and 2605 adults in studies conducted in South-East Asia. The left side shows the relative importance of the clinical syndrome of severe falciparum malaria by age, and Venn diagrams on the right show the mortality in children and adults associated with manifestations of cerebral, malaria renal impairment and metabolic acidosis alone or in combination (John and Sons, 2014).

1.2.3.1 Uncomplicated malaria

All symptoms of uncomplicated malaria can occur early or late in the course of the disease. This is characterized by fever in the presence of peripheral parasitaemia. Other frequently occurring features may include chills, profuse sweating (associated with a paroxysm of fever), muscle pains, joint pains, abdominal pain, diarrhoea, nausea, vomiting, irritability and refusal to feed and splenomegaly. Thrombocytopenia and anaemia are associated with malaria, particularly in children. These features may occur singly or in combination (MPHS, 2010). Symptomatic uncomplicated malaria may appear in children under 5 years, pregnant

women, people who are HIV positive and travellers from non-malaria endemic regions (WHO, 2010).

1.2.3.2 Severe *falciparum* malaria

Plasmodium falciparum is the most common cause of severe malaria causing organ dysfunction and even mortality, while other species of malaria rarely cause death (Trampuz *et al.*, 2003; Newton and Krishna, 1998). Severe malaria is mainly occurs in children (under 6 years old) and is less common in older children and adults, due to the acquisition of partial immunity, giving increasing protection against the parasite. It is estimated that greater than 80% of the world's severe and fatal malaria affects children in sub-Saharan Africa (John and Sons, 2014). While malaria may affect any age group, the symptoms and manifestations of severe *falciparum* malaria vary widely, depending on age and malaria transmission intensity, which varies across different sites in Africa (Jallow *et al.*, 2012; Dondorp *et al.*, 2008). In areas of a high transmission, severe malaria is predominantly a disease of infants and very young children, where severe anaemia is the characteristic presentation. Severe malaria does not occur in adults because of the early acquisition of protective immunity (Trampuz *et al.*, 2003; Dondorp *et al.*, 2008). In areas of lower transmission, severe malaria occurs in both adults and children, but is more common in adults who often present with cerebral malaria, renal failure, severe jaundice, and pulmonary edema. Life-threatening complications occur most commonly in travellers and migrant workers who have not developed any protective immunity (John and Sons, 2014). The major complications of severe malaria include cerebral malaria, severe anemia, Acidosis and hypoglycaemia, and acute renal failure.

Cerebral malaria is one of the most common features of severe malaria, and it represents a neurological complication of acute *Plasmodium falciparum*, characterized by unrousable coma (Idro *et al.*, 2010). In Africa, an estimated 17 to 50% of hospital admissions for severe

malaria are a result of cerebral malaria. The case fatality rate ranging from 30% in adults to 20% in children, with 1 in 4 survivors developing neurological complications and cognitive disability and thus this represents a very serious complication of malaria infection (Solomon *et al.*, 2014; WHO, 2000). Cerebral malaria can be attributed to an isolate of infected red blood cells in the deep blood vessels of the brain, hence blocking the cerebral microcirculation, thus causing tissue damage and death (WHO, 2000).

Anaemia is an important and commonly life threatening complication of *falciparum* malaria in children. The majority of infants and young children who suffer from severe malarial anaemia reside in holoendemic regions (Figure 1.6) (John and Sons, 2014; WHO, 2000). The World Health Organization (WHO) defines severe anaemia as haemoglobin <5 g/dL or haematocrit <15% (Perkins *et al.*, 2011). Anaemia may develop rapidly in endemic areas especially when association with cerebral malaria or any other complication of *P. falciparum* infection (White *et al.*, 2014; WHO, 2000). Severe anaemia occurs as a result of lysis of infected and uninfected RBCs dyserythropoiesis and bone marrow suppression (Perkins *et al.*, 2011).

Acidosis is an important risk factor for mortality in severe *falciparum* malaria in both adults and children (Figure 1.6). It results from the accumulation of organic acids such as lactic acid, usually as a result of ketoacidosis in children and renal dysfunction in adults. Thus, elevated lactate (hyperlactataemia) is indicative of an obstruction of micro circulatory flow causing hypoperfusion, a common feature in infected children (John and Sons, 2014; White *et al.*, 2014). The normal range for plasma lactate, defined by the World Health Organization is up to 2 mmol/L. A plasma lactate level >5 mmol/L is an indication of severe malaria (WHO, 2000; Dhabangi *et al.*, 2013).

Hypoglycaemia and associated lactic acidosis are the most common metabolic complications of malarial infection (Trampuz *et al.*, 2003). Which results from decreased glucose

production by gluconeogenesis in liver hepatocytes and an increase in consumption of tissue glucose. Hypoglycaemia can develop rapidly and progress to coma and death especially in children and pregnant women (White *et al.*, 2014). In *falciparum* malaria, the majority of episodes of hypoglycaemia are due to an important adverse effect of plasma quinine, which induces insulin secretion through its capacity to induce hyperinsulinaemia. Plasma quinine is detectable during hypoglycaemia and it is particularly associated with pregnancy and severe diseases (WHO, 2000). Hypoglycemia was identified as predictive (blood glucose below 2.2 mmol/L, less than 40 mg/dL) and is an indicator of mortality risk coma, shock, and hyperparasitemia in children (Elased and Playfair, 1994; Osonuga *et al.*, 2011). Women in late pregnancy are more likely than other adults to develop hypoglycaemia. In Africa, 153,000-267,000 malaria related mortalities are attributed due to hypoglycemia, estimate 8% of adults, 30% of children and 50% of pregnant women (Osonuga *et al.*, 2011).

Acute kidney injury occurs as a complication of *P. falciparum* malaria leading to high mortality, especially in adults with severe malaria and when the disease is not diagnosed early (Figure 1.6) (Mishra *et al.*, 2002; Abdul *et al.*, 2006). The diagnosis of acute renal failure in malaria is usually based on symptoms alongside high values of serum muscular enzymes, for instance: creatine kinase and myoglobin; plasma creatinine concentration above than 3 mg/dL (265 mol/L), oliguric renal failure (about < 400 ml in day). Acute tubular necrosis is the principal pathological factor in malaria induced acute renal failure. In acute tubular necrosis, haemoglobin granules may be observed in the tubular cells and may be associated with convulsions, anaemia, jaundice, hypoglycaemia, and coma (Mishra *et al.*, 2002; Yong *et al.*, 2012). Other nonspecific mechanisms may also contribute to acute renal failure seen in malaria, including: catecholamine release, cytoadherence of parasitized erythrocytes, dehydration, intravascular haemolysis and intravascular coagulation (Abdul *et al.*, 2006).

1.2.4 Strategies for malaria control

a. Vector control

The role of vector control efforts is very important in the prevention and treatment of malaria (White *et al.*, 2014). Deployment of indoor residual spraying and vector control interventions contribute to a decreased density of mosquito vectors and thus decline in malaria morbidity and mortality and that represents about 60% of global investment in malaria control (WHO, 2013). The increased deployment of insecticide treated nets (ITNs) has decreased malaria mortality rates in children (< 5 years) by 55%, in *Plasmodium falciparum* endemic settings (Eisele *et al.*, 2010), such as deployment of pyrethroid-insecticide-treated mosquito nets in agriculture, ITNs protect people by killing anopheline mosquitoes and should be deployed in endemic areas (White *et al.*, 2014).

Based on data from national malaria control programmes (NMCPs), in 2013, about 49% of people in communities at risk had access to an ITNs in their household while in 2004 this was just 3% (Figure 1.7). In 2013 about 44% were sleeping under an ITN while in 2004 there were only 2% (WHO, 2014).

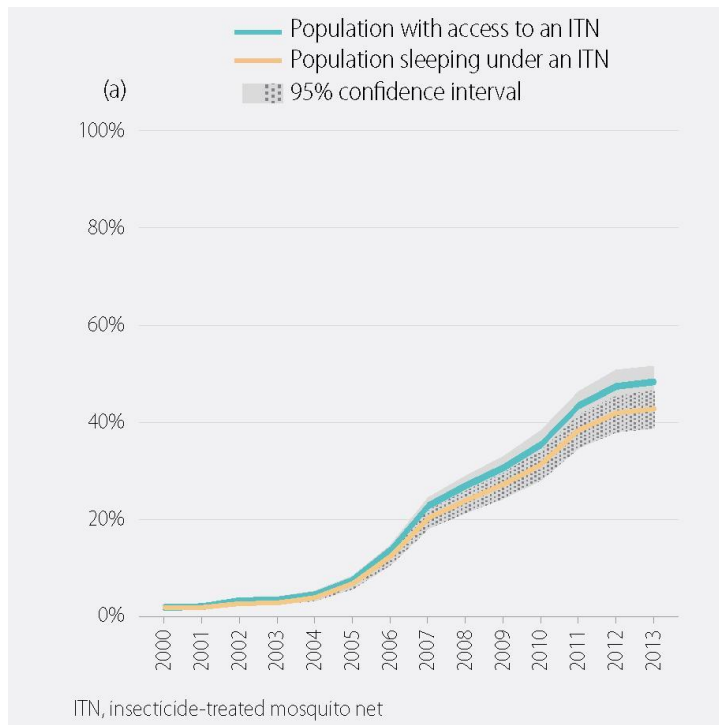


Figure 1.7: Rate of population with access to an ITN and proportion sleeping under an ITN, sub-Saharan Africa, 2000–2013. Source: ITN coverage model from the Malaria Atlas Project.

b. Chemoprophylaxis and chemoprevention

Chemoprophylaxis is advised to effectively protect the millions of tourists at risk of exposure to the malarial parasite (Chen *et al.*, 2006). Drugs such as atovaquone–proguanil, doxycycline, primaquine and mefloquine that are all highly effective against *P. falciparum* are used (White *et al.*, 2014). Intermittent preventive treatment in pregnancy (IPTp) with two course of sulfadoxine–pyrimethamine during the second and third trimester of pregnancy to prevent severe anaemia, has been shown to reduce the proportion of both low birth weight and infant mortality (Kalanda *et al.*, 2006).

Seasonal malaria chemoprevention (SMC) consists of a therapeutic course of an antimalarial within the malaria season. This action is important to prevent millions of cases and thousands of deaths in children aged 3–59 months. In order for this to be effective it is important to maintain therapeutic concentrations of drugs in the blood throughout the period of the

epidemic. In countries where epidemics of malaria exist The World Health Organization (WHO) recommends SMC with sulfadoxine-pyrimethamine and amodiaquine (SP+AQ) (Zongo, 2014).

Mass drug administration (MDA) is described as the administration of antimalarial drugs to whole populations. MDA is used in many different areas using several different approaches and therefore it is difficult to estimate its effect on the reduction of the burden of clinical malaria (Seidlein and Greenwood, 2003).

MDA had marked effect on vector control that reduced parasite spread and clinical malaria. However this was only shown to be the case transiently and rarely interrupts transmission, for MDA or to control the disease and maybe encourage the spread of drug-resistant parasites (Seidlein and Greenwood, 2003). Nevertheless, the resurrection of MDA in the management of epidemics and malaria elimination in areas with a very short transmission season has reawakened attention in this field (Greenwood, 2010). Several studies of MDA, occasionally in combination with vector control, were carried out in the 1950s, 1960s and 1970s and showed that MDA, especially if given repeatedly, could reduce parasite prevalence and the incidence of clinical malaria substantially, but that this effect was only transitory and MDA rarely interrupts transmission (Seidlein and Greenwood, 2003).

c. Vaccination

The RTS,S-subunit vaccine is the most effective vaccine still in late development for infants and young children living in endemic areas as part of the expanded programme on immunisation (EPI). It targets the circumsporozoite protein of *P. falciparum* and therefore prevents the parasite from maturing and infecting hepatocytes (Shahinas *et al.*, 2013; White *et al.*, 2014). Previous studies have shown promising results of RTS,S (approximately 30% rate of protection) in infants and young children. The studies by Bejon *et al.*, (2008) and

Abdulla *et al.*, (2008) were confirmed that RTS,S can promise as a candidate protect against clinical malaria infection.

1.2.5 Overview of Antimalarial Drugs

Over the last 60 to 70 years the antimalarials used have primarily fallen into the following seven classes: 4-Aminoquinolines, Aryl amino alcohols, 8-Aminoquinolines, Artemisinins, Antifolates, Inhibitors of the respiratory chain and antibiotics (Schlitzer, 2008; Grimberg and Mehlotra, 2011). The evolution and spread of resistance to one or, in the case of multidrug resistance, more than one of these classes poses a significant health risk to populations living in malaria endemic regions. Table (1.1) shows the first reported resistance to some antimalarial drugs.

Table 1.1: First reported resistance to some antimalarial drugs (Sinha *et al.*, 2014).

Antimalarial drug	Introduction date	First reported resistance	Difference (years)
Quinine	1632	1910	278
Chloroquine	1945	1957	12
Proguanil	1948	1949	1
Sulfadoxine +Pyrimethamine	1967	1967	0
Mefloquine	1977	1982	5
Halofantrine	1988	1993	5
Atovaquone	1996	1996	0
Artemisinin	1971	1980	9
Artesunate	1975	2008	33
Artesunate +Mefloquine	2000	2009	9

1.2.5.1 Chloroquine (CQ)

CQ (4-aminoquinoline) has been one of the most effective antimalarial drug since its introduction in the 1940s (Figure 1.8). However, CQ-resistant strains began to emerge in the 1950's and its usefulness has been dramatically reduced in different regions of the world where malaria is endemic (Grimberg and Mehlotra, 2011). CQ resistant *P. falciparum* malaria was reported for the first time in Southeast Asia (Thai-Cambodian border) and South America (Colombia) in the late 1950s (Farooq and Mahajan, 2004). Today, about 80% of field isolates are resistant against CQ (Schlitzer, 2008).

The chloroquine-sensitive strains of *P. falciparum* tend to concentrate the drug to higher concentrations in the parasite's digestive vacuole than do CQ resistant parasites (Krogstad *et al.*, 1987). Here, CQ inhibits haem polymerization by forming complexes with haem. Haem polymerization detoxifies this moiety, creating haemozoin (also known as malaria pigment as it can be directly observed in infected erythrocytes), otherwise the toxic haem is available to cause damage to cellular membranes that ultimately kill the parasite (Combrinck *et al.*, 2013).

CQ resistance in *P. falciparum* principally arises from mutations in the genes encoding transport proteins such as PfCRT (the chloroquine resistance transporter) and PfMDR1 (the multidrug resistance transporter) (Juge *et al.*, 2015). Moreover, mutations in PfMDR1 cause cross resistance to other antimalarials such as mefloquine, quinine and artemisinin derivatives (Eyasu, 2015). The PfCRT K76T mutation, located in the parasite's digestive vacuole membrane, showing a resistance to CQ (Ecker *et al.*, 2012).

1.2.5.2 Quinine

Quinine (6-methoxycinchonan-9-ol) is a cinchona alkaloid that belongs to the aryl amino alcohol group of drugs (Figure 1.8) and is one of the oldest antimalarial drugs and has been used for the treatment of uncomplicated malaria. It is often the last resort for the treatment of severe malaria because preparations for intravenous applications are only available (Grimberg and Mehlotra, 2011; Petersen *et al.*, 2011). Quinine has a short serum half-life of 8–10 h (Petersen *et al.*, 2011). Clinical resistance to quinine was first reported in South America nearly a century ago and around the Thai-Cambodian border in the mid-1960s. A combination of quinine with tetracycline or doxycycline is recommended to enhance its effectiveness. Quinine use is limited due to side effects, for example its arrhythmogenic potential and the release of insulin lead to hypoglycemia and this occur in about 32% of patients receiving QN as a drug (Dondorp *et al.*, 2005; Schlitzer, 2008). In a recent study, hypoglycemia has been reported approximately 3% of adults and 2.8% of African children of receiving quinine (Dondorp *et al.*, 2010; Dondorp *et al.*, 2005). Moreover, more serious effects side of quinine includes skin eruptions, asthma, thrombocytopenia, hepatic injury and psychosis these effects are less frequent (Achan *et al.*, 2011).

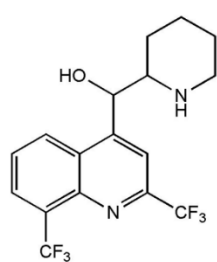
QN acts as Similar to CQ by binding to haem. QN accumulation in the parasite's food vacuole inhibits haem detoxification (Mharakurwaa *et al.*, 2011). However, polymorphisms in several proteins have been associated with resistance to QN, including PfCRT, PfMDR1 and PfNHE1 (sodium/hydrogen exchanger 1) (Cheruiyot *et al.*, 2014).

1.2.5.3. Mefloquine (MQ)

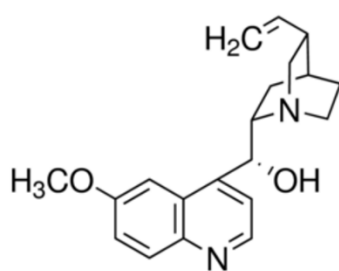
MQ is a 4-methanolquinoline with a long serum half-life of 14–18 days (Figure 1.8) (Petersen *et al.*, 2011), MQ was introduced in the 1970s. It was used against most CQ resistant *Plasmodium* strains (Schlitzer, 2008). MQ resistance was first reported at the

beginning of 1980s near the Thai-Cambodian border where MQ was used intensively, and then in some parts of Southeast Asia as well as in the in the Amazon region of South America and intermittently in Africa (Farooq and Mahajan, 2004; Dasonville-Klimpt *et al.*, 2011; Meshnick *et al.*, 1996). The effects side due to use of MQ include insomnia, depression and panic attacks (Schlitzer, 2008). Also the increase of resistance to MQ has limited its use. The primary determinant conferring resistance to MQ is associated with amplification of the *pfmdr1* gene (Saifi *et al.*, 2013; Preechapornkul *et al.*, 2009). MQ has been used with artesunate as a drug combination or MQ/artemether in an effort to overcome the development of resistance to MQ (Price *et al.*, 1995; Dasonville-Klimpt *et al.*, 2011).

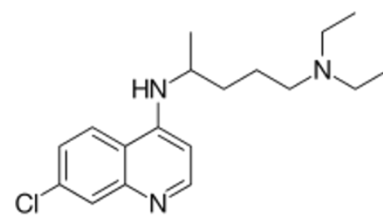
Mode of action for MQ has been shown to inhibit the accumulation of hemozoin a similar or less efficiency than CQ in infected cells. Also, MQ is given the lower basicity which leads it to accumulate less than CQ (Mharakurwaa *et al.*, 2011).



Mefloquine



Quinine



Chloroquine

Figure 1.8: Chemical structure of mefloquine, quinine and chloroquine

1.2.5.4. Artemisinin

Artemisinin is a sesquiterpene lactone endoperoxide. The most common semi-synthetic derivatives of artemisinin are used clinically (dihydroartemisinin (DHA), artesunate and artemether) (Grimberg and Mehlotra, 2011). Artesunate and artemether are transformed to dihydroartemisinin which has a short serum half-life (<1 hour) (Schlitzer, 2008). Artemisinin derivatives have endoperoxide bridge (C-O-O-C) (Figure 1.9) which is a specific feature and essential for antimalarial activity (Cui and Su, 2009).

In 2001, the WHO recommended the sole use of artemisinin-based combination therapies (ACTs) for treating *P. falciparum* malaria in all endemic areas where resistance to monotherapies is prevalent (Grimberg and Mehlotra, 2011). Artemisinins are usually combined with a long-acting partner antimalarial drug (e.g., artemether-lumefantrine, artesunate-amodiaquine and artesunate-mefloquine) in order to increase ACT efficacy overall and achieve effective treatment over a 3 days period (Beeson *et al.*, 2015; Bloland, 2001). ACTs are used as the first line in antimalarial chemotherapy worldwide, due to act rapidly upon erythrocyte stages and reduce the parasite biomass rapidly (Grimberg and Mehlotra, 2011).

The mechanism of antimalarial endoperoxides depends on two-steps (Figure 1.10): activation of artemisinin, this step involves the peroxide bridge cleaves by haem iron form a highly reactive free radical such as oxygen radicals, or of a C-centred radical of artemisinin itself, followed by specific alkylation. Covalent adducts are formed between the drug and parasite proteins, thus interfering with their detoxification leading to produce lethal damage to the parasite (Meshnick *et al.*, 1996). Number of mutations seems to be responsible for alterations of *Plasmodium* sensitivity to artemisinins. These include PfCRT, pfmdr1 and PfATP6 (*P. falciparum* calcium-dependent ATPase) (Ding *et al.*, 2011; Zakeri *et al.*, 2012)

It has been proposed that artemisinins might targeted inhibition of PfATP6 which considered a membrane transporter in the parasite's endoplasmic reticulum, and plays an important role in calcium homeostasis for parasite survival (David-Bosne *et al.*, 2013). Also, there has been a number of genes suspected in change of artemisinin sensitivity (Zakeri *et al.*, 2012). The study by (Jambou *et al.*, 2005) suggested that Single Nucleotide Polymorphism (SNP), in particular, pfatpase6 S769N gene has been associated with artemether resistance in *P. falciparum*. In addition to this, it has been found that the S769N mutation is contributed with increased IC₅₀ value of artemether isolates from French Guiana.

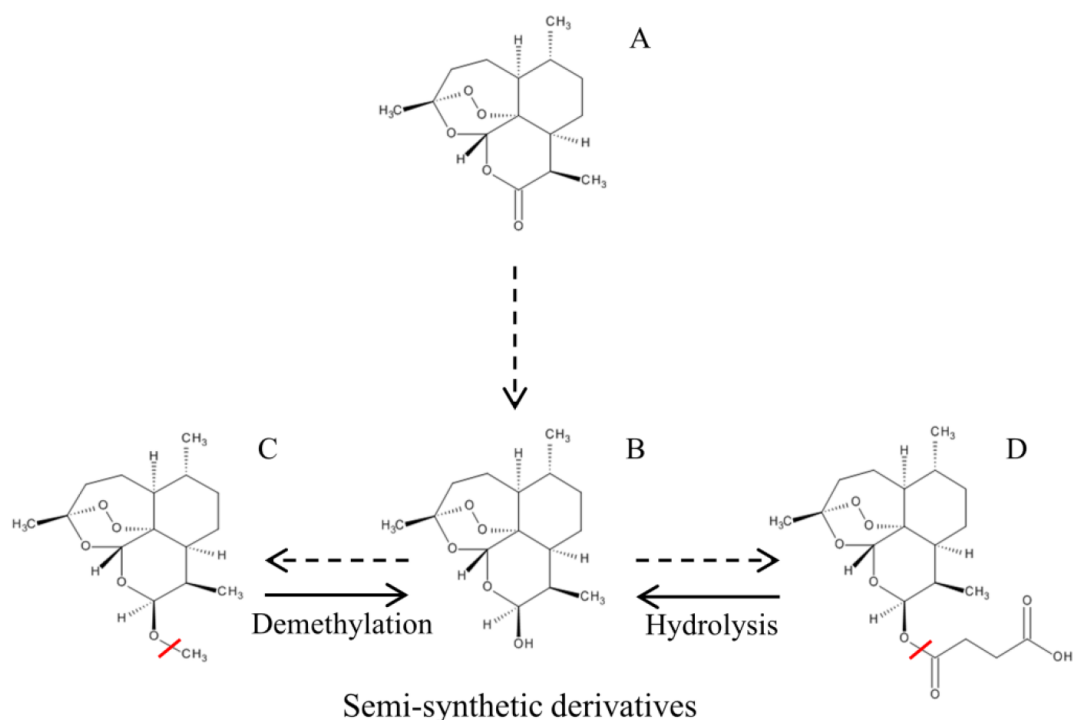


Figure 1.9: Chemical structures of (A) artemisinins (B) dihydroartemisinin, (C) artemether and (D) artesunate (Ericsson, 2014).

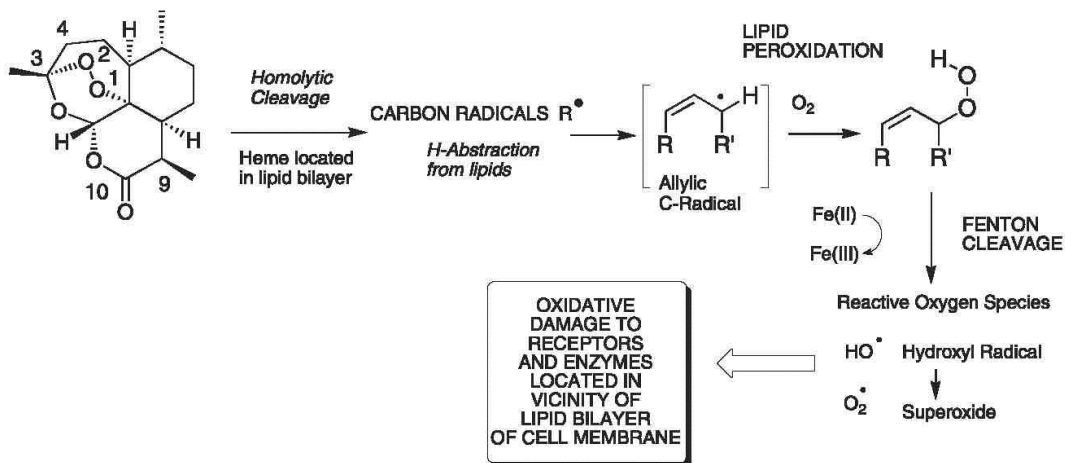


Figure 1.10: Proposed mechanism of action for artemisinin (Bray *et al.*, 2005).

1.3 Human African Trypanosomiasis (HAT)

1.3.1 Background of the Disease

HAT is a neglected tropical disease that is caused by *Trypanosoma brucei*, a protozoan parasite. This disease is transmitted to humans through the bite of a tsetse fly of the genus *Glossina*. Three species of the parasite are responsible for different types of disease. *T. b. gambiense*, found in western and central Africa, is responsible for a chronic disease, of which humans are the main reservoir host. In contrast, *T. b. rhodesiense*, has zoonotic transmission and is associated with a more acute clinical presentation in Eastern and Southern Africa (Simarro *et al.*, 2010). Also, animal African trypanosomiasis (AAT) disease of mammalian livestock, also known as Nagana, is caused by infection with *T. b. brucei*, which is not pathogenic to humans (Kagira *et al.*, 2007). In recent years, *T. brucei gambiense* has caused >95% of reported HAT cases for more than 20 countries (WHO, 2010x; WHO, 2017a).

The symptoms of the disease occur in two sequential stages: the first stage is hemato-lymphatic, while the second stage is meningo-encephalitic. The symptoms of the first stage

are fever, pruritus, arthralgia, enlarged lymph nodes, fatigue and headaches, whereas the second stage is related to various and progressive neuropsychiatric symptoms and signs that ultimately lead to coma and death (Blum *et al.*, 2006; WHO, 2013a). The burden of this disease differs from one to another country with variations in different localities within the same country. In 2015, there were 2804 cases recorded to WHO, of these 2733 were *gambiense* HAT and 71 were *rhodesiense* HAT. These cases were diagnosed in both endemic and non-endemic countries (Büscher *et al.*, 2017). Three countries were reported to have more than 50 cases of the *gambiense* HAT per year, and these are the Democratic Republic of the Congo (86% of cases) followed by the Central African Republic and Chad (52% and 2% of cases respectively) (Figure 1.11).

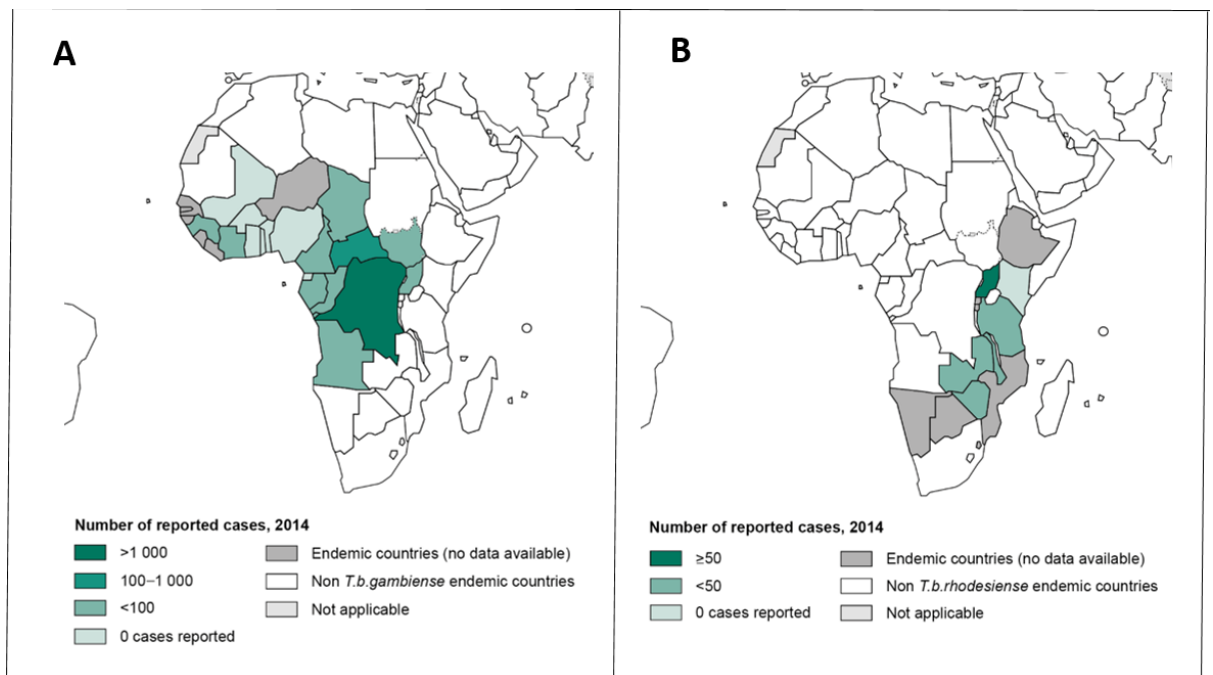


Figure 1.11: Geographic distribution of Human African trypanosomiasis (A) *T. b gambiense* and (B) *T. b. rhodesiense*. Source- modified from WHO, available at: http://www.who.int/trypanosomiasis_african/country/en/

1.3.2 The life cycle of *Trypanosoma brucei*

The infection of mammalian hosts begins when the metacyclic *T. brucei* together with tsetse saliva, are injected into the skin during blood meal (Figure 1.12). After several days of multiply by binary fission, the metacyclic trypomastigote transforms into a long slender form and establishes a bloodstream infection. The long slender forms spread via the lymph or blood vessels to a different body fluids (such as blood, lymphatic or spinal fluid) and variety of peripheral organs and tissues. Later of this stage, the parasites invade the brain parenchyma and cause local inflammation and neurological damage, producing the typical symptoms associated with Trypanosomiasis (Kristensson *et al.*, 2013). At this stage, the parasites regulate an important immunological reactions, some of which are pathogenic, induced by parasite and the tsetse fly saliva (Stijlemans *et al.*, 2016).

On the other hand, the disease can be spread by another tsetse fly when taking a blood meal on an infected mammalian host. Inside the fly, the parasites transform into procyclic trypomastigotes in the fly's midgut and multiply by binary fission. The procyclic trypomastigotes leave the midgut, and transform into epimastigotes. Finally, the epimastigotes migrate to the salivary glands and continue multiplication by binary fission, and finally transform into metacyclic trypomastigotes in preparation for their transmission to mammalian host (Matthews, 2005; Matthews *et al.*, 1995). The cycle in the fly takes about three weeks.

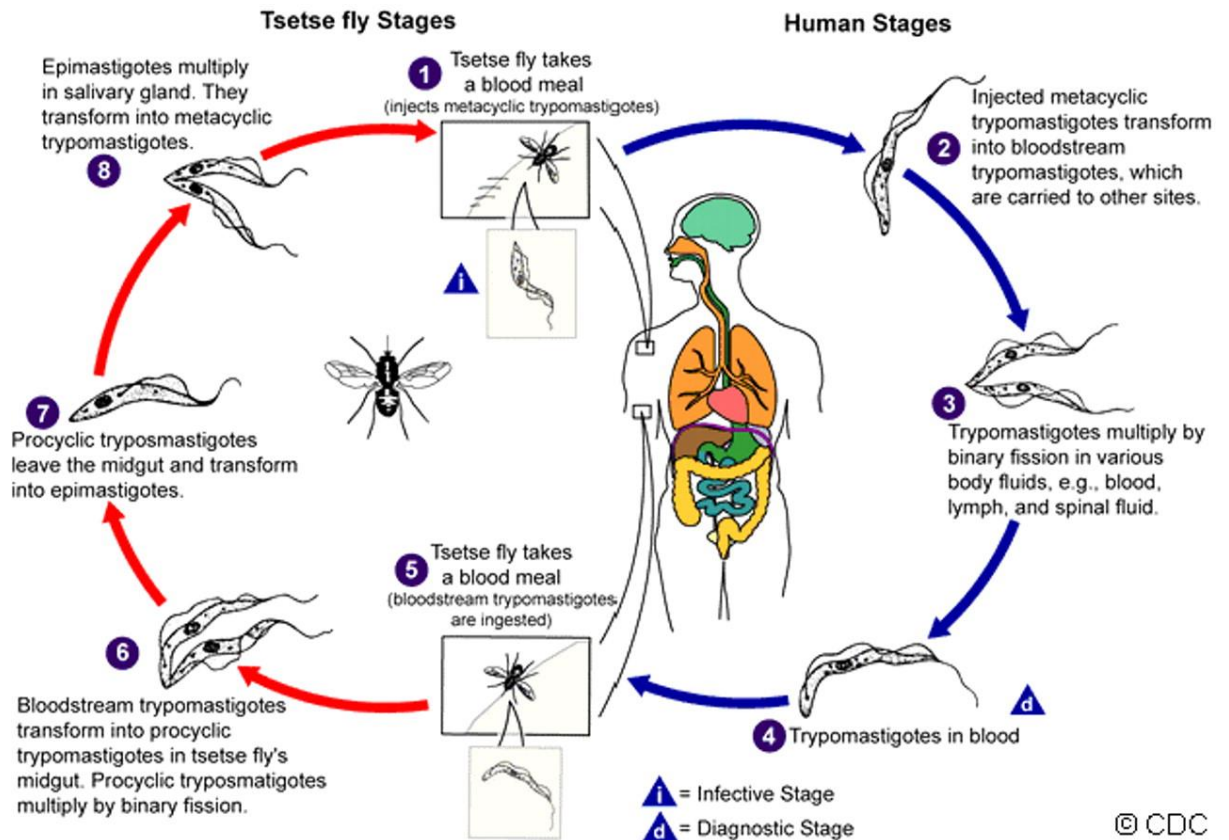


Figure 1.12: Lifecycle of the human African trypanosomiasis. *Source- modified from CDC, available at: <https://www.cdc.gov/parasites/sleepingsickness/biology.html>*

In the recent studies by Capewell *et al.* (2016), they found that the skin is a reservoir for *T. brucei* in animals and people, even when none were detected in the bloodstream. Their study revealed that the mice developed bloodstream infections within a several days after injection of *T. brucei* into the abdominal cavity. And after less than 2 weeks, the *T. brucei* detected in patches of the skin of mice, and persisted throughout the infection. That suggests that the *T. brucei* spread from the blood into the skin. Also, they confirmed that these parasites were viable (slender forms) in the skin. The trypanosomes can be spread by another tsetse bites also persist in the skin (Caljon *et al.*, 2016).

1.3.3 The clinical features of HAT

The clinical manifestations of HAT have been attributed to the parasite subspecies, host response and disease stage (MacLean *et al.*, 2010). Both forms (*gambiense* HAT and *rhodesiense* HAT) lead to death if they are left untreated (Jamonneau *et al.*, 2012). *Rhodesiense* HAT is an acute disease, within a few weeks changing to the second stage and leading to death within 6 months (Checchi *et al.*, 2008). The infection of *gambiense* HAT follows a chronic progressive course, with a mean period of time about 3 years, with high variability between patients (Checchi *et al.*, 2008a). The HAT disease progresses through two stages, a first, hemo-lymphatic stage, and then followed by a second, meningo-encephalitic stage when trypanosomes invade the central nervous system (CNS). A spectrum of neurological disturbances is observed, including sleep disorder and psychiatric disorders, while the most signs and symptoms are common to the two stages (Kennedy, 2004). First stage *gambiense* HAT includes intermittent fever, headache, pruritus, and lymphadenopathy. The second stage presents neuropsychiatric disorders in addition to the first-stage features. Other neurological signs include hyper- or hypo-tonicity, tremor of hands, motor weakness, and speech disorders (Blum *et al.*, 2006).

1.3.4 Pharmacological treatment of HAT

Five drugs are currently used in HAT treatment: suramin and pentamidine to treat early first-stage, and melarsoprol, eflornithine and nifurtimox for late stage of disease. The choice of drug therapy depends on the causative agent and the stage of disease (Table 1.2; Figure 1.13). The first-line treatment for the early-stage *T. b gambiense* HAT is pentamidine, which was first used in 1940 and which is usually managed by the intramuscular (also can be used intravenously) (Atouguia and Kennedy, 2000; Brun *et al.*, 2010). This drug is usually

effective but has adverse events such as hyperglycaemia or hypoglycaemia, hypotension, and abdominal pain and gastrointestinal problems (Brun *et al.*, 2010; Pohlig *et al.*, 2016). Moreover, suramin has been used for the early-stage *T. b rhodesiense* HAT since 1920 and is usually administered by an intravenous. The potential side effects for this drug include renal failure, skin lesions, anaphylactic shock, bone marrow toxicity, and neurological complications such as peripheral neuropathy (Kennedy, 2004; Brun *et al.*, 2010). The early stage drugs will generally not be effective for late stage disease, and late stage drugs are not justified in first stage because the drugs used are more toxic. Effective treatment of late stage disease requires drugs that cross the blood-brain barrier and these drugs present to be toxic and complicated to administer.

The first-line treatment for late-stage *T. b rhodesiense* infection is melarsoprol, which was first used in 1949 and is usually administered by multiple intramuscular injections (Babokhov *et al.*, 2013). Injection with Melarsoprol is painful and the drug is toxic, producing a post-treatment reactive encephalopathy in 5–18% of treated patients, and is fatal in 10–70% of affected patients (Seixas, 2004). A post-injection syndrome characterized by fever, rapid onset of neurological disorders, and abnormal behaviour (Pépin *et al.*, 1994).

Eflornithine has been given in monotherapy for late-stage *T. b. gambiense* HAT since 1981, and has proved effective with a cure rate about 90-95% (Priotto *et al.*, 2009; Franco *et al.*, 2014; Jamonneau *et al.*, 2015). Potential adverse events include fever, pruritus, hypertension, nausea, vomiting, diarrhoea, abdominal pain, headaches, and anemia.

An important advance was the development of the first line treatment for second stage *gambiense* HAT is nifurtimox–eflornithine combination therapy (NECT). In 2009, WHO was incorporated the NECT into the essential medicines list. NECT has higher rates of cure (accounting for 59% of all cases treated in 2010), lower rates of fatality, less severe side

effects and easier administration, compared to melarsoprol or eflornithine monotherapy (Simarro *et al.*, 2012; Alirol *et al.*, 2012). WHO supplies NECT in endemic countries, free of charge (Yun *et al.*, 2010). NECT includes of oral nifurtimox and intravenous eflornithine. The treatment regimen of NECT involves 15 mg/kg/day three daily oral doses x 10 days of nifurtimox and 400 mg/kg/day intravenously of eflornithine for a total of 7 days (Table 1.2). The main drawback of treatment with NECT is complicated to administer due to the dosing regimen requires a minimum of four nurses to give the eflornithine infusions to the patient, the patient requires to monitor for any adverse reactions after prescribe the therapy by a doctor, which is not optimal, given that patients often live in remote areas with few health resources (Tong *et al.*, 2011; Schmid *et al.*, 2012). As such, Fexinidazole, which involves a simplified, short-course regimen that could be offered a potential new safe oral treatment, was rediscovered to-use *T. brucei gambiense* treatment (Torreele *et al.*, 2010; Mogk *et al.*, 2014). Preclinical studies revealed oral effectiveness in curing both chronic and late stages of the disease in mice (Tarral *et al.*, 2014). The first studies in the human showed with oral combination therapies of fexinidazole, a 2-substituted 5-nitroimidazole was safe and effective to prevent trypanocidal activity. Fexinidazole causes damaging of DNA, protein and lipid by doing as a prodrug releasing cytotoxic metabolites by enzyme-mediated reduction by nitro-reductases (Sundar and Singh, 2016). The treatment exposure could be obtained with a well tolerated 10-day treatment regimen that included a loading dose of 1800 mg per day for 4 days followed by a 1200 mg per day regimen for 6 days given with a simple, locally adapted meal (Kaiser *et al.*, 2011; Tarral *et al.*, 2014). Fexinidazole is metabolized rapidly by some of cytochrome P450 enzymes, such as CYPs 1A2, 2B6, 2C19, 3A4 and 3A5, and flavin-containing mono-oxygenase into two active metabolites: fexinidazole sulfoxide and fexinidazole sulfone (Burrell-Saward *et al.*, 2017).

Table 1.2: Drugs used in treatment of human African trypanosomiasis. i.m., intramuscularly; i.v., intravenously. (Büscher *et al.*, 2017).

HAT B12:E18age	First-line treatment	Dosage	Alternative treatment
<i>T. b gambiense</i>			
First-stage	Pentamidine	4 mg/kg/day i.m. or i.v. (diluted in normal saline, in 2-h infusions) x 7 days	
Second-stage	Nifurtimox eflornithine combination therapy (NECT)	Nifurtimox 15 mg/kg/day orally in three doses x 10 days Eflornithine 400 mg/kg/day i.v. in two 2- h infusions (each dose diluted in 250 ml water for injection) ^a x 7 days	Eflornithine 400 mg/kg/day i.v. in four 2-h infusions (each dose diluted in 100 ml water for injection) ^a x 14 days Third-line (e.g. treatment for relapse): Melarsoprol 2.2 mg/kg/day i.v. x 10 days
<i>T. b rhodesiense</i>			
First-stage	Suramin	Test dose of 4–5 mg/kg i.v. (day 1), then 20 mg/kg i.v. weekly x 5 weeks (maximum 1 g /injection) (e.g. days 3, 10, 17, 24, 31)	Pentamidine 4 mg/kg/day i.m. or i.v. (diluted in normal saline, in 2-h infusions) x 7 days
Second-stage	Melarsoprol	2.2 mg/kg/day i.v. x 10 days	

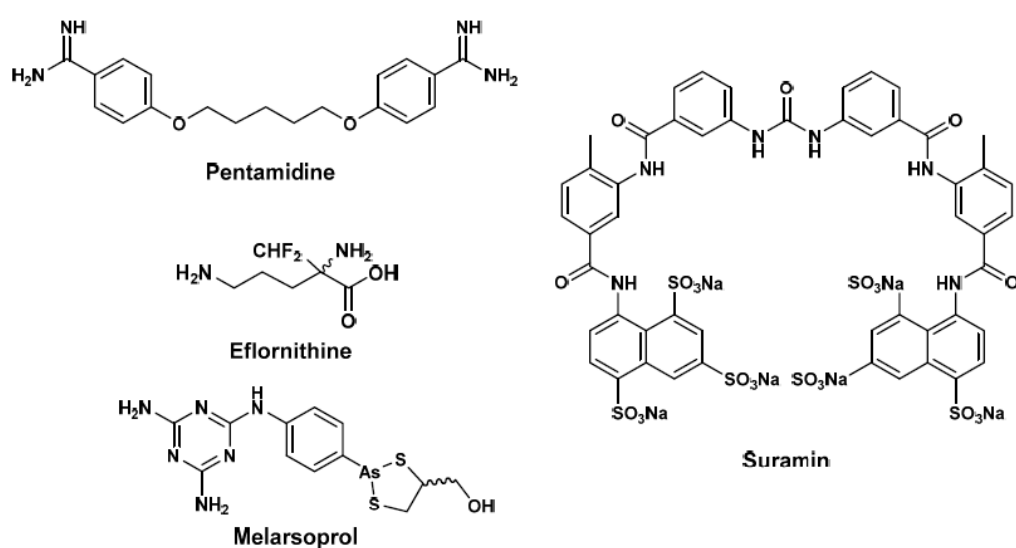


Figure 1.13: Antitrypanosomal drugs in clinical use.

1.4 Leishmaniasis

1.4.1 Background of the Disease

Leishmaniasis is a group of diseases with a wide epidemiological and clinical diversity, caused by intracellular protozoa parasite from over 20 leishmania species that are known to be transmitted to humans. leishmania is classified under the Kinetoplastidae kingdom, family Trypanosomatidae from the genus *Leishmania*. The parasite is transmitted to humans by the bite of approximately 30 species of *phlebotomine* sandflies, and infects the macrophages of the mammalian host, such as dogs or rodents, or human beings (Ouellette *et al.*, 2004; Bates, 2007). It is considered as the second most prevalent parasitic disease next to malaria according to the World Health Organization (WHO). Thus, it has become a major focus of concern in global health and economic mainly in the poorer sections of the world (WHO, 2013; Singh *et al.*, 2014). The disease has recently demonstrated geographical expansion of the tropics, subtropics and the Mediterranean basin patterns (Rose *et al.*, 2004; Faiman *et al.*, 2013). leishmania has been reported in 98 countries, covering 3 territories and 5 continents, with estimation around 15 million people around the world are infected, and nearly 350 million people are at risk of contracting the diseases (Alvar *et al.*, 2012; Roberts *et al.*, 2015). An estimated 1.5 to 2 million new cases annually, and there are an estimated ~70,000 deaths every year due to the disease (Reithinger *et al.*, 2007).

Currently, the burden of Leishmaniasis is increasing due to different factors including; HIV, climate change, disruption of health systems in endemic areas and massive population displacement. For instance in Syria, the numbers of CL cases began to increase even further especially after the onset of the Syrian Civil War in 2011, with new cases appearing into non-endemic regions (Du *et al.*, 2016). Under these favorable conditions to the parasite

transmission, this disease has the ability to spread in non-endemic countries of the world (Dujardin *et al.*, 2006; Ready, 2008; Okwor and Uzonna, 2016).

1.4.2 Clinical forms of Leishmaniasis

Leishmaniasis consists of three main clinical manifestations of the disease according to the observed clinical symptom presentations; cutaneous leishmaniasis; muco-cutaneous leishmaniasis and visceral leishmaniasis (Table 1.3) (Handman, 2001).

Table 1.3: Leishmania species and their clinical manifestation (Bates, 2007; McCall *et al.*, 2013).

Syndrome		Species
Cutaneous Leishmaniasis	Common	<i>L. major</i> <i>L. tropica</i> <i>L. amazonensis</i> <i>L. mexicana</i> <i>L. braziliensis</i> <i>L. aethiopica</i>
	Rare	<i>L. infantum</i> <i>L. donovani</i> <i>L. peruviana</i>
Mucocutaneous Leishmaniasis	Common	<i>L. braziliensis</i>
	Rare	<i>L. panamensis</i> <i>L. guyanensis</i> <i>L. amazonensis</i>
Visceral Leishmaniasis	Common	<i>L. donovani</i> <i>L. infantum</i> <i>L. infantum chagasi</i>
	Rare	<i>L. tropica</i> <i>L. amazonensis</i>

1.4.2.1 Visceral Leishmaniasis

Visceral leishmaniasis (VL) also known as kala-azar, Burdwan fever, dum-dum fever, black sickness, black fever, is considered the most severe of the forms of leishmaniasis. *L. donovani* and *L. infantum* are the main causative species of VL. The symptoms of VL are characterized by irregular fever, weight loss (cachexia), swelling of the liver and spleen, anaemia, and hypergammaglobulinaemia (mainly IgG from polyclonal B cell activation) with hypoalbuminaemia, and is usually fatal if left untreated (Herwaldt, 1999; McCall *et al.*, 2013). Mostly, VL encompasses a broad range of manifestations of infection that shows no symptoms or, might be acute, subacute, or chronic course. Starvation, immune suppression, and HIV infection enhance the risk of leishmania infection. VL occurs in Central and South America, the Mediterranean basin, Central Asia, Indian subcontinent, Middle East and Africa (Figure 1.14).

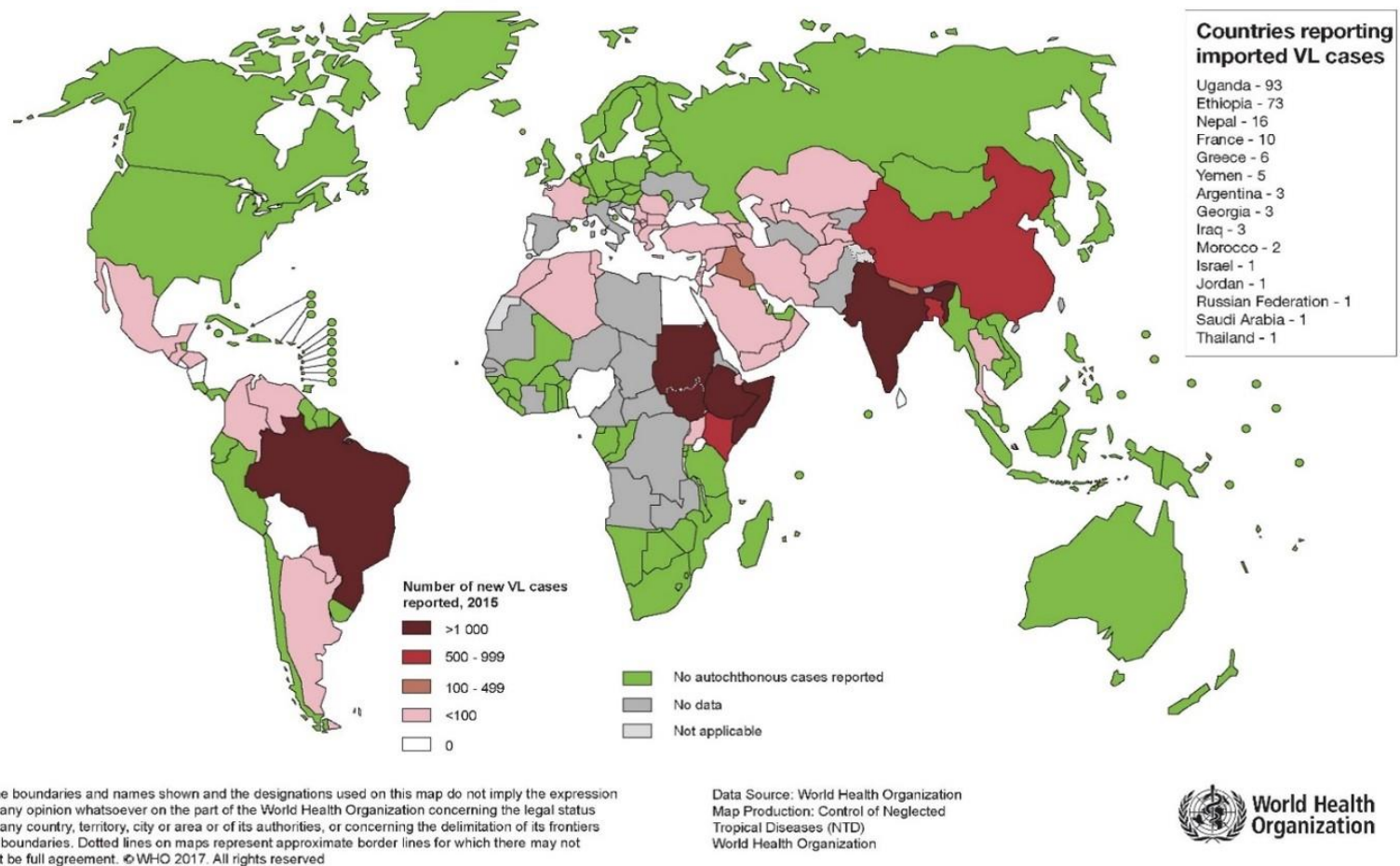
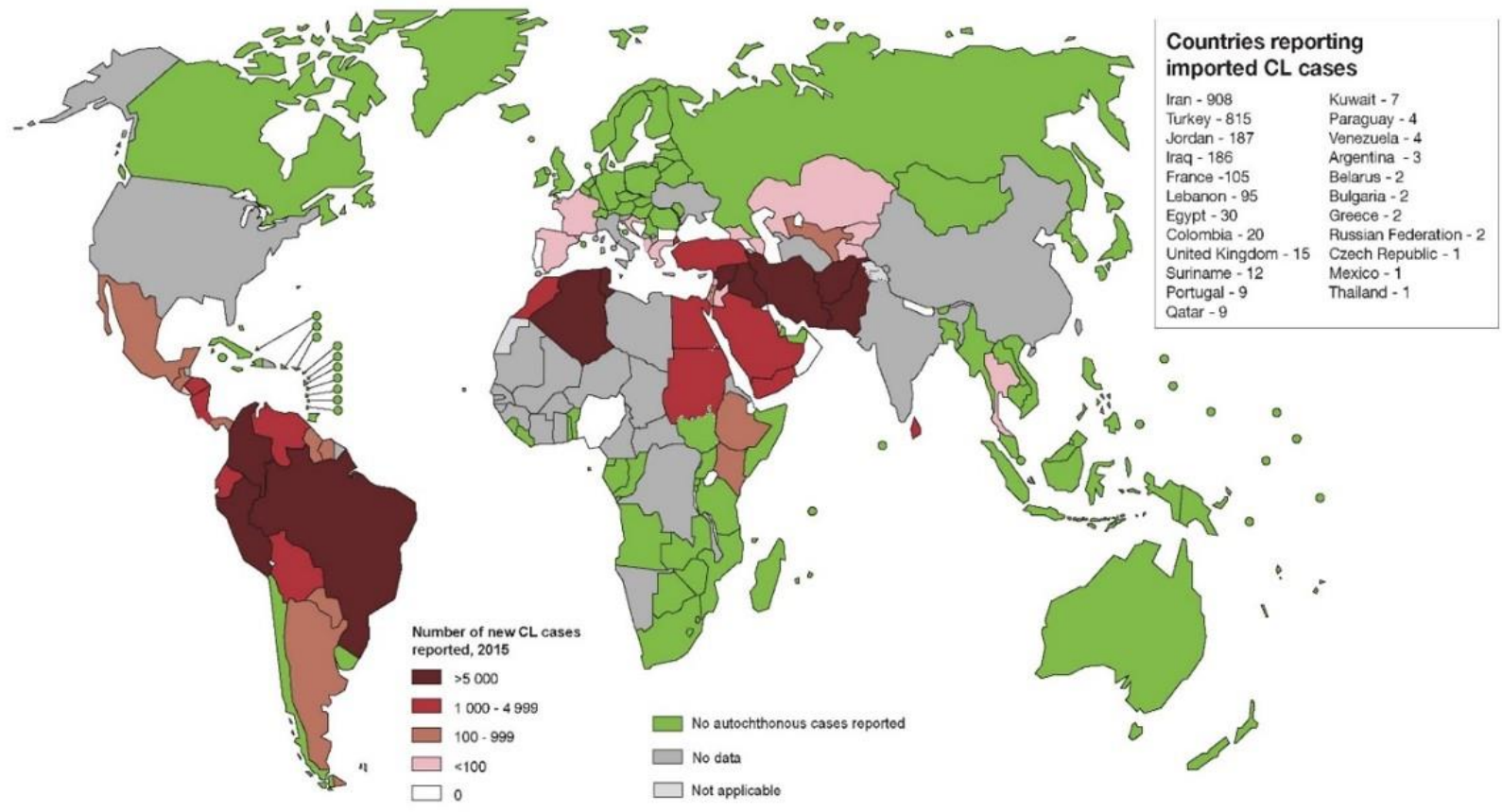


Figure 1.14: Distribution and endemicity of visceral leishmaniasis (VL) worldwide according to 2015 annual country reports. The majority of VL cases occur in just six countries — Bangladesh, Brazil, Ethiopia, India, Nepal and Sudan (source: WHO Global Health Observatory Link and access date).

1.4.2.2 Cutaneous Leishmaniasis

Cutaneous leishmaniasis (CL) is the most common form of leishmaniasis, known as ‘Oriental sore’. It has been estimated that CL represents about 75% of leishmania cases globally (Alvar *et al.*, 2012). CL is visually characterized by the cutaneous lesions which appear as a persistent insect bite on the exposed parts of the body. The lesions of uncomplicated localized cutaneous leishmaniasis, which self heal without treatment after a few months but leaves scars (Pearson and Sousa, 1996; Scorza *et al.*, 2017). The Global Burden of Disease Study 2013 determined that disability-adjusted life-years (DALYs) for CL was 0.58 per 100,000 people (Karimkhani *et al.*, 2016). CL is caused mainly by different of leishmania species (e.g. *L. major*, *L. tropica*, and *L. aethiopica* in old world and *L. amazonensis*, *L. mexicana*, and *L. braziliensis* in the new world) (Alvar *et al.*, 2012). CL represents an important public health concern in various geographical regions mainly in Central and South America (Colombia, Brazil and Peru), Africa, Indian Subcontinent, and countries of the Middle East including Iran (WHO, 2010) (Figure 1.15). There are many factors play an important role in increasing transmission of CL which include inadequate vector and reservoir control, urbanization, ecological changes, natural disasters, population movement, poor sanitation and garbage disposal system, human behavioral risk factors and resistance to standard drugs (Daszak *et al.*, 2001, Macpherson, 2005, Croft *et al.*, 2006).



The boundaries and names shown and the designations used on this map do not imply the expression of any opinion whatsoever on the part of the World Health Organization concerning the legal status of any country, territory, city or area or of its authorities, or concerning the delimitation of its frontiers or boundaries. Dotted lines on maps represent approximate border lines for which there may not yet be full agreement. ©WHO 2017. All rights reserved

Data Source: World Health Organization
 Map Production: Control of Neglected Tropical Diseases (NTD)
 World Health Organization



Figure 1.15: Distribution and endemicity of cutaneous leishmaniasis, (CL) worldwide according to 2015 country reports. (Source: WHO Global Health Observatory).

1.4.2.3 Mucocutaneous Leishmaniasis (MCL)

Mucocutaneous Leishmaniasis (MCL) is also known as “espundia”. In the majority of mucosal pathology develops following skin lesions, and affect the mucous membranes of the nose, mouth and throat with severely disfiguring lesions, which may lead to destruction of the infected tissues of the body (Lessa *et al.*, 2007; Diniz *et al.*, 2011). MCL is caused by *L. braziliensis*, *L. panamensis* and, less frequently, *L. amazonensis*. ML is mainly present in South American countries i.e. Bolivia, Brazil and Peru (Chandra and Mahesh, 2017).

1.4.3 The life cycle of leishmania

The survival of the leishmanial parasite is sustained by the interactions between two hosts, the sand flies of genera *Phlebotomus* and the vertebrate host (Banuls *et al.*, 2007; Pace, 2014). Leishmanial parasites exist in two forms according to the host: the amastigotes in vertebrate hosts and promastigotes in sandfly vector (Figure 1.16) (Dawit *et al.*, 2013).

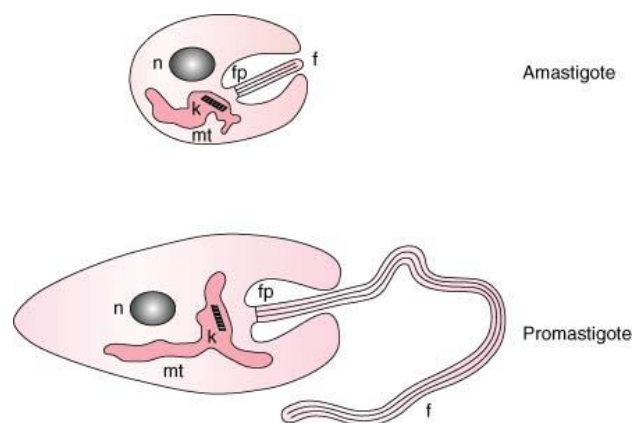


Figure 1.16: Developmental forms of promastigote and amastigote. Each form has a nucleus (n) and kinetoplast (k) in the single mitochondrion (mt). The flagellum (f) arises from the flagellar pocket (fp). Source: (Bates, 2015).

The host infection begins when the metacyclic promastigotes from proboscis of a female sand fly are injected into a host during a blood meal. The metacyclic promastigotes are characterized by the small slender bodies with 15-20 μ m in long and possess long free flagella (Bates, 2008). Which aid the motility of the parasite inside the bloodstream of the host. The promastigotes invade the macrophages through phagocytosis and they transform into amastigotes (Figure 1.17).

In addition, in the vertebrate host, the non-motile amastigotes are ovoid (aflagellar), with 3-5 μ m in long and reside in the parasitophorous vacuole of macrophages, at this stage the parasite become infectious. The amastigotes develop and multiply by binary fission until they are released by cell lysis in order to invade other macrophages (Banuls *et al.*, 2007). The amastigotes are then transported to the draining lymph nodes from the site of bite by the dendritic cells (Moll *et al.*, 1993). The life cycle is complete after digestion of a blood meal from macrophages infected with amastigotes. On the other hand, in the sandfly, amastigotes released from the macrophages and differentiate into procyclic promastigotes in the gut, and then migrate towards the proboscis and are ready to inoculate during the next blood meal (Schlein *et al.*, 1992). The life cycle continues when the sandfly releases the promastigotes into the skin of the host, and then access into macrophages cells during blood meal (Dawit *et al.*, 2013; CDC, 2013). The process takes from six to nine days depending on the species of leishmania. Transmission of leishmanial parasites can be zoonotic (i.e., from animals such as dogs and rodents to humans) or anthroponotic (i.e., from infected humans to non-infected humans) (CDC, 2013). This complex life cycle could be exploited for drug design optimization and development (Hammarton *et al.*, 2003).

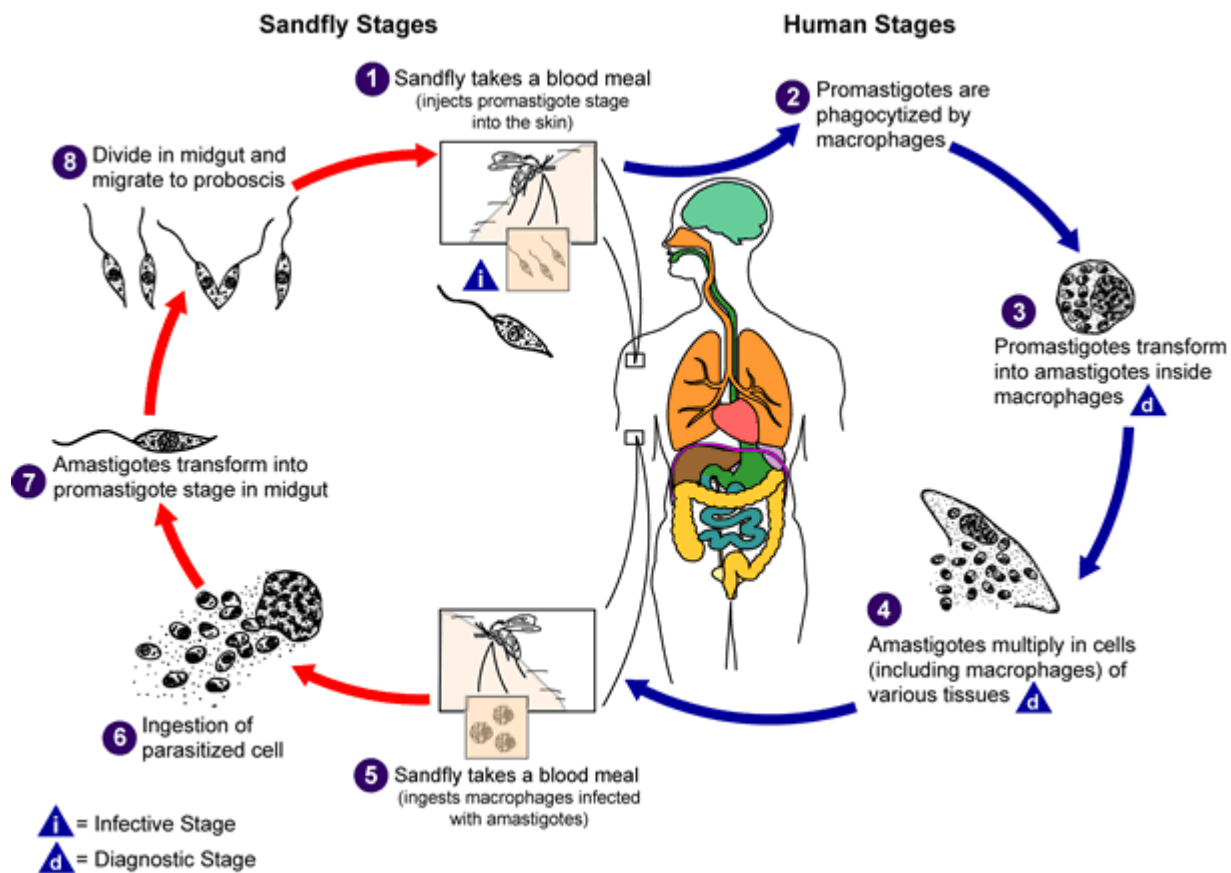


Figure 1.17: Life Cycle of leishmanial parasite. (CDC, 2013)

<https://www.cdc.gov/parasites/leishmaniasis/biology.html>

1.4.4 Control strategies for Visceral Leishmaniasis

Early diagnosis and treatment of leishmaniasis is vital in order to reduce parasite transmission, morbidity and mortality for the community (Matlashewski *et al.*, 2011).

Furthermore, antileishmania vaccines in both human and veterinary medicine are still being developed, and no vaccines licensed for human use against leishmaniasis (Cecílio *et al.*, 2017). In the past few decades, several vaccine candidates have been identified against VL. Some were presented to be immunogenic in rodent models, while most of them have not shown any positive potential in large animals (Kumar *et al.*, 2014). There are three veterinary

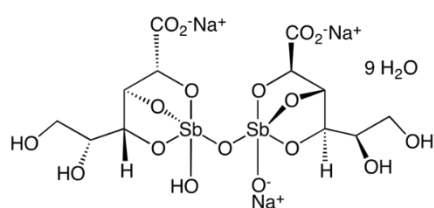
vaccines in clinical use include a recombinant single-protein antigen (Leish-Tec1), a secreted/excreted antigen (Canileish1), and a recombinant polypeptide antigen (Letifend1) (Miró *et al.*, 2017). The manufacturer's recommendations for these vaccines are to vaccinate only animals to elicit an adequate immune response that will prevent progression of disease upon infection. Epidemiologic studies have been shown that successful canine vaccination would greatly decrease of leishmania transmission and mortality in both dogs and people (Alvar *et al.*, 2013; Dye, 1996).

Commonly, targeting the vector is the most effective strategy to control vector-borne diseases, by reducing or eliminating the human-vector contact. There are 500 known Phlebotomine species, of these 30 have been identified as vectors of the disease. Vector control measures are primarily based on insecticide-treated nets (ITNs) and indoor residual spraying (IRS) (Killick-Kendrick, 1999). This will greatly reduce the incidence of leishmaniasis (Bern *et al.*, 2008). In the 1950s, after using an effective antimalarial insecticide (dichloro-diphenyl-trichloroethane (DDT)), VL was almost completely eliminated in northeastern Bihar . Unfortunately, as soon as these spraying campaigns were stopped, a resurgence of the disease predominantly in the 1970s, with an explosive epidemic in the early 1990s (Barnett *et al.*, 2005).

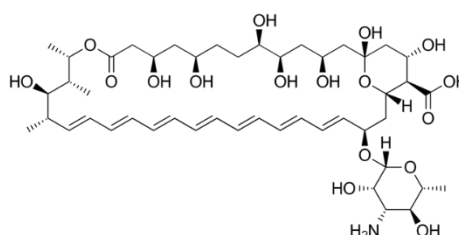
In Sudan and other endemic countries in East Africa, transmission occurs mainly, but not exclusively, outside villages, during shepherding for example. Indoor residual spraying for disease control is therefore unlikely to be as efficient in this region. Resistance of *P. argentipes* still limited to DDT, but has been reported in Bihar (Picado *et al.*, 2010). However, previous report showed that ITNs have a limited effect on sandfly exposure in VL endemic areas such as India and Nepal (Gidwani *et al.*, 2011).

1.4.5 Treatment of Leishmaniasis

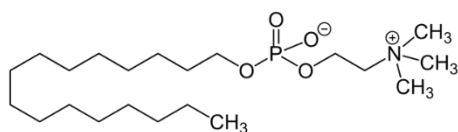
Chemotherapy is still the most effective way to treatment leishmania infection. Unfortunately, the available drugs are costly, have high toxicity, there is a long duration of treatment, and the resistance has emerged as a serious problem, which has compelled the search for new antileishmanial agents (Rajasekaran and Chen, 2015, Freitas-Junior *et al.*, 2012). There are a limited number of drugs are available and currently recommended to treat leishmaniasis include the Pentavalent Antimonials, Amphotericin B, Miltefosine and recently, Paromomycin. The main features of these treatments are summarised in Table 1.4 and Figure 1.18.



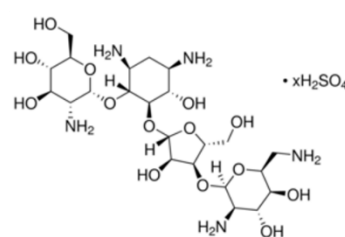
Sodium Stibogluconate



Amphotericin B



Miltefosine



Paromomycin

Figure 1.18: Chemical structure of current antileishmania drugs

Table 1.4: Antileishmania drugs properties. i.v. = intravenous. i.m. = intramuscular. CID = PubChem Compound Identifier

	Sodium Stibogluconate (VL)	Liposomal Amphotericin B (VL, ML)	Miltefosine (VL, CL)	Paromomycin (VL, CL)
Administration	i.v. infusion	i.v. infusion	Oral	i.m.
Regimen	20 mg/kg/day for 28 days	2 mg/kg/day for 5 days or 1 single injection of 7.5 mg/kg	100 (bodyweight >25kg) mg/day for 28 days	15mg/kg/day for 21 days
Toxicity	High toxicity, possible cardiac arrhythmia, Nephrotoxicity and hepatotoxicity	Limited nephrotoxicity and mild procedure side effects	Teratogenicity, mild gastrointestinal toxicity, nephrotoxicity and hepatotoxicity	Nephrotoxicity, hepatotoxicity both extremely rare
Treatment failure	>60% in the ISC	10%	6%	<5%
Cost of the drug (USD)*	21	675 (2-4d) or 900 (1d)	150	15
Advantages	Cheap	Highest therapeutic index of all the VL drugs, short	Oral route is a plus on the field, no need of hospitalisation	Cheapest drug available, no need for prolonged hospitalisation since the injection can be given as ambulatory care
Disadvantages	Prolonged cure with painful injection, requires high quality control, highly toxic and high parasite resistance in the ISC	Expensive, requires excellent preservation (<25°C) and Requires i.v. infusion	Low compliance, relatively expensive, possible teratogenicity makes it forbidden for pregnant women, resistance (?)	Low efficiency in monotherapy in East Africa, potential for resistance (?) and prolonged treatment favours non termination

1.4.5.1 Pentavalent antimonials [Sb(V)]

For more than 70 years, pentavalent antimony (sodium stibogluconate and meglumine antimoniate) have been the first-line of treatment for all forms of leishmaniasis in South America, North Africa, Turkey, Bangladesh, and Nepal (Franco *et al.*, 2016).

There are lots of problems of antimonials, and the main problem is their requirement for treatment intramuscular or intravenous injection every day for about one month, also the major side-effects of antimonials are toxicity such as: cardiotoxicity, pancreatitis, nausea, abdominal pain and cardiac arrhythmia (de Moura *et al.*, 2016). However, they are still in use in other regions of the world, including Latin America and East Africa (Mitropoulos *et al.*, 2010).

Moreover, Pentavalent antimonial compounds was no longer recommended to use in North Eastern India due to high levels of arsenic in groundwater which made parasites cross-resistant to antimony in this region (Perry *et al.*, 2011). This has been assessed in a retrospective epidemiological survey performed in Bihar, India, the results of which suggest that arsenic-contaminated groundwater may well be associated with antimony treatment failure (Perry *et al.*, 2015).

The mode of action of antimony is still unclear. Pentavalent antimony (Sbv) enters the macrophage cells and reduction to trivalent antimonials SbIII form in the cytosol, or can enter as such in the amastigotes. The entry of Sb (III) occurs through the aquaglyceroporin AQP1 transporter but the route of entry of Sb (V) is not known (Marquis *et al.*, 2005) (Figure 1.19). Within the parasite, the conversion Sbv to the active form Sb(III) will increase by either thiols, or by the action of the reductases, ACR2 (an homolog of the yeast arsenate reductase) and TDR1 (Thiol Dependent Reductase). SbIII is combined with thiol-containing

molecules including cysteine, glutathione (GSH) and trypanothione (T(SH)₂) to produce the Sb(III)-thiol complex before being exported outside of the cell. Moreover, antimony induces efflux of the intracellular trypanothione, and also Inhibition of trypanothione reductase (TR) leading to an accumulation of the reduced form of trypanothione (Wyllie *et al.*, 2011). Based on these two mechanisms, Sb(III) enhances oxidative stress and leads to the accumulation of reactive oxygen species (ROS) that ends by apoptosis. There are few mechanisms have been led to explain Leishmania resistance to antimonials: reduced conversion of Sb(V) to the Sb(III) active form, reduced uptake of Sb(III) by reducing the expression of transporters which mediate the uptake of Sb(III), and increased efflux the level of conjugation Sb(III) with thiols by the ABC transporter MRPA (Frézard *et al.*, 2009; Rai *et al.*, 2013; Ghorbani and Farhoudi, 2018).

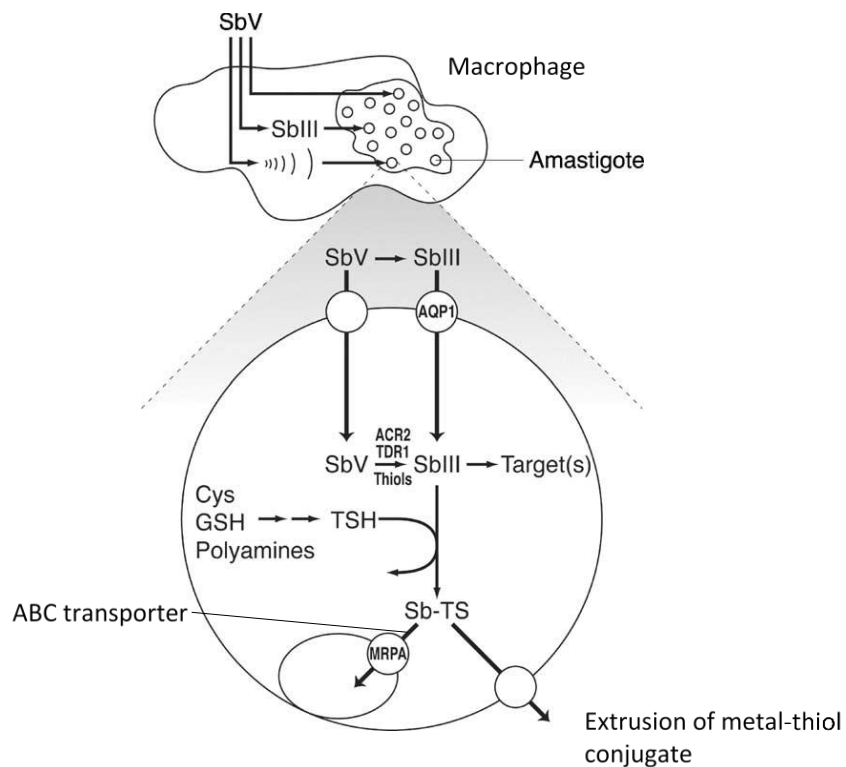


Figure 1.19: Mode of action and resistance for pentavalent antimony in leishmania amastigotes.

1.4.5.2 Amphotericin B (AmB)

AmB was first used as an antifungal macrolide antibiotic produced by *Streptomyces nodosus* in 1956. It is often used as a second line drug for leishmaniasis since the early 1960s (Almeida *et al.*, 2017). Its ability to bind to ergosterol-related sterols in cell membranes explains its specificity (Lemke *et al.*, 2005). AmB was the first combined with deoxycholate to increase the solubility and allowed intravenous administration (Thakur *et al.*, 1996). This combination therapy showed side effects particularly renal toxicity (Botero *et al.*, 2014). To reduce the side effects and increase the half life time of the compound, liposomal-amphotericin B (LAmB) was developed to allow a higher concentration of the drug, thereby greatly reducing the time for hospitalization. Studies have assessed the activity and the feasibility of a single-dose LAmB injection of 20 mg/kg. In India, the results from an implementation trial which was underway, carried out by DNDi and partners, led the government to change the treatment guidelines in 2014, abandoning miltefosine as a monotherapy in favour of single-dose AmBisome as first-line and a combination of paromomycin/miltefosine as second-line treatment (DNDi, 2017a). The main drawback of LAmB remains the costs, therefore some developing countries such as Brazil, use the first and the second lines of therapy versus LAmB (Mistro *et al.*, 2016).

The AmB mechanism of action on parasite membrane sterols and inserts in ergosterol of the cell wall resulting in an increase in permeability for protons and monovalent cations as K^+ , Ca^{2+} , and Mg^{2+} , resulting in cell death (Figure 1.20) (Romero *et al.*, 2009). Ergosterol is important for endocytosis, vacuole fusion and stabilization of proteins at the cell membrane, therefore the binding of AmB with ergosterol could account for kill the parasite by mechanism of ergosterol sequestration (Heese-Peck *et al.*, 2002; Zhang *et al.*, 2010). Another mode of action by which AmB could affect the cells by formation of reactive

oxygen species (ROS) (Moreira *et al.*, 2011). The accumulation of free radicals lead to deleterious effects on the cell (membrane, proteins, DNA and mitochondria) resulting in cell death. The absence of ergosterol in the resistant parasite's membranes and the upregulated AmB efflux and ROS scavenging machinery are having a cumulative effect in conferring resistance against AmB to the Leishmania parasite. These cumulative effects of an altered membrane profile, evolved MDR1, and the tryparedoxin cascade may be responsible for making the *L. donovani* parasite resistant to AmB (Kumar *et al.*, 2011).

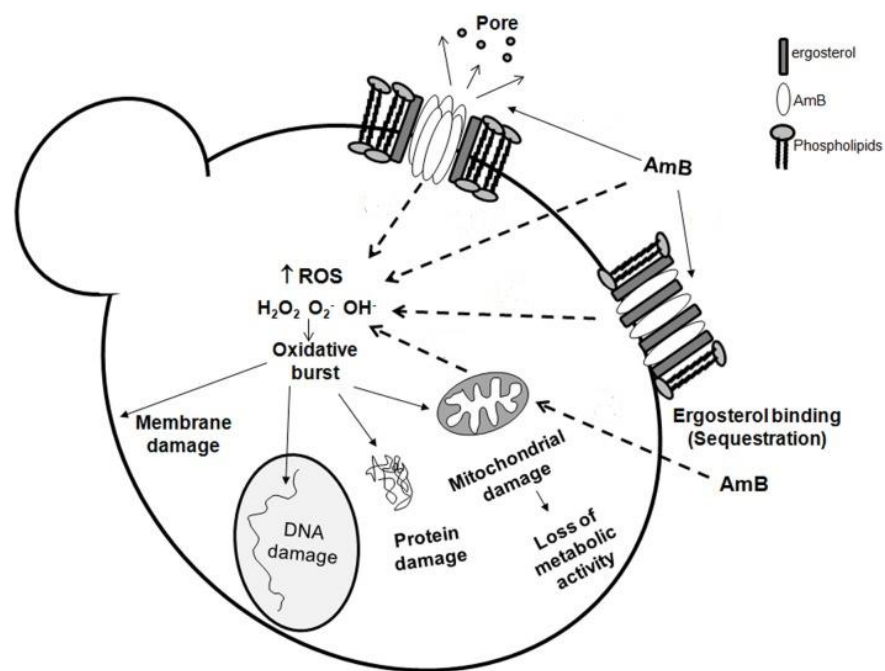


Figure 1.20: The mode of action of amphotericin B against leishmanial parasites

1.4.5.3 Miltefosine

Miltefosine, an alkylphosphocholine, was initially developed as an antineoplastic agent of breast cancer, is the first oral treatment against leishmaniasis (Smorenburg *et al.*, 2000; Dorlo *et al.*, 2012). Antileishmanial activity was first reported in 1987 against *L. donovani* *in vitro* and *in vivo* experimental models (Achterberg and Gercken, 1987) (Croft *et al.*, 1987). Efficacy of miltefosine has been registered in India since 2002 for oral treatment against VL, followed by Germany in 2004 (Davies, CR *et al.*, 2003; Berman, 2008). In 2005 in Colombia, the use of miltefosine to treat cutaneous leishmaniasis has recorded over % 91 cure rates (Soto and Soto 2006).

The main side effect of miltefosine is its teratogenicity properties, so miltefosine should not be administered to pregnant women (Rakotomanga *et al.*, 2005; Dorlo *et al.*, 2008). Additionally, gastrointestinal symptoms such as anorexia, nausea, vomiting and diarrhea (Sundar *et al.*, 2002). Another drawback, miltefosine has long half-life ~7 days, which could promote development of drug resistance as a result of the drug being present in the bloodstream after the end of treatment (Chappuis *et al.*, 2007; Bryceson 2001).

The mode of action of miltefosine described in chapter 4.

1.4.5.4 Paromomycin

Paromomycin, an aminoglycoside antibiotic, was first isolated from filtrates of *Streptomyces krestomuceticus* in the 1950s. Interestingly it was introduced in 1960s and shown to have antileishmania activities. In 1980, renewed interest of paromomycin led to development of topical formulations effective against CL, and a parenteral formulation was also developed against VL (Croft, SL and Yardley, V 2002). In 2006, paromomycin injection was licenced

based on the results of a clinical trial for treatment of VL performed in India (Sundar *et al.*, 2007; Davidson *et al.*, 2009). Paromomycin has shown a cure rate of 93% against VL in a daily injection at 15 mg.kg⁻¹ for 21 days (Musa *et al.*, 2010).

The mode of action of paromomycin has not been fully determined, it has been suggested that PMM binds to the ribosomal subunit of cytoplasmic forms, thus inhibiting protein synthesis (Croft and Yardley, 2002). Paromomycin also would dysfunction of mitochondrial activity acting, leading to decrease ATP production, and appears to have other effects such as decreases membrane fluidity and permeability (Berg *et al.*, 2013).

1.4.5.6 Combination therapy

The current antileishmania drugs target different biological pathways inside the parasites but also present different side effects. Combination regimens in visceral Leishmaniasis was implemented over the last few years for several reasons.

First, combining therapies from different chemical structures could reduce the dose of total drug treatment duration, limit the toxicity, higher compliance, reducing the cost of treatment, and also provide less burden on long term for the health system (Alvar *et al.*, 2006; Van Griensven *et al.*, 2010). Moreover, combination therapy may limit the emergence of drug resistance. Previous studies have been shown that selection of parasite resistance *in vitro* against two combination drugs is too difficult for the parasite especially if the two drugs target different biological pathways (Berg *et al.*, 2013; Hendrickx *et al.*, 2017). Ideally the design of combination chemotherapy regimens should be made of a rapid acting drug and a slow-acting drug to reduce the parasites burden on the short term and to elimination of the

parasites on the long term (Mondal *et al.*, 2010). For example, combined therapies were tested such as liposomal AmB and miltefosine, miltefosine and paromomycin and liposomal AmB and paromomycin and with more than a 94% success rate for all of them in Indian and Bangladesh (Table 1.5) (Sundar *et al.*, 2011; Rahman *et al.*, 2017). There were very few side effects reported and no relapse or Post Kala azar dermal (PKDL) was confirmed at 6 months post-treatment (Rahman *et al.*, 2017).

Table 1.5: Combination therapy of antileishmania drugs

Combination	Dosage	Cure rate	
		India (Bihar)	Bangladesh
L-AmB + Miltefosine	Single injection of 5 mg.kg ⁻¹ LAmB + 7 days 50-100 mg miltefosine	97.50%	94.40%
Miltefosine + paromomycin	50-100 mg.day ⁻¹ miltefosine + 11 mg.kg ⁻¹ per day paromomycin for 10 days	98.70%	97.90%
L-AmB + paromomycin	Single injection of 5 mg.kg ⁻¹ LAmB + 10 days 11 mg.kg ⁻¹ intramuscular paromomycin	97.50%	99.40%

1.4.5.7 New hope for novel drugs for leishmaniasis

Drug development efforts spearheaded by the Drugs for Neglected Diseases initiative (DNDi) have now shown encouraging progress in several novel classes. Two entirely new chemical entities (NCEs) were nominated as pre-clinical candidates in animal models against both visceral (VL) and cutaneous leishmaniasis (CL), DNDI-6148 from the oxaborole class and DNDI-0690 from the nitroimidazole class have entered in pre-clinical development. Phase I studies for both NCEs will be conducted throughout 2018 to 2019. Results will serve for both VL and CL as oral drugs (Figure 1.21) (DNDi, 2017 and 2018). Other compounds, such as DNDi 5561, will be expected to be nominated as preclinical candidates in late 2018 or early 2019 (DNDi, 2018).

In addition, final results of the preclinical in vivo efficacy study showed an improved outcome for CpG-D35, an immunomodulator to stimulate the innate immune system against CL. This system was used either alone or as an adjunct to drug therapy with pentavalent antimony, for progression to Phase 1 clinical studies (DNDi, 2017 and 2018). Furthermore, the efficacy of combination therapy using thermotherapy (TT) (one application, 50°C for 30") and miltefosine (2.5 mg/kg/day for 21 days) was tested to treatment of uncomplicated CL in Peru and Colombia. In 2017, 72 subjects (47 from Peru and 25 from Colombia) were enrolled into the study. after an interim analysis conducted by the Data Safety Monitoring Board (DSMB) in 2018 allowed to continue with this study and start planning a phase III in both New and Old World (DNDi, 2015 and 2018).

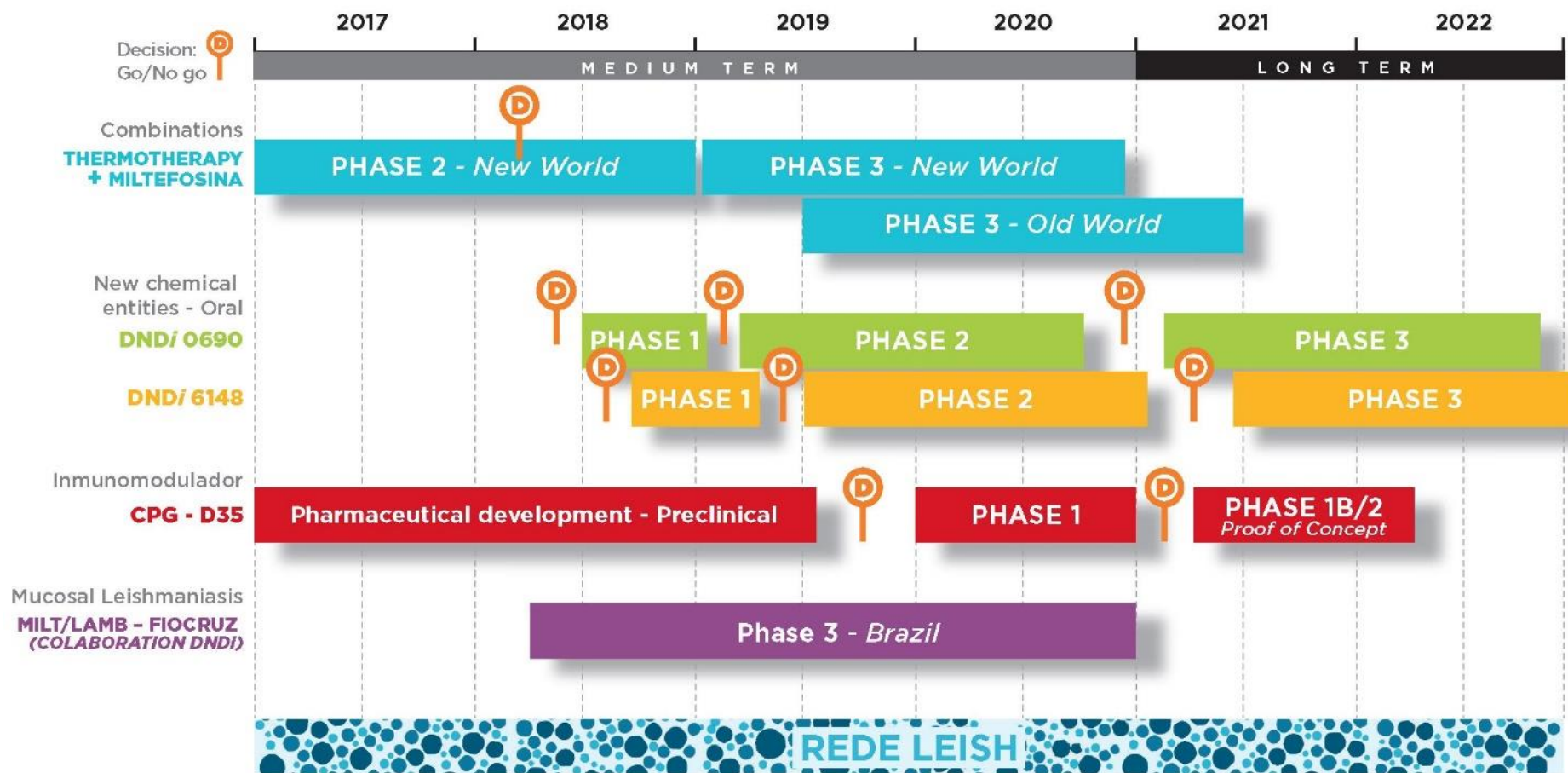


Figure 1.21: DNDi planning activities in CL

1.6 The search for new drugs includes natural products

Natural products (secondary metabolites) have historically been used to control and treat diseases, and serve as a successful source for many pharmaceuticals used today since they contain a quantity of metabolites with a great variety of chemical structures and pharmacological activities (Ginsburg and Deharo, 2011). Between 1981 and 2006, a study of natural products (or semi-synthetics) as sources of new drugs was estimated at 62% of new small molecule drugs (Newman and Cragg, 2007). As only approximately 10% of the biodiversity in the world has been evaluated for biological activity, there is an immense potential for natural compounds that are, as yet, undiscovered (Dias *et al.*, 2012; Meshnick *et al.*, 1996). Quinine, an aminoquinoline alkaloid isolated from the cinchona tree bark of the 17th century, was first purified as the active component in 1820. Quinine remained an important anti-malarial drug until 1920s (Wells, 2011; Achan *et al.*, 2011) when its widespread use was replaced by synthetic quinoline derivatives. Artesunate was isolated from the sweet wormwood plant *Artemisia annua* in 1971 (Wells, 2011) and its derivatives are the current front-line antimalarial in the form of artemisinin combination therapies. Others have been synthetic antimalarial drugs produced using natural products belonging to the classes of 4- and 8-aminoquinolines, such as chloroquine, amodiaquine and primaquine, which have all been extensively used over the last century (Carvalho and Krettli, 1991; Batista *et al.*, 2009). Moreover, theophylline, penicillin G, morphine, paclitaxel and vitamin A among many other examples that are derived from natural products (Clark, 1996). Analysis of functionality and physiochemical properties of recently developed small molecule natural-product-derived drugs has revealed that 50% of them met Lipinski's rules-of-five for orally available drugs (Ganesan, 2008).

Over the last decades, natural products (secondary metabolites) have been studied due to the great variety and amount of bioactive compounds they synthesize. Active natural products include several groups of alkaloids, terpenoids, sterol, flavanoid, and quinones stand out because of their biological activities and potential health benefits (Table 1.6) (Wink, 2012).

Alkaloids are an organic compounds characterized by basic nitrogen atoms as a part of heterocyclic system (Bribi, 2018).

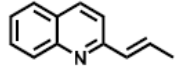
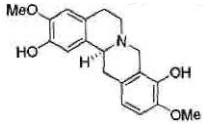
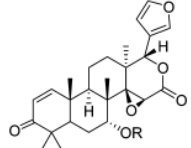
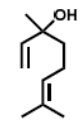
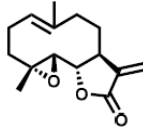
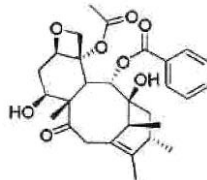
Terpenoids are a large and diverse class of natural products derived from C₅ unit like as isoprene. They are classified as hemiterpenes (C₅), monoterpenes (C₁₀), sesquiterpenes (C₁₅), diterpenes (C₂₀), sesterpenes (C₂₅), triterpenes (C₃₀), tetraterpenes (C₄₀), and polyterpenes (>C₄₀). Terpenoids can be found in numerous sources of living organisms, especially plants, fungi, and marine animals (Sülsen *et al.*, 2017). Many terpenoids possess the pharmaceutical properties reported such as cancer preventive effects and analgesic, anti-inflammatory, antimicrobial, antifungal, antiviral, and antiparasitic activities (Singh and Sharma, 2014).

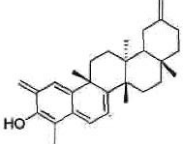
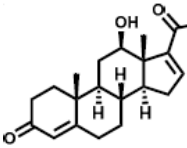
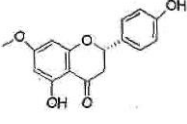
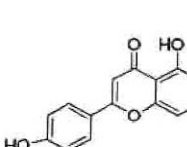
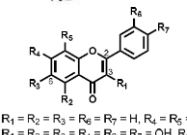
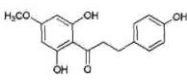
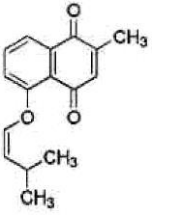
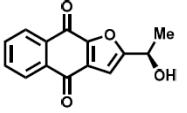
Flavonoids are hydroxylated phenolic compounds (which consists of two phenyl rings and heterocyclic ring) that are present in plants. They are classified into different classes into flavonoids, isoflavonoids and neoflavonoids. Flavonoids present a wide range of biological activities such as antioxidant and anti-inflammatory activities (Mamadalieva *et al.*, 2011; Kumar and Pandey, 2014).

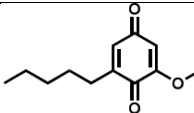
Quinones are a class of organic compounds, characterized by two carbonyl groups linked to a carbocyclic backbone. Quinones have been extensively studied as potential antimicrobial and anticancer agents, functioning either as inhibitors of essential redox pathways or as prodrugs (Hall *et al.*, 2012a).

The number of recent studies regarding the effectiveness of natural products against different pathogens have been summarized in Table 1.6.

Table 1.6: Antiparasitic activity of natural product sources

Sources	Identifications	Structure	Author
Alkaloids	Chimanine B isolated from <i>Galipea longiflora</i> (Rutaceae) have demonstrated strong therapeutic efficacy against experimental CL and VL. When administered to <i>L. amazonensis</i> infected BALB/c mice (50 mg/kg body weight x 5 injections at intervals of 4 days). Chimanine B reduced the parasite load by 90% while the lesion weight was reduced by 74%.	 Chimanine B	Fournet <i>et al.</i> , 1996
	Scoulerine isolated from <i>Corydalis dubia</i> showed activity against two different strains of <i>P. falciparum</i> (TM4/8.2 and K1CB1, with IC ₅₀ values of 5.4 μM and 3.1 μM, respectively)		Wangchuk <i>et al.</i> , 2012
Terpenoids	Triterpenoid compound from the fruits of Neem, <i>Azadirachta indica</i> showed activity against D10 (CQ-S) and W2 (CQ-R) Strains of <i>P. falciparum</i> with EC ₅₀ values between 0.03 μM and 9.4μM		Chianese <i>et al.</i> , 2010
	Monoterpene (inalool) isolated from a plant <i>Croton cajucara</i> (Euphorbiaceae) showed strong antileishmanial activity against <i>L. amazonensis</i> promastigotes and intracellular amastigotes—LD ₅₀ = 0.028 and 0.14 μM respectively.		Rosa <i>et al.</i> , 2003
	Sesquiterpene lactone—parthenolide isolated from a crude extract of plant <i>Saussurea costus</i> (Asteraceae) showed activity against <i>T. brucei rhodesiense</i> with EC ₅₀ = 0.8 2 μM and SI = 6.5 against rat skeletal myoblast L6 cells		Julianti <i>et al.</i> , 2011
	Deacetylbaccatin III isolated from <i>Taxus baccata</i> (European yew tree) exhibited strong antileishmanial activity against (intracellular amastigotes) <i>L. donovani</i> with an EC ₅₀ value of 70 nM		Georgopoulou <i>et al.</i> , 2007

	compound LLD-3, obtained from <i>Lophanthera lactescens</i> exhibited activity against <i>L. amazonensis</i> with an EC ₅₀ of 0.41 μM		Danell <i>et al.</i> , 2009
	6,7-dihydroneeridienone (sterol) isolated from <i>Pentalinon andrieuxii</i> displayed antileishmania potential against <i>L. mexicana</i> with EC ₅₀ = 0.03 μM, and negligible cytotoxicity on health bone marrow macrophages from C57BL/6 mice.		Pan <i>et al.</i> , 2012
Flavonoids	sakuranetin from the dichloromethane fraction of <i>Baccharis retusa</i> exhibited antileishmania potential against <i>L. amazonensis</i> , <i>L. braziliensis</i> , <i>L. major</i> , and <i>L. chagasi</i> with EC ₅₀ values ranging between 43-52 μg/mL		Grecco <i>et al.</i> , 2012
	Quercetin isolated from the leaves of <i>Morinda morindoides</i> (Rubiaceae) exhibited high anti-plasmodium activity against the <i>P. falciparum</i> (Congolese chloroquine-sensitive strain) with an EC ₅₀ value of 19.20 μM		Cimanga <i>et al.</i> , 2009
	2 phenolic compounds isolated from different subclasses of flavonoids demonstrated submicromolar potency against <i>T. brucei rhodesiense</i> with EC ₅₀ (= 0.16 and 0.8 μM) and SI (= 1019 and 571 (adenocarcinoma cells (HT-29)), respectively.	 R ₁ = R ₂ = R ₃ = R ₆ = R ₇ = H, R ₄ = R ₅ = OH R ₁ = R ₂ = R ₃ = R ₄ = R ₆ = R ₇ = OH, R ₅ = H	(Răz, 1998)
dihydrochalcones (chalcone) obtained from <i>Piper elongatum</i> exhibited antileishmania potential (<i>in vitro</i>) against the promastigotes of <i>L. braziliensis</i> , <i>L. tropica</i> and <i>L. infantum</i> with EC ₅₀ value of 28.47, 3.82 and 6.35 μg/mL respectively		Hermoso <i>et al.</i> , 2003	
Quinones	Prenyloxy naphthoquinone obtained from the roots of <i>P. zeylanica</i> showed leishmanicidal activity against <i>L. donovani</i> amastigote and promastigote with EC ₅₀ = 1.9 and 3.46 μM, respectively.		Mishra <i>et al.</i> , 2013
	furanonaphthoquinone isolated from the stem bark and root bark extracts exhibit activity against <i>T. brucei rhodesiense</i> with EC ₅₀ = 0.045 μM,		Moideen <i>et al.</i> , 1999

	Primin isolated from the leaves of <i>Miconia lepidota</i> exhibit activity against <i>T. brucei rhodesiense</i> with $EC_{50} = 0.14 \mu\text{M}$, and moderate cytotoxicity ($CC_{50} = 15.4 \mu\text{M}$) against mammalian L6 cell lines.		Gunatilaka <i>et al.</i> , 2001
--	--	---	---------------------------------

1.7 The objective of this study

Through a Materials Transfer Agreement with PhytoQuest Ltd, I was provided with the Phyt PURE natural product library – a novel collection of 643 natural products isolated from plants distributed within temperate zones. As such, natural products from these plants will not have any tradition of being used as medicines for the treatment of trypanosomiasis, malaria or leishmaniasis. In this thesis, I describe the screening of this library against three parasites; the intraerythrocytic stages of *Plasmodium falciparum*, axenic amastigotes of *Leishmania mexicana* and the bloodstream form of *Trypanosoma brucei brucei*. Data on their activity and selectivity when compared to human cell line(s) is presented.

Where a Phyt PURE compound is evaluated as a potential hit, the objective will then be to attempt to generate a resistant line in order to facilitate a comparative study of morphology before and after compound action in order to explore its action. Further, the molecular basis of drug action and resistance will be explored.

A final objective is the evaluation and validation of a novel *L. mexicana* transgenic cell line that expresses the NanoLuc luciferase reporter. This validation exploits the Medicine for Malaria Venture (MMV) Pathogen Box as a resource as well as an evaluation of the utility of luciferase expressing transgenic parasites in the more relevant intramacrophage assay.

Chapter 2: Materials and methods

2.1 Materials (source of stocks and reagents)

Unless specified, all plastic were sourced commercially from either Greiner Bio One or Starlab. Unless specified, all chemicals were provided by Sigma and ThermoFisher scientific. Compound libraries were provided by either Phyto-Quest Ltd or the Medicines for Malaria Venture (MMV) Pathogen Box. Lastly, the human blood was provided to professor Paul Horrocks as an approved user by The National Blood and Transplant Service (NBTS) account H064, and maintained under the Human Tissue Authority (HTA) License 12349 for the Institute for Science and Technology in Medicine (ISTM) at Keele University.

2.2 Cell culture methods

2.2.1 *Plasmodium falciparum*

2.2.1.1 Preparation of growth medium for *P. falciparum* culture

The complete growth medium consists of 500 mL RPMI (Roswell Park Memorial Institute) -1640 medium supplemented with 37.5 mM HEPES buffer solution, 5 mM sodium hydroxide solution, filter sterilised (0.5 µM) 10 mM D-glucose, 2 mM L-Glutamine, , 100 µM hypoxanthine solution, 25 mg/mL gentamicin sulfate, 5% for both human serum and albumax-II.

Incomplete growth medium was prepared the same way as the complete medium, but without 5% of albumax-II or human serum.

2.2.1.2 Preparation of normal human erythrocytes

NBTS UK supplied fresh human red blood cells type-O-Rhesus positive (ORh+). Human blood was aliquoted in to a 50 mL tube and stored at 4°C for 2-3 weeks. To prepare 50% haematocrit blood cell (RBC) solution for cell culture, a 50 mL aliquot was centrifuged at 1160 g at room temperature (RT) for 10 minutes. The upper serum phase was removed and an equal volume of incomplete growth medium was added to the pelleted RBCs. The RBCs were re-suspended and then pelleted by centrifugation at 850 g RT for 5 minutes. The process of washing the RBC pellet was repeated twice more as describe above to ensure the complete removal of serum, preservatives and white blood cells (WBCs). To complete the process, an equal volume of incomplete growth medium was added to ensure there was an equal volume of blood and supernatant in the tube. The RBCs at 50% haematocrit (HCT) were stored for up to 10 at 4C°.

2.2.1.3 *In vitro* intraerythrocytic culture of *P. falciparum*

Two clones of *P. falciparum* were used in this study; *Pf* 3D7 is derived from *P. falciparum* NF54 isolated from a Dutch malaria patient, which is chloroquine sensitive (Delemarre and Van der Kaay, 1979; Walliker *et al.*, 1987), and *Pf*Dd2^{Luc} transgenic parasite line is a clone derived from genetic modification of AHE1 (Hasenkamp *et al.*, 2013). Which has a *pfpcna*/luciferase expression cassette introduced (Wong *et al.*, 2011), and is chloroquine resistant.

The *P. falciparum* strain 3D7 and Dd2^{Luc} were continuously cultured at a 2% HCT and 2% parasitemia as previously described (Trager and Jensen, 1976; Freese *et al.*, 1988). Cultures are maintained at 37°C in an atmosphere of 1% O₂, 3% carbon dioxide and 96% nitrogen. Light microscopy was used to assess the growth and stages of the parasite. Parasite density was controlled by diluting cultures with complete medium, RBC and infected red blood cells

(iRBCs) as necessary to between 2-4% HCT and 0.5-5 % parasitaemia (PCT) depending on the requirements of the assays.

2.2.1.4 Assessment of Parasitaemia with Giemsa Staining

Parasite density was assessed daily. Thin blood smears were prepared on glass slides and fixed with 100% absolute methanol for 1 minute. The slide was air dried, then covered with 10% giemsa stain (filtered through a 0.45 μ M pore filter) and left for 10 minutes. The dye was washed with water and allowed to dry. Parasitemia and life cycle staging were assessed by light microscopy (oil immersion objective lens) at x1000 magnification (Olympus).

2.2.1.5 *P. falciparum* culture synchronisation using sorbitol-lysis method

P. falciparum culture synchronisation with sorbitol was originally described by Lambros and Vanderberg (1979). Cells were grown until the culture displays predominantly ring stage parasites in 0-18 hours post RBC infection. The iRBC cell pellet was collected from the parasite culture by centrifugation at 300 g, RT, RT for 5 minutes. The supernatant was discarded and 5 volumes of pre-warmed 5% w/v sorbitol solution was added to the cell pellet and 5 minutes incubation at 37°C. Synchronised iRBC were collected by centrifugation of the culture at 850 g RT for 5 minutes the supernatant was removed and the cell pellet (iRBC represents early ring stage parasites). The culture was put in a flask with the appropriate volume of complete medium, gassed and returned to the incubator at 37 °C.

2.2.2 *Trypanosoma brucei*

2.2.2.1 *In vitro* culture of *T. brucei*

The procyclic forms of *T. brucei* 427 SMWT strain cells were maintained in HMI-9 medium (a stock of HMI-9 was prepared by dissolving 16 g of HMI-9, 1.51 g of sodium bicarbonate (NaHCO₃) and 7 µL of 2M β-mercaptoethanol in 400 mL dH₂O), supplemented with 10% (v/v) foetal calf serum, 2 mM L-glutamine (Gibco) and 100 U/mL penicillin (Gibco) and 100 µg/mL streptomycin (Gibco) at 37°C with 5% CO₂ (Hirumi and Hirumi, 1989; Sullivan *et al.*, 2015). Cell cultures were diluted 1:20 into fresh medium every 3 days to maintain the cell densities between 10⁵ and 10⁶ cells/mL.

2.2.3 *Leishmania mexicana*

2.2.3.1 *In vitro* culture of *L. mexicana*

Procyclic *L. mexicana* promastigotes (strain MNYC/BZ/62/M379) were maintained in Schneider's medium (Gibco) pH 7.0 with 10% FBS (Fetal Bovine Serum) (Gibco), 100 U/mL penicillin (Lonza) and 100 µg/mL streptomycin (Lonza) at 26°C. Differentiation to axenic amastigotes were performed by a 1 in 10 dilution of stationary phase promastigotes into Schneider's medium pH 5.5 supplemented with 10% FBS, 100 U/mL penicillin and 100 µg/mL streptomycin (complete Schneider's media pH 5.5) at 32°C (Heather *et al.*, 1997).

The density of parasite growth was determined by the addition an equal volume of culture and 2% formaldehyde (v/v) in phosphate buffered saline (PBS), and counted in a Neubauer haemocytometer under Light microscopy.

2.2.3.2 Generation of plasmid constructs and *L. mexicana* transfection

Transgenic *L. mexicana* NanoLuc and NanoLuc-PEST provided by Dr. Berry and described in (Berry *et al.*, 2018). Briefly, NanoLuc and NanoLuc-PEST open reading frames were amplified by PCR from plasmid DNA templates: pNL1.1, pNL1.2 (Promega). All oligonucleotide sequences are provided in Table 2.1. Amplified genes were digested with *Bam*HI and *Kpn*I and ligated into pSSU-No (Oyola *et al.*, 2012) to produce the constructs pSSU-NanoLuc and pSSU-NanoLuc-PEST, for constitutive expression in *Leishmania mexicana*. The pSSU expression vector contains flanking regions for integration into the rDNA locus of the parasite genome. The constructs (*Pac*I/*Mss*I digested) were transfected into mid-log *L. mexicana* procyclic cells by nucleofection using a 4b Nucleofector system (Lonza), as described previously (Burkard *et al.*, 2007). Transformants were selected after 24 hours by the addition of 40 µg/ml Geneticin (Life Technologies). Integration of the construct into the genome was assessed by PCR amplification of 160-200 ng genomic DNA, using the oligonucleotide primers pSSU-F (region of the 18S gene) and pSSU-R (splice acceptor site in the pSSU vector). Genomic DNA was purified from mid-log promastigote cells using the DNeasy Blood and Tissue Kit (Qiagen).

Table 2.1: Oligonucleotide sequences for cloning and integration.

Name	Purpose	Sequence
<i>NanoLuc-F</i>	Amplification of NLuc and NLucP for pSSU-	5' -GTTGGTGGATCCACCATGGTCTTCACAC-3'
<i>NanoLuc-R</i>		5' -GCCCGGTACCAGAGTCGCGGCCTTACG-3'
<i>NanoLuc-PEST-R</i>	Neo cloning	5' -GCCCGGTACCAGAGTCGCGGCCTTAG-3'

2.2.3.3 Long term storage of promastigote cells culture

500 µl promastigote cells culture was mixed with 500 µl Schneiders medium pH 7 and 10% DMSO in sterile freezing vials. The vials were stored -80°C overnight before storage for long term in liquid nitrogen.

To defrost cells: A vial of frozen promastigote cells were thawed at 37°C in water bath. The cells were then transferred to 1.5 mL eppendorf tube and centrifuged for 5 minutes at 300 g to remove the DMSO. The cell pellet was resuspended in 10 mL Schneiders medium pH 7 and incubated at 26°C.

2.3 Drug assays

2.3.1 Drug stocks preparation

a. Phytopure compounds library:

PhytoQuest Ltd has provided a Diversity library of 643 non polar compounds (1mg/mL in DMSO). This library represent a novel source of purified natural products isolated from temperate zone plants across a diversity of chemotypes, which are tested here for their anti-parasitic activity. This library was stored at -20°C.

b. Pathogen Box compounds:

The MMV Pathogen Box resource, comprising 400 diverse drug-like molecules were obtained from the Medicines for Malaria Venture (MMV; Geneva, Switzerland). The Pathogen Box compounds were supplied at a concentration 10 mM (in 10 µl DMSO) in 96-well plates. All compounds were stored at -20°C.

2.3.2 Malaria SYBR-green (MSF) assay

This protocol was adapted from Smilkstein *et al.* (2004). A stock MSF lysis buffer was prepared by mixing 20mM Tris pH7.5, 5mM EDTA, 0.008% Saponin and 0.08% Triton X-100 with 5000X SYBR-green 1 (to produce a 1x final concentration) and placed in the dark at RT until needed. To perform the assay, 100 µl of the re-suspended iRBC culture (from drug dilution experiment) was transferred to a black 96-well plates (Greiner, UK) and combined with 100 µl of MSF lysis buffer with 1x SYBR-green. The black plate was incubated for an hour in the dark at RT. After 1 hour, the fluorescence signal of the samples were detected by using the GloMax Microplate Luminometer (Promega, UK), using the blue fluorescence module filter (excitation, and emission).

2.3.3 Standard protocol for AlamarBlue (AlamarBlue) assay

This protocol was developed by Raz *et al.* (1997). AlamarBlue (ThermoFisher) was diluted 1:10 per well of 96-well plate containing cells culture. The fluorescence signal was measured at 570 nm using a Glomax multi-detection System after 6 h incubation in the dark at 32°C, with 5% CO₂.

2.3.4 Luciferase assay

All bioluminescence reagents are from Promega unless otherwise stated. This protocol was adapted from that originally described by Hasenkamp *et al.*, 2012. 40 µl of *P. falciparum* culture were transferred to wells on a white 96-well plates in triplicate, and 10 µl passive lysis buffer (Promega, UK) was added into each well and homogenized by shaking. Then 50 µl of Luciferase Substrate was added and mixed by shaking the plate. After 2 minutes, the bioluminescent signal was measured using the Glomax Multi Detection System.

2.3.5 Nano-Glo Luciferase Assay

20 µl of treated axenic amastigote culture was transferred in duplicate to a white 96-well plates and 20 µl of luciferase reagent (Nano-Glo Luciferase Assay buffer and Nano-Glo Luciferase Assay substrate, 200:1) was added to each well. After 3 minutes, the bioluminescent signal was measured using a Glomax Multi Detection System. Results were analysed using GraphPad Prism 5.0.

2.3.6 Drug screening experiments against *P. falciparum*

2.3.6.1 Initial screening of intraerythrocytic *P. falciparum*

These experiments were employed using the *Pf* Dd2^{luc} strain in trophozoite stage. Initial screening of all 633 compounds were screened at 10-fold dilution between 20 µM and 2 µM concentrations in duplicate with two technical replicates to provide n=4. An equal volume (100 µL) of Mastermix (4% haematocrit, 1% trophozoite parasitemia and complete medium) was added into all wells and mixed by shaking. Both positive (2 µM Chloroquine CQ) and negative (equivalent volume of DMSO) controls were made in 100 µl of complete medium and 100 µl of Mastermix of each plate. 200 µl incomplete growth medium was added to the perimeter wells of the plate 96-well to minimize edge effects from evaporation. The 96-well plates were incubated at 37°C for 48 hours in a humidified airtight box with an atmosphere of 1% O₂, 3% CO₂ and 96% N₂. The Malaria SYBR-green Fluorescence Assay (2.3.2) was used to assess the inhibitory effect of each compound.

2.3.6.2 Determination of the 50% effect concentration (EC₅₀)

Drug sensitivity was determined by measuring the 50% effective concentration (EC₅₀), 50% lethal dose (LD₅₀) and rate of kill on the Dd2 parasite strain. All these assays were performed in 96-well plates in triplicate at least three independent biological replicates, unless otherwise indicated.

For EC₅₀ assay, the specific concentration for each compound was serially diluted (1:2), nine times in 100 µl complete growth medium (Figure 2.1). Subsequently, 100 µL of Mastermix (4% haematocrit, 1% trophozoite parasitemia and complete medium) was seeded into all wells. Untreated controls were provided by cultures exposed to a 1% DMSO (100% growth) with a drug-treated control provided by exposure to 2µM CQ (0% growth). 200 µl incomplete growth medium was transferred to the perimeter wells of the plate 96-well. The plates were incubated at 37 °C for 48 hours in a 1% O₂, 3% CO₂ and 96% N₂ atmosphere. After that a malaria SYBR-green fluorescence assay (2.3.2) was used to assess the inhibitory effect of each compound. The 50% effect concentration (EC₅₀) was determined by analysis of a log₁₀ transformed drug concentration versus the percentage of parasites growth using GraphPad Prism software (v5.0).

2.3.6.3 Determination of the 50% lethal dose (LD₅₀)

The 50% Lethal Dose (LD₅₀) was determined according to the bioluminescent assay as previously described by Ullah *et al.* (2017).

To measure LD₅₀ was used the same protocol for EC₅₀ as described in (2.3.7) although with a higher starting concentration, with the following modification:

The plates were incubated at 37 °C for 6 hours (rather than 48 hours) in a 1% O₂, 3% CO₂ and 96% N₂ atmosphere (Figure 2.1 B). After that, the LD₅₀ was measured using the standard

protocols for Luciferase (rather than SYBR-green fluorescence assay) as described in (2.3.4).

2.3.6.4 Bioluminescent Relative Rate of Kill (BRRoK) assay

The BRRoK was determined according to the bioluminescent assay as previously described by Ullah *et al.* (2017).

The specific concentration for each compound was serially diluted (1:3), four times in 100 μ l complete growth medium (Figure 2.1 C). Subsequently, 100 μ L of Mastermix (4% haematocrit, 1% parasitemia of early trophozoite-stage and complete medium) was seeded into all wells. A positive control was made of 100 μ l Mastermix with 100 μ l complete medium. To minimize edge effects from evaporation, 200 μ l of incomplete medium was added to the outermost wells on each plate. The plate was placed in a humidified airtight box, gassed (to maintain an atmosphere of 1% O₂, 3% CO₂ and 96% N₂) and incubated for 48 hours at 37 °C (Figure 2.1 C). The RoK was measured after 3, 6 and 48 hours of incubations respectively using the standard protocols for Luciferase 2.3.4.

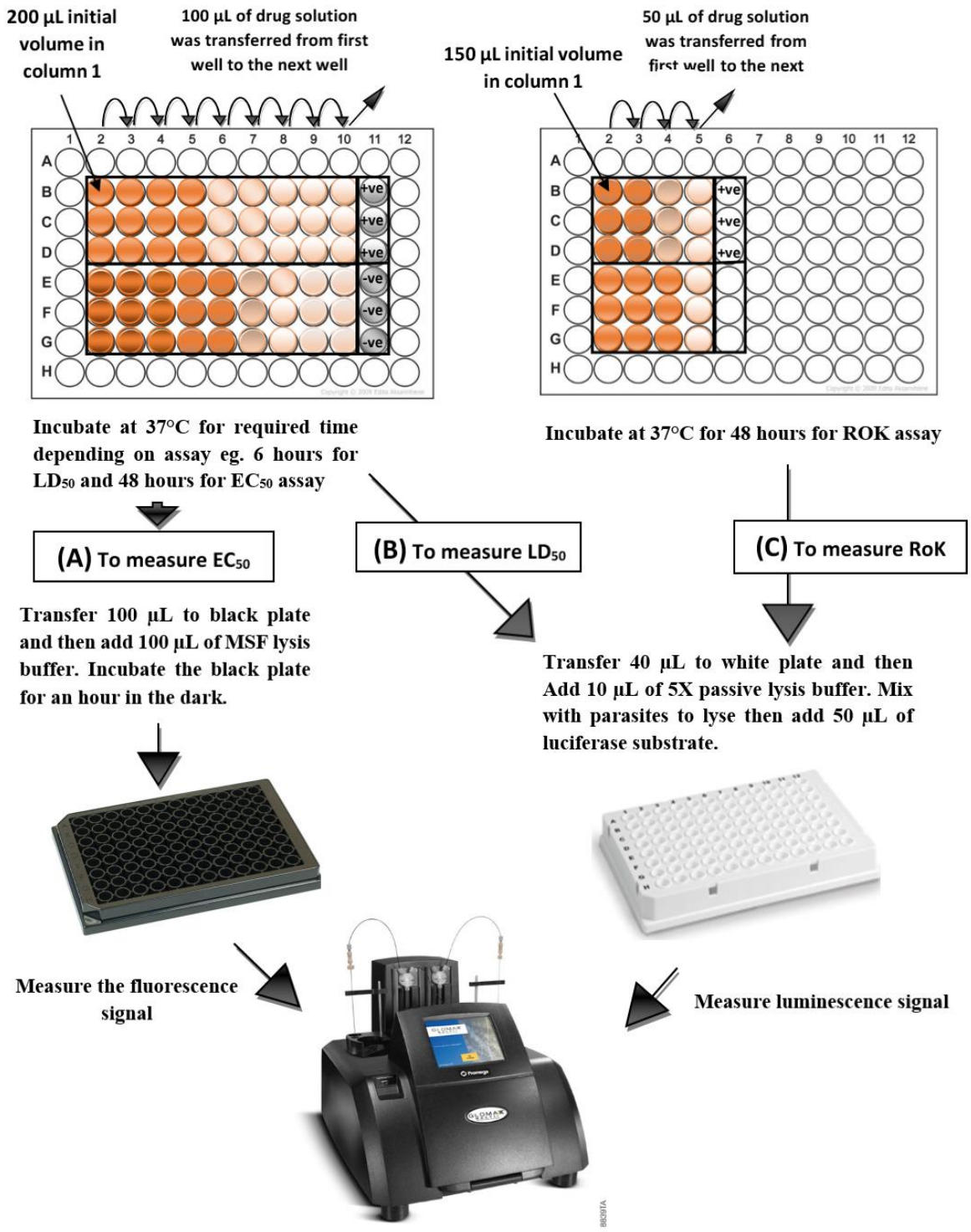


Figure 2.1: Schematic representation of a bioluminescence assay (to measure LD₅₀ and RoK) and fluorescence assay (to measure EC₅₀).

2.3.6.5 Cytotoxicity assay

The toxic effect of PhytoQuest compounds on hepatoblastoma cell line (HepG2) was assessed using AlamarBlue.

HepG2 cells were cultured in DMEM medium supplemented with 10% (v/v) foetal bovine serum and 0.2% (v/v) of a penicillin (10 U/mL)/streptomycin (10 µg/mL) solution at 37 °C with 5% CO₂. The cultures were diluted in in DMEM medium every 4 days to maintain the cell density between 4 x 10⁵ cells/mL and 4 x 10⁶ cells/mL (Aldulaimi *et al.*, 2017).

Assays were performed in 96-well plates. The required concentration for each compound was diluted serially 1:2, eight times in 100 µl DMEM medium, in triplicate.

After that, 100 µL of HepG2 cells at a density of 1×10⁵ cells/mL were seeded to the wells. Untreated controls were provided by cultures exposed to a 1% DMSO (100% growth) with a drug-treated control provided by exposure to 1 µM actinomycin D (0% growth).

The treated cells were incubated for 48 hours at 37°C in an atmosphere of 5% CO₂. After that, HepG2 viability of each compound was assessed by using AlamarBlue fluorescence method as described in (2.3.3). The 50% cytotoxicity concentration (CC₅₀) was determined by analysis of a log transformed concentration versus normalized fluorescence signal curve using GraphPad Prism software (v5.0).

2.3.7 Drug screening experiments against *Trypanosoma brucei*

2.3.7.1 *In vitro* drug screening experiments

In vitro antitrypanosomal activity were assessed using an AlamarBlue assay. The screening of PhytoQuest compounds was performed at 2 µM in each well of 96-well plates. Plates were incubated with 100 µL of *T. brucei* at a density of 1 x 10⁵ cells/mL in HMI-9 medium from a 3 days old culture at 37°C with 5% CO₂ for 48 hours. Assays were screened in triplicate with two biological replicates to perform (n=6). Both positive (2 µL of 2 µM Amphotericin

B (Gibco)) and negative (equivalent volume of DMSO) controls were included on each plate. Following incubation, fluorescence method was used to assess the inhibitory effect of each compound depending on AlamarBlue assay 2.3.3.

2.3.7.2 *In vitro* determination of antitrypanosomal activity

In vitro antitrypanosomal activities of the PhytoQuest compounds were assessed against *T. brucei* using fluorescence method AlamarBlue as described in 2.3.3. The effective concentration 50% (EC₅₀) was measured for candidate compounds according to inhibit of parasite growth as described in 2.4.4.

Assays were performed in 96-well plates. The specific concentration for each compound was diluted serially 1:2, eight times in 100 µl HMI-9 medium, in triplicate. Plates were incubated with 100 µL of *T. brucei* at a density of 2×10^5 cells/mL in HMI-9 medium for 48 hours at 37°C with 5% CO₂. Following incubation, EC₅₀s was measured using AlamarBlue assay, described in 2.3.3. Both positive (2 µl of 2 µM Amphotericin B) and negative (equivalent volume of DMSO) controls were included for each plate. All experiments were performed on a minimum of three independent biological replicates, unless otherwise indicated.

The EC₅₀ was determined by analysis of a log transformed concentration versus normalized fluorescence signal curve using GraphPad Prism software (v5.0).

2.3.8 Drug screening experiments against *Leishmania mexicana*

2.3.8.1 *In vitro* drug screening experiments

Initial screening of PhytoQuest compounds was performed at 2 µM in each well of 96-well plates. Assays were screened in triplicate, with two biological replicates (n=6). 200 µL of axenic amastigotes at a density of 1×10^6 cells/mL were seeded to each well. Both positive

(2 μ l of 2 μ M Amphotericin B) and negative (equivalent volume of DMSO) controls were included on each plate. Cells were incubated for 72 hours at 32°C. The fluorescence method AlamarBlue (2.3.3) was used to assess the inhibitory effect of each compound.

2.3.8.2 *In vitro* determination of antileishmanial activity

In vitro antileishmanial activities of the PhytoQuest compounds were assessed against *L. mexicana* (axenic amastigotes) using fluorescence method AlamarBlue as described in 2.3.3. The EC₅₀ was measured for the candidate compounds according to inhibit of parasite growth, as described in 2.5.4.

Assays were performed in 96-well plates. The specified concentration of each compound was diluted serially in eight different concentrations in 100 μ l Schneider's medium pH 5.5 for each well of 96-well plates, in triplicate at a 2 fold dilution. Plates were incubated with 100 μ L of axenic amastigotes at a density of 2 x 10⁶ cells/mL in Schneider's medium pH 5.5 for 72 hours at 32°C. Following incubation, EC₅₀s was measured using AlamarBlue assay, described in 2.3.3. Both positive (2 μ l of 2 μ M Amphotericin B) and negative (equivalent volume of DMSO) controls were made up on each plate. All experiments were prepared from at least three independent biological replicates, unless otherwise indicated.

The 50% effect concentration (EC₅₀) was determined by analysis of a log transformed concentration versus normalized fluorescence signal curve using GraphPad Prism software (v5.0).

2.3.8.3 Macrophages (THP-1) cell line cytotoxicity assay

The cytotoxicity of the PhytoQuest compounds hits were tested against human acute monocytic leukemia cell line (Tsuchiya *et al.*, 1980, Auwerx, 1991). The human monocyte cell line THP-1 was cultured at density 1x10⁵ cell/mL in RPMI-1640 medium (Gibco)

supplemented with 10% (v/v) FBS and 2 mM L-glutamine (Gibco) (complete RPMI media) at 37°C in an atmosphere of 5% CO₂. The cells were diluted 1:10 into RPMI-1640 medium every 3 days to maintain cell density between 3×10^5 and 8×10^5 cells/mL (Barilli *et al.*, 2011).

Assays were performed in 96-well plates. The required concentration for each compound was serially diluted 1:2, eight times in 100 µL RPMI-1640 medium, in triplicate. After that, 100 µL of THP1 cells at a density of 5×10^4 cells/mL were seeded in each well. Negative controls were provided by cultures exposed to a 1% DMSO (100% growth), and positive controls provided by exposure to 1 µM actinomycin D (0% growth) were included in each experiment. The treated plates were incubated for 48 hours at 37°C with 5% CO₂. Cytotoxicity was determined using fluorescence assay AlamarBlue (2.3.3). Cytotoxic concentration 50% (CC₅₀) was estimated with Graph Pad Prism (5.0). The selectivity index (SI) was calculated through the expression: $SI = CC_{50}/EC_{50}$.

2.3.8.4 Infected macrophages and treatments

The activity of PhytoQuest compounds were tested against intracellular infected macrophages. Differentiation of THP-1 cells was performed by seeding 2.5×10^5 cells/mL in complete RPMI media, supplemented with 20 ng/mL phorbol 12-myristate 13-acetate (PMA) (Invitrogen) (Jain *et al.*, 2012). THP-1 cells were plated onto chamber slides (200 µL/well) (Thermo Scientific), and allowed to adhere for 24 hours incubation at 37°C with 5% CO₂. Following incubation, adherent macrophages were carefully washed once with PBS to remove non-adherent cells. Macrophages were infected with axenic amastigotes at a ratio of 10:1 (parasites:macrophages cells) in complete RPMI medium, and incubated at 32°C

with 5% CO₂ for 16 hours. The macrophages were washed 4 times with PBS to remove extracellular parasites.

Infected cultures were re-incubated for 72 hours at 37°C, 5% CO₂, with compounds (700022, 700107, 700136 and 700240 at 1x, 3x and 9x EC₅₀) or amphotericin b (AmB) (at 1x, 3x EC₅₀), in duplicate. The treated cells were then washed 3 times with PBS, and the plastic chambers was removed from the slides. Infected and uninfected macrophages controls were included in each chamber slide. The cells were then fixed by immersing the slides in 100% absolute methanol for 30 seconds. The slides were dried and then incubated with 5x SYBR-green stain in the dark for 15 minutes. The dye was washed off with PBS and allowed to dry. THP-1 cells were examined under EVOS FL cell imaging system (ThermoFisher Scientific) fluorescence microscope with a 100x lens. The percentage of infected THP-1 was determined by counting the average number of amastigotes per macrophages for each well based on SYBR-green stain. Two biological replicates were performed for each assay.

2.3.8.5 *In vitro* drug screening of MMV Pathogen Box against *L. mexicana* NanoLuc-PEST-transgenic line

Initial screening of the MMV Pathogen Box library was performed at two concentrations (10 μM and 2 μM) μM in each well of 96-well plates. Assays were screened in duplicate, with two biological replicates (n=4). Axenic amastigotes of *L. mexicana* NanoLuc-PEST-transgenic line were seeded at a density of 2 x 10⁶/mL in duplicate (100 μl/well). Both positive (2 μl of 2 μM Amphotericin B) and negative (equivalent volume of DMSO) controls were included on each plate. Cells were incubated for 72 hours at 32°C and a bioluminescence based assay was used to assess the relative cell growth as described in 2.3.5.

2.4 Generating drug-resistance

In vitro, *L. mexicana* (strain MNYC/BZ/62/M379) resistant to 700022 was obtained by growing promastigotes in complete Schneider's medium pH 7.0 at 26°C, under drug pressure in stepwise selection process (Seifert *et al.*, 2003). Promastigotes at a density of 1×10^6 cells/mL were initially treated at 11.5 μ M (the EC₅₀ concentration of 700022) in triplicate. The compound concentration was gradually increased every 48 hours for 28 weeks until they were resistant to 85 μ M. Promastigote growth was monitored every 48 hours using a haemocytometer. The resistance levels of promastigotes were monitored during their establishment by measuring EC₅₀ value as described in 2.5.5 with the following modification: Promastigotes at a density of 1×10^5 cells/mL in complete Schneider's medium pH 7.0 at 26°C were used in assay rather than amastigotes.

L. mexicana amastigotes resistant to 700022 were obtained by culturing resistants stationary phase promastigotes into complete Schneider's media pH 5.5 at 32°C. Once transformed, the resistance levels of axenic amastigotes were detected by measuring the EC₅₀ value.

The stability of the promastigotes resistance line to 700022 was studied by maintaining the resistant culture in Schneider's complete medium pH 7.0, in the absence of drug pressure. The EC₅₀ was re-tested, and these lines remained resistant to 700022 for at least two months.

2.5 Morphological and ultrastructural analysis of the *Leishmanial* parasite

2.5.1 Immunofluorescence assay

The stationary phase metacyclic promastigotes (5×10^7 cells/mL) were treated with 85 μ M and 170 μ M of compound 700022 and incubated for 24 hours. The untreated control was made up with Schneiders medium. After treatment, the cells were washed twice in 100 μ l of

1x PBS (phosphate buffered saline), and settled onto a polysine slide (thermo scientific) for 10 minutes at RT. The excess liquid was removed, and the cells permeabilized with 0.1% triton™ X-100 (100 µl/slide) (Sigma) for 15 minutes, then blocked with one drop of Image iT FX Signal Enhancer (Life Technologies) for 30 minutes in a humid chamber. Cells were then incubated with 100 µl primary antibodies mouse-anti- α -Tubulin (ThermoFisher Scientific) (diluted 1:250 in PBS) for 1 hour. After washing three times with 1x PBS, the cells were incubated with 100 µl goat-anti-mouse secondary antibodies conjugated to Alexa Fluor 488 (diluted 1:200 in PBS) (Invitrogen) for 1 hour in a humid chamber in the dark. Slides were washed twice in PBS, and the cellular DNA was then stained with 100 µl of 0.01 mg/mL 4,6-diamino-2-phenylindole (DAPI) (Invitrogen) for 5 minutes at RT, and then washed twice in PBS before covering with a coverslip. The cells were then analysed using the EVOS FL cell imaging system (ThermoFisher Scientific).

The parameters of length flagellum and body surface area of 200 randomly cells were measured using the ImageJ software (version 1.48).

2.5.2 Scanning electron microscopy (SEM) of metacyclic promastigotes

Before seeding the cells, the coverslips (12 mm, circular) were washed in ethanol. 75 µl of 0.1 mg/mL poly-L-lysine (in PBS) was added onto each coverslip and allowed to stand for 25 minutes at RT. The coverslips were then washed with 100 µl PBS, and kept hydrated in 100 µL PBS overnight.

The stationary phase metacyclic promastigotes (5×10^7 cells/mL) were treated with 85 µM and 170 µM of 700-22 and incubated for 24 hours. The control group was cultivated with Schneiders medium, pH 7 only.

After treatment, promastigotes were rinsed three times in serum free Schneiders and once with PBS. The cell pellets were washed and re-suspended in 100 µL PBS. The cells were

transferred onto a coverslip and incubated at RT for 30 minutes within 12-well plate. Cells were then washed twice with 1 mL PBS, then fixed with 1 mL of 2.5% glutaraldehyde in 0.1 M sodium cacodylate trihydrate ($(\text{CH}_3)_2\text{AsO}_2\text{Na}\cdot 3\text{H}_2\text{O}$) (pH 7.4) for 2 hours in a fume hood. *L. mexicana* promastigotes were then presented for either scanning electron microscopy (SEM) or transmission electron microscopy (TEM). EM and SEM were performed by Karen Walker, Central Electron Microscope Unit/Keele University. This assay was performed in promastigotes wild-type and resistance line.

2.5.3 Transmission Electron Microscopy (TEM)

For TEM was used the same protocols for SEM as described in 2.7.3 with the following modification: Aclar films were used rather than coverslips. Aclar film was cut into squares that fit easily into a well in a 12-well plate.

2.6 Molecular Biology Techniques

2.6.1 Isolation of Genomic DNA

Genomic DNA was isolated from a pellet of stationary-phase promastigotes of *L. mexicana* (strain MNYC/BZ/62/M379) and resistant line for the same strain using DNeasy blood and tissue kits (Qiagen). 1×10^9 cells/mL were harvested and centrifuged at 300 g for 5 minutes. The pellets were resuspended in 200 μl PBS. 20 μl of 20 mg/mL proteinase K and 200 μl buffer AL were added. The mixture was vortexed, and incubated at 56°C for 10 minutes. The samples were extracted with 200 μl ethanol (96-100%) and mixed thoroughly by pulse-vortexing for 20 seconds. The DNA extracted was placed into mini spin column (in a 2 mL collection tube provided in the kit) and centrifuged at 6000 g for 1 minute. The flow-through

and collection tube were then discarded. 500 µl buffer AW1 was added and subjected to a centrifuge at 20,000 g for 1 minute, and then mini spin column was placed in a new 2 mL collection tube and discard the tube containing the filtrate (this step was repeated using 500 µl buffer AW2 rather than AW1 to dry the DNeasy membrane). The column was re-centrifuged for 1 minute at 20,000 g to ensure that no residual ethanol was carried over during the elution. The final step is to transfer the spin column to a new 1.5 mL microcentrifuge tube. 100 µl buffer AE (10mM Tris-Cl, 0.5 mM EDTA, pH 8.5) was added to the center of the spin column membrane to elute the DNA, incubated at RT for 2 minutes, and centrifuged for 1 minute at 10,000 g. Take 10 µl to the PCR amplification. The DNA concentration was measured using a NanoDrop 1000 spectrophotometer (Thermo Scientific).

2.6.2 Amplification reactions

The miltefosine transporter *LmRos3* gene (LmxM.31.0510) and LmMT gene (LmxM.13.1530) were amplified from genomic DNA of both *L. mexicana* promastigotes wild type and *L. mexicana* promastigotes resistance to compound 700022, using the oligonucleotide shown in Table 2.2.

Reactions were performed in a final volume of 100 µl using 50 ng genomic DNA, 10 µl of 10X buffer, 6 µl of 10 mM deoxynucleotide dNTPs, 10 µL of (25mM) MgSO₄ Solution, 3 µl of 1 µM of each oligonucleotide, 56 µl dH₂O and 5 U/µL *Taq* DNA Polymerase. Negative controls (without genomic DNA) were prepared in each reaction. The PCR amplification reaction was performed using a thermocycler PTC-200 (MJ Research). The PCR reaction was carried out under the following conditions: initial denaturation at 95°C for 2 minutes and 34 cycles at 95°C for 30 seconds, 55°C to 65°C for 30 seconds and 72°C for 2 minutes, and a final elongation step at 70°C for 10 minutes.

Table 2.2: List of genes and oligonucleotide sequences used for gene sequences. All the oligonucleotides were bought from Eurofins Genomics.

Gene / Clone	Oligonucleotide sequence	Band size (bp)
LmxM.31.0510	F 5'-CGTGGGCCAAATCATGGCGT-3' R 5'-TGCATTTTGGCTTCACGAGAAAGGCG-3'	1153
LmxM.13.1530	F1 5'-CCTGCTCCGTTTCATATACCCCC-3' R1 5'-CCGTACGGTCCAGCGCCACACG-3'	3430
	F1 5'-GCCGCTGTCCTTCGTGCTCCTGG-3' R1 5'-GGCTATGATAAAGTAGTTCAGC-3'	589
	F2 5'-CCAGAACATAACGCTGTGGGGG-3' R2 5'-GCATCCAAATGATCACACCGGCG-3'	1013
	F3 5'-GAGCGGCGCTGCACCTTGATCATCG-3' R3 5'-CGCTGAACACGAGCGTGCCGGTCTC-3'	741

2.6.3 PCR product analysis

PCR products were verified using a 2% agarose gel. Agarose was dissolved in to TAE buffer (0.04 mol/L Tris acetate, 0.001 mol/L EDTA), and stained with 0.5 mg/mL ethidium bromide. Following electrophoresis, the gel was and photographed under an ultraviolet light. 2-Log DNA Ladder (0.1-10.0 kb) was used as a molecular marker to determine the band size of samples.

2.6.4 Ligation:

The PCR product was subcloned into the PCR™2.1 TOPO® vector (Invitrogen). The ligation reaction was set up as follows: 4 µL PCR product was added into 1 µL TOPO® vector and mixed with 1 µL salt solution (1.2 M NaCl; 0.06 M MgCl₂ provided in the kit) and the ligation reaction was incubated at RT for 2 hours.

2.6.5 Transformation of bacteria

The ligation product was transformed into *E. coli* cells (Invitrogen™ Competent *E. Coli*) to amplify the confute get large quantities of the gene insert. 3 µL of the ligation product was

added to 50 μ l competent *E. coli* cells, mixed gently and incubated on ice for 10 minutes. The cells were heat shocked at 42°C for 45 seconds, then put on ice for 1-2 minutes. 200 μ l of S.O.C medium (2% tryptone, 0.5% yeast extract, 10 mM NaCl, 2.5 mM KCl, 10 mM MgCl₂, 10 mM MgSO₄, and 20 mM glucose) was added to the cells and incubated at 37°C for 1 hour. 150 μ L of this solution was plated out on LB agar plates containing 100 μ g/mL ampicillin and incubated at 37°C overnight.

2.6.6 Selecting transformed colonies

Positive colonies were grown in 5 mL Lysogeny broth (LB) (Sigma) containing 100 μ g/mL ampicillin. Cultures were incubated at 37°C overnight with shaking at 300 g to obtain large quantities of the plasmid. Plasmid DNA was isolated using the plasmid miniprep kit. Then cloning was verified by restriction enzyme digestion to check the insert cloned into the vector.

2.6.7 Purification of plasmid DNA

Plasmid DNA was purified from the harvested cells using a QIAprep Spin Miniprep kit (Qiagen), according to the manufacturer's protocol. 2 mL of overnight *E. coli* culture was centrifuged at 300 g for 5 minutes into microcentrifuge tube. The pellet was resuspended in 250 μ l buffer P1 (50 mM Tris-Cl, pH8.0; 10 mM EDTA and 100 μ g/mL RNase A) and then 250 μ l of buffer P2 (200mM NaOH and 1 % ww/v NaOH) was added and mixed thoroughly. 350 μ l of buffer N3 (25-50% guanidinium hydrochloride and 10-25% acetic acid) and mix immediately by pulse-vortexing, followed by centrifugation at 10,000 g for 10 minutes. The supernatant was placed in a QIASpin column and centrifuged at 6000 g for 1 minute. The column was washed with 750 μ L buffer PE and centrifuged for 30–60 seconds. 50 μ l buffer EB was added to the centre of the spin column membrane to elute the plasmid DNA, and

centrifuged for 1 minute at 10,000 g. Plasmid DNA was quantified using a NanoDrop 2000c spectrophotometer (Thermo Scientific).

2.6.8 Digestion of plasmid with restriction enzyme

Purified plasmid was digested using EcoRI restriction enzyme (Thermo Scientific) to confirm of the insert. The digestion reactions were set up as described in table 2.3.

Table 2.3: EcoRI digestion reaction

Reagent	Final concentration	Final volume in 20 μ l
Plasmid DNA		
10X FastDigest Green Buffer	1x	2 μ l
EcoRI (10 U/ μ l)	5 U	1 μ l
ddH ₂ O	To give a final volume of 20 μ l	

The reaction mixture was incubated at 37°C for 30 minutes-1 hr.

The restriction digests were analyzed by gel electrophoresis.

2.6.9 Genomic DNA sequencing of LmMT and LmRos3

The LmMT and LmRos3 genes for both *L. mexicana* wild-type and r-*L. mexicana* resistant to 700022 were implemented using commercial DNA sequences (Eurofins Genomics).

2.6.10 Sequence analysis

Multiple alignment of nucleotide sequences were performed by using the Clusta omega (<https://www.ebi.ac.uk/Tools/msa/clustalo/>). ID of *L. mexicana* orthologs is available at TriTrypDB (<http://tritrypdb.org/tritrypdb/>). Swiss institute of bioinformatics (SIB) tool was

used to translate nucleotide (DNA/RNA) sequence to a protein sequence (<https://web.expasy.org/translate/>).

Genome sequencing analysis was done to determine if there any differences between the reference sequence and the gene that has already been sequenced.

2.7 Data analysis

The data was converted to Excel spreadsheets using Instinct software (Promega). Data was analysed and bar charts plotted on GraphPad Prism v5.0.

2.8 Chemical laboratories

Chemical structures of the tested compounds were drawn using ChemDraw software and SMILES code reported. Chemoffice and Molinspiration softwares were used to find out compound's names with physicochemical properties such as Molecular weight (MW), Log_p (octanol-water partition coefficient), Log_s (water solubility), hydrogen bond acceptors (HBA), hydrogen bond donors (HBD), total polar surface area (TPSA), number of rotatable bonds (NROT_B) and molecular volume.

Chapter 3: Screening of Phytopure library compounds against *P. falciparum*, *T. brucei* and *L. mexicana*

3.1 Introduction

Diseases such as malaria, leishmaniasis and trypanosomiasis continue to be the cause of suffering for many millions of people living in tropical and subtropical areas of the world. There is an urgent need to identify and evaluate novel chemical scaffolds to seed the drug discovery pipeline for these parasitic diseases to meet the challenges of emerging resistance to available drugs, risks of toxicity and the cost of these treatments. There has been a significant investment in international efforts in the screening of massive small-chemical libraries with several million compounds have been screened in phenotypic assays against malarial parasite, which has resulted in a solid pipeline of novel candidates in clinical and preclinical development (Kaiser *et al.*, 2015; Preston *et al.*, 2016; Burrows *et al.*, 2013). In addition, the Drugs for Neglected Diseases initiative (DNDi) is a patient-needs driven, non-profit drug research and development (R&D) to provide new treatments for neglected diseases, notably leishmaniasis, sleeping sickness (human African trypanosomiasis, HAT) and Chagas' disease (Don and Ioset, 2013).

In addition to massive libraries of synthetic compounds, activity screening also includes natural products, recognizing that they offer a potential source of new antiparasitic therapies. Natural products are derived from a wide array of organisms such as animals, fungi and the higher plants have been shown to contain secondary metabolites with a variety of underexplored chemical entities and pharmacological activities (Yamthe *et al.*, 2017; Zulfiqar *et al.*, 2017). Generally, natural products are more complex, when compared to

synthetic molecules with the structures of natural products having greater numbers of carbon, oxygen and hydrogen atoms, as well as a generally high polarity and molecular weight. Recent efforts to elucidate the chemical structure and biological function of the active chemical structure within anti-parasitic natural product extracts have detected molecules with the potential to treat some Neglected Tropical Diseases (Cheuka *et al.*, 2016). For instance, recently, the antiparasitic activity of alkamide (deca-2E,4E-dienoic acid 2-phenylethylamide isolated from *Anacyclus pyrethrum* roots) has been tested against *L. donovani*, *T. b. rhodesiense*, *T. cruzi* and *P. falciparum* with EC₅₀ of between 3 to 5 µg/ml across these diverse species (Althaus *et al.*, 2017). Moreover, the anti-kinetoplastid activity of 472 natural products based library has been screened against *L. donovani* DD8, *T. b. brucei* and *T. cruzi*, and identified several compounds with novel activities (Zulfiqar *et al.*, 2017). The utility of natural products as drugs is well established, and it has been estimated that approximately 50% of current registered drugs are derived from natural products or developed on the basis of natural compounds; such as camptothecin, lovastatin, maytansine, paclitaxel, reserpine and silibinin (Harvey *et al.*, 2015; Pérez-Moreno *et al.* 2016; Ruiz-Torres *et al.*, 2017). This is also perhaps best exemplified in malaria treatment, with artemisinin and quinine both good examples of drugs developed from a natural product (Ginsburg and Deharo, 2011). There are large numbers of studies that report phenotypic screens of antiparasitic activity from plant extracts chosen on the basis of ethnopharmacology reviews of the use of traditional medicines (Simoben *et al.*, 2018; Zulfiqar *et al.*, 2017; Pérez-Moreno *et al.*, 2016; Harvey *et al.*, 2015; Ibrahim *et al.*, 2014). Although from this starting point, unless there is ethnopharmacological evidence of the use of a traditional medicine for the treatment of a parasitic disease (or the symptoms of that disease, e.g. fever), many other natural products produced by plants, marine invertebrates and fungi etc will not have been evaluated for their antiparasitic activity (Yang *et al.*, 2011;

Davis *et al.*, 2011; Choomuenwai *et al.*, 2015). Going some way to address this issue has been the creation of natural product libraries – a means to exploit the success of high throughput screening of synthetic compound libraries. A library of 96 compounds and 120 extracts from traditional Chinese medicines have been screened against *P. falciparum* (Nonaka *et al.*, 2018), with the identification of new antiplasmodial activity in two medicinal plants. In Spain, a natural product extract collection (MEDINA) comprising 130000 extracts from soil bacteria and fungi has been prepared and a subset of 20000 extracts screened against *P. falciparum* resulting in the discovery of three new antiplasmodial compounds, albeit with moderate μM activities (Pérez-Moreno *et al.*, 2016). Using the same MEDINA library, a second study screened a second subset of 5976 against the kinetoplastids *T. cruzi*, *L. donovani* and *T. brucei brucei*, with 48 fractions selected for follow up studies (Annang *et al.*, 2014). The Davis open access natural product-based library contains 472 compounds, the majority of which are natural products that have been obtained from a diverse range of Australian natural sources. A similar kinetoplast screen to that described above for the MEDINA library, identified a single compound, lissoclinotoxin E, with low μM activity against all three parasites, although this compound showed low selectivity against *T. brucei brucei*. Whilst these natural product screens have yet to provide a lead for development, they do illustrate well how natural product libraries can facilitate a more efficient throughput in screening multiple parasites – a process that may lead to a scaffold that could be amenable to medicinal chemistry.

In this chapter, I report a similar multiple parasite screen of a proprietary library of purified natural products, the Phytopure library. PhytoQuest, a UK small to medium enterprise SME, has produced a library of approximately 1000 *Molecules*, isolated predominantly from temperate zone plants, this resource developed from work of the founder Professor Nash at the Royal Botanical Gardens and Institute of Grasslands and Environment

(<http://www.phytoquest.co.uk/>). As such, the source plants are unlikely to be known in any literature of traditional medicines for parasitic tropical diseases given they are from temperate zone plants. The library encompasses a wide range of chemical classes, two thirds of which are novel, and the remaining third not commercially available. Critically, the library consists of isolated compounds, overcoming common issues with screening fractions of complex mixes where the active moiety is unknown and may be acting in synergy/antagonism with other unknown compounds. This library therefore represents a unique resource for lead discovery of high value chemicals from temperate zone plants against antimicrobial pathogens.

In this regard, 643 compounds within Phytopure library have been selected and provided to Keele University as part of a BBSRC High Value Chemicals from Plants initiative for screening against human parasitic diseases. These compounds have also been selected on the basis of their development potential: they have a high degree of functionality and physiochemical properties that meet Lipinski's rules-of-five. The activity of these compounds were screened against intraerythrocytic *Plasmodium falciparum*, the blood-stream form of *Trypanosoma brucei brucei* and axenic *Leishmania mexicana*. The key aims of this work were to;

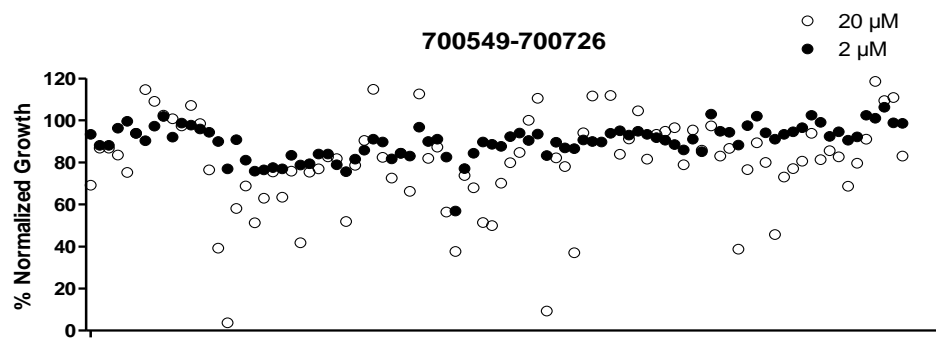
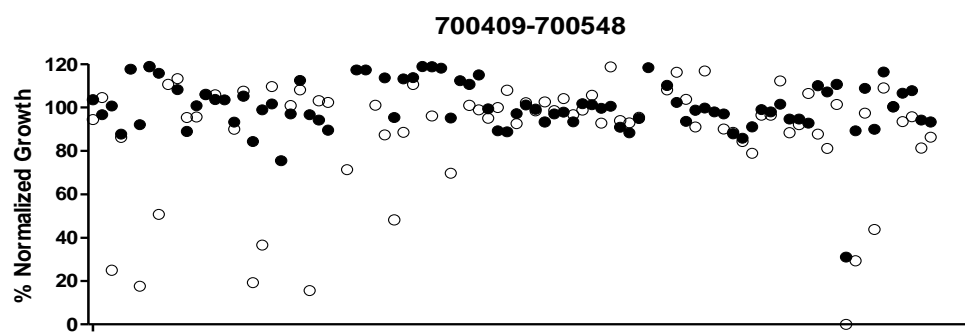
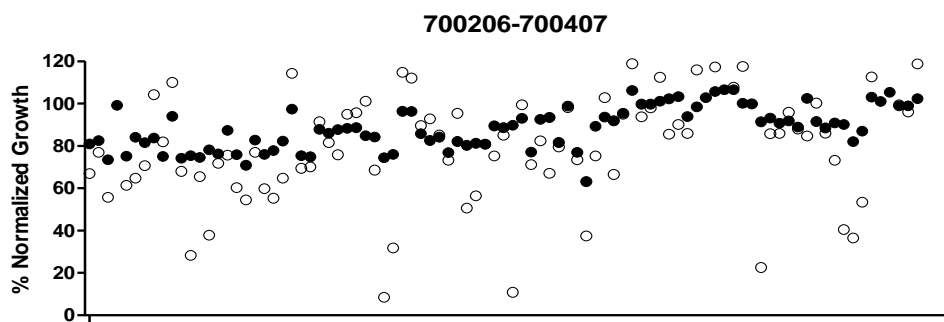
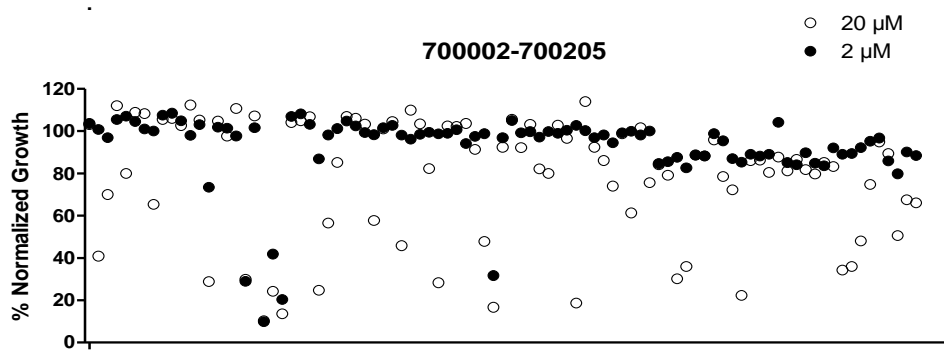
1. Screen and compare the growth inhibitory activity of the Phytopure library compounds against *P. falciparum*, *T. brucei* and *L. mexicana*.
2. Identify priorities for determination of their EC₅₀
3. Provide initial toxicity data by determination of the compounds selectivity when compared to HepG2 cell lines, and the THP-1 cell line where appropriate.

3.2 Results

3.2.1 Antiplasmodial activity

3.2.1.1 Initial screening of intraerythrocytic *P. falciparum*

The Phytopure library of 633 compounds was provided under a Materials Transfer Agreement with Phytopure, Ltd. Antiplasmodial activity for these compounds was determined against the intraerythrocytic trophozoite stages of *P. falciparum* (Dd2 clone) over 48 hours. Compounds were screened at two concentrations, 20 μM and 2 μM , in duplicates with 2 biological replicates (n=4 were performed). The inhibitory effect of each compound was assessed using Malaria SYBR-green fluorescence assay (MSF) with untreated wells serving as a 100% growth control and wells treated with 10 μM chloroquine as the 0% growth control. Table appendix 1 report the mean relative growth data for each compound in the library. A series of dot plot graphs reporting the mean of the normalized growth for each compound at both 20 μM and 2 μM is shown in Figure 3.1.



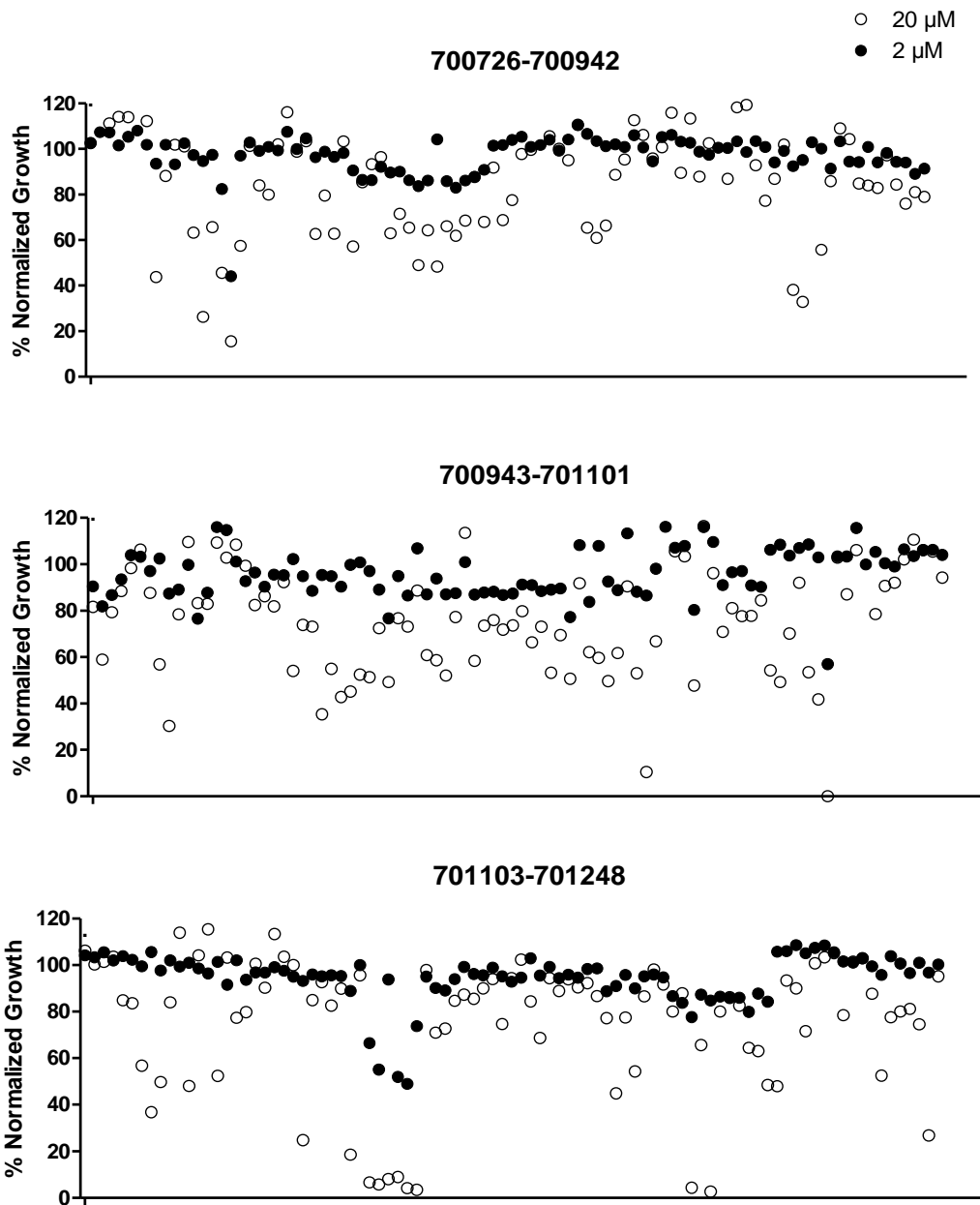


Figure 3.1: Screening the Phytopure library against *P. falciparum*. Dot plot graphs reporting the mean % normalized growth (n=4) obtained from intraerythrocytic trophozoite stages of *P. falciparum* exposed to 20 μM (open circle) and 2 μM (filled circle) of compounds over 48 hours. The range of compound ID reported on each dot plot is above of each chart (note that no detail on actual compound ID shown on x-axis, this is provided in table appendix 1).

A total of 70 compounds were identified with mean normalized growth of $< 50\%$ at a concentration of $20\ \mu\text{M}$, giving a hit rate of 11% . The mean normalized growth at $20\ \mu\text{M}$ and $2\ \mu\text{M}$ for these 70 compounds were plotted against each other (Figure 3.2). This graph allows us to identify compounds in the lower left quadrant as priorities for EC_{50} determination, with a total of 14 compounds (shown in red, all with 50% or less normalized growth at $2\ \mu\text{M}$) selected to determine their EC_{50} value using Dd2 *P. falciparum* trophozoite stages.

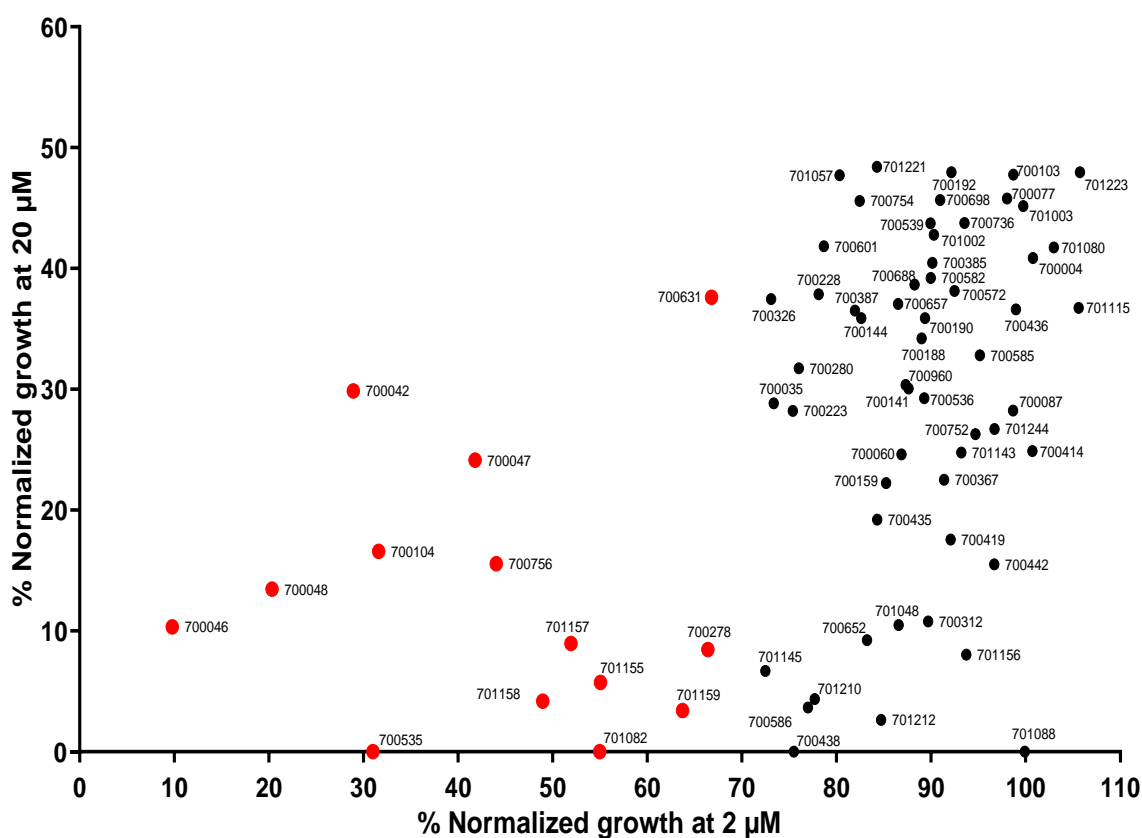


Figure 3.2: Prioritizing compounds for EC_{50} determination in *P. falciparum*. The scatter plot compares the % normalized growth following exposure to $20\ \mu\text{M}$ or $2\ \mu\text{M}$ for 70 Phytopure library compounds (see ID starting 70xxxx). Fourteen compounds (shown in red) were selected for EC_{50} determination.

The EC₅₀ values for these 14 compounds were less than 6 μM after the first biological repeat (Figure 3.3). Of these, 12 were available to take forward for two additional biological replicates to determine their EC₅₀. Compounds 700047 and 700756 were excluded at this point due to lack of material for further analysis. Table 3.1 reports the EC₅₀ values (and their 95% confidence intervals where three biological repeats are available) determined from these log concentration normalized response curves.

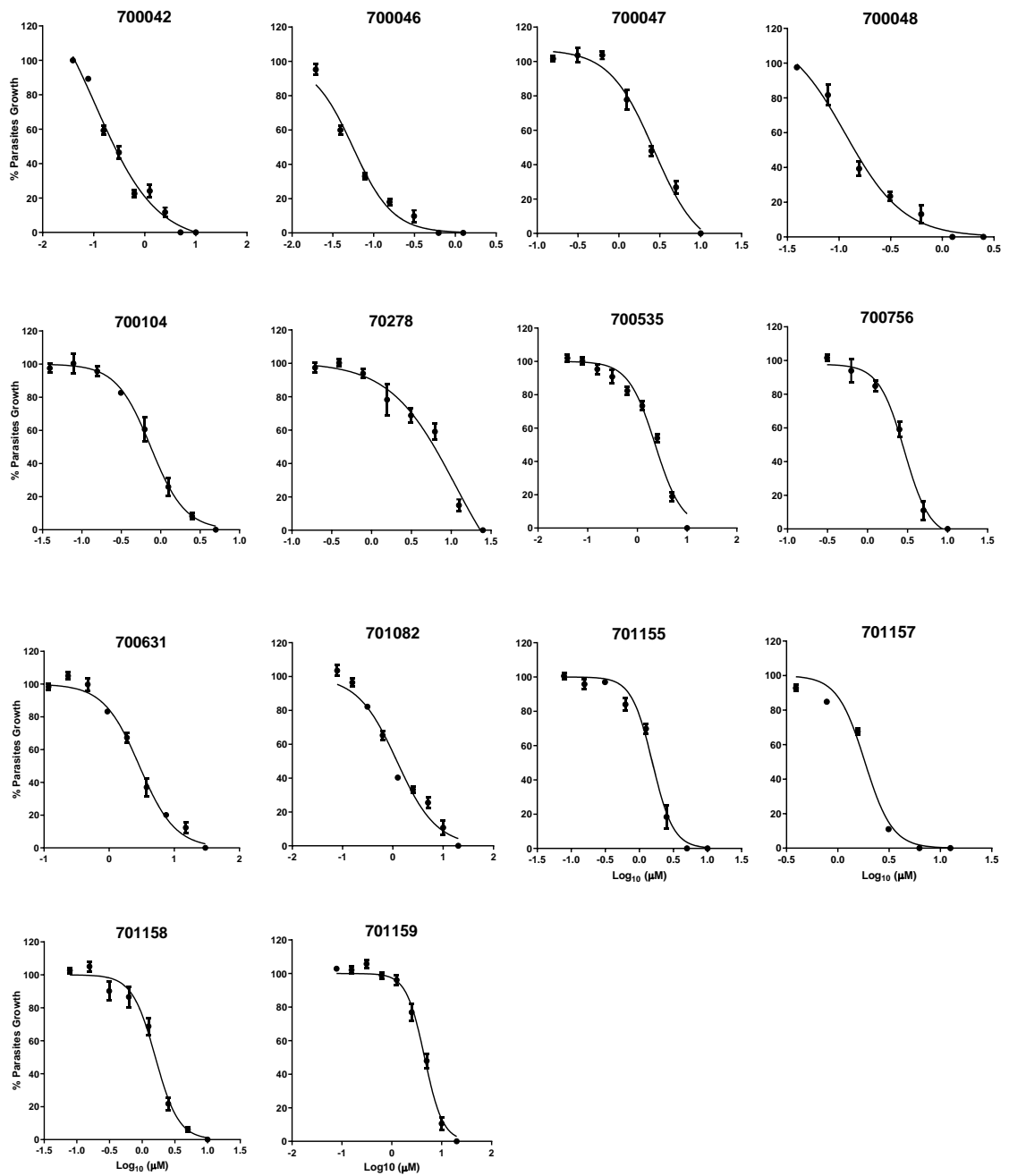


Figure 3.3: Log concentration normalized response curves for 30 Phytopure compounds used to estimate EC_{50} values in intraerythrocytic *P. falciparum*. (A) Reports compounds with EC_{50} determined $< 6\mu\text{M}$. The data show a mean \pm StDev of $n=9$ measurements.

Table 3.1: EC₅₀ data of 14 Phytopure compounds obtained from intraerythrocytic *P. falciparum* with an EC₅₀ of <6μM determined from three independent biological repeats (highlighted in green). The 95% confidence intervals (95% CI) are reported for the the EC₅₀ of these 12 compounds.

Compounds ID	EC ₅₀ (μM)	
	Mean	(95% CI)
70042	0.29	0.26-0.32
70046	0.055	0.054-0.056
70047	2.69	nd
70048	0.14	0.135-0.157
70104	0.74	0.74-0.79
70278	5.51	5.11-7.32
70535	2.28	1.81-2.58
70631	2.94	2.81-3.4
71082	1.2	1.11-1.42
7100756	2.88	nd
71155	1.56	1.49-1.73
71157	1.83	1.71-2.03
71158	1.59	1.43-1.91
71159	4.56	4.15-4.72

3.2.1.2 Confirmation of EC₅₀ determination in a second *P. falciparum* strain (3D7)

The EC₅₀ of the 12 compounds were determined using a 48 hours MSF assay format against a second, genetically distinct, 3D7 strain of *P. falciparum*. This was done to explore the general activity of these compounds against a chloroquine sensitive clone (3D7), compared to the Dd2 clone which is chloroquine resistant. The compounds were exposed using a 2-fold dilution in triplicate with three biological repeats performed. The EC₅₀ values were

determined using a log concentration normalized response curves for each of 12 compounds and are shown in green on Figure 3.4. For comparison, the same data derived against Dd2 is shown on each graph in black. The mean EC₅₀ with 95% CI determined against the *P. falciparum* 3D7 strain are reported in Table 3.2.

The log concentration normalized response curves for 3D7 and Dd2 were very similar for all 12 compounds, suggesting that there is no apparent difference in activity for these 12 compounds in these two strains. A linear regression analysis (Figure 3.5) of the mean EC₅₀ values in Dd2 and 3D7 strains revealed a strong and statistically significant correlation between these values (slope = 0.96, $r^2 = 0.92$ and p value <0.0001). The source species, class of compound and structure of each of these 12 Phytopure compounds is shown in Table 3.3.

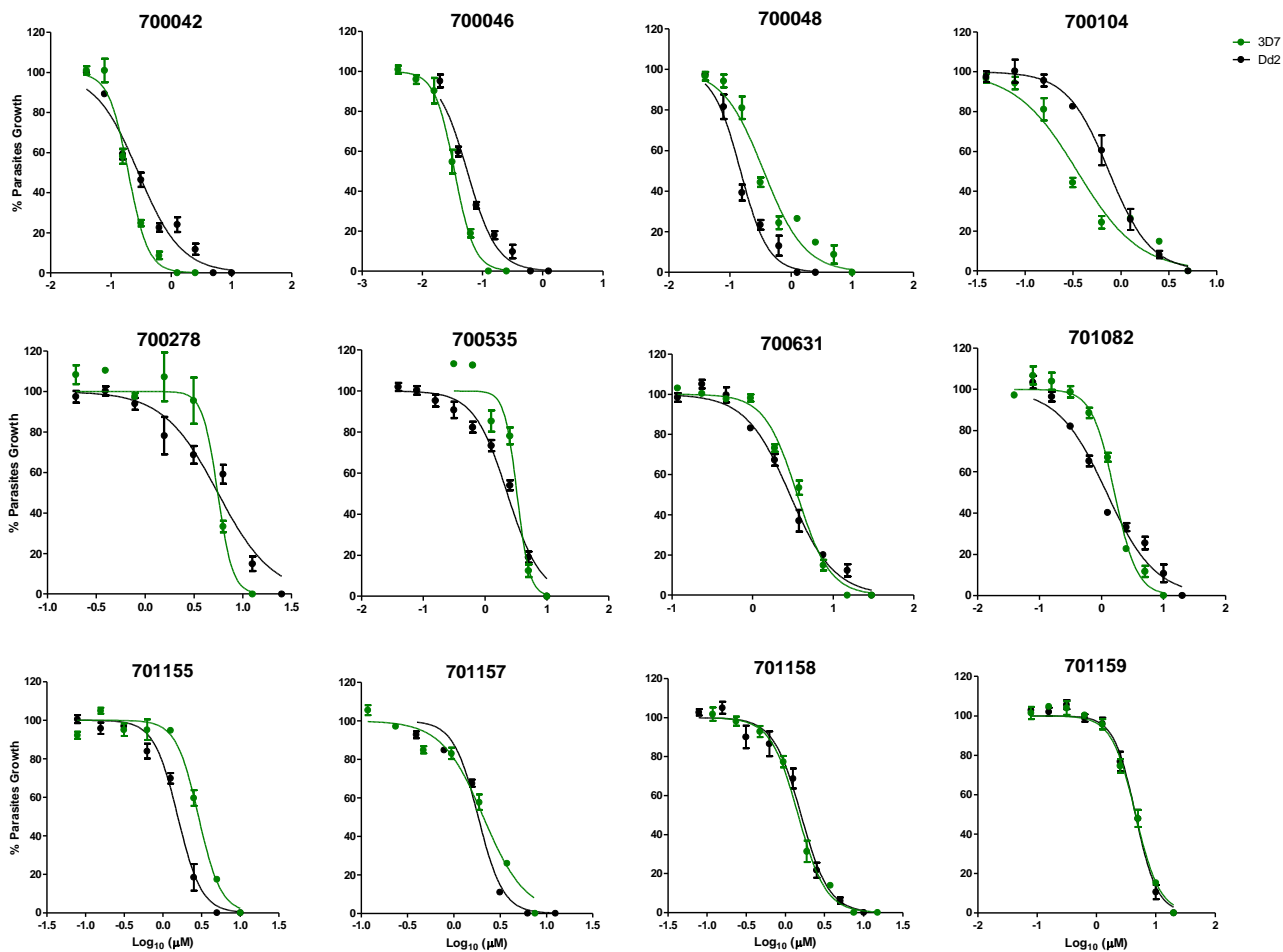


Figure 3.4: Log concentration normalized response curves for 12 Phytopure compounds in two strains of *P. falciparum*. The data show a mean \pm StDev from three biological replicates. Non-linear regression curves in green are for the 3D7 strain and in black for the Dd2 strain. The EC_{50} with 95% CI values are shown in Table 3.2.

Table 3.2: EC₅₀ in Dd2 and 3D7 strains of *P. falciparum* for 12 Phytopure compounds.

Compound ID	EC ₅₀ (μM)	
	Dd2	3D7
	Mean (95% CI)	Mean (95% CI)
700042	0.29 (0.26-0.32)	0.19 (0.18-0.19)
700046	0.055 (0.054-0.056)	0.034 (0.032-0.038)
700048	0.14 (0.135-0.157)	0.35 (0.31-0.4)
700104	0.74 (0.74-0.79)	0.35 (0.33-0.44)
700278	5.53 (5.11-7.32)	5.52 (5.1-6.57)
700535	2.28 (1.81-2.58)	3.27 (3.1-3.4)
700631	2.91 (2.81-3.4)	3.6 (3.26-3.94)
701082	1.2 (1.11-1.42)	1.62 (1.58-1.6)
701155	1.55 (1.49-1.73)	2.9 (2.88-3.12)
701157	1.83 (1.71-2.03)	2.08 (1.89-2.1)
701158	1.59 (1.43-1.91)	1.45 (1.37-1.6)
701159	4.53 (4.15-4.72)	4.56 (3.74-4.8)

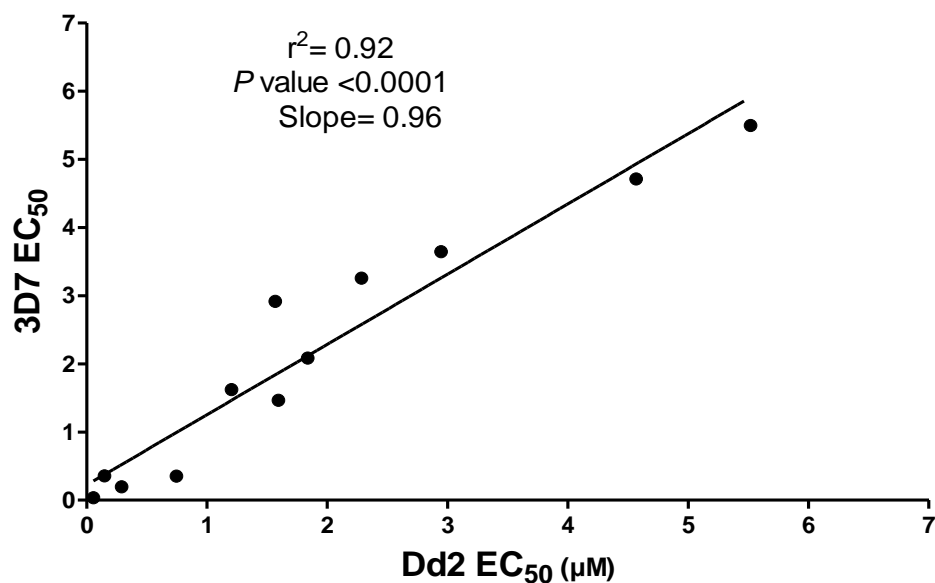


Figure 3.5: Correlation between EC_{50} values determined in two strains of *P. falciparum*. The mean EC_{50} value of 12 Phytopure compounds from 3D7 and Dd2 strains are plotted with the results of a linear regression analysis.

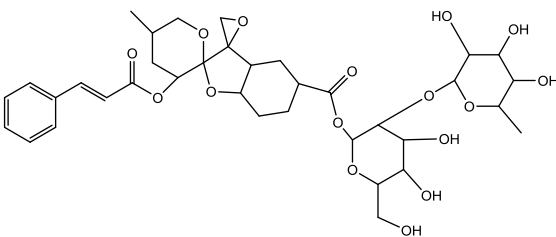
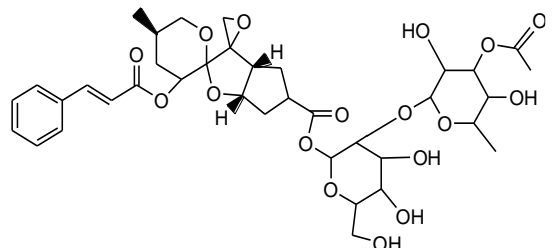
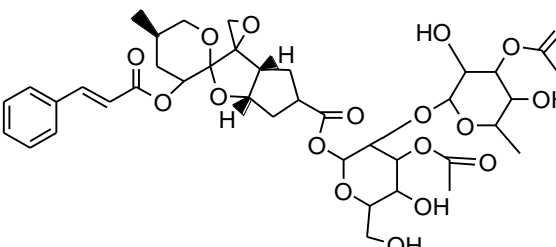
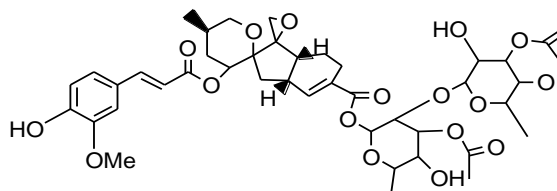
Table 3.3: A, information generated from PhytoQuest for high interest compounds against *P. falciparum*. B, the structure of each compound.

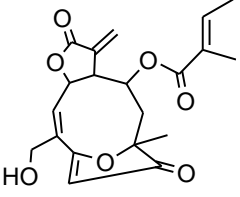
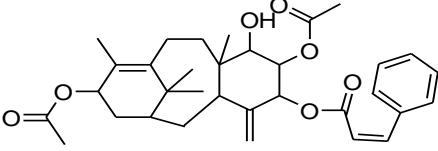
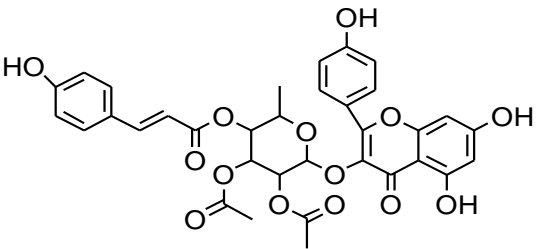
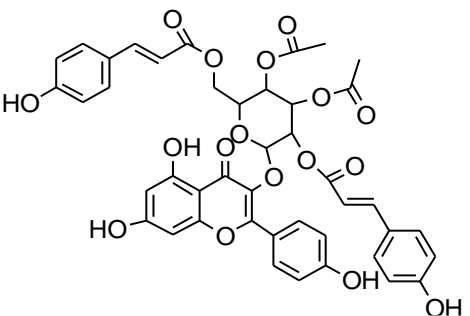
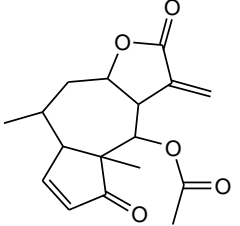
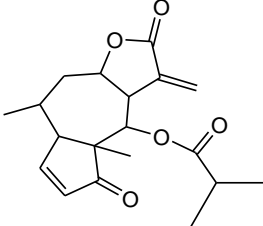
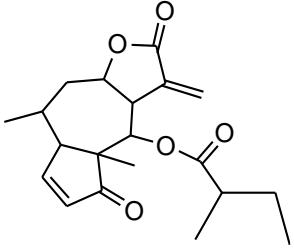
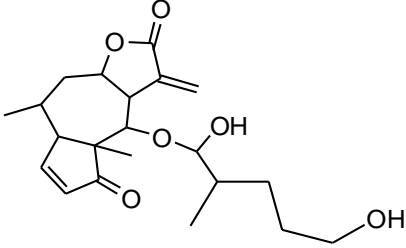
(A)

PQ number	Class	plant common name	Genus	Species	Formula	Mwt
700042	Phyllanthocin		<i>Phyllanthus</i>	<i>accuminatus</i>	C ₃₆ H ₄₈ O ₁₆	736.77
700046	Phyllanthocin		<i>Phyllanthus</i>	<i>accuminatus</i>	C ₃₈ H ₅₀ O ₁₇	778.81
700048	Phyllanthocin		<i>Phyllanthus</i>	<i>accuminatus</i>	C ₄₀ H ₅₂ O ₁₈	820.85
700104	Phyllanthocin		<i>Phyllanthus</i>	<i>accuminatus</i>	C ₄₂ H ₅₄ O ₁₈	846.88
700278	Sesquiterpene	Dwarf sunflower	<i>Helianthus</i>	<i>annuus</i>	C ₂₀ H ₂₂ O ₇	374.39

700535	Taxane	Yew	<i>Taxus</i>	<i>baccata</i>	C33H42O7	550.69
700631	Flavonoid	Bog myrtle	<i>Myrica</i>	<i>gale</i>	C34H30O14	662.61
701082	Flavonoid	Holm oak	<i>Quercus</i>	<i>llex</i>	C43H36O17	824.75
701155	Sesquiterpene	Arnica	<i>Arnica</i>	<i>montana</i>	C17H20O5	304.34
701157	Sesquiterpene	Arnica	<i>Arnica</i>	<i>montana</i>	C19H24O5	332.4
701158	Sesquiterpene	Arnica	<i>Arnica</i>	<i>montana</i>	C20H26O5	346.42
701159	Sesquiterpene	Arnica	<i>Arnica</i>	<i>montana</i>	C21H30O6	378.46

(B)

Structures of compounds	
<p>700042</p> 	<p>700046</p> 
<p>700048</p> 	<p>700104</p> 
<p>700278</p>	<p>700535</p>

	
<p>700631</p> 	<p>701082</p> 
<p>701155</p> 	<p>701157</p> 
<p>701158</p> 	<p>701159</p> 

3.2.1.3 Determination of estimated 50% lethal dose (LD₅₀) in Dd2^{luc} using bioluminescence assay

The EC₅₀ of a drug represents its inhibitory effect on growth, a process that combines both the cytotoxic and cytostatic effect of the drug. Measurement of the cytotoxic effect of the drug alone requires the determination of the 50% lethal dose, LD₅₀, which is estimated here using a bioluminescence-based assay of concentration-response adapted from the protocol originally described by Paguio *et al.* (2011). The Paguio assay utilizes a 6 hours drug bolus, washing off the drug and regrowth of the surviving parasites in the absence of drug for 48 hours to determine the LD₅₀ using a MSF assay. However, a bioluminescence assay to estimate LD₅₀ was refined by Imran Ullah from the Horrocks laboratory (Ullah *et al.*, 2017). This assay provides the ability to determine the LD₅₀ immediately after the 6 hours of drug exposure as the intrinsic instability of the luciferase reporter protein, compared to the stability of DNA measured in a MSF assay, allows both concentration and time dependent effects on the luciferase signal to be monitored robustly (Ullah *et al.*, 2017).

The 12 selected compounds were exposed to a serial 2-fold dilution of compounds and the bioluminescent signal as a proportion of the untreated control (100%) determined. Experiments were carried out as technical triplicates with three biological repeats carried out. The mean (n=9) and StDev for each concentration are used to plot a log concentration normalized response curve with a non-linear regression providing the LD₅₀ value (and 95% CI). Figure 3.6 reports the data used to determine the LD₅₀ value (open circles and dotted lines) with the EC₅₀ determined using the 48 hours MSF assay plotted for comparison (filled circles and full line). The mean LD₅₀ with 95% CI for *P. falciparum* Dd2 strain for these 12 compounds are reported in Table 3.4 along with the same data previously reported for benchmark antimalarials (Ullah *et al.*, 2017).

The majority of the 12 Phytopure compounds show a right shift of the LD₅₀ curves when compared against the EC₅₀ curves – this is expected as it represents the higher concentration of compound required to kill over the 6 hours window of the shorter LD₅₀ assay. In Ullah *et al.* (2017) it was shown that antimalarial compounds with a rapid initial rate of kill, such as artemisinin, have a LD₅₀/EC₅₀ ratio of close to 1 (see Table 3.4). As we move through compounds in terms of their initial rate of kill, chloroquine is faster than quinine which is faster than atovaquone, the LD₅₀/EC₅₀ ratio increases. The LD₅₀/EC₅₀ ratios reported for all 12 Phytopure compounds indicate that they all exert an initial cytotoxic effect (0.75 to 3.12), and likely they have an initial rate of kill that falls between those of chloroquine and artemisinins (1.12 to 5.24). Interestingly, three Phytopure compounds, 701082, 700631 and 700104, share a LD₅₀/EC₅₀ ratio similar to that of dihydroartemisinin, suggesting they exert an extremely rapid cytotoxic action. Given this apparent rapid cytotoxic action, these compounds were selected for an evaluation of their initial rate of kill.

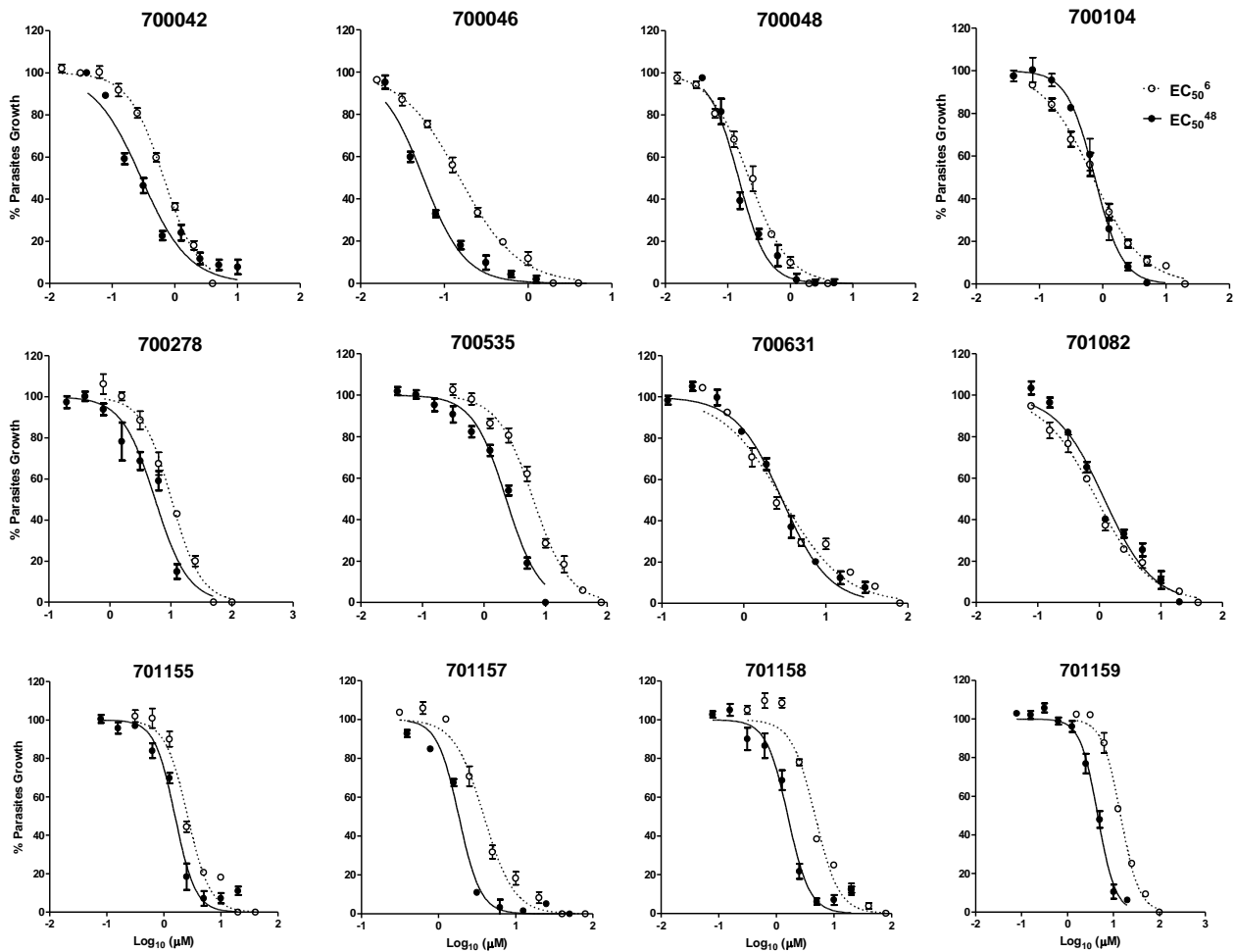


Figure 3.6: Log concentration normalized response curves comparing LD₅₀ and EC₅₀ values determined for 12 Phytopure compounds. The normalised 6 hour bioluminescence response is used to determine the LD₅₀ (open circles and dotted lines) with the normalized 48 hours fluorescence curves being used to determine the EC₅₀ (filled circles and full line). The data shown is a mean ± StDev from three independent biological replicates (n=9).

Table 3.4: Estimates of EC₅₀ and LD₅₀ of 12 Phytopure compounds in the Dd2 strain of *P. falciparum*. The data shown for benchmark antimalarial drugs chloroquine (CQ), quinine (QN), atovaquone (ATQ) and dihydroartemisinin (DHA) were obtained from Ullah *et al.* (2017).

Compounds ID	EC ₅₀ (μM) ^{48hr}	LD ₅₀ (μM) ^{6hr}	LD ₅₀ /EC ₅₀ ratio
	Dd2 ^{LUC}	Dd2 ^{LUC}	
	Mean	Mean(95% CI)	
700042	0.29	0.69 (0.67-0.71)	2.37
700046	0.055	0.15 (0.10-0.16)	2.72
700048	0.14	0.22 (0.19-0.26)	1.57
700104	0.74	0.71 (0.52-0.71)	0.95
700278	5.53	10.28 (9.53-11.9)	1.85
700535	2.28	6.30 (5.70-6.40)	2.76
700631	2.91	2.99 (2.46-2.60)	1.02
701082	1.2	0.90 (0.77-0.93)	0.75
701155	1.55	2.63 (2.39-2.69)	1.69
701157	1.83	3.89 (2.87-0.39)	2.12
701158	1.59	4.75 (3.65-0.48)	2.98
701159	4.53	14.3 (12.97-15.14)	3.12
CQ	0.2	1.091	5.24
QN	0.24	1.861	7.75
ATQ	0.0026	nd	
DHA	0.0041	0.00461	1.12

3.2.1.4 *In vitro* determination of Bioluminescence Relative Rate of Kill (BRRoK)

An estimate of the Rate of Kill (RoK) for a potential antimalarial compound provides important information for its priority for development. There is an urgent demand to identify novel compounds that kill the intraerythrocytic parasite at least as fast as chloroquine (Ullah *et al.*, 2016), noting the LD₅₀/EC₅₀ ratios for the compounds above are within the range for these drugs (Table 3.4). As previously shown, the killing rates for different antimalarial drugs was measured *in vitro* by Sanz *et al.*, (2012) based on the re-growth of drug-treated parasites using a fluorescence-based assay. Here, parasite growth is monitored after 3-4 weeks and poses a significant limitation on its feasibility to routinely assess the rate of kill for a large number of different compounds. Our laboratory developed a Bioluminescence Relative Rate of Kill (BRRoK) assay that can be used from as soon as three hours of compound exposure up to 48 hours (Ullah *et al.*, 2017). The principle of RoK assay depends on the dynamic response of the luciferase enzyme ($t_{1/2}$ of 1-2 hours). Following drug treatment, a time and concentration-dependent loss of bioluminescence is measured – importantly, this data then compared to the same data developed for a number of benchmark antimalarial drugs where the *in vivo* and *in vitro* rate of kill is known. In this way, the initial rate of kill for a compound can be compared to these benchmarks and a relative assessment of their rate of kill established ie as fast as artemisinin, slower than chloroquine etc.

The BRRoK activity of compounds were determined against Dd2^{luc} parasites using a three-fold serial dilution of compounds added at 0.33, 1, 3 and 9 xEC₅₀ (Ullah *et al.*, 2017). The normalized bioluminescent signal, compared to an untreated control, was measured after 3, 6 and 48 hours to ensure the completion of one full intraerythrocytic cycle (Figure 3.7). The BRRoK assay was performed as three technical repeats in three independent biological

repeats (n=9). At each concentration, the mean and StDev of the n=9 bioluminescent signal data are determined and plotted.

The time-and concentration-dependent on loss of bioluminescence signal for the 12 Phytopure compounds were compared against the same data from a range of benchmark antimalarial drugs (Ullah *et al.*, 2017). These were; dihydroartemisinin (DHA, very rapid initial rate of kill), chloroquine (CQ, rapid initial rate of kill), quinine (QN, moderate initial rate of kill) and atovaquone (ATQ, slow initial rate of kill) (Figure 3.7 B). The majority of the 12 Phytopure compounds reveal to have a rapid initial cytotoxic affect, with the curves for the three different timepoints appearing to be more similar to DHA and CQ than for QN and ATQ. At this point, these data appear to agree with the initial cytotoxic activity estimated from the LD₅₀/EC₅₀ ratios previously determined.

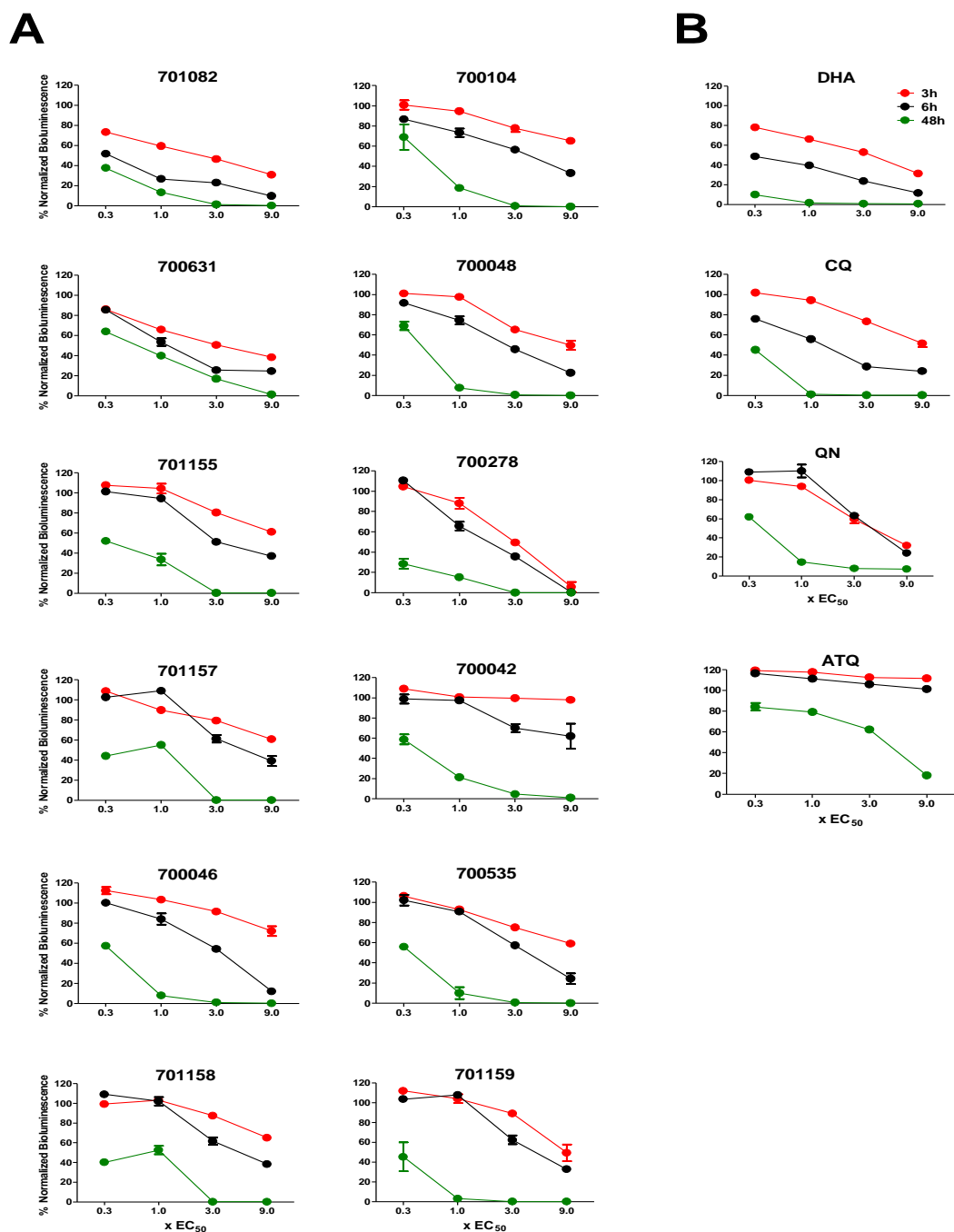


Figure 3.7: BRRoK assays for 12 Phytopure compounds. Each curves represent the concentration-dependant killing effects for (A) the indicated Phytopure compounds or (B) a benchmark antimalarials. The BRRoK was measured after 3 hours (red line), 6 hours (black line) and 48 hours (green line) with the mean and StDev (n=9) of normalised bioluminescence signal reported. The

Phytopure compound data are plotted (top to bottom, predicted fastest to slowest) according to the ratio of LD₅₀/EC₅₀ from Table 3.4.

In the Ullah *et al.* (2017) study, the relative ordering of compounds from the MMV Malaria Box was possible following a principle component analysis of the available data for 400 compounds. This study only has data for 12 compounds, and these data are relatively similar to each other. To see if some ranking order could be determined, the mean bioluminescent signal obtained following exposure at each concentration of compound at 6 hours were plotted against each other (Figure 3.8). In this way, the data for each compound can be compared against the four benchmark drugs (shown in red) when comparing all combinations of compound concentrations used, and also being able to draw on the 6 hour analysis presented in Ullah *et al.* (2017). Linear regression of the 16 data points (12 compounds and four benchmark antimalarials) reveal that, as expected, the strongest and most significant correlations ($r^2 > 0.7$ and $p < 0.001$) exist when concentrations immediately adjacent to each other are compared; i.e. 9X ν 3X EC₅₀, 3X ν 1X EC₅₀ and 1X ν 0.33X EC₅₀. Taking these three panels with strong and significant correlations, the six compounds that would be ranked the fastest acting based on their LD₅₀/EC₅₀ ratio; 701082, 700631, 700104, 700631, 700048 and 701155 (shown in green) all consistently group together with the DHA and CQ benchmarks in these analyses. Further support is provided by the data for compound 7001082, this compound has the lowest LD₅₀/EC₅₀ ratio of 0.75 and is located immediately adjacent to DHA on all comparisons, irrespective of the strength of the regression analysis reported (Figure 3.8).

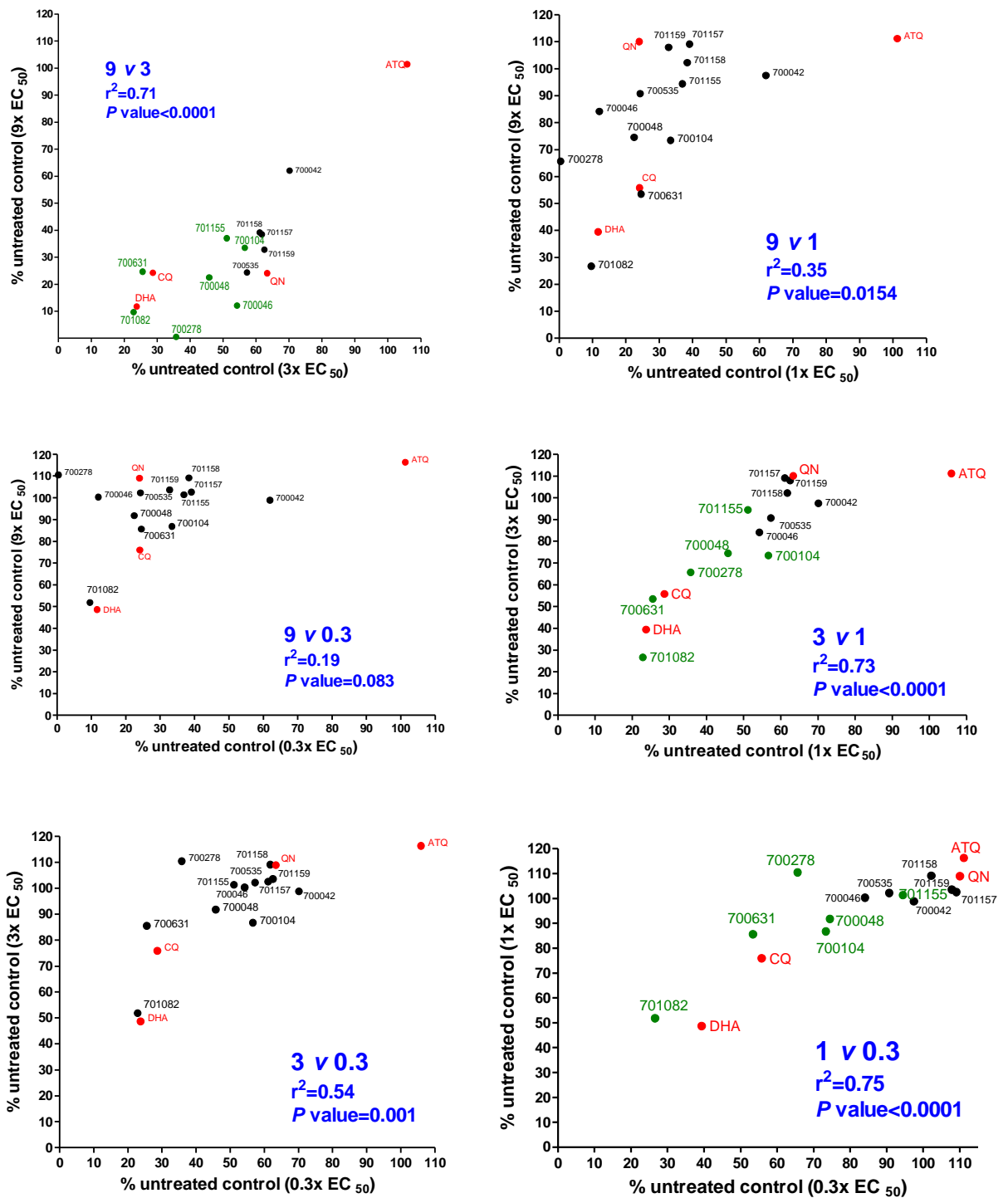


Figure 3.8: Correlation of BRRoK assay data to determine the relative rates of kill for the 12 Phytopure compounds. Each chart relates the indicated correlation between 9x, 3x, 1x and 0.3x EC₅₀ data at 6hours (e.g. top left compares 9X v. 3X EC₅₀ data). The filled red circles represent benchmark antimalarial drugs, green circles represent the six Phytopure compounds with LD₅₀/EC₅₀

ratio < 2, black circles represent the six Phytopure compounds with LD₅₀/EC₅₀ ratio > 2. Note all *p* values and *r*² for a linear regression of the 16 data points are reported on each graph.

3.2.1.5 *In vitro* determination of cytotoxic effects against the human HepG2 cell line

Understanding at an early stage the potential toxic liabilities of a candidate is important. The antiproliferative effect of the 12 Phytopure compounds on a human hepatoma cell line (HepG2) was assessed using the Alamar Blue viability assay. The mechanism of the assay depends on viable HepG2 cells producing NADPH, NADH and FADH which can reduce resazurin (a non-fluorescent indicator blue dye) to resorufin (a pink fluorescent molecule) in live cells via mitochondrial enzymes (Rampersad, 2012). HepG2 cells were exposed for 48 hours to a serial 2-fold dilution of the Phytopure compounds in technical triplicate, with three independent biological repeats (n=9) for 48 hours. The fluorescence signal was normalized against an untreated control (100% growth) and the mean ± StDev of relative growth plotted (Fig. 3.9) as a green line. For comparison on the same graphs, the EC₅₀ antiplasmodial data against Dd2 is also plotted. The 50% cytotoxic concentration (CC₅₀) was estimated using a log concentration normalized response curves for each compound and are reported with their 95% CI in Table 3.5. The selective index (SI) of the 12 Phytopure compounds when comparing activity against the *P. falciparum* Dd2 and 3D7 strains compared to HepG2 was calculated based on CC₅₀/EC₅₀ ratios as described by Be'zivin *et al.* (2003) (Table 3.5).

Of the 12 compounds tested, almost all appear to have low μM CC₅₀ activity in HepG2, with compound 700535 apparently the least toxic with a CC₅₀ of 52.1 μM. In general, there appears to be minimal selectivity for these compounds when comparing their antiproliferative activity against *P. falciparum* and HepG2, a feature apparent from the relative closeness of the curves in Figure 3.9. The highest selectivity (SI between 36 to 59)

is shown by compound 700046, although the compound is actually reasonably toxic against HepG2 at relatively low concentrations (CC₅₀ of 2µM). The next most selective compound is 700535 (SI between 16 to 23), a limitation here is that this compound is only moderately active against *P. falciparum* (EC₅₀ of 2 to 3 µM). For comparison, the same data for the benchmark antimalarial drugs tested here are included using data developed in other studies (Lelièvre *et al.*, 2012) are reported on the same table 3.5.

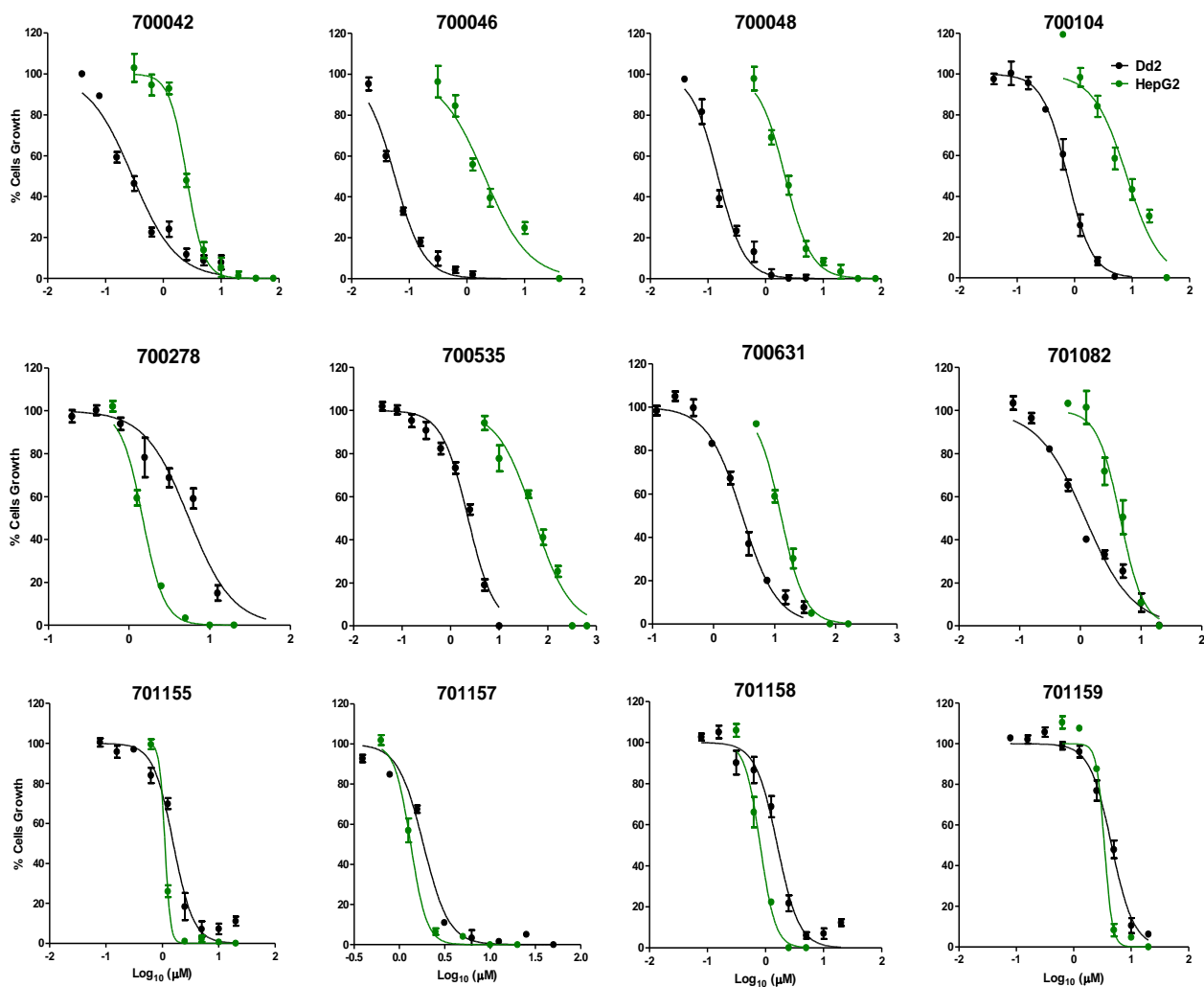


Figure 3.9: Initial determination of cytotoxicity of the 12 Phytopure compounds against HepG2 cells. Log concentration normalized growth curves were fitted for HepG2 (green lines) and *P. falciparum* (black line) Dd2 strain. The data shown is a mean ($n=9$) \pm StDev from at three independent biological replicates.

Table 3.5: *In vitro* antiplasmodial activity (EC₅₀) and cytotoxicity (CC₅₀) against HepG2 cells for the 12 Phytopure compounds. SI^A, is calculated as CC₅₀/EC₅₀ using Dd2 strain, whilst SI^B is calculated using the 3D7 strain. (Ullah, 2017)¹, (Lelievre *et al.*, 2012)².

Compound ID	EC ₅₀ (μM)		CC ₅₀ (μM)	SI ^A	SI ^B
	Dd2 ^{LUC}	3D7	HepG2		
	Mean	Mean	Mean (95% CI)		
700042	0.29	0.19	2.51 (2.21-2.60)	9	13.2
700046	0.055	0.034	2.01 (1.89-2.32)	36.5	59.1
700048	0.14	0.35	2.16 (1.73-2.26)	15.4	6.2
700104	0.74	0.35	8.00 (7.30-7.90)	10.8	22.9
700278	5.53	5.52	1.47 (1.38-1.39)	0.3	0.3
700535	2.28	3.27	52.1 (68.13-70.37)	22.8	16
700631	2.91	3.6	12.6 (12.51-12.60)	4.3	3.5
701082	1.21	1.62	4.55 (5.61-6.56)	3.8	2.8
701155	1.55	2.9	1.11 (1.07-1.09)	0.7	0.4
701157	1.83	2.08	1.33 (1.26-1.34)	0.7	0.6
701158	1.59	1.45	0.80 (0.70-0.95)	0.5	0.5
701159	4.53	4.56	3.42 (3.36-4.43)	0.8	0.8
CQ	0.2081 ¹	-	51.842	249	-
QN	0.2451 ¹	-	>50 ²	>204	-
ATOVA	0.00261 ¹	-	>40 ²	>15384	-
DHA	0.00411 ¹	-	>50 ²	>12195	-

3.2.2 Antitrypanosomal activity

3.2.2.1 Optimization of the proliferation assay

An initial determination of the initial blood stream form *T. b. brucei* (hereafter *T. brucei*) seeding density in the proposed 96-multiwell screening plate format was made, ensuring that the density initially seeded did not reach a confluence that would affect the rate of cell division within the 48 hours assay period. Blood stream form *T. brucei* were diluted serially from 4.5×10^5 to 0.035×10^5 cells/mL before leaving 48 hours at 37°C in normal growth conditions (n=3 replicates). Following this incubation, the resulting cell numbers were estimated using an Alamar Blue fluorescence assay to determine the activity of viable (still generate reduced cofactors) parasites (Figure 3.10). This analysis indicates that an initial seeding of 1×10^5 cells/mL of *T. brucei* blood stream form provides for the maximum growth of *T. brucei* within 48 hours without growth being affected by saturation effects (Figure 3.10). All subsequent growth inhibition assays assumed this initial seeding density.

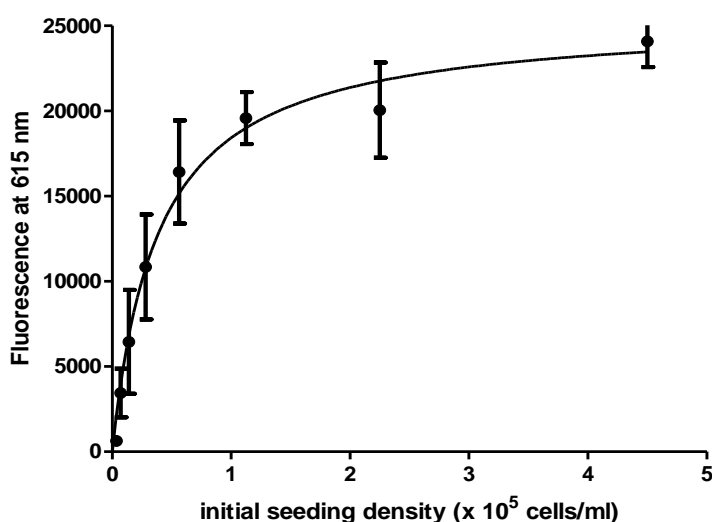


Figure 3.10: Determination of initial blood stream form *T. brucei* seeding density. The graph plots a logarithmic growth regression analysis of a 48 hours Alamar Blue assay (fluorescence at 615nm) versus the initial seeding density to optimize the selection of conditions for a 96-well multiplate growth assay. Data represents the mean \pm StDev of n=3.

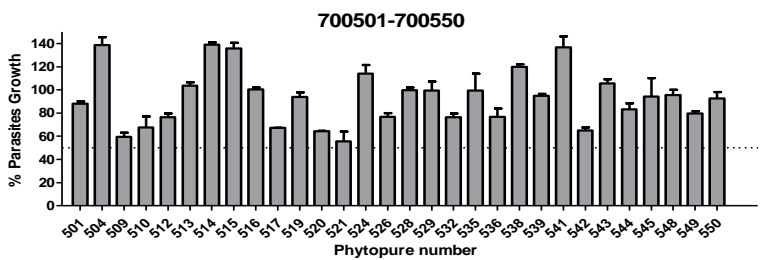
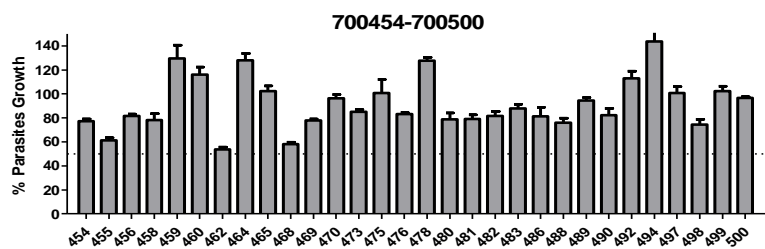
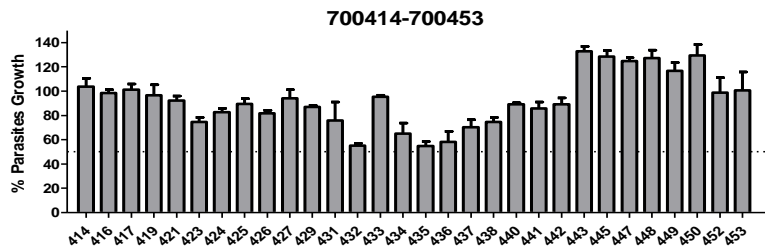
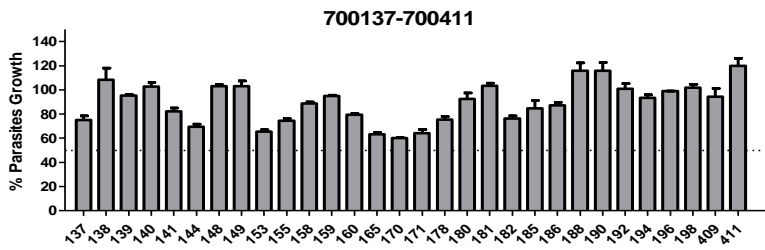
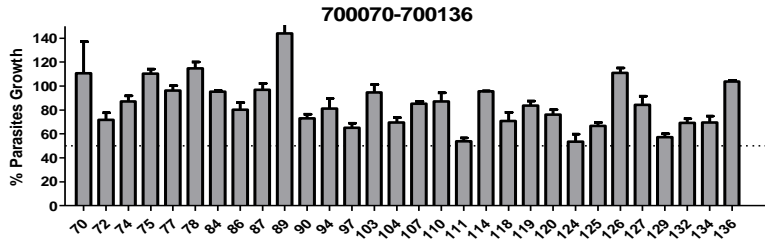
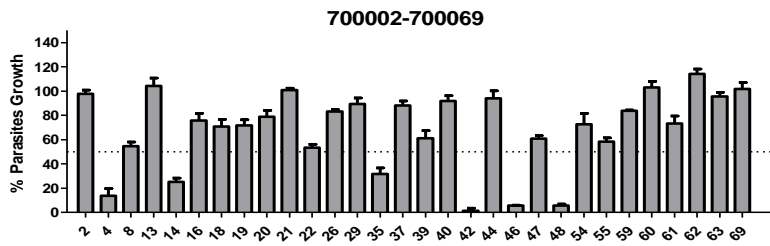
3.2.2.2 Screening of Phytopure library against *T. brucei*

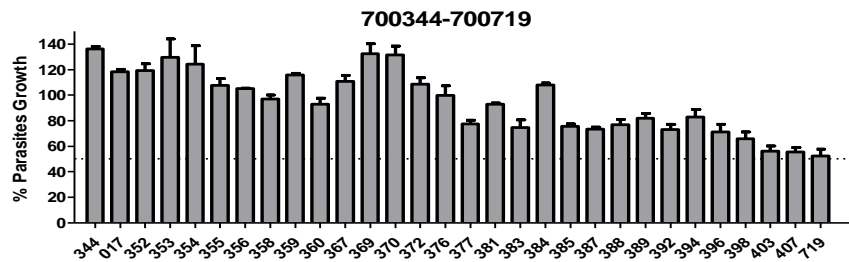
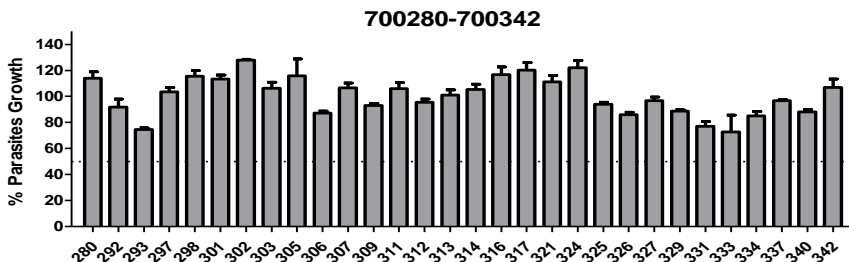
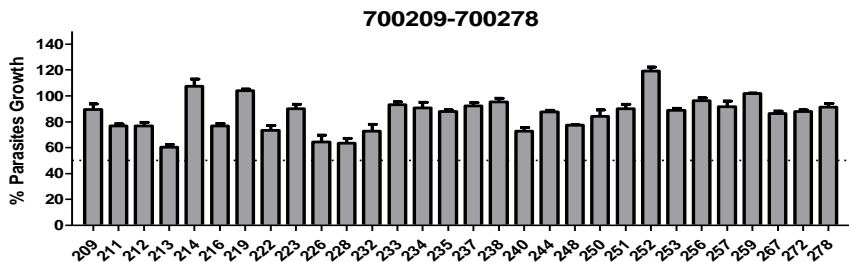
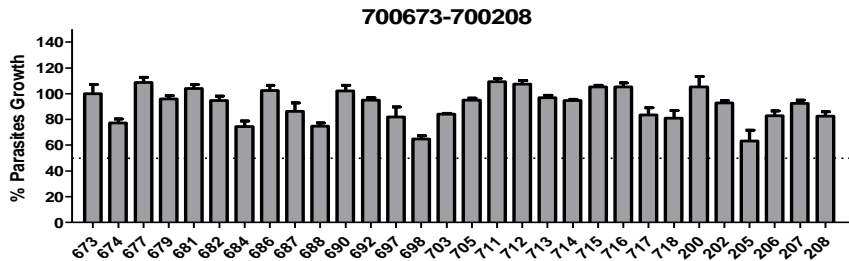
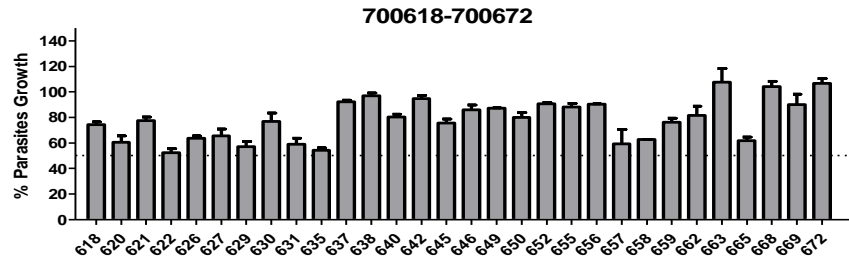
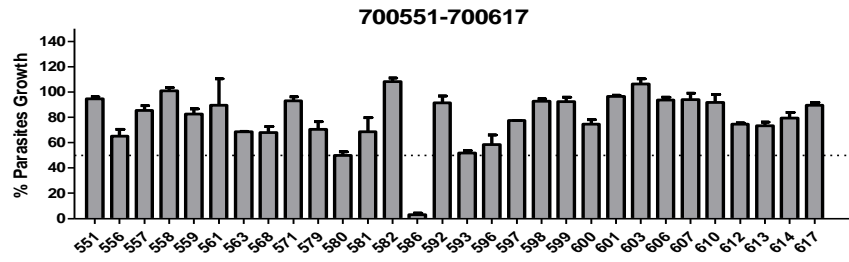
The screening of the 643 Phytopure library compounds was assessed against the strain 427 SMWT *T. brucei* blood stream forms over 48 hours at 37 °C with 5% CO₂. Compounds were tested at a single concentration of 2µM in duplicates with 2 independent biological replicates done (n=4). The inhibitory effect of each compound was assessed using Alamar Blue fluorescence assay and growth normalized against an untreated control. Figure 3.11 presents a series of panels that plots the mean ± StDev of the normalized growth for the compounds indicated above the chart. These data are also provided in Table appendix 1.

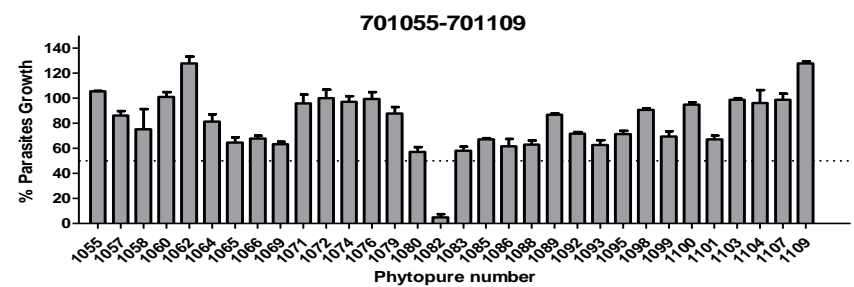
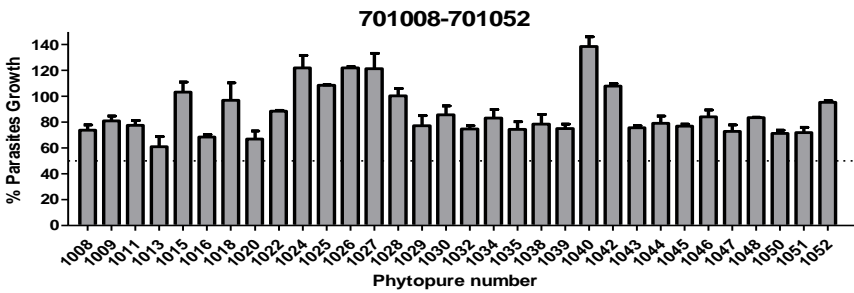
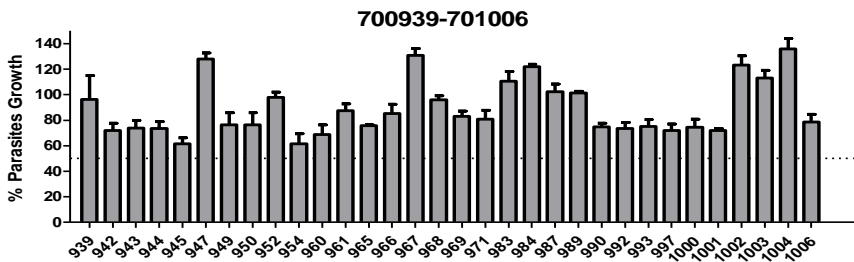
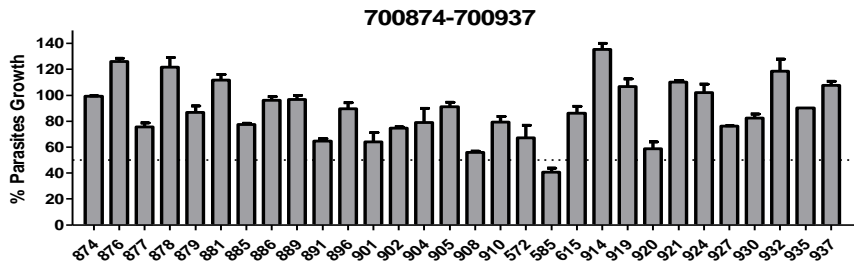
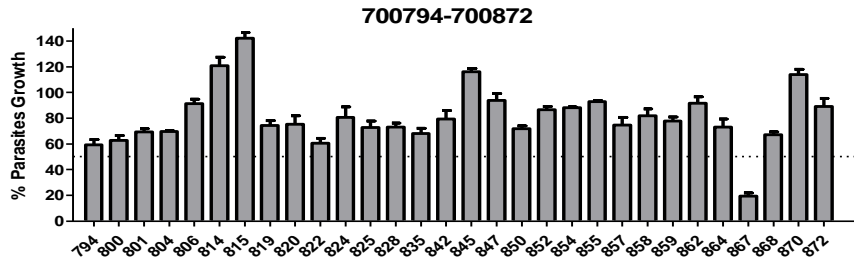
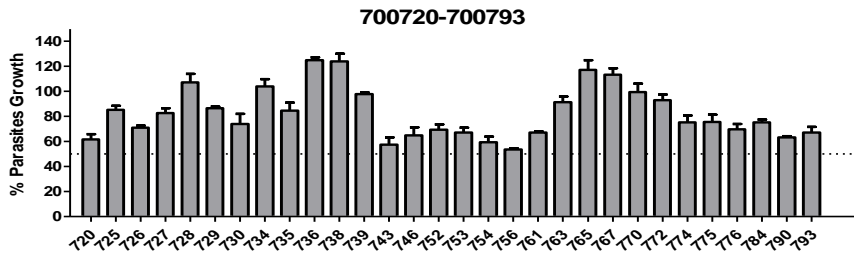
Note that ten additional compounds compared to the *P. falciparum* screen were done here. These ten synthetic compounds were provided by PhytoQuest as they are synthetic derivatives of the *T. brucei* hits 701241 and 701249, two closely related compounds isolated from *Chrysanthemum segetum*.

3.2.2.3 Determination of EC₅₀ values of 25 hits from Phytopure library screen by using Alamar Blue viability assay

Analysis of the initial screen identifies 25 compounds, a hit rate of 3.8%, with a > 50% growth inhibition recorded at 2 µM. All these 25 compounds were taken forward to determine their EC₅₀ in 2-fold dilution series Alamar Blue growth inhibition assays. These assays were carried out for each compound using technical triplicates in three independent biological repeats (n=9). These data were plotted in log concentration normalized response curves (black lines on Figure 3.12) and the EC₅₀ and 95% CI determined from a non-linear regression curve and reported in Table 3.6. These data report good to moderate antiproliferative activities ranging between 0.16 to 2.71 µM.







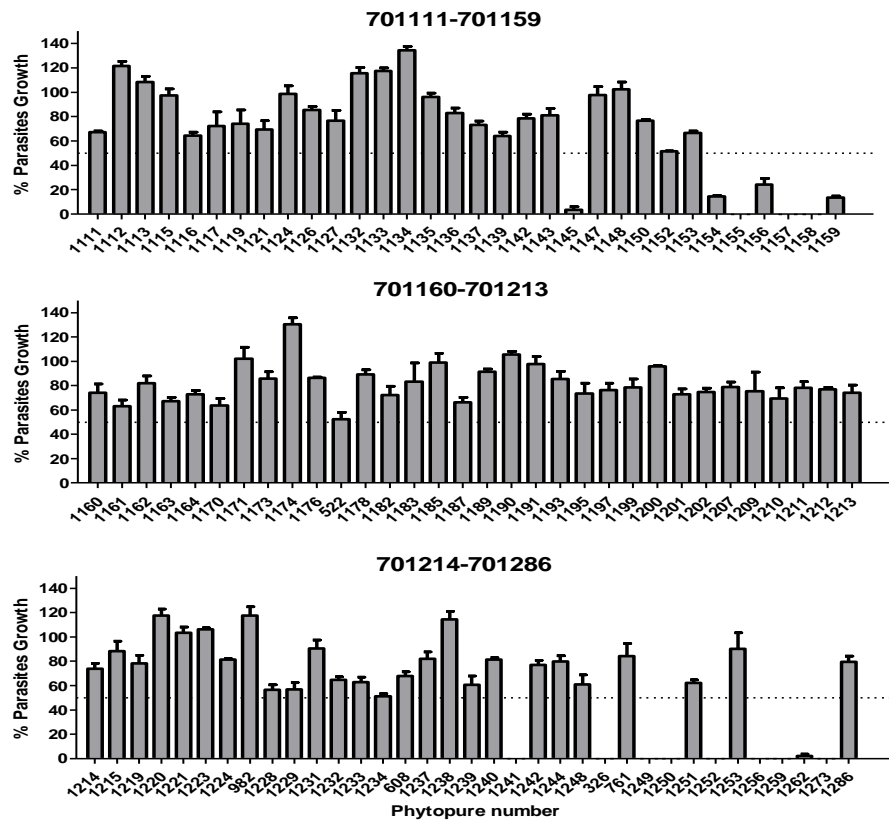


Figure 3.11: Screening the Phytopure library compounds against *T. brucei*. Each panel reports the mean \pm StDev (n=4) of normalized parasite growth when exposed to $2\mu\text{M}$ of the indicated compound. The Compound ID is 700-xxx with the suffix listed for each compound on the x-axis.

3.2.2.4 *In vitro* determination of cytotoxic effects against the human HepG2 cell line

The potentially toxic effects of these 25 Phytopure compounds against a human hepatoma cell line HepG2 was assessed using the Alamar Blue viability assay. The Phytopure compounds were exposed to a serial 2-fold dilution in triplicate, with three independent biological repeats (n=9) done. Following 48 hours of incubation the fluorescence signal was determined and normalized against an untreated control (100% growth) and the mean \pm SD of relative growth plotted (green lines on Fig. 3.12) on log concentration normalized

response graphs. Using this data, the 50% cytotoxic concentration (CC₅₀) was determined and is reported in Table 3.6.

The selectivity of these 25 compounds against *T. brucei* compared to HepG2 was calculated based on the ratio of the HepG2 CC₅₀ and *T. brucei* EC₅₀ data (the selective index SI) and reported in Table 3.6. For comparison, the same data for pentamidine is also reported. Whilst in general, many of the Phytopure compounds were poorly selective, three compounds have a SI that is the same or better than that of pentamidine (26.7). Two of these compounds have a nanomolar activity against *T. brucei*; 700035 (EC₅₀ of 350nM and SI of 43.3) and 701145 (EC₅₀ of 520nM and SI of 53.5). The sources for these 25 Phytopure compounds as well as their structures are shown in Table 3.7.

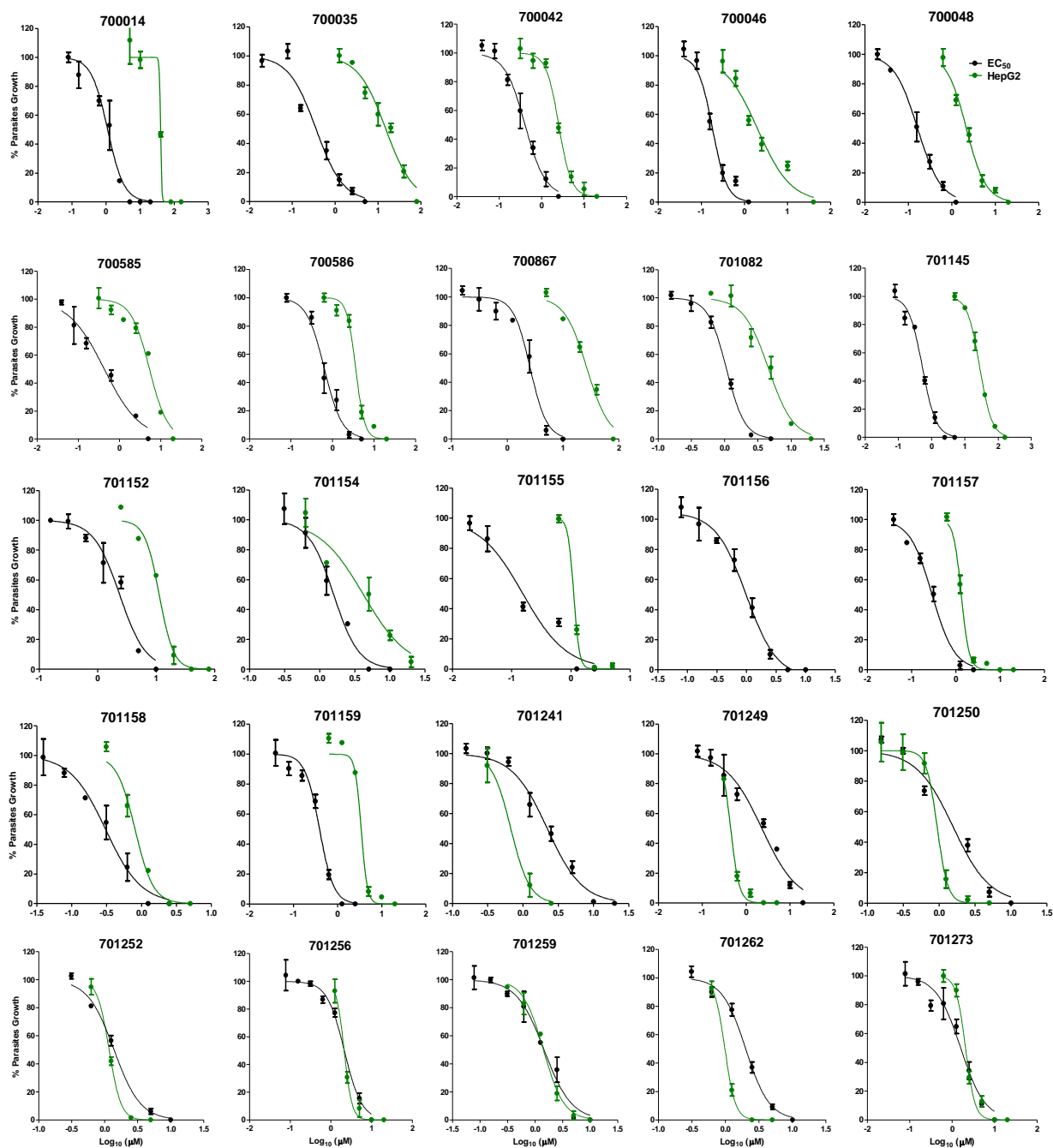


Figure 3.12: EC₅₀ activity of 25 Phytopure compounds against *T. brucei* and initial determination of cytotoxicity. Log concentration normalised response curves to determine EC₅₀ activity against *T. brucei* (black curves) and CC₅₀ against HepG2 cells (green curves) for the indicated Phytopure compounds. The data shown is a mean ± StDev of n=9. There was no CC₅₀ assay done for compound 701156.

Table 3.6: *In vitro* antitrypanosomal activity (EC₅₀) and cytotoxicity (CC₅₀) against HepG2 cells of 25 Phytopure compounds. SI*, is calculated as CC₅₀/EC₅₀. (Thao *et al.*, 2014)¹.

Compounds ID	EC ₅₀ (μM)	CC ₅₀ (μM)	SI*
	95% CI		
	<i>T. brucei</i>	HepG2 cell line	
700014	1.11 (1.05-1.22)	39.79 (39.86-47.95)	35.8
700035	0.35 (0.29-0.45)	15.15 (15.23-15.27)	43.3
700042	0.40 (0.39-0.43)	2.51 (2.20-12.60)	6.3
700046	0.18 (0.18-0.21)	2.01 (1.89-2.32)	11
700048	0.16 (0.13-0.18)	2.16 (1.73-2.26)	13.5
700585	0.42 (0.35-0.47)	5.33 (5.41-7.01)	12.6
700586	0.63 (0.58-0.77)	3.59 (3.61-4.10)	5.7
700867	2.58 (2.65-3.27)	26.75 (25.78-26.76)	10.4
701082	1.06 (0.94-1.11)	4.55 (4.41-5.12)	4.2
701145	0.52 (0.51-0.88)	27.83 (23.3-27.42)	53.5
701152	2.3 (1.96-2.71)	11.29 (11.14-11.39)	4.9
701154	1.58 (1.65-1.87)	4.18 (2.30-5.23)	2.6
701155	0.15 (0.15-0.17)	1.11 (1.07-1.09)	7.4
701156	0.99 (0.89-1.11)	ND	ND
701157	0.29 (0.22-0.30)	1.33 (1.26-1.30)	4.5
701158	0.30 (0.31-0.32)	0.80 (0.70-0.95)	2.6
701159	0.38 (0.35-0.37)	3.42 (3.36-4.43)	9
701241	2.21 (2.06-2.94)	0.67 (0.6-0.98)	0.3
701249	2.28 (2.10-2.43)	0.44 (0.28-0.39)	0.2
701250	1.57 (1.38-2.65)	0.94 (0.79-1.13)	0.6
701252	1.38 (1.35-1.40)	1.16 (1.07- 1.178)	0.8
701256	2.13 (2.10-2.20)	2.1 (2.06-2.60)	1
701259	1.45 (1.34-1.56)	1.41 (1.34-1.60)	1
701262	2.01 (1.3-2.00)	0.98 (0.88-0.92)	0.5
701273	1.58 (1.56-1.98)	2.06 (2.03-2.32)	1.3
Pentamidine ¹	0.015	< 0.40	<26.7

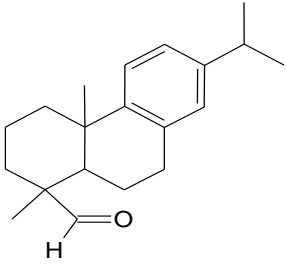
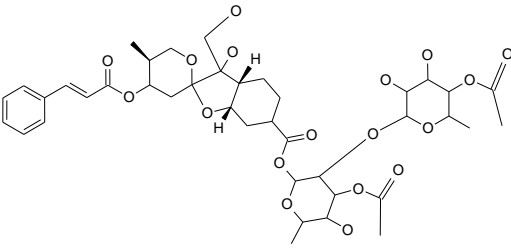
Table 3.7: (A) Source information and (B) structure of 25 hit compounds from Phytopure library against *T. brucei*.

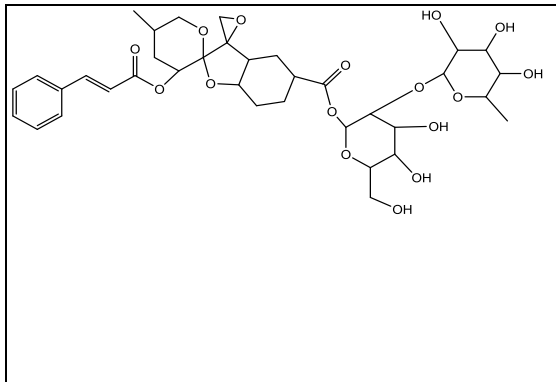
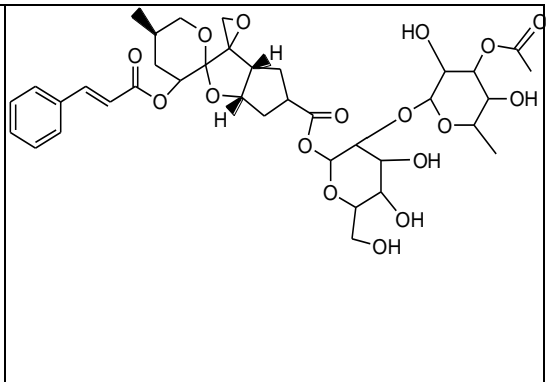
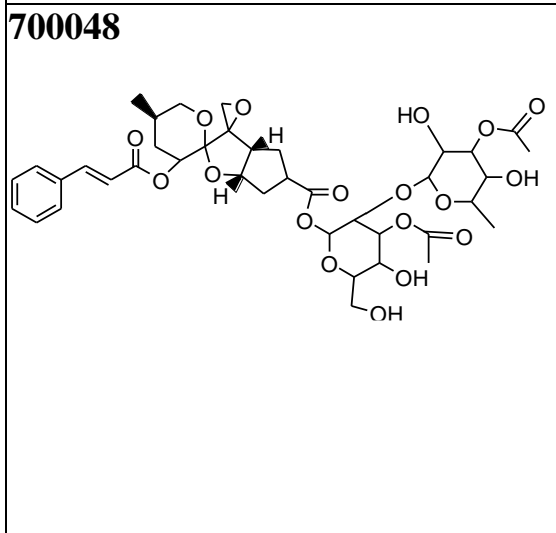
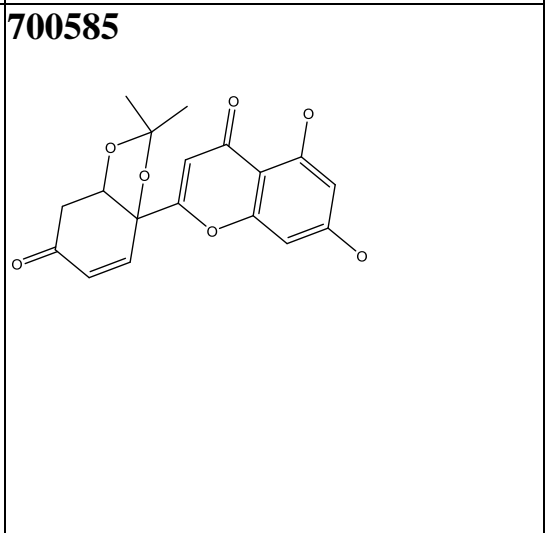
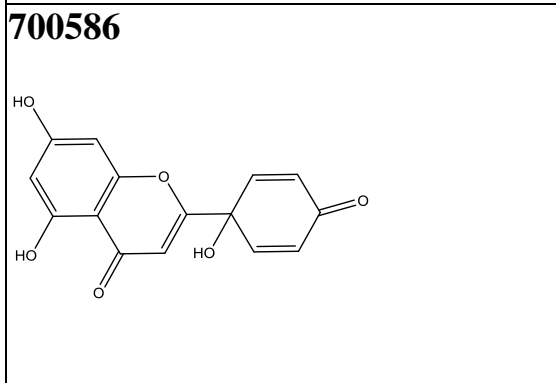
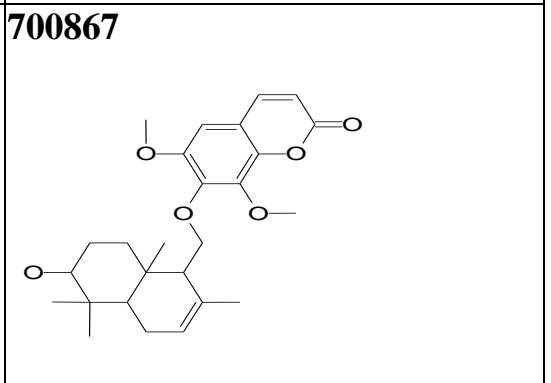
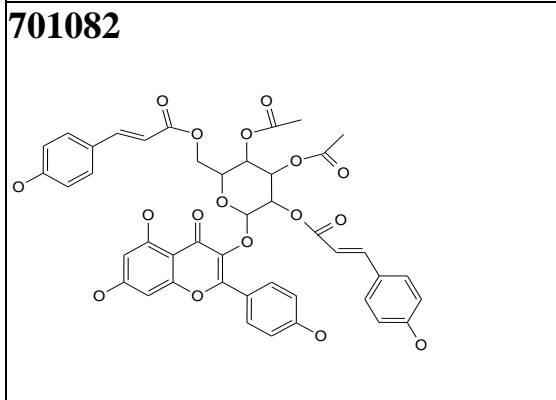
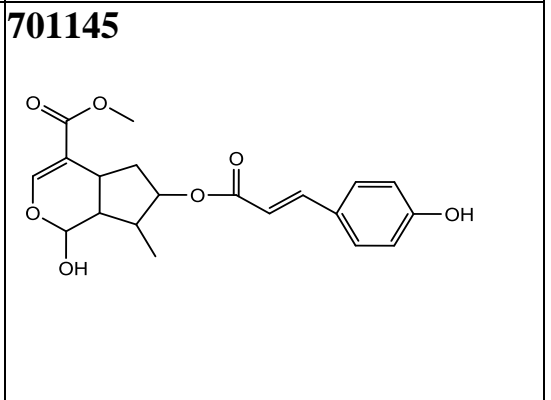
(A)

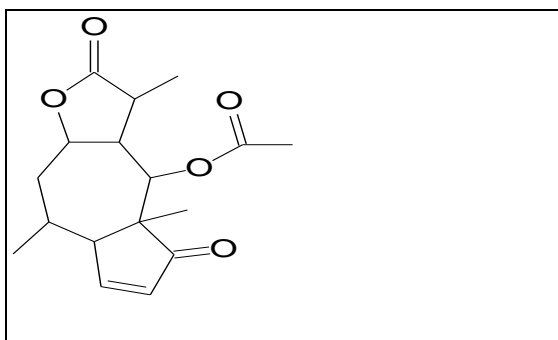
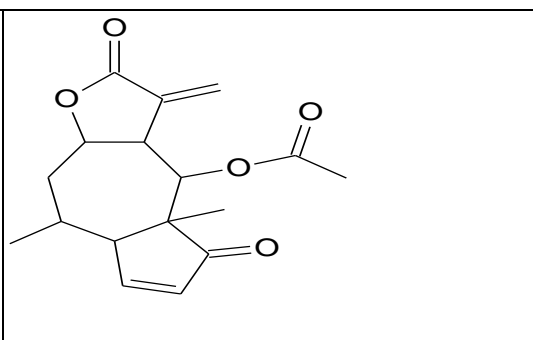
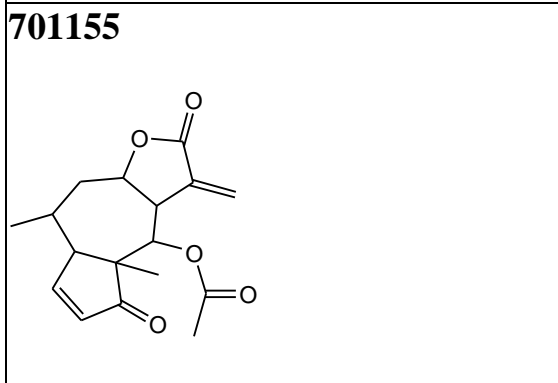
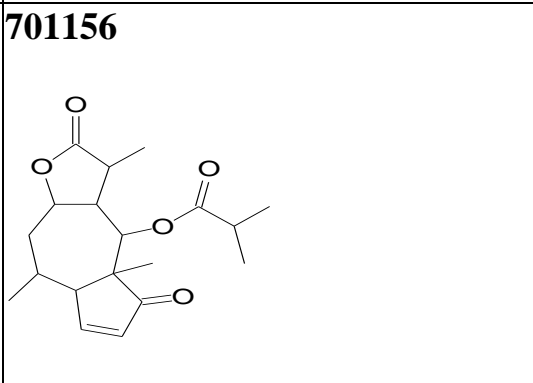
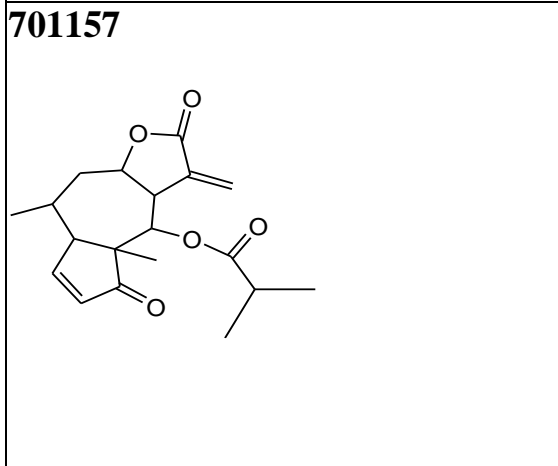
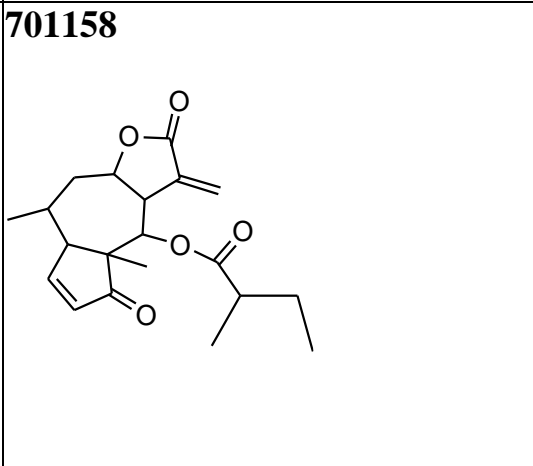
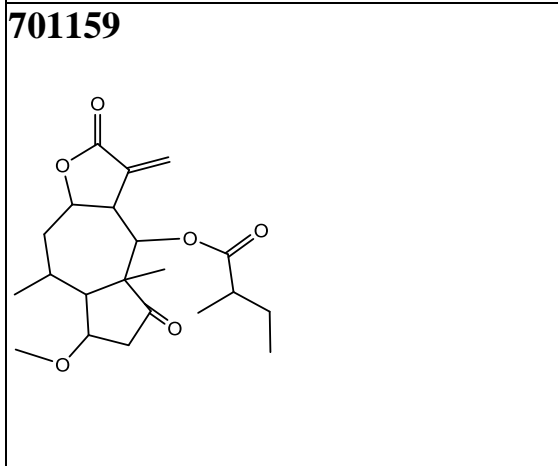
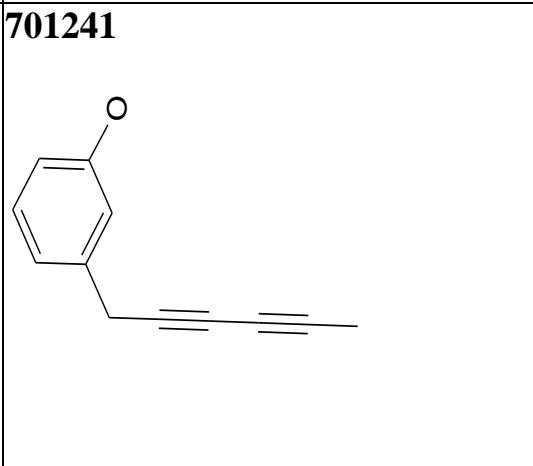
PQ number	Class	plant name	genus	species	Mwt	mol formula
700014	abietic diterpene	Noble fir	<i>Abies</i>	<i>procera</i>	284.443	C20H28O
700035	phyllanthocin		<i>Phyllanthus</i>	<i>acuminatus</i>	822.854	C40H54O18
700042	phyllanthocin		<i>Phyllanthus</i>	<i>acuminatus</i>	736.764	C36H48O16
700046	phyllanthocin		<i>Phyllanthus</i>	<i>acuminatus</i>	778.801	C38H50O17
700048	phyllanthocin		<i>Phyllanthus</i>	<i>acuminatus</i>	820.838	C40H52O18
700585	flavonoid	Common horsetail	<i>Equistum</i>	<i>arvense</i>	344.319	C18H16O7
700586	flavonoid	Common horsetail	<i>Equistum</i>	<i>arvense</i>	286.239	C15H10O6
700867	Coumarin					C26H33O6
701082	flavonoid		<i>Phyllanthus</i>	<i>acuminatus</i>	824.744	C43H36O17
701145	sesquiterpene	Bogbean	<i>Menyanthese</i>	<i>trifoliata</i>	374.389	C20H22O7
701152	Sesquiterpene	Arnica	<i>Arnica</i>	<i>montana</i>	302.34	C17H18O5
701154	sesquiterpene	Arnica	<i>Arnica</i>	<i>montana</i>	304.342	C17H20O5
701155	sesquiterpene	Arnica	<i>Arnica</i>	<i>montana</i>	304.34	C17H20O5
701156	sesquiterpene	Arnica	<i>Arnica</i>	<i>montana</i>	334.4	C17H22O5
701157	sesquiterpene	Arnica	<i>Arnica</i>	<i>montana</i>	332.4	C17H20O5
701158	sesquiterpene	Arnica	<i>Arnica</i>	<i>montana</i>	346.42	C20H26O5
701159	sesquiterpene	Arnica	<i>Arnica</i>	<i>montana</i>	378.465	C21H30O6

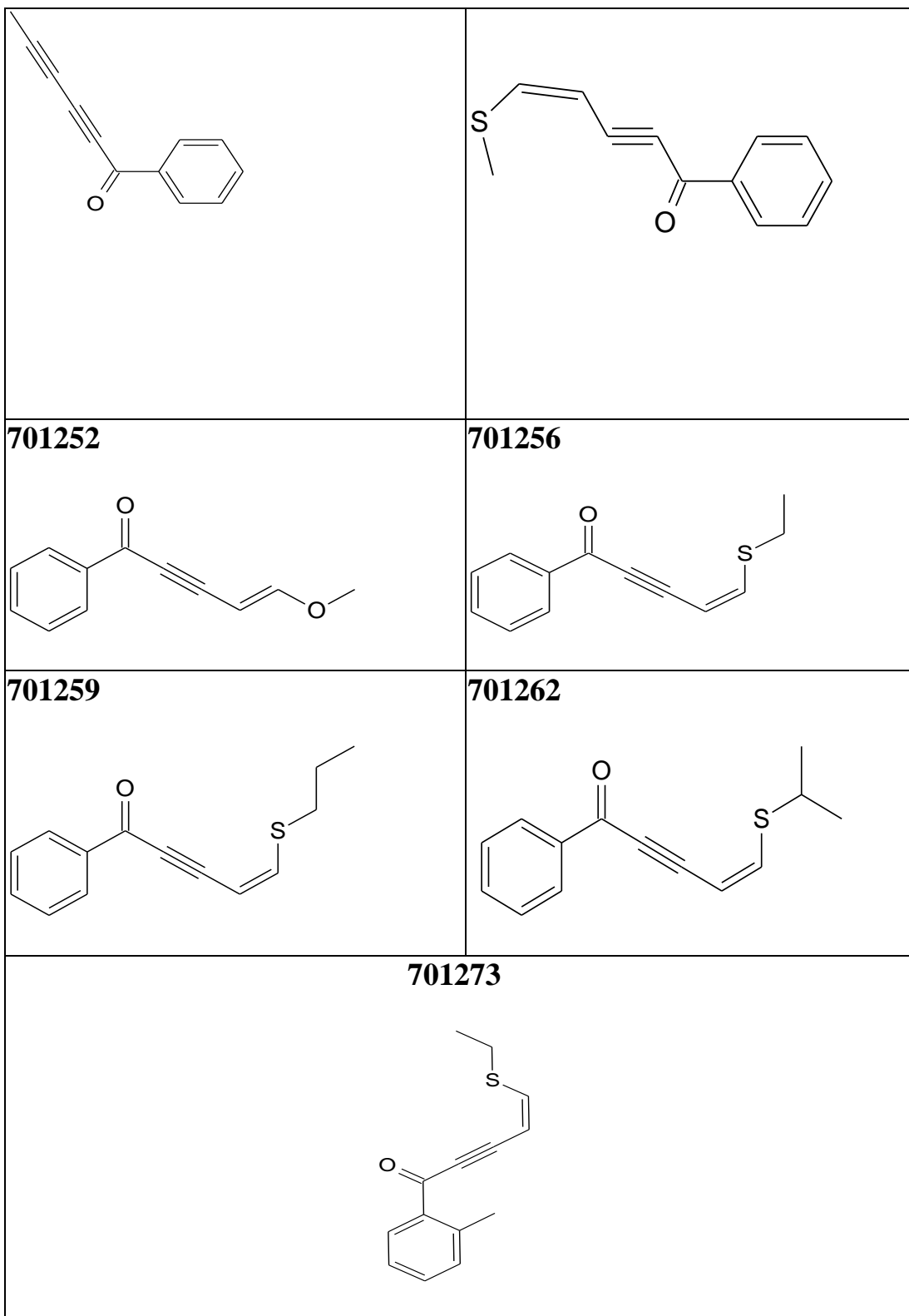
701241	aromatic	Corn marigold	<i>Chrysanthemum segetum</i>	170.211	C ₁₂ H ₁₀ O
701249	aromatic	Corn marigold	<i>Chrysanthemum segetum</i>	168.195	C ₁₂ H ₈ O
701250	aromatic	Synthetic		202.275	C ₁₂ H ₁₀ OS
701252	aromatic	Synthetic		186.21	C ₁₂ H ₁₀ O ₂
701256	aromatic	Synthetic		216.302	C ₁₃ H ₁₂ OS
701259	aromatic	Synthetic		230.329	C ₁₄ H ₁₄ OS
701262	aromatic	Synthetic		230.329	C ₁₄ H ₁₄ OS
701273	aromatic	Synthetic		230.329	C ₁₄ H ₁₄ OS

(B)

Structure of compound	
700014 	700035 
700042	700046

	
<p>700048</p> 	<p>700585</p> 
<p>700586</p> 	<p>700867</p> 
<p>701082</p> 	<p>701145</p> 
<p>701152</p>	<p>701154</p>

	
<p>701155</p> 	<p>701156</p> 
<p>701157</p> 	<p>701158</p> 
<p>701159</p> 	<p>701241</p> 
<p>701249</p>	<p>701250</p>



3.2.3 Antleishmanial activity

3.2.3.1 Optimization of the proliferation assay

An initial determination of the initial *L. mexicana* axenic amastigotes MNYC/BZ/62/M379 strain seeding density in the proposed 96-multiwell screening plate format was made, ensuring that the density initially seeded did not reach a confluence that would affect the rate of cell division within the 72 hours assay period. Axenic *L. mexicana* amastigotes were diluted serially from 1.5×10^7 to 0.012×10^7 cells/mL before leaving for 72 hours at 37°C in normal growth conditions (n=3 replicates). Following this incubation, the resulting cell numbers were estimated using an Alamar Blue fluorescence assay to determine the activity of viable (still generate reduced cofactors) parasites (Figure 3.13). This analysis indicates that an initial seeding of 1×10^6 cells/mL of *L. mexicana* axenic amastigotes provides for the maximum growth within 72 hours without growth being affected by saturation effects (Figure 3.13). All subsequent growth inhibition assays assumed this initial seeding density.

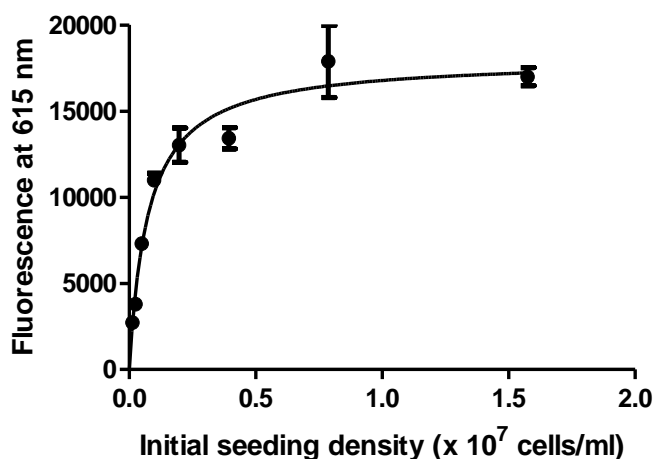
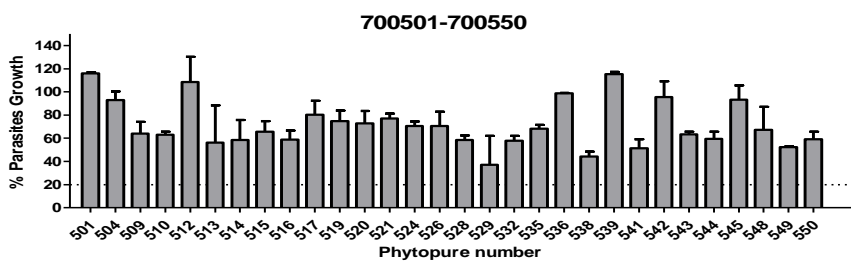
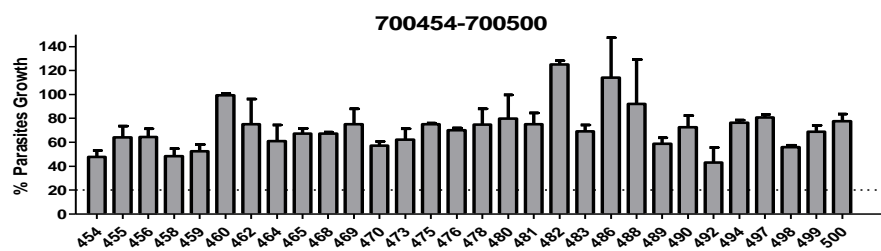
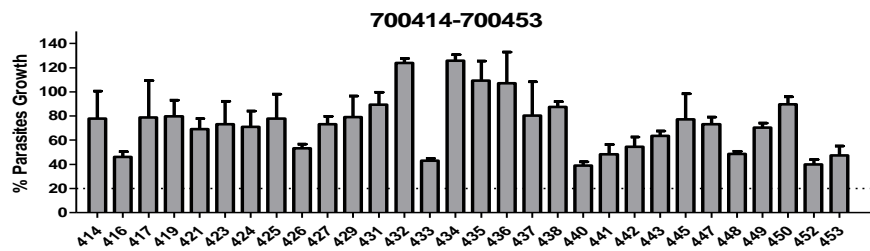
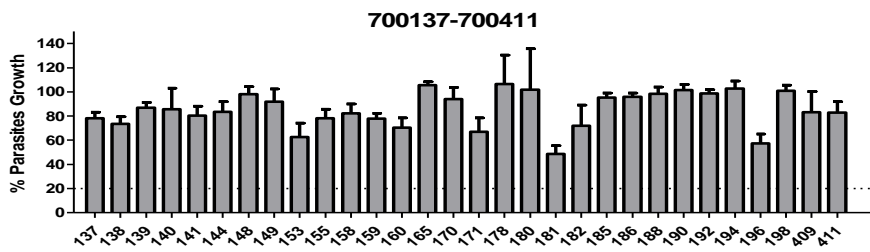
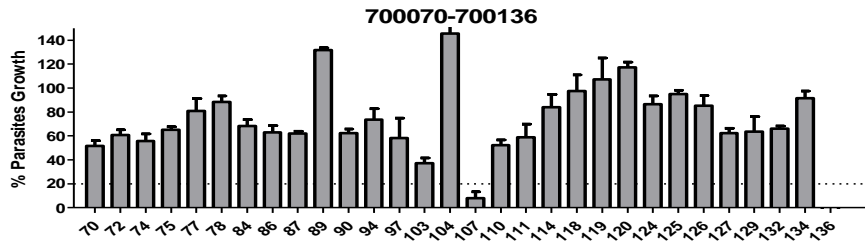
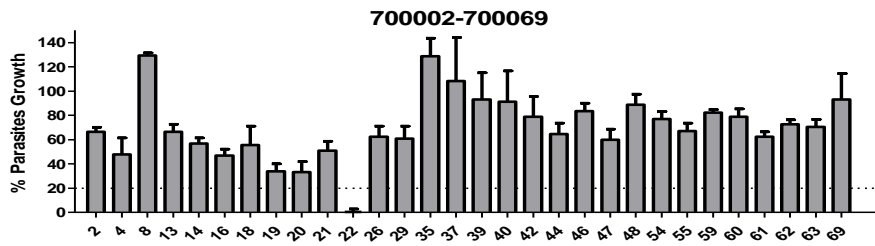
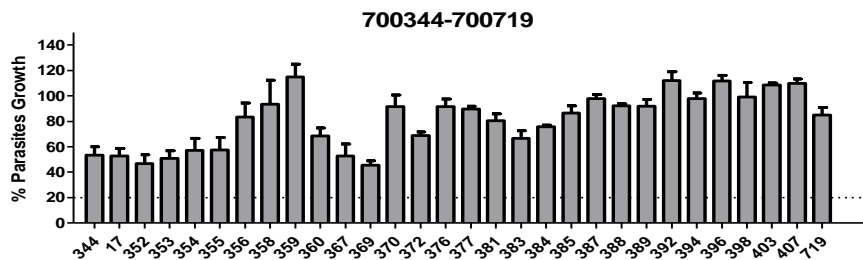
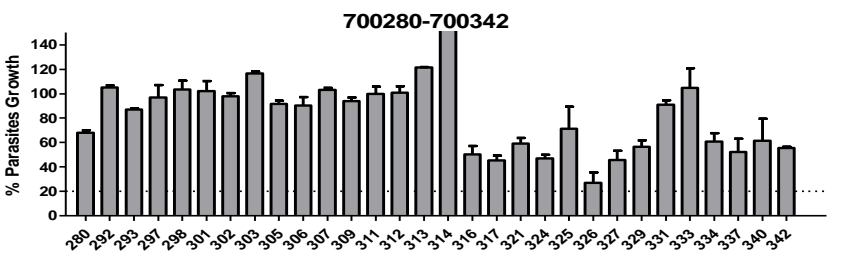
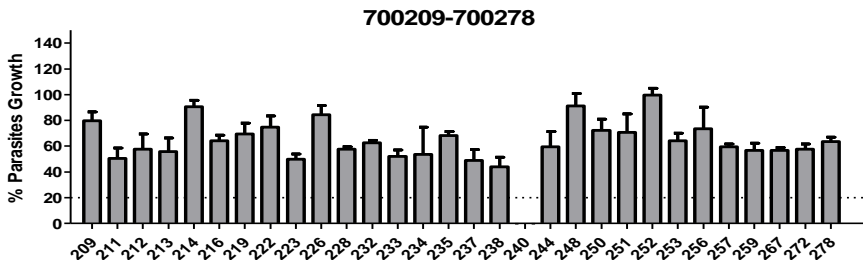
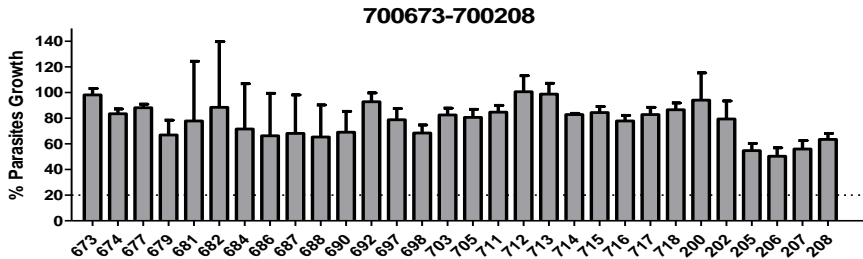
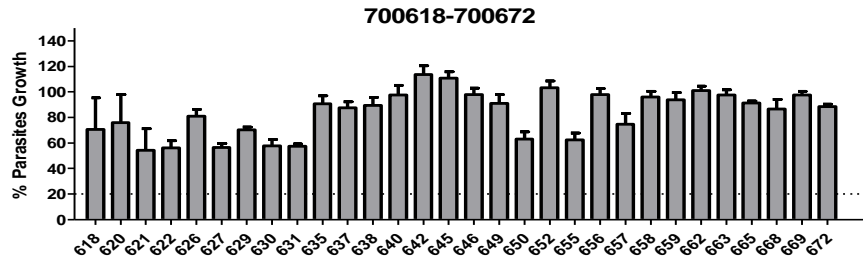
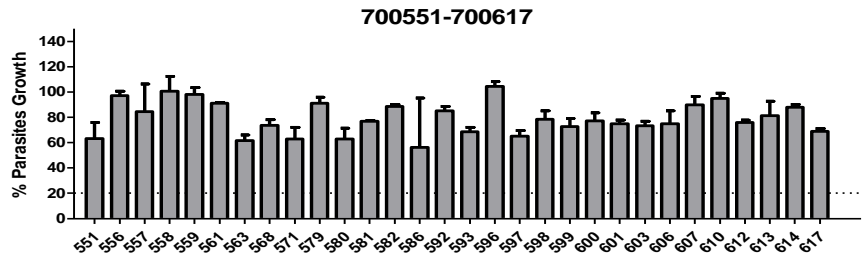


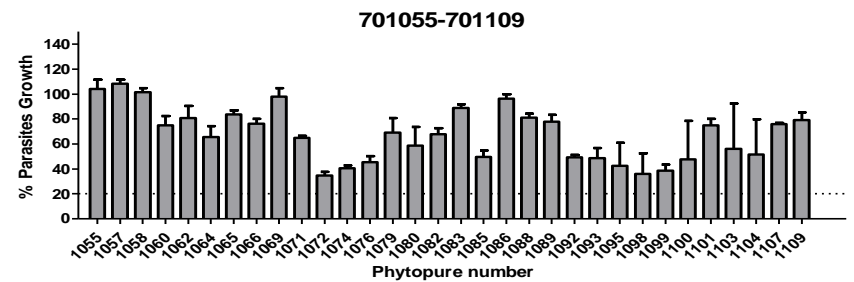
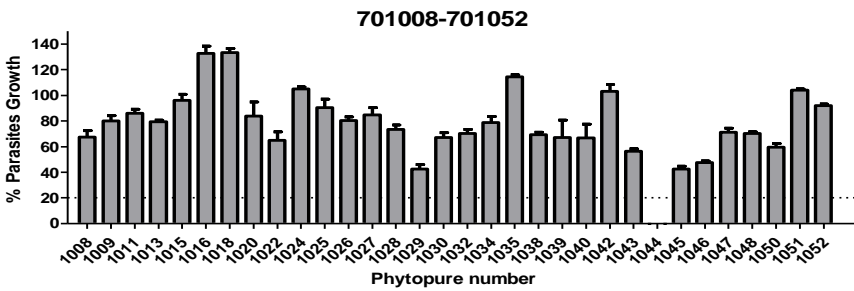
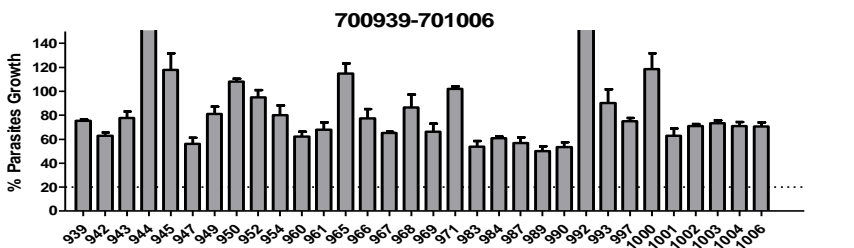
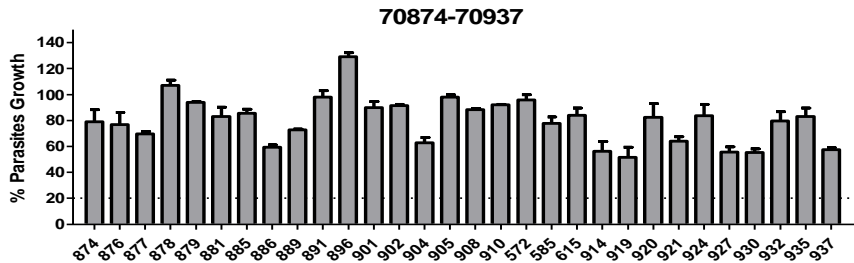
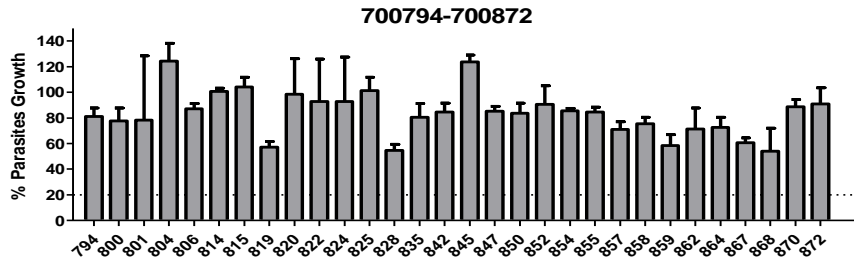
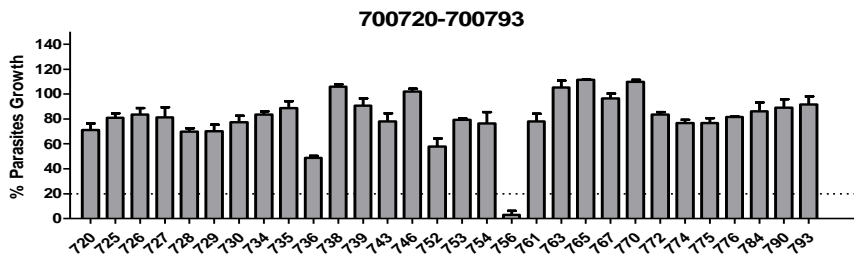
Figure 3.13: Determination of initial *L. mexicana* axenic amastigote seeding density. The graph plots a logarithmic growth regression analysis of a 72 hours Alamar Blue assay (fluorescence at 615nm) versus the initial seeding density to optimize the selection of conditions for a 96-well multiplate growth assay. Data represents the mean \pm StDev of n=3.

3.2.3.2 Screening of Phytopure library against *L. mexicana*

The screening of 643 Phytopure library compounds was assessed against *L. mexicana* axenic amastigotes strain MNYC/BZ/62/M379 over 72 hours at 37 °C with 5% CO₂. Compounds were tested at a single concentration of 2 μM in duplicates with 2 independent biological replicates (n=4). The inhibitory effect of each compound was assessed using Alamar Blue fluorescence assay and growth normalized against an untreated control. Figure 3.14 presents a series of panels that plots the mean ± StDev of the normalized growth for the compounds indicated above the chart. These data are also provided in Table appendix 1.







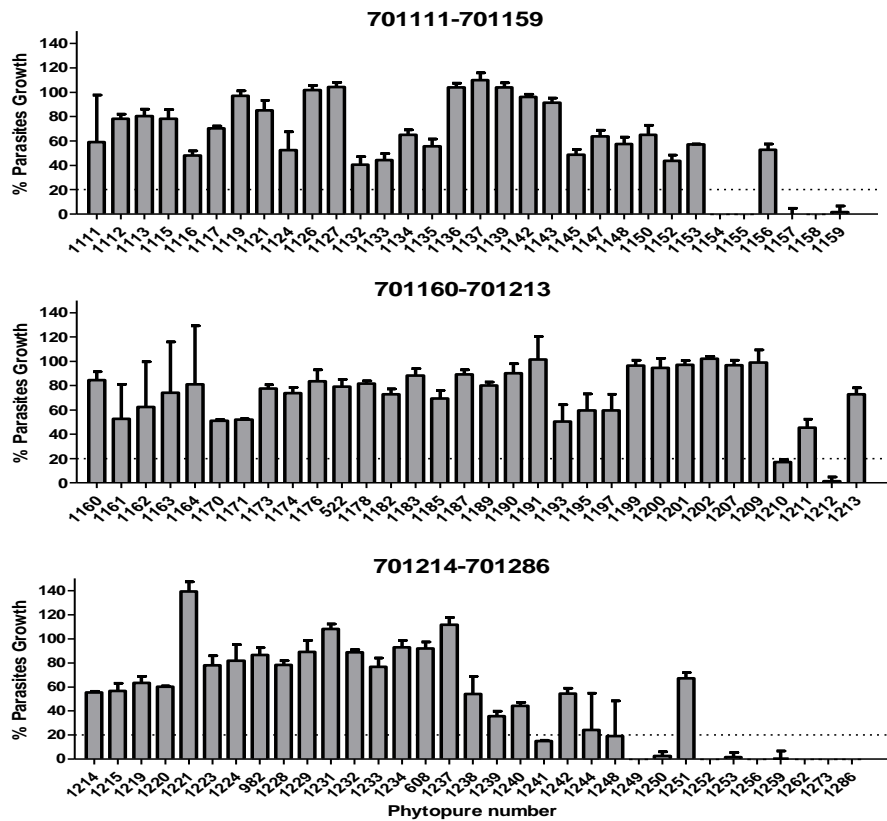


Figure 3.14: Screening the Phytopure library compounds against *L. mexicana*. Each panel reports the mean \pm StDev (n=4) of normalized parasite growth when exposed to 2 μ M of the indicated compound. The Compound ID is 700-xxx with the suffix listed for each compound on the x-axis.

3.2.3.3 Determination of EC₅₀ values of 23 hits from Phytopure screens by using Alamar Blue viability assay

A total of 38 compounds reduce parasite growth by 50% or more at 2 μM , giving a hit rate of 5.9%. However, of these 38, 23 of them reduced parasite growth by 80% or more at 2 μM (a revised hit rate of 3.5%). In order to manage the subsequent assays required, these 23 compounds were selected to study their activity in more detail against *L. mexicana*.

The EC₅₀ of the 23 compounds were determined using a 72 hours Alamar Blue assay format *L. mexicana* axenic amastigotes strain MNYC/BZ/62/M379. The compounds were exposed in technical triplicate to a 2-fold dilution of each compound, with three independent biological repeats carried out (n=9). These data were plotted in log concentration normalized response curves (black lines on Figure 3.15) and the EC₅₀ and 95% CI determined from a non-linear regression curve and reported in Table 3.8. As controls, amphotericin B and miltefosine were included (Figure 3.15). These compounds provided the expected EC₅₀ against axenic *L. mexicana* of approximately 0.25 μM and 1 μM , respectively. These data report very good antiproliferative activities for the Phytopure compounds ranging between 0.15 to 1 μM , perhaps expected as a higher threshold for their selection was applied.

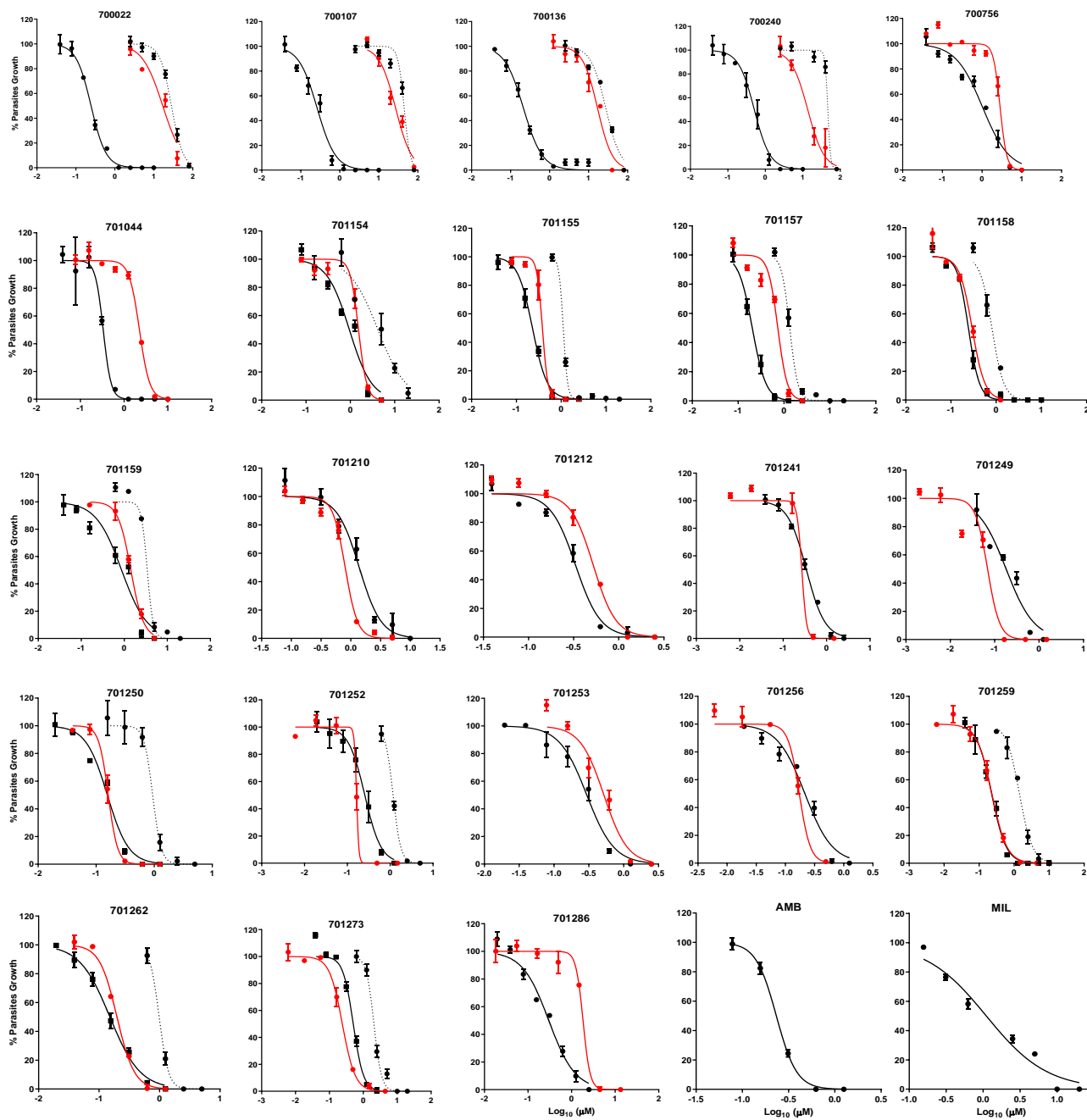


Figure 3.15: EC₅₀ activity of 23 Phytopure compounds against *L. mexicana* and initial determination of cytotoxicity. Log concentration normalised response curves to determine EC₅₀ activity against *L. mexicana* (black curves) and CC₅₀ against THP-1 cells (red curves) or HepG2 (dotted curves) for the indicated Phytopure compounds. The data shown is a mean ± StDev of n=9. HepG2 assays were not carried out for all compounds.

Table 3.8: *In vitro* antileishmanial activity (EC₅₀), and cytotoxicity (CC₅₀) against THP-1 cell line and HepG2 cell line for 23 Phytopure compounds. SI, is calculated as CC₅₀/EC₅₀. (Mehta *et al.*, 2010)¹; (Escudero-Martínez *et al.*, 2017)²

Compounds ID	EC ₅₀ (μM) (95% CI)	CC ₅₀ (μM) (95% CI)	SI	CC ₅₀ (μM) (95% CI)	SI
	<i>L. mexicana</i> amastigotes	THP-1 cell line		HepG2 cell line	
700022	0.24 (0.21-0.25)	16.97 (15.1-7.38)	70.7	28.37 (27.7-30.8)	118
700107	0.26 (0.24-0.28)	27.00 (20.78-7.9)	103.6	44.8 (46.3-46.8)	169
700136	0.21 (0.22-0.27)	16.96 (13.4-20.13)	80.7	27.6 (29.1-31.1)	131
700240	0.5 (0.46-0.52)	13.54 (10.6-15.00)	27	46.5 (52.7-57.1)	93
700756	1 (0.98-1.01)	2.83 (2.5-3.73)	2.8	-	-
701044	0.33 (0.27-0.3)	2.24 (1.5-2.25)	6.78	-	-
701154	0.95 (0.93-0.98)	1.52 (1.46-1.73)	1.5	4.18 (2.30-5.23)	4.4
701155	0.22 (0.19-0.23)	0.38 (0.407-0.43)	1.7	1.11 (1.07-1.09)	5
701157	0.2 (0.16-0.19)	0.73 (0.65-0.91)	3.6	1.33 (1.26-1.3)	6.65
701158	0.24 (0.28-0.31)	0.29 (0.29-0.33)	1.2	0.80 (0.70-0.95)	3.3
701159	0.88 (0.64-1.26)	1.42 (1.2-1.63)	1.5	3.42 (3.36-4.43)	3.8
701210	1.38 (1.39-1.51)	0.8 (0.66-0.96)	0.57	-	-
701212	0.33 (0.30-0.34)	0.52 (0.46-0.67)	1.5	-	-
701241	0.34 (0.28-0.34)	0.26 (0.26-0.29)	0.7	-	-
701249	0.18 (0.18-0.21)	0.06 (0.04-0.067)	0.3	-	-

701250	0.15 (0.12-0.15)	0.16 (0.14-0.16)	1	0.94 (0.79-1.13)	6.2
701252	0.25 (0.19-0.26)	0.16 (0.15-0.16)	0.64	1.16 (1.07-1.178)	4.6
701253	0.29 (0.26-0.30)	0.51 (0.5-0.87)	1.75	-	-
701256	0.21 (0.19-0.21)	0.17 (0.168-0.18)	0.8	-	-
701259	0.22 (0.12-0.21)	0.23 (0.18-0.24)	1	1.41 (1.34-1.6)	6.4
701262	0.15 (0.15-0.36)	0.19 (0.18-0.185)	1.2	0.98 (0.88-0.92)	6.5
701273	0.5 (0.51-0.64)	0.24 (0.25-0.31)	0.48	2.06 (2.03-2.32)	4.1
701286	0.29 (0.27-0.28)	1.83 (1.3-1.8)	6.3	-	-
AmB	0.23 (0.23-0.29)	>100	>434	>100	>434
Miltefosine	1.11 (0.99-1.16)	40.5±12.0 ¹	36	50.4 ± 4.3 ²	45.4

3.2.3.4 *In vitro* determination of cytotoxic effects against the human THP-1 and HepG2 cell lines

The potentially toxic effects of these 23 Phytopure compounds was initially determined against a human leukemia monocytic cell line THP-1. These were selected as in subsequent experiments this monocyte cell line is differentiated into macrophages using phorbol 12-myristate 13-acetate (PMA) for intramacrophage assays. The Phytopure compounds were exposed to THP-1 as a serial 2-fold dilution in triplicate, with three independent biological repeats (n=9) done. Following 48 hours of incubation the fluorescence signal was determined and normalized against an untreated control (100% growth) and the mean ± SD of relative

growth plotted (red lines on Fig. 3.15) on log concentration normalized response graphs. Using this data, the 50% cytotoxic concentration (CC_{50}) was determined and is reported in Table 3.8. Note that published data for amphotericin B and miltefosine are included for comparison.

In general, these Phytopure compounds show low μM to nM antiproliferative activities and thus very poor selectivity against the parasite compared to the THP-1 cells. Four compounds, closely related triterpenes from *Abies procera*, had CC_{50} between 13 to $27\mu\text{M}$ and thus SI of between 27-104. Using the same HepG2 assay as described earlier for the *T. brucei* hits, the CC_{50} of these four compounds were measured. These data are plotted as green curves on Figure 3.15 and the CC_{50} data and estimated SI reported in Table 3.8. These data were promising with CC_{50} between 28 to $47\mu\text{M}$ and SI of between 93-169, suggesting these four related compounds may provide selectivity against axenic stages of *L. mexicana* over these two human cell lines. Note, where HepG2 data is available for a *L. mexicana* from the previous *T. brucei* HepG2 screen, these data were added to Figure 3.15 and Table 3.8. In all cases, the observed poor selectivity against the THP-1 cell line was similarly observed for the HepG2 cell line. The sources and structures of these 23 Phytopure compounds are shown in Table 3.9.

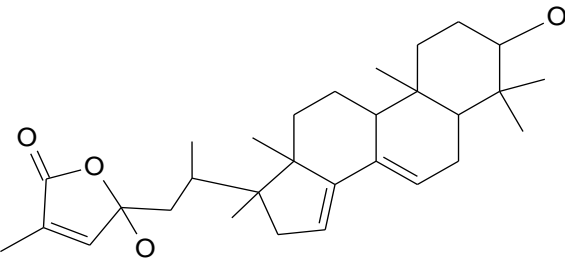
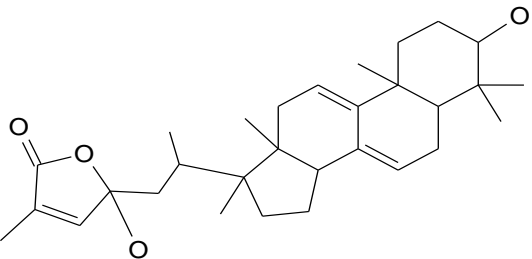
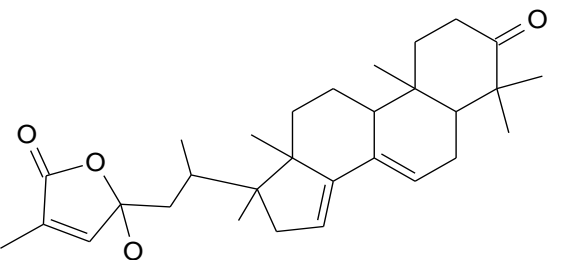
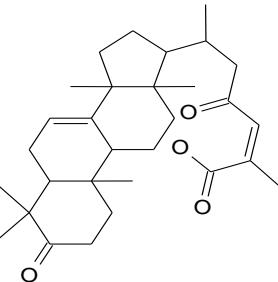
Table 3.9: A, information generated from PhytoQuest for high interest compounds against *L. mexicana*. B, the structure of each compound.

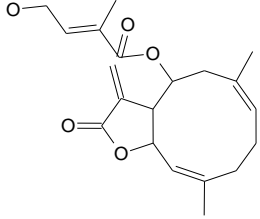
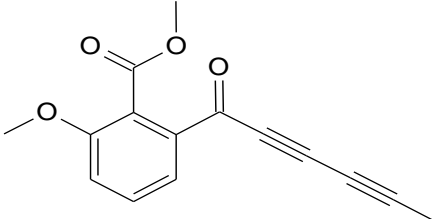
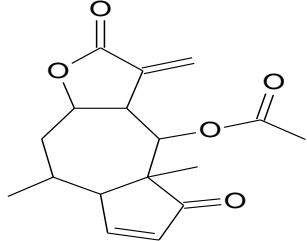
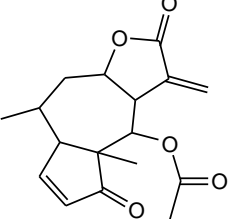
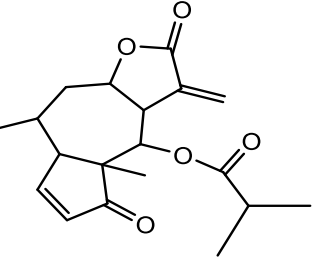
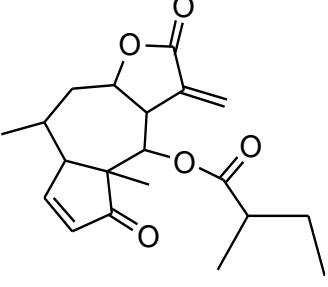
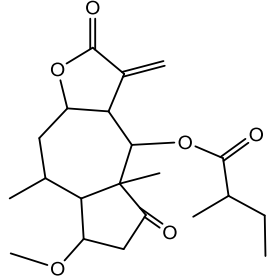
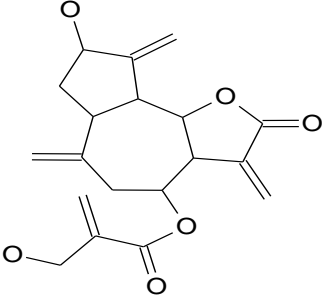
(A)

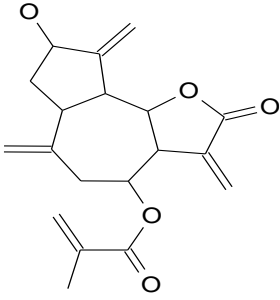
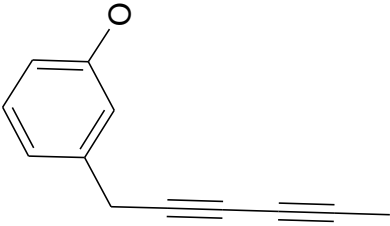
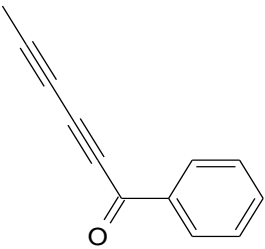
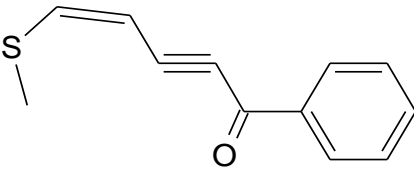
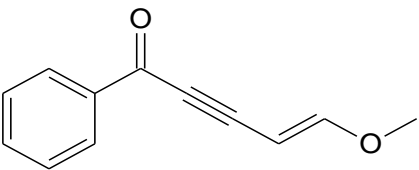
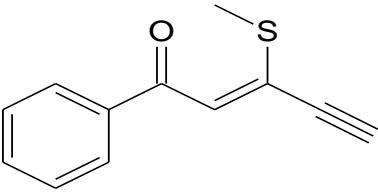
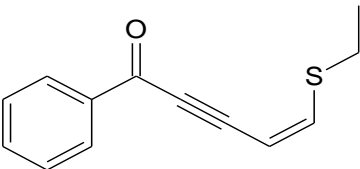
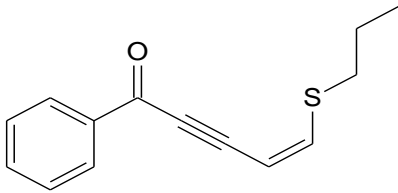
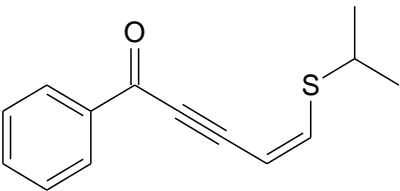
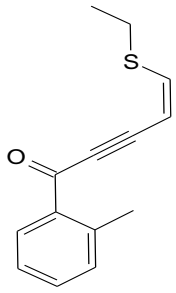
PQ number	Class	plant name	genus	species	Mwt	mol formula
700022	triterpene	Noble fir	<i>Abies</i>	<i>procera</i>	468.678	C30H44O4
700107	triterpene	Noble fir	<i>Abies</i>	<i>procera</i>	468.678	C30H44O4
700136	triterpene	Noble fir	<i>Abies</i>	<i>procera</i>	466.662	C30H42O4
700240	triterpene	Grand fir	<i>Abies</i>	<i>grandis</i>	468.678	C30H44O4
700756	sesquiterpene	Hemp agrimony	<i>Eupatorium</i>	<i>cannabinum</i>	346.423	C20H26O5
701044	aromatic	Marguerite	<i>Argyranthemum</i>	<i>frutescens</i>	256.257	C15H12O4
701154	sesquiterpene	Arnica	<i>Arnica</i>	<i>montana</i>	304.342	C17H20O5
701155	sesquiterpene	Arnica	<i>Arnica</i>	<i>montana</i>	304.34	C17H20O5
701157	sesquiterpene	Arnica	<i>Arnica</i>	<i>montana</i>	332.4	C19H24O5
701158	sesquiterpene	Arnica	<i>Arnica</i>	<i>montana</i>	346.42	C20H26O5
701159	sesquiterpene	Arnica	<i>Arnica</i>	<i>montana</i>	378.465	C21H30O6
701210	sesquiterpene	Artichoke	<i>Cynara</i>	<i>cardunculus</i>	346.379	C19H22O6
701212	sesquiterpene	Artichoke	<i>Cynara</i>	<i>cardunculus</i>	330.38	C19H22O5
701241	aromatic	Corn marigold	<i>Chrysanthemum</i>	<i>segetum</i>	170.211	C12H10O
701249	aromatic	Corn marigold	<i>Chrysanthemum</i>	<i>segetum</i>	168.195	C12H8O
701250	aromatic	Synthetic			202.275	C12H10OS
701252	aromatic	Synthetic			186.21	C12H10O2
701253	aromatic	Synthetic			202.275	C12H10OS

701256	aromatic	Synthetic			216.302	C13H12OS
701259	aromatic	Synthetic			230.329	C14H14OS
701262	aromatic	Synthetic			230.329	C14H14OS
701273	aromatic	Synthetic			230.329	C14H14OS
701286	aromatic	Synthetic			234.298	C17H14O

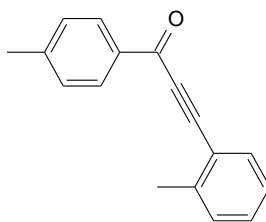
(B)

Structure of compound	
<p>700022</p> 	<p>700107</p> 
<p>700136</p> 	<p>700240</p> 
<p>700756</p>	<p>701044</p>

	
<p>701154</p> 	<p>701155</p> 
<p>701157</p> 	<p>701158</p> 
<p>701159</p> 	<p>701210</p> 
<p>701212</p>	<p>701241</p>

	
<p>701249</p> 	<p>701250</p> 
<p>701252</p> 	<p>701253</p> 
<p>701256</p> 	<p>701259</p> 
<p>701262</p> 	<p>701273</p> 

701286



3.2.3.5 Validation of the four *L. mexicana* hits against *L. donovani*

The EC₅₀ of the four apparently selective compounds (700022, 700107, 700136 and 700240) against axenic *L. mexicana* ranged between 210-500 nM. To validate the potency of these compounds, the EC₅₀ was determined against the axenic amastigotes of *L. donovani* strain LdBoB – a species responsive for the visceral form of leishmaniasis. The same Alamar Blue protocol was used over 72 hours, each compound tested as a technical triplicate and three independent biological repeats done (n=9). These data were plotted in log concentration normalized response curves (dotted black lines on Figure 3.16) and the EC₅₀ and 95% CI determined from a non-linear regression curve and reported in Table 3.10. To help with the comparison with previous data, the *L. mexicana* EC₅₀ data (black curve) and CC₅₀ data from THP-1 (red curve) and HepG2 (green curve) are also plotted, the CC₅₀ values used to determine the SI for *L. donovani* compared to both human cell line (Table 3.10) The antiproliferative activity of 700022, 700107, 700136 and 700240 is also present in a second *Leishmania* species at comparable EC₅₀ activities (140-330nM), which provide the same, if not slightly improved, SI values against both human cell lines tested.

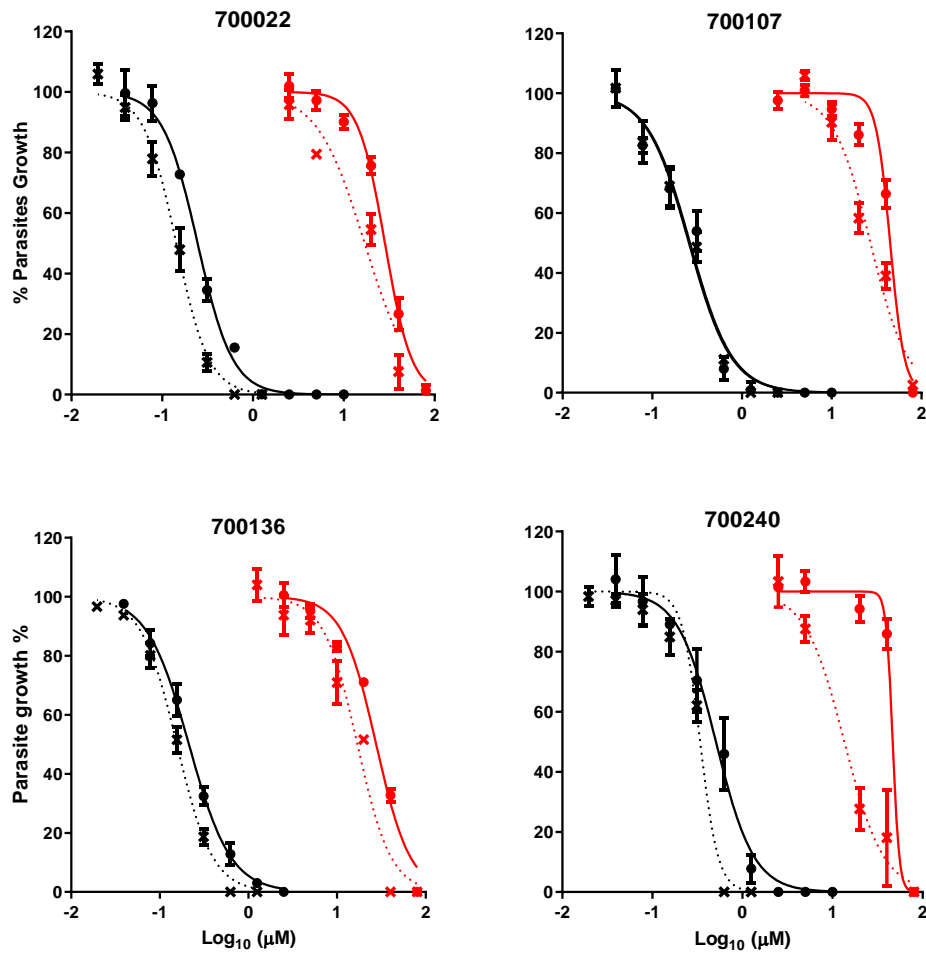


Figure 3.16: EC₅₀ activity of 700022, 700107, 700136 and 700240 Phytopure compounds against *L. donovani*. Log concentration normalised response curves to determine EC₅₀ activity against *L. donovani* (black dotted curves). To aid comparison, the EC₅₀ activity against *L. mexicana* (black full line curve) and CC₅₀ against THP-1 cells (red curves) or HepG2 (green curves) are also shown for the indicated Phytopure compounds. The data shown is a mean \pm StDev of n=9. Note the EC₅₀ curves for 700107 are overlapping.

Table 3.10: *In vitro* antileishmanial activity, and cytotoxicity of compounds (700022, 700107, 700136 and 700240) against *L. donovani* amastigotes, THP-1 cells and HepG2 cells. SI, is calculated as CC_{50}/EC_{50} .

ID	EC ₅₀ (μM)	CC ₅₀ (μM)	SI	CC ₅₀ (μM)	SI
	axenic amastigotes of <i>L. donovani</i>	THP1		HepG2	
	Mean (95% CI)	Mean (95% CI)		Mean (95% CI)	
700022	0.14 (0.13-0.19)	16.97 (15.1-17.38)	121.2	28.37 (27.7-30.8)	189
700107	0.25 (0.18-0.29)	27.00 (20.78-27.9)	108	44.8 (46.3-46.8)	186
700136	0.15 (0.12-0.15)	16.96 (13.4-20.13)	113	27.6 (29.1-31.1)	276
700240	0.33 (0.3-0.35)	13.54 (10.6-15.00)	41	46.5 (52.7-57.1)	172

3.2.3.6 Validation of the four *L. mexicana* hits against an intracellular macrophage model

The activity of Phytopure compounds 700022, 700107, 700136 and 700240 were tested against the more clinically relevant intracellular macrophage assay to explore the potential effect on antiproliferative activity when the target parasite resides within a lipid bound vesicle, with an acidic environment, within another cell. THP-1 monocyte cell lines were differentiated into macrophages using PMA. These differentiated macrophages were infected with amastigote stage parasites and then exposed to 72 hours of 1x, 3x and 9xEC₅₀ concentrations derived using axenic stage amastigotes, of each compound. The higher concentrations recognizing that the antiproliferative effects of these compounds may be less potent against the intramacrophage amastigote. As a control, untreated cultures were also maintained as well as two cultures exposed to either 1x or 3xEC₅₀ concentrations of

amphotericin B (0.25 and 0.75 μ M, respectively). The experiments were carried out as duplicates with two independent biological replicates.

Following incubation, cultures are stained with the nuclear staining SYBR Green 1 (Figure 3.17) and fluorescent imaging of cultures done. In the first case, the proportion of differentiated THP-1 cells containing intracellular macrophages was determined. Based on the counting of 200 THP-1 cells, the proportion that shows punctate staining peripheral to the THP-1 nucleus, these being the nuclei of intracellular *L. mexicana* amastigotes, were counted. From the untreated controls, the two biological repeats show quite different efficiencies in amastigote infection into the differentiated THP-1. The first experiment (Figure 3.18A) shows some 80% of differentiated THP-1 infected, with approximately half that rate achieved in the second experiment (Figure 3.18B). Thus, the proportions of differentiated THP-1 infected following treatment with the different concentrations of amphotericin B or 700022, 700107, 700136 or 700240 are shown separately before a % infected normalized to the control for each experiment is shown in Figure 3.18B.

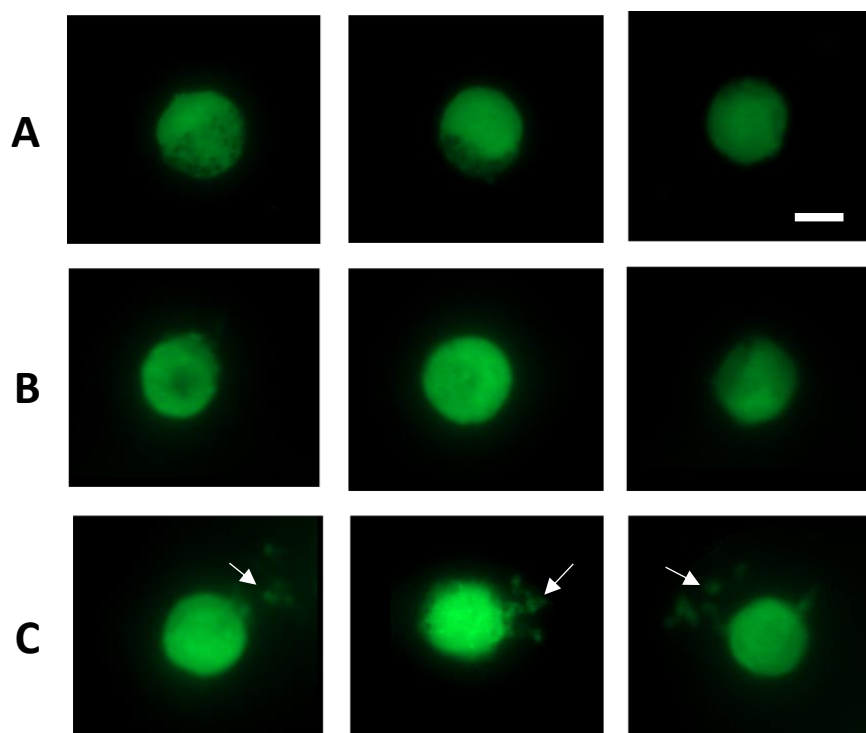


Figure 3.17: Scoring *L. mexicana* infected THP-1. The panels represent fluorescent imaging of Sybr Green I staining of nuclear material imaged using an EVOS fluorescence imaging system. (A) Images from the uninfected differentiated THP-1 control. Images from the 0.75 μ M amphotericin B treatment of infected differentiated THP-1 where (B) intracellular *L. mexicana* amastigotes are not evident or (C) are evident (white arrows). Bar = 100 μ m.

The potency of amphotericin B against intramacrophage parasites is evident from an apparent 60% reduction in infected THP-1 when exposed to a 1xEC₅₀ concentration of this drug and greater than 90% reduction at a 3xEC₅₀ concentration (Figure 3.18C). All four of the selected Phyt PURE compounds show some evidence of a concentration-dependent reduction in the proportion of infected THP-1 cells, particularly when the effects between 9x and 1x the EC₅₀ concentration are compared and at a 9xEC₅₀ concentration all these compounds reduce the proportion of infected THP-1 by greater than 70%. Clearly, however, these compounds do not appear to cause the same extent of effect in the two biological

replicates presented here (Figure 3.18 A and B) and illustrates a challenge in biological repeats of this assay method.

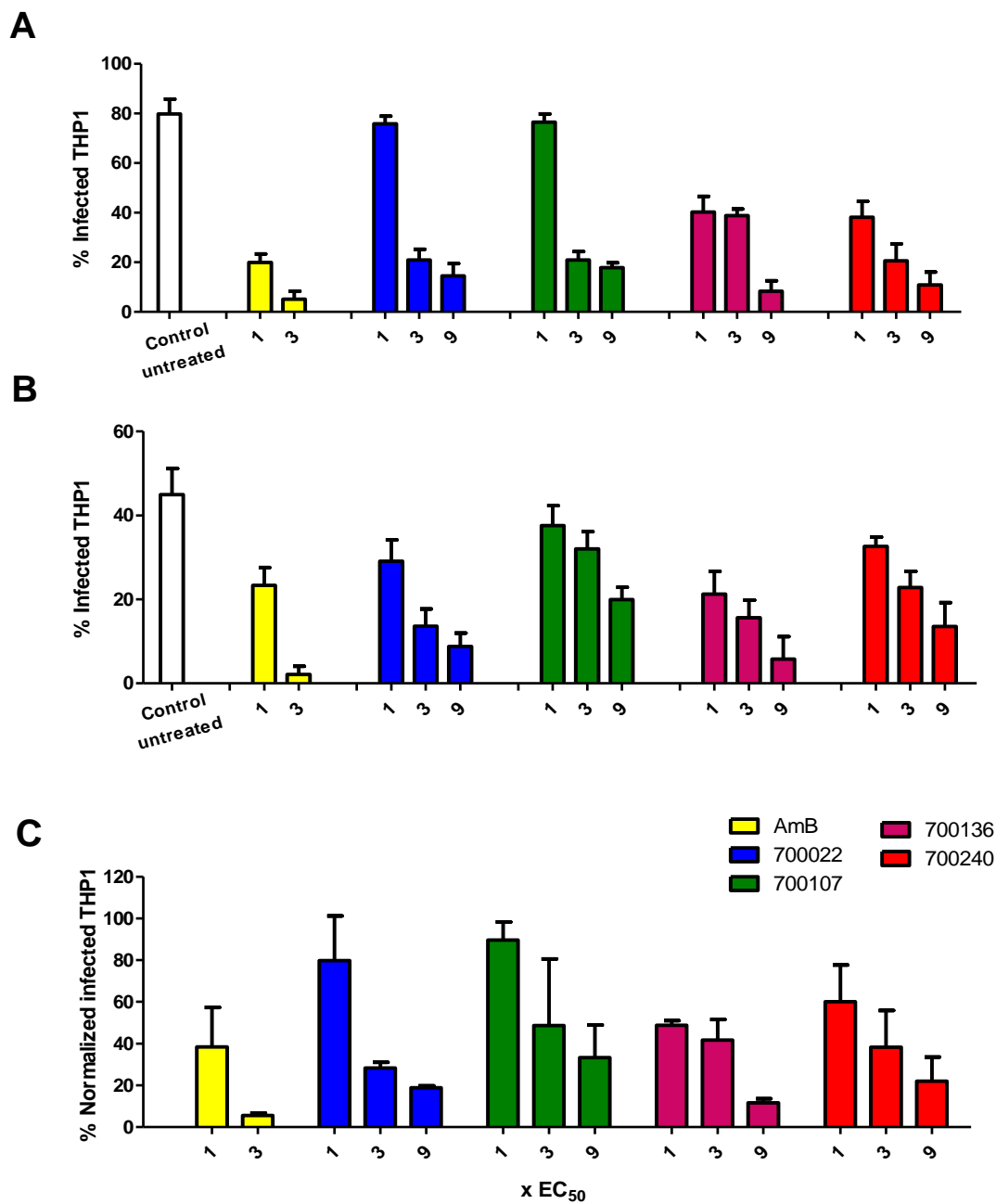


Figure 3.18: Compounds 700022, 700107, 700136 and 700240 are effective against *L. mexicana* intramacrophage amastigotes. (A and B) illustrate the proportion of differentiated THP-1 that show evidence of intramacrophage amastigotes following exposure to the fold EC₅₀ concentration of amphotericin B (AmB) or the four Phytoquest compounds from two independent biological repeats.

Each graph represents the mean \pm range from two technical repeats. (C) Illustrates these two data sets, normalized in each case against their respective mean untreated control, combined together to show the mean \pm StDev (n=4).

To explore whether in addition to a reduction in the proportion of THP-1 infected with *L. mexicana*, I explored whether there was also a reduction in parasite burden per infected THP-1 cell. To do this, the number of the punctate signals representing the nuclei of *L. mexicana* intramacrophage amastigotes peripheral to the infected THP-1 nucleus were counted. For the cultures exposed to no treatment or 1xEC₅₀ concentrations of amphotericin B or the four Phytopure compounds, the total of punctate signals from 95 infected THP-1 were counted. As the proportion of infected THP-1 decreased with increasing concentration of test compounds, the total number of cells counted decreased (the lowest was 15 infected THP-1 following exposure to 3xEC₅₀ concentration of amphotericin B). The distribution of these parasite counts per infected THP-1 is shown in Figure 3.19. Using a one-way ANOVA test of variance, a Dunnett's post-test revealed that significantly ($p < 0.05$) lower parasite counts, compared to the untreated control, were found only following exposure to 3xEC₅₀ concentrations of (i) amphotericin B, (ii) 700022 or (iii) 700136. As the 9xEC₅₀ concentration of all four Phytoquest compounds did not cause a significant reduction in parasite number per infected THP-1, some caution must be applied to these observations. Whilst a significant reduction in parasite numbers per infected THP-1 would be expected following exposure to a 3xEC₅₀ concentration of amphotericin B, there was no 9xEC₅₀ data measured to show if this trend was real.

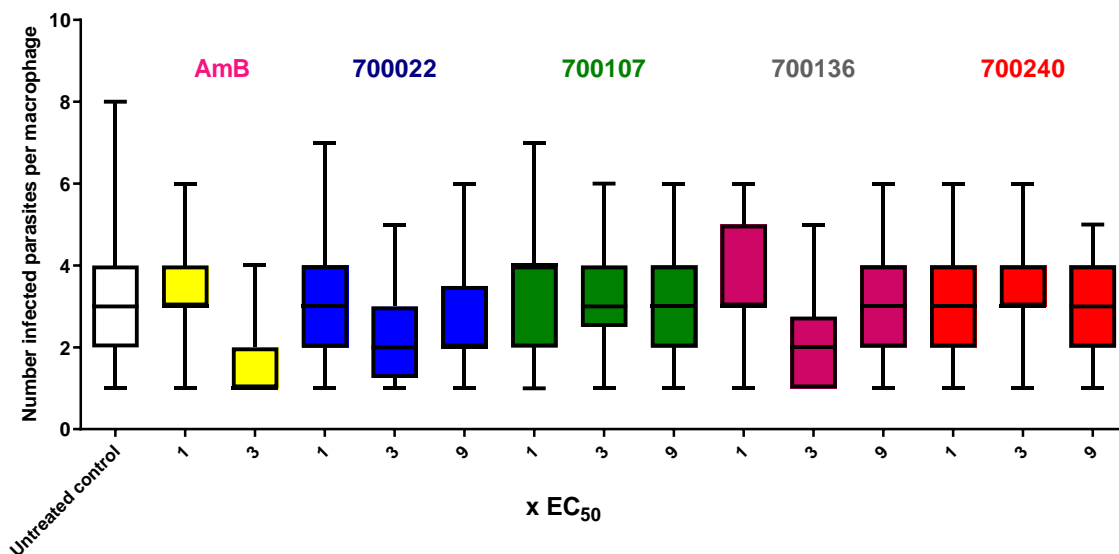


Figure 3.19: Distribution of *L. mexicana* parasite count in infected macrophages. Box and whisker plots of counts of intramacrophage amastigotes in infected differentiated THP-1 following exposure to the treatment shown on the x-axis. The box represents the 25-75% mean distribution with the central line as the mean. Whiskers show the total distribution of the counts of intramacrophage amastigotes. AmB; amphotericin B.

3.2.4 An investigation of the biophysical properties the of Phytopure compound hits

33 compounds with $EC_{50} < 2\mu\text{M}$ were identified against *L. mexicana*, *T. brucei* and *P. falciparum*. Key aspects of their physicochemical properties were determined using ChemDraw and Molinspiration software and are shown in Table 3.11. The reported biophysical properties for these compounds are important with regards to their potential as drug development targets that will be orally bioavailable (Oprea, 2002). A rule of five (Ro5) to determine if a chemical compound has biophysical properties that would predict for oral availability of drugs in humans was derived by Lipinski *et al.* (2001). The Ro5 is used to predict an orally active drug depends on the following physicochemical criteria:

- a molecular weight of less than 500 Daltons
- Less than 10 hydrogen bond acceptors (HBA)
- No more than 5 hydrogen bond donors (HBD)
- An octanol-water partition coefficient (LogP) of less than 5

Thus, if any compound follows these conditions: $MW > 500$, $\text{LogP} > 5$, $\text{HBD} > 5$, and $\text{HBA} > 10$, this would predict that this compound would have poorer membrane permeability or absorption properties in the human gut. Additional rules for predicting bioavailability were later suggested by Veber *et al.* (2002), they assessed three additional parameters for assessing structural properties that were linked to increased oral bioavailability in rats in an analysis of over 1100 drug candidates, specifically: the number of rotatable bonds ($\text{nrotb} < 5$), total polar surface area ($\text{PSA} \leq 140 \text{ \AA}^2$) and a total hydrogen bond count (sum of H-bond acceptors and donors) of ≤ 12 . Of the 33 compounds listed here, 22 compounds follow all of the Ro5 and Veber's rules (Table 3.11), 5 compounds violated one rule, 4 compounds violated two and 2 compounds exhibited three violations.

Table 3.11: Exploring 33 compounds properties depending on Lipinski's Rule of Five and Veber's rules.

ID	LogP	TPSA (Å ²)	MW	HBA	HBD	nrotb	Volume (Å ³)	violations
700014	6.25	17.07	284.44	1	0	2	298.26	1
700022	6.61	66.76	468.68	4	2	3	468.05	1
700035	2.28	252.53	822.85	18	5	14	723.17	2
700042	1.41	232.68	736.76	16	6	10	640.52	3
700046	1.79	238.75	778.8	17	5	13	677.03	2
700048	2.5	244.83	820.84	18	4	15	713.54	2
700104	3.23	244.83	846.88	18	4	14	740.45	2
700107	6.61	66.76	468.68	4	2	3	468.05	1
700136	6.43	63.6	466.66	4	1	3	462.19	1
700240	5.89	71.44	468.68	4	1	5	472.74	1
700585	2.56	107.7	357.34	7	0	3	305.27	0
700586	0.73	107.97	286.24	6	3	1	232.12	0
700756	4.89	72.84	346.42	5	1	4	332.24	0
701044	2.82	52.61	256.26	4	0	4	233.9	0
701082	5.83	255.04	824.74	17	5	16	690.8	3
701145	2.82	102.3	374.39	7	2	6	332.21	0
701154	2.82	102.3	374.39	7	2	6	332.21	0
701155	1.05	69.68	304.34	5	0	2	277.3	0
701157	1.96	69.68	332.4	5	0	3	310.69	0
701158	2.46	69.68	346.42	5	0	4	327.5	0
701159	0.96	93.07	378.46	6	2	6	358.42	0
701210	0.9	93.07	346.38	6	2	4	314.38	0
701212	2.14	72.84	330.38	5	1	3	306.12	0
701241	3.38	17.06	169.2	1	0	1	166.97	0
701249	3.03	17.07	168.19	1	0	1	163.88	0
701250	2.76	17.07	202.28	1	0	2	187.28	0
701252	2.22	26.3	186.21	2	0	2	178.13	0
701253	2.39	17.07	202.28	1	0	3	187.39	0
701256	3.13	17.07	216.31	1	0	3	204.08	0
701259	3.64	17.07	230.33	1	0	4	220.88	0
701262	3.5	17.07	230.33	1	0	3	220.67	0
701273	3.54	17.07	230.33	1	0	3	220.64	0
701286	4.13	17.07	234.3	1	0	1	229.7	0

3.3 Discussion

I report here the screen of 643 Phytopure library compounds against intraerythrocytic *Plasmodium falciparum*, the blood-stream form of *Trypanosoma brucei brucei* and axenic amastigotes of *Leishmania mexicana* to determine their inhibitory effects. These initial screens are followed up with assays against human cell lines to establish whether there is selectivity for the compound against the parasite in question. In the discussion I will address the results of each parasite screen and then do a comparison of data across the three parasite species tested.

3.3.1 Intraerythrocytic *P. falciparum*:

Twelve compounds were shown to have activity against intraerythrocytic asexual stages of *P. falciparum* with EC₅₀ values <6 µM. Of these 12 compounds, compounds 700035, 700042, 700046 and 700048 from *Phyllanthus accuminatus* were identified (Table 3.4). Previous studies have reported the activity of extracts from *Phyllanthus* spp. against a range of pathogens (Mao *et al.*, 2016). The extracts of *Phyllanthus emblica* exhibit activities against *P. falciparum* with EC₅₀ values ranging between 0.25 to 15.4 µg/ml, and with selectivity indices (SI) ranging from between from 11 to 17 against the monkey kidney epithelial Vero cell line (Pinmai *et al.*, 2010). Likewise, extracts of *Phyllanthus simplex* show activity against *Trypanosoma evansi* with an EC₅₀ value of 96 µg/ml, although these appear toxic as there is an SI of 1 when compared to the human MRC-5 cell line (Bawn, 2010). Aqueous extracts from *Phyllanthus amarus* and *Phyllanthus muellerianus* have antileishmanial activities (Onocha *et al.*, 2010) with an aqueous extract from *Phyllanthus orbicularis* showing antiviral activity against bovine and human infective viruses (del Barrio and Parra, 2000). Of note is the antiviral activities of a range of sesquiterpenoid glycosides (for example

phyllaembicillin C) that are structurally related to the four phyllanthocins identified in this study (Lv *et al.*, 2014; Zhang *et al.*, 2000).

In general, the 12 selected compounds either showed low levels of selectivity against *P. falciparum* over the human HepG2 line – or where selectivity was demonstrated (eg. for 700046 or 700104), the absolute CC_{50} value of $<10\mu\text{M}$ suggested the compounds were broadly toxic to humans. The only compound of relative interest left was the taxane 700535 from the English Yew (*Taxus baccata*) tree, which showed selective activity against *P. falciparum* with SI (16-22), but with a CC_{50} against HepG2 of $52\mu\text{M}$ (Table 3.5). Whilst extracts of *T. baccata* have been shown to have antimicrobial properties (Erdemoglu and Sener, 2001), the best known medicinal use of this tree is from the microtubule-targeting drug paclitaxel, with a structure similar to 7000535, which is widely used as an anticancer drug.

Using the BRRoK assays to determine the immediate cytotoxic effect of these twelve compounds showed that they, in general, showed an immediate cytotoxic effect *in vitro*. Given that there were two flavonoids, five sesquiterpenes and four sesquiterpenoid glycosides (phyllanthocins), the initial cytotoxic activities of each were compared to others with related structures (Figure 3.20). Whilst the initial rate of kill for the two related flavonoids (both flavanol subclass), there are some distinct structural differences of 700631 and 701082 outside of the flavanol core structure that may mean that they are not acting on the same target. Interestingly, of the five sesquiterpenes, the four most closely related; 701155, 701157, 701158 and 701159, which are all guaianolides isolated from *Arnica montana* are structurally similar to 11,13-Dehydromatricarin (Kraft *et al.*, 2003) of *Artemisia afra* with an antiparasitic EC_{50} of $12.5\mu\text{g/ml}$ in Dd2 parasites. These four guaianolides are structurally distinct to the less potent 700278 sesquiterpene from the Dwarf sunflower (*Helianthus annuus*), and show a distinct initial rate of cytotoxic activity which suggests that these two groups of compounds have distinct targets in the parasite. The similar initial rates

of kill for three of the four sesquiterpenoid glycosides; 700046, 700048 and 700104 isolated from *P. accuminatus* appears distinct to 700042 – which is also isolated from *P. accuminatus* and is closely structurally related. This would suggest that 700046, 700048 and 700104, at least, share a similar target in the parasite.

Ten synthetic compounds (701249, 701250, 701251, 701252, 701253, 701256, 701259, 701262, 701273 and 701286) were provided by PhytoQuest Ltd after the *P. falciparum* screen; hence only 631 compounds were tested. However, as these compounds showed high toxicity against HepG2 cells (Table 3.6) in later work, I did not determine their antiplasmodial effect.

Target Candidate Profiles (TCP) for potential compounds to be included in future antimalarial drugs have been developed by the Medicine for Malaria Venture (Burrows *et al.*, 2017; Burrows *et al.*, 2013). For all the compounds identified as hits against *P. falciparum*, these hits are neither potent enough nor selective enough to warrant further investigation here. Compound 700046 was by far the most potent hit, with EC₅₀ potency in the 30-50nM range. Unfortunately it was quite toxic to the human cell line HepG2 (CC₅₀ of 2µM) and with a molecular mass of >500 and 17 hydrogen bond acceptors, it fails two of the Ro5 criteria to predict a compound that would be orally bioavailable.

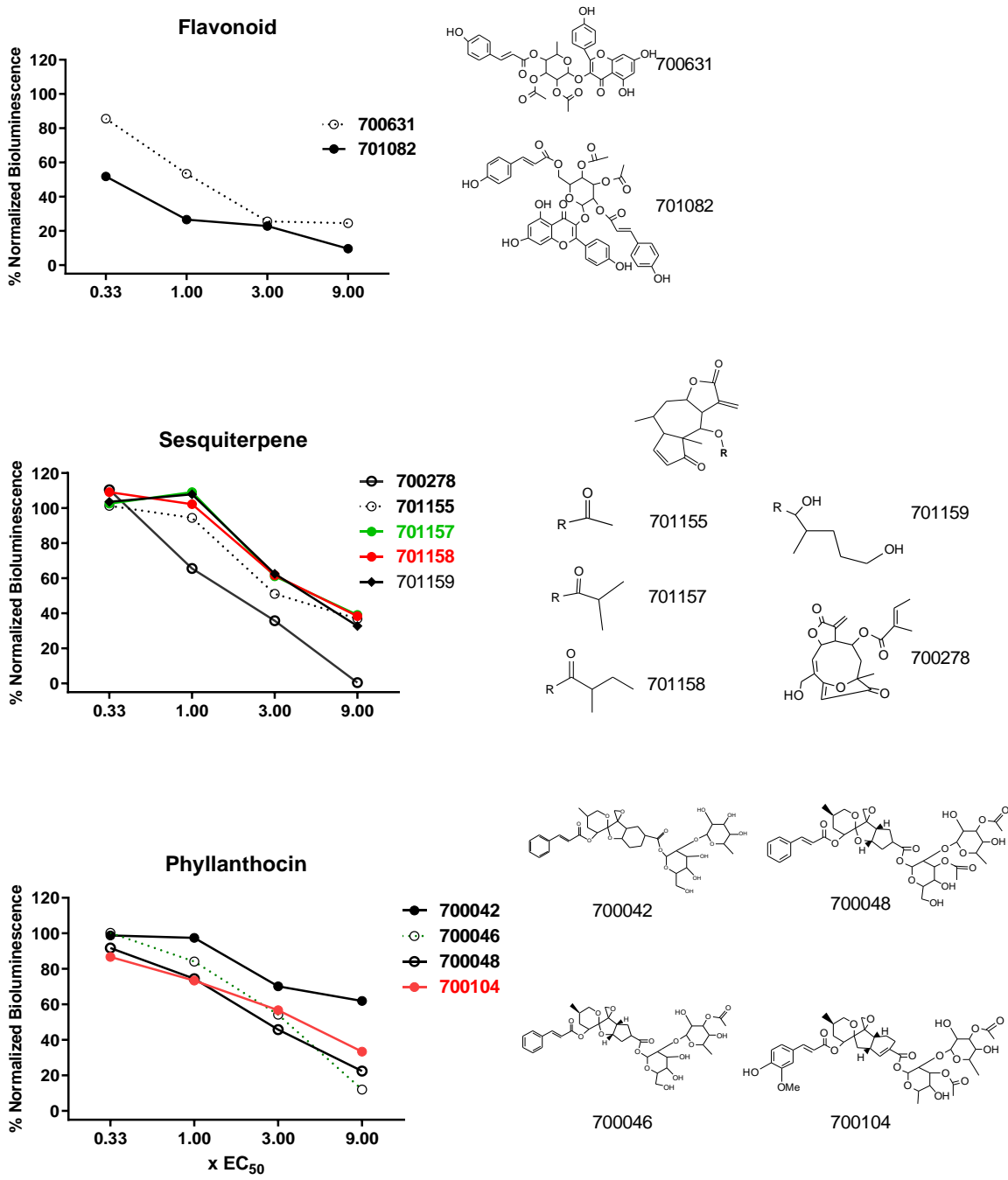


Figure 3.20: Comparison of 6 hours BRRoK data for structurally related Phytopure compounds.

Comparison of mean normalized bioluminescence signals (from Figure 3.7) clustered by compound structure. Structures for the indicated compounds are shown to the right.

3.3.2 *T. brucei* bloodstream stages:

The criteria used to define a hit in this screen was a >50% inhibition of growth at 2 μM , this criteria providing 25 hits. The EC_{50} of these compounds ranged from 0.16 to 2.71 μM , indicating a good range of potency against the bloodstream form of *T. brucei*, although the majority of these compounds (21 of 25) did not show appreciable selectivity for the parasite over the HepG2 cell line (SI values between 0.2 and 13.5). Only three compounds showed a selectivity for the parasite over HepG2 that was at least as good as that for pentamidine (benchmark antitrypanosomal SI 26.7 see Table 3.6). These were; (i) 700014 an abietic diterpene from *Abies procera* (SI of 35.8), (ii) 700035 a sesquiterpenoid glycoside from *P. acuminatus* (SI of 43.3) that is structurally closely related to the four sesquiterpene glycosides that are hits for *P. falciparum* and although 700035 has a similar HepG2 CC_{50} to these other four compounds, there appears to be some exclusivity between the sesquiterpene glycosides targeting *P. falciparum* or *T. brucei*, but not both (iii) and 701145 a sesquiterpenoid from *Menyanthes trifoliata* with an SI 53.5. Previous studies revealed that the extracts of Noble fir (*Abies procera*) from North America showed potent activity against *T. brucei*, >99% kill, at 20 $\mu\text{g}/\text{mL}$ (Jain *et al.*, 2016). The related dehydroabietic acid also shows activity against kinetoplastid parasites; for example, derivatives of dehydroabietic acid were screened against *L. donovani* and *T. cruzi*, with EC_{50} values ranging between 2.3 and 9 μM against *L. donovani*, while 1.4 and 5.8 μM against *T. cruzi*, as well as demonstrating good selectivity against the THP-1 cell line (Vahermo *et al.*, 2016). The abietane quinone P-1 showed activity against extracellular and intracellular of *L. braziliensis*, *L. infantum* and *T. cruzi* with EC_{50} values ranging between 14.2 and 24.5 μM (Ramírez-Macías *et al.*, 2012).

There is an urgent demand for new antitrypanosomal drugs to treat both human African trypanosomiasis (HAT) as well as American trypanosomiasis, Chagas disease (Field *et al.*, 2017 and Scarim *et al.*, 2018; Cullen and Mocerino, 2017). Challenges include resistance to

current drugs, toxicity as well as new classes of drugs that can effectively cross the blood brain barrier to target the advanced disease stage where the central nervous system is affected. As shown above, the classes of compounds described as hits here have been reported in the literature. These data were also developed at the same time as the *L. mexicana* screen, and given the progress in that area (see next section), work on *T. brucei* was halted for lack of time.

3.3.3 *L. mexicana* parasites:

Due to the potency of the Phytopure compounds against *L. mexicana* axenic amastigotes, an increased threshold of greater than 80% inhibition in parasite growth at 2 μ was used here to prioritize 23 hits. The EC₅₀ values determined ranged between 0.15 and 1.38 μ M, with the improved potency a reflection of the higher criteria being applied. The inhibitory effect of these 23 compounds was first established against the human cell line (THP-1) used to produce macrophages for intramacrophage assays. This data showed that 19 of these compounds displayed cytotoxicity with low SI values <6.7. The four compounds 700022, 700107, 700136 and 700240 remaining displayed both the best potency and selectivity of the hits (SI > 27) (Table 3.8). These compounds also showed good selectivity when compared to a second, HepG2, human cell line. All four compounds are structurally related triterpenes isolated from the Noble Fir (*Abies procera*) or Grand fir (*Abies grandis*) see table 3.9) with EC₅₀ between 0.24 to 0.5 μ M, activities similar to that of amphotericin B (Table 3.8 and 3.10). These four triterpenes are steroid like in structure, with 700022, 700107 and 700136 structurally related to cardenolides such as digitoxigenin and ouabain. These cardenolides, through targeting of sodium-potassium pumps can be toxic to humans through their effect on cardiac cells (cells not tested here), although ouabain is not toxic to *L. amazonensis* (De Almeida-Amaral *et al.*, 2008). Disappointingly, these compounds did not

show the same activity against *P. falciparum* as the new generation of PfATP4 targeting drugs (Spillman *et al.*, 2013) which disrupt sodium ion transport. An evaluation of these cardenolides synergy with spiro indolines may have been interesting.

Triterpene compounds have previously reported to have antileishmanial activity, such as ursolic acid was used to eliminate *L. amazonensis* promastigotes with an EC₅₀ of 6.4 µg/mL (Yamamoto *et al.*, 2015). Also, these correlate with previously published of quinonemethide triterpenes (maytenin and pristimerin) presented antileishmanial activity with an EC₅₀ values <0.88 nM and antitrypanosomal activity with an EC₅₀ <0.3 nM, these compounds showed low toxicity against BALB/c macrophages for *L. amazonensis* and *L. chagasi* according to SI values 243.65 and 46.61 for maytenin and 193.63 and 23.85 for pristimerin (Dos Santos *et al.*, 2013). The activity of triterpenes compounds (700022, 700107, 700136 and 700240) were also evaluated on HepG2 cell line and exhibited less toxicity against these mammalian cells (Table 3.10). The lack of toxicity of these compounds at the doses used in human cell line and that is consistent with the previously study of triterpenes such as ursolic acid and oleanolic acid (isolated from leaves of *Petiveria alliaceae*) were showed low toxicity against different experimental models (Yamamoto *et al.*, 2015).

The antileishmanial activity of these four triterpene compounds was further confirmed against intracellular *L. mexicana* amastigotes in a cellular image-based intramacrophage assay. To be active against intracellular parasite, compounds must be able to cross membrane barriers (cellular membrane of the macrophage and phagolysosome vacuole membrane) and maintain stability in the presence of reactive oxygen species in the phagolysosome environment and under low pH- all these factors increase the attrition rate of axenic amastigote hits when compared to the amastigote intracellular assay (Siqueira-Neto *et al.*, 2012). The microscopic counting assay used here determined the proportion of parasite-infected THP-1 cells, an assay that required the counting of parasite nuclei adjacent to the

macrophage nuclei. Some caution must be applied to our interpretation of the assay data here as this assay has limitations based on the expertise of the user. That said, the experiments showed that the triterpene compounds exhibited some efficacy against intracellular *L. mexicana* infection at a 9xEC₅₀ concentration. For instance, compounds 700022 and 700136 showed activity against intracellular infection at 9x EC₅₀, with an activity comparable to amphotericin B when used at 3x EC₅₀. Some reports have described that nitric oxide (NO) produced by macrophage cells inhibits intracellular amastigotes of *L. amazonensis* (Laurenti *et al.*, 2014; Campos *et al.*, 2015; Carneiro *et al.*, 2015) and that nitric oxide production can be triggered by natural products (Lin *et al.*, 2014). Previously, Yamamoto *et al.*, 2015 and You *et al.*, 2001 reported that the treatment of *L. amazonensis* infected macrophages with the steroidal triterpene (ursolic acid purified from *Petiveria alliaceae*) eliminated intracellular amastigotes as a result of nitric oxide in a dose-dependent manner. Moreover, ursolic acid and oleanolic acid isolated from *Pourouma guianensis* showed high activity against intracellular amastigotes of *L. amazonensis* with EC₅₀ values of 27 µg/ml and 11 µg/ml, respectively (Passero *et al.*, 2011). These studies show that triterpenes are able to eliminate parasites, suggesting that ursolic acid and oleanolic acid have multispectral action against *Leishmania* spp. In our study, the antileishmanial activity of these steroidal triterpene compounds isolated from the Noble Fir (*Abies procera*) represent a novel and interesting point to develop in the next chapter.

3.3.4 Comparison of activity across parasites tested – a cautionary note

To enable a comparison of potential cross-species activity, activity in any species was defined as an EC₅₀ < 2 µM. A list of these compounds is produced in Table 3.12 below. Comparison of activity in these parasites shows seven compounds (701154, 701159, 701250, 701252, 701259, 701262 and 701273) as demonstrating activity against both of the

kinetoplastids *T. brucei* and *L. mexicana* (Figure 3.21 green), four compounds (700042, 700046, 700048 and 701082) which were active in both *T. brucei* and *P. falciparum* (Figure 3.21 blue) and 3 compounds (701155, 701157 and 701158), all sesquiterpenoid glycosides isolated from *P. accuminatus* sesquiterpenes, exhibited significant activity against all three parasites tested (Figure 3.21 red).

One factor considered was that compounds that showed a broad activity across multiple parasites may in fact represent a general antiproliferative capacity that would reflect a toxicity challenge. Of note, the sesquiterpenoid glycosides 701155, 701157 and 701158 were toxic against HepG2 cell lines in this study, with related sesquiterpenoid lactones described as having broad antiparasitic activity but with limited selectivity (François *et al.* 1996; Pedersen *et al.*, 2009; Berger *et al.*, 2001; Villaescusa *et al.* 2000; Fuchino *et al.* 2001; Perez-Victoria *et al.* 1999; Koshimizu *et al.* 1994 and Mahiou *et al.* 1995). Compounds with selectivity indices of >20 for the parasite indicated when compared to human cell lines are indicated with boxes in Figure 3.21. These compounds are shown in boxes in Figure 3.21 and, except the dotted box for 700046 which was only selective in *P. falciparum* but also active against *T. brucei*, they all identify single species hits.

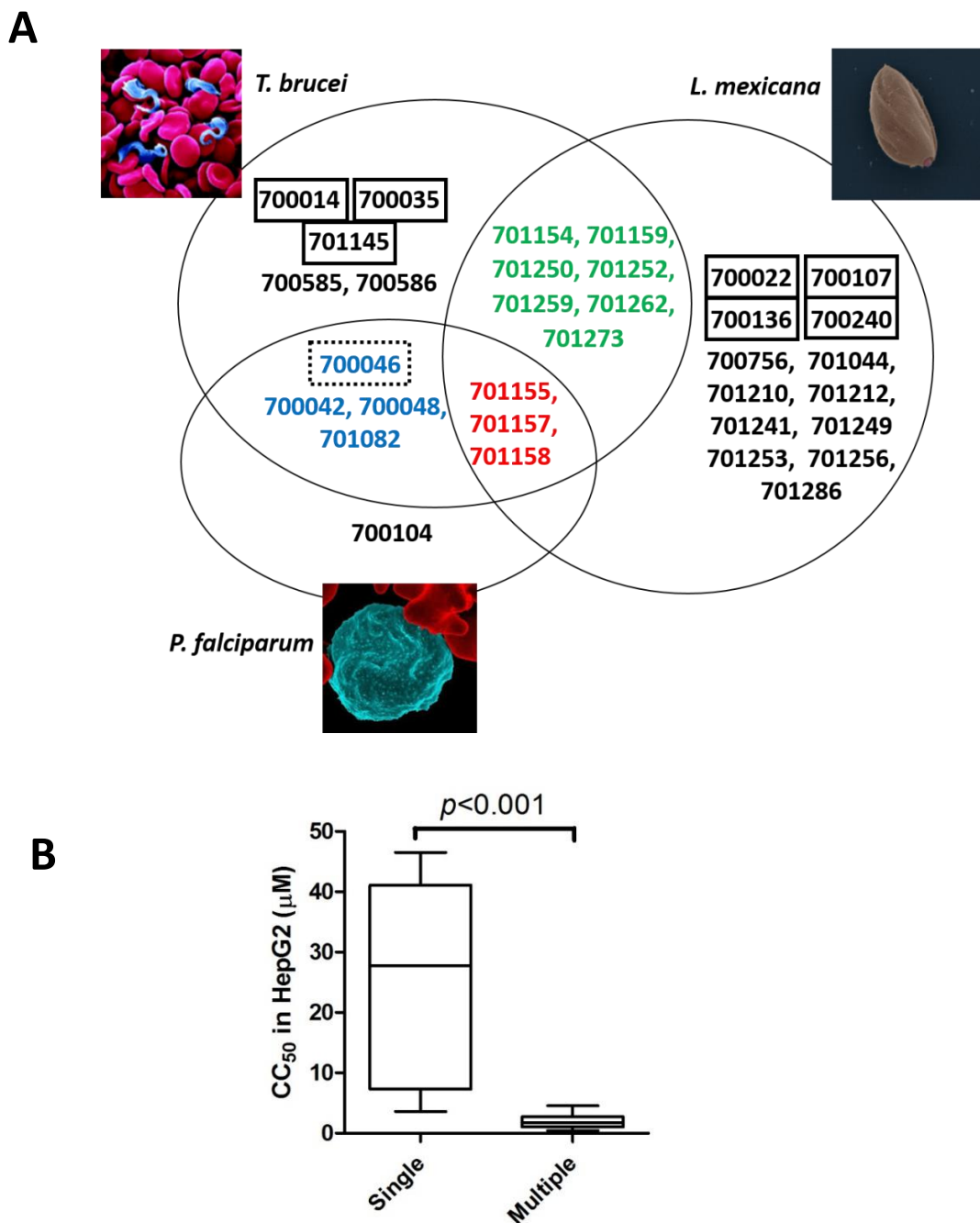


Figure 3.21: Phytopure compound activity across multiple species (A) A Venn diagram of the compounds identified to have an $EC_{50} < 2 \mu M$ activity in one or more of the indicated species (B) Bar chart reporting the distribution of HepG2 CC_{50} values of compounds that target a single species or multiple (two or three species) in this study. Boxes, compounds with selectivity indices of >20 . Dotted box, 700046 has a selectivity against *P. falciparum* and *T. brucei*. Significance is determined from an unpaired t-test of distribution.

Table 3.12: Table reporting most active compounds.

PQ number	Common name	Genus (species)	Plant part	Mwt	Formula	Class
700022	Noble fir	<i>Abies (procera)</i>	aerial parts	468.67	C30H44O4	triterpene
700107	Noble fir	<i>Abies (procera)</i>	aerial parts	468.67	C30H44O4	triterpene
700136	Noble fir	<i>Abies (procera)</i>	aerial parts	466.66	C30H42O4	triterpene
700014	Noble fir	<i>Abies (procera)</i>	aerial parts	284.44	C20H28O	abietic diterpene
700240	Grand fir	<i>Abies (grandis)</i>	branch	468.67	C30H44O4	triterpene
700035		<i>Phyllanthus (acuminatus)</i>	aerial parts	822.85	C40H54O18	phyllanthocin
700104		<i>Phyllanthus (acuminatus)</i>	aerial parts	846.87	C42H54O18	phyllanthocin
700046		<i>Phyllanthus (acuminatus)</i>	aerial parts	778.80	C38H50O17	phyllanthocin
700042		<i>Phyllanthus (acuminatus)</i>	aerial parts	736.76	C36H48O16	phyllanthocin
700048		<i>Phyllanthus (acuminatus)</i>	aerial parts	820.83	C40H52O18	phyllanthocin
701082		<i>Phyllanthus (acuminatus)</i>	aerial parts	824.74	C43H36O17	flavonoid
700585	Common horsetail	<i>Equisetum (arvense)</i>	aerial parts	344.31	C18H16O7	flavonoid
700586	Common horsetail	<i>Equisetum (arvense)</i>	aerial parts	286.23	C15H10O6	flavonoid
700756	Hemp agrimony	<i>Eupatorium (cannabinum)</i>	aerial parts	346.42	C20H26O5	sesquiterpene
701145	Bogbean	<i>Menyanthes (trifoliata)</i>	Fruit & seed	374.38	C20H22O7	sesquiterpene
701154	Arnica	<i>Arnica (montana)</i>	flowers	304.34	C17H20O5	sesquiterpene
701155	Arnica	<i>Arnica (montana)</i>	flowers	304.3	C17H20O5	sesquiterpene
701157	Arnica	<i>Arnica (montana)</i>	flowers	332.4	C19H24O5	sesquiterpene
701158	Arnica	<i>Arnica (montana)</i>	flowers	346.42	C20H26O5	sesquiterpene
701159	Arnica	<i>Arnica (montana)</i>	flowers	378.46	C21H30O6	sesquiterpene
701210	Artichoke	<i>Cynara (cardunculus)</i>	leaves	346.37	C19H22O6	sesquiterpene
701212	Artichoke	<i>Cynara (cardunculus)</i>	leaves	330.38	C19H22O5	sesquiterpene

701044	Marguerite	<i>Argyranthemum (frutescens)</i>	roots	256.257	C15H12O4	aromatic
701241	Corn marigold	<i>Segetum (Chrysanthemum)</i>	whole plant	170.211	C12H10O	aromatic
701249	Corn marigold	<i>Segetum (Chrysanthemum)</i>	whole plant	168.195	C12H8O	aromatic
701250	Synthetic			202.275	C12H10OS	aromatic
701252	Synthetic			186.21	C12H10O2	aromatic
701253	Synthetic			202.275	C12H10OS	aromatic
701256	Synthetic			216.302	C13H12OS	aromatic
701259	Synthetic			230.329	C14H14OS	aromatic
701262	Synthetic			230.329	C14H14OS	aromatic
701273	Synthetic			230.329	C14H14OS	aromatic
701286	Synthetic			234.298	C17H14O	aromatic

Chapter 4: Initial studies exploring the action of, and resistance to, compound 700022 in *Leishmania mexicana*.

4.1 Introduction

For more than 70 years, the antimonials glucantime and Pentostam (SbV) were used as a first-line therapy across South America, North Africa, Turkey, Bangladesh, and Nepal for the treatment of all forms of leishmaniasis (Franco *et al.*, 2016). The second-line therapy against visceral leishmaniasis is based on the use of amphotericin B or pentamidine (Kumar *et al.*, 2011; Sundar *et al.*, 2015). Local variations in the use of antileishmanial drugs are due to regional increases in the number cases of primary resistance, or several in relapses after several courses of treatment (Burza *et al.*, 2014; Sundar and Chakravarty, 2015). In 2002, the efficacy of miltefosine was recognised with a registration in India as the first oral treatment for visceral leishmaniasis (Dorlo *et al.*, 2012). Although miltefosine displays good efficacy, its use can lead to serious adverse effects on the liver and kidney (de Menezes *et al.*, 2015). More recently, the liposomal preparation of amphotericin B, has been used as a first-line treatment in Asia, Africa and Europe (WHO, 2010).

Despite their widespread use, the mechanism of action for these drugs against different leishmania spp. is relatively poorly understood (Gazanion *et al.*, 2016). The amphotericin B mode of action appears to be primarily mediated through the generation of channel-like pores spanning the lipid bilayer after binding to ergosterol (the main sterol in the membrane), resulting in an increase in permeability for protons and monovalent cations as K^+ , Ca^{2+} , and Mg^{2+} , hence leading to cells death (Pourshafie *et al.*, 2004; Romero *et al.*, 2009). Similarly, several studies suggest that miltefosine is able to target glycosylphosphatidylinositol (GPI) biosynthesis, and the interference with other phospholipid metabolisms through the

inhibition of alkyl lysophosphatidylcholine specific acyltransferase (Luque-Ortega and Rivas, 2007; Rakotomanga *et al.*, 2007). The effects of miltefosine treatment on lipid modifications in promastigotes of *L. donovani* have also been observed to diminishing phosphatidylcholine (PC), while sphingolipids and sterols increased (Rakotomanga *et al.*, 2007; Armitage *et al.*, 2018). To study the viability of *L. major* promastigotes without sphingolipid biosynthesis through loss of the serine palmitoyl transferase gene (Δ LCB2) were matched by substantial alterations in sterol content. These data indicate that sphingolipids and ergosterol are important for miltefosine sensitivity and presented 3-fold less sensitive to miltefosine than wild-type parasites (Denny *et al.*, 2004; Zhang *et al.*, 2007). It was suggested that the ergosterol of the Leishmania plasma membrane replaces cholesterol as the primary membrane sterol, could enable this (Fridberg *et al.*, 2008).

Given that both amphotericin B and miltefosine affect lipids in cellular membranes, research on their mode of resistance typically explores changes in lipid profiles in resistant parasites (Mbongo *et al.*, 1998; Barratt *et al.*, 2009).

Generating drug resistant parasites has been used to study the mechanism of action of antileishmanial drugs, and has contributed to identification of drug resistance gene loci in parasitic protozoa following whole genome sequencing (Muller and Hemphill, 2011; Hefnawy *et al.*, 2017). Drug resistance associated with a decrease in the effectiveness of antileishmanial drugs may be the result of either natural or adaptive changes to the genetic structure of the parasite, enabling the selection of appropriate protective mechanisms against these drugs. These genetic changes include alterations in the gene encoding the primary drug target, such as mutations, rearrangements, or amplifications that lead to variation in the level of gene expression or the development/recruitment of existing processes to reduce exposure to the drug, such as efflux pathways (Vanaerschot *et al.*, 2014; Garcia-Hernandez *et al.*, 2015). To explore drug action and resistance pathways *in vitro*, drug resistant lines can be

obtained by chemical mutagenesis followed by selection by the drug of interest, or by culturing wild-type parasites under a stepwise increase in the drug concentration, selecting resistant parasites that arise as a result of the plasticity of the genome (Laffitte *et al.*, 2016). New techniques for expediting the identification of drug targets and resistance mechanisms in leishmania would aid the reassessment of current antileishmanial drugs and the development of new effective drugs (Hefnawy *et al.*, 2017). Recently, functional cloning has been successfully applied for identification of drug target and resistance in leishmania (Clos and Choudhury, 2006; Gazanion *et al.*, 2016). Cosmid-based functional cloning have been applied to study mutants defective in the biosynthesis of lipophosphoglycan (LPG) in *L. donovani* (Ryan *et al.*, 1993) and later successfully implemented for isolating nucleoside transporters (Vasudevan *et al.*, 1998; Carter *et al.*, 2000) and a miltefosine translocator (Pérez-Victoria *et al.*, 2003). Similarly, genes involved within phospholipid translocation and ergosterol biosynthesis contribute to miltefosine resistance in *L. infantum* (Gazanion *et al.*, 2016). This approach has also been used to study mechanisms of drug resistance. Examples include, the isolation of a novel protein (which belongs to the superfamily of leucine-rich repeat (LRR) proteins) that is linked to antimonial resistance in *L. infantum* amastigotes (Genest *et al.*, 2008), modulation of the aquaglyceroporin AQP1 transcript levels as a key determinant in the accumulation of antimonials in leishmania resistant lines (Marquis *et al.*, 2005), and isolation of genes involved directly in resistance to antifolates in *L. tarentolae* (Kündig *et al.*, 1999). Next-generation sequencing (NGS) technologies are also being used to identify drug targets and elucidate drug resistance mechanisms (Horn and Duraisingh 2014). In *Leishmania* spp., copy number variation and single-nucleotide polymorphism were detected in miltefosine drug-resistant parasites using NGS (Downing *et al.*, 2011; Coelho *et al.*, 2012).

As an example of this, miltefosine resistance results from a reduction in the intracellular drug concentration as a result of an impairment to a miltefosine transporter complex (Perez Victoria *et al.*, 2006a). The acquisition of point mutations in the miltefosine transporter (MT) and/or an associated subunit Ros3 has been shown to drastically increase miltefosine resistance in *in vitro* and *in vivo* experiments (Figure 4.1) (Perez-Victoria *et al.*, 2006; Seifert *et al.*, 2007; Shaw *et al.*, 2016). *In vitro* studies in a *L. donovani* promastigote line resistant to miltefosine was generated by increasing drug pressure in stepwise selection process. The EC₅₀ value for the resulting miltefosine-resistant cells was 15 times higher than that for the original wild-type line (Perez-Victoria *et al.*, 2003b). In clinical isolates, a reduced expression of the MT-Ros3 complex has also been shown to represent a miltefosine-resistant marker in *L. braziliensis* strains (Sanchez-Canete *et al.*, 2009). Clinical resistance to miltefosine in *L. donovani* demonstrated a 10-fold-increase in EC₅₀ over clinically sensitive strains (Srivastava *et al.*, 2017).

Here I describe my initial studies that explore the action of compound 700022 against *L. mexicana*. This work includes the selection of a 700022 resistant line using a process of step-wise increases in exposure to 700022. The phenotype of wild-type and drug resistant parasites are also investigated using immunofluorescent (IF) assays and electron microscopy.

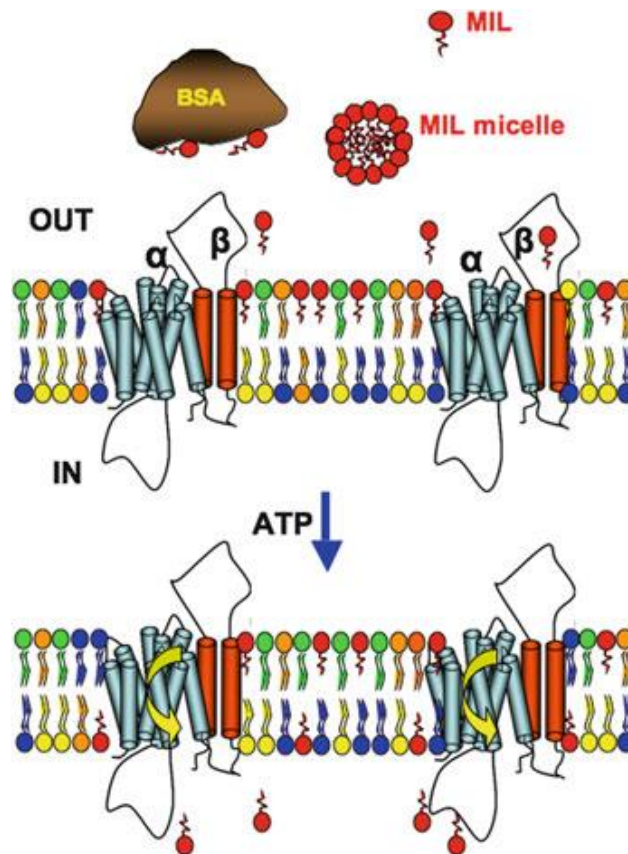


Figure 4.1: Binding and uptake of miltefosine (MIL) in *Leishmania* spp. A schematic representing the uptake of MIL across a membrane by the MT/Ros3 MIL transporter. The hydrophobic MIL is typically bound to serum albumin (represented here is a tissue culture system using bovine serum albumin, BSA) which acts as a reservoir. The translocation of MIL from the outer to the inner leaflet of the plasma membrane is facilitated by the *Leishmania* miltefosine transporter (MT), a P4-ATPase subfamily flipase shown here as the α -unit termed *L. donovani* miltefosine transporter (LdMT), with its β -subunit termed Ros3 (Perez-Victoria *et al.*, 2003).

4.2 Results

4.2.1 Generation of 700022-resistant *L. mexicana*

A *L. mexicana* (strain MNYC/BZ/62/M379) resistant to compound 700022 was obtained by propagating promastigotes *in vitro* under increasing selective pressure through a stepwise increase in exposure to 700022. At the start, *L. mexicana* promastigotes (termed here now as wild-type) at 1×10^6 cells/ml were exposed to 11.5 μ M of 700022 (the EC₅₀ value). *In vitro* promastigotes were passaged for a period of time, until the rate of growth increased to that typical of the wild-type strain not under drug selection. Thus, as the 700022-exposed parasites adapted to exposure to 700022, the period of time between each dilution back to an initial 1×10^6 cells/ml decreased. At this time, the EC₅₀ for 700022 promastigotes would be determined in an AlamarBlue assay. This data being used to start the next phase of selection. In subsequent rounds of selection, one culture of *L. mexicana* promastigotes would be maintained at the previous concentration (as well as an aliquot stored in liquid nitrogen) and two cultures exposed to a new increased concentration (based on the EC₅₀ for 700022 determined after the previous round of selection). Parasite lines at intermediate stages during each step of the selection were also stored in liquid nitrogen.

In this way, over a period of 28 weeks, *L. mexicana* promastigotes were serially exposed to 11.5 μ M, 20.5 μ M, 41 μ M, 77 μ M and finally 85.6 μ M of compound 700022 (Figure 4.2). This figure illustrates the windows of 700022-selection pressure over the timecourse of the resistance-selection experiment (Figure 4.2A). At each of the indicated points on Figure 4.2, the EC₅₀ of 700022 against the selected promastigotes was determined using Log concentration normalized response graphs. Examples of these are shown from weeks 0, 10, 15, 25 and 28 of the selection process – these data being used to determine the next phase of the incremental 700022-selection process (Figure 4.2B). At each of these timepoints, the

promastigotes were also transformed to provide axenic amastigotes, and the EC₅₀ of 700022 against this stage of the life cycle also determined (Figure 4.2C). Over the 28 weeks of increasing concentration selection process, a wild type *L. mexicana* (EC₅₀ promastigotes 11.5 μM, amastigotes 0.24 μM) was used to derive a 700022-resistant strain (EC₅₀ promastigotes 85.6 μM, amastigotes 10.1 μM) that provided a 7.5-fold and 42-fold increase in EC₅₀ potency in promastigotes and axenic amastigotes, respectively. This appears to be a stable resistance phenotype as promastigotes of the 700022-resistant line were cultured for 60 days in the absence of 700022 and the EC₅₀ measured at 10.23 μM and 86.54 μM for axenic amastigote and promastigote respectively (Figure 4.3).

Early during the selection process, at week 8, axenic promastigotes were derived from the promastigotes under selection and the EC₅₀ of the triterpene compounds 700107, 700136 and 70240 closely structurally related to 700022 were measured. Due to the limiting material (all remaining samples of these three compounds were used), this experiment had to be done with the more sensitive axenic amastigotes and could not be repeated later following additional selection with 700022. Assays were carried out using the AlamarBlue assay, each experiment carried out as technical triplicates and three independent biological repeats done. The mean ± Stdev of the normalized fluorescent response was plotted against log concentration (Figure 4.4) to allow EC₅₀ and their 95% confidence intervals to be determined and are reported in Table 4.1. Following 8 weeks of selection to 700022, the axenic amastigotes showed a 4.2-fold increase (RI, resistance index) in the EC₅₀ to 700022. At the same time, these 700022-selected parasites showed between a 4.1-5.3 RI for the three related triterpenes. This similar RI for all compounds, and their structural similarity, suggests that they likely share a similar mechanisms of resistance and mode of action.

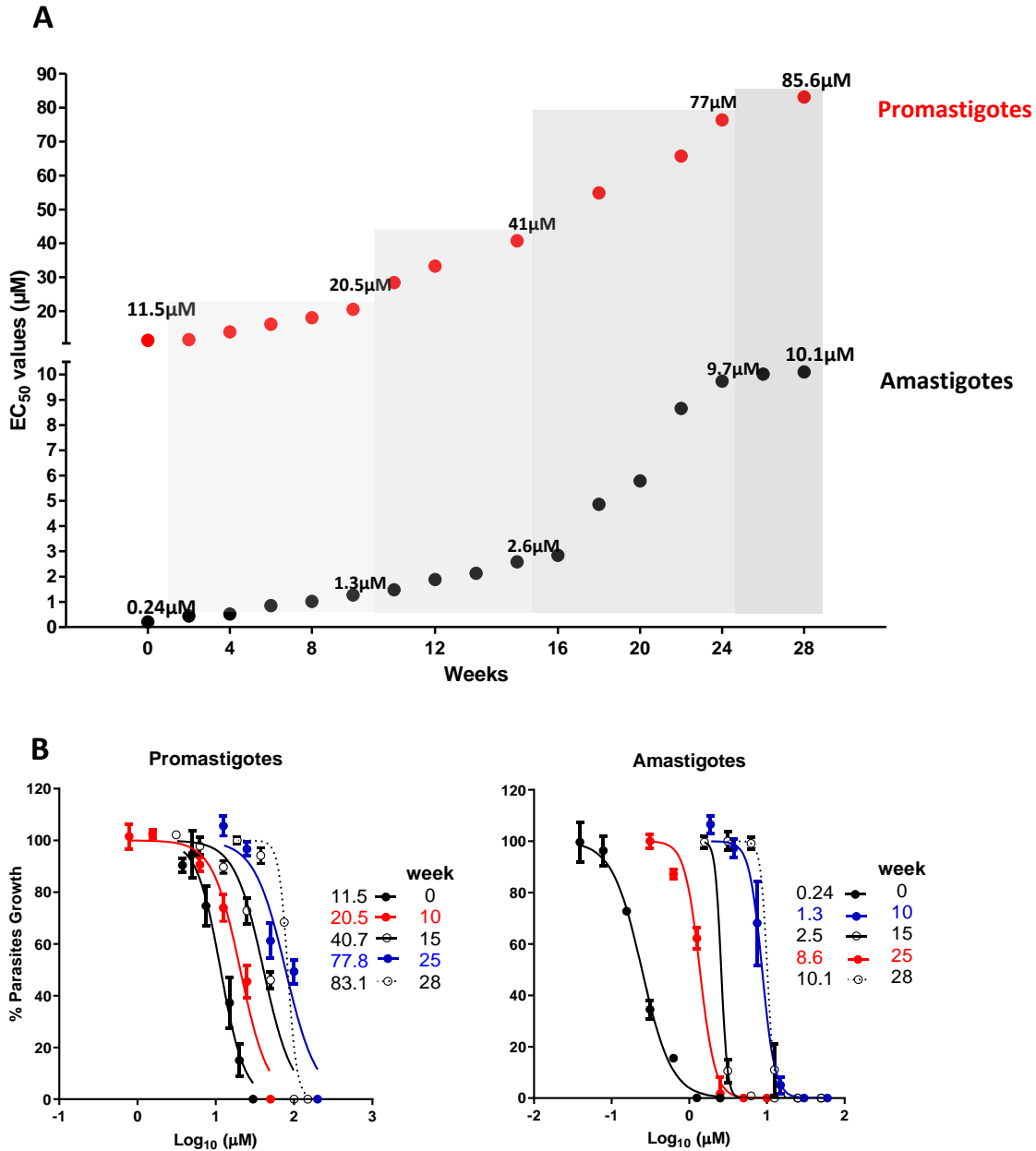


Figure 4.2: Selection of a 700022-resistant line in *L. mexicana*. (A) Promastigote cultures are exposed sequentially to the indicated concentration of 700022 (increasing tone of gray to show increase in concentration). These concentrations of 700022 are based on the EC₅₀ in promastigotes determined at start of week 0, 10, 15 and 25. At the indicated points (circles) the EC₅₀ of 700022 was determined in promastigotes (red, note y-axis is split with different concentration ranges indicated) or axenic amastigotes (black) prepared from the promastigote culture under selection. Log concentration normalized response graphs to determine the EC₅₀ in promastigotes (B) or axenic

amastigotes (C). The key indicates the weeks of selection as well as the EC_{50} (in μM). The mean \pm StDev (n=9) are reported.

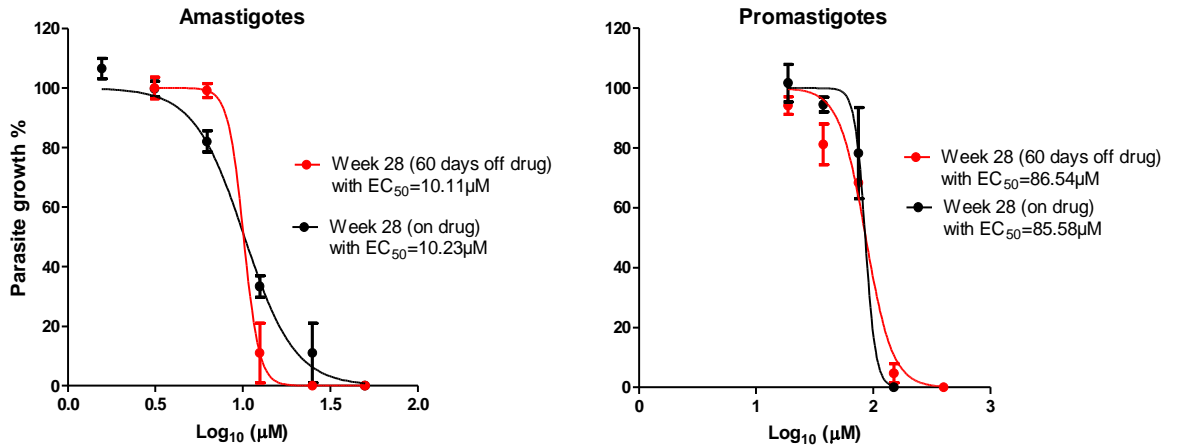


Figure 4.3: Observation of resistance stability for *L. mexicana* axenic amastigotes and promastigotes under compound pressure in stepwise concentrations after 28 weeks (black), and 60 days after removal from compound pressure (red).

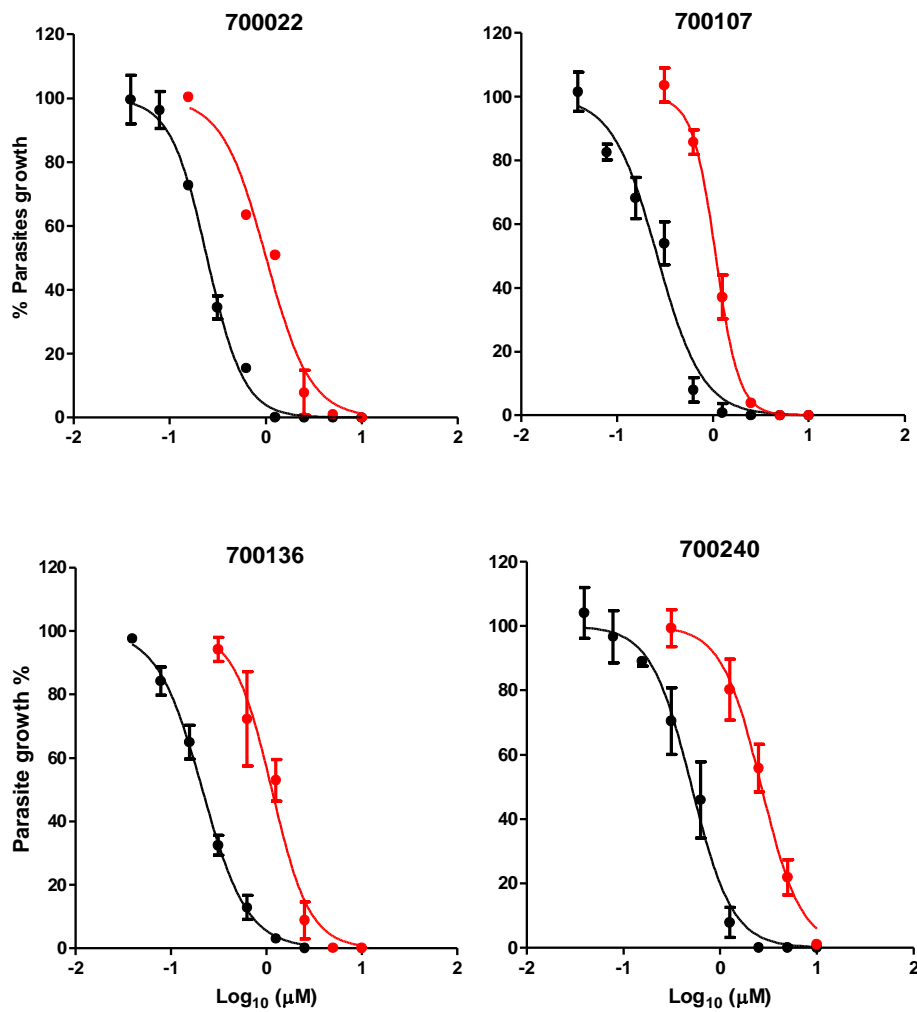


Figure 4.4: 700022-resistant *L. mexicana* axenic amastigotes showed decreased sensitivity to related triterpenes. Log concentration-normalised response curves for the related triterpenes 700022, 700107, 700136 and 700240. Response curves for axenic parasites before exposure to 700022 (black lines) and after 8 weeks of selection (red lines). The mean \pm StDev (n=9) are reported.

Table 4.1: Cross-resistance to related triterpenes in 700022-resistant *L. mexicana*. Resistance index, RI is a ratio of the mean EC₅₀ after 8 weeks selection compared to that in WT (unselected) parasites

Compounds	EC ₅₀ (μM)		RI
	WT axenic amastigotes	700022-resistant axenic amastigotes	
	Mean (95% CI)	Mean (95% CI)	
700022	0.24 (0.21-0.25)	1.00 (0.95-1.23)	4.2
700107	0.26 (0.24-0.28)	1.07 (0.92-1.31)	4.1
700136	0.21 (0.22-0.27)	1.13 (1.11-1.29)	5.3
700240	0.50 (0.46-0.52)	2.67 (2.21-2.96)	5.3

4.2.2 Comparative morphological examination of 700022-resistant and wild-type *L. mexicana*

An initial comparison of morphology between wild-type (unselected) *L. mexicana* and the same culture following 28 weeks of selection to increasing concentrations of 700022 (700022-resistant) was made using an indirect immunofluorescence assay. α -tubulin within microtubules are an abundant protein within *Leishmania spp*, labelling the cell body and flagellum. Wild-type and 700022-resistant promastigotes and axenic amastigotes were fixed and labelled using a mouse α -tubulin antibody and then subsequently labelled with an Alexa-Fluor (488nm, green) labelled anti-mouse antibody (Figure 4.5). The cultures were also counter-stained with DAPI to label the DNA within the nucleus and kinetoplast.

The imaging of α -tubulin in some 200 parasites for each culture, divided over four independent staining experiments, reveals a typical morphology for metacyclic promastigotes in the wild-type parasites, with nuclear staining identifying a single nuclear and kinetoplast compartment. The same staining of the 700022-resistant promastigotes reveals the same nuclear compartments, but also that there is a much shorter flagellum. No clear differences in the morphology of the axenic amastigotes is apparent. Images of these

200 parasites for each stage and 700022-resistance phenotype were digitally captured and analysed using tools within the freeware Image J analysis package (www.imagej.nih.gov). Here the area tool was used to measure the surface area of both promastigotes and axenic amastigotes. The length tool was used to measure the length of the flagellum from the base of the main body of the parasite to the end of the flagellum. Example ImageJ images used to capture these parameters are shown in Figures 4.6 and 4.7.

Taking the 200 sets of data for the wild-type and 700022-resistant parasites, distribution plots (box and whisker) were used to compare cell size (based on cell surface) and for promastigotes, the length of the flagellum (Figure 4.8). The significance of the differences in the distributions are analysed using a two-sample t-test (GraphPad PRISM). Table 4.2 reports the mean and standard deviation of these measurements.

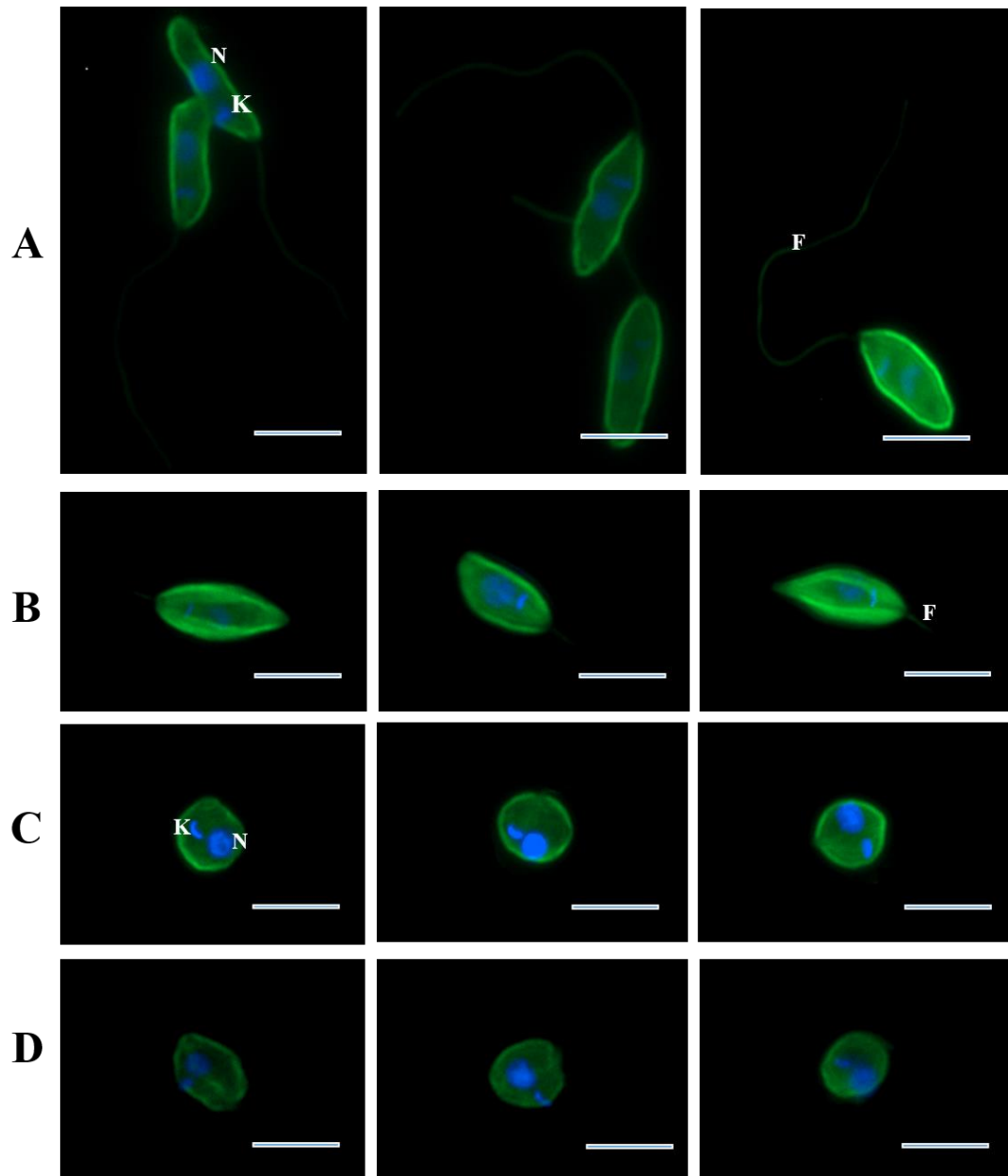


Figure 4.5: Comparative immunofluorescence microscopy analysis wild-type and 700022 resistant *L. mexicana*. Representative images of promastigotes from wild-type (A) and 700022-resistant (B) stained for α -tubulin (green) and DNA (blue). Note the absence of flagellum in the 700022-resistant promastigotes. The same staining was applied to wild-type (C) and 700022-resistant (D) axenic amastigotes. N, nucleus; F, flagellum; K, kinetoplast. Bars = 10 μ m

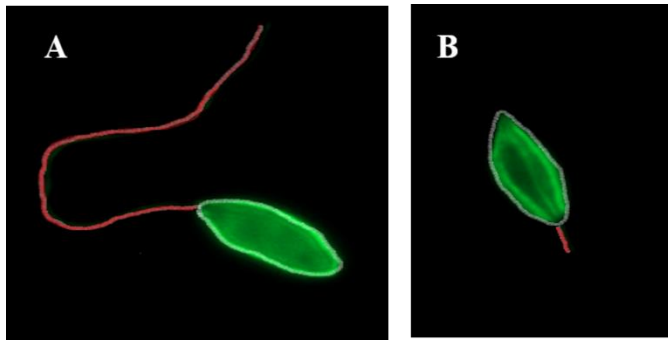


Figure 4.6: ImageJ analysis of *L. mexicana* promastigotes stained for α -tubulin content. Using the area tool (white) the area of the promastigote cell is outlined in wild-type (A) and 700022-resistant cells. Using the length tool (red), the length of the flagellum is indicated in the same images.

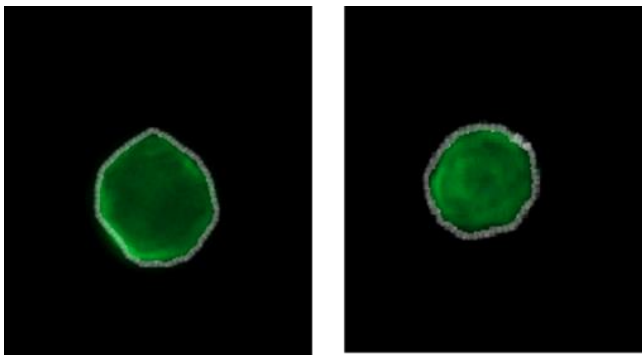


Figure 4.7: ImageJ analysis of *L. mexicana* axenic amastigotes stained for α -tubulin content. Using the area tool (white) the area of the amastigote cell is outlined in wild-type (A) and 700022-resistant cells.

There is a significant reduction in the mean length of the flagellum in 700022-resistant promastigotes, now approximately $2.3\mu\text{M}$ in length compared to $13.7\mu\text{M}$ – a reduction in length by some 85%. Interestingly, this analysis revealed a slight, but significant reduction in the size of both the 700022-resistant promastigote and axenic amastigote. Whilst not obvious from the initial inspection of the immunofluorescent images, there appears to be a one third reduction in size of both life cycle stages.

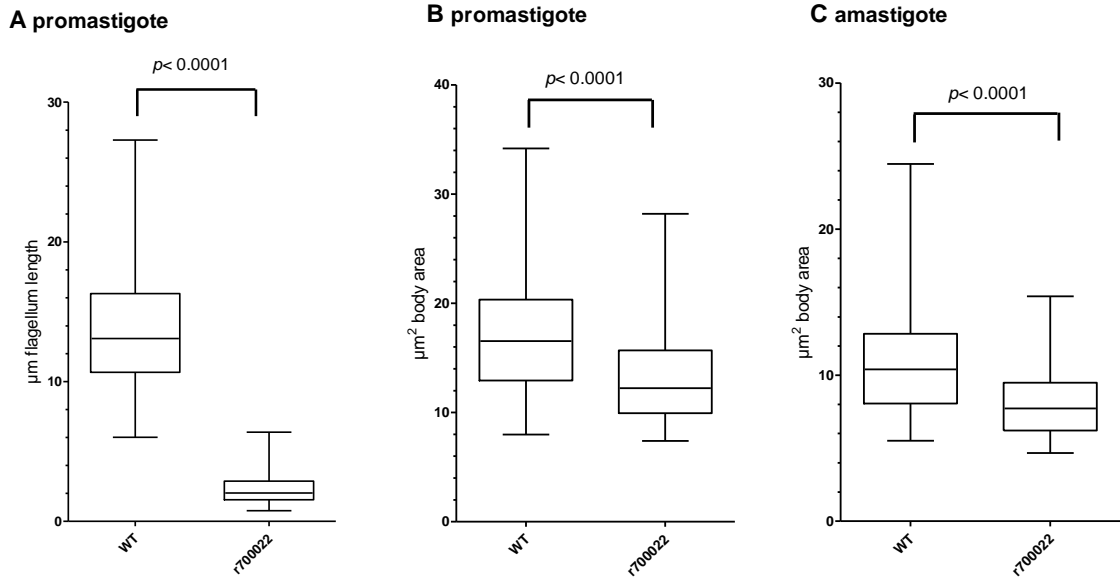


Figure 4.8: Scatterplots of the distribution of cell body size and flagellum length in wild type and 700022-resistant *L. mexicana*. Box and whisker plots (boxes illustrate 25 to 75% distribution and median, with whiskers showing range of data). (A) Compares the distribution of flagellar length (μm) in wild-type (WT) and 700022-resistant (r700022) promastigotes. (B) and (C) compare the surface area (μm^2), a surrogate determination of cell size, in promastigotes and axenic amastigotes, respectively. The significance of the difference in means is shown (two-way t-test).

Table 4.2: Measurements of morphological forms; cells surface area and flagellum length for *L. mexicana* WT and resistant line

	Mean surface area (μm^2) \pm stdev	Mean flagellum length (μm) \pm stdev
<i>L. mexicana</i> promastigote WT	17.03 \pm 5.30	13.73 \pm 3.98
<i>L. mexicana</i> amastigote WT	10.76 \pm 3.22	-
<i>L. mexicana</i> promastigote resistant line	12.62 \pm 3.94	2.27 \pm 1.15
<i>L. mexicana</i> amastigote resistant line	8.04 \pm 2.28	-

To further explore the comparative morphology, scanning and transmission electron micrographs of wild-type and 700022-resistant promastigotes were prepared. In addition to preparing images from untreated promastigotes, images were also prepared after the wild-type and 700022-resistant promastigotes were exposed to a 1xEC₅₀ concentration of 700022 for 24 hours.

Scanning electron micrographs of untreated wild-type promastigotes and those exposed to 11.4µM 700022 show how exposure to the compound causes the cell body to round up and start to show an irregular shape (Figure 4.9 A and B). A similar effect on the cell body is observed on the 700022-resistant parasites exposed to 85.6µM of 700022 (Figure 4.9 C and D). Also apparent in Figure 4.9 C is that the untreated 700022-resistant promastigotes have a very short flagellum compared to the WT promastigotes of Figure 4.9A.

Using the same approach, untreated and 700022 treated promastigotes were prepared for transmission electron microscopy. Osmium-stained fixed-sections of untreated wild type promastigotes reveals a characteristic ultrastructural morphology. Organelles readily identified include the nucleus, mitochondria, kinetoplast, flagellar pocket, flagellum, and vesicles termed acidocalcisomes (Figure 4.10 A). As expected, the kinetoplast body is positioned immediately adjacent to the flagellar pocket. Exposure to 700022 for 24 hours resulted in the loss of much of the defined ultrastructure morphology, with the only defined feature in all the micrographs of a nucleus that appears to be smaller in size and with a dense content, likely condensed chromatin, a characteristic feature of dying cells (Figure 4.10 B). The micrographs of the 700022-resistant untreated promastigotes, whilst not as clear as those of the wild type parasites, do show the kinetoplast, nucleus and vesicles described as acidocalcisomes (Figure 4.11A).

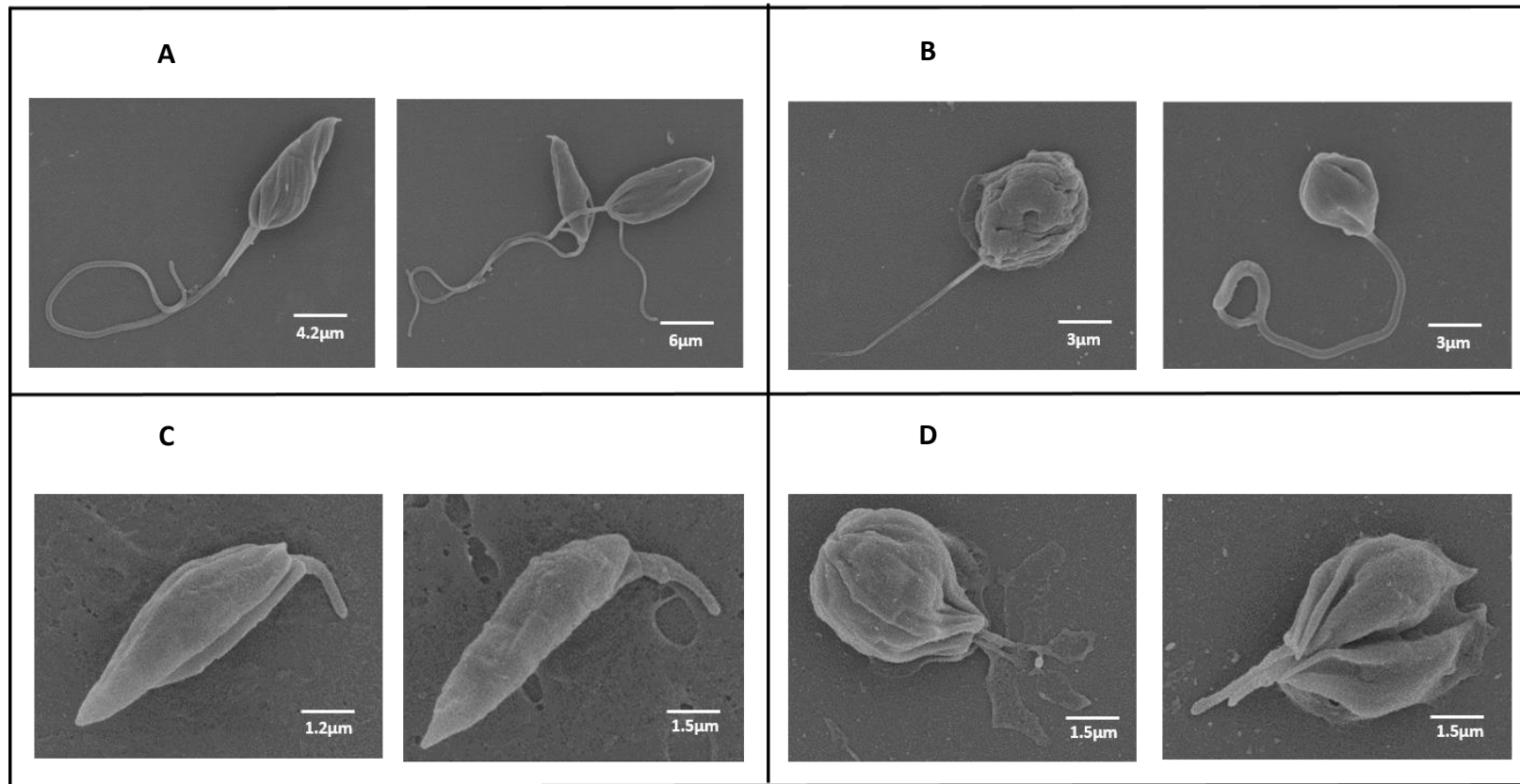


Figure 4.9: Scanning electron microscopy of *L. mexicana* promastigotes. Wild-type promastigotes that are (A) untreated or (B) exposed to 1x EC₅₀ (11.4 μM) of 700022. 700022-resistant promastigotes that are (C) untreated or (D) exposed to 1x EC₅₀ (85.6 μM) of 700022C.

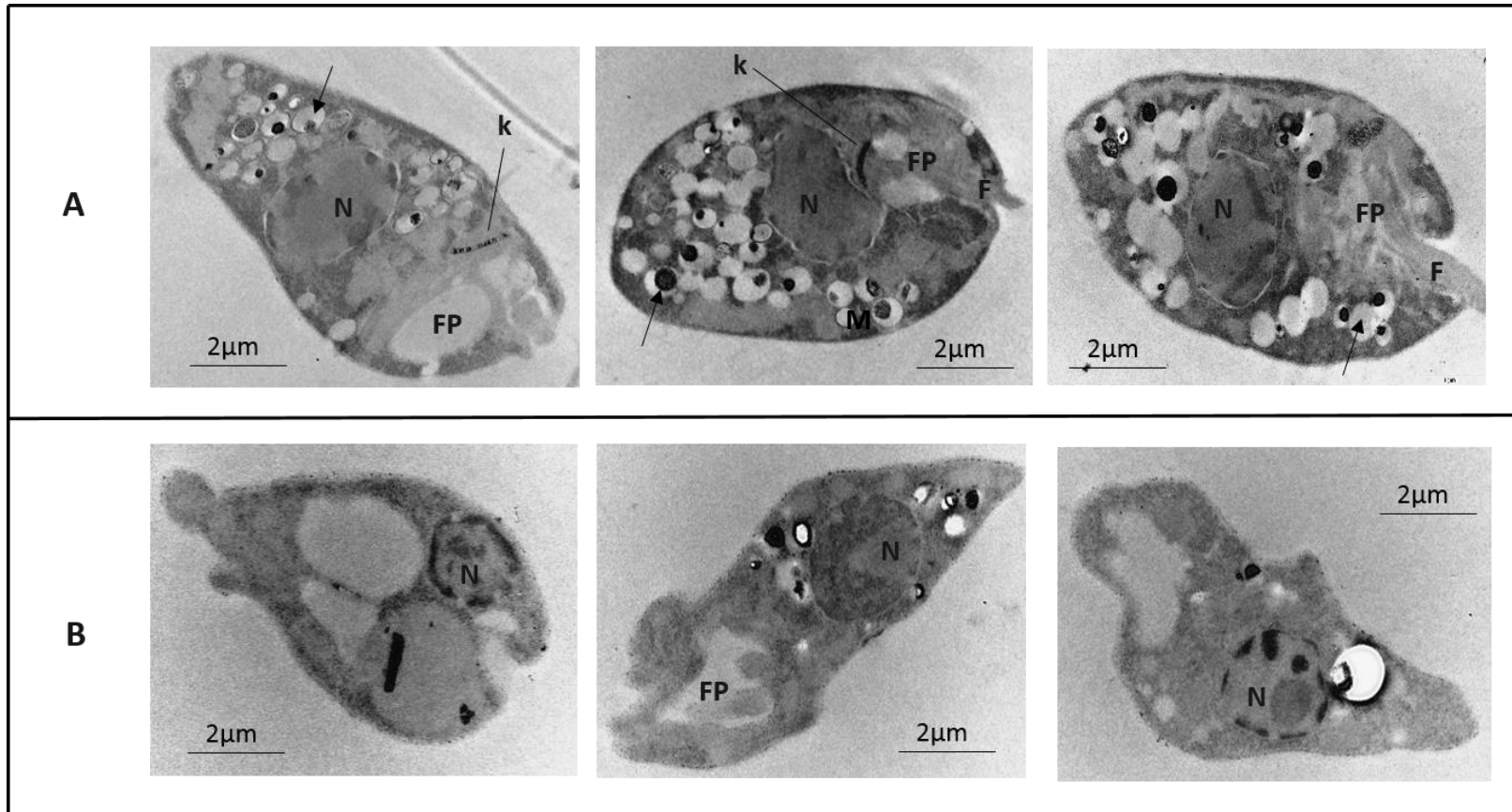


Figure 4.10: Transmission electron microscopy of wild type *L. mexicana* promastigotes. Wild-type promastigotes that are (A) untreated or (B) exposed to 1x EC₅₀ (11.4µM) of 700022 for 24 hours. N, nucleus; K, kinetoplast; M, mitochondria; FP, flagellar pocket; F, flagellar; acidocalcisomes (black arrows).

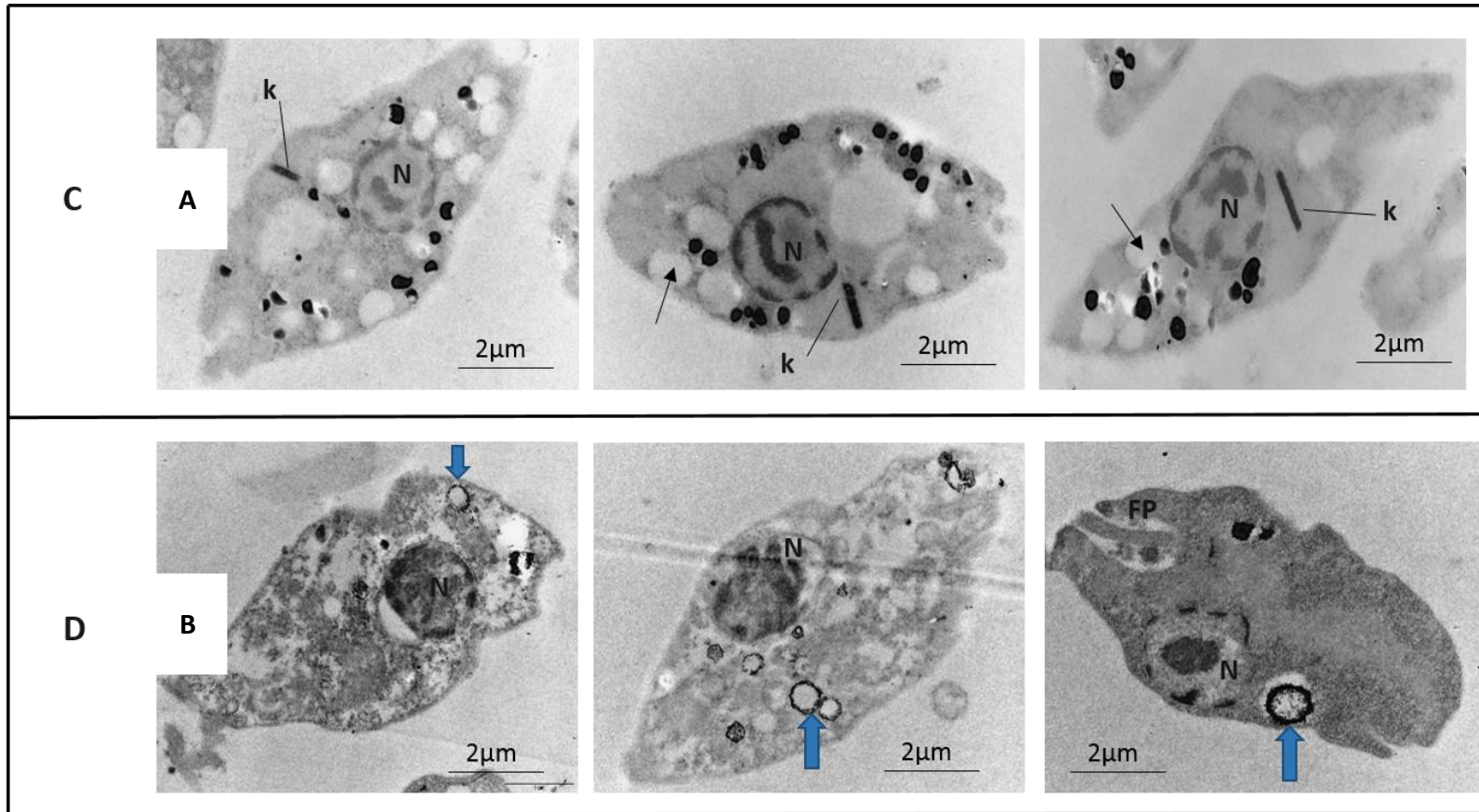


Figure 4.11: Transmission electron microscopy of 700022-resistant *L. mexicana* promastigotes. 700022-resistant promastigotes that are (A) untreated or (B) exposed to 1x EC₅₀ (85.6. 4µM) of 700022 for 24 hours. N, nucleus; K, kinetoplast; acidocalcisomes appear as vacuoles or with an electron-dense inclusion (black arrows) following exposure to 700022.

The quality of the images meant that a clear identification of organelles such as the flagellar pocket or the mitochondria could not be made though. As with the wild-type parasites, treatment with an EC₅₀ concentration of 700022 for 24 hours led to a disruption of the internal ultrastructure and the potential condensation of the nucleus (Figure 4.11 B). One interesting feature is a consistent pattern of thickening of the electron dense material around acidocalcisome vesicles – with several examples present in all images shown (Figure 4.11 B). These structures are not observed in the untreated promastigotes – although there may be examples of these in the 700022-treated wild type parasites in the central panel of Figure 4.10 B.

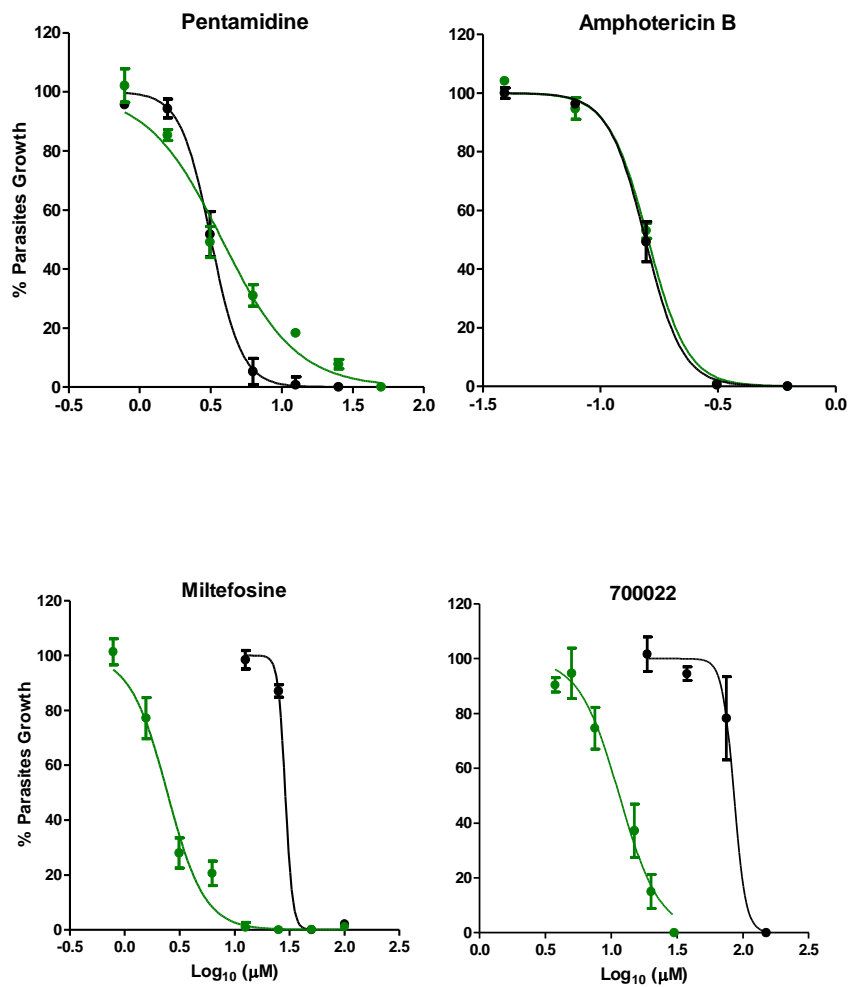
4.2.3 Investigating the molecular basis of the 700022 resistant phenotype

The limited amount of 700022 materials available made a comprehensive molecular analysis of the 700022 resistant phenotype unachievable. Ideally, multiple independent clones would be exposed to 700022, or left untreated, with whole genome analysis of all these clones supporting an investigation of mutations (SNPs, indels, duplication) associated with the resistant clones. Our approach would facilitate the whole genome sequencing of parasite clones isolated during the drug selection process, and this was considered at the outset as the most likely route forward. With time becoming a limiting factor, and subsequent data suggesting that the concentration required for 700022 to kill intramacrophage stages was quite high (see final chapter), the time to complete this approach was not considered as the best use of my time.

However, it was decided to explore whether the 700022-resistant *L. mexicana* parasite line was cross-resistant to any other antileishmanial drug for which specific gene targets that could be easily followed up were known. Both promastigotes and axenic amastigotes of the wild type and 700022-resistant lines had the EC₅₀ of amphotericin B, miltefosine and

pentamidine determined using log concentration normalised response from AlamarBlue assays. Experiments were done as technical triplicates, at least two biological repeats done. The mean \pm StDev of these data were plotted (Figure 4.12) and the EC₅₀ reported in Table 4.3.

A Promastigotes



B Amastigotes

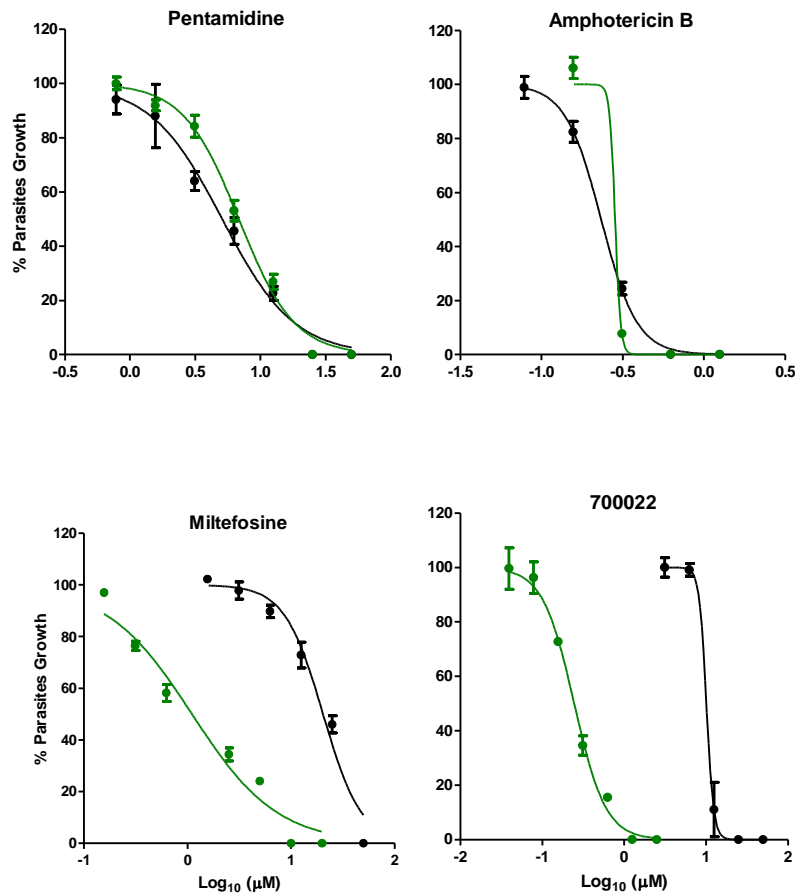


Figure 4.12: Exploring cross-resistance in 700022-resistant *L. mexicana*. (A) Log concentration-response curves used to estimate EC₅₀ of the indicated compound/drug in wild type (green curve) and 700022-resistant promastigotes (black curve). (B) Log concentration-response curves used to estimate EC₅₀ of the indicated compound/drug in wild type (green curve) and 700022-resistant axenic amastigotes (black curve). The data shown is a mean ± StDev from at least two biological replicates. See also Table 4.3.

A ratio of the EC₅₀ in the 700022-resistant line compared to the wild type line provides a resistance index (RI, Table 4.3). This was shown earlier in this chapter to provide a RI for 700022 of 7.5 and 42 for promastigotes and axenic amastigotes, respectively. Looking at these data for pentamidine and amphotericin B showed that for both promastigotes and

axenic amastigotes that the EC₅₀ determined in either the wild type or 700022 resistant lines was essentially the same (RI between 0.74 and 1.2). The data for miltefosine, however, was of particular interest. Both the promastigotes (RI of 11.8) and axenic amastigotes (RI of 17.8) of the 700022-resistant line now appears to be resistant to miltefosine.

Table 4.3: Cross resistance of 700022-resistant *L. mexicana* promastigotes and amastigotes towards other antileishmanial drugs. Resistance Index (RI) is the ratio between the EC₅₀ of resistant line/the EC₅₀ for the wild-type strain. 700022-r, *L. mexicana* resistant to 700022.

Compounds	<i>L. mexicana</i> promastigotes EC ₅₀ (μM)			<i>L. mexicana</i> amastigotes EC ₅₀ (μM)		
	WT	700022-r	RI	WT	700022-r	RI
	Mean 95% CI	Mean 95% CI		Mean 95% CI	Mean 95% CI	
700022	11.40 9.05-11.63	85.60 83.13-85.64	7.5	0.24 0.21-0.25	10.11 10.02-11.43	42
Miltefosine	2.44 1.81-3.13	28.9 27.88-28.43	11.8	1.14 0.99-1.16	20.37 18.98-21.12	17.8
Pentamidine	3.78 2.80-3.51	3.17 3.00-4.01	0.8	6.82 6.11-7.35	5.09 4.22-5.63	0.74
AmB	0.16 0.15-0.162	0.15 0.15-0.158	0.9	0.23 0.23-0.29	0.28 0.2-0.29	1.2

Given this apparent cross-resistance of the 700022-resistant line to miltefosine, it was decided to explore whether mutations within the genes encoding the two major subunits of the miltefosine transporter could be linked to the 700022-resistant phenotype. Mutations (stop codons and non-synonymous mutations) in both the α unit of the miltefosine transporter (MT) and the β unit ROS3 have been associated with *in vitro* resistance to miltefosine (Perez-Victoria *et al.*, 2006; Seifert *et al.*, 2007; Mondelaers *et al.*, 2017).

Genomic DNA was isolated from promastigotes of both WT and 700022-resistant *L. mexicana*. PCR was carried out to amplify the whole of the miltefosine transporter LmRos3 gene (LmxM.31.0510) located on chromosome 31 (Figure 4.13). This provided a fragment

of the correct size that was subsequently cloned into the PCRTM2.1 TOPO vector and nine independent clones recovered and sent for commercial sequencing (Eurofins GmbH). The same amplification over the whole 3315bp of LmMT (LmxM.13.1530) from chromosome 13 was not successful even after different attempts to adjust temperature, magnesium/template concentration and changing the polymerase used in the PCR. Review of the literature regarding mutations in the MT gene across five *Leishmania* spp. (Table 4.4), was used to determine where these mutations had been previously mapped. Using this data mapped onto the 3315bp gene, three regions called fragments 1 to 3 were identified as containing all these previously mapped mutations. PCR oligonucleotides were designed to amplify each of these regions (Figure 4.13 and 4.14) and the products cloned into the PCRTM2.1 TOPO vector and six independent clones from each recovered and sent for commercial sequencing (Eurofins GmbH).

Table 4.4: Mutations identified in MT miltefosine transporter genes in *Leishmania* spp

	Gene Accession number	AA change	References
<i>L. donovani</i>	LdBPK_131590.1	T420N & L856P	(Pérez-Victoria <i>et al.</i> , 2003; Turner <i>et al.</i> , 2015)
<i>L. infantum</i>	LinJ.13.1590	E216Q, R853C & L768P. Stop codon (L140, K229 & Y964)	(Laffitte <i>et al.</i> , 2016)
<i>L. amazonensis</i>	MF150.3	G852E, L856P, G852D and L832F	(Adriano <i>et al.</i> , 2014)
<i>L. major</i>	LmjF13.1530	(G852D, M547del)	(Turner <i>et al.</i> , 2015)
<i>L. braziliensis</i>	LbrM.13.1380	T420N, L856P	(Obonaga <i>et al.</i> , 2014)

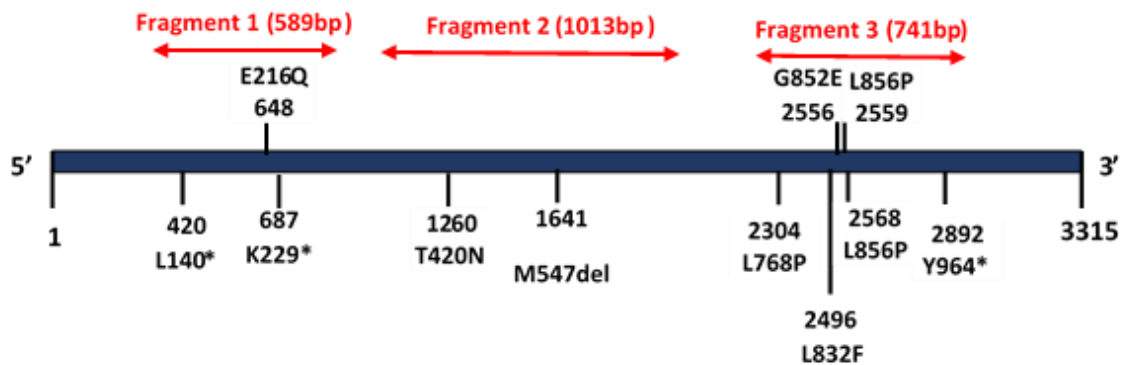


Figure 4.13: Schematic illustrating the mapping of mutations in *Leishmania* MT gene associated with miltefosine resistance, as previously discibed (see Table 4.4). Fragments 1 to 3 were chosen to amplify from *L. mexicana* genomic DNA.

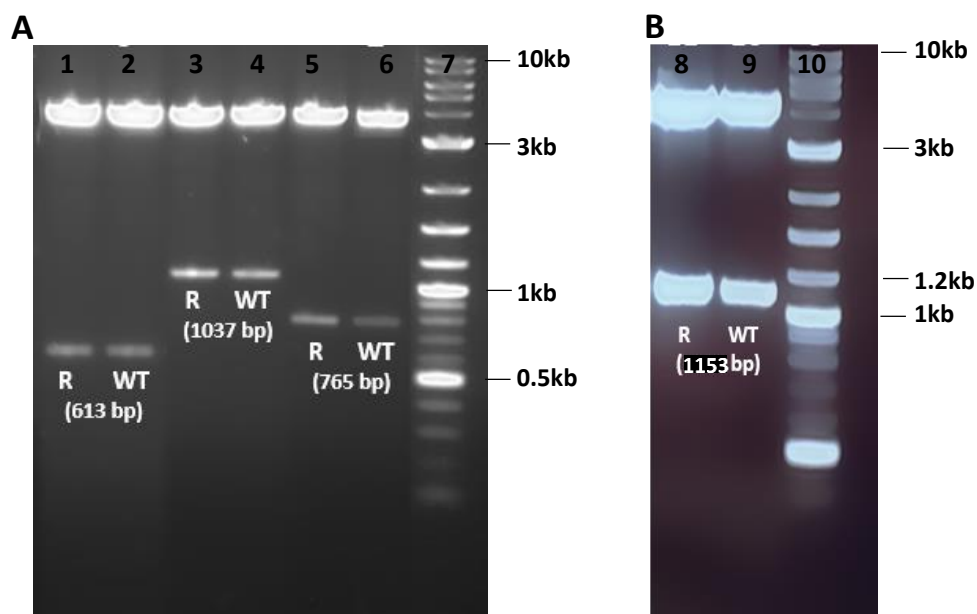


Figure 4.14: Verification of PCR amplification from (A) *LmMT* and (B) *LmROS3* genes. Size fractionation of *EcoRI* restricted plasmid clone containing the following PCR product; 1&2 are fragment 1, 3&4 are fragment 2 and 5&6 are fragment 3 of *LmMT* gene; 7 and 10 are 100bp markers (Bioline); 8 and 9 are of *LmROS3*. R; 700022-resistant line; WT, wild type. Note that fragment sizes are larger than in Figure 4.13 as include flanking regions with restriction sites.

4.2.3.1 Sequence analysis of LmMT

Six independent clones for each fragment of LmxM.13.1530 were sequenced using forward and reverse primers to the TOPO vector. Nucleotide sequences were aligned against LmxM.13.1530, using complementary reverse where required, using freeware online tools from Bioinformatics.org. Where there were differences to LmxM.13.1530, the sequence files provided by Eurofins were visually inspected to confirm the difference on both forward and reverse reads of that position. No insertions or deletions were identified, a number of single nucleotide polymorphisms (SNP) were confirmed (see Appendix 2 and Table 4.5). DNA sequences were translated and compiled using freeware from the ExPASy site (see Appendix 3).

Prior to 700022-selection, the wild type clones revealed two allele types of fragment 1 (see schematic in Figure 4.15). This may be expected as the *L. mexicana* line used was not clonal. One allele type was the same as the LmxM.13.1530 sequence and was found in 4/6 sequenced clones. One clone each had a single nonsynonymous (NS) SNP; that for H158R was novel, with the second K229R being novel although in *L. infantus* a stop codon in this position has been reported in a miltefosine resistant line (Laffitte *et al.*, 2016). These SNP are not sequencing errors, but could be artefacts introduced during the PCR. Following 700022 selection, these NS SNP are lost, with 5/6 clones having the same sequence as LmxM.13.1530 and a single clone with a R135R synonymous SNP. This loss of the NS SNP from the pre-selection population may reflect a purifying selection pressure on an allele variant that lacks them, or that they were PCR artifacts. There are no mutations in fragment 1 after selection that are linked with to the resistant phenotype. Sequence analysis of fragment 2 revealed no variation in the sequenced clones from LmxM.13.1530.

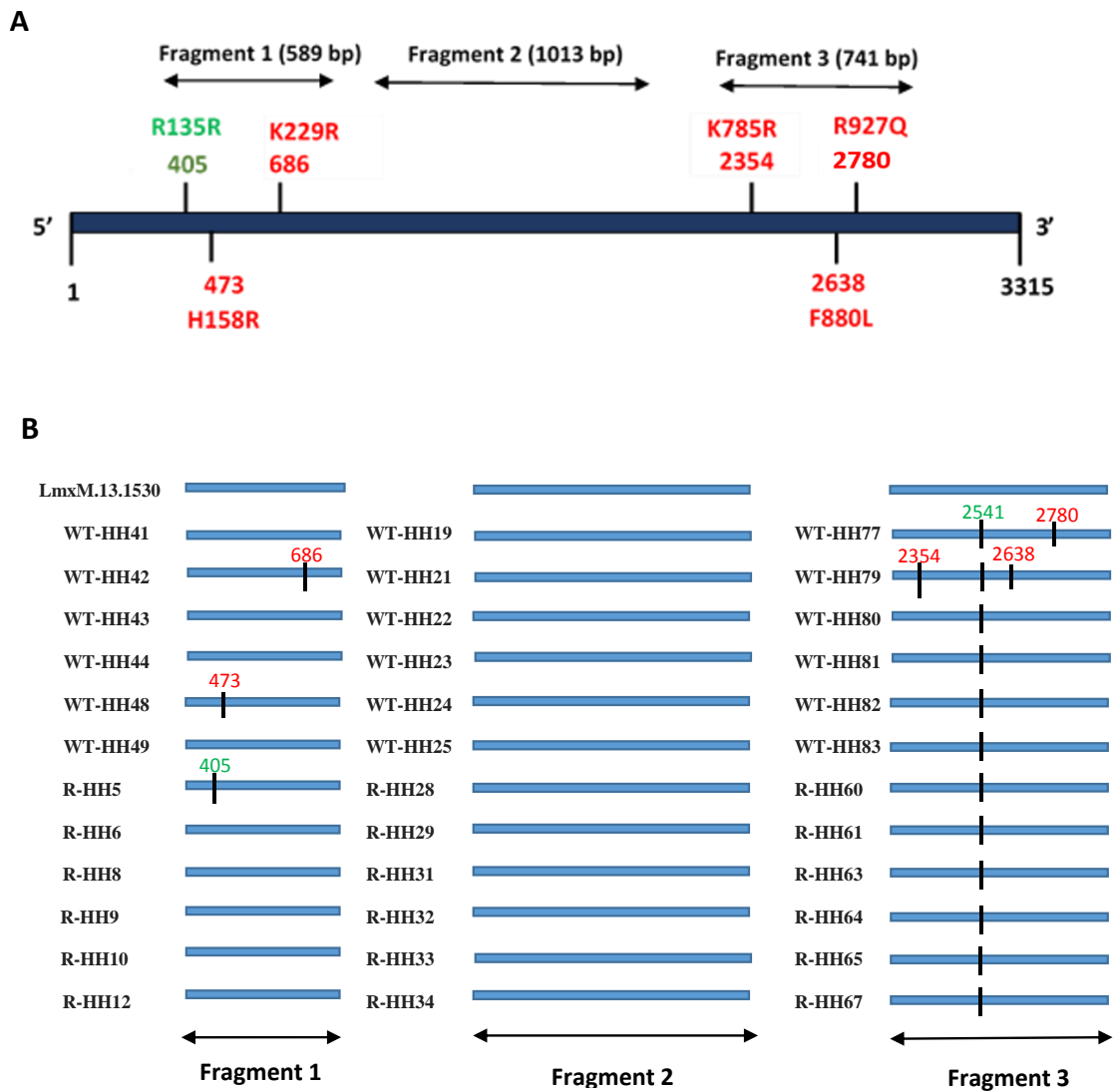


Figure 4.15: Schematic representing sequence analysis of LmMT gene. (A) A summary of all SNP identified in various clones after sequencing. The nucleotide position of each SNP is indicated by a bar, with the effect on amino acid sequence shown adjacent. For ease, NS SNP are shown in red throughout, with synonymous SNP in green. (B) A summary of the 12 clones for each fragment of LmMT sequenced compared LmxM.13.1530. The WT-prefix is for the pre-selection wild type and the R-prefix for 700022-selected parasites. The HH code uniquely identifies the PCR clone sequenced. Note that the synonymous G2541A SNP in all fragment 3 clones sequenced is marked only once in the schematic.

All PCR clones sequenced from fragment 3 contain a NS SNP (nucleotide G2541A) – which suggests this SNP is present in the WT clone used here and is distinct to the *L. mexicana* clone sequenced for the genome project. The pre-selection clones again indicate the presence of three allele variants (Figure 4.15). Two clones contained NS SNP; R927Q in one and both K785R and F880L in a second. Again, there is the potential for PCR artefacts, but also that this is a region of the MT gene that is susceptible to mutations in miltefosine resistant lines (Table 4.4). Again, on 700022-selection, these NS SNP were not seen in the resulting clones and suggests that purifying selection of alleles that lack them may have occurred. There were no mutations in Fragment 3 associated with the 700022-resistant phenotype.

4.2.3.2 Sequence analysis of LmRos

Nine independent clones for each fragment of LmxM.31.0510 were sequenced using forward and reverse primers to the TOPO vector. As above, nucleotide sequences were aligned and checked against LmxM.31.0510 using freeware online tools from Bioinformatics.org. In all nine clones, no insertions or deletions were identified, a number of single nucleotide polymorphisms (SNP) were confirmed (see Appendix 4 and Table 4.5) with a protein sequence alignment provided in Appendix 5.

Before 700022 selection there appear to be four alleles; one that is identical to the reference sequence in LmxM.31.0510, with three single PCR clones that each contain one synonymous SNPs (Figure 4.16). Note than none of these NS SNP variant alleles are found after 700022-selection. Instead, there are two different allele variants, both of which contain at least one NS SNP (Table 4.5). In this case, NS SNP only found in the LmROS3 gene in 700022-resistant have been described here.

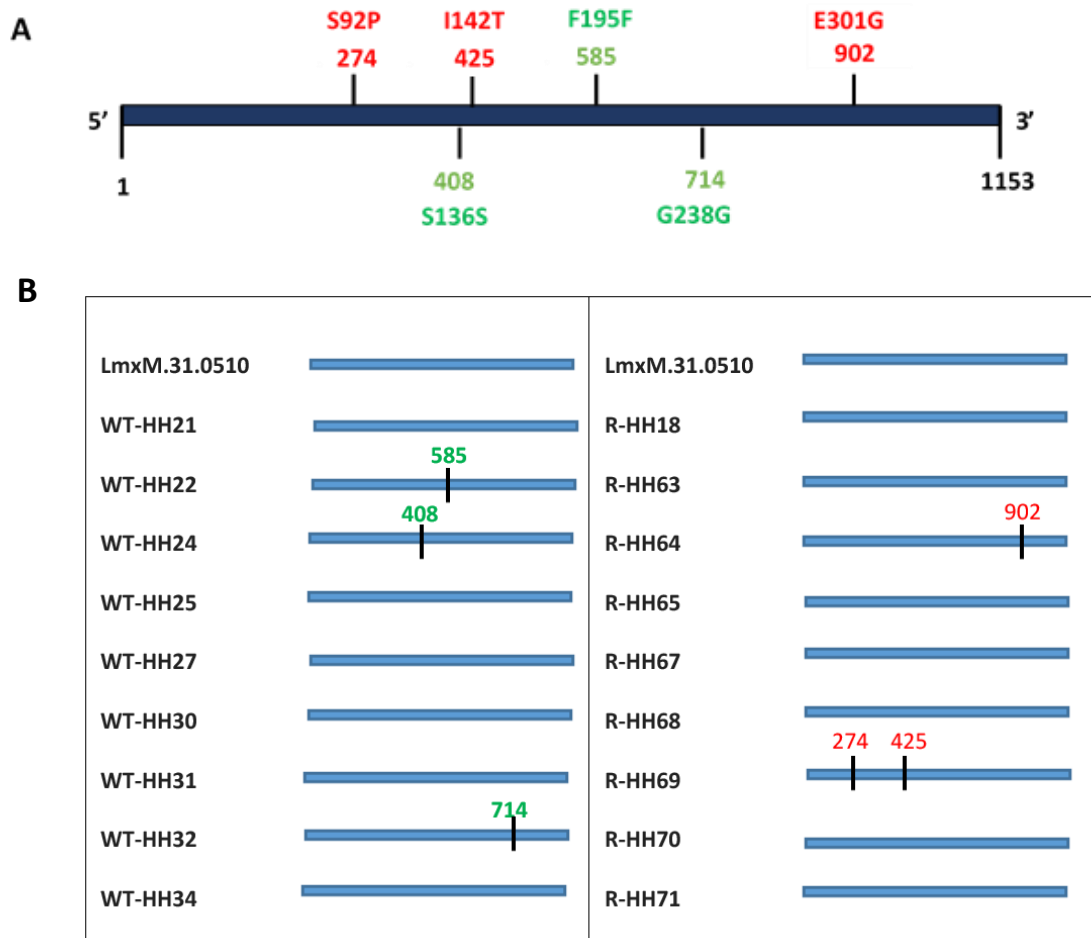


Figure 4.16: Schematic representing sequence analysis of LmROS3 gene. (A) A summary of all SNP identified in various clones after sequencing. The nucleotide position of each SNP is indicated by a bar, with the effect on amino acid sequence shown adjacent. For ease, NS SNP are shown in red throughout, with synonymous SNP in green. (B) A summary of the 9 clones for LmROS3 sequenced compared to LmxM.31.0510. The WT-prefix is for the pre-selection wild type and the R-prefix for 700022-selected parasites. The HH code uniquely identifies the PCR clone sequenced.

Table 4.5 Mutations identified in miltefosine transporter genes LmROS3 and LmMT in this study. WT, wild type pre-selection; R, 700022-resistant; Syn, synonymous; Non-syn, non-synonymous; AA, amino acid.

Gene Accession number	Chromosome no	Sample	WT/R	Nucleotide change	SNP type	AA change
LmROS3 LmxM.31.0510	31	HH22	WT	C585T	Syn	F195F
	31	HH24	WT	C408T	Syn	S136S
	31	HH32	WT	T714C	Syn	G238G
	31	HH69	R	T274C T425C	Non-syn Non-syn	S92P I142T
	31	HH64	R	A902G	Non-syn	E301G
LmMT LmxM.13.1530	13	HH5	R	T405C	Syn	R135R
	13	HH42	WT	A686G	Non-syn	K229R
	13	HH48	WT	A473G	Non-syn	H158R
	13	HH77	WT	G2780A	Non-syn	R927Q
	13	HH79	WT	A2354G T2638C	Non-syn Non-syn	K785R F880L

4.3 Discussion

In this chapter, *L. mexicana* promastigotes resistant to 700022 were generated using a stepwise drug selection pressure to support a series of studies to explore the activity of 700022 against *L. mexicana*. This approach has similarly been successfully used with antileishmanial drugs in studies to determine drug targets following genome sequencing of amphotericin B-resistant lines of *L. mexicana* (Al-Mohammed *et al.*, 2005), antimony-resistant lines of *L. donovani* (Singh *et al.*, 2010) and miltefosine-resistant lines of *L. donovani* (Seifert *et al.*, 2003).

The 700022 resistant parasite line was 7.5 times more resistant to the effect of the compound than the wild type. Eventually, after 28 weeks of selection, *L. mexicana* promastigotes of the 700022 resistant line were capable of growth in concentrations of 85.6 μ M. The key challenge to this study was that I did not have sufficient compound 700022 - with material

that was eventually only enough for one attempt at drug selection. I recognise this as a major limitation in the studies undertaken, but pursued the morphological and molecular analysis of the single resistant line that I did develop, but have introduced the necessary caution in the interpretation of my data.

After doing this study once, I have identified a research plan that should be put in place to ensure the preparation of resistant parasite clones that would be suitable for a molecular analysis of the 700022/miltefosine resistant phenotype;

- (i) To reduce the heterogeneity of the WT *L. mexicana* line before drug selection, several independent clones should be prepared using an approach such as limited dilution or the use of a semi-solid agar (Iovannisci and Ullman, 1984). This will help overcome the variation in allele types that may arise when parasites are left uncloned over a long period of continuous culture.
- (ii) Several of these WT clones need to be independently placed under 700022 selection pressure. Ideally, a second group of clones should be placed under selection pressure with a structurally related triterpenes (eg 700104) to establish whether 700104 resistant lines are also resistant to 700022 (this being likely as the reverse is true) and miltefosine, and whether mutations in the same gene(s) are associated with these resistant phenotypes.
- (iii) Whole genome sequencing of multiple WT and resistant clones should be used to explore any association of the resistant phenotypes with insertions, deletion or non-synonymous SNPs. Further, gene duplications and/or rearrangements would need to be assessed. Ideally, a further round of high throughput RNA sequencing (RNASeq) could be used to establish whether there are any variations in the levels of gene expression associated with a drug resistant phenotype.

The process to select a 700022 resistant line was relatively simple. We did not need to induce DNA changes using a mitogenic agent, and within 8 weeks the EC₅₀ values to 700022 (and related compounds) increased 4-5 fold. This relatively simple induction and selection of the resistant phenotype *in vitro* would be of concern for any future development of 700022 as a lead irrespective of the fact that there was a coselection of resistance to a leading current frontline antileishmanial drug miltefosine.

The initial comparative morphological studies between the wild-type and 700022 resistant line were done with an understanding of their limitations. The first features of the 700022 resistant line identified was the lack of a flagellum in the promastigote, with subsequent image analysis also revealing a significant decrease in the cell body area for both promastigotes and axenic amastigotes. The lack of a flagellum in a drug-selected line has been previously reported by Al-Mohammed *et al.* (2005) with their report of an aflagellate amphotericin B-resistant *L. mexicana* promastigote isolated from BALB/c mice. This suggests that loss of the flagellum may provide some fitness benefit that is exploited under drug selection pressure. Interestingly, amastigotes of the amphotericin B-resistant lines were noninfective to mice, lesions did not develop, and amastigotes could not be recovered from the injection site (Al-Mohammed *et al.* 2005). Injection of promastigotes from the same resistant line did lead to the development of cutaneous lesions with parasites reisolated from these lesions, and their AMB sensitivities were assessed and the results were highly resistant to AMB. Whether there is a similar fitness cost in terms of the infectivity of 700022 resistant promastigotes was not investigated here. Whilst mouse models would not be appropriate here as there are no plans to develop 700022 as a lead compound, the *in vitro* infectivity of 700022 resistant promastigotes into PMA-treated THP-1 could be compared against that of the wild-type parasites. The reduction in cell body size by approximately 25% in both 700022 resistant axenic amastigotes and promastigotes could be a reflection of a more rapid

cell proliferation rate – with cells dividing earlier and thus when smaller in size. This idea was tested, although only as a single biological repeat, where the cell density of axenic amastigotes and promastigotes were compared between the wild type (WT) and 700022 resistant lines when grown in medium without drug pressure (Figure 4.17). In both life stages, there appears to be a faster proliferation rate for the 700022 resistant line that could start to account for the smaller sized cell phenotype.

The lack of flagellum was confirmed using SEM. A more focussed analysis of ultrastructure morphology between the resistant and wild type parasites gave mixed results as the image quality was poor for some parasite preparations and time was not available to do more. The transmission electron microscopy of wild type parasites clearly showed a kinetoplast located at the posterior end of the cell near the basal body of the flagellum (Matthews, 2005). The TEM of the 700022 resistant cells appeared to indicate that the kinetoplast was more centrally located, and there was no apparent flagellar pocket adjacent to this. Unfortunately, the quality

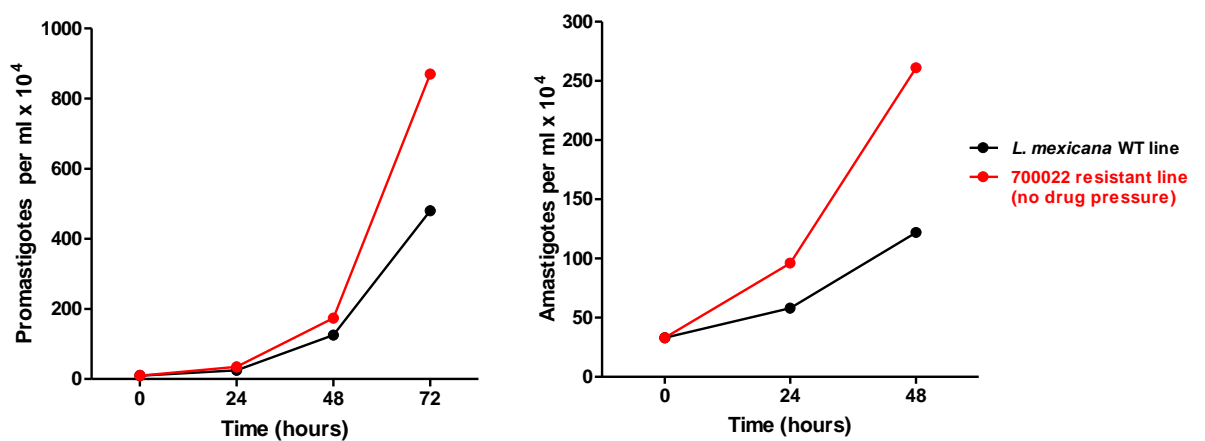


Figure 4.17: Comparison of the effect of parasite growth between *L. mexicana* WT and 700022 resistant line. The number of parasites were counted over a 72 hours for *L. mexicana* promastigotes, and over a 48 hours for *L. mexicana* amastigotes. The growth of resistant cells was two times more

than to the *L. mexicana* wild type of both forms promastigotes and amastigotes over a 72 hours and 48 hours period respectively.

and number of images means that nothing conclusive can be said. However, it would be interesting to produce additional EM imaging of the 700022 resistant parasite to see whether the lack of a flagellum does affect the positioning of the kinetoplast.

On addition of 700022, SEM analysis revealed that the early stage of cell death, ie 24 hours, was characterized by a rounding up of the promastigote cell body. A previous study by Da Silva *et al.* (2015) similarly shows that promastigotes of *L. amazonensis* treated with 100 µg/mL AEPa (isolated from *Physalis angulata*) for 72 hours was accompanied by a rounding up of the parasite body. These alternatives presented as well with *L. amazonensis* promastigotes when treated with 1x EC₅₀ of 4-nitrobenzaldehyde thiosemicarbazone (BZTS) (Britta *et al.*, 2014). TEM analysis after 700022 treatment showed loss of clearly defined organelle structure, and perhaps evidence of nuclear condensation on cell death. Interestingly, the 700022 resistant line showed a vacuolar structure with an electron dense lining after 700022 treatment. These vacuoles potentially represent calciosomes and are similarly lined acidocalcisomes have been reported in studies of *L. mexicana* and *L. amazonensis* promastigotes when moved between different culture media (Miranda *et al.*, 2004). Acidocalcisomes are intracellular stores of Ca²⁺ and as well as miltefosine activating Ca²⁺ channels in the plasma membrane it is also predicted to affect Ca²⁺ storage within the acidocalcisomes by inducing the rapid alkalization of these important organelles (Pinto-Martinez *et al.*, 2017). 700022 action may therefore be centred around these organelles. To explore this in more detail, additional and improved EM imaging of parasites are required to define what ultrastructural changes do occur. In addition to the use of 700022 on the WT and resistant strains, it would also be useful to include an additional triterpene as well as miltefosine in this comparative study. In addition, it would be useful to determine whether

the action of miltefosine and 700022 is antagonistic or synergistic, this information potentially providing some link to suggest that their modes of action are the same (or related) and how this may therefore link to their co-resistance. As such, exploring and comparing the movement of Ca²⁺ ions within untreated and 700022/miltefosine treated parasites using the Fluo-4 AM indicator with fluorescence microscopy (Schneidereit et al., 2016) could be potentially interesting. Likewise, given that there may be a repositioning of the kinetoplast in the 700022 resistant parasite as well as changes to the control of cell cycle during division, based on their smaller size, an analysis of kinetoplast and DNA content (Schneidereit et al., 2016) could also be interesting.

Molecular analysis of the LmMT and LmROS3 genes identified three non-synonymous SNPs found only in PCR clones from LmROS3 gene in 700022-resistant parasites. Unfortunately, these were each only seen once, and these non-synonymous mutations may have been generated as a result of artifacts during PCR amplification. As the SNPs were confirmed by sequencing of both strands of DNA, they were not the result of sequencing errors. As we were cloning directly into the TOPO TA vector, a non-proofreading Taq was used, and this could have accounted for any errors – although not why they were all non-synonymous SNPs after 700022 selection (McInerney *et al.*, 2014). The way forward would be to confirm by sequencing more clones whether these non-synonymous SNPs can be found more than once each. Should this then be the case, and they become candidate mutations that could account for the 700022 and/or miltefosine resistance then we would consider to use of gene replacement or gene editing (Zhang *et al.*, 2017) to replace a mutated version of LmRos3 units into wild type parasites and then explore their effect on the resistance phenotypes.

A recent paper from the Mottram group suggests that a specific section of the *L. infantum* genome (termed the Miltefosine Sensitivity Locus MSL) is different in some Brazilian

strains of the parasite making them less susceptible to the drug miltefosine (Carnielli *et al.*, 2018). The MSL was found in the Old World parasites *L. infantum* and *L. donovani*, where miltefosine can have a cure rate > 93%. Of relevance here is that the MSL contains four genes on chromosome 31 that could be studied in our 700022 resistant line. The failure of miltefosine treatment in the Brazilian samples, despite the fact that miltefosine has not been used for VL treatment in Brazil suggests that a natural resistance to miltefosine exists within the circulating population of *L. infantum* in Brazil. Given that we used a natural product here to generate a miltefosine resistant line, it would be interesting to understand and explore whether the use of natural products as antileishmanial traditional medicines in Brazil has potentially created this natural resistance. These data have been shared with Jeremy Mottram and small amount of compound 700022 provided to him by PhytoQuest to start addressing this.

Chapter 5: Validation of bioluminescence screening and intramacrophage assays using *L. mexicana* expressing a NanoLuc-PEST reporter

*Declaration: Research describing the validation of NanoLuc and NanoLuc-PEST *L. mexicana* transgenic parasites and their use in the screening of the MMV Pathogen Box Open Access library in this chapter has been published (Berry SL, Hameed H, Thomason A, Maciej-Hulme ML, Saif Abou-Akkada S, Horrocks P, Price HP. 2018. **Development of NanoLuc-PEST expressing *Leishmania mexicana* as a new drug discovery tool for axenic- and intramacrophage-based assays.** PLoS Negl Trop Dis, vol. 12(7), e0006639). These parasite lines were provided to me by Dr Sarah Berry, the research described in this chapter, and published in this paper, were carried out by me with support from Dr Berry in maintenance of the cell lines.*

5.1 Introduction

Over the last years, efforts have greatly increased to identify novel compounds with antileishmanial properties, or to resource existing drugs to expand the therapeutic options against this disease (Allarakhia, 2013). Efficient compound screening is dependent on the availability of highly robust, sensitive and reproducible assays that are suitable for high throughput application. The use of fluorescent-based assays, including AlamarBlue, are useful for studying the parasite alone, but cannot distinguish between the parasite and macrophage cells in an *in vitro* cell infection model. Compound screening in the intracellular macrophage model is more clinically relevant and is likely to provide a better validation of potential hits as this assay takes into account the multiple membranes a compound must

transit and the acidic environment within the parasitophorous vacuole in which the parasite resides.

One technology that can overcome this hurdle is the use of bioluminescence, where transgenic parasites (and not the host cell) expresses a luciferase reporter; a diverse group of enzymes that generate photons in the visible spectrum in the presence of a specific substrate. Such luciferase-based assays have been used extensively in *Plasmodium falciparum* and proven a robust and sensitive reporter in drug screens (Ullah *et al.*, 2017; Che *et al.*, 2012; Lucumi *et al.*, 2010; Cui *et al.*, 2008; Ekland *et al.*, 2011). My host laboratory has utilised bioluminescence in *P. falciparum* over a number of years to explore gene expression, transfection efficiency, drug assay screening and more recently assays of the dynamics of drug action (Horrocks and Lanzer, 1999; Ullah *et al.*, 2017). Bioluminescent reporter genes have also been used in kinetoplastid systems. A study by Lang and co-workers (2005) demonstrated that a luciferase expressing *L. amazonensis* strain was useful for rapid and high throughput screening of drugs against amastigote infected macrophages. This same approach has also been used with *L. major* (Buckner and Wilson, 2005) and *L. infantum* (Serenio *et al.*, 2001).

As well as the more common luciferases from the North American firefly (*Photinus pyralis*) and the sea pansy (*Renilla reniformis*) being used for drug screening (Claes *et al.*, 2009; Myburgh *et al.*, 2013; Reimao *et al.*, 2015; Sadeghi *et al.*, 2015), other luciferases with differing properties are now being explored. A luciferase isolated from the deep sea shrimp (*Oplophorus gracilirostris*), known as NanoLuc, is a relatively small (19.1 kDa) and stable enzyme which produces a high intensity, glow-type bioluminescence (Hall *et al.*, 2012). A modified form of the enzyme, NanoLuc-PEST, retains the high enzymatic activity but has a reduced intracellular half-life due to fusion of a PEST sequence which marks the molecule for rapid proteosomal degradation (Hall *et al.*, 2012). The term PEST coming from the

enrichment of proline (P), glutamic acid (E), serine (S), and threonine (T) residues in the proteasome targeting sequence (Rogers *et al.*, 1986; Rechsteiner and Rogers, 1996). NanoLuc has been successfully expressed in *Plasmodium spp* (Azevedo *et al.*, 2014; De Niz *et al.*, 2016) with the first report of expression of NanoLuc in kinetoplastids done by the Price research group at Keele University (Berry *et al.*, 2018). In the Berry *et al.* (2018) study, *L. mexicana* were genetically modified to express either NanoLuc or NanoLuc-PEST. Both these parasite lines were made available to me as part of this study.

Here I evaluate and describe the use of NanoLuc and NanoLuc-PEST *L. mexicana* transgenic lines in for use as a drug discovery screening tool for both axenic amastigotes and infected macrophages systems. For the evaluation of the NanoLuc and NanoLuc-PEST *L. mexicana* transgenic, I report a screen of the MMV Pathogen Box. This open access drug discovery resource was developed following the success of the MMV (Medicine for Malaria Venture) Malaria Box, particularly when this box of compounds that initially developed for antimalarial drug discovery were now screened against other pathogens (van Voorhis *et al.*, 2016) (Table 5.1). That a compound library developed for malaria research could be readily repurposed for screening a number of diseases, lead to the MMV developing and releasing a second open access library resource to the community – the MMV Pathogen Box. Pathogen Box compounds were selected from screens against a wide range of pathogenic organisms, from mycobacteria, through single cell eukaryotes to worms and these were pooled for screening in these and other organisms (Duffy *et al.*, 2017; Preston *et al.*, 2016) (Table 5.1). These compounds are provided in a library of 400 compounds, which include a number of reference compounds (drugs used currently to treat a wide range of diseases) along with data on their structure and toxicity. Full information about these compounds is available online via (<https://www.pathogenbox.org/>).

Table 5.1: Studies reporting the screening of the MMV Pathogen Box and Malaria Box libraries

Author	Library	Pathogen	Identifications
Spalenka <i>et al.</i> (2018)	Pathogen Box	<i>Toxoplasma gondii</i>	8 compounds with an EC ₅₀ < 2 µM and CC ₅₀ on Vero cells ranged from 1.69 to 15.92 µM. The best SI value of 275 was detected for MMV675968.
Mayer and Kronstad (2017)	Pathogen Box	Human fungal	MMV688271 showed activity against both <i>C. neoformans</i> and <i>C. albicans</i> with EC ₅₀ of 250 nM, and nontoxic to human cells such as (lung tissue cell line, peritoneal murine macrophages (PMM), and HepG2 cell line.
Vila and Lopez-Ribot (2016)	Pathogen Box	<i>Candida albicans</i> biofilm formation	Compound MMV688768 was displayed the most potent to increase anti-biofilm activity, with high selectivity index in liver hepatocellular cells.
Preston <i>et al.</i> (2016)	Pathogen Box	<i>Haemonchus contortus</i>	MMV688934 revealed to inhibit xL3 motility and L4 motility, growth and development, with EC ₅₀ values between 0.02 and 3 mM.
Partridge <i>et al.</i> (2018)	Pathogen Box	<i>Caenorhabditis elegans</i>	Tolfenpyrad, Auranofin, Mebendazole and Isradipine showed activity against <i>Caenorhabditis elegans</i> with an EC ₅₀ values between 0.2 and 1.6 µM.
Hennessey <i>et al.</i> (2018)	Pathogen Box	<i>Giardia lamblia</i>	MMV687807, MMV688262, MMV688978 and MMV688978 displayed activity against <i>G. lamblia</i> with EC ₅₀ values (0.51 µM, 0.55 µM, 2.30 µM and 3.74 µM respectively), and SI= (<10, >73, > 17 and 0.13 respectively) in liver hepatocellular cells.
Stadelmann <i>et al.</i> (2016)	Malaria Box	Alveolar echinococcosis (AE)	MMV665807 displayed activity against EA with EC ₅₀ value <2 µM, and showed less toxic for human foreskin fibroblasts and Reuber rat hepatoma cells.
Hostettler <i>et al.</i> (2016)	Malaria Box	<i>Theileria annulata</i>	5 compounds identified as anti-theilerial activities.
Kaiser <i>et al.</i> (2015)	Malaria Box	Trypanosomatids	Novel Active Scaffolds were identified against <i>T. brucei</i> , <i>T. cruzi</i> , and <i>L. donovani</i> and <i>L. infantum</i> .
Bessoff <i>et al.</i> (2014).	Malaria Box	<i>Cryptosporidium parvum</i>	3 novel compounds derived from the quinolin-8-ol, allopurinol-based, and 2,4-diaminoquinazoline chemical scaffolds that exhibited submicromolar potency against <i>C. parvum</i> .
Khraiweh <i>et al.</i> (2016)	Malaria Box	<i>L. major</i>	14 compounds identified to have antileishmanial activity.

5.2 Results

5.2.1 Evaluation of NanoLuc assay parameters

In Berry *et al.* (2018) the use of the NanoLuc assay to monitor expression of the different reporters as well as growth of the transgenic parasites was reported. These assays, however, used 100 μ L of NanoLuc reagent and my initial experiments attempted to reduce the volume of reagent to reduce the cost of library screening. Axenic amastigotes expressing either NanoLuc or NanoLuc-PEST were seeded at a density of 1×10^5 /mL in 96-microwell plates. The cells were treated with 0.2 μ M Amphotericin B (AmB at approximately $1 \times EC_{50}$ concentration) and incubated for 72 hours at 32°C. Control wells with an equivalent volume of DMSO solvent (100% growth) were included on all plates. Following incubation, samples of control and AmB-treated cultures were titrated into a fixed volume of 50 μ L using Schneider's medium and transferred into a white 96-multiwell plate and 50 μ L of the Nano-Glo reagent (lysis buffer and substrate, diluted 200:1) was added to each well (Table 5.2). After 3 minutes, the bioluminescence signal from three technical replicates was measured using the Glomax Multi Detection System. Correlation of the resulting bioluminescence against the volume of parasite culture included in each well shows a strong linear correlation with $r^2 = 0.98$ and $p \text{ values} < 0.0001$ between these two parameters (Figure 5.1) for both AmB-treated and control experiments with both NanoLuc reporter lines. As expected, the bioluminescent signal from the more stable NanoLuc reporter was evident (Figure 5.1). From this data, it was decided that experiments using 20 μ L of parasite culture would be selected, being within the linear range and a readily manageable volume for consistent pipetting.

Table 5.2: Table reporting volumes used to evaluate NanoLuc assay

Total volume (50μL)		Nano-Glo assay substrate volume
Axenic amastigotes	Schneider's medium	
-	50 μ L	50 μ L
5 μ L	45 μ L	50 μ L
10 μ L	40 μ L	50 μ L
20 μ L	30 μ L	50 μ L
30 μ L	20 μ L	50 μ L
40 μ L	10 μ L	50 μ L
50 μ L	-	50 μ L

The Nano-Glo reagent contains both a lysis buffer and bioluminescent substrate and at least one volume is required for lysis according to the manufacturer. To determine if 20 μ L of this reagent would be sufficient, or whether more would be required, volumes of between 20 to 50 μ L were added to 20 μ L of AmB-treated axenic amastigotes, in triplicates, and the bioluminescent signal measured (Figure 5.1). There was no significant difference in bioluminescent signal as the volume of Nano-Glo reagent was increased, indicating sufficient lysis and substrate concentration was available when a 20 μ L 1:1 parasite:Nano-Glo assay is used.

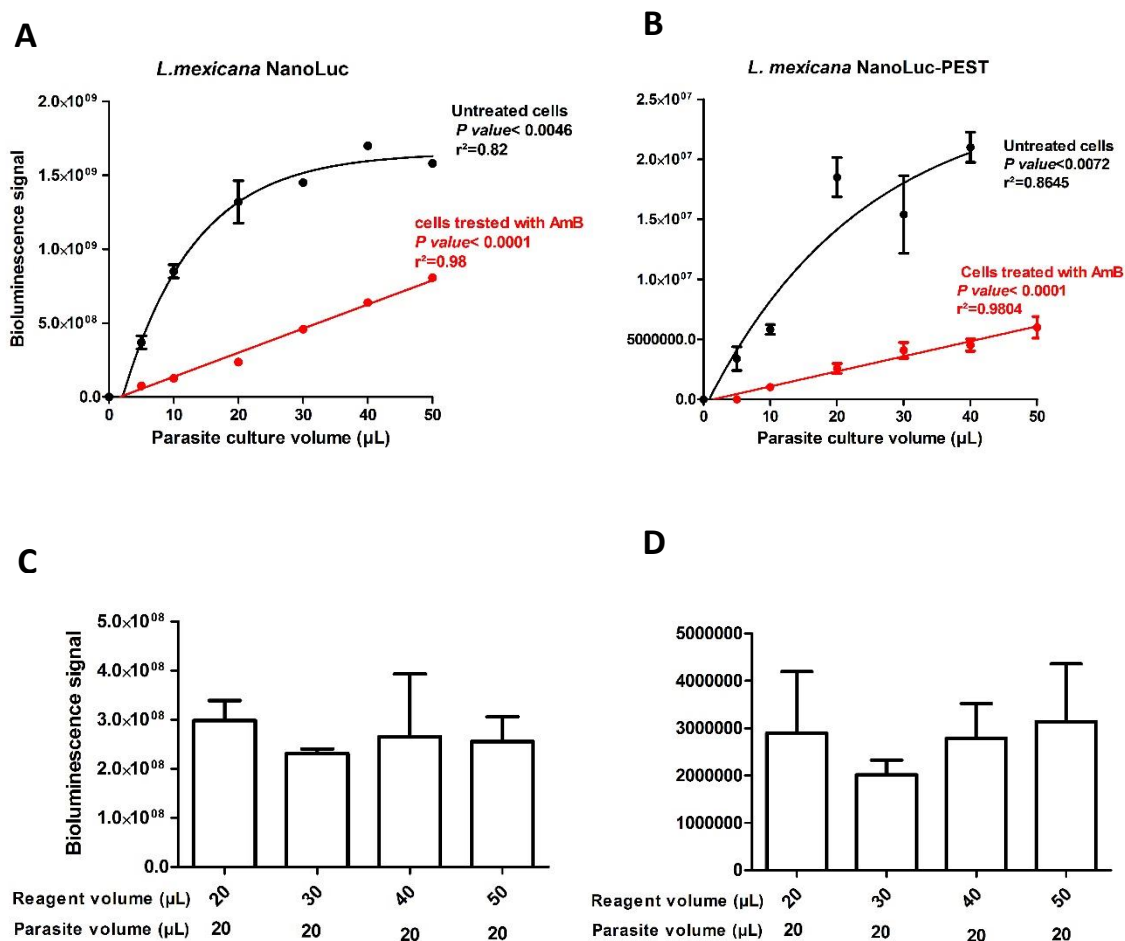


Figure 5.1: Optimizing assay volumes for bioluminescence assays with NanoLuc and NanoLuc-PEST transgenic *L. mexicana*. Correlating bioluminescence signal with parasite volume for (A) NanoLuc and (B) NanoLuc-PEST transgenic *L. mexicana*. Black lines represent untreated control parasites, and Red lines represent parasites exposed to 0.2 μM AmB. Data represent mean ± StDev of n=3 technical replicates. Charts C and D report the bioluminescent signal from 20 μL of NanoLuc and NanoLuc-PEST transgenic *L. mexicana* (respectively) with increasing volumes of Nano-Glo reagent. Bars show mean ± StDev of n=3 technical replicates.

To assess the two NanoLuc enzymes as a reporter of antileishmanial drug activity in axenic amastigote stage, the two bioluminescent enzymes were compared against a standard resazurin-based fluorescent viability assay using Amphotericin B. Here a concentration-normalized response assay was used to determine the EC₅₀ of Amphotericin B using both a fluorescence assay and a bioluminescence assay of the respective NanoLuc variant (Figure

5.2). In addition, the use of supralethal Amphotericin B ($2\mu\text{M}$ for 0% growth) and untreated parasites (100% growth) allowed for assay parameters such as the Z' , a statistical evaluation of the robustness of a high throughput assay (Zhang *et al.*, 1999), and signal:background (S:B) ratio to be determined and compared (Table 5.3). Each experiment was carried out as a technical triplicate with at least two biological repeats.

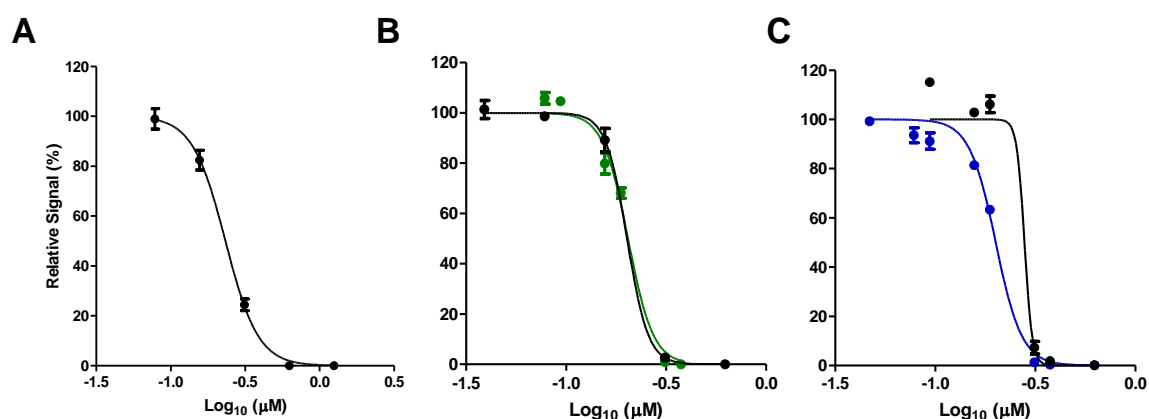


Figure 5.2: Amphotericin B concentration-normalized response profiles. Graphs depicting the concentration-response to amphotericin B in the (A) parental, (B) NanoLuc and (C) NanoLuc-PEST *L. mexicana* lines. The black line on each graph represents the response as determined using the fluorescent-based AlamarBlue assay. The green and blue lines represent the bioluminescent activity in the respective (B) NanoLuc and (C) NanoLuc-PEST *L. mexicana* lines. Mean values \pm StDev (n=6) are shown. Data are reported in Table 5.3.

The EC₅₀ values for amphotericin-B in the parental and transgenic lines were essentially indistinguishable (overlapping 95% CI) irrespective of the assay format used (Table 5.3), with the range of 0.20-0.27 μM reported comparable to the value of $0.30 \pm 0.02 \mu\text{M}$ previously described for *L. mexicana* axenic amastigotes (Callahan *et al.*, 1997) using the AlamarBlue assay. As expected, all assays report a robust assay performance with a Z' factor

value of ≥ 0.64 , with neither the fluorescence nor bioluminescence assays showing a marked improvement in their performance. The S:B ratios, however, do show some differences in assay performance. The bioluminescence-based assays performed on the transgenic NanoLuc and NanoLuc-PEST lines displayed S:B ratios approximately 4-fold and 100-fold higher, respectively, than those for the standard fluorescence-based assay on the same lines. Also, the S:B ratios for the NanoLuc-PEST transgenic was approximately 25-time greater than that for NanoLuc transgenic line. This difference reflects the short half-life of this protein that is targeted using a PEST sequence to the proteasome, providing an indication of the greater dynamic range achieved using this reporter. Based on these data, the same experiments were repeated using a second antileishmanial drug, milofosine (Figure 5.3). The same observations in terms of the same (or close to the same) EC_{50} values determined using the fluorescence and bioluminescence assays, robust assay performance (all $Z' > 0.68$) and vastly increased S:B ratio for the NanoLuc-PEST bioluminescence compared to fluorescence assay were all observed (Table 5.4). Based on these findings, it was decided to take the NanoLuc-PEST transgenic line forward to screen the MMV Pathogen Box library.

Table 5.3: Comparison of the EC_{50} , Z' and Signal:Background (S:B) values of amphotericin B (AmB) activity against wild-type and NanoLuc-expressing *L. mexicana* in fluorescent and bioluminescence assays.

Strain	Assay	AmB EC_{50} (μ M)		Z'	S:B
		Mean	95% CI		
Parental	Fluorescence	0.23	0.23-0.29	0.64-0.88	3.2-3.6
NanoLuc	Fluorescence	0.20	0.20-0.28	0.88-0.91	3.6-4.6
	Bioluminescence	0.20	0.18-0.19	0.84-0.85	13.2-14.4
NanoLuc-PEST	Fluorescence	0.27	20.7-0.28	0.72-0.88	2.4-5.1
	Bioluminescence	0.20	0.18-0.20	0.79-0.90	322.5-369.8

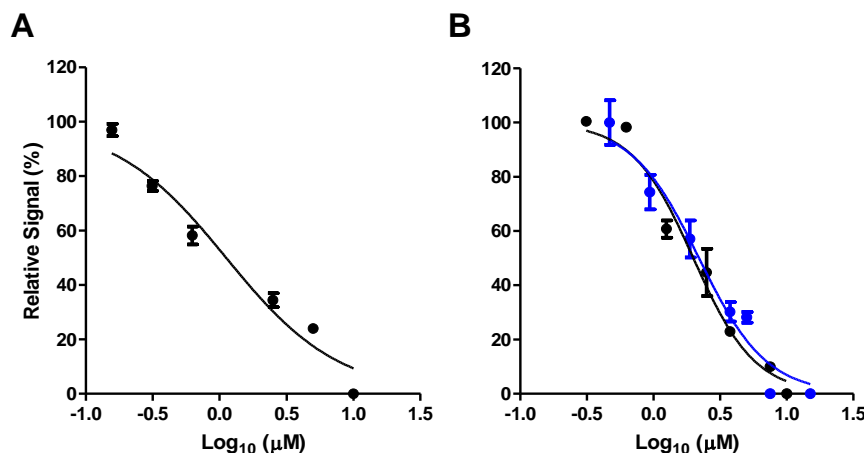


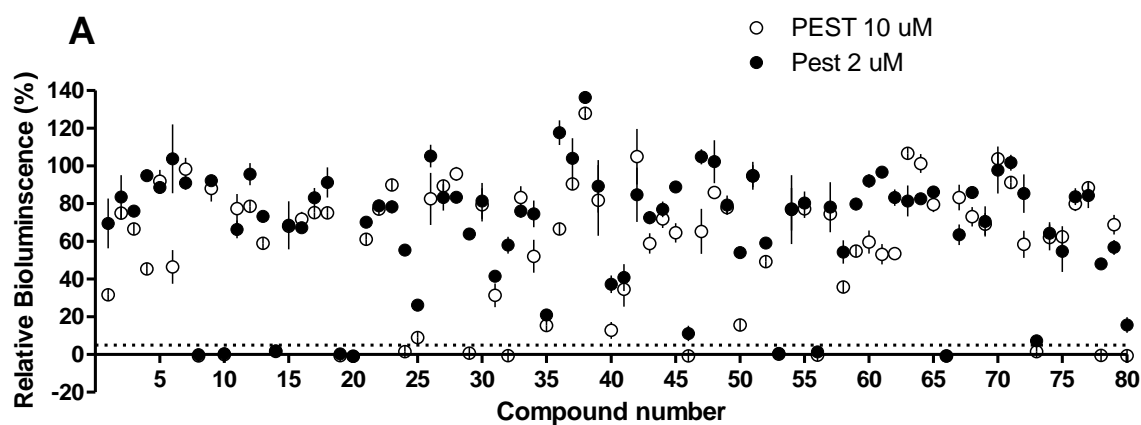
Figure 5.3: Miltefosine concentration-normalized response profiles. (A) Concentration-response curve of the parental *L. mexicana* cell line, measured using the fluorescence-based AlamarBlue assay. (B) Concentration-response curve of the transgenic NanoLuc-PEST expressing *L. mexicana* clone measured using both the fluorescence-based AlamarBlue assay (black) and the bioluminescence-based assay (blue). Mean values are shown ($n=6$) \pm StDev. EC₅₀ values for the parental and NanoLuc-PEST cell lines are reported in Table 5.4.

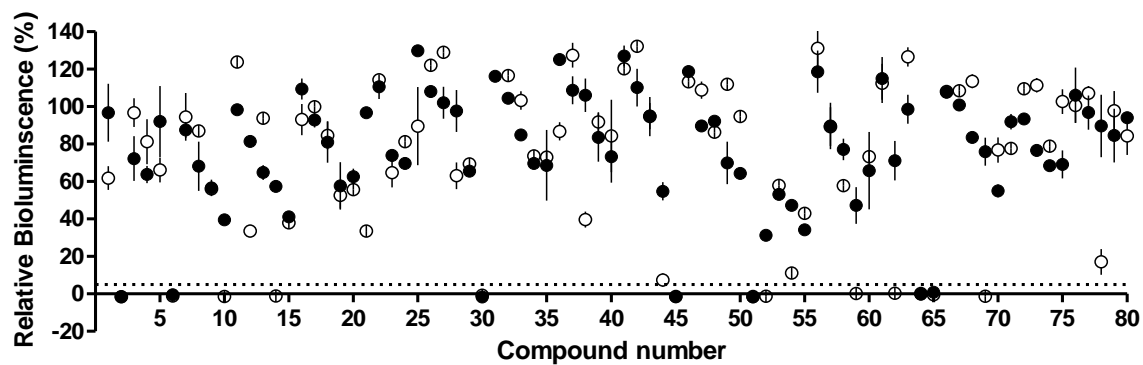
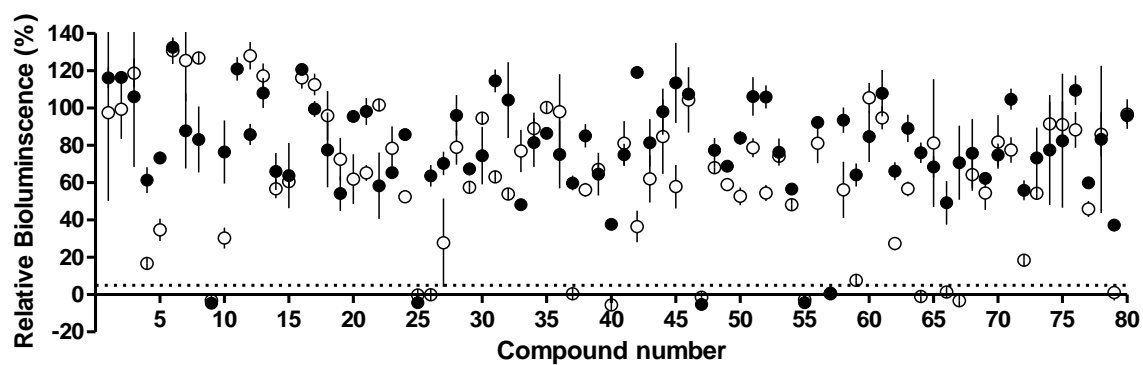
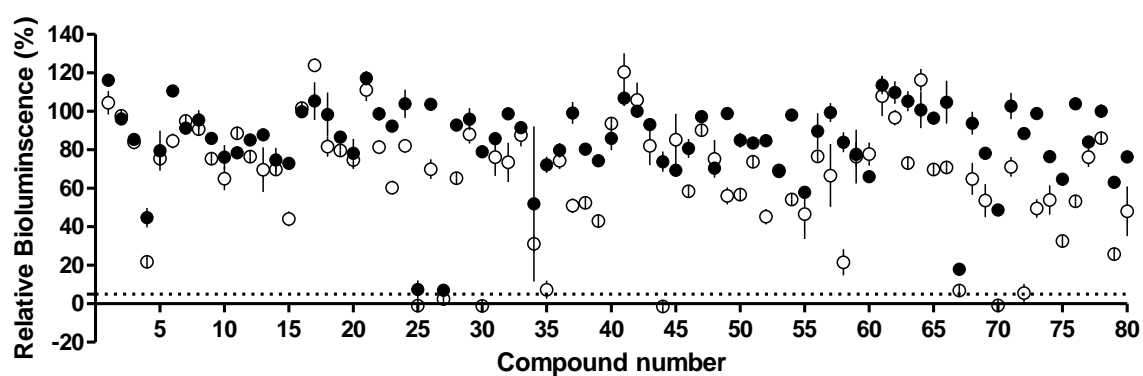
Table 5.4: Comparison of the EC₅₀, Z' and Signal:Background (S:B) values of miltefosine (MIL) (AmB) activity against wild-type and NanoLuc-PEST expressing *L. mexicana* in fluorescence and bioluminescence assays.

Strain	Assay	MIL EC ₅₀ (μM)		Z'	S:B
		Mean	95% CI		
Parental	Fluorescence	1.1	0.99-1.16	0.68-0.72	2.2-3.3
NanoLuc-PEST	Fluorescence	1.99	1.8-2.06	0.70-0.83	4.2-4.5
	Bioluminescence	2.19	2.07-2.35	0.84-0.86	192.7-211.5

5.2.3 Screening of MMV Pathogen Box against *L. mexicana* NanoLuc-PEST-transgenic line

The MMV Pathogen Box library was screened at two concentrations (10 μ M and 2 μ M) for activity against *L. mexicana* NanoLuc-PEST axenic amastigotes. Assays were performed in duplicate with two biological replicates (n=4). Axenic amastigotes were seeded at a density of 2×10^6 /mL in duplicate (100 μ l/well). Both no growth controls (2 μ M Amphotericin B) and solvent control (equivalent volume of DMSO) controls were made up on each plate. Cells were incubated for 72 hours at 32°C and a bioluminescence based assay was used to assess the relative cell growth as described in 2.3.5. These data are presented in Figure 5.4 as a dot plot of the mean of the normalized growth plotted for each compound at 20 μ M and 2 μ M. Table appendix 6 reports the data for each compound.



B**C****D**

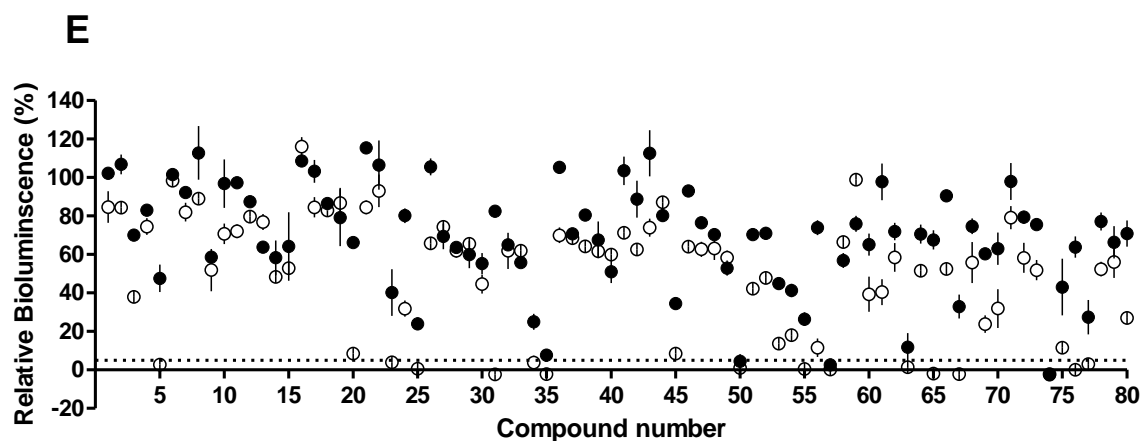


Figure 5.4: MMV Pathogen Box screening using the NanoLuc-PEST assay. The library is provided as five plates labelled A to E (and as shown here), each with 80 compounds – shown here on the x-axis (see also Table S2). The relative bioluminescence of the NanoLuc-PEST expressing *L. mexicana* when screened against 2 μ M (filled circle) or 10 μ M (open circle) is shown with the lines marking the StDev. The dashed line shows the point at which a 95% reduction in relative bioluminescence, ie a 95% kill, was achieved.

Using a scatterplot, the mean relative bioluminescence signals from each concentration were plotted to correlate the data. Using a colour code for the indicated disease the compounds were originally selected (Figure 5.5A), the distribution for the highly active compounds (>95% reduction at both concentrations, Figure 5.5B) in the MMV Pathogen Box reveals that of these 23 compounds, twelve were selected from antituberculosis screens and four from anti-kinetoplastid parasite screens. These 23 hits represent a hit rate of 5.75%, with all of these 23 hits selected to determine their EC_{50} .

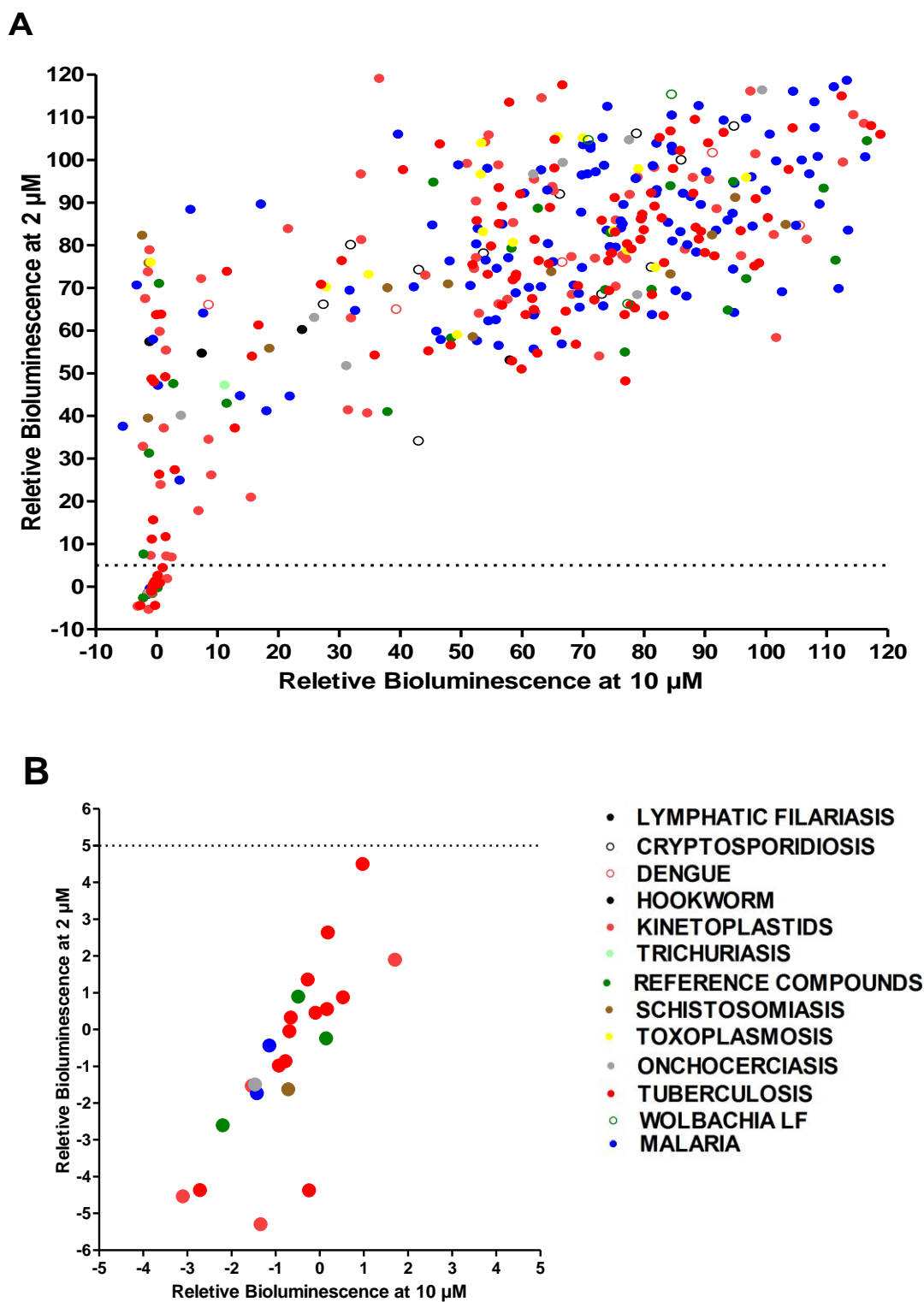


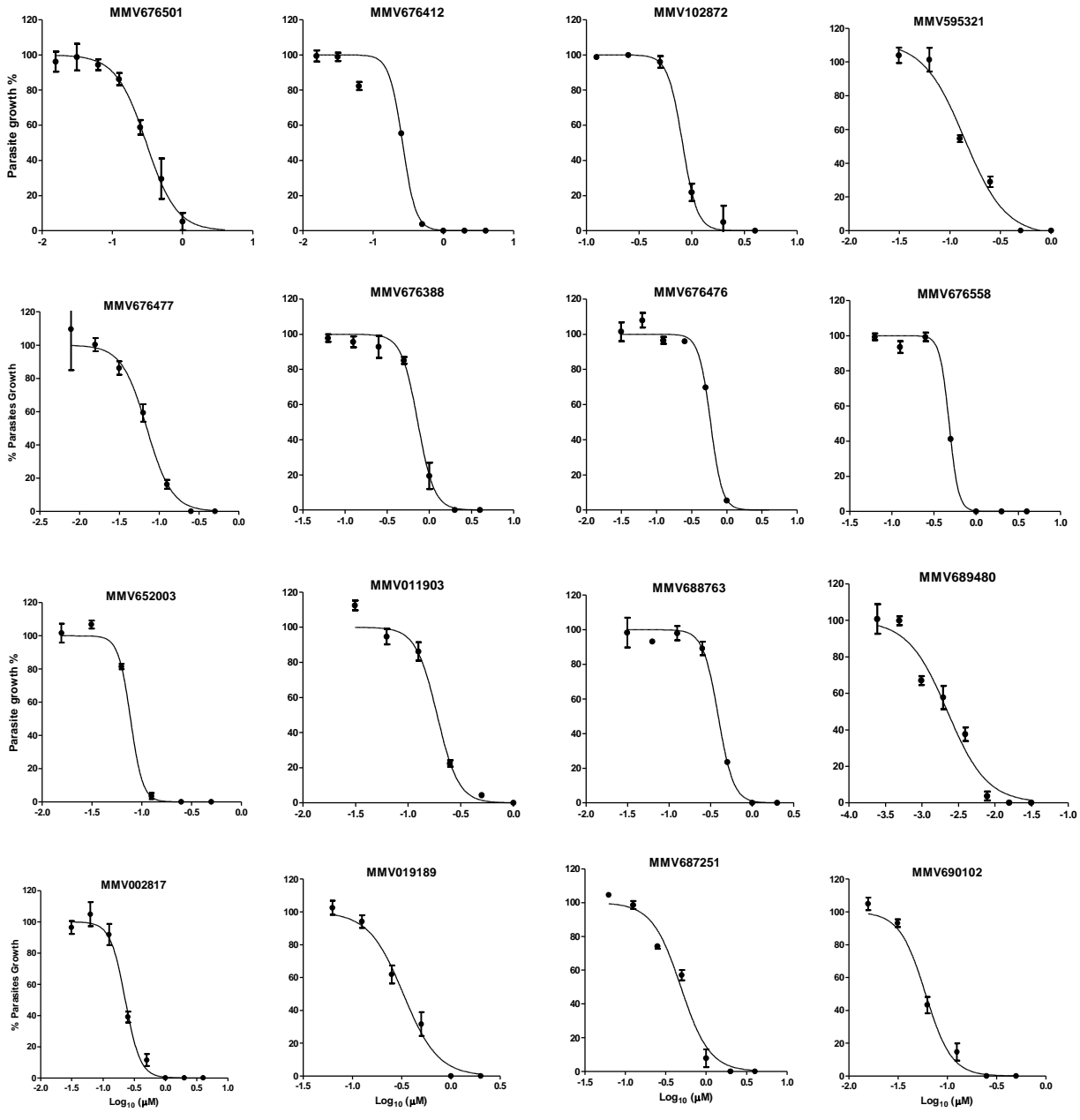
Figure 5.5: Screening the MWV Pathogen Box using the NanoLuc-PEST-based bioluminescence assay. Scatterplot correlating the mean bioluminescence following exposure to the indicated concentration of compounds. The mean (n=4) bioluminescence signal is shown, with the

key illustrating the disease screen that identified the compound for inclusion in the library (www.pathogenbox.org) (A) Illustrates the full library dataset with (B) providing an inset of the most potent compounds from the MMV Pathogen Box screen.

5.2.4 Determination of EC₅₀ values of selected compounds

The EC₅₀ of the 23 hit compounds were determined against axenic amastigote of *L. mexicana* NanoLuc-PEST-expressing transgenic line. Two-fold dilution series were prepared in triplicate and 100 µL of axenic amastigotes at a density of 2 x 10⁶ cells/mL incubated for 72 hours at 32°C. In addition, the use of a supralethal Amphotericin B (2µM for 0% growth) and untreated parasites (100% growth) were included on each plate and a bioluminescence based assay was used to assess the viability of cells (as described in 2.3.5). The 50% effective concentration (EC₅₀) was determined by analysis of a log transformed concentration versus normalized bioluminescence signal curves (Figure 5.6, except mebendazole as initial data suggested EC₅₀ >5µM) and are reported in Table 5.5.

Out of these 23 compounds, eight displayed an EC₅₀ value less than that observed for Miltefosine (2.19 µM). Of these eight compounds, two of them were the reference compounds (current drugs included in the MMV Pathogen Box) Buparaguone and Auranofin). I next took the most potent reference compound (Buparaguone) and the remaining six hit compounds forward to screen in a novel bioluminescence based intramacrophage assay.



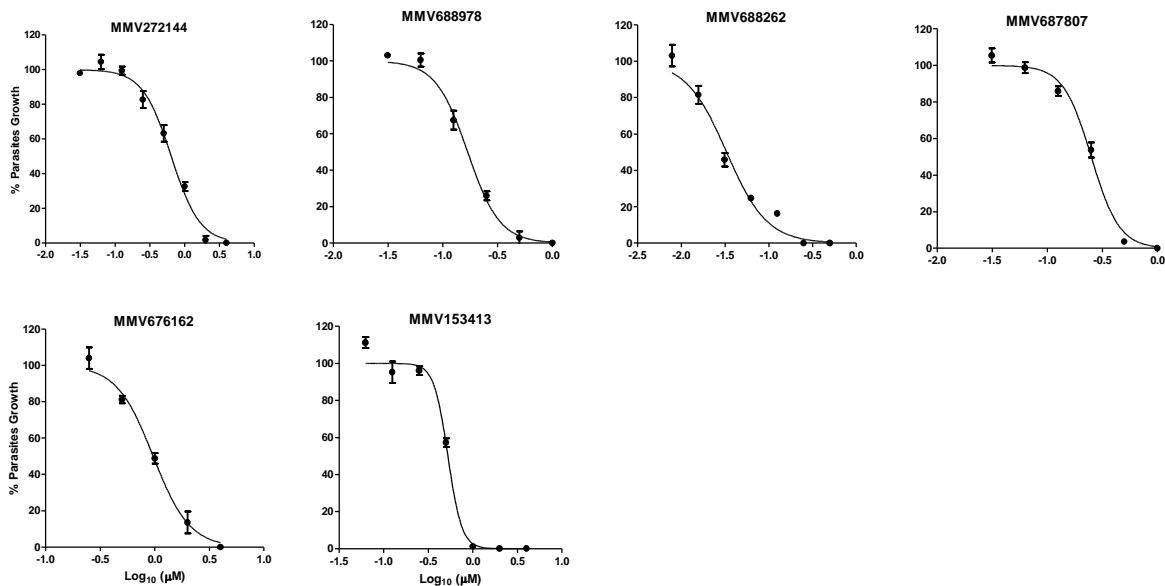


Figure 5.6: Log-concentration response curves for MMV Pathogen Box hits. Concentration-normalised bioluminescence response curves for 22 hits against axenic *L. mexicana* amastigotes. The data shown is a mean \pm StDev from at least three biological replicates. EC₅₀ estimates are reported in Table 5.5.

Table 5.5: EC₅₀ values for MMV Pathogen box hits against axenic *L. mexicana* amastigotes.

COMPOUND ID	MMV DISEASE SET	COMMON NAME	AXENIC AMASTIGOTES	
			EC ₅₀ (µM)	95% CI
<i>MMV689480</i>	REFERENCE COMPOUNDS	BUPARVAQUONE	0.0022	0.0017-0.002
<i>MMV688262</i>	TUBERCULOSIS	DELAMANID	0.03	0.031-0.031
<i>MMV690102</i>	KINETOPLASTIDS		0.06	0.038-0.054
<i>MMV676477</i>	TUBERCULOSIS		0.07	0-06-0.072
<i>MMV652003</i>	KINETOPLASTIDS		0.07	0.048-0.095
<i>MMV595321</i>	KINETOPLASTIDS		0.15	0.13-0.25
<i>MMV688978</i>	REFERENCE COMPOUNDS	AURANOFIN	0.17	0.16-0.18
<i>MMV011903</i>	MALARIA		0.18	0.12-0.15
<i>MMV002817</i>	ONCHOCERCIASIS	IDOQUINOL	0.22	0.21-0.23

MMV687807	TUBERCULOSIS		0.25	0.18-0.24
MMV676412	TUBERCULOSIS		0.26	0.19-0.28
MMV676501	TUBERCULOSIS		0.3	0.26-0.34
MMV019189	MALARIA		0.32	0.29-0.40
MMV688763	SCHISTOSOMIASIS		0.38	0.39 -0.48
MMV676558	TUBERCULOSIS		0.47	0.37-0.49
MMV687251	TUBERCULOSIS		0.48	0.48-0.49
MMV153413	TUBERCULOSIS		0.52	0.45-0.57
MMV676476	TUBERCULOSIS		0.58	0.53-0.73
MMV272144	TUBERCULOSIS		0.64	0.59-0.87
MMV676388	TUBERCULOSIS		0.73	0.54-0.69
MMV102872	TUBERCULOSIS		0.81	0.80-1.44
MMV688776	KINETOPLASTIDS		0.9	0.86-0.95
MMV003152	REFERENCE COMPOUNDS	Mebendazole	5>	-
AmB	NA		0.201	0.18-0.20
MIL	NA		2.19	2.07-2.35

5.2.5 Intracellular macrophage assay

The activity of the seven MMV Pathogen Box compounds, as well as amphotericin B and miltefosine, against intracellular *L. mexicana* NanoLuc-PEST-transgenic amastigotes in a macrophage cell line were assessed using a bioluminescence assay. Differentiation of THP-1 cells was performed by seeding 2.5×10^5 cells/mL in complete RPMI media supplemented with 20 ng/mL phorbol 12-myristate 13-acetate (PMA) to induce differentiation into a macrophage lineage (Jain *et al.*, 2012). These PMA-treated THP-1 cells were plated onto 96-well plates (200 μ L/well) and incubated for 24 hours at 37°C with 5% CO₂. Following incubation, adherent macrophages were carefully washed once with PBS to remove non-adherent cells. The adherent macrophages were then infected with axenic amastigotes at a ratio of 10:1 (parasites:macrophages) in complete RPMI medium, and incubated at 32°C

with 5% CO₂ for 16 hours. At this time, the infected cells were washed 4 times with PBS to remove extracellular parasites.

The specified concentration of each compound was diluted in a serial two-fold series and applied to the infected THP-1 cells as a technical triplicate. A non-drug treated control was included to represent 100% and uninfected THP-1 as a 0% control. These were incubated for 72 hours at 37°C and 5% CO₂ before a bioluminescence based assay was used to assess the signal relative to these controls (as described in 2.3.5). The 50% effective concentration (EC₅₀) was determined by analysis of a log transformed concentration versus normalized bioluminescence signal curve (Figure 5.7) with all experiments were prepared from at least three independent biological replicates (dotted lines). For comparison, on each curve, the data for the same compound on axenic amastigotes are shown using full lines. These intramacrophage EC₅₀ data are reported in Table 5.6.

The EC₅₀ values of selected compounds were less potent in intramacrophage *L. mexicana* amastigotes compared to the EC₅₀ values against free parasites, and the ratios of these values are ranged between 1.78 and 69.27 (Table 5.6). Compound MMV690102 presented the best value to reduction the infected macrophages, and has ratio of EC₅₀ (intramacrophage) to EC₅₀ (axenic amastigotes) of 1.78 and this in between 0.52 and 4.96 for AmB and MIL respectively (Table 5.6).

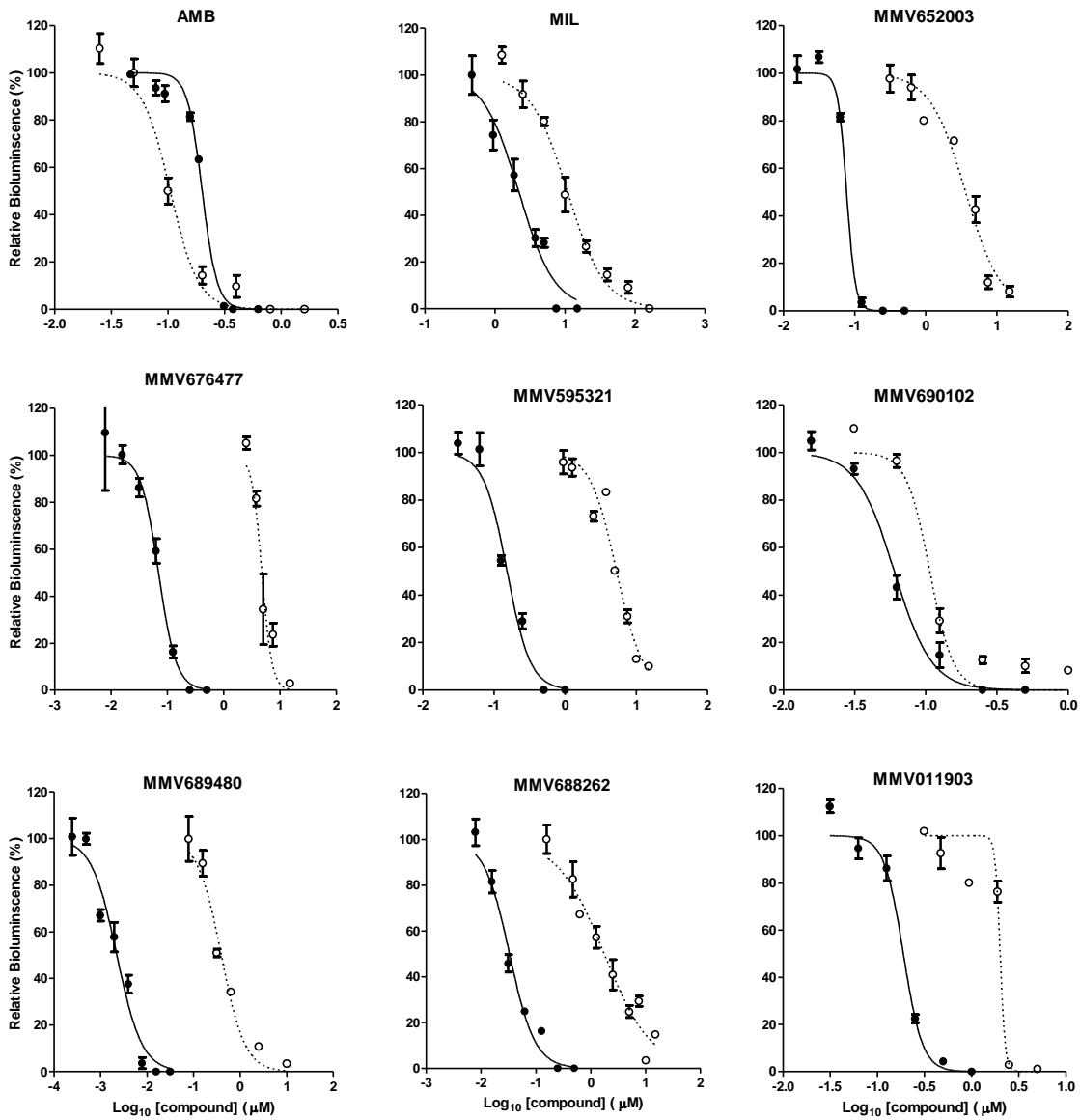


Figure 5.7: Bioluminescence assays of intracellular activity of MMV Pathogen Box compounds.

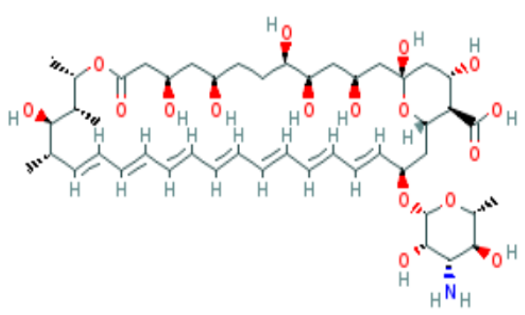
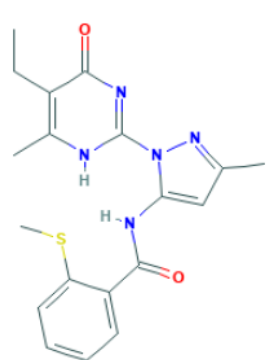
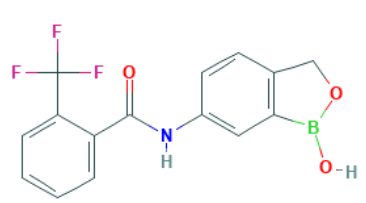
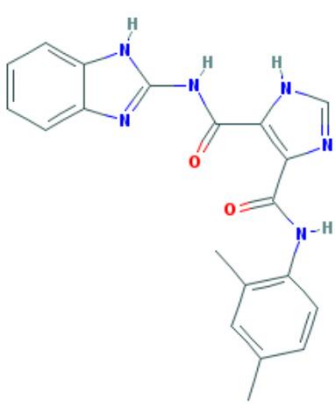
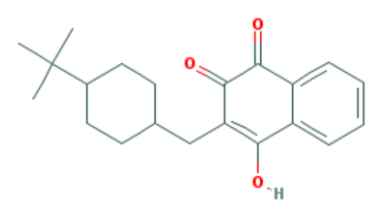
The concentration response curves (mean \pm StDev of n=9) for the indicated MMV Pathogen Box compound, amphotericin B (AmB) or miltefosine (MIL) against intracellular amastigotes in THP-1 (dotted lines) or axenic amastigotes (full line).

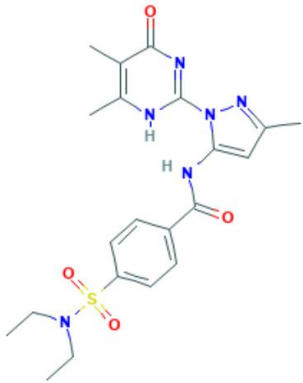
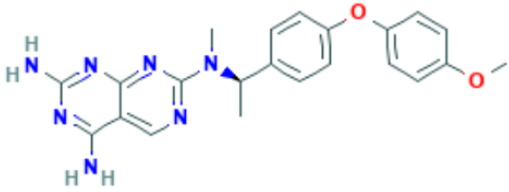
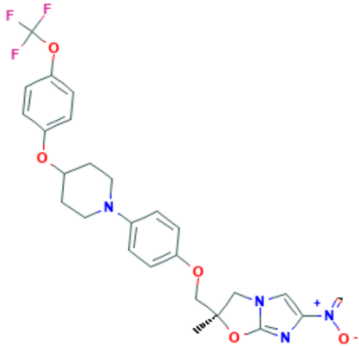
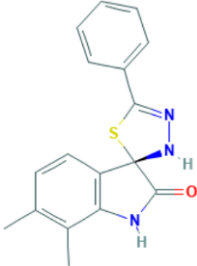
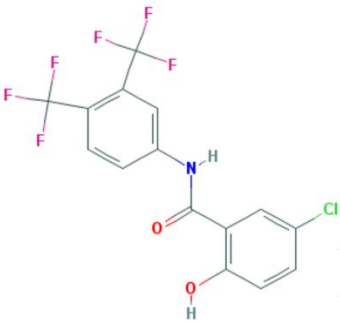
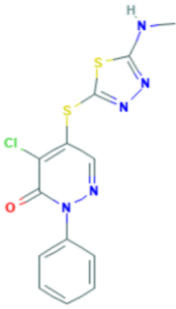
Table 5.6: A, activity of the most potent MMV compounds against axenic and intra-macrophage amastigotes using a bioluminescence assay. B, structure of compounds

A

Compound	EC ₅₀ ¹ (μM)	EC ₅₀ ² (μM)	The ratio of EC ₅₀ ² / EC ₅₀ ¹
	Axinec amastigotes	Intra- macrophage	
		Amastigotes Mean (95% CL)	
AMPHOTERICIN B	0.201	0.105 (0.86-1.03)	0.52
MILTEFOSINE	2.19	10.87 (9.89-11.12)	4.96
<i>MMV676477</i>	0.069	4.78 (4.85-5.53)	69.27
<i>MMV652003</i>	0.077	3.63 (2.98-4.24)	47.14
<i>MMV011903</i>	0.189	2.015 (0.96-1.42)	10.66
<i>MMV689480</i>	0.002	0.39 (0.40-0.46)	195
<i>MMV595321</i>	0.153	5.29 (4.50-6.01)	35.26
<i>MMV690102</i>	0.060	0.107 (0.87-0.20)	1.78
<i>MMV688262</i>	0.03	1.75 (1.50-2.12)	58.33
<i>MMV019189</i>	0.32	11.26	35.18
<i>MMV687807</i>	0.25	14.55	58.2
<i>MMV688763</i>	0.38	9.73	25.6

B

Structure of compound	
Amphotericin b 	Miltefosine 
MMV676477 	MMV652003 
MMV011903 	MMV689480 

<p style="text-align: center;">MMV595321</p>  <p>The structure of MMV595321 features a central pyrimidopyrimidine core. It is substituted with a methyl group at the 2-position, a methyl group at the 4-position, and a methyl group at the 6-position. A hydrogen atom is attached to the nitrogen at the 5-position. This core is linked via an amide bond to a para-substituted benzene ring, which is further connected to a diethylsulfonamide group.</p>	<p style="text-align: center;">MMV690102</p>  <p>The structure of MMV690102 consists of a fused pyrimidopyrimidine system. It has a methyl group at the 2-position and a methyl group at the 4-position. A hydrogen atom is attached to the nitrogen at the 5-position. This core is linked via a secondary amine to a para-substituted benzene ring, which is further connected to a 4-methoxyphenyl group.</p>
<p style="text-align: center;">MMV688262</p>  <p>The structure of MMV688262 is a complex molecule. It features a central pyrimidopyrimidine core with a methyl group at the 2-position and a methyl group at the 4-position. A hydrogen atom is attached to the nitrogen at the 5-position. This core is linked via an amide bond to a para-substituted benzene ring, which is further connected to a piperidine ring. The piperidine ring is also linked to another para-substituted benzene ring, which is further connected to a trifluoromethoxy group.</p>	<p style="text-align: center;">MMV019189</p>  <p>The structure of MMV019189 features a central pyrimidopyrimidine core with a methyl group at the 2-position and a methyl group at the 4-position. A hydrogen atom is attached to the nitrogen at the 5-position. This core is linked via a secondary amine to a para-substituted benzene ring, which is further connected to a phenyl group.</p>
<p style="text-align: center;">MMV687807</p>  <p>The structure of MMV687807 features a central pyrimidopyrimidine core with a methyl group at the 2-position and a methyl group at the 4-position. A hydrogen atom is attached to the nitrogen at the 5-position. This core is linked via an amide bond to a para-substituted benzene ring, which is further connected to a trifluoromethyl group. The benzene ring is also linked to a chlorine atom and a hydroxyl group.</p>	<p style="text-align: center;">MMV688763</p>  <p>The structure of MMV688763 features a central pyrimidopyrimidine core with a methyl group at the 2-position and a methyl group at the 4-position. A hydrogen atom is attached to the nitrogen at the 5-position. This core is linked via a secondary amine to a para-substituted benzene ring, which is further connected to a chlorine atom and a hydroxyl group.</p>

5.2.6 *In vitro* cell cytotoxicity assay

There was only sufficient material available from the MMV Pathogen Box for three compounds (MMV011903, MMV676477 and MMV595321) to explore their cytotoxicity against the THP-1 cell line. However, for all three compounds, no effect against THP-1 was measured using a resazurin viability assay at concentrations up to 50 μ M, therefore suggesting that their CC₅₀ is > 50 μ M (data not shown). The MMV Pathogen Box library has been tested for cytotoxicity against a number of other human cell lines, and this information is available online at www.pathogenbox.org/about-pathogen-box/supporting-information. For example, HepG2 cytotoxicity data is available for compounds MMV011903, MMV676477 with MRC5 (lung fibroblast cell line) cytotoxicity data is available for compound MMV652003. These varied human cell line cytotoxicity data are reported in Table 5.7 and then compared against the same activity against the axenic and intracellular amastigotes. From the THP-1 data generated here, there appears to be a moderate selectivity against the intracellular amastigotes (SI between 9-30), although for at least one of these compounds (MMV676477) there appears to be cytotoxicity against HepG2. Using the data available from the MMV, compounds MMV688262 and MMV690102 show some selectivity against intracellular amastigotes compared to HepG2 or MRC5, respectively, although for both no other human cell line data is available to corroborate this potential selectivity.

Table 5.7: Human cytotoxicity data for selected MMV Pathogen Box compounds.

MMV ID	EC ₅₀ (μM) ^b		HepG2 CC ₅₀ (μM) ^a	SI		MRC5 CC ₅₀ (μM) ^a	SI		THP1 EC ₅₀ (μM) ^b	SI	
	Axenic amastigotes	Intracellular amastigotes		CC ₅₀ /EC ₅₀ axenic	CC ₅₀ /EC ₅₀ intracellular		CC ₅₀ /EC ₅₀ axenic	CC ₅₀ /EC ₅₀ intracellular		CC ₅₀ /EC ₅₀ amastigotes	CC ₅₀ /EC ₅₀ intracellular
<i>MMV011903</i>	0.189	2.015	>10	>53	>5	-	-	-	>50	>264	>24.8
<i>MMV676477</i>	0.069	4.783	1.3	18.8	0.27	-	-	-	>50	>724	>10.45
<i>MMV595321</i>	0.153	5.295	-	-	-	-	-	-	>50	>326	>9.44
<i>MMV689480</i>	0.002	0.394							12.03 ^c	6015	30.53
<i>MMV688262</i>	0.03	1.75	72.5	2416	41.42	-	-	-	-	-	-
<i>MMV652003</i>	0.077	3.637	-	-	-	>32	>415	>8.8	-	-	-
<i>MMV690102</i>	0.060	0.107	-	-	-	5.4	90	50.46	-	-	-

^a Data provided with the MMV Pathogen Box. ^b Data obtained as part of this study. -, no data available. ^c (Jamal *et al.*, 2015)

5.2.7 Evaluation the initial cytotoxic effect of antileishmanial reference compounds

The Horrocks laboratory have used the unstable luciferase reporter to measure the immediate cytotoxic effect of compounds against intraerythrocytic *P. falciparum* (Ullah *et al.*, 2017), and led to the BRRoK assay as used here in Chapter 3. Here, the short half-life of the reporter allows the effect of compounds in reducing viability (ie they stop making new luciferase to replace that degraded) to be measured as a timecourse of the initial cytotoxic effect. This is important in antimalarial drugs, where a rapid reduction in parasite load is important for malaria treatment. As yet, there is no rapid rate of kill requirement for antileishmanial drugs, but here I explore whether the initial cytotoxic timecourse can be measured due to the short half-life (c 16 mins, Berry *et al.*, 2018) of the NanoLuc-PEST in *L. mexicana*. The effect of antileishmanial reference drugs (AmB, MIL and pentamidine) and the antibiotic hygromycin B (an inhibitor of protein translation in eukaryotes) on *L. mexicana* NanoLuc-Pest transgenic line were measured at a series of fold-EC₅₀ values of each drug (1, 3 and 9 x EC₅₀). These EC₅₀ data were measured on the *L. mexicana* NanoLuc-Pest transgenic line using a bioluminescence concentration-normalized response assay (Figure 5.8) and are reported in Table 5.8. The concentration and time-dependent loss of viability (bioluminescence signal normalized to an untreated control) was assessed at these three concentrations over a period of 6, 24, 48 and 72 hours. The assay was done as three biological repeats with the mean normalized bioluminescent signal \pm StDev (n=9) plotted against fold-EC₅₀ for each timepoint (Figure 5.9).

Whilst all compounds show both a time and concentration dependent loss in bioluminescence (Figure 5.9), although less pronounced between 3x and 9x EC₅₀ as the timecourse extends to 48 and 72 hours, there is some differentiation between the loss of viability profiles for the different drugs. Pentamidine apparently has the most pronounced

loss of viability followed by miltefosine, then amphotericin B, with the rate of loss of signal least for hygromycin B. At 6hours, the rate of bioluminescent signal loss for hygromycin B follows a pattern that suggests that the drug is weakly cytotoxic at best and quite likely to be cytostatic.

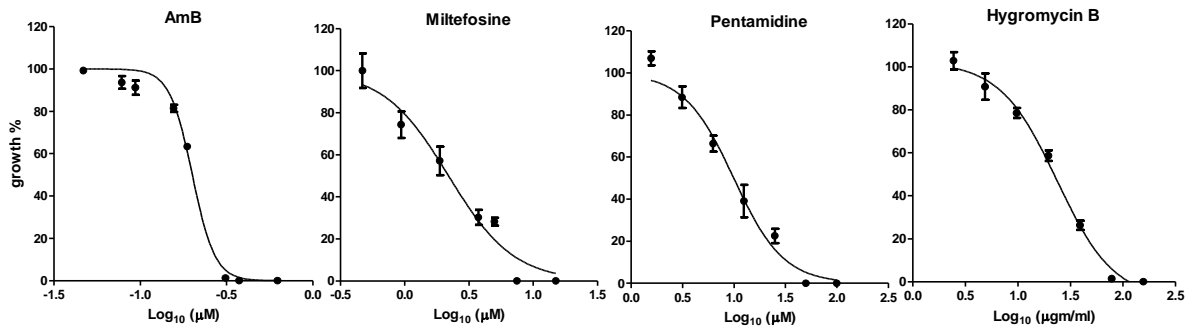


Figure 5.8: EC₅₀ responses to Amphotericin B (AmB), Miltefosine (MIL), Pentamidine and Hygromycin B in axenic *L. mexicana* amastigotes expressing NanoLuc-PEST. Mean values are shown (n=4) ± StDev.

Table 5.8: Comparison the EC₅₀ values between antileishmanial drugs

	EC ₅₀ (μM)	
	Mean	95% CI
Amphotericin B	0.2	0.18-0.20
Miltefosine	2.19	2.07-2.35
Pentamidine	9.94	10.08-1.39
Hygromycin B	32.65	21.12-24.23

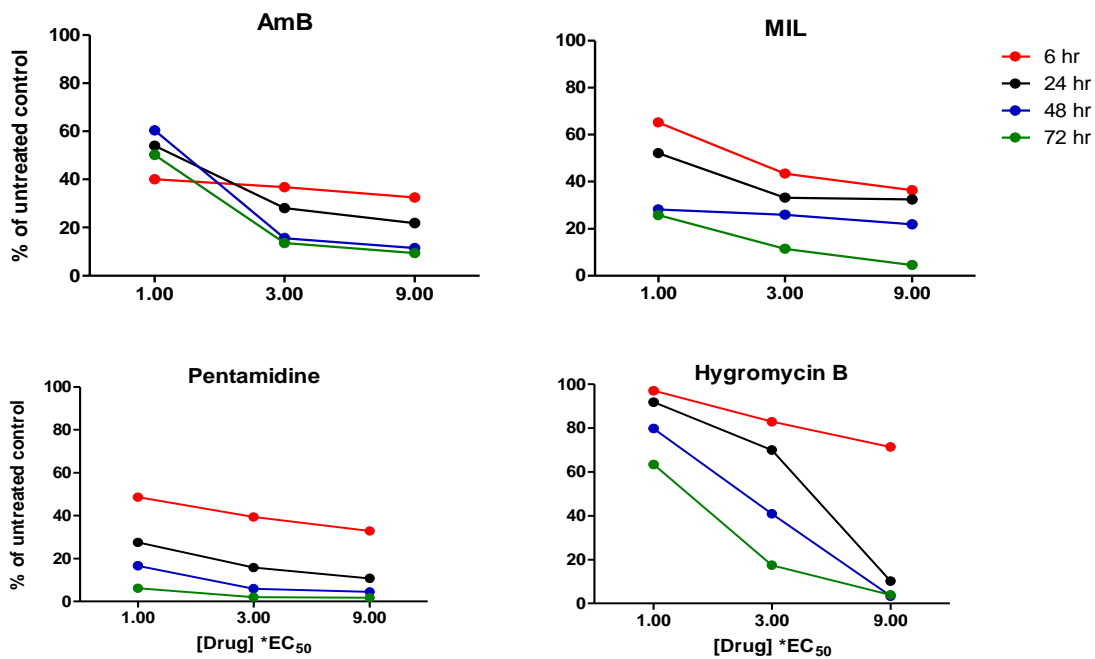


Figure 5.9: Time and concentration-dependent loss of bioluminescence representing a timecourse of cytotoxic activity for antileishmanial drugs. The mean normalized bioluminescent signal from *L. mexicana* NanoLuc-Pest transgenic lines exposed to increasing fold-EC50 concentrations of amphotericin B (AmB), miltefosine (MIL), pentamidine and hygromycin B. The key indicates the time for each concentration-reponse reported on each graph. Data represent mean \pm StDev (n=9).

5.3 Discussion

Over the last years the ability to use transgenic leishmanial parasites that express one or more luciferases has offered new methods for screening compounds and is an approach that has been applied to a number of other infectious disease models (Lang *et al.*, 2005, Mandal *et al.*, 2009; Plock *et al.*, 2001). For example, a bioluminescent *L. amazonensis* parasites expressing firefly luciferase has been used for drug screening against infected macrophages (Lang *et al.*, 2005). In this thesis, I report the evaluation of the NanoLuc luciferase. This new luciferase is a small enzyme (19.1kDa) which produces a high intensity bioluminescence using a furimazine substrate and does not require ATP to catalyse the oxidation process that results in light emission (Figure 5.10). The NanoLuc enzyme is very stable in *L. mexicana*, with a long half-life of greater than 8 hours (Berry *et al.*, 2018). A modified form of the enzyme, NanoLucPEST, retains the high enzymatic activity of NanoLuc but has a much shorter half-life of 16 mins – this instability, coupled to the high signal intensity producing an assay of antiproliferative action with a high S:B ratio that was exploited here in the screen of the MMV Pathogen Box (Berry *et al.*, 2018).

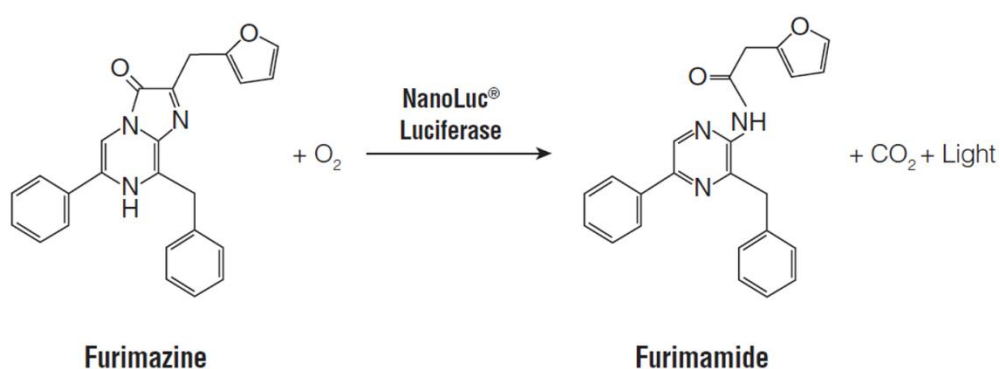


Figure 5.10: The bioluminescent reaction catalyzed by NanoLuc luciferase. (Source: Promega)

I tested the MMV Pathogen Box against a *L. mexicana* NanoLucPest transgenic line (generated by Dr Berry of the Price Laboratory) using a bioluminescent assay as a drug discovery screening tool. A total of 23 hits were identified, giving a hit rate of 5.75%. These hits included three reference compounds (Buparvaquone, Mebendazole and Auranofin), four compounds previously identified as targeting kinetoplasts, twelve compounds identified in a tuberculosis screen (52% of total selected compounds), two compounds active against *Plasmodium* spp., and one compound each identified in onchocerciasis and schistosomiasis screens (Figure 5.5). The activity of compounds identified against *Mycobacterium tuberculosis* have been proposed to be likely of benefit in screening against Leishmanial parasites as they are required to be able to transit multiple membrane barriers as well as target a pathogen within an acidic compartment (Russell *et al.*, 2010). The higher hit rate here against *Mycobacterium tuberculosis* screen compounds in the MMV Pathogen Box is not likely as a result of this, as axenic amastigotes were initially screened, but is perhaps a bias introduced by chance because 29% of the Pathogen Box compounds are from TB screening programmes.

Importantly in this study, a number of the most potent hits were taken forward to evaluate a NanoLuc based assay of intramacrophage activity. As perhaps expected, the EC₅₀ values in intramacrophage for all seven compounds were higher than those obtained from the screen of the axenic amastigotes alone (Table 5.6; Figure 5.7). This a result of the compound traversing an additional two membranes before it reaches the *Leishmania* amastigote. However, all seven compounds displayed an EC₅₀ < 5 µM, which is below the 10 µM limit suggested as an initial threshold for hits against *L. donovanni* intramacrophage stages (Katsuno *et al.*, 2015). As well as these compounds being active against *L. infantum* intramacrophage amastigotes (the screen used for their inclusion in the MMV Pathogen Box), their cytotoxicity against MRC5 cells (Table 5.9) was provided with the resource

(<https://www.pathogenbox.org/about-pathogen-box/supporting-information>). Of note is that the relative order of activity of their EC₅₀ activity, and thus selectivity when compared to this human cell line, is the same in the two species for three of the compounds for which data is available.

Table 5.9: Activity of selected kinetoplastid hits against *L. infantum* intracellular macrophage and cytotoxicity

Kinetoplastid compounds	MRC5 CC ₅₀ (μM)	<i>L. mexicana</i> in intra-macrophages EC ₅₀ (μM) ^a	SI CC ₅₀ /EC ₅₀	<i>L. infantum</i> in intra-macrophages EC ₅₀ (μM) ^b	SI CC ₅₀ /EC ₅₀
<i>MMV690102</i>	5.4	0.107	50.4	0.03	180
<i>MMV652003</i>	>32	3.63	8.8	1.4	23
<i>MMV595321</i>	6.6	5.29	1.2	6.9	1
<i>MMV688776</i>	>64	-	-	44	1.5

^a Data obtained as part of this study. ^b Data provided with the MMV Pathogen Box

Of the seven compounds taken to intramacrophage assays, three compounds (MMV652003, MMV689480 and MMV688262) were previously known to be active against kinetoplastids. The results for MMV688262 correlate well with the existing data, despite this previous data being gathered against intracellular *L. donovani* with EC₅₀ values 0.087 μM (Patterson *et al.*, 2016). However, the EC₅₀ results for MMV689480 (Buparvaquone) of 0.394 μM in the intracellular assay is at least three times lower than the previously reported values (1.25 μM) against *L. mexicana* infected macrophages (Mäntylä *et al.*, 2004). This may indicate a difference resulting from the types of intracellular assay used – and I discuss below more about this aspect of the bioluminescence based assays. The remaining MMV652003 compound is active against *T. brucei* with EC₅₀ values as low as 0.02 μg/mL (Ding *et al.*, 2010; Jacobs *et al.*, 2011).

The main advantage of the bioluminescent technique in an infected macrophage model, a method which has already been shown to be advantageous for studying intracellular stages of *Plasmodium falciparum* and *Mycobacterium tuberculosis* (Ullah *et al.*, 2017; Andreu *et al.*, 2012) is the simplicity of the assay format. This allows screening programmes to assess compound activity against the intracellular parasite to be developed that reduce the time burden, a requirement for specialist equipment and post-assay processing associated with the current microscopy based high content imaging techniques.

As an example of this, in chapter 3 the intramacrophage *L. mexicana* activity of amphotericin B was determined using a Sybr-Green I fluorescent microscopy assay, with a NanoLuc-PEST evaluation of the same activity in Chapter 5. There was a good correlation between the bioluminescence- and microscopy-based assays (Figure 5.11). However, the luminescent signal decreased by >99%, whilst the fluorescent counting assay still reported ~20% infected macrophages (Figure 5.11). One interpretation is that the bioluminescence-based assay is more sensitive than the microscopy-based technique, as only viable parasites produce bioluminescence and are therefore detected. In comparison, the standard microscopy based counting assay relies on either nuclear staining using DAPI or Sybr Green I, or parasite-specific antibodies (for example HASPB) (De Muylder *et al.*, 2011; Jain *et al.*, 2012). Not only can parasite nuclear staining can be obscured by the macrophage nucleus, but these protocols only detect the presence of the parasite, not its viability. The NanoLuc-PEST expressing cell line therefore may provide a unique opportunity to assess compound efficacy against intracellular parasites without the need for laborious, less sensitive, microscopy-based counting assays.

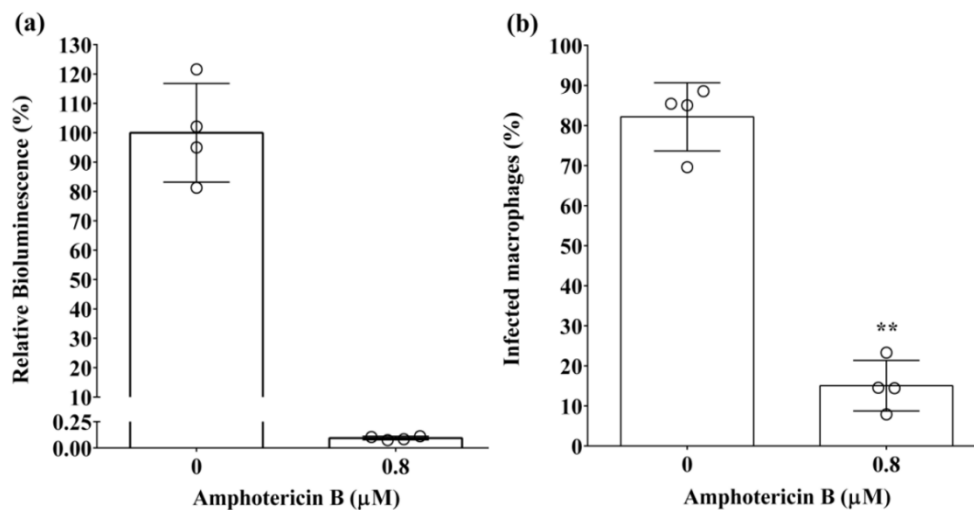


Figure 5.11: Comparison of bioluminescence- and microscopy-based intra-macrophage infection assays following treatment with Amphotericin B. (a) Infection of PMA-differentiated THP-1 was assessed by the NanoLuc-PEST-expressing transgenic *L. mexicana*, using the novel bioluminescence-based assay. Infected cells were exposed to 0.8 μM amphotericin B, or left untreated, for 72 hours. Relative bioluminescence is shown after each treatment, calculated against the average value for the untreated cells. Mean values are shown (n=4) ± SD. Results were analysed by Paired T Test on raw data ($p < 0.001$). (b) Infection of PMA-differentiated THP-1 macrophages was assessed by the NanoLuc-PEST-expressing transgenic *L. mexicana*, using the standard microscopy-based counting assay. Infected cells were exposed to 0.8 μM amphotericin B, or left untreated, for 72 hours.

Moreover, using the dynamic response of NanoLuc-PEST expressing parasites, I evaluated the initial cytotoxic activity of a range of antileishmanial reference drugs against amastigote NanoLuc-Pest transgenic line using concentration and time based assays similar to those developed previously in our laboratory to explore the initial action of antimalarial drugs (Ullah et al., 2017). The key to the *P. falciparum* study was that *in vivo* data for a small number of drugs are available to compare against the *in vitro* data. Thus, this study represented a start in defining the relative order of the rate of *in vitro* cytotoxic action. The reference compounds selected were pentamidine, miltefosine, hygromycin B and

amphotericin B – as either antileishmanial drugs or a selection marker with known mode of action. Pentamidine, miltefosine and amphotericin B were all shown as having a cytotoxic effect on *L. mexicana* NanoLuc-Pest transgenic line when tested at 3x and 9x EC₅₀ as the timecourse extended to 48 and 72 hours, whilst hygromycin B was slow-acting/cytostatic in its killing effect. The data further suggested that pentamidine has the most pronounced loss of viability followed by miltefosine, then amphotericin B, with the rate of loss of signal least for hygromycin B. These observations are in line with a recent study by Kerkhof *et al*, (2018), a short time-to-kill (defined as completely eliminating amastigotes) for intracellular amastigotes was observed for miltefosine of at least 72 hours for *L. infantum* and 96 hours for *L. donovani* at 5× EC₅₀ (20 μM). While amphotericin B took at least 192 hours in both *L. infantum* and *L. donovani* (Table 5.10). A short rate of kill was also observed in another study for miltefosine, of at least 168 hours at 2× EC₅₀ (10 μM) for *L. infantum* and >240 hours for amphotericin B at 2× EC₅₀ (2 μM). While the initial cytotoxic activity for miltefosine and amphotericin B took more than 240 hours at 2× EC₅₀ against *L. donovani* for both of them (Table 5.10) (Maes *et al.*, 2017).

Table 5.10: *In vitro* time-to-kill for current antileishmanial reference compounds. (Van den Kerkhof *et al.*, 2018)¹ (Maes *et al.*, 2017)²

Drug	Concentration 5 x EC ₅₀ μM	Concentration 2 x EC ₅₀ μM	<i>L. infantum</i>	<i>L. donovani</i>
			TTK (h)	TTK (h)
MIL ¹	20	-	72	96
AmB ¹	5	-	192	192
MIL ²	-	10	168	>240
AmB ²	-	2	>240	>240

The initial cytotoxic activity of antileishmanial drugs are still a relatively under reported pharmacodynamic property. The determination of initial cytotoxic activities may, however, help in the design of drug combination therapies that would reduce the development and spread of drug resistance and/or reduce treatment schedules - something that could increase

compliance and reduce drug costs (Sundar *et al.*, 2015; Jha *et al.*, 2013). The dynamic response of the NanoLucPEST system reported here may, with more *in vivo* data, help develop a validated *in vitro* system to screen this pharmacodynamics property. *In vitro* rate of kill assays are increasingly being developed and tested in a range of pathogens, including antibacterials (Nielsen *et al.*, 2007), antifungals (Gil-Alonso *et al.*, 2016) and antimalarials (Ullah, 2017) but its novelty in leishmaniasis is reported here for the first time.

Chapter 6 General discussion

Here I report a screen of the antiproliferative activities of 643 Phytopure library compounds against three different parasites. These parasites represent aetiological agents, or models, of malaria, trypanosomiasis and leishmaniasis. The library represented a unique resource for lead discovery of high value chemicals from temperate zone plants, recognising that these plants are highly unlikely to have been used as a traditional medicine for these diseases endemic in tropical and subtropical zones. Whilst the evaluation of potential hit compounds against each pathogen did not definitively identify a potent and selective activity within this library, these 643 compounds represent an incredibly small fraction of phytochemicals likely available from temperate zone plants. The potential for plant-derived natural products, and particularly those that have been used in traditional medicines, is recognised as an important part of public health in developing countries (Carlos, 2002) and there is a WHO strategy for their use (WHO, 2013). However, plant-based natural products, representing the majority of traditional medicines, are only one source of natural products that don't recognise opportunities available from microorganisms, marine sources or even animal sources.

The phytopure library was screened here against intraerythrocytic *P. falciparum*, blood-stream forms of *T. b brucei* and axenic amastigotes of *L. mexicana*. Other work in the laboratory has used the same library against bloodstream forms of *Trypanosoma evansi*, the aetiological agent of Surra in camels (H. Price, personal communication) and the same library has been screened in Aberystwyth against schistosomules of *Schistosoma mansoni* (Hoffmann, personal communications). Recognising that the biological activities of these natural products need not only be as antiparasitics, a new project to screen the library at Keele University against aphids to look for natural insecticide agents will shortly start. These projects together illustrate the utility of natural product libraries, and this library in particular

given that the natural products are purified and are not fractions prepared using a range of aqueous and organic solvents and often contain a complex mix of phytochemicals.

Given the size of the library, it was perhaps not surprising to not have an active and selective hit against any of the parasites screened. Screening of massive compound libraries to generate the Tres Cantos antimalaria compound set, some 30000 hits from 5 million compounds, represents one hit per 166 compounds screened (Gamo *et al.*, 2010; Guiguemde *et al.*, 210). This would suggest three potent hits against *P. falciparum* – and whilst there were several, they did not show the level of selectivity (and/or lack of toxicity against HepG2) that would be required to take them forward. The chemical diversity in the 5 million compounds screened is also greater than that within the Phytopure library. The four related triterpenes 700022, 700107, 700136 and 700240 did show both activity and selectivity against the *L. mexicana* axenic amastigotes. These compounds also showed activity against axenic amastigotes of *L. donovani*, an aetiological agent of visceral leishmaniasis in the Old World and would perhaps suggest that they may have a broad antileishmanial activity – although not anti-kinetoplastid activity as are not all hits against *T. brucei* nor *T. evansi*. Data presented in chapter 3 indicates that several of these triterpenes were active against intramacrophage amastigotes – although high concentrations (9xEC₅₀) had to be used. Following the work described here in Chapter 5, specifically the development of a NanoLuc-PEST assay for intramacrophage amastigotes, the same assay was used to determine the EC₅₀ of 700022 (Figure 6.1). The log concentration-response curve of intramacrophage amastigotes is shifted towards the right of the axenic amastigotes – as would be expected for a majority of compounds when their axenic *v* intramacrophage activity is compared (see several examples from the MMV Pathogen Box in Chapter 5). Plotting the antiproliferative activity curves of 700022 against THP1 and HepG2 human cell lines on the same graph

illustrates how the more relevant assessment of 700022 activity against *L. mexicana* now illustrates potential issues with cytotoxicity as the selective indices shrink from 30-50 to 1.6-2.6 (Table 6.1).

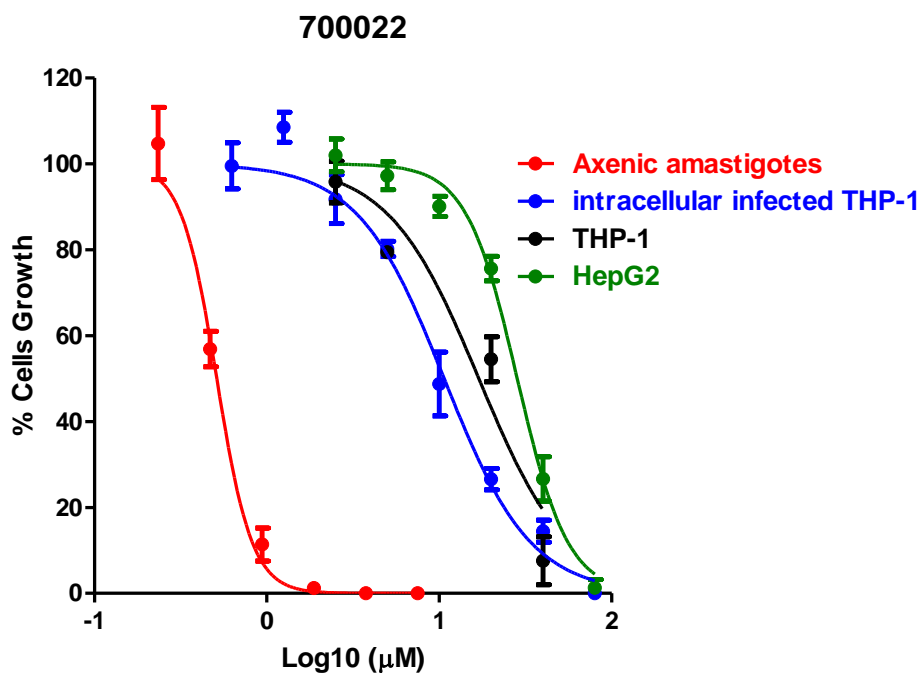


Figure 6.1: Comparing 700022 activity between axenic amastigotes (red) and intramacrophage amastigotes (blue). Concentration–response curves for compound 700022 against: intracellular *L. mexicana* NanoLuc-PEST-transgenic line (blue), axenic amastigotes of NanoLuc-PEST-transgenic line (red) as well as the human cell lines HepG2 (green) and THP-1 (black). Most data from chapter 5. The data for the intracellular *L. mexicana* NanoLuc-PEST-transgenic line represent one biological repeat of three technical repeats.

Table 6.1: Activity of Phytopure compound 700022 against intracellular and extracellular *L. mexicana* amastigotes using luminescence assay. SI¹, is calculated as CC₅₀/EC₅₀ using axenic amastigotes whilst SI² is calculated using intra-macrophage amastigote data.

	EC ₅₀ (μM)		CC ₅₀ (μM)	SI ¹	SI ²	CC ₅₀ (μM)	SI ¹	SI ²
	Axenic amastigotes ¹	Intra-macrophage amastigotes ²	THP1			HepG2		
700022	0.51	10.69	16.97	33.27	1.58	28.37	55.62	2.65

The limitations of the materials provided did not allow for a more complete analysis of 700022 drug action. In chapter 4, I outline how, with more material, additional studies could be used to explore the action of 700022 as well as the molecular basis of resistance in the 700022 resistant *L. mexicana* line. Molecular studies reported here may provide a start with a confirmation of the association of the mutations in LmROS3 with 700022 resistance – the data reported here needing additional validation. In addition, potential resistance markers associated with the miltefosine sensitivity locus identified in *L. infantum* (Carnielli *et al.*, 2018), specifically the 3'-nucleotidase, 3' nuclease, helicase-like protein and 3,2-trans-enoyl-CoA enolase. However, perhaps the most interesting line of research that could evolve from this work is whether the miltefosine resistant parasites, such as the *L. infantum* from Brazil lacking the miltefosine sensitivity locus, are cross resistant to 700022 (or other related triterpenes). As discussed in chapter 5, that exposure to natural products, perhaps through a commonly used traditional medicine used in the Amazon, may have led to the insensitivity of miltefosine is not only an interesting scientific question, but also may act as a note of warning for future drug releases where natural products have previously been widely used.

In this thesis I also report an evaluation of a transgenic *L. mexicana* expressing a NanoLuc-PEST luciferase as a simple, rapid and sensitive assay system. The utility of a bioluminescent assay screen has been demonstrated for a variety of parasite systems, including;

Cryptosporidium parvum (Hennessey *et al.*, 2018), *Toxoplasma gondii* (Radke *et al.*, 2018) as well as *P. falciparum* early stage gametocytes (Lucantoni *et al.*, 2013).

The validation of this assay system against the MMV Pathogen Box was used in recognition of the importance of this compound library in repurposing compounds in the search for drugs against diseases for which large chemical screens are not being done (Mi-Ichi *et al.*, 2018; Spalenka *et al.*, 2018; Partridge *et al.*, 2018; Hennessey *et al.*, 2018; Mayer and Kronstad, 2017; Preston *et al.* 2016). Full information about these compounds is available online via (<https://www.pathogenbox.org/>). The MMV Pathogen Box is an important tool in open-access drug discovery model, and includes compounds identified from screens against a range of different pathogens, such as *P. falciparum*, Mycobacterium, kinetoplastid parasites (*Leishmania* spp., and *Trypanosoma cruzi*), *Schistosoma*, *Toxoplasma*, *Cryptosporidium* and helminths. These compounds are provided in a library of 400 compounds, which include a set of 26 reference compounds with activity associated with one or more of these pathogens with data on their structure and toxicity.

Screening the MMV Pathogen Box against the axenic amastigotes identified 23 compounds that reduced bioluminescence to $\leq 5\%$ of the untreated controls at 2 μM . The seven most potent compounds were then screened in the intracellular infection model in parallel with amphotericin B and miltefosine as controls. This subsequent screen in the infected macrophage screen showed that all seven compounds displayed an $\text{EC}_{50} < 5 \mu\text{M}$. Of these seven compounds, three compounds (MMV652003, MMV689480 and MMV688262) were known to be active against kinetoplastids. However, for the majority of these compounds, they were some 10 to 70-fold less active in the intramacrophage assay. One compound, however, MMV690102 (Figure 6.2), had an EC_{50} of 100nM against the intramacrophage amastigote compared to 60nM activity against the axenic amastigote. Picked to be included

in the MMV Pathogen Box based on a screen against *L. infantum*, this compound has also been shown to be active against *L. donovani* and *T. cruzi* (Duffy *et al.*, 2017). MMV690102 is a pyrimido[4,5-d]pyrimidine-2,4,7-triamine, with a prediction that this compound targets the dihydrofolate reductase enzyme (Duffy *et al.*, 2017). Two closely structurally related compounds, MMV690103 and MMV689437, that have been shown to have activity against *L. infantum*, *L. donovani* and *T. cruzi* (Duffy *et al.*, 2017), are not, however, identified as one of the 23 hits in this screen of *L. mexicana*.

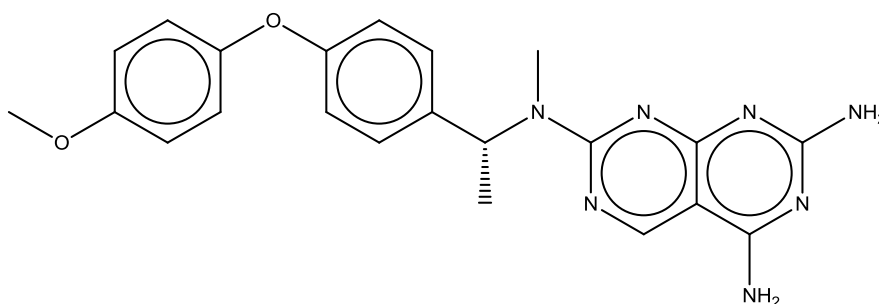


Figure 6.2. Structure of MMV690102.

Bringing together the large natural compound library and the validation of the bioluminescence-based screening approach in *L. mexicana* highlights opportunities for moving forward from the research presented in this thesis. The genetic construct used to generate the NanoLuc-PEST is based on the integration into a rRNA locus (Berry *et al.*, 2018) and is capable to being readily modified for other leishmanial and trypanosomal parasite systems. This then offers a simple, sensitive and robust screen of antiparasitic activity that could be capable of being scaled up for high-throughput screens. For example, assessment of whether the 72 hours assay time needed for *L. mexicana* could be robustly reduced to say 48 or 24 hours would help in throughput. More importantly would be scaling

the assay to enable 384-well or even 1536-well plates to be used, an opportunity that is supported by the high signal intensity from NanoLuc accompanied by the rapid loss of signal on death (providing excellent signal:background ratio). In this way, rapid screens of the axenic amastigote *L. mexicana*, or other parasites, could be performed against tens of thousands (or more) of compounds.

To scale this as an opportunity for discovery of natural products, it would be useful to generate compilations of existing libraries from natural resources including plants, bacteria, marine and terrestrial microorganisms. For example, these materials are available in different libraries (ex: Albany Molecular Research Inc., AnalytiCon Discovery, BioAustralis, Biosortia Pharmaceuticals, Caithness Biotechnologies Ltd—Phytotitre Natural Product Extract Library, ChromaDex® Natural Compound Library, Cyano Biotech, Greenpharma, InterLink Biotechnologies and Quality Phytochemicals) and are highlighted as a resource through the USA National Center for Complementary and Integrative Health (nccih.nih.gov/grants/naturalproducts/libraries). Ideally, these should be libraries of purified compounds – or at least subfractions that are predominantly a single compound – to reduce the complexity of the hit selection process. That said, it is clear that the support for maintaining a library that requires a living source to produce the library components is a significant challenge (Butler *et al.*, 2014), and likely expensive to generate, store and distribute the materials.

Using such a resource, a high throughput screen against axenic amastigotes of *L. mexicana* using bioluminescence as an output would be performed. Choice of the screening concentration is important here. These needs to be high enough to capture a diversity of hits (recognising that the most potent hits may not be the best leads for development), but not too low so that large numbers of low affinity compounds are included in the hit list. In

Chapter 3, experience with *P. falciparum* showed that the 2 μ M screen was sufficient to identify the hits taken forward and that the 20 μ M screen added little to the selection process. Comparison of the thresholds used is also important – the *L. mexicana* screens in Chapters 3 and 5 used increasingly higher thresholds, and as a result the hits characterised were more potent. Obviously, with larger libraries, the screening concentration and threshold can be adjusted to produce a manageable list of potent hits for subsequent assays. In the case of the transgenic NanoLuc *L. mexicana* screens, the next step would be an assay of the intramacrophage amastigotes. This is a more complex assay process, requiring THP-1 differentiation and then invasion, with wash steps, before exposure to the compound of interest. That said, this is key data to demonstrate activity against a clinically-relevant parasite life-stage. One possible additional innovation here would be to include a constitutive expression of a second luciferase reporter in the THP-1 cell line. Reports using luciferase as a reporter system in THP-1 reveal that this is likely possible (Ilg, 2017; Hong *et al.*, 2011; Sau *et al.*, 2003) Using a luciferase reporter that uses a substrate different to that of NanoLuc would allow both the effect of the compound on the parasite and the host THP-1 cell line, an indication of potential toxicity, in a simple stop-start assay that would only require the use of a microinjection device to the bioluminometer.

References list

Abdul, M., Junejo H. A. and Manohar L. 2006. Acute renal failure associated with malaria. *Journal of Ayub Medical College*, 18(4): 47–52.

Abdulla, S., Oberholzer, R., Juma, O., Kubhoja, S., Machera, F., Membi, C., Omari, S., Urassa, A., Mshinda, H., Jumanne, A., Salim, N., Shomari, M., Aebi, T., Schellenberg, D.M., Carter, T., Villafana, T; Demoitié, M.A., Dubois, M.C., Leach, A., Lievens, M., Vekemans, J., Cohen, J., Ballou, W.R., and Tanner, M. 2008. Safety and immunogenicity of RTS,S/AS02D malaria vaccine in infants. *The New England Journal of Medicine*, 359:2533-2544.

Achan, J., Talisuna, A. O., Erhart, A., Yeka, A., Tibenderana, J. K., Baliraine, F. N. and D'Alessandro, U. 2011. Quinine, an old anti-malarial drug in a modern world: role in the treatment of malaria. *Malaria Journal*, 10(144), 1-12.

Achan, J., Talisuna, A. O., Erhart, A., Yeka, A., Tibenderana, J.K., Baliraine, F.N. and D'Alessandro, U. 2011. Quinine, an old anti-malarial drug in a modern world: role in the treatment of malaria. *Malaria Journal*, 10(144), 1-12.

Achterberg, V. and Gercken G.1987. Cytotoxicity of ester and ether lysophospholipids on *Leishmania donovani* promastigotes. *Molecular and Biochemical Parasitology*, 23(2): 117-22. doi:10.1016/0166-6851(87)90146-0

Adriano, C.C., Trinconi, C.T., Costa, C.H.N., and Uliana, S. R. B. 2014. *In vitro* and *in vivo* miltefosine susceptibility of a *Leishmania amazonensis* isolate from a patient with diffuse cutaneous leishmaniasis. *PLoS Neglected Tropical Diseases*, 8(7), e2999. doi:10.1371/journal.pntd.0002999

Aldulaimi O., Uche F.I., Hameed H., Mbye H., Ullah I., Drijfhout F., Claridge T.D.W., Horrocks P., and Li W.W. 2017. A characterization of the antimalarial activity of the bark of *Cylicodiscus gabunensis* Harms. *Journal of Ethnopharmacology*, 198, 221–225. doi:10.1016/j.jep.2017.01.014

Alirol, E., Schrumph, D., Amici Heradi, J., Riedel, A., de Patoul, C., Quere, M., and Chappuis, F. 2012. Nifurtimox-Eflornithine combination therapy for second-stage *Gambiense* human african trypanosomiasis: médecins sans frontières experience in the democratic republic of the Congo. *Clinical Infectious Diseases*, 56(2), 195–203. doi:10.1093/cid/cis886

Allarakhia, M. 2013. Open-source approaches for the repurposing of existing or failed candidate drugs: learning from and applying the lessons across diseases. *Drug Design, Development and Therapy*, 753. doi:10.2147/dddt.s46289

Allotey, P., Reidpath, D. D., and Pokhrel, S. 2010. Social sciences research in neglected tropical diseases 1: the ongoing neglect in the neglected tropical diseases. *Health Research Policy and Systems*, 8(1). doi:10.1186/1478-4505-8-32

- Al-Mohammed, H.I., Chance, M.L., and Bates, P.A. 2005. Production and characterization of stable amphotericin-resistant amastigotes and promastigotes of *Leishmania mexicana*. *Antimicrobial Agents and Chemotherapy*, 49(8), 3274–3280. doi:10.1128/aac.49.8.3274-3280.2005
- Althaus, J.B., Malyszek, C., Kaiser, M., Brun, R., and Schmidt, T. J. 2017. Alkamides from *anacyclus pyrethrum* L. and their *in vitro* antiprotozoal activity. *Molecules*, 22(5), 796. doi:10.3390/molecules22050796
- Alvar J., Croft S., and Olliaro P. 2006. Chemotherapy in the treatment and control of leishmaniasis. *Advances in Parasitology*, 61: 223–274.
- Alvar, J., Croft, S. L., Kaye, P., Khamesipour, A., Sundar, S., and Reed, S. G. 2013. Case study for a vaccine against leishmaniasis. *Vaccine*, 31, B244–B249. doi:10.1016/j.vaccine.2012.11.080
- Alvar, J., Vélez, I. D., Bern, C., Herrero, M., Desjeux, P., Jorge Cano J., Jannin J., den Boer M., and Cano, J. 2012. Leishmaniasis worldwide and global estimates of its incidence. *PLoS ONE*, 7(5), e35671. doi:10.1371/journal.pone.0035671
- Andreu, N., Fletcher, T., Krishnan, N., Wiles, S., and Robertson, B. D. 2011. Rapid measurement of antituberculosis drug activity *in vitro* and in macrophages using bioluminescence. *Journal of Antimicrobial Chemotherapy*, 67(2), 404–414. doi:10.1093/jac/dkr472
- Angrisano, F., Yan-Hong T., Sturm A., Geoffrey I. and Mcfaddenc, J. B. 2012. Malaria parasite colonisation of the mosquito midgut - placing the *Plasmodium* ookinete centre stage. *International Journal for Parasitology*, 42(6): 519–527.
- Anil, K. G. and Marcelo J. 2019. *Plasmodium* sporozoite invasion of the mosquito salivary gland. *Current Opinion in Microbiology*, 12(4): 394–400. doi:10.1016/j.mib.2009.06.010
- Annang, F., Pérez-Moreno, G., García-Hernández, R., Cordon-Obras, C., Martín, J., Tormo, J. R., Rodríguez L., de Pedro N., Gómez-Pérez V., Valente M., Reyes F., Genilloud O., Vicente F., Castanys S., Ruiz-Pérez L. M., Navarro M., Gamarro F., and González-Pacanowska, D. 2014. High-throughput screening platform for natural product-based drug discovery against 3 neglected tropical diseases. *Journal of Biomolecular Screening*, 20(1), 82–91. doi:10.1177/1087057114555846
- Armitage, E. G., Alqaisi, A. Q. I., Godzien, J., Peña, I., Mbekeani, A. J., Alonso-Herranz, V., López-González A., Martín J., Gabarro R., Denny P.W., Barrett M.P., and Barbas, C. 2018. Complex Interplay between Sphingolipid and Sterol Metabolism Revealed by Perturbations to the *Leishmania* Metabolome Caused by Miltefosine. *Antimicrobial Agents and Chemotherapy*, 62(5). doi:10.1128/aac.02095-17
- Ashley E.A., Pyae Phyo A., and Woodrow C.J. 2018. Malaria. *Lancet*, 21;391(10130):1608-1621. doi: 10.1016/S0140-6736(18)30324-6.

Atouguia J.L.M., and Kennedy P.G.E. 2000. Neurological aspects of human African trypanosomiasis. In: Davis LE, Kennedy PGE, eds. Infectious diseases of the nervous system. *Oxford: Butterworth-Heinemann*, 321–72.

Auwerx, J. 1991. The human leukemia cell line, THP-1: a multifaceted model for the study of monocyte-macrophage differentiation. *Experientia*, 47(1), 22–31. doi:10.1007/bf02041244

Azevedo M.F., Nie C.Q., Elsworth B., Charnaud S.C., Sanders P.R., Crabb B.S., and Gilson P.R. 2014. *Plasmodium falciparum* transfected with ultra bright NanoLuc luciferase offers high sensitivity detection for the screening of growth and cellular trafficking inhibitors. *PLoS ONE*, 9(11):e112571. doi.org/10.1371/journal.pone.0112571

Babokhov, P., Sanyaolu, A.O., Oyibo, W.A., Fagbenro-Beyioku, A.F., and Iriemenam, N.C. 2013. A current analysis of chemotherapy strategies for the treatment of human African trypanosomiasis. *Pathogens and Global Health*, 107(5), 242–252. doi:10.1179/2047773213y.0000000105

Bannister, L. and Mitchell, G. 2003. The ins, outs and roundabouts of malaria. *Trends in Parasitology*, 19(5): 209–213.

Banuls, A.L., Hide, M., and Prugnolle, F. 2007. Leishmania and the leishmaniases: a parasite genetic update and advances in taxonomy, epidemiology and pathogenicity in humans. *Advances in Parasitology*, 1–458. doi:10.1016/s0065-308x(06)64001-3

Barilli, A., Rotoli, B.M., Visigalli, R., Bussolati, O., Gazzola, G.C., and Dall'Asta, V. 2011. Arginine transport in human monocytic leukemia THP-1 cells during macrophage differentiation. *Journal of Leukocyte Biology*, 90(2), 293–303. doi:10.1189/jlb.0910510

Barnett, P., Singh, S., Bern, C., Hightower, A., and Sundar, S. 2005. Virgin soil: the spread of visceral leishmaniasis into uttar pradesh, India. *The American Journal of Tropical Medicine and Hygiene*, 73(4), 720-5.

Barratt G., Saint-Pierre-Chazalet M., and Loiseau P.M. 2009. Cellular transport and lipid interactions of miltefosine. *Current drug metabolism*, 10(3):247–55. doi:10.2174/138920009787846332

Barry, M. A., Simon, G. G., Mistry, N., and Hotez, P. J. 2013. Global trends in neglected tropical disease control and elimination: impact on child health. *Archives of Disease in Childhood*, 98(8), 635–641. doi:10.1136/archdischild-2012-302338

Bates, P. 2015. Leishmania. *Encyclopedia of Life Sciences*, 11, 1-10. doi: 10.1002/9780470015902.a0001968.pub3

Bates, P. 2008. Leishmania sand fly interaction: Progress and challenges. *Current Opinion in Microbiology*, 11(4), 340-344. doi:10.1016/j.mib.2008.06.003

Bates, P.A. 2007. Transmission of *Leishmania* metacyclic promastigotes by phlebotomine sand flies. *International Journal for Parasitology*, 37: 1097-1106. doi:10.1016/j.ijpara.2007.04.003

- Batista, R., Silva, A., and Alaíde, B.A. 2009. Plant-derived antimalarial agents: new leads and efficient phytomedicines. Part II. Non-alkaloidal natural products. *Molecules*, 14, 3037-3072.
- Baumeister, S., Winterberg, M., Przyborski, J. M. and Lingelbach, K. 2010. The malaria parasite *Plasmodium falciparum*: cell biological peculiarities and nutritional consequences. *Protoplasma*, 240(1): 3–12. doi:10.1007/s00709-009-0090-3
- Bawn S. 2010. Studies on antitrypanosomal activity of medicinal plants. Hokkaido university, PhD thesis.
- Be' zivin, C., Tomasi, S., Lohe' zic-Le De' ve' hat, F. and Boustie, J. 2003. Cytotoxic activity of some lichen extracts on murine and human cancer cell lines. *Phytomedicine*, 10, 499–503.
- Beeson, G. J., Boeuf, P. and Fowkes, J. F. 2015. Maximizing antimalarial efficacy and the importance of dosing strategies. *BMC Medicine*, 13(110), 1-4.
- Bejon, P., Lusingu, J., Olotu, A., and von Seidlein L. 2008. Efficacy of RTS,S/AS01E: clinical malaria in 5 to 17 month old children. *The New England Journal of Medicine*, 359: 2521-2532.
- Belachew, E.B. 2018. Immune Response and Evasion Mechanisms of Plasmodium falciparum Parasites. *Journal of Immunology Research*, 1–6. doi:10.1155/2018/6529681
- Berg M., Vanaerschot M., Jankevics A., Cuypers B., Maes I., Mukherjee S., Khanal B., Rijal S., Roy S., Opperdoes F., Breitling R., and Dujardin J.C. 2013. Metabolic adaptations of *Leishmania donovani* in relation to differentiation, drug resistance, and drug pressure. *Mol Microbiol*, 90: 428–42. doi: 10.1111/mmi.12374.
- Berger, I., Passreiter, C.M., Cáceres, A., Kubelka, W., 2001. Antiprotozoal activity of *Neurolaena lobata*. *Phytotherapy Research*, 15, 327–330. doi.org/10.1002/ptr.782
- Berman J.J. 2008. Treatment of leishmaniasis with miltefosine: 2008 status. *Expert Opinion on Drug Metabolism & Toxicology*, 4(9), 1209–1216. doi:10.1517/17425255.4.9.1209
- Bern, C., Maguire, J. H., and Alvar, J. 2008. Complexities of assessing the disease burden attributable to leishmaniasis. *PLoS Neglected Tropical Diseases*, 2(10), e313. doi:10.1371/journal.pntd.0000313
- Berry, S. L., Hameed, H., Thomason, A., Maciej-Hulme, M. L., Saif Abou-Akkada, S., Horrocks, P., and Price, H. P. 2018. Development of NanoLuc-PEST expressing *Leishmania mexicana* as a new drug discovery tool for axenic- and intramacrophage-based assays. *PLoS Neglected Tropical Diseases*, 12(7), e0006639. doi:10.1371/journal.pntd.0006639
- Bessoff, K., Spangenberg, T., Foderaro, J. E., Jumani R.S., Ward G.E., and Huston CD. 2014. Identification of *Cryptosporidium parvum* active chemical series by repurposing the

open access malaria box. *Antimicrobial Agents and Chemotherapy*, 58, 2731–2739. doi:10.1128/aac.02641-13

Betterton-lewis, D. G. 2007. Alarial arasites. *Medical Journal of Therapeutics Africa*, 1(1): 45–46.

Bloland, P. B. 2001. Drug resistance in malaria drug resistance in malaria. *World Health Organazation*. Available at: https://www.cdc.gov/malaria/resources/pdf/drug_resistance/bloland_who2001.pdf

Blum J., Schmid C., and 2006. Burri C. Clinical aspects of 2541 patients with second stage human African trypanosomiasis. *Acta Tropica*, 97(1):55-64. doi:10.1016/j.actatropica.2005.08.001

Booth, M. 2018. Climate change and the neglected tropical diseases. *Advances in Parasitology*, 39–126. doi:10.1016/bs.apar.2018.02.001

Botero, A., Keatley, S., Peacock, C., and Thompson, R. C. A. 2017. *In vitro* drug susceptibility of two strains of the wildlife trypanosome, *Trypanosoma copemani*: A comparison with *Trypanosoma cruzi*. *International Journal for Parasitology: Drugs and Drug Resistance*, 7(1), 34–41. doi:10.1016/j.ijpddr.2016.12.004

Botero, M.C., Puentes-Herrera, M., and Cortés, J.A. 2014. Lipid formulations of amphotericin. *Revista Chilena de Infectologia*, 31, 518–527.

Bozdech, Z., Llinás M., Pulliam B. L., Wong E. D., Zhu J., and DeRisi J. L. 2003. Thetranscriptome of the intraerythrocytic developmental cycle of *Plasmodium falciparum*. *PLoS Biology*, 1(1), 1–16.

Bribi N., 2018. Pharmacological activity of alkaloids: a review. *Asian Journal of Botany*, 1, 1-6. DOI: 10.63019/ajb.v1i2.467

Britta E.A. Scariot D.B., Falzirolli H., Ueda-Nakamura T., Silva C.C., Filho B.P., Borsali R., and Nakamura C.V. 2014. Cell death and ultrastructural alterations in *Leishmania amazonensis* caused by new compound 4-Nitrobenzaldehyde thiosemicarbazone derived from S-limonene. *BMC Microbiology*, 14:236, 1-12. doi:10.1186/s12866-014-0236-0

Brun R., Blum J., Chappuis F., and Burri C. 2010. Human African trypanosomiasis. *Lancet*, 375: 148–59.

Bryceson A. 2001. A policy for leishmaniasis with respect to the prevention and control of drug resistance. *Tropical Medicine and International Health*, 6(11),928–934. doi:10.1046/j.1365-3156.2001.00795.x

Buckner F.S., and Wilson A.J. 2005. Colorimetric assay for screening compounds against leishmania amastigotes grown in macrophages. *The American Journal of Tropical Medicine and Hygiene*, 72(5), 600–605.

Burkard G., Fragoso C.M., and Roditi I. 2007. Highly efficient stable transformation of bloodstream forms of *Trypanosoma brucei*. *Molecular and Biochemical Parasitology*, 153: 220-3.

Burrell-Saward H., Harris A.J., de LaFlor R., Sallam H., Alavijeh M.S., Ward T.H., and Croft S.L. 2017. Dose-dependent effect and pharmacokinetics of fexinidazole and its metabolites in a mouse model of human African trypanosomiasis. *International Journal of Antimicrobial Agents*, 50(2):203-209. doi: 10.1016/j.ijantimicag.2017.01.038.

Burrows, J. N., Duparc, S., Gutteridge, W. E., Hooft van Huijsduijnen, R., Kaszubska, W., Macintyre, F., Mazzuri .S, Möhrle J.J. and Wells, T. N. C. 2017. New developments in anti-malarial target candidate and product profiles. *Malaria Journal*, 16(1), 1-29. doi:10.1186/s12936-016-1675-x

Burrows, J. N., Hooft van Huijsduijnen, R., Möhrle, J. J., Oouvray, C., and Wells, T. N. 2013. Designing the next generation of medicines for malaria control and eradication. *Malaria Journal*, 12(187), 1-20. doi:10.1186/1475-2875-12-187

Burza, S., Sinha, P. K., Mahajan, R., Lima, M. A., Mitra, G., Verma, N., Balasegaram M., and Das, P. 2014. Five-year field results and long-term effectiveness of 20 mg/kg liposomal amphotericin B (ambisome) for visceral leishmaniasis in Bihar, India. *PLoS Neglected Tropical Diseases*, 8(1), e2603. doi:10.1371/journal.pntd.0002603

Burza S., Croft S.L., and Boelaert M. 2018. Leishmaniasis. *Lancet*, 15;392(10151):951-970. doi: 10.1016/S0140-6736(18)31204-2. Epub 2018 Aug 17.

Büscher P., Cecchi G., Jamonneau V., and Priotto G. 2017. Human African trypanosomiasis. *The Lancet*, 25;390(10110):2397-2409. doi: 10.1016/S0140-6736(17)31510-6

Butler M.S., Fontaine F., and Cooper M.A. 2014. Natural product libraries: assembly, maintenance, and screening. *Planta Medica*, 80(14): 1161-1170. DOI: 10.1055/s-0033-1360109

Caljon, G., Van Reet, N., De Trez, C., Vermeersch, M., Pérez-Morga, D., and Van Den Abbeele, J. 2016. The dermis as a delivery Site of *Trypanosoma brucei* for tsetse flies. *PLoS Pathogens*, 12(7), e1005744. doi:10.1371/journal.ppat.1005744

Callahan, H. L., Portal, A. C., Devereaux, R., and Grogl, M. 1997. An axenic amastigote system for drug screening. *Antimicrobial Agents and Chemotherapy*, 41(4), 818–822. doi:10.1128/aac.41.4.818

Campos B.L., Silva T.N., Ribeiro S.P., Carvalho K.I., Kallás E.G., Laurenti M.D., Passero L.F. 2015. Analysis of iron superoxide dismutase-encoding DNA vaccine on the evolution of the *Leishmania amazonensis* experimental infection. *Parasite Immunology*, 37(8): 407–16. doi: 10.1111/pim.12206 PMID: 26040192

Capewell P., Cren-Travaillé C., Marchesi F., Johnston P., Clucas C., Benson R. A., Gorman T. A., Calvo-Alvarez E., Crouzols A., Jouvion G., Jammoneau V., Weir W., Stevenson M. L., O'Neill K., Cooper A., Swar N. K., Bucheton B., Ngoyi D. M., Garside P., Rotureau B. and MacLeod A. 2016. The skin is a significant but overlooked anatomical reservoir for vector-borne African trypanosomes. *eLife*, 5:e17716. 1-17. doi: 10.7554/eLife.177161 of 17SHORT REPORT

Carlos M. 2002. Protection and promotion of traditional medicine - implications for public health in developing countries. *Correa University of Buenos Aires*. Available at: <http://apps.who.int/medicinedocs/pdf/s4917e/s4917e.pdf>

Carneiro M.B., Lopes M.E., Vaz L.G., Sousa L.M., Santos L.M., Souza C.C., Campos A.C., Gomes D.A., Gonçalves R., Tafuri W.L., Vieira L.Q. 2015. IFN- γ -dependent recruitment of CD4+ T cells and macrophages contributes to pathogenesis during *Leishmania amazonensis* infection. *Journal of Interferon and Cytokine Research*, 35(12), 935–947. doi:10.1089/jir.2015.0043

Carnielli, J. B. T., Crouch, K., Forrester, S., Silva, V. C., Carvalho, S. F. G., Damasceno, J. D., Brown E., Dickens N.J., Costa D.L., Costa C.H.N., Dietze R., Jeffares D.C. and Mottram, J. C. 2018. A *Leishmania infantum* genetic marker associated with miltefosine treatment failure for visceral leishmaniasis. *EBioMedicine*. doi:10.1016/j.ebiom.2018.09.029

Carter, N.S., Drew, M.E., Sanchez, M., Vasudevan, G., Landfear, S.M., and Ullman, B. 2000. Cloning of a novel inosine-guanosine transporter gene from *Leishmania donovani* by functional rescue of a transport-deficient mutant. *Journal of Biological Chemistry*, 275(27), 20935–20941.

Carvalho, L.H., and KrettliA, U. 1991. Antimalarial chemotherapy with natural products and chemically defined molecules. *Memórias Do Instituto Oswaldo Cruz*, 86(suppl 2), 181–184. doi:10.1590/s0074-02761991000600041

Carvalho, L., Lopez, L., Fajardo, J.E., Jaureguiberry-Bravo, M., Fiser, A., and Berman, J.W. 2017. HIV-Tat regulates macrophage gene expression in the context of neuroAIDS. *PLOS ONE*, 12(6), e0179882. doi:10.1371/journal.pone.0179882

CDC 2013. Parasites - Leishmaniasis. *Centers for Disease Control and Prevention*. Available: <http://www.cdc.gov/parasites/leishmaniasis/>

Cecílio P., Pérez-Cabezas B., Fernández L., Moreno J., Carrillo E., Requena J.M., Fichera E., Reed S.G., Coler R.N., Kamhawi S., Oliveira F., Valenzuela J.G., Gradoni L., Glueck R., Gupta G., Cordeiro-da-Silva A. 2017. Pre-clinical antigenicity studies of an innovative multivalent vaccine for human visceral leishmaniasis. *PLoS Neglected Tropical Diseases*, 27;11(11):e0005951. doi:10.1371/journal.pntd.0005951.

Ch'ng, J.-H., Kotturi, S. R., Chong, A. G.-L., Lear, M. J., and Tan, K. S.-W. 2010. A programmed cell death pathway in the malaria parasite *Plasmodium falciparum* has general features of mammalian apoptosis but is mediated by clan CA cysteine proteases. *Cell Death and Disease*, 1(2), e26–e26. doi:10.1038/cddis.2010.2

Chandra A.R., and Mahesh S. 2017. Cutaneous leishmaniasis. *Journal of Pathology of Nepal*, 7, 1212 -1217.

Chappuis, F., Loutan, L., Simarro, P., Lejon, V., and Buscher, P. 2005. Options for field diagnosis of human african trypanosomiasis. *Clinical Microbiology Reviews*, 18(1), 133–146. doi:10.1128/cmr.18.1.133-146.2005

Chappuis, F., S. Sundar, A. Hailu, H. Ghalib, S. Rijal, R. W. Peeling, J. Alvar and M. Boelaert 2007. Visceral leishmaniasis: what are the needs for diagnosis, treatment and control?. *Nature Reviews Microbiology*, 5(11): 873-82. doi:10.1038/nrmicro1748z

Che P, Cui L, Kutsch O, Li Q. 2012. Validating a firefly luciferase-based high-throughput screening assay for antimalarial drug discovery. *Assay and Drug Development Technologies*, 10(1):61±8. Epub 2011/11/03.doi.org/10.1089/adt.2011.0378

Checchi, F., Filipe, J.A., Haydon, D. T., Chandramohan, D., and Chappuis, F. 2008. Estimates of the duration of the early and late stage of *gambiense* sleeping sickness. *BMC Infectious Diseases*, 8(1). doi:10.1186/1471-2334-8-16

Checchi, F., Filipe, J.A.N., Barrett, M.P., and Chandramohan, D. 2008a. The natural progression of *Gambiense* sleeping sickness: what is the evidence?. *PLoS Neglected Tropical Diseases*, 2(12), e303. doi:10.1371/journal.pntd.0000303

Chen, L. H., Wilson M. E. and Schlagenhauf P. 2006. Prevention of malaria in long-term travellers. *The Journal of the American Medical Association*, 8;296(18):2234-44.

Cheruiyot, J. Luicer, A., Ingasia, A. A. Omondi, D. W. Juma, B. H. Opot, J. M., Ndegwa, J. M., Agnes, C., Cheruiyot, R. Y., Charles O., Peninah, M., Ngalah, S. B., Lorna, J. C., Paul O. A., Fredrick L. E., Jacob D. J., Wallace D. B., Ben, A., Hoseah, M. A. and Edwin, K. 2014. Polymorphisms in *Pfmdr1*, *Pfcrt*, and *Pfnhe1* Genes Are Associated with Reduced *in Vitro* Activities of Quinine in *Plasmodium falciparum* Isolates from Western Kenya. *Antimicrobial Agents and Chemotherapy*, 58 (7), 3737–3743.

Cheuka, P., Mayoka, G., Mutai, P., and Chibale, K. 2016. The role of natural products in drug discovery and development against neglected tropical diseases. *Molecules*, 22(1), 58. doi:10.3390/molecules22010058

Chianese, G., Yerbanga, S.R., Lucantoni, L., Habluetzel, A., Basilico, N., Taramelli, D., Fattorusso, E., and Tagliatalata-Scafati, O. 2010. Antiplasmodial triterpenoids from the fruits of Neem, *Azadirachta indica*. *Journal of Natural Products*, 73, 1448-1452. doi:10.1021/np100325q

Choomuenwai, V., Beattie, K.D., Healy, P.C., Andrews, K. T., Fechner, N., and Davis, R.A. 2015. Entonalactams A–C: isoindolinone derivatives from an Australian rainforest fungus belonging to the genus *Entonaema*. *Phytochemistry*, 117, 10–16. doi:10.1016/j.phytochem.2015.05.018

Cimanga, R.K., Tona, G.L., Kambu, O.K., and Mesia, G.K., Muyembe, J.J.T., Apers S., Totte, J., Pieters, L., and Villetinck A.J. 2008. Antimalarial activity of some extracts and

isolated constituents from *Morinda morindoides* leaves. *Journal of Natural Remedies*, 8/2, 191-202.

Claes F, Vodnala SK, van Reet N, Boucher N, Lunden-Miguel H, Baltz T, , Goddeeris B.M., scher P.B., and Rottenberg M.E. 2009. Bioluminescent imaging of *Trypanosoma brucei* shows preferential testis dissemination which may hamper drug efficacy in sleeping sickness. *PLoS Neglected Tropical Diseases*, 3(7):e486. doi.org/10.1371/journal.pntd.0000486

Clark, A.M. 1996. Natural products as a resource for new drugs. *Pharmaceutical Research*, 13(8), 1133–1141.

Clos J., and Choudhury K. 2006. Functional cloning as a means to identify leishmania genes involved in drug resistance. *Mini-Reviews in Medicinal Chemistry*, 6(2), 123–129. doi:10.2174/138955706775476028

Coelho A.C., Boisvert S., Mukherjee A., Leprohon P., Corbeil J., and Ouellette M. 2012. Multiple mutations in heterogeneous miltefosine-resistant *Leishmania major* population as determined by whole genome sequencing. *PLoS Neglected Tropical Diseases*, 2012; 6(2):e1512.

Combrinck, J. M., Mabothe, T. E., Ncokazi, K. K., Ambele, M. A., Taylor, D., Smith, P.J., Hoppe, H. C. and Egan, T.J. 2013. Insights into the role of heme in the mechanism of action of antimalarials. *ACS Chemical Biology*, 8(1), 133–137. doi:10.1021/cb300454t

Conteh, L., Engels, T., and Molyneux, D. H. 2010. Socioeconomic aspects of neglected tropical diseases. *The Lancet*, 375(9710), 239–247. doi:10.1016/s0140-6736(09)61422-7

Cowman, A.F., Berry, D. and Baum, J. 2012. The cellular and molecular basis for malaria parasite invasion of the human red blood cell. *Journal of Cell Biology*, 198 (6): 961–71.

Cox, F. E. 2010. History of the discovery of the malaria parasites and their vectors. *Parasites and Vectors*, 3(5): 1-9. doi:10.1186/1756-3305-3-5

Croft S.L., Sundar S., and Fairlamb A.H. 2006. Drug resistance in leishmaniasis. *Clinical Microbiology Reviews*, 19(1):111-26.

Croft, S.L., and Yardley V. 2002. Chemotherapy of leishmaniasis. *Curr Pharm*
Croft, S.L., Neal R.A., Pendergast W., and Chan J.H. 1987. The activity of alkyl phosphorylcholines and related derivatives against *Leishmania donovani*. *Biochem Pharmacol*, 36(16): 2633-6.

Cromwell, E. A., and Fullman, N. 2018. Preventive chemotherapy coverage for neglected tropical diseases: does one metric fit all?. *The Lancet Global Health*, 6(9), e936–e937. doi:10.1016/s2214-109x(18)30345-0

Cui L., Miao J., Wang J., and Li Q. 2008. *Plasmodium falciparum*: development of a transgenic line for screening antimalarials using firefly luciferase as the reporter. *Experimental Parasitology*, 120(1):80-87. doi:10.1016/j.exppara.2008.05.003

- Cui, L. and Su, X. 2009. Discovery, mechanisms of action and combination therapy of artemisinin. *Expert Review of Anti-Infective Therapy*, 7(8), 999–1013. doi:10.1586/eri.09.68
- Cullen D.R., and Mocerino M. 2017. A brief review of drug discovery research for human african trypanosomiasis. *Current Medicinal Chemistry*, 24(7):701-717. doi: 10.2174/0929867324666170120160034.
- Da Silva, R.R.P., da Silva, B.J.M., Rodrigues, A.P.D., Farias, L.H.S., da Silva, M.N., Alves, D.T.V., Bastos G.N.T., do Nascimento J.L.M and Silva, E.O. 2015. *In vitro* biological action of aqueous extract from roots of *Physalis angulata* against Leishmania (*Leishmania amazonensis*). *BMC Complementary and Alternative Medicine*, 15(1). doi:10.1186/s12906-015-0717-1
- Danell, M., Soares, D., Abreu, H., Peçanha, L., and Saraiva, E. 2009. Leishmanicidal effect of LLD-3 (1), a nor-triterpene isolated from *Lophanthera lactescens*. *Phytochemistry*, 70 (5), 608-614.
- Dassonville-Klimpt, A., Jonet, A., Pillon, M., Mullié, C. and Sonnet, P. 2011. Mefloquine derivatives: synthesis, mechanisms of action, antimicrobial activities. *Science against Microbial Pathogens*, 23–35.
- Daszak, P., Cunningham, A.A., and Hyatt, A.D. 2001. Anthropogenic environmental change and the emergence of infectious diseases in wildlife. *Acta Tropica*, 78(2), 103–116. doi:10.1016/s0001-706x(00)00179-0
- David-Bosne, S., Florent, I., Lund-Winther AM, Hansen, B. J., Buch-Pedersen, M., Machillot, P., Maire, M. and Jaxel, C. 2013. Antimalarial screening via large-scale purification of *Plasmodium falciparum* Ca²⁺-ATPase 6 and *in vitro* studies. *FEBS Journal*, 280 (21), 5419–5429.
- Davidson R.N., den Boer M., and Ritmeijer K. Paromomycin. *Transactions of The Royal Society of Tropical Medicine and Hygiene*, 103: 653–60.
- Davies, C.R., Kaye P., Croft S.L. and Sundar S. 2003. Leishmaniasis: new approaches to disease control. *Bmj*, 326(7385): 377-82.
- Davis, R. A., Sykes, M., Avery, V. M., Camp, D., and Quinn, R. J. 2011. Convolutamines I and J, antitrypanosomal alkaloids from the bryozoan *Amathia tortusa*. *Bioorganic and Medicinal Chemistry*, 19(22), 6615–6619. doi:10.1016/j.bmc.2011.06.006
- Dawit G., Girma Z., and Simenew K. 2013. A Review on biology, epidemiology and public health significance of leishmaniasis. *Journal of Bacteriology & Parasitology*, 4: 166.
- De Almeida-Amaral, E. E., Caruso-Neves, C., Pires, V. M. P., and Meyer-Fernandes, J. R. 2008. *Leishmania amazonensis*: characterization of an ouabain-insensitive Na⁺-ATPase activity. *Experimental Parasitology*, 118(2), 165–171.

De Almeida L., Fujimura T.A., Del Cistia L.M., Fonseca-Santos B., Imamura B.K., Michels A.M. P, Chorilli M, and Graminha A.S.M. 2017. Nanotechnological strategies for treatment of leishmaniasis—a review. *Journal of Biomedical Nanotechnology*, 13(2):117-133.

De Menezes, J. P. B., Guedes, C.E.S., Petersen, A.L. de O. A., Fraga, D.B. M., and Veras, P.S.T. 2015. Advances in development of new treatment for leishmaniasis. *BioMed Research International*, 1–11. doi:10.1155/2015/815023

De Moura T.R., Santos M.L., Braz J.M., Santos L.F., Aragão M.T., de Oliveira F.A., Santos P.L., da Silva Â.M., de Jesus A.R., and de Almeida R.P. 2016. Cross-resistance of *Leishmania infantum* isolates to nitric oxide from patients refractory to antimony treatment, and greater tolerance to antileishmanial responses by macrophages. *Parasitology Research*, 115(2):713-21. doi:10.1007/s00436-015-4793-4

De Muylder G., Ang K.K., Chen S., Arkin M.R., Engel J.C., and McKerrow J.H. 2011. A screen against *Leishmania* intracellular amastigotes: comparison to a promastigote screen and identification of a host cell-specific hit. *PLoS Neglected Tropical Diseases*, 5(7), e1253. doi:10.1371/journal.pntd.0001253

De Niz, M., Ullrich, A.-K., Heiber, A., Blancke Soares, A., Pick, C., Lyck, R., Keller D., Kaiser G., Prado M., Flemming S., Del Portillo H., Janse C.J., Heussler V., Spielmann T. and Spielmann, T. 2016. The machinery underlying malaria parasite virulence is conserved between rodent and human malaria parasites. *Nature Communications*, 7, 11659. doi:10.1038/ncomms11659

Denny P.W., Goulding D., Ferguson M.A.J., Smith D.F. 2004. Sphingolipid free *Leishmania* are defective in membrane trafficking, differentiation and infectivity. *Molecular Microbiology*, 52:313–327.

del Barrio G., and Parra F. 2000. Evaluation of the antiviral activity of an aqueous extract from *Phyllanthus orbicularis*. *Journal of Ethnopharmacology*, 72(1-2):317-22.

Delemarre B.J., and van der Kaay H.J. 1979. Tropical malaria contracted the natural way in the Netherlands. *Nederlands Tijdschrift voor Geneeskunde*, 123:1981–1982.

Derbyshire, E. R., Prudencio, M., Mota, M. M., and Clardy, J. 2012. Liver-stage malaria parasites vulnerable to diverse chemical scaffolds. *Proceedings of the National Academy of Sciences*, 109(22), 8511–8516. doi:10.1073/pnas.1118370109

Dhabangi, A., Mworozzi E., Lubega I. R., Cserti-Gazdewich C. M., Maganda A. and Dzik, W. H. 2013. The effect of blood storage age on treatment of lactic acidosis by transfusion in children with severe malarial anaemia: a pilot, randomized, controlled trial. *Malaria Journal*, 12(55): 1-7.

Dias, D. A., Urban, S., and Roessner, U. 2012. A historical overview of natural products in drug discovery. *Metabolites*, 2(2), 303–336.

Ding, C. X., Beck, H. and Raso, G. 2011. *Plasmodium* sensitivity to artemisinins: magic bullets hit elusive targets. *Trends in Parasitology*, 27(2), 73-81.

Ding, D., Zhao, Y., Meng, Q., Xie, D., Nare, B., Chen, D., Bacchi C.J., Yarlett N., Zhang Y.K., Hernandez V., Xia Y., Freund Y., Abdulla M., Ang K.H., Ratnam J., McKerrow J.H., Jacobs R.T., Zhou H., and Plattner, J.J. 2010. Discovery of novel benzoxaborole-based potent antitrypanosomal agents. *ACS Medicinal Chemistry Letters*, 1(4), 165–169. doi:10.1021/ml100013s

Dinko B., Pradel G. Immune evasion by *Plasmodium falciparum* parasites: converting a host protection mechanism for the parasite's benefit. *Advances in Infectious Diseases*. 2016;6 (2, article 67759) doi: 10.4236/aid.2016.62011.

Diniz J.L., Costa M.O., and Gonçalves D.U. 2011. Mucocutaneous leishmaniasis: clinical markers in presumptive diagnosis. *Braz J Otorhinolaryngol*, 77(3):380-4. doi.org/10.1016/j.exppara.2008.05.003

DNDi Annual Report 2015. Adapted treatments for the benefit of neglected patients. DNDi Annual Report. Available at: https://www.dndi.org/wp-content/uploads/2016/08/DNDi_AR_2015_2.pdf

DNDi Annual Report 2017. New hope for novel drugs for leishmaniasis. Update of DNDi's leishmaniasis R&D pipeline. Available at: https://www.dndi.org/wp-content/uploads/2017/05/DNDi_LeishmaniasisPipeline_2017.pdf

DNDi. 2017. Leishmaniasis. Available at: https://www.dndi.org/wp-content/uploads/2016/10/Factsheet_2015_Leish.pdf

DNDi Annual Report 2018. InfoLEISH. RredeLEISH newsletter-3rd edition. DNDi Annual Report. Available at: https://www.dndi.org/wp-content/uploads/2018/07/InfoLeish_Newsletter_June2018_ENG.pdf

Don, R., and Ioset, J.-R. 2013. Screening strategies to identify new chemical diversity for drug development to treat kinetoplastid infections. *Parasitology*, 141(01), 140–146. doi:10.1017/s003118201300142x

Dondorp, A. M., Fanello, I. C., Hendriksen, I. C., Gomes, E., Seni, A., Chhaganlal, D. K., Bojang, K., Olaosebikan, R., Anunobi, N., Maitland, K., Kivaya, E., Agbenyega, T., Nguah, B. S., Evans, J., Gesase, S., Kahabuka, C., Mtove, G., Nadjm, B., Deen, J., Mwangi-Amumpaire, J., Nansumba, M., Karema, C., Umulisa, N., Uwimana, A., Mokuolu, A. O., Adedoyin, T. O., Johnson, B. W., Tshefu, K. A., Onyamboko, A. M., Sakulthaew, T., Ngum, P. W., Silamut, K., Stepniewska, K., Woodrow, J. C., Bethell, D., Wills, B., Onoko, M., Peto, E. T., Seidlein, V. L., Day, P. N. and White, J. N. 2010. Artesunate versus quinine in the treatment of severe falciparum malaria in African children (AQUAMAT): an open-label, randomised trial. *Lancet*, 13; 376(9753), 1647–1657.

Dondorp, A. M., Lee S. J., Faiz M. A., Mishra S., Price R., Tjitra E., Than M., Htut Y., Mohanty S., Bin Y. E., Rahman R., Nosten F., Anstey N. M. and Lee S. J. 2008. The relationship between age and the manifestations of and mortality associated with severe malaria. *Clinical Infectious Diseases*, 47: 151–157.

Dondorp, A., Nosten, F., Stepniewska, K., Day, N., and White, N. 2005. Artesunate versus quinine for treatment of severe falciparum malaria: a randomised trial. *Lancet*, 366 (9487), 717–25.

Dorlo, T.P.C., Balasegaram, M., Beijnen, J.H., and de Vries, P.J. 2012. Miltefosine: a review of its pharmacology and therapeutic efficacy in the treatment of leishmaniasis. *Journal of Antimicrobial Chemotherapy*, 67(11), 2576–2597. doi:10.1093/jac/dks275

Dorlo, T.P.C., Balasegaram, M., Beijnen, J.H., and de Vries, P.J. 2012. Miltefosine: a review of its pharmacology and therapeutic efficacy in the treatment of leishmaniasis. *Journal of Antimicrobial Chemotherapy*, 67(11), 2576–2597. doi:10.1093/jac/dks275

Dorlo, T.P.C., van Thiel, P.P.A. M., Huitema, A.D.R., Keizer, R.J., de Vries, H.J.C., Beijnen, J.H., and de Vries, P.J. 2008. Pharmacokinetics of miltefosine in old world cutaneous leishmaniasis patients. *Antimicrobial Agents and Chemotherapy*, 52(8), 2855–2860. doi:10.1128/aac.00014-08.

Dos Santos, V., Leite, K., da Costa Siqueira, M., Regasini, L., Martinez, I., Nogueira, C., Galuppo M.K., Stolf B.S., Pereira A.M., Cicarelli R.M., Furlan M., and Graminha M.A. 2013. Antiprotozoal activity of quinonemethide triterpenes from *Maytenus ilicifolia* (Celastraceae). *Molecules*, 18(1), 1053–1062. doi:10.3390/molecules18011053

Dowdle, W. R., and Cochi, S. L. 2011. The principles and feasibility of disease eradication. *Vaccine*, 29, D70–D73. doi:10.1016/j.vaccine.2011.04.006

Downing T., Imamura H., Decuyper S., Clark T.G., Coombs G.H., Cotton J.A., Hilley J.D., de Doncker S., Maes I., Mottram J.C., Quail MA, Rijal S., Sanders M., Schonian G., Stark O., Sundar S., Vanaerschot M., Hertz-Fowler C., Dujardin J.C., and Berriman M. 2011. Whole genome sequencing of multiple *Leishmania donovani* clinical isolates provides insights into population structure and mechanisms of drug resistance. *Genome Research*, 21:2143-2156.10.1101/gr.123430.111

Du, R., Hotez, P. J., Al-Salem, W. S., and Acosta-Serrano, A. 2016. Old world cutaneous leishmaniasis and refugee crises in the middle east and north Africa. *PLoS Neglected Tropical Diseases*, 10(5), e0004545. doi:10.1371/journal.pntd.0004545

Duffy, S., Sykes, M.L., Jones, A.J., Shelper, T. B., Simpson, M., Lang, R., Poulsen S.-A., Sleebs B.E. and Avery, V.M. 2017. Screening the medicines for malaria venture pathogen box across multiple pathogens reclassifies starting points for open-source drug discovery. *Antimicrobial Agents and Chemotherapy*, 61(9). doi:10.1128/aac.00379-17

Dujardin, J.-C. 2006. Risk factors in the spread of leishmaniasis: towards integrated monitoring? *Trends in Parasitology*, 22(1), 4–6. doi:10.1016/j.pt.2005.11.004

Dye C. 1996. The logic of visceral leishmaniasis control. *The American Journal of Tropical Medicine and Hygiene*, 55:125–130.

Ecker, A., Lehane, A.M., Clain, J., and Fidock, D.A. 2012. PfCRT and its role in antimalarial drug resistance. *Trends in Parasitology*, 28(11), 504–514. doi:10.1016/j.pt.2012.08.002

Eisele, T.P., Larsen, D. and Steketee, R.W. 2010. Protective efficacy of interventions for preventing malaria mortality in children in *Plasmodium falciparum* endemic areas. *International Journal of Epidemiology*, 39: i88–i101.

Ekland E.H., Schneider J., and Fidock D.A. 2011. Identifying apicoplast-targeting antimalarials using high-throughput compatible approaches. *The FASEB Journal*, 25(10):3583±93. doi.org/10.1096/fj.11-187401

Elased, K. and Playfair J. H. L. 1994. Hypoglycemia and hyperinsulinemia in rodent models of severe malaria infection. *Infection and Immunity*, 62(11): 5157–5160.

Erdemoglu, N., and Sener, B. 2001. Antimicrobial activity of the heartwood of *Taxus baccata*. *Fitoterapia*, 72(1), 59–61. doi:10.1016/s0367-326x(00)00233-1

Ericsson, T. 2014. *In vitro* and *in vivo* studies of artemisinin endoperoxides. *Institute of Neuroscience and Physiology; University of Gothenburg*, 1-76.

Escudero-Martínez, J. M., Pérez-Pertejo, Y., Reguera, R. M., Castro, M. Á., Rojo, M. V., Santiago, C., Abad A., García P.A., Lopez-Perez J.L., Feliciano AS., and Balaña-Fouce, R. 2017. Antileishmanial activity and tubulin polymerization inhibition of podophyllotoxin derivatives on *Leishmania infantum*. *International Journal for Parasitology: Drugs and Drug Resistance*, 7(3), 272–285. doi:10.1016/j.ijpddr.2017.06.003

Eyasu, M. 2015. Antimalarial drug resistance: In the past, current status and future perspectives mebrahtu. *British Journal of Pharmacology and Toxicology*, 6(1), 1-15.

Faiman, R., Abbasi, I., Jaffe, C., Motro, Y., Nasereddin, A., Schnur, L.F., Torem, M., Pratlong, F., Dedet, J-P., and Warburg, A. 2013. A newly emerged cutaneous leishmaniasis focus in northern Israel and two new reservoir hosts of *Leishmania major*. *PLoS Neglected Tropical Diseases*, 7(2): e2058.

Farooq, U. and Mahajan, R. C. 2004. Drug resistance in malaria. *Journal of Vector Borne Diseases*, 41(3-4), 45–53.

Field, M. C., Horn, D., Fairlamb, A. H., Ferguson, M. A. J., Gray, D. W., Read, K. D., De Rycker M., Torrie S.L., Wyatt P. G., Wyllie S., and Gilbert, I. H. 2017. Anti-trypanosomatid drug discovery: an ongoing challenge and a continuing need. *Nature Reviews Microbiology*, 15(7), 447–447. doi:10.1038/nrmicro.2017.69

Fournet, A., Ferreira, M.E., de Arias, A.R., Ortiz, S.T., Fuentes, S., Nakayama, H., Schinini, A., and Hocquemiller, R. 1996. *In vivo* efficacy of oral and intralésional administration of 2-substituted quinolines in experimental treatment of new world cutaneous leishmaniasis caused by *Leishmania amazonensis*. *Antimicrobial Agents and Chemotherapy*, 40, 2447–2451.

Franco J.R., Simarro P.P., Diarra A., and Jannin J.G. 2014. Epidemiology of human African trypanosomiasis. *Clinical Epidemiology*, 6:257-75. doi:10.2147/cep.s39728

Franco, A. M. R., Grafova, I., Soares, F. V., Gentile, G., Wyrepkowski, C. D. C., Bolson, M. A., Sargentini É., J.r., Carfagna C., Leskelä M., and Grafov A. 2016. Nanoscaled hydrated antimony (V) oxide as a new approach to first-line antileishmanial drugs. *International Journal of Nanomedicine*, Volume 11, 6771–6780. doi:10.2147/ijn.s121096

François, G., Passreiter, C., Woerdenbag, H., and Van Looveren, M. 1996. Antiplasmodial activities and cytotoxic effects of aqueous extracts and sesquiterpene lactones from *Neurolaena lobata*. *Planta Medica*, 62(02), 126–129. doi:10.1055/s-2006-957833

Freitas-Junior L.H., Chatelain E., Kim H.A., and Siqueira-Neto J.L. 2012. Visceral leishmaniasis treatment: what do we have, what do we need and how to deliver it?. *International Journal for Parasitology: Drugs and Drug Resistance*, 2, 11–19. doi:10.1016/j.ijpddr.2012.01.003

Frézard, F., Demicheli, C., and Ribeiro, R. 2009. Pentavalent Antimonials: New Perspectives for Old Drugs. *Molecules*, 14(7), 2317–2336. doi:10.3390/molecules14072317

Fridberg A., Olson C.L., Nakayasu E.S., Tyler K.M., Almeida I.C., and Engman D.M. 2008. Sphingolipid synthesis is necessary for kinetoplast segregation and cytokinesis in *Trypanosoma brucei*. *Journal of Cell Science*, 121:522–535.

Fuchino, H., Koide, T., Takahashi, M., Sekita, S., Satake, M., 2001. New sesquiterpene lactones from *Elephantopus mollis* and their leishmanicidal activities. *Planta Medica*, 67, 647–653

Gamo F.J., Sanz L.M., Vidal J., de Cozar C., Alvarez E., Lavandera J.L., Vanderwall D.E., Green D.V., Kumar V., Hasan S., Brown J.R., Peishoff C.E., Cardon L.R., and Garcia-Bustos J.F. 2010. Thousands of chemical starting points for antimalarial lead identification. *Nature*, 465(7296):305–10.

Ganesan, A. 2008. The impact of natural products upon modern drug discovery. *Current Opinion in Chemical Biology*, 12(3), 306–317. doi:10.1016/j.cbpa.2008.03.016

García-Hernández, R., Gómez-Pérez, V., Castanys, S., and Gamarro, F. 2015. Fitness of *Leishmania donovani* parasites resistant to drug combinations. *PLoS Neglected Tropical Diseases*, 9(4), e0003704. doi:10.1371/journal.pntd.0003704

Gazanion, É., Fernández-Prada, C., Papadopoulou, B., Leprohon, P., and Ouellette, M. 2016. Cos-seq for high-throughput identification of drug target and resistance mechanisms in the protozoan parasite leishmania. *Proceedings of the National Academy of Sciences*, 113(21), E3012–E3021. doi:10.1073/pnas.1520693113

Genest, P.A., Haimeur, A., Légaré, D., Sereno, D., Roy, G., Messier, N., Papadopoulou B., and Ouellette, M. 2008. A protein of the leucine-rich repeats (LRRs) superfamily is implicated in antimony resistance in *Leishmania infantum* amastigotes. *Molecular and Biochemical Parasitology*, 158(1), 95–99. doi:10.1016/j.molbiopara.2007.11.008

Georgopoulou, K., Smirlilis, D., Bisti, S;Xingl, E., Skaltsounis L., and Soteriadou, K. 2007. *In vitro* activity of 10-deacetylbaocatin III against *Leishmania donovani* promastigotes and intracellular amastigotes. *Planta Medica*, 73 (10), 1081-1088.

- Gidwani, K., Picado, A., Rijal, S., Singh, S. P., Roy, L., Volfova, V., Andersen E.W., Uranw S., Ostyn B., Sudarshan M., Chakravarty J., Volf P., Sundar S., Boelaert M., and Rogers, M. E. 2011. Serological markers of sand fly exposure to evaluate insecticidal nets against visceral leishmaniasis in India and Nepal: a cluster-randomized trial. *PLoS Neglected Tropical Diseases*, 5(9), e1296. doi:10.1371/journal.pntd.0001296
- Gil-Alonso, S., Jauregizar, N., Ortega, I., Eraso, E., Suárez, E., & Quindós, G. 2016. *In vitro* pharmacodynamic modelling of anidulafungin against *Candida* spp. *International Journal of Antimicrobial Agents*, 47(3), 178–183. doi:10.1016/j.ijantimicag.2015.12.011
- Ginsburg, H., and Deharo, E. 2011. A call for using natural compounds in the development of new antimalarial treatments – an introduction. *Malaria Journal*, 10(Suppl 1):S1, 1-7 doi:10.1186/1475-2875-10-s1-s1
- Ghorbani M., and Farhoudi R. 2018. Leishmaniasis in humans: drug or vaccine therapy?. *Drug Design, Development and Therapy*, 12: 25–40.
- Gould, M. K., Vu, X. L., Seebeck, T., and de Koning, H. P. 2008. Propidium iodide-based methods for monitoring drug action in the kinetoplastidae: Comparison with the Alamar Blue assay. *Analytical Biochemistry*, 382(2), 87–93. doi:10.1016/j.ab.2008.07.036
- Grecco, S.S., Relmão, J.Q., Tempone, A.G. 2012. Sartorelli, P: Cunha, R. L;Romoft, P.;Ferreira, M. J.; Fávero, O. A;Lago, I. H. G, *In vitro* antileishmanial and antitrypanosomal activities of flavanones from *Baccharis retusa* DC (*Asteraceae*). *Experimental Parasitology*, 130 (2), 141-145
- Greenwood, B. 2010. Anti-malarial drugs and the prevention of malaria in the population of malaria endemic areas. *Malaria Journal*, 9 (Suppl 3):S2, 1-7.
- Grimberg, B. T. and Mehlotra, R. K. 2011. Expanding the antimalarial drug arsenal-now, but how?. *Pharmaceuticals*, 4(5), 681–712.
- Grondin, K., Kundig, C., Roy, G., and Ouellette, M. 1998. Linear amplicons as precursors of amplified circles in methotrexate-resistant *Leishmania tarentolae*. *Nucleic Acids Research*, 26(14), 3370–3378. doi:10.1093/nar/26.14.3370
- Guantai, E., and Chibale, K. 2011. How can natural products serve as a viable source of lead compounds for the development of new/novel anti-malarials? *Malaria Journal*, 10(Suppl 1):S2, 1-8.
- Guiguemde W.A., Shelat A.A., Bouck D., Duffy S., Crowther G.J., Davis P.H., *et al.* Chemical genetics of *Plasmodium falciparum*. *Nature*, 2010;465(7296):311–5.
- Guintran, J., Delacollette C. and Trigg P. 2006. Systems for the early detection of malaria epidemics in Africa: An analysis of current practices and future priorities. World Health Organization, Geneva.
- Gunatilaka, A.A.L., Berger, J.M., Evans, R., Miller, J.S., Wisse, J.H., Neddermann, K.M., Bursuker, I., and Kingston, D.G.I. 2001. Isolation, synthesis, and structure activity

relationships of bioactive benzoquinones from *Miconia lepidota* from the suriname rainforest. *Journal of Natural Products*, 64, 2–5.

Hall M.P., Unch J., Binkowski B.F., Valley M.P., Butler B.L., Wood M.G., Otto P., Zimmerman K., Vidugiris G., Machleidt T., Robers M.B., Benink H.A., Eggers C.T., Slater M.R., Meisenheimer P.L., Klaubert D.H., Fan F., Encell L.P., and Wood K.V. 2012. Engineered luciferase reporter from a deep sea shrimp utilizing a novel imidazopyrazinone substrate. *ACS Chemical Biology*, 7(11):1848-1857. doi.org/10.1021/cb3002478

Hall, B. S., Meredith, E.L., and Wilkinson, S.R. 2012a. Targeting the substrate preference of a type I nitroreductase to develop antitrypanosomal quinone-based prodrugs. *Antimicrobial Agents and Chemotherapy*, 56(11), 5821–5830. doi:10.1128/aac.01227-12.

Hammarton, T.C., Mottram, J.C., Doerig, C., 2003. The cell cycle of parasitic protozoa: potential for chemotherapeutic exploitation. *Progress in Cell Cycle Research*, 5, 91–101.

Handman E. 2001. Leishmaniasis: current status of vaccine development. *Clinical Microbiology Reviews*, 14:229-243.

Harvey, A. L., Edrada-Ebel, R., and Quinn, R. J. 2015. The re-emergence of natural products for drug discovery in the genomics era. *Nature Reviews Drug Discovery*, 14(2), 111–129. doi:10.1038/nrd4510

Hasenkamp, S., Russell, K.T. and Horrocks, P., 2012. Comparison of the absolute and relative efficiencies of electroporation-based transfection protocols for *Plasmodium falciparum*. *Malaria Journal*, 11(210), 1-5.

Hasenkamp, S., Sidaway, A., Devine, O., Roye, R. and Horrocks, P., 2013. Evaluation of bioluminescence-based assays of anti-malarial drug activity. *Malaria Journal*, 12(58), 1-10.

Heese-Peck, A., Pichler, H., Zanolari, B., Watanabe, R., Daum, G., and Riezman, H. 2002. Multiple functions of sterols in yeast endocytosis. *Journal of Molecular Biology*, 13, 2664–2680.

Hefnawy, A., Berg, M., Dujardin, J.-C., and De Muylder, G. 2017. Exploiting knowledge on leishmania drug resistance to support the quest for new drugs. *Trends in Parasitology*, 33(3), 162–174. doi:10.1016/j.pt.2016.11.003

Hellemond, J. v.,Marijke R.,Rob K., Anne-Marie Z.,Jaco J. V., Pieter J. W., Clemens H. K. and Perry J.J. 2009. Human *Plasmodium knowlesi* infection detected by rapid diagnostic tests for malaria. *Emerging Infectious Diseases*, 15(9): 1478–1480. doi: 10.3201/eid1509.090358

Hendrickx S., Van den Kerkhof M., Mabile D., Cos P., Delputte P., Maes L., and Caljon G. 2017. Combined treatment of miltefosine and paromomycin delays the onset of experimental drug resistance in *Leishmania infantum*. *PLoS Neglected Tropical Diseases*, 11: e0005620.

Hennessey, K. M., Rogiers, I. C., Shih, H.-W., Hulverson, M. A., Choi, R., McCloskey, M. C., Whitman R.G, Barrett L.K., Merritt E.A., Paredez A.R. and Ojo, K. K. 2018. Screening

of the pathogen box for inhibitors with dual efficacy against *Giardia lamblia* and *Cryptosporidium parvum*. *PLoS Neglected Tropical Diseases*, 12(8), e0006673. doi:10.1371/journal.pntd.0006673

Henry J. K. 2011. The global malaria epidemic. *U.S. Global Health Policy*. The Kaiser Family Foundation's website at www.kff.org.

Hermoso, A. 2003. Jiménez L.A.; Mamani, Z A.; Bazzocchi, LL, Pinero, J. E.; Ravelo, A G., Valladares, B., Antileishmanial activities of dihydrochalcones from *Piper elongatum* and synthetic related compounds Structural requirements for activity. *Bioorganic and Medical Chemistry*, 11(18), 3975-3980.

Herricks, J. R., Hotez, P. J., Wanga, V., Coffeng, L. E., Haagsma, J. A., Basáñez, M.-G., Buckle G., Budke C.M., Carabin H., Fèvre E.M., Fürst T., Halasa Y.A., King C.H., Murdoch M.E., Ramaiah k.D., Shepard D.S., Stolk W.A., Undurraga E.A., Stanaway J.D., Naghavi M., and Murray, C.J.L. 2017. The global burden of disease study 2013: What does it mean for the NTDs? *PLoS Neglected Tropical Diseases*, 11(8), e0005424. doi:10.1371/journal.pntd.0005424

Herwaldt B.L. 1999. Leishmaniasis. *Lancet*, 2:354:1191-1199

Hirumi, H., and Hirumi, K. 1989. Continuous cultivation of *Trypanosoma brucei* blood stream forms in a medium containing a low concentration of serum protein without feeder cell layers. *Journal of Parasitology*, 75: 985–989.

Hong C., Walczak R., Dhamko H., Bradley M.N., Marathe C., Boyadjian R., Salazar J.V., and Tontonoz P. 2011. Constitutive activation of LXR in macrophages regulates metabolic and inflammatory gene expression: identification of ARL7 as a direct target. *Journal of Lipid Research*, 52(3): 531–539. doi: [10.1194/jlr.M010686]

Horn, D., and Duraisingh, M.T. 2014. Antiparasitic chemotherapy: from genomes to mechanisms. *Annual Review of Pharmacology and Toxicology*, 54(1), 71–94. doi:10.1146/annurev-pharmtox-011613-135915

Horrocks, P., and Lanzer, M. 1999. Mutational analysis identifies a five base pair cis-acting sequence essential for GBP130 promoter activity in *Plasmodium falciparum*. *Molecular and Biochemical Parasitology*, 99(1), 77–87. doi:10.1016/s0166-6851(98)00182-0

Hostettler I., Müller J., and Hemphill A. 2016. *In vitro* Screening of the Open-Source Medicines for Malaria Venture Malaria Box Reveals Novel Compounds with Profound Activities against *Theileria annulata* Schizonts. *Antimicrob Agents Chemother*, 23;60(6):3301-8. doi: 10.1128/AAC.02801-15.

Hotez, P. J., Fenwick, A., Savioli, L., and Molyneux, D. H. 2009. Rescuing the bottom billion through control of neglected tropical diseases. *The Lancet*, 373(9674), 1570–1575. doi:10.1016/s0140-6736(09)60233-6

Hotez, P.J., David H. Molyneux, Alan F., Jacob K., Sonia E.S., Jeffrey D.S., and Lorenzo S. 2007. Control of neglected tropical diseases. *The New England Journal of Medicine*, 357:1018–27.

Houweling T.A.J., Karim-Kos H.E., Kulik M.C., Stolk W.A. , Haagsma J.A. ,Lenk E.J. , Richardus J.H. and de Vlas S.J. Socioeconomic inequalities in neglected tropical diseases: a systematic review. *PLoS Neglected Tropical Diseases*, 2016; 10: e0004546.

Ibrahim MA, Mohammed A, Isah MB, Aliyu AB. 2014. Anti-trypanosomal activity of African medicinal plants: a review update. *Journal of Ethnopharmacology*, 4, 28;154(1):26-54. doi: 10.1016/j.jep.2014.04.012.

Idro, R., Kakooza-Mwesige A., Balyejjussa S., Mirembe G., Mugasha C., Tugumisirize J., and Byarugaba J. 2010. Severe neurological sequelae and behaviour problems after cerebral malaria in Ugandan children. *BMC Research Notes*, 3(104): 1-6.

Ilg, T. 2017. Investigations on the molecular mode of action of the novel immunostimulator ZelNate: activation of the cGAS-STING pathway in mammalian cells. *Molecular Immunology*, 90, 182–189. doi:10.1016/j.molimm.2017.07.013.

Iovannisci D.M., and Ullman B. 1984. Single cell cloning of leishmanial parasites in purine-defined medium: isolation of drug-resistant variants. *Advances in Experimental Medicine and Biology*, 165 Pt A:239-43.

Jacobs, R. T., Plattner, J. J., Nare, B., Wring, S. A., Chen, D., Freund, Y., Gaukel E.G., Orr M.D., Perales J.B., Jenks M., Noe R.A., Sligar J.M., Zhang Y.-K., Bacchi C.J., Yarlett N., and Don, R. 2011. Benzoxaboroles: a new class of potential drugs for human African trypanosomiasis. *Future Medicinal Chemistry*, 3(10), 1259–1278. doi:10.4155/fmc.11.80

Jain S K., Jacob M., Walker L. and Tekwani B. 2016. Screening North American plant extracts *in vitro* against *Trypanosoma brucei*, the causative agent for human african trypanosomiasis. *BMC Complementary and Alternative Medicine*, 18;16:131. doi: 10.1186/s12906-016-1122-0.

Jain, S. K., Sahu, R., Walker, L. A., & Tekwani, B. L. 2012. A parasite rescue and transformation assay for antileishmanial screening against intracellular *Leishmania donovani* Amastigotes in THP1 human acute monocytic leukemia cell line. *Journal of Visualized Experiments*, (70), 1-14. doi:10.3791/4054

Jallow, M., Casals-Pascual C., Ackerman H., Walther B., Walther M., Pinder M. and Kwiatkowski D. 2012. Clinical features of severe malaria associated with death: a 13-year observational study in the Gambia. *PLoS ONE*, 7(9): 1-8.

Jamal Q., Khan N.H., Wahid S., Awan M.M., Sutherland C., and Shah A. 2015. *In-vitro* sensitivity of Pakistani leishmania tropica field isolate against buparvaquone in comparison to standard antileishmanial drugs. *Experimental Parasitology*, 154:93-7. doi: 10.1016/j.exppara.2015.04.017

Jamonneau V., Ilboudo H., Kaboré J., Kaba D., Koffi M., Solano P., Garcia A., Courtin D., Laveissière C., Lingue K., Büscher P., AND Bucheton B. 2012. Untreated human infections

by *Trypanosoma brucei gambiense* are not 100% fatal. *PLoS Neglected Tropical Diseases*, 6(6): e1691. doi.org/10.1371/journal.pntd.0001691

Jha, R.K., Sah A.K., Shah D.K., and Sah P. 2013. The treatment of visceral leishmaniasis: safety and efficacy. *Journal of Nepal Medical Association*, 52(192):645-51.

John, W. and Sons. 2014. Severe malaria. *Tropical Medicine and International Health*, 19 (Suppl. 1): 7–131.

Juge, N., Moriyama, S., Miyaji, T., Kawakami, M., Iwai, H., Fukui, T., et al. 2015. Plasmodium falciparum chloroquine resistance transporter is a H⁺-coupled polyspecific nutrient and drug exporter. *Proceedings of the National Academy of Sciences*, 112(11), 3356–3361. doi:10.1073/pnas.1417102112

Julianti, T., Hata, Y., Zimmermann, S., Kaiser, M., Hamburger, M., and Adams, M. 2011. Antitrypanosomal sesquiterpene lactones from *Saussurea costus*. *Fitoterapia*, 82, 955–959.

Kagira, J.M., Ngotho, M. and Thuita, J. 2007. Development of a rodent model for late stage rhodesian sleeping sickness. *The Journal of protozoology research*, 17:48–56.

Kaiser, M., Maes, L., Tadoori, L.P., Spangenberg, T., and Ioset, J.-R. 2015. Repurposing of the open access malaria box for kinetoplastid diseases identifies novel active scaffolds against trypanosomatids. *Journal of Biomolecular Screening*, 20(5), 634–645. doi:10.1177/1087057115569155

Kaiser M., Bray M.A., Cal M., Bourdin Trunz B., Torreele E., and Brun R. 2011. Antitrypanosomal activity of fexinidazole, a new oral nitroimidazole drug candidate for treatment of sleeping sickness. *Antimicrob Agents Chemother*, 55: 5602–08.

Kalanda, G. C., Hill J., Verhoeff F. H., Brabin B. J. 2006. Comparative efficacy of chloroquine and sulphadoxine-pyrimethamine in pregnant women and children: a meta-analysis. *Tropical Medicine and International Health*, 11(5): 569-577.

Katsuno, K., Burrows, J.N., Duncan, K., van Huijsduijnen, R. H., Kaneko, T., Kita, K., Charles E., Mowbray, Schmatz D., Warner P., and Slingsby, B.T. 2015. Hit and lead criteria in drug discovery for infectious diseases of the developing world. *Nature Reviews Drug Discovery*, 14(11), 751–758. doi:10.1038/nrd4683

Keenan J.D., Bailey R.L., West S.K., Arzika A.M., Hart J., Weaver J., Kalua K., Mrango Z., Ray K.J., Cook C., Lebas E., O'Brien K.S., Emerson P.M., Porco T.C., and Lietman T.M. 2018. Azithromycin to reduce childhood mortality in sub-saharan Africa. *The New England Journal of Medicine*, 378: 1583–92.

Kennedy P.G.E. 2004. Human African trypanosomiasis of the CNS: current issues and challenges. *Journal of Clinical Investigation*, 113: 496–504.

Kerkhof, V.-d.M., Mabile, D., Chatelain, E., Mowbray, C. E., Braillard, S., Hendrickx, S., Maes, G., and Caljon, G. 2018. *In vitro* and *in vivo* pharmacodynamics of three novel antileishmanial lead series. *International Journal for Parasitology: Drugs and Drug Resistance*, 8(1), 81–86. doi:10.1016/j.ijpddr.2018.01.006

Kheir, A. 2011. Factors influencing evolution to antimalarial drug resistance in *P. falciparum* in Sudan and the Gambia. *Dissertation, Department of Medical Biochemistry and Microbiology*, Box 582, Uppsala University, 1-56.

Khraiwesh, M., Hudson, T., Johnson, J., Leed, S., Hickman, M., Roncal, N., Johnson J., Sciotti R., Smith P., Read L., Paris R, Hudson T., Hickman M., and Grogl M. 2016. Antileishmanial activity of compounds derived from the medicines for malaria venture Open access box against intracellular *Leishmania major* amastigotes. *The American Journal of Tropical Medicine and Hygiene*, 94(2), 340–347. doi:10.4269/ajtmh.15-0448

Killick-Kendrick, R. 1999. The biology and control of *Phlebotomine* sand flies. *Clinics in Dermatology*, 17(3), 279-289.

Kiszewski, A. E., and Teklehaimanot A. 2004. A review of the clinical and epidemiologic burdens of epidemic malaria. *American Journal of Tropical Medicine and Hygiene*, 71(SUPPL 2), 128–35.

Koshimizu, K., Ohigashi, H., Huffman, M.A., 1994. Use of *Vernonia amygdalina* by wild chimpanzee: possible roles of its bitter and related constituents. *Physiology & Behavior*, 56(6), 1209–1216.

Kraft, C., Jenett-Siems, K., Siems, K., Jakupovic, J., Mavi, S., Bienzle, U., and Eich, E. 2003. *In vitro* antiplasmodial evaluation of medicinal plants from Zimbabwe. *Phytotherapy Research*, 17(2), 123–128. doi:10.1002/ptr.1066

Kristensson, K., Masocha, W., and Bentivoglio, M. 2013. Mechanisms of CNS invasion and damage by parasites. *Handbook of Clinical Neurology*, 11–22. doi:10.1016/b978-0-444-53490-3.00002-9

Krogstad, D. J., Schlesinger H. P. and Herwaldt B. 1987. Efflux of chloroquine from *Plasmodium falciparum*: mechanism of chloroquine resistance. *American Society for Microbiology*, 32(6), 799-801.

Kumar A., Nandi N., Sardar H.A., Das S., Kumar S., Pandey K., Ravidas V., Kumar M., De T., Singh D., and Dasa P. 2011. Mechanism of amphotericin B resistance in clinical isolates of *Leishmania donovani*. *Antimicrobial Agents and Chemotherapy*. p. 1031–1041. doi:10.1128/AAC.00030-11

Kumar A, Nandi N, Sardar H A, Das S, Kumar S, Pandey K, Ravidas V, Kumar M, De T, Singh D, and Dasa P. 2011. Mechanism of Amphotericin B Resistance in Clinical Isolates of *Leishmania donovani* Bidyut Purkait, *Antimicrobial Agents and Chemotherapy*, 56(2), 1031–1041. doi:10.1128/aac.00030-11

Kumar R., and Engwerda C. 2014. Vaccines to prevent leishmaniasis. *Clinical & Translational Immunology*, 3(3):e13. doi: 10.1038/cti.2014.4.

Kündig, C., Haimeur, A., Légaré, D., Papadopoulou, B., and Ouellette, M. 1999. Increased transport of pteridines compensates for mutations in the high affinity folate transporter and

contributes to methotrexate resistance in the protozoan parasite *Leishmania tarentolae*. *The EMBO Journal*, 18(9), 2342–2351. doi:10.1093/emboj/18.9.2342

Laffitte M.C., Leprohon P., Légaré D., and Ouellette M. 2016. Deep-sequencing revealing mutation dynamics in the miltefosine transporter gene in *Leishmania infantum* selected for miltefosine resistance. *Parasitology Research*, 115(10):3699-703. doi: 10.1007/s00436-016-5195-y.

Laffitte M.N., Leprohon P., Papadopoulou B., and Ouellette M. 2016. Plasticity of the leishmania genome leading to gene copy number variations and drug resistance. *F1000Research Journal*, 20;5:2350. doi: 10.12688/f1000research.9218.1.

Lambros, C. and Vanderberg, J.P., 1979. Synchronization of *Plasmodium falciparum* erythrocytic stages in culture. *The Journal of Parasitology*, 65(3), 418-420.

Lang, T., Goyard, S., Lebastard, M., and Milon, G. 2005. Bioluminescent *Leishmania* expressing luciferase for rapid and high throughput screening of drugs acting on amastigote-harbouring macrophages and for quantitative real-time monitoring of parasitism features in living mice. *Cellular Microbiology*, 7(3), 383–392. doi:10.1111/j.1462-5822.2004.00468.x

Laurenti M.D., Passero L.F., Tomokane T.Y., Franceschini Fde C., Rocha M.C., Gomes C.M., Corbett C.E., Silveira F.T. 2014 Dynamic of the cellular immune response at the dermal site of *Leishmania (L.) amazonensis* and *Leishmania (V.) braziliensis* infection in *Sapajus apella* primate. *BioMed Research International*, 134236. doi: 10.1155/2014/134236 PMID: 25309902

Leera, S., Hyacinth C. O. and Victoria D. 2014. Understanding human malaria: further review on the literature, pathogenesis and disease control. *Report and Opinion*, 6(6): 55–63.

Lelièvre, J., Almela, M. J., Lozano, S., Miguel, C., Franco, V., Leroy, D., and Herreros, E. 2012. Activity of clinically relevant antimalarial drugs on *Plasmodium falciparum* mature gametocytes in an ATP bioluminescence “transmission blocking” assay. *PLoS ONE*, 7(4), e35019. doi:10.1371/journal.pone.0035019

Lemke A., Kiderlen A.F. and Kayser O. 2005. Amphotericin B. *Appl Microbiol Biotechnol*, 68(2):151-62.

Li, Y., Liu, D., Cheng, Z., Proksch, P., and Lin, W. 2017. Cytotoxic trichothecene-type sesquiterpenes from the sponge-derived fungus *Stachybotrys chartarum* with tyrosine kinase inhibition. *RSC Advances*, 7(12), 7259–7267. doi:10.1039/c6ra26956g

Lin X., Chen Z., Zhang Y., Gao X., Luo W., Li B. 2014. Interactions among chemical components of Cocoa tea (*Camellia ptilophylla* Chang), a naturally low caffeine-containing tea species. *Food & Function*, 5 (6): 1175–85. doi: 10.1039/c3fo60720h PMID: 24699984

Lipinski, C.A., Lombardo, F., Dominy, B.W. and Feeney, P.J. 2001. Experimental and computational approaches to estimate solubility and permeability in drug discovery and development settings. *Advanced Drug Delivery Reviews*, 1(46), 3-26.

Lucantoni L., Duffy S., Adjalley S.H., Fidock D.A., and Avery V.M. 2013. Identification of MMV malaria box inhibitors of *Plasmodium falciparum* early -stage gametocytes using a luciferase -based high -throughput assay. *Antimicrob Agents Chemother*, 57:6050-62.

Lucumi E., Darling C., Jo H., Napper A.D., Chandramohanadas R., Fisher N., Shone A.E., Jing H., Ward S.A., Biagini G.A., DeGrado W.F., Diamond S.L. and Greenbaum D.C. 2010. Discovery of potent small-molecule inhibitors of multidrug-resistant *Plasmodium falciparum* using a novel miniaturized highthroughput luciferase-based assay. *Antimicrob Agents Chemother*, 54(9):3597-3604. doi.org/10.1128/AAC.00431-10

Luque-Ortega, J. R., and Rivas, L. 2007. Miltefosine (hexadecylphosphocholine) inhibits cytochrome c oxidase in *Leishmania donovani* promastigotes. *Antimicrobial Agents and Chemotherapy*, 51(4), 1327–1332. doi:10.1128/aac.01415-06

Lv, J.-J., Wang, Y.-F., Zhang, J.-M., Yu, S., Wang, D., Zhu, H.-T., Cheng R.-R., Yang C.-R., Xu M., and Zhang, Y.-J. 2014. Anti-hepatitis B virus activities and absolute configurations of sesquiterpenoid glycosides from *Phyllanthus emblica*. *Organic & Biomolecular Chemistry*, 12(43), 8764–8774. doi:10.1039/c4ob01196a

Mackey, T. K., Liang, B. A., Cuomo, R., Hafen, R., Brouwer, K. C., and Lee, D. E. 2014. Emerging and reemerging neglected tropical diseases: a review of key characteristics, risk factors, and the policy and innovation environment. *Clinical Microbiology Reviews*, 27(4), 949–979. doi:10.1128/cmr.00045-14

MacLean, L.M., Odiit, M., Chisi, J.E., Kennedy, P. G. E., and Sternberg, J.M. 2010. Focus-specific clinical profiles in human African trypanosomiasis caused by *Trypanosoma brucei rhodesiense*. *PLoS Neglected Tropical Diseases*, 4(12), e906. doi:10.1371/journal.pntd.0000906

Macpherson, C.N. L. 2005. Human behaviour and the epidemiology of parasitic zoonoses. *International Journal for Parasitology*, 35(11-12), 1319–1331. doi:10.1016/j.ijpara.2005.06.004

MacPherson, D.W., Gushulak B.D., Baine W.B., Bala, S., Gubbins P.O., Holtom P., Segarra-Newnham M. 2009. Population mobility, globalization, and antimicrobial drug resistance. *Emerging Infectious Diseases*, 15: 1727–1732.

Maes L., Beyers J., Mondelaers A., Van den Kerkhof M., Eberhardt E., Caljon G., and Hendrickx S. 2017. *In vitro* 'time-to-kill' assay to assess the cidal activity dynamics of current reference drugs against *Leishmania donovani* and *Leishmania infantum*. *Journal of Antimicrobial Chemotherapy*, 72(2):428-430. doi: 10.1093/jac/dkw409.

Mahiou, V., Roblot, F., Hocquemiller, R., Cave´, A., Barrios, A.A., Fournet, A., Ducrot, P.H., 1995. Piperogalin, a new prenylated diphenol from *Peperomia galioides*. *Journal of Natural Products*, 58, 324–328.

- Maier, A. G., Rug, M., O'Neill, M. T., Brown, M., Chakravorty, S., Szeszak, T., Cowman, A. F. 2008. Exported proteins required for virulence and rigidity of *Plasmodium falciparum*-infected human erythrocytes. *Cell*, 134(1): 48–61.
- Mamadalieva, N.Z., Herrmann, F., El-Readi, M.Z., Tahrani, A., Hamoud, R., Egamberdieva, D.R., Azimovaa S.S., and Wink, M. 2011. Flavonoids in *Scutellaria immaculate* and *S. ramosissima* (Lamiaceae) and their biological activity. *Journal of Pharmacy and Pharmacology*, 63(10), 1346–1357. doi:10.1111/j.2042-7158.2011.01336.x
- Mandal S., Maharjan M., Ganguly S., Chatterjee M., Singh S., Buckner F.S., and Madhubala R. 2009. High-throughput screening of amastigotes of *Leishmania donovani* clinical isolates against drugs using a colorimetric betalactamase assay. *Indian Journal of Experimental Biology*, 47:475– 479
- Mäntylä, A., Garnier, T., Rautio, J., Nevalainen, T., Vepsäläinen, J., Koskinen, A., Croft S.L. and Järvinen, T. 2004. Synthesis, *in vitro* evaluation, and antileishmanial activity of water-soluble prodrugs of buparvaquone. *Journal of Medicinal Chemistry*, 47(1), 188–195. doi:10.1021/jm030868a
- Mao X., Wu L.-F., Guo H.-L, Chen W.-J., Cui Y.-P., Qi Q., Li S., Liang W.-Y., Yang G.-H., Shao Y.-Y., Zhu D., She G.-M., You Y., and Zhang L.-Z. 2016. The genus phyllanthus: an ethnopharmacological, phytochemical, and pharmacological review. *Evidence-Based Complementary and Alternative Medicine*, Article ID 7584952, 1-36. doi.org/10.1155/2016/7584952
- Marquis, N., Gourbal, B., Rosen, B.P., Mukhopadhyay, R., and Ouellette, M. 2005. Modulation in aquaglyceroporin AQP1 gene transcript levels in drug-resistant *Leishmania*. *Molecular Microbiology*, 57(6), 1690–1699. doi:10.1111/j.1365-2958.2005.04782.x
- Matlashewski, G., Arana, B., Kroeger, A., Battacharya, S., Sundar, S., Das, P., Sinha P.K., Rijal S., Mondal D., Zilberstein D., and Alvar, J. 2011. Visceral leishmaniasis: elimination with existing interventions. *The Lancet Infectious Diseases*, 11(4), 322–325. doi:10.1016/s1473-3099(10)70320-0
- Matthews, K. R. 2005. The developmental cell biology of *Trypanosoma brucei*. *Journal of Cell Science*, 118(2), 283–290. doi:10.1242/jcs.01649
- Mayer, F. L., and Kronstad, J. W. 2017. Discovery of a novel antifungal agent in the pathogen box. *mSphere*, 2(2). doi:10.1128/msphere.00120-17
- Mbongo N., Loiseau P.M., Billion M.A., and Robert-Gero M. 1998. Mechanism of amphotericin B resistance in *Leishmania donovani* promastigotes. *Antimicrobial Agents and Chemotherapy*, 42(2):352–7. Epub 1998/04/04. PMID: 9527785
- McCall, L.I., Zhang, W.W., and Matlashewski, G. 2013. Determinants for the development of visceral leishmaniasis disease. *PLoS Pathogens*, 9(1), e1003053. doi:10.1371/journal.ppat.1003053

McInerney P., Adams P., and Hadi M.Z. 2014. Error rate comparison during polymerase chain reaction by DNA polymerase. *Molecular Biology International*, Article ID 287430, 1-8. doi.org/10.1155/2014/287430.

Mehta, S.R., Zhang, X.Q., Badaro, R., Spina, C., Day, J., Chang, K.P., and Schooley, R.T. 2010. Flow cytometric screening for antileishmanials in a human macrophage cell line. *Experimental Parasitology*, 126(4), 617–620. doi:10.1016/j.exppara.2010.06.007

Meshnick, S. R., Taylor, T. E. and Kamchonwongpaisan, S. 1996. Artemisinin and the antimalarial endoperoxides: from herbal remedy to targeted chemotherapy. *Microbiological Reviews*, 60(2), 301–315.

Mharakurwaa, S., Kumwendaa, T., Mkulamaa, A. P., Musapaa, M., Chishimbaa, S., Shiffb, J. C., Sullivanb, J. D., Thumaa, E. P., Liub, K. and Agreb, P. 2011. Malaria antifolate resistance with contrasting *Plasmodium falciparum* dihydrofolate reductase (DHFR) polymorphisms in humans and Anopheles mosquitoes. *PNAS*, 108(46), 18796–18801.

Mi-Ichi F., Miyake Y., Tam V.K., and Yoshida H. 2018. A flow cytometry method for dissecting the cell differentiation process of entamoeba encystation. *Frontiers in Cellular and Infection Microbiology*, 8:250, 1-16. doi: 10.3389/fcimb.2018.00250.

Ministry of Public Health and Sanitation MPHS. 2010. National guidelines for the diagnosis, treatment and prevention of malaria in Kenya. Third Edition. Available at: https://www.thecompassforsbc.org/sites/default/files/project_examples/Kenya_Malaria_Tx_Guideline_2010.pdf

Miranda, K., Docampo, R., Grillo, O., Franzen, A., Attias, M., Vercesi, A., Helmut Plattner H., Hentschel J. and de Souza, W. 2004. Dynamics of polymorphism of acidocalcisomes in leishmanial parasites. *Histochemistry and Cell Biology*, 121(5), 407–418. doi:10.1007/s00418-004-0646-4

Miró, G., Petersen, C., Cardoso, L., Bourdeau, P., Baneth, G., Solano-Gallego, L., Pennisi M.G., Ferrer L. and Oliva, G. 2017. Novel areas for prevention and control of canine leishmaniosis. *Trends in Parasitology*, 33(9), 718–730. doi:10.1016/j.pt.2017.05.005

Mishra, B.B., Gour, J.K., Kishore, N., Singh, R.K., Tripathi, V., and Tiwari, V.K. 2013. An antileishmanial prenyloxy-naphthoquinone from roots of *Plumbago zeylanica*. *Natural Product Research*, 27(4-5), 480–485.

Mishra, S. K, Shradhanand M. and Sanjib M. 2002. Acute renal failure in *falciparum* malaria. *Journal, Indian Academy of Clinical Medicine*, 3(2): 141-147

Mistro S., Rodrigues M., Rosa L., Camargo M., Badaró R. 2016. Liposomal amphotericin B drug access for the treatment of leishmaniasis in Brazil. *Tropical Medicine and International Health*, 21(6):692-3.

Mitropoulos P., Konidas P. and Durkin-Konidas M. 2010. New World cutaneous leishmaniasis: updated review of current and future diagnosis and treatment. *Journal of the American Academy of Dermatology*, 63(2):309-22.

- Mogk, S., Meiwes, A., Boßelmann, C. M., Wolburg, H., and Duszenko, M. 2014. The lane to the brain: how African trypanosomes invade the CNS. *Trends in Parasitology*, 30(10), 470–477. doi:10.1016/j.pt.2014.08.002
- Moideen, S.V.K., Houghton, P.J., Rock, P., Croft, S.L., and Aboagye-Nyame, F. 1999. Activity of extracts and naphthoquinones from *Kigelia pinnata* against *Trypanosoma brucei brucei* and *Trypanosoma brucei rhodesiense*. *Planta Medica*, 65, 536–540. doi:10.1055/s-1999-14011
- Moll, H., Fuchs, H., Blank, C., and Röllinghoff, M. 1993. Langerhans cells transport *Leishmania major* from the infected skin to the draining lymph node for presentation to antigen-specific T cells. *European Journal of Immunology*, 23(7), 1595–1601. doi:10.1002/eji.1830230730
- Mondal S., Bhattacharya P., and Ali N. 2010. Current diagnosis and treatment of visceral leishmaniasis. *Expert Review of Anti-Infective Therapy*, 8: 919–944.
- Mondelaers, A., Hendrickx, S., Van Bockstal, L., Maes, L., and Caljon, G. 2017. Miltefosine-resistant *Leishmania infantum* strains with an impaired MT/ROS3 transporter complex retain amphotericin B susceptibility. *Journal of Antimicrobial Chemotherapy*, 73(2), 392–394. doi:10.1093/jac/dkx407
- Moreira, W., Leprohon, P., and Ouellette, M. 2011. Tolerance to drug-induced cell death favours the acquisition of multidrug resistance in *Leishmania*. *Cell Death & Disease*, 2(9), e201–e201. doi:10.1038/cddis.2011.83
- Muller, J., and Hemphill, A., 2011. Drug target identification in intracellular and extracellular protozoan parasites. *Current Topics in Medicinal Chemistry*, 11, 2029-2038
- Mundwiler-Pachlatko, E., and Beck, H.-P. 2013. Maurer's clefts, the enigma of *Plasmodium falciparum*. *Proceedings of the National Academy of Sciences of the United States of America*, 110(50): 19987–94.
- Musa, A. M., Younis, B., Fadlalla, A., Royce, C., Balasegaram, M., Wasunna, M., Hailu A., Edwards T., Omollo R., Mudawi M., Kokwaro G., El-Hassan A., and Khalil, E. 2010. Paromomycin for the treatment of visceral leishmaniasis in Sudan: a randomized, open-label, dose-finding study. *PLoS Neglected Tropical Diseases*, 4(10), e855. doi:10.1371/journal.pntd.0000855
- Mwamtobe, P. M, Shirley A., Tchuente J. M. and Kasambara A. 2014. Optimal (control of) intervention strategies for malaria epidemic in Karonga district , Malawi. *Abstract and Applied Analysis*, Article ID 594256: 1-20. doi:10.1155/2014/594256
- Myburgh E., Coles J.A., Ritchie R., Kennedy P.G., McLatchie A.P., Rodgers J., Taylor M.C., Barrett M.P., Brewer J.M., and Mottram J.C. 2013. *In vivo* imaging of trypanosome-brain interactions and development of a rapid screening test for drugs against CNS stage trypanosomiasis. *PLoS Neglected Tropical Diseases*, 7(8), e2384. doi:10.1371/journal.pntd.0002384

National Institute of Allergy and Infectious Diseases (NIH). 2007. Understanding malaria and fighting an ancient scourge. *NIH Publication*, No. 07-7139: 1-32.

Newman, D. J., and Cragg, G. M. 2007. Natural products as sources of new drugs over the last 25 years. *Journal of Natural Products*, 70(3), 461–477.

Newton, C. R., and Krishna S. 1998. Severe *falciparum* malaria in children: current understanding of pathophysiology and supportive treatment. *Pharmacology and Therapeutics*, 79(1): 1–53.

Nguitragool, W., Bokhari, A. a B., Pillai, A. D., Rayavara, K., Sharma, P., Turpin, B., Desai, S. a. 2011. Malaria parasite clag3 genes determine channel-mediated nutrient uptake by infected red blood cells. *Cell*, 145(5): 665–677.

Nielsen E.I., Viberg A., Lowdin E. Cars O., Karlsson M.O., and Sandström M. 2007. Semimechanistic pharmacokinetic/pharmacodynamic model for assessment of activity of antibacterial agents from time-kill curve experiments. *Antimicrob Agents Chemother*, 51(1):128–136.

Njuguna, P., and Newton, C. 2004. Management of severe falciparum malaria. *Journal of Postgraduate Medicine*, 50(1): 45–50.

Nonaka, M., Murata, Y., Takano, R., Han, Y., Kabir, M.H.B., and Kato, K. 2018. Screening of a library of traditional Chinese medicines to identify anti-malarial compounds and extracts. *Malaria Journal*, 17(1). doi:10.1186/s12936-018-2392-4

Oberli, A., Slater, L. M., Cutts, E., Brand, F., Mundwiler-Pachlatko, E., Rusch, S. and Vakonakis, I. 2014. A *Plasmodium falciparum* PHIST protein binds the virulence factor PfEMP1 and comigrates to knobs on the host cell surface. *FASEB Journal*, 28 (10): 4420-4433.

Obonaga, R., Fernández, O.L., Valderrama, L., Rubiano, L.C., Castro, M. del M., Barrera, M.C., Gomez M.A., and Gore Saravia, N. 2013. Treatment failure and miltefosine susceptibility in dermal leishmaniasis caused by leishmania subgenus Viannia species. *Antimicrobial Agents and Chemotherapy*, 58(1), 144–152. doi:10.1128/aac.01023-13

Okwor, I., and Uzonna, J. 2016. Social and economic burden of human leishmaniasis. *The American Journal of Tropical Medicine and Hygiene*, 94(3), 489–493. doi:10.4269/ajtmh.15-0408

Olmo, A., Arrebola, R., Bernie, V., González-Pacanowska, D., and Ruiz-Pérez, L. M. 1995. Co-existence of circular and multiple linear amplicons in methotrexate-resistant *Leishmania*. *Nucleic Acids Research*, 23(15), 2856–2864. doi:10.1093/nar/23.15.2856

Onocha P., and Ali M., 2010. Antileishmaniasis, phytotoxicity and cytotoxicity of Nigerian euphorbiaceous plants 2: *Phyllanthus amarus* and *Phyllanthus muellerianus* extracts. *African Scientist*, 11:79–83

Oprea, I. T. 2002. Virtual screening in lead discovery: a viewpoint. *Molecules*, 7, 51–62. doi:10.3390/70100051

Orem, J. N., Kirigia J. M, Azairwe R., Kasirye I. and Walker O. 2012. Impact of malaria morbidity on gross domestic product in Uganda. *International Archives of Medicine*, 5(12): 1-8.

Osonuga, O. A., Osonuga A. A., Osonuga I. O., Osonuga A. and Derkyi K. L. 2011. Prevalence of hypoglycemia among severe malaria children in a rural African population. *Asian Pacific Journal of Tropical Disease*, 1(3), 192–194. doi:10.1016/s2222-1808(11)60026-1

Ouellette, M., Drummelsmith, J., and Papadopoulou, B. 2004. Leishmaniasis: Paaijmans, K. 2014. Antimalarial drug delivery to the mosquito: an option worth exploring?. *Future Microbiol*, 9(5): 579–582.

Oyola O.S., Evans J.k., Smith K.T., Smith A.B., Hilley D.J., Mottram C.J., Kaye M.P., and Smith F.D. 2012. Functional analysis of *Leishmania* cyclopropane fatty acid synthetase. *PLoS One*, 7: e51300.

Pace, D. 2014. Leishmaniasis. *Journal of Infection*, 69, S10-S18.

Paguio, M. F., Bogle, K. L., and Roepe, P. D. 2011. *Plasmodium falciparum* resistance to cytotoxic versus cytostatic effects of chloroquine. *Molecular and Biochemical Parasitology*, 178(1-2), 1–6. doi:10.1016/j.molbiopara.2011.03.003

Pan, L., Lezama-Davila, C.M., Isaac-Marquez, A.P., Calomeni, E.P., Fuchs, J. R., Satoskar, A.R., and Kinghorn, A. D. 2012. Sterols with antileishmanial activity isolated from the roots of *Pentalinon andrieuxii*. *Phytochemistry*, 82, 128–135.

Partridge F.A. , Brown A. E , Buckingham S.D. , Willis N.J., Wynne G.M. , Forman R., Else K.J. , Morrison A.A. , Matthews J.B. , Russell A.J. , Lomas D.A., and Sattelle D.B. 2018. An automated high-throughput system for phenotypic screening of chemical libraries on *Caenorhabditis elegans* and parasitic nematodes. *International Journal for Parasitology: Drugs and Drug Resistance*, 8(1): 8–21. doi: [10.1016/j.ijpddr.2017.11.004]

Passero, L.F.D., Bonfim-Melo, A., Corbett, C.E.P., Laurenti, M.D., Toyama, M.H., de Toyama, D.O., Romoff P., Fávero O.A., dos Grecco S.S., Zalewsky C.A., and Lago, J.H.G. 2011. Antileishmanial effects of purified compounds from aerial parts of *Baccharis uncinella* C. DC. (*Asteraceae*). *Parasitology Research*, 108(3), 529–536. doi:10.1007/s00436-010-2091-8

Patterson S., Wyllie S., Norval S., Stojanovski L., Simeons F.R., Auer J.L., Osuna-Cabello M., Read M.D., and Fairlamb A.H. 2016. The anti-tubercular drug delamanid as a potential oral treatment for visceral leishmaniasis. *Elife*, 5. Epub 2016/05/24.

Pedersen, M. M., Chukwujekwu, J. C., Lategan, C. A., Staden, J. van, Smith, P. J., and Staerk, D. 2009. Antimalarial sesquiterpene lactones from *Distephanus angulifolius*. *Phytochemistry*, 70(5), 601–607. doi:10.1016/j.phytochem.2009.02.005

Pépin J., Milord F., Khonde A., Niyonsenga T., Loko L., and Mpia B. 1994. *Gambiense* trypanosomiasis: frequency of, and risk factors for, failure of melarsoprol therapy. *The Royal Society of Tropical Medicine and Hygiene*, 88:447-52.

Pérez-Moreno G., Cantizani J., Sánchez-Carrasco P., Ruiz-Pérez L.M., Martín J., el Aouad N., Pérez-Victoria I., Tormo J.R., González-Menendez V., González I., de Pedro N., Reyes F., Genilloud O., Vicente F., González-Pacanowska D. 2016. Discovery of new compounds active against *Plasmodium falciparum* by high throughput screening of microbial natural products. *PLOS ONE*. 11(1): e0145812. P 1-16. doi:10.1371/journal.pone.0145812

Pérez-Victoria F.J., Gamarro F., Ouellette M., and Castanys S. 2003. Functional cloning of the miltefosine transporter: a novel P-type phospholipid translocase from *Leishmania* involved in drug resistance. *Journal of Biological Chemistry*, 278(50):49965–49971

Perez-Victoria F.J., Sanchez-Canete M.P., Castanys S., and Gamarro F. 2006a. Phospholipid translocation and miltefosine potency require both *L. donovani* miltefosine transporter and the new protein LdRos3 in *Leishmania* parasites. *Journal of Biological Chemistry*, 281:23766-23775.

Pérez-Victoria F.J., Sánchez-Cañete M.P., Seifert K., Croft S.L., Sundar S., Castanys S., and Gamarro F. 2006. Mechanisms of experimental resistance of *Leishmania* to miltefosine: Implications for clinical use. *Drug Resistance Updates*, 9(1-2), 26–39. doi:10.1016/j.drug.2006.04.001

Perez-Victoria, F.J., Gamarro, F., Ouellette, M., and Castanys, S., 2003b. Functional cloning of the miltefosine transporter: a novel P-type phospholipid translocase from *Leishmania* involved in drug resistance. *Journal of Biological Chemistry*, 278(50), 49965–49971. doi:10.1074/jbc.m308352200

Perez-Victoria, J.M., Tincusi, B.M., Jimenez, I.A., Bazzocchi, I.L., Gupta, M.P., Castanys, S., Gamarro, F., Ravelo, A.G., 1999. New natural sesquiterpenes as modulators of daunomycin resistance in a multidrug-resistant *leishmania tropica* line. *Journal of Medicinal Chemistry*, 42, 4388–4393.

Perkins, D. J., Were T., Davenport G. C., Kempaiah P., Hittner J. B. and Ongandapos J. M. 2011. Severe malarial anemia: innate immunity and pathogenesis. *International Journal of Biological Sciences*, 7(9): 1427–1442.

Perry M.R., Prajapati V.K., Menten J., Raab A., Feldmann J., Chakraborti D., Sundar S., Fairlamb A.H., Boelaert M. and Picado A. 2015. Arsenic exposure and outcomes of antimonial treatment in visceral leishmaniasis patients in Bihar, India: a retrospective cohort study. *PLoS Neglected Tropical Diseases*, 9(3):e0003518.

Perry M.R., Wyllie S., Prajapati V.K., Feldmann J., Sundar S., Boelaert M. and Fairlamb A.H. 2011. Visceral leishmaniasis and arsenic: an ancient poison contributing to antimonial treatment failure in the Indian subcontinent? *PLoS Neglected Tropical Diseases*, 5(9):e1227.

Petersen, I., Eastman, R. and Lanzer, M. 2011. Drug-resistant malaria: Molecular mechanisms and implications for public health. *Biochemistry for Tomorrow's Medicine*, 585(11), 1551–1562.

Picado, A., Singh, S. P., Rijal, S., Sundar, S., Ostyn, B., Chappuis, F., Uranw S., Gidwani K., Khanal B., Rai M., Paudel I.S., Das M.L., Kumar R., Srivastava P., Dujardin J.C., Vanlerberghe V., Andersen E.W., Davies C.R. AND Boelaert, M. 2010. Longlasting insecticidal nets for prevention of *Leishmania donovani* infection in India and Nepal: paired cluster randomised trial. *BMJ*, 341(dec29 1), c6760–c6760. doi:10.1136/bmj.c6760

Pinmai K., Hiriote W., Soonthornchareonnon N., Jongsakul K., Sireeratawong S., and Tor-Udom S. 2010. *In vitro* and *In vivo* antiplasmodial activity and cytotoxicity of water extracts of *Phyllanthus emblica*, *Terminalia chebula*, and *Terminalia bellerica*. *Journal of the Medical Association of Thailand*, 93 (Suppl 7):S120-6.

Pinto-Martinez, A. K., Rodriguez-Durán, J., Serrano-Martin, X., Hernandez-Rodriguez, V., and Benaim, G. 2017. Mechanism of action of miltefosine on *Leishmania donovani* involves the impairment of acidocalcisome function and the activation of the sphingosine-dependent plasma membrane Ca²⁺ channel. *Antimicrobial Agents and Chemotherapy*, 62(1). doi:10.1128/aac.01614-17

Plock A., Sokolowska-Kohler W., and Presber W. 2001. Application of flow cytometry and microscopical methods to characterize the effect of herbal drugs on leishmania spp. *Experimental Parasitology*, 97:141–153.

Pohlig, G., Bernhard, S. C., Blum, J., Burri, C., Mpanya, A., Lubaki, J.-P. F., Mpotu A.M., Munungu B.F., N'tombe P.M., Deo G.K., Mutantu P.N., Kuikumbi F.M., Mintwo A.F., Munungi A.K., Dala A., Macharia S., Bilenge C.M., Mesu V.K., Franco J.R., Dituvanga N.D., Tidwell R.R., and Olson, C. A. 2016. Efficacy and safety of pafuramidine versus pentamidine maleate for treatment of first stage sleeping sickness in a randomized, comparator-controlled, international phase 3 clinical trial. *PLoS Neglected Tropical Diseases*, 10(2), e0004363. doi:10.1371/journal.pntd.0004363

Pourshafie M., Morand S., Virion A., Rakotomanga M., Dupuy C., and Loiseau P.M. 2004. Cloning of S-adenosyl-Lmethionine:C-24-Delta-sterol-methyltransferase (ERG6) from *Leishmania donovani* and characterization of mRNAs in wild-type and amphotericin B-Resistant promastigotes. *Antimicrobial Agents and Chemotherapy*, 48(7):2409–14. doi: 10.1128/AAC.48.7.2409-2414.2004 PMID: 15215088

Preechapornkul, P., Imwong, M., Chotivanich, K., Pongtavornpinyo, W., Dondorp, M. A., Day, P. J., White, J. N. and Pukrittayakamee, S. 2009. *Plasmodium falciparum* pfm-dr1 Amplification, Mefloquine Resistance, and Parasite Fitness. *Antimicrobial agent and chemotherapy*, 53(4), 1509–1515.

Preston, S., Jiao, Y., Jabbar, A., McGee, S. L., Laleu, B., Willis, P., Wells T.N.C., and Gasser, R.B. 2016. Screening of the “Pathogen Box” identifies an approved pesticide with major anthelmintic activity against the barber’s pole worm. *International Journal for Parasitology: Drugs and Drug Resistance*, 6(3), 329–334. doi:10.1016/j.ijpddr.2016.07.004

Price, R., Nosten, F., Luxemburger, C., Kham, A., Brockman, A., Chongsuphajaisiddhi, T., White, N. 1995. Artesunate versus artemether in combination with mefloquine for the treatment of multidrug-resistant *falciparum* malaria. *Transactions of the Royal Society of Tropical Medicine and Hygiene*, 89(5),523–527.

Priotto, G., Kasparian, S., Mutombo, W., Ngouama, D., Ghorashian, S., Arnold, U., Ghabri S., Baudin E., Buard V., Kazadi-Kyanza S., Ilunga M., Mutangala W., Pohlig G., Schmid C., Karunakara U., Torreele E., and Kande V. 2009. Nifurtimox-eflornithine combination therapy for second-stage African *Trypanosoma brucei gambiense* trypanosomiasis: a multicentre, randomised, phase III, non-inferiority trial. *The Lancet*, 374(9683), 56–64. doi:10.1016/s0140-6736(09)61117-x

Prudêncio, M., Rodriguez A. and Mota M. M. 2006. The silent path to thousands of merozoites: the *plasmodium* liver stage. *Microbiology*, 4(11): 849–856.

Public Health England (PHE). 2013. Guidelines for Malaria Prevention in Travellers from the UK. *PHE publications gateway number*, 2014237: 1-97.

Purkait, B., Kumar, A., Nandi, N., *et al.* 2011. Mechanism of Amphotericin B Resistance in Clinical Isolates of *Leishmania donovani*. *Antimicrobial Agents and Chemotherapy*, 56(2), 1031–1041. doi:10.1128/aac.00030-11

Raz B, Iten M, Grether-Bühler Y, Kaminsky R, Brun R. 1997. The Alamar Blue assay to determine drug sensitivity of African trypanosomes (*T. b. rhodesiense* and *T. b. Gambiense*) *in vitro*. *Acta Tropica*, 68(2):139-147.

Radke, J.B., Burrows, J.N., Goldberg, D.E., and Sibley, L.D. 2018. Evaluation of current and emerging antimalarial medicines for inhibition of *Toxoplasma gondii* growth *in vitro*. *ACS Infectious Diseases*, 4(8), 1264–1274. doi:10.1021/acsinfecdis.8b00113

Rahman R., Goyal V., Haque R., Jamil K., Faiz A., Samad R., Ellis S., Balasegaram M., Boer M.D., Rijal S., Strub-Wourgaft N., Alves F., Alvar J., and Sharma B. 2017. Safety and efficacy of short course combination regimens with AmBisome, miltefosine and paromomycin for the treatment of visceral leishmaniasis (VL) in Bangladesh. *PLoS Neglected Tropical Diseases*, 30;11(5):e0005635. doi: 10.1371/journal.pntd.0005635.

Rai, S., Bhaskar, Goel, S. K., Nath Dwivedi, U., Sundar, S., and Goyal, N. 2013. Role of Efflux Pumps and Intracellular Thiols in Natural Antimony Resistant Isolates of *Leishmania donovani*. *PLoS ONE*, 8(9), e74862. doi:10.1371/journal.pone.0074862

Rajasekaran R., and Chen Y.P. 2015. Potential therapeutic targets and the role of technology in developing novel antileishmanial drugs. *Drug Discov Today*, 20(8):958–968.

Rakotomanga M., Blanc S., Gaudin K., Chaminade P., and Loiseau P.M. 2007. Miltefosine affects lipid metabolism in *Leishmania donovani* promastigotes. *Agents Chemother*, 51:1425–1430.

Rakotomanga M., Saint-Pierre-Chazalet M., and Loiseau P.M. 2005. Alteration of fatty acid and sterol metabolism in miltefosine-resistant *Leishmania donovani* promastigotes and

consequences for drug-membrane interactions. *Antimicrob Agents Chemother*, 49:(7):2677-86.

Rakotomanga, M., Blanc, S., Gaudin, K., Chaminade, P., and Loiseau, P.M. 2007. Miltefosine affects lipid metabolism in *Leishmania donovani* promastigotes. *Antimicrobial Agents and Chemotherapy*, 51(4), 1425–1430. doi:10.1128/aac.01123-06

Ramírez-Macías, I., Marín, C., Es-Samti, H., Fernández, A., Guardia, J. J., Zentar, H., Agil A., Chahboun R., Alvarez-Manzaneda E. and Sánchez-Moreno, M. 2012. Taiwaniaquinoid and abietane quinone derivatives with trypanocidal activity against *T. cruzi* and *Leishmania* spp. *Parasitology International*, 61(3), 405–413. doi:10.1016/j.parint.2012.02.001

Rampersad, S.N., 2012. Multiple applications of Alamar Blue as an indicator of metabolic function and cellular health in cell viability bioassays. *Sensors*, 12(9), pp.12347-12360.

Räz, B. 1998. Isolation and evaluation of antiparasitic lead compounds from African medicinal plants. *Ph.D. Thesis*, Universität Basel, Basel, Switzerland.

Raz, B., Iten M., Grether-Buhler Y., Kaminsky R., and Brun R. 1997. The Alamar Blue assay to determine drug sensitivity of African trypanosomes (*T.b. rhodesiense* and *T.b. gambiense*) *in vitro*. *Acta Tropica*, 68(2): 139-47

Ready, P.D. 2008. Leishmaniasis emergence and climate change. *Revue scientifique et technique*, 27, 399–412.

Rechsteiner M., and Rogers S.W. 1996. PEST sequences and regulation by proteolysis. *Trends in Biochemical Sciences*, 21(7):267-271.

Reimao J.Q., Oliveira J.C., Trinconi C.T., Cotrim P.C., Coelho A.C., and Uliana S.R. 2015. Generation of luciferase expressing *Leishmania infantum chagasi* and assessment of miltefosine efficacy in infected hamsters through bioimaging. *PLoS Neglected Tropical Diseases*, 9(2):e0003556. doi.org/10.1371/journal.pntd.

Reithinger R., Dujardin J., Louzir H., Pirmez C., Alexander B., and Brooker S. 2007. Cutaneous leishmaniasis. *The Lancet Infectious Diseases*, 7(9): 581–96. *rhodesiense*. *Planta Medica*, 65, 536–540.

Roberts, T., Barratt, J., Sandaradura, I., Lee, R., Harkness, J., Marriott, D., Ellis, J., Stark, D. 2015. Molecular epidemiology of imported cases of leishmaniasis in Australia from 2008 to 2014. *PLoS ONE*, 10(3): e0119212.

Rogers S., Wells R., and Rechsteiner M. 1986. Amino acid sequences common to rapidly degraded proteins: the PEST hypothesis. *Science*, 234(4774):364±8.

Romero E.A., Valdivieso E., and Cohen B.E. 2009. Formation of two different types of ion channels by amphotericin B in human erythrocyte membranes. *The Journal of Membrane Biology*, 230:69-81.

Rosa, M.d.S.S., Mendonca-Filho, R.R., Bizzo, H.R., Rodrigues, I.d.A., Soares, R.M.A., Souto-Padron, T., Alviano, C.S., and Lopes, A.H.C.S. 2003. Antileishmanial activity of a

linalool-rich essential oil from *Croton cajucara*. *Antimicrobial Agents and Chemotherapy*, 47, 1895–1901

Rose, K., Curtis, J., Baldwin, T., Mathis, A., Kumar, B., Sakthianandeswaren, A., Spurck, T., Choy, J. and L., Handman, E. 2004. Cutaneous leishmaniasis in red kangaroos: isolation and characterisation of the causative organisms. *International Journal for Parasitology*, 34: 655-664.

Ruiz-Torres, V., Encinar, J., Herranz-López, M., Pérez-Sánchez, A., Galiano, V., Barrajión-Catalán, E., and Micol, V. 2017. An updated review on marine anticancer compounds: the use of virtual screening for the discovery of small-molecule cancer drugs. *Molecules*, 22(7), 1037. doi:10.3390/molecules22071037

Russell, D.G., VanderVen, B.C., Lee, W., Abramovitch, R.B., Kim, M., Homolka, S., Niemann S., and Rohde, K.H. 2010. Mycobacterium tuberculosis Wears What It Eats. *Cell Host and Microbe*, 8(1), 68–76. doi:10.1016/j.chom.2010.06.002

Ryan K.A., Garraway L.A., Descoteaux A., Turco S.J., and Beverley S.M. 1993. Isolation of virulence genes directing surface glycosyl-phosphatidylinositol synthesis by functional complementation of *Leishmania*. *Proceedings of the National Academy of Sciences of the United States of America*, 90(18):8609–8613.

Sadeghi S., Seyed N., Etemadzadeh M.H., Abediankenari S., Rafati S., and Taheri T. 2015. *In vitro* infectivity assessment by drug susceptibility comparison of recombinant *Leishmania major* expressing enhanced green fluorescent protein or EGFP-luciferase fused genes with wild-type parasite. *The Korean Journal of Parasitology*, 53(4):385±94. doi.org/10.3347/kjp.2015.53.4.385.

Saifi, A. M., Beg, T., Harrath, A., Altayalan, S. F. and Al-Quraishy S. 2013. Antimalarial drugs: mode of action and status of resistance. *African Journal of Pharmacy and Pharmacology*, 7(5), 148-156

Sanchez-Canete, M.P., Carvalho, L., Perez-Victoria, F.J., Gamarro, F., and Castanys, S. 2009. Low plasma membrane expression of the miltefosine transport complex renders *Leishmania braziliensis* refractory to the drug. *Antimicrobial Agents and Chemotherapy*, 53(4), 1305–1313. doi:10.1128/aac.01694-08

Sanz, L. M., Crespo, B., De-Cózar, C., Ding, X. C., Llergo, J. L., Burrows, J. N., Garcí'a-Bustos J.F. and Gamó, F.-J. 2012. *P. falciparum* *in vitro* killing rates allow to discriminate between different antimalarial mode of action. *PLoS ONE*, 7(2), e30949. doi:10.1371/journal.pone.0030949

Sau K., Mambula S.S., Latz E., Henneke P., Golenbock D.T., and Levitz S.M. 2003. The antifungal drug amphotericin B promotes inflammatory cytokine release by a toll-like receptor- and CD14-dependent mechanism. *The Journal of Biological Chemistry*, 278(39), 37561–37568.

Scarim, C.B., Jornada, D.H., Chelucci, R.C., de Almeida, L., dos Santos, J. L., and Chung, M. C. 2018. Current advances in drug discovery for chagas disease. *European Journal of Medicinal Chemistry*, 155, 824–838. doi:10.1016/j.ejmech.2018.06.040

Schlitzer, M. 2008. Antimalarial drugs – what is in use and what is in the pipeline. *Archiv Der Pharmazie*, 341(3), 149–163.

Schmid C., Kuemmerle A., Blum J., Ghabri S., Kande V., Mutombo W., Ilunga M., Lumpungu I., Mutanda S., Nganzobo P., Tete D., Mubwa N., Kisala M., Blesson S., and Mordt O.V. 2012. In-hospital safety in field conditions of nifurtimox eflornithine combination therapy (nifurtimox eflornithine combination therapy) for *T. b. gambiense* sleeping sickness. *PLoS Neglected Tropical Diseases*, 6(11):e1920. doi: 10.1371/journal.pntd.0001920.

Schneidereit, D., Vass, H., Reischl, B., Allen, R. J., and Friedrich, O. 2016. Calcium sensitive fluorescent dyes fluo-4 and furared under pressure: behaviour of fluorescence and buffer properties under hydrostatic pressures up to 200 MPa. *PLOS ONE*, 11(10), e0164509. doi:10.1371/journal.pone.0164509

Scorza, B., Carvalho, E., and Wilson, M. 2017. Cutaneous manifestations of human and murine leishmaniasis. *International Journal of Molecular Sciences*, 18(6), 1296. doi:10.3390/ijms18061296

Seidlein, V. L. and Greenwood, M. B. 2003. Mass administrations of antimalarial drugs. *Trends in Parasitology*. 19(10): 452-460.

Seifert K., Matu S., Pe´rez-Victoria F., Castany S., Gamarro F., Croft S.L. 2003. Characterisation of *Leishmania donovani* promastigotes resistant to hexadecylphosphocholine (miltefosine). *International Journal of Antimicrobial Agents*, 22: 380–387. doi:10.1016/s0924-8579(03)00125-0

Seifert, K., Pérez-Victoria, F.J., Stettler, M., Sánchez-Cañete, M.P., Castanys, S., Gamarro, F., and Croft, S.L. 2007. Inactivation of the miltefosine transporter, LdMT, causes miltefosine resistance that is conferred to the amastigote stage of *Leishmania donovani* and persists *in vivo*. *International Journal of Antimicrobial Agents*, 30(3), 229–235. doi:10.1016/j.ijantimicag.2007.05.007

Seixas J.B.A. 2004. Investigation on the encephalopathic syndrome during melarsoprol treatment of human African trypanosomiasis. *Universidade Nova de Lisboa*, University of Basel.

Sereno D., Roy G., Lemesre J.L., Papadopoulou B., and Ouellette M. 2001. DNA transformation of *Leishmania infantum* axenic amastigotes and their use in drug screening. *Antimicrob Agents Chemother*, 45: 1168–1173.

Shadab, M., Jha, B., Asad, M., Deepthi, M., Kamran, M., and Ali, N. 2017. Apoptosis-like cell death in *Leishmania donovani* treated with KalsomeTM10, a new liposomal amphotericin B. *PLOS ONE*, 12(2), e0171306. doi:10.1371/journal.pone.0171306

Shahinas, D., Folefoc A. and Pillai D. 2013. Targeting *Plasmodium falciparum* Hsp90: towards reversing antimalarial resistance. *Pathogens*, 2(1): 33–54.

Shaw, C.D., Lonchamp, J., Downing, T., Imamura, H., Freeman, T. M., Cotton, J.A., Sanders M., Blackburn G., Dujardin J.C., Rijal S., Khanal B., Illingworth C.J., Coombs G.H., and Carter K.C. 2016. *In vitro* selection of miltefosine resistance in promastigotes of *Leishmania donovani* from Nepal: genomic and metabolomic characterization. *Molecular Microbiology*, 99(6), 1134–1148. doi:10.1111/mmi.13291

Simarro, P. P., Cecchi, G., Paone, M., Franco, J. R., Diarra, A., Ruiz, J. A., Fèvre E.M., Courtin F., Mattioli R.C., and Jannin, J. G. 2010. The atlas of human African trypanosomiasis: a contribution to global mapping of neglected tropical diseases. *International Journal of Health Geographics*, 9(1), 57. doi:10.1186/1476-072x-9-57

Simarro, P.P., Franco, J., Diarra, A., Postigo, J.A.R., and Jannin, J. 2012. Update on field use of the available drugs for the chemotherapy of human African trypanosomiasis. *Parasitology*, 139(07), 842–846. doi:10.1017/s0031182012000169

Simoben C.V., Ntie-Kang F., Akone S., and Sippl W. 2018. Compounds from African medicinal plants with activities against selected parasitic diseases: schistosomiasis, trypanosomiasis and leishmaniasis. *Natural Products and Bioprospecting*, 8:151–169.

Singh, B., and Sharma, R. A. 2014. Plant terpenes: defense responses, phylogenetic analysis, regulation and clinical applications. *Biotech*, 5(2), 129–151. doi:10.1007/s13205-014-0220-2

Singh, R., Kumar, D., Duncan, R. C., Nakhasi, H. L., and Salotra, P. 2010. Overexpression of histone H2A modulates drug susceptibility in leishmanial parasites. *International Journal of Antimicrobial Agents*, 36(1), 50–57. doi:10.1016/j.ijantimicag.2010.03.012

Sinha, S., Medhi, B., and Sehgal, R. 2014. Challenges of drug-resistant malaria. *Parasite*, 21(61), 3-15.

Siqueira-Neto J.L., Moon S., Jang J., Yang G., Lee C., Moon H.K., Chatelain E., Genovesio A., Cechetto J., Freitas-Junior L.H. 2012. An image-based high-content screening assay for compounds targeting intracellular *Leishmania donovani* amastigotes in human macrophages. *PLoS Neglected Tropical Diseases*, 6:e1671. doi:10.1371/journal.pntd.0001671.

Smilkstein, M., Sriwilajaroen, N., Kelly, J.X., Wilairat, P. and Riscoe, M. 2004. Simple and inexpensive fluorescence-based technique for high-throughput antimalarial drug screening. *Antimicrobial Agents and Chemotherapy*, 48(5), 1803-1806.

Smorenburg C.H., Seynaeve C., Bontenbal M., Planting A.S., Sindermann H., and Verweij J. 2000. Phase II study of miltefosine 6% solution as topical treatment of skin metastases in breast cancer patients. *Anticancer Drugs*, 11: 825–8.

Solomon, W., Wilson N. O., Anderson L., Pitts S., Patrickson J., Liu M., Byron D. F. and Stiles J. K. 2014. Neuregulin-1 attenuates mortality associated with experimental cerebral malaria. *Journal of Neuroinflammation*, 11(9): 1-13.

Soto J., and Soto P. 2006. Miltefosine: oral treatment of leishmaniasis. *Expert Review of Anti-Infective Therapy*, 4:177–185

Spalenka, J., Escotte-Binet, S., Bakiri, A., Hubert, J., Renault, J.-H., Velard, F., S., Aubertad D., Huguenin A., and Villena, I. 2017. Discovery of new inhibitors of *Toxoplasma gondii* via the pathogen box. *Antimicrobial Agents and Chemotherapy*, 62(2). doi:10.1128/aac.01640-17

Spillman, N.J., Allen, R.J.W., McNamara, C.W., Yeung, B.K.S., Winzeler, E. A., Diagona, T.T., and Kirk, K. 2013. Na⁺ regulation in the malaria parasite *Plasmodium falciparum* involves the cation ATPase PfATP4 and is a target of the spiroindolone antimalarials. *Cell Host and Microbe*, 13(2), 227–237. doi:10.1016/j.chom.2012.12.006

Srivastava S., Mishra J., Gupta A.K., Singh A., Shankar P., and Singh S. 2017. Laboratory confirmed miltefosine resistant cases of visceral leishmaniasis from India. *Parasite Vectors*, 10(1):49. <https://doi.org/10.1186/s13071-017-1969-z> PMID: 28137296

Stadelmann, B., Rufener, R., Aeschbacher, D., Spiliotis, M., Gottstein, B., and Hemphill, A. 2016. Screening of the open source malaria box reveals an early lead compound for the treatment of alveolar echinococcosis. *PLoS Neglected Tropical Diseases*, 10(3), e0004535. doi:10.1371/journal.pntd.0004535

Stijlemans, B., Caljon, G., Van Den Abbeele, J., Van Ginderachter, J. A., Magez, S., and De Trez, C. 2016. Immune evasion strategies of *Trypanosoma brucei* within the mammalian host: progression to pathogenicity. *Frontiers in Immunology*, 7. doi:10.3389/fimmu.2016.00233

Sullivan, J.A., Tong, J.L., Wong, M., Kumar, A., Sarkar, H., Ali, S., Hussein I., Zaman I., Meredith EL., Helsby NA., Hu L., and Wilkinson, S.R. 2015. Unravelling the role of SNM1 in the DNA repair system of *Trypanosoma brucei*. *Molecular Microbiology*, 96(4), 827–838. doi:10.1111/mmi.12973

Sülsen, V. P., Lizarraga, E., Mamadalieva, N.Z., and Lago, J.H.G. 2017. Potential of terpenoids and flavonoids from *Asteraceae* as anti-Inflammatory, antitumor, and antiparasitic agents. *Evidence-Based Complementary and Alternative Medicine*, 2017, 1–2. doi:10.1155/2017/6196198

Sundar, S., and Singh, A. 2016. Recent developments and future prospects in the treatment of visceral leishmaniasis. *Therapeutic Advances in Infectious Disease*, 3(3-4), 98–109. doi:10.1177/2049936116646063

Sundar S, Singh A, Rai M, Chakravarty J. Single-dose indigenous liposomal amphotericin B in the treatment of Indian visceral leishmaniasis: a phase 2 study. *The American Journal of Tropical Medicine and Hygiene*, 2015; 92: 513–17.

Sundar S, and Chakravarty J. 2015. An Update on Pharmacotherapy for Leishmaniasis. *Expert Opin Pharmacother*, 16(2): 237–252. doi: 10.1517/14656566.2015.973850

Sundar S., Jha T.K., Thakur C.P., Sinha P.K., and Bhattacharya S.K. 2007. Injectable paromomycin for visceral leishmaniasis in India. *The New England Journal of Medicine*, 356:2571-2581.

Sundar S., Sinha P.K., Rai M., Verma D.K., Nawin K., Alam S., Chakravarty J., Vaillant M., Verma N., Pandey K., Kumari P., Lal C.S., Arora R., Sharma B., Ellis S., Strub-Wourgaft N., Balasegaram M., Olliaro P., Das P., and Modabber F. 2011. Comparison of short-course multidrug treatment with standard therapy for visceral leishmaniasis in India: An open-label, non-inferiority, randomised controlled trial. *Lancet*, 5;377(9764):477–486.

Sundar, S., Jha, T. K., Thakur, C. P., Engel, J., Sindermann, H., Fischer, C., Junge K., Bryceson A., and Berman, J. 2002. Oral miltefosine for Indian visceral leishmaniasis. *New England Journal of Medicine*, 347(22), 1739–1746. doi:10.1056/nejmoa021556

Tarral A., Blesson S., Mordt O.V., et al. 2014. Determination of an optimal dosing regimen for fexinidazole, a novel oral drug for the treatment of human African trypanosomiasis: first-in-human studies. *Clinical Pharmacokinetics*, 53: 565–80.

Thakur C.P., Sinha G.P., and Pandey A.K. 1996. Comparison of regimens of amphotericin B deoxycholate in kala-azar. *Indian Journal of Medical Research*, 103: 259–63.

Tarral A., Blesson S., Mordt O.V., Torreele E., Sassella D., Bray M.A., Hovsepian L., Evène E., Gualano V., Felices M., and Strub-Wourgaft N. 2014. Determination of an Optimal Dosing Regimen for Fexinidazole, a Novel Oral Drug for the Treatment of Human African Trypanosomiasis: First-in-Human Studies. *Clinical Pharmacokinetics*, 53(6), 565–580. doi:10.1007/s40262-014-0136-3

Thao, N., No, J., Luyen, B., Yang, G., Byun, S., Goo, J., Kim K.T., Cuong N.X., Nam N.H., Minh C.V., Schmidt T.J., Kang J.S., and Kim, Y. 2014. Secondary metabolites from vietnamese marine invertebrates with activity against *Trypanosoma brucei* and *T. cruzi*. *Molecules*, 19(6), 7869–7880. doi:10.3390/molecules19067869

Tong, J., Valverde, O., Mahoudeau, C., Yun, O., and Chappuis, F. 2011. Challenges of controlling sleeping sickness in areas of violent conflict: experience in the Democratic Republic of Congo. *Conflict and Health*, 5(1), 7. doi:10.1186/1752-1505-5-7

Torreele E., Bourdin Trunz B., Tweats D., Kaiser M., Brun R., Mazué G., Bray M.A., and Pécoul B. 2010. Fexinidazole—a new oral nitroimidazole drug candidate entering clinical development for the treatment of sleeping sickness. *PLoS Neglected Tropical Diseases*, 4(12), e923. doi:10.1371/journal.pntd.0000923

Trager, W. and Jensen, J.B., 1976. Human malaria parasites in continuous culture. *Science*, 193(4254), pp.673-675.

Trampuz, A., Matjaz J., Igor M. and Rajesh M. P. 2003. Clinical review: severe malaria. *Critical care (London, England)*, 7(4): 315–323.

Tsuchiya, S., Yamabe, M., Yamaguchi, Y., Kobayashi, Y., Konno, T., and Tada, K. 1980. Establishment and characterization of a human acute monocytic leukemia cell line (THP-1). *International Journal of Cancer*, 26(2), 171–176. doi:10.1002/ijc.2910260208

Turner K.G., Vacchina P., Robles-Murguía M., Wadsworth M., McDowell M.A., and Morales M.A. 2015. Fitness and phenotypic characterization of miltefosine-resistant *Leishmania major*. *PLoS Neglected Tropical Diseases*, 31;9(7):e0003948. doi: 10.1371/journal.pntd.0003948.

- Tuteja, R. 2007. Malaria—an overview. *The FEBS Journal*, 274: 4670–4679.
- Ullah, I., Sharma, R., Biagini, G. A., and Horrocks, P. 2016. A validated bioluminescence-based assay for the rapid determination of the initial rate of kill for discovery antimalarials. *Journal of Antimicrobial Chemotherapy*, dkw449. doi:10.1093/jac/dkw449
Updates, 7(4-5), 257-266.
- Vahermo M., Krogerus S., Nasereddin A., Kaiser M., Brun R., Jaffe C.L., Yli-Kauhaluoma J., and Moreira V. M. 2016. Antiprotozoal activity of dehydroabiestic acid derivatives against *Leishmania donovani* and *Trypanosoma cruzi*. *Journal of Medicinal Chemistry*, 7, 457. DOI: 10.1039/c5md00498e
- Van Dooren, G. G., Marti, M., Tonkin, C. J., Stimmler, L. M., Cowman, A. F. and McFadden, G. I. 2005. Development of the endoplasmic reticulum, mitochondrion and apicoplast during the asexual life cycle of *Plasmodium falciparum*. *Molecular Microbiology*, 57(2): 405–419.
- van Eijk A. M., Hill J., Larsen D. A., Webster J., Steketee R. W, Eisele T. P. and ter Kuile F. O. 2013. Coverage of intermittent preventive treatment and insecticide-treated nets for the control of malaria during pregnancy in sub-saharan Africa: a synthesis and meta-analysis of national survey data, 2009-11. *The Lancet Infectious Diseases*, 13(12): 1029–42.
- van Griensven J., Balasegaram M., Meheus F., Alvar J., Lynen L., and Boelaert M. 2010. Combination therapy for visceral leishmaniasis. *The Lancet Infectious Diseases*, Mar;10(3):184-94. doi: 10.1016/S1473-3099(10)70011-6.
- Van Voorhis, W. C., Adams, J. H., Adelfio, R., Ahyong, V., Akabas, M. H., Alano, P., et al. 2016. Open source drug discovery with the malaria box compound collection for neglected diseases and beyond. *PLOS Pathogens*, 12(7), e1005763. doi:10.1371/journal.ppat.1005763
- Vanaerschot, M., Huijben, S., Van den Broeck, F., and Dujardin, J.-C. 2014. Drug resistance in vectorborne parasites: multiple actors and scenarios for an evolutionary arms race. *FEMS Microbiology Reviews*, 38(1), 41–55. doi:10.1111/1574-6976.12032
- Vasudevan, G., Carter, N.S., Drew, M.E., Beverley, S.M., Sanchez, M.A., Seyfang, A., Ullman B., and Landfear, S M. 1998. Cloning of leishmania nucleoside transporter genes by rescue of a transport-deficient mutant. *Proceedings of the National Academy of Sciences*, 95(17), 9873–9878. doi:10.1073/pnas.95.17.9873
- Vaughan, A. M., Mikolajczak S. a, Wilson E. M., Grompe M., Kaushansky A., Camargo N. and Kappe S. H. I. 2012. Complete *Plasmodium falciparum* liver stage development in liver-chimeric mice. *The Journal of Clinical Investigation*, 122(10), 3618–3628.
- Veber, D.F., Johnson, S.R., Cheng, H.-Y., Smith, B.R., Ward, K.W., and Kopple, K.D. 2002. Molecular properties that influence the oral bioavailability of drug candidates. *Journal of Medicinal Chemistry*, 45(12), 2615–2623. doi:10.1021/jm020017n

Vila, T., and Lopez-Ribot, J. L. 2016. Screening the pathogen box for identification of *Candida albicans* biofilm inhibitors. *Antimicrobial Agents and Chemotherapy*, 61(1). doi:10.1128/aac.02006-16

Villaescusa, L., Diaz-Lanza, A.M., Gasquet, M., Dlemas, F., Ollivier, E., Bernabe, M., Faure, R., Elisa, R., Galansard, G., 2000. Antiprotozoal activity of sesquiterpene from *Jasonia glutinosa*. *Pharmaceutical Biology*, 38 (3), 176–180.

Walliker D., Quakyi I.A., Wellems T.E., McCutchan T.F., Szarfman A., London W.T., Corcoran L.M., Burkot T.R., and Carter R. 1987. Genetic analysis of the human malaria parasite *Plasmodium falciparum*. *Science*, 236:1661–1666.

Wangchuk P., Keller, P.A., Pyne, S.G., Willis, A.C. 2-12. Kamchonwongpalsan, S, antimalarial alkaloids from a bhutanese traditional medicinal plant *Corydalis dubia*. *Journal of Ethnopharmacology*, 143 (1), 310-313.

Weatherall D., Miller L., Baruch D., Marsh K., Doumbo O., Casals-Pascual C. and Poberts D. 2002. Malaria and the red cell. *American society of haematology*, 35-57.

Wells, T.N. 2011. Natural products as starting points for future anti-malarial therapies: going back to our roots?. *Malaria Journal*, 10(Suppl 1), S3.1-12.

Wheeler, R. J., Gull, K., and Gluenz, E. 2012. Detailed interrogation of trypanosome cell biology via differential organelle staining and automated image analysis. *BMC Biology*, 10(1), 1. doi:10.1186/1741-7007-10-1

White, N. 1999. Antimalarial drug resistance and combination chemotherapy. *Philosophical Transactions of the Royal Society B: Biological Sciences*, 354(1384), 739–749. doi:10.1098/rstb.1999.0426

White, N. J., Pukrittayakamee S., Hien T. T., Faiz M. A., Mokuolu O. a.and Dondorp A. M. 2014. Malaria. *The Lancet*, 383(9918): 723–735.

WHO, 2013. WHO traditional medicine strategy: 2014-2023. Available at: http://www.who.int/traditional-complementary-integrative-medicine/publications/trm_strategy14_23/en/

WHO, 2016. World malaria report. <http://apps.who.int/iris/bitstream/handle/10665/252038/9789241511711-eng.pdf?sequence=1>

WHO, 2017a. Human African trypanosomiasis. Available at http://www.who.int/trypanosomiasis_african/resources/Human_African_trypanosomiasis_Review_June_2017.pdf

WHO. 2013. Sustaining the drive to overcome the global impact of neglected tropical diseases. *World Health Organization*, Geneva, Switzerland http://www.who.int/neglected_diseases/9789241564540/en/

WHO. 2017a. World malaria report 2017. Available at <http://www.who.int/malaria/publications/world-malaria-report-2017/en/>

WHO. Crossing the billion. Lymphatic filariasis, onchocerciasis, schistosomiasis, soil-transmitted helminthiasis and trachoma: preventive chemotherapy for neglected tropical diseases. Geneva: *World Health Organization*, 2017.

WHO. World Malaria Report 2013, (March). Available at http://www.who.int/malaria/publications/world_malaria_report_2013/en/

WHO. World malaria report 2013, (March). Available at http://www.who.int/malaria/publications/world_malaria_report_2013/en/

Wink, M. 2012. Medicinal Plants: A source of anti-Parasitic secondary metabolites. *Molecules*, 17(11), 12771–12791. doi:10.3390/molecules171112771

Wong, E.H., Hasenkamp, S. and Horrocks, P., 2011. Analysis of the molecular mechanisms governing the stage-specific expression of a prototypical housekeeping gene during intraerythrocytic development of *P. falciparum*. *Journal of Molecular Biology*, 408(2), 205-221.

World Health Organization, 2013c. Sustaining the drive to overcome the global impact of neglected tropical diseases, second WHO report on neglected tropical diseases, “Diseases”, *Leishmaniasis*, 67-71.

World Health Organization. 2000. Severe falciparum malaria. Communicable Diseases Cluster, 1211 Geneva 27, Switzerland. *Transactions of the Royal Society of Tropical Medicine and Hygiene*, 94, Supplement 1.

World Health Organization. 2010. Guidelines for the treatment of malaria, 2nd Edition. WHO: 194p. Available at <http://apps.who.int/medicinedocs/en/d/Js19105en/>

World Health Organization. 2010x. Control of the leishmaniases. Report of a meeting of the WHO expert committee on the control of the leishmaniases. Geneva. *World Health Organization technical report series*.

World Health Organization. 2010x. Working to overcome the global impact of neglected diseases: first WHO report on neglected tropical diseases. WHO; Geneva, Switzerland, p. 82-90

World Health Organization. 2013a. Control and surveillance of human African trypanosomiasis. WHO Technical Report Series. (984). WHO; Geneva, Switzerland.

World Health Organization. 2010. Control of the leishmaniases. Report of a meeting of the WHO expert committee on the control of the leishmaniases. Geneva. *World Health Organization technical report series*.

World Health Organization. 2010x. Working to overcome the global impact of neglected diseases: first WHO report on neglected tropical diseases. *WHO*; Geneva, Switzerland. 82-90

World malaria report, 2014. Available at http://www.who.int/malaria/publications/world_malaria_report_2014/wmr-2014-no-profiles.pdf

Wyllie S, Mandal G, Singh N, Sundar S, Fairlamb AH, Chatterjee M (2011) Elevated levels of trypanothione peroxidase in antimony unresponsive *Leishmania donovani* field isolates. *Molecular and Biochemical Parasitology*, 173:162-164.

Yamamoto, E. S., Campos, B. L. S., Jesus, J. A., Laurenti, M. D., Ribeiro, S. P., Kallás, E. G., Rafael-Fernandes M., SantosGomes G., Silva M.S., Sessa D.P., Lago J.H.G., Levy D., Luiz F. and Passero, L. F. D. 2015. The effect of ursolic acid on *Leishmania amazonensis* is related to programmed cell death and presents therapeutic potential in experimental cutaneous leishmaniasis. *PLOS ONE*, 10(12), e0144946. doi:10.1371/journal.pone.0144946

Yamthe, T.L., Appiah-Opong, R., Tsouh Fokou, P., Tsabang, N., Fekam Boyom, F., Nyarko, A., and Wilson, M. 2017. Marine algae as source of novel antileishmanial drugs: a review. *Marine Drugs*, 15(11), 323. doi:10.3390/md15110323

Yang, X., Feng, Y., Duffy, S., Avery, V., Camp, D., Quinn, R., and Davis, R. 2011. A new quinoline epoxide from the Australian plant *Drummondita calida*. *Planta Medica*, 77(14), 1644–1647. doi:10.1055/s-0030-1270963

Yong, K. P., Ban H. T. and Chian Y. L. 2012. Severe falciparum malaria with dengue coinfection complicated by rhabdomyolysis and acute kidney injury: an unusual case with myoglobinemia, myoglobinuria but normal Serum creatine kinase. *BMC infectious diseases*, 12(364): 1-5

You, H.J., Choi, C.Y., Kim, J. Y., Park, S. J., Hahm, K.-S., and Jeong, H.G. 2001. Ursolic acid enhances nitric oxide and tumor necrosis factor- α production via nuclear factor- κ B activation in the resting macrophages. *FEBS Letters*, 509(2), 156–160. doi:10.1016/s0014-5793(01)03161-1

Yun, O., Priotto, G., Tong, J., Flevaud, L., and Chappuis, F. 2010. NECT is next: implementing the new drug combination therapy for *Trypanosoma brucei gambiense* sleeping sickness. *PLoS Neglected Tropical Diseases*, 4(5), e720. doi:10.1371/journal.pntd.0000720

Zakeri, S., Hemati, S., Pirahmadi, S., Afsharpad, M., Raeisi, A., and Djadid, D. N. 2012. Molecular assessment of atpase 6 mutations associated with artemisinin resistance among unexposed and exposed *Plasmodium falciparum* clinical isolates to artemisinin-based combination therapy. *Malaria Journal*, 11(373), 1-8.

Zhang J.H., Chung T.D., and Oldenburg K.R. 1999. A simple statistical parameter for use in evaluation and validation of high throughput screening assays. *Journal of Biomolecular Screening*, 4(2):67±73. doi.org/10.1177/108705719900400206

Zhang, W.-W., Lypaczewski, P., and Matlashewski, G. 2017. Optimized CRISPR-Cas9 genome editing for leishmania and its use to target a multigene family, induce chromosomal translocation, and study DNA break repair mechanisms. *mSphere*, 2(1). doi:10.1128/msphere.00340-16

Zhang K., Pompey J.M., Hsu F-F., Key P., Bandhuvula P., Saba J.D., Turk J., and Beverley S.M. 2007. Redirection of sphingolipid metabolism toward de novo synthesis of ethanolamine in Leishmania. *The EMBO Journal*, 26:1094 –1104.

Zhang, Y.-J., Tanaka, T., Iwamoto, Y., Yang, C.-R., and Kouno, I. 2000. Novel norsesquiterpenoids from the roots of phyllanthus emblica. *Journal of Natural Products*, 63(11), 1507–1510. doi:10.1021/np000135i

Zongo, I. 2014. Efficacy, safety, tolerability of dihydroartemisinin-piperaquine and sulfadoxine-pyrimethamine plus amodiaquine for seasonal malaria chemoprevention (SMC) in children in Burkina Faso. Available at. http://researchonline.lshtm.ac.uk/2026584/1/2014_EPH_PhD_Zongo_Issaka.pdf

Zulfiqar, B., Jones, A., Sykes, M., Shelper, T., Davis, R., and Avery, V. 2017. Screening a natural product-based library against kinetoplastid parasites. *Molecules*, 22(10), 1715. doi:10.3390/molecules22101715

Appendix 1 (Chapter 3)

Normalized growth (%) following the 643 Phytopure compounds screen at 10 μ M and 2 μ M against intraerythrocytic *P. falciparum*, and at 2 μ M against the blood-stream form of *T. b. brucei* and axenic amastigotes of *L. mexicana*.

Compound ID	<i>P. falciparum</i>		<i>L. mexicana</i>	<i>T. b. brucei</i>
	% Normalized growth			
	20 μ M	2 μ M	2 μ M	2 μ M
700002	103.01	103.61	66.57	97.78
700004	40.86	100.76	48.07	13.95
700008	69.98	96.88	129.39	54.7
700013	112	105.41	66.51	104.39
700014	79.94	107.12	56.9	25.2
700016	108.83	104.46	47.07	75.71
700018	108.28	100.92	55.62	70.76
700019	65.37	100.02	33.89	71.97
700020	105.57	107.54	33.26	79.1
700021	105.88	108.44	50.99	100.85
700022	102.6	104.89	0.54	53.52
700026	112.33	97.93	62.46	83.31
700029	105.19	102.96	60.99	89.57
700035	28.85	73.36	128.81	31.83
700037	104.72	101.83	108.44	88.33
700039	97.58	101.4	93.34	61.31
700040	110.66	97.66	91.24	91.89
700042	29.86	28.92	79.08	1.55
700044	107.13	101.6	64.7	94.03
700046	10.33	9.79	83.38	5.63
700047	24.15	41.79	60	61.01
700048	13.47	20.33	88.98	5.75
700054	104.08	106.9	77.22	72.72
700055	104.82	108.16	67.21	58.38
700059	106.83	103.17	82.15	83.95
700060	24.62	86.86	79.04	103.01
700061	56.5	98.14	62.59	73.42
700062	85.18	101.17	72.86	114.17
700063	106.91	104.78	70.49	95.59
700069	106.14	102.44	93.26	101.98
700070	103.28	99.32	51.83	110.81
700072	57.66	98.24	60.94	71.92

700074	100.92	101.58	55.97	87.12
700075	104.44	102.68	65.36	110.37
700077	45.78	98.02	80.98	96.34
700078	109.86	96.1	88.28	114.74
700084	103.42	98.47	68.47	95.27
700086	82.3	99.47	63.03	80.25
700087	28.23	98.67	61.93	96.86
700089	102.4	98.89	131.9	143.91
700090	102.26	100.56	62.4	73.01
700094	103.56	94.12	73.86	81.27
700097	91.3	97.48	58.33	65.34
700103	47.76	98.7	37.13	94.68
700104	16.6	31.61	145.51	69.66
700107	92.3	96.84	8.07	85.19
700110	105.48	104.98	52.4	87.17
700111	92.13	99.15	59.02	53.98
700114	103.23	99.67	83.9	95.62
700118	82.06	97.12	97.45	70.92
700119	79.98	99.78	107.4	83.72
700120	102.78	98.98	117.48	76.33
700124	96.53	100.39	86.38	53.6
700125	18.66	102.72	95.16	66.71
700126	113.94	100.24	85.44	110.96
700127	92.34	96.85	62.45	84.33
700129	86.1	98.2	63.62	57.27
700132	73.96	94.47	66.16	69.44
700134	98.61	99.13	91.56	69.65
700136	61.22	99.87	-0.41	103.96
700137	101.54	98.17	78.35	75.12
700138	75.64	99.96	73.73	108.59
700139	84.11	84.64	86.83	95.41
700140	79.05	85.43	85.86	102.81
700141	30.07	87.62	80.43	82.44
700144	35.89	82.61	83.58	69.44
700148	88.72	88.59	98.29	103.08
700149	88.21	88.26	91.83	103.15
700153	95.8	98.71	62.74	65.41
700155	78.54	95.36	78.2	74.48
700158	72.21	86.88	82.33	88.65
700159	22.25	85.25	77.89	95.15
700160	85.93	89.08	70.5	79.51
700165	86.21	88.21	105.59	63.21

700170	80.43	89.07	94.01	60.25
700171	87.68	104.12	67.12	64.24
700178	81.1	85.06	106.59	75.55
700180	86.54	83.99	101.85	92.61
700181	81.75	89.71	48.74	103.56
700182	79.69	84.79	72.05	76.37
700185	85.14	83.5	95.46	84.89
700186	83.21	92.03	96.06	87.34
700188	34.21	89.01	98.39	115.94
700190	35.9	89.35	101.59	115.91
700192	47.97	92.13	98.78	100.91
700194	74.71	95.16	102.99	93.61
700196	94.82	96.71	57.6	98.96
700198	89.31	85.9	100.87	101.77
700409	94.49	103.62	83.35	94.34
700411	104.53	96.66	82.82	119.81
700414	24.89	100.7	77.86	103.76
700416	86.15	87.75	46.17	98.42
77417	121.44	117.67	78.81	101.27
700419	17.56	92.05	79.84	96.52
700421	118.98	118.68	69.16	92.39
700423	50.68	115.75	73.28	74.74
700424	110.66	120.58	71.15	82.54
700425	113.27	108.24	77.79	89.53
700426	95.39	89.01	53.42	81.81
700427	95.69	100.82	73.31	94.2
700429	106.13	105.94	79.08	87.18
700431	105.78	103.72	89.54	75.88
700432	121.25	103.53	124	55.16
700433	90.05	93.26	43.2	95.45
700434	107.57	105.22	125.96	64.91
700435	19.22	84.3	109.38	54.98
700436	36.61	98.96	107.02	58.16
700437	109.71	101.64	80.56	70.33
700438	-10.61	75.49	87.69	74.74
700440	100.86	97	39.11	89.37
700441	108.1	112.48	48.46	85.87
700442	15.51	96.66	54.61	89.25
700443	103.1	94.16	63.51	132.83
700445	102.33	89.5	77.31	128.57
700447	122.24	122.65	73.3	124.77
700448	71.35	123.72	48.86	127.36

700449	121.5	117.3	70.51	116.65
700450	128.75	117.29	89.65	129.46
700452	101.03	120.31	40.1	98.81
700453	87.37	113.7	47.27	100.86
700454	48.14	95.36	47.88	77.28
700455	88.54	113.13	64.32	61.26
700456	110.62	113.73	64.38	81.51
700458	122.19	118.9	48.46	78.15
700459	96.15	118.75	52.38	129.74
700460	126.04	118.14	99.51	116.32
700462	69.64	95.12	75.28	53.87
700464	123.77	112.43	60.89	128.02
700465	100.94	110.63	67.13	102.41
700468	98.93	115.01	67.46	28.03
700469	95.07	99.42	75.07	77.77
700470	100.01	89.24	57.31	96.61
700473	107.99	88.73	62.32	85.19
700475	92.51	97.16	75.14	100.8
700476	102.19	101.18	70.03	83.34
700478	98.45	99.23	74.81	127.88
700480	102.57	93.34	79.8	78.79
700481	98.57	96.99	75.27	79.19
700482	104.04	97.85	125.05	81.7
700483	96.73	93.42	69.09	88.05
700486	98.87	101.7	114.24	81.31
700488	105.6	101.26	92.33	75.99
700489	92.79	99.58	58.94	94.48
700490	118.67	100.56	72.52	82.32
700492	93.94	90.94	43.19	113.22
700494	92.9	88.28	76.32	143.85
700497	95.43	94.94	80.8	100.63
700498	124.78	118.36	55.89	74.5
700499	123.82	120.58	68.96	102.43
700500	108.17	110.15	77.7	96.77
700501	116.25	102.32	115.88	88.17
700504	103.76	93.56	92.98	138.81
700509	90.95	98.75	63.98	59.66
700510	116.85	99.72	63.12	67.6
700512	125.72	97.98	108.67	76.32
700513	90.08	96.98	56.48	103.67
700514	88.54	87.93	58.53	139.05
700515	84.31	85.88	65.66	135.98

700516	78.86	91.07	59.03	100.41
700517	96.54	99.08	80.36	67.22
700519	96.37	97.94	74.92	94.05
700520	112.18	101.53	72.95	64.34
700521	88.35	94.72	77.04	55.84
700524	92.07	94.71	70.63	113.88
700526	106.45	92.84	70.74	76.69
700528	87.67	110.06	58.38	99.89
700529	81.14	107.19	37.03	99.33
700532	101.4	110.61	57.87	76.48
700535	-35.14	31	68.2	99.44
700536	29.26	89.26	98.96	76.85
700538	97.36	108.83	44.13	119.99
700539	43.74	89.93	115.29	95.04
700541	108.98	116.34	51.29	136.72
700542	100.33	100.36	95.38	65.12
700543	93.47	106.61	63.38	105.62
700544	95.73	107.77	59.48	83.13
700545	81.26	94.17	93.14	94.19
700548	86.36	93.28	67.27	95.62
700549	69.15	93.31	52.27	79.62
700550	86.76	88.07	59.24	92.5
700551	86.84	88.11	63.2	94.86
700556	83.48	96.29	97.27	65.19
700557	75.21	99.52	84.6	85.4
700558	93.86	93.91	100.7	101.07
700559	114.62	90.33	98.2	82.82
700561	108.96	97.15	91.24	89.55
700563	102.47	101.88	61.81	68.58
700568	100.8	92.05	73.85	68.09
700571	97.34	98.71	63.03	93.24
700579	107.03	97.73	91.09	70.63
700580	98.48	95.95	62.92	50.1
700581	76.46	94.3	76.82	68.55
700582	39.21	89.97	88.81	108.47
700586	3.67	76.97	56.47	3.14
700592	58.03	90.8	85.14	91.74
700593	68.84	81.01	68.77	52.06
700596	51.26	75.87	104.54	58.61
700597	62.89	76.44	65.14	77.39
700598	75.47	77.52	78.62	92.84
700599	63.4	76.9	72.99	92.39

700600	75.83	83.31	77.22	74.74
700601	41.84	78.68	74.96	96.65
700603	75.38	79.38	73.5	106.42
700606	76.93	84.06	75.17	93.76
700607	82.62	84.02	90.1	94.1
700610	81.76	78.91	95.12	91.88
700612	51.82	75.62	76.07	74.63
700613	78.57	81.64	81.31	73.6
700614	90.45	85.89	88.07	79.6
700617	114.75	91.08	68.93	89.66
700618	82.33	89.77	70.7	74.28
700620	72.53	81.7	76.01	60.64
700621	84.28	84.39	54.16	77.66
700622	66.24	82.96	56.08	52.37
700626	112.54	96.84	80.88	63.56
700627	81.88	89.88	56.49	65.48
700629	87.32	91.02	70.15	57.15
700630	56.3	82.6	57.83	76.96
700631	37.62	66.8	57.38	58.88
700635			90.87	54.42
700637	67.91	84.44	87.45	92.24
700638	51.41	89.73	89.59	97
700640	49.93	88.7	97.58	80.49
700642	70.19	87.62	113.83	94.88
700645	79.88	92.26	110.65	75.52
700646	84.73	94.02	97.9	85.88
700649	100.07	90.41	91.02	87.26
700650	110.6	93.49	63.1	80.06
700652	9.25	83.22	103.14	90.65
700655	82.18	89.53	62.37	88.28
700656	77.98	86.94	97.82	90.43
700657	37.06	86.5	74.85	59.28
700658	94.08	90.74	96.02	62.76
700659	111.66	89.93	93.89	76.32
700662	127.74	89.75	101.1	81.51
700663	111.84	93.77	97.68	107.6
700665	83.84	95.08	91.26	61.87
700668	91.14	93.06	86.61	104.31
700669	104.58	94.87	97.75	90.07
700672	81.56	93.29	88.39	106.68
700673	93.28	91.73	98.23	99.98
700674	94.85	90.64	83.4	77.47

700677	96.48	88.49	88.07	108.71
700679	78.91	85.95	66.91	96.12
700681	95.48	91	77.92	104.24
700682	85.74	85.06	88.6	94.65
700684	97.34	103.02	71.53	74.5
700686	82.99	94.91	66.22	102.43
700687	86.67	94.32	68.1	86.26
700688	38.67	88.24	65.45	74.81
700690	76.59	97.46	69.16	102.02
700692	89.33	101.93	92.78	94.91
700697	79.99	94.05	78.71	82.06
700698	45.66	90.96	68.34	64.89
700703	73.11	93.36	82.52	84.04
700705	77.04	94.61	80.69	95.04
700711	80.53	96.49	84.51	109.49
700712	93.82	102.43	100.67	107.42
700713	81.33	99.08	98.82	96.91
700714	85.55	92.38	82.88	94.82
700715	82.7	94.54	84.38	105.25
700716	68.67	90.51	77.88	105.31
700717	79.66	92.2	82.96	83.43
700718			86.61	81.17
700200	50.47	79.78	93.92	105.2
700202	67.47	90.09	79.28	92.84
700205	66.03	88.39	54.5	63.15
700206	66.91	80.92	50.27	82.82
700207	76.92	82.47	55.9	92.38
700208	55.6	73.46	63.58	82.54
700209	126.87	99.13	79.67	89.53
700211	61.35	75.14	50.53	76.86
700212	64.75	84.05	57.63	76.8
700213	70.65	81.49	55.89	60.44
700214	104.19	83.73	90.53	107.59
700216	81.93	75.05	64.23	76.76
700219	109.95	93.99	69.6	104.22
700222	67.93	74.14	74.69	73.26
700223	28.22	75.37	49.96	90.13
700226	65.43	74.57	84.4	64.55
700228	37.87	78.1	57.85	63.51
700232	71.74	76.21	62.68	72.94
700233	75.6	87.34	52.12	93.16
700234	60.33	75.9	53.87	90.85

700235	54.5	70.85	68.2	87.89
700237	76.97	82.74	49.04	92.24
700238	59.77	75.99	44.07	95.38
700240	55.3	77.85	-10.09	72.93
700244	64.71	82.31	59.65	87.58
700248	114.23	97.38	91.39	77.39
700250	69.39	75.37	72.21	84.35
700251	70.07	74.82	70.83	90.22
700252	91.43	87.8	99.63	119.37
700253	81.52	85.92	64.26	88.81
700256	75.74	87.69	73.47	96.32
700257	94.96	88.28	59.5	91.84
700259	95.63	88.57	56.7	101.97
700267	101.05	84.78	56.9	86.27
700272	68.56	84.25	57.74	88.09
700278	8.46	74.42	63.63	91.27
700280	31.75	76.02	67.92	114.02
700292	114.68	96.36	105.07	91.88
700293	112	96.2	87.1	74.63
700297	89.51	85.72	97.03	103.66
700298	92.73	82.6	103.6	115.63
700301	85.14	84.14	102.06	113.43
700302	73.13	76.89	97.99	127.8
700303	95.38	82.13	116.84	106.49
700305	50.61	80.26	91.83	116.07
700306	56.42	81.2	90.47	87.17
700307	80.83	80.86	103.18	106.77
700309	75.23	89.42	94.06	93.1
700311	84.99	88.56	100.04	106.04
700312	10.78	89.7	100.82	95.73
700313	99.4	92.99	121.62	101.17
700314	71.11	77.02	150.58	105.4
700316	82.39	92.55	50.19	116.84
700317	67.03	93.41	45.19	120.16
700321	79.5	81.55	59.2	111.32
700324	98.07	98.88	47.11	122.05
700325	73.45	76.93	71.17	93.91
700326	37.46	63.08	26.99	-8.93
700327	75.17	89.27	45.65	96.64
700329	102.77	93.63	56.47	88.9
700331	66.46	91.85	91.16	77.02
700333	94.94	95.41	104.75	72.63

700334	118.78	106.18	60.68	85.02
700337	93.66	99.71	52.26	96.77
700340	97.93	99.71	61.51	88.17
700342	112.38	101.1	55.43	106.96
700344	85.46	102.23	53.34	136.15
700017	90.16	103.26	52.75	118.29
700352	85.88	93.78	46.76	119.37
700353	115.93	98.47	50.9	129.84
700354	146.43	102.77	57.17	124.48
700355	117.23	105.72	57.43	107.84
700356	127.12	106.45	83.49	105.1
700358	107.73	106.44	93.42	96.96
700359	117.55	100.1	114.77	115.83
700360	141.3	99.85	68.68	93.07
700367	22.5	91.37	52.91	110.64
700369	85.78	93.17	45.54	132.41
700370	85.91	90.67	91.54	131.48
700372	95.82	91.79	68.91	108.53
700376	88	88.83	91.74	99.98
700377	84.73	102.43	89.68	77.47
700381	100.21	91.47	80.62	92.84
700383	85.92	88.47	66.5	74.63
700384	73.17	90.84	75.99	108.1
700385	40.46	90.14	86.69	75.55
700387	36.5	81.96	97.96	73.42
700388	53.44	86.91	92.37	76.78
700389	112.55	103.02	92.02	82.04
700392	121.93	100.94	112.23	73.19
700394	127.73	105.3	97.95	82.86
700396	99.32	98.92	112	71.18
700398	96.06	98.96	99.26	65.9
700403	118.65	102.3	108.63	56.24
700407	118.59	100.98	110.06	55.39
700719	109.36	106.2	84.98	52.45
700720	110.8	98.84	71.17	61.73
700725	82.97	98.53	80.79	85.29
700726	102.7	102.46	83.4	71.12
700727	127	107.39	81.45	82.77
700728	111.23	107.27	69.79	107.29
700729	114.14	101.54	70.33	86.69
700730	113.98	105.32	77.57	74.01
700734	120.04	108.04	83.64	103.93

700735	112.23	101.85	88.63	84.71
700736	43.77	93.53	48.91	124.92
700738	88.18	101.83	105.92	124.25
700739	101.82	93.22	90.75	97.9
700743	101.13	102.52	78.18	57.54
700746	63.21	97.33	102.2	65.04
700752	26.29	94.68	57.86	69.37
700753	65.68	97.41	79.38	67.22
700754	45.58	82.44	76.49	59.41
700756	15.57	44.03	2.93	53.74
700761	57.42	97.03	77.99	67.35
700763	101.31	102.82	105.44	91.47
700765	84.05	99.2	111.47	117.42
700767	79.92	100.94	96.42	113.26
700770	102	99.38	109.9	99.57
700772	116.13	107.51	83.73	93.09
700774	98.84	99.95	76.73	75.16
700775	103.31	104.68	76.65	75.52
700776	62.69	96.38	81.6	69.82
700784	79.52	98.87	86.08	75.34
700790	62.78	96.58	89	63.31
700793	103.34	98.24	91.72	67.04
700794	57.18	90.59	81.04	59.26
700800	85.36	86.45	77.8	62.75
700801	93.39	86.36	78.36	69.46
700804	96.45	92.1	124.3	69.86
700806	62.97	89.67	87.04	91.4
700814	71.5	90.08	100.69	120.77
700815	65.48	86.24	104.13	142.27
700819	48.91	83.66	57.1	74.42
700820	64.21	86.12	98.56	75.5
700822	48.34	104.29	92.8	60.67
700824	66.05	85.86	93	80.51
700825	61.84	82.97	101.37	72.75
700828	68.55	86.19	54.8	73.16
700835	87.68	87.73	80.54	68.09
700842	68	90.87	84.87	79.39
700845	91.89	101.49	123.67	116.07
700847	68.74	101.74	85.41	93.84
700850	77.5	103.98	83.8	72
700852	97.8	105.34	90.85	86.72
700854	99.54	100.98	85.6	88.31

700855	122.29	101.78	84.71	92.84
700857	105.67	104.02	71.09	74.63
700858	100.05	99.29	75.4	81.77
700859	95.04	104.18	58.62	77.89
700862	110.61	110.47	71.54	91.85
700864	65.43	106.62	72.51	73.24
700867	60.92	103.47	60.68	19.33
700868	66.39	101.24	53.99	67.07
700870	88.68	102.01	88.72	113.97
700872	95.32	100.8	91.02	89.21
700874	112.63	106.06	79.09	99.16
700876	106.19	100.67	76.97	125.96
700877	95.89	94.53	69.66	75.56
700878	100.71	105.23	107.15	121.51
700879	115.9	106.19	94.01	86.69
700881	89.51	103.26	82.92	111.71
700885	113.35	102.76	85.46	77.62
700886	87.83	98.86	59.41	96.26
700889	102.57	97.41	72.82	96.65
700891	120.83	100.59	98.09	64.67
700896	86.81	100.5	129.01	89.63
700901	118.28	103.39	90.1	64.17
700902	119.35	98.69	91.56	74.79
700904	92.84	103.44	62.83	79.1
700905	77.29	100.88	98.19	91.22
700908	86.83	94.18	88.4	55.99
700910	101.94	99.13	92.23	79.45
700572	38.14	92.47	95.81	67.05
700585	32.82	95.17	77.98	40.81
700615	126.32	102.97	84.11	86.04
700914	55.72	100.15	56.3	135.39
700919	85.81	91.38	51.53	106.86
700920	109.05	103.31	82.29	58.82
700921	104.35	94.48	64.02	110.08
700924	84.82	94.22	83.51	102.2
700927	83.96	100.85	55.83	76.19
700930	82.8	94.14	55.49	82.26
700932	97.23	98.22	79.81	118.63
700935	84.37	94.34	83.07	90.18
700937	75.91	94.06	57.39	107.64
700939	81.07	89.06	75.53	96.27
700942	78.91	91.4	62.94	72.04

700943	81.67	90.44	77.84	73.81
700944	58.99	81.81	166.14	73.74
700945	79.34	86.71	118.08	61.49
700947	88.42	93.44	56.35	127.93
700949	98.39	103.99	81.16	76.43
700950	106.34	103.3	108.09	76.41
700952	87.66	97.07	95.1	97.96
700954	56.86	102.45	80.16	61.72
700960	30.35	87.32	62.48	68.7
700961	78.46	89.09	68.17	87.47
700965	109.68	99.72	114.79	75.67
700966	83.29	76.54	77.5	85.15
700967	82.93	87.71	65.4	130.92
700968	109.32	116.05	86.43	96.03
700969	102.84	114.8	66.14	83
700971	108.5	101.12	102.16	80.8
700983	99.31	92.76	53.95	110.71
700984	82.43	96.46	61.1	122.06
700987	86.3	90.39	56.97	102.34
700989	81.88	95.6	50.1	101.39
700990	92.33	95.21	53.54	74.9
700992	54.08	102.23	161.84	73.66
700993	73.85	94.89	90.43	75.03
700997	73.16	88.51	75.08	72.09
701000	35.34	95.33	118.55	74.54
701001	54.99	94.82	63.11	71.98
701002	42.78	90.3	70.97	123.28
701003	45.16	99.75	73.58	113.37
701004	52.46	100.86	71.1	136.11
701006	51.39	97.09	70.81	78.63
701008	72.45	89.03	67.44	73.77
701009	49.26	76.61	79.98	81.06
701011	76.75	95	86	77.55
701013	73.11	86.56	79.6	60.9
701015	88.63	106.85	96.23	103.32
701016	60.87	87.02	182.84	68.45
701018	58.65	93.83	153.48	97.1
701020	52.07	87.09	83.91	67.04
700122	77.21	87.54	64.77	88.51
701024	113.58	100.91	104.95	142.11
701025	58.4	87	90.47	108.46
701026	73.54	87.81	80.36	141.89

701027	75.99	88.12	84.7	131.44
701028	71.85	86.75	73.29	100.58
701029	73.63	87.34	42.59	77.13
701030	79.71	91.25	67.19	85.82
701032	66.32	91.04	70.37	74.65
701034	73.04	88.41	78.69	83.16
701035	53.26	89.07	114.51	74.45
701038	69.44	89.6	69.45	78.45
701039	50.69	77.23	67.12	75.18
701040	91.89	108.22	66.92	138.54
701042	62.13	83.77	102.97	108.1
701043	59.69	108	56.39	75.55
701044	49.6	92.56	-4.46	79.26
701045	61.74	88.83	42.43	77.12
701046	90.4	113.3	47.68	84.12
701047	53.02	88.16	71.32	72.94
701048	10.49	86.57	70.34	83.73
701050	66.89	98.01	59.67	71.13
701051	121.26	116.17	104.1	71.86
701052	105.58	107.14	92.24	95.35
701055	103.45	107.83	104.25	105.48
701057	47.71	80.34	108.19	86.32
701058	116.48	116.09	101.57	75.3
701060	96.13	109.69	74.82	101.06
701062	70.8	91.09	80.9	127.78
701064	81.01	96.54	65.39	81.24
701065	77.61	97.04	83.87	64.38
701066	77.71	90.8	76.19	67.63
701069	84.4	90.23	97.79	63.45
701071	54.29	106.23	64.94	95.89
701072	49.22	108.47	34.69	100.2
701074	70.15	103.74	40.5	97.11
701076	92.04	107.1	45.46	99.41
701079	53.41	108.53	69.16	87.84
701080	41.74	102.96	58.86	57.2
701082	-24.64	76.98	67.78	4.98
701083	102.83	103.4	89.1	58.19
701085	87.06	103.33	49.68	67.35
701086	106.19	115.63	96.29	61.77
701088	-6.02	99.91	81.13	63.04
701089	78.55	105.35	77.97	86.72
701092	90.65	100.42	49.46	71.64

701093	92.04	99	48.83	62.73
701095	102.13	106.49	42.67	71.26
701098	110.64	103.51	36.1	90.67
701099	106.2	106.04	38.81	69.37
701100	105.5	106.27	47.85	94.89
701101	94.22	104.06	74.86	67.32
701103	106.18	104.13	56.27	98.79
701104	100.23	103.34	51.72	96.25
701107	101.34	105.47	76.01	98.85
701109	103.56	101.9	79.19	127.66
701111	84.82	103.85	59.21	67.35
701112	83.59	102.27	78.33	121.54
701113	56.75	99.42	80.47	108.41
701115	36.74	105.6	78.35	97.57
701116	49.75	97.67	48.03	64.58
701117	83.99	101.91	70.26	72.31
701119	113.85	99.36	96.93	74.03
701121	48.05	100.95	85.32	69.52
701124	104.2	98.56	52.46	98.84
701126	115.37	96.34	101.82	85.58
701127	86.94	98.97	104.14	76.71
701132	52.38	101.34	40.74	115.63
701133	103.28	91.52	44.35	117.49
701134	77.32	102.08	64.91	134.46
701135	79.75	93.62	55.63	96.02
701136	90.29	96.79	104.08	83
701137	113.38	99.02	109.8	73.37
701139	103.56	97.58	103.97	64.22
701142	99.96	95.07	96.1	78.53
701143	24.76	93.2	91.37	81.1
701145	84.94	95.97	48.85	3.43
701147	92.66	95.12	63.98	97.77
701148	82.53	95.56	57.46	102.45
701150	89.88	95.2	64.95	76.63
701152	18.54	88.89	43.76	51.46
701153	95.51	99.98	57.2	66.56
701154	6.69	66.49	-0.64	14.74
701155	5.74	55.07	-0.28	-0.81
701156	8.04	93.72	52.74	24.25
701157	8.97	51.93	0.07	-1.82
701158	4.19	48.96	-1.72	-1.34
701159	3.41	83.73	1.54	13.68

701160	97.85	95.01	84.73	74.2
701161	70.9	90.14	52.68	63.22
701162	72.63	89.02	62.64	82.22
701163	84.63	93.96	74.14	67.33
701164	87.27	99.11	81.2	72.94
701170	85.5	96.18	51.27	63.92
701171	89.95	95.53	52.33	102.22
701173	93.97	98.87	77.65	85.9
701174	74.68	95.2	73.97	130.55
701176	94.4	92.85	83.64	86.48
700522	102.33	94.52	79.27	52.52
701178	84.34	102.83	81.75	89.34
701182	68.6	95.45	73.1	72.49
701183	94.37	99.11	88.48	83.18
701185	88.88	94.36	69.42	99.04
701187	93.81	95.81	89.23	66.42
701189	90.43	94.53	80.22	91.56
701190	92.23	98.26	90.23	105.56
701191	86.68	98.51	101.38	97.9
701193	77.12	88.72	50.39	85.58
701195	44.84	90.92	59.87	73.57
701197	77.49	95.73	59.74	76.46
701199	54.22	89.91	96.75	78.66
701200	86.58	95.11	94.62	95.79
701201	98.05	95.92	97.01	72.77
701202	91.65	94.7	102.34	74.69
701207	80.06	86.65	96.86	78.86
701209	87.9	83.75	99.23	75.3
701210	4.35	77.69	23.3	69.45
701211	65.68	87.27	45.7	78.36
701212	2.63	84.71	1.47	77.12
701213	80.06	86.46	72.76	74.3
701214	86.16	85.88	55.58	73.77
701215	82.57	85.97	56.87	88.48
701219	64.46	79.8	63.31	78.39
701220	63.01	87.79	60.3	117.7
701221	48.42	84.27	139.5	103.55
701223	47.97	105.74	77.98	106.29
701224	93.38	105.96	81.67	81.32
700982	89.96	108.53	86.44	117.57
701228	71.56	105.07	78.48	56.52
701229	100.78	107.32	89.19	57.11

701231	103.33	108.32	108.15	90.58
701232	105.14	105.44	88.74	64.93
701233	78.45	101.52	76.64	62.84
701234	101.48	101	93.12	51.2
700608	102.95	102.89	92.08	68.11
701237	87.62	99.42	111.77	82.09
701238	52.49	95.79	54.37	114.58
701239	77.52	103.74	35.86	60.84
701240	80.07	100.65	44.16	81.38
701241	81.12	96.52	15.02	-1.91
701242	74.56	100.97	54.5	76.88
701244	26.72	96.71	24.43	79.9
701248	95.12	100.24	19.15	60.9
701249			-1.71	-7.6
701250			2.77	-3.13
701251			67.32	22.36
701252			-0.18	-2.16
701253			1.9	90.28
701256			-3.07	-2.12
701259			0.49	-0.72
701262			-1.02	2.2
701273			-0.14	-0.09
701286			-1.54	79.71

Appendix 2 (Chapter 4)

Multiple sequence alignment for each fragment of LmMT gene.

A summary of the 12 clones for each fragment of LmMT sequenced compared LmxM.13.1530. The WT-prefix is for the pre-selection wildtype and the R-prefix for 700022-selected parasites. The HH code uniquely identifies the PCR clone sequenced.

Fragment 1 (589bp)

LmxM.13.1530	CCGCTGAATCCGGCGACAGC ATTGCGCCGCTGTCCCTTCGTGCTCCTGGTGGCAATCATC	360
WT- HH41	CCGCTGAATCCGGCGACAGCATTGCGCCGCTGTCCCTTCGTGCTCCTGGTGGCAATCATC	360
WT- HH42	CCGCTGAATCCGGCGACAGCGATGCGCCGCTGTCCCTTCGTGCTCCTGGTGGCAATCATC	360
WT- HH43	CCGCTGAATCCGGCGACAGCGATGCGCCGCTGTCCCTTCGTGCTCCTGGTGGCAATCATC	360
WT- HH44	CCGCTGAATCCGGCGACAGCGATGCGCCGCTGTCCCTTCGTGCTCCTGGTGGCAATCATC	360
WT- HH48	CCGCTGAATCCGGCGACAGCGTTGCGCCGCTGTCCCTTCGTGCTCCTGGTGGCAATCATC	360
WT- HH49	CCGCTGAATCCGGCGACAGCATTGCGCCGCTGTCCCTTCGTGCTCCTGGTGGCAATCATC	360
R-HH5	CCGCTGAATCCGGCGACAGCGATTGCGCCGCTGTCCCTTCGTGCTCCTGGTGGCAATCATC	360
R-HH6	CCGCTGAATCCGGCGACAGCGATTGCGCCGCTGTCCCTTCGTGCTCCTGGTGGCAATCATC	360
R-HH8	CCGCTGAATCCGGCGACAGCGATTGCGCCGCTGTCCCTTCGTGCTCCTGGTGGCAATCATC	360
R-HH9	CCGCTGAATCCGGCGACAGCGATTGCGCCGCTGTCCCTTCGTGCTCCTGGTGGCAATCATC	360
R-HH10	CCGCTGAATCCGGCGACAGCGATTGCGCCGCTGTCCCTTCGTGCTCCTGGTGGCAATCATC	360
R-HH12	CCGCTGAATCCGGCGACAGCGATTGCGCCGCTGTCCCTTCGTGCTCCTGGTGGCAATCATC	360

LmxM.13.1530	AAGGAGGCTGTGGAGGACATCAAGCGACATCGGGCCGATAACCGTGCCAACCTCGGTTTTA	420
WT- HH41	AAGGAGGCTGTGGAGGACATCAAGCGACATCGGGCCGATAACCGTGCCAACCTCGGTTTTA	420
WT- HH42	AAGGAGGCTGTGGAGGACATCAAGCGACATCGGGCCGATAACCGTGCCAACCTCGGTTTTA	420
WT- HH43	AAGGAGGCTGTGGAGGACATCAAGCGACATCGGGCCGATAACCGTGCCAACCTCGGTTTTA	420
WT- HH44	AAGGAGGCTGTGGAGGACATCAAGCGACATCGGGCCGATAACCGTGCCAACCTCGGTTTTA	420
WT- HH48	AAGGAGGCTGTGGAGGACATCAAGCGACATCGGGCCGATAACCGTGCCAACCTCGGTTTTA	420
WT- HH49	AAGGAGGCTGTGGAGGACATCAAGCGACATCGGGCCGATAACCGTGCCAACCTCGGTTTTA	420
R-HH5	AAGGAGGCTGTGGAGGACATCAAGCGACATCGGGCCGATAACCGTGCCAACCTCGGTTTTA	420
R-HH6	AAGGAGGCTGTGGAGGACATCAAGCGACATCGGGCCGATAACCGTGCCAACCTCGGTTTTA	420
R-HH8	AAGGAGGCTGTGGAGGACATCAAGCGACATCGGGCCGATAACCGTGCCAACCTCGGTTTTA	420
R-HH9	AAGGAGGCTGTGGAGGACATCAAGCGACATCGGGCCGATAACCGTGCCAACCTCGGTTTTA	420
R-HH10	AAGGAGGCTGTGGAGGACATCAAGCGACATCGGGCCGATAACCGTGCCAACCTCGGTTTTA	420
R-HH12	AAGGAGGCTGTGGAGGACATCAAGCGACATCGGGCCGATAACCGTGCCAACCTCGGTTTTA	420

LmxM.13.1530	ACGCAGGTAATGCGAAAAGGCAAGCTCGTCTCGGTGCACAGCAAGGACATCCACCCTGGT	480
WT- HH41	ACGCAGGTAATGCGAAAAGGCAAGCTCGTCTCGGTGCACAGCAAGGACATCCACCCTGGT	480
WT- HH42	ACGCAGGTAATGCGAAAAGGCAAGCTCGTCTCGGTGCACAGCAAGGACATCCACCCTGGT	480
WT- HH43	ACGCAGGTAATGCGAAAAGGCAAGCTCGTCTCGGTGCACAGCAAGGACATCCACCCTGGT	480
WT- HH44	ACGCAGGTAATGCGAAAAGGCAAGCTCGTCTCGGTGCACAGCAAGGACATCCACCCTGGT	480
WT- HH48	ACGCAGGTAATGCGAAAAGGCAAGCTCGTCTCGGTGCACAGCAAGGACATCCACCCTGGT	480
WT- HH49	ACGCAGGTAATGCGAAAAGGCAAGCTCGTCTCGGTGCACAGCAAGGACATCCACCCTGGT	480
R-HH5	ACGCAGGTAATGCGAAAAGGCAAGCTCGTCTCGGTGCACAGCAAGGACATCCACCCTGGT	480
R-HH6	ACGCAGGTAATGCGAAAAGGCAAGCTCGTCTCGGTGCACAGCAAGGACATCCACCCTGGT	480
R-HH8	ACGCAGGTAATGCGAAAAGGCAAGCTCGTCTCGGTGCACAGCAAGGACATCCACCCTGGT	480
R-HH9	ACGCAGGTAATGCGAAAAGGCAAGCTCGTCTCGGTGCACAGCAAGGACATCCACCCTGGT	480
R-HH10	ACGCAGGTAATGCGAAAAGGCAAGCTCGTCTCGGTGCACAGCAAGGACATCCACCCTGGT	480
R-HH12	ACGCAGGTAATGCGAAAAGGCAAGCTCGTCTCGGTGCACAGCAAGGACATCCACCCTGGT	480

LmxM.13.1530	GACGTCGTACGTATCAAGAACAGTGAGGAGGTGCACGCCGATGTCGTCATGCTCTCCTCG	540
WT- HH41	GACGTCGTACGTATCAAGAACAGTGAGGAGGTGCACGCCGATGTCGTCATGCTCTCCTCG	540
WT- HH42	GACGTCGTACGTATCAAGAACAGTGAGGAGGTGCACGCCGATGTCGTCATGCTCTCCTCG	540
WT- HH43	GACGTCGTACGTATCAAGAACAGTGAGGAGGTGCACGCCGATGTCGTCATGCTCTCCTCG	540
WT- HH44	GACGTCGTACGTATCAAGAACAGTGAGGAGGTGCACGCCGATGTCGTCATGCTCTCCTCG	540
WT- HH48	GACGTCGTACGTATCAAGAACAGTGAGGAGGTGCACGCCGATGTCGTCATGCTCTCCTCG	540
WT- HH49	GACGTCGTACGTATCAAGAACAGTGAGGAGGTGCACGCCGATGTCGTCATGCTCTCCTCG	540
R-HH5	GACGTCGTACGTATCAAGAACAGTGAGGAGGTGCACGCCGATGTCGTCATGCTCTCCTCG	540
R-HH6	GACGTCGTACGTATCAAGAACAGTGAGGAGGTGCACGCCGATGTCGTCATGCTCTCCTCG	540
R-HH8	GACGTCGTACGTATCAAGAACAGTGAGGAGGTGCACGCCGATGTCGTCATGCTCTCCTCG	540
R-HH9	GACGTCGTACGTATCAAGAACAGTGAGGAGGTGCACGCCGATGTCGTCATGCTCTCCTCG	540

R-HH10	GACGTCGTACGTATCAAGAACAGTGAGGAGGTGCACGCCGATGTCGTCATGCTCTCCTCG	540
R-HH12	GACGTCGTACGTATCAAGAACAGTGAGGAGGTGCACGCCGATGTCGTCATGCTCTCCTCG *****	540
LmxM.13.1530	TCCCTCGAGGAGGGACAGGCCTTTATAGACACGTGCAACCTGGACGGCGAGTCGAACCTG	600
WT- HH41	TCCCTCGAGGAGGGACAGGCCTTTATAGACACGTGCAACCTGGACGGCGAGTCGAACCTG	600
WT- HH42	TCCCTCGAGGAGGGACAGGCCTTTATAGACACGTGCAACCTGGACGGCGAGTCGAACCTG	600
WT- HH43	TCCCTCGAGGAGGGACAGGCCTTTATAGACACGTGCAACCTGGACGGCGAGTCGAACCTG	600
WT- HH44	TCCCTCGAGGAGGGACAGGCCTTTATAGACACGTGCAACCTGGACGGCGAGTCGAACCTG	600
WT- HH48	TCCCTCGAGGAGGGACAGGCCTTTATAGACACGTGCAACCTGGACGGCGAGTCGAACCTG	600
WT- HH49	TCCCTCGAGGAGGGACAGGCCTTTATAGACACGTGCAACCTGGACGGCGAGTCGAACCTG	600
R-HH5	TCCCTCGAGGAGGGACAGGCCTTTATAGACACGTGCAACCTGGACGGCGAGTCGAACCTG	600
R-HH6	TCCCTCGAGGAGGGACAGGCCTTTATAGACACGTGCAACCTGGACGGCGAGTCGAACCTG	600
R-HH8	TCCCTCGAGGAGGGACAGGCCTTTATAGACACGTGCAACCTGGACGGCGAGTCGAACCTG	600
R-HH9	TCCCTCGAGGAGGGACAGGCCTTTATAGACACGTGCAACCTGGACGGCGAGTCGAACCTG	600
R-HH10	TCCCTCGAGGAGGGACAGGCCTTTATAGACACGTGCAACCTGGACGGCGAGTCGAACCTG	600
R-HH12	TCCCTCGAGGAGGGACAGGCCTTTATAGACACGTGCAACCTGGACGGCGAGTCGAACCTG *****	600
LmxM.13.1530	AAGCCACGCAAGGCTTTGGAGGTGACCTGGGGCCTCTGC GAAATTGAGACAATCATGAAT	660
WT- HH41	AAGCCACGCAAGGCTTTGGAGGTGACCTGGGGCCTCTGC GAAATTGAGACAATCATGAAT	660
WT- HH42	AAGCCACGCAAGGCTTTGGAGGTGACCTGGGGCCTCTGC GAAATTGAGACAATCATGAAT	660
WT- HH43	AAGCCACGCAAGGCTTTGGAGGTGACCTGGGGCCTCTGC GAAATTGAGACAATCATGAAT	660
WT- HH44	AAGCCACGCAAGGCTTTGGAGGTGACCTGGGGCCTCTGC GAAATTGAGACAATCATGAAT	660
WT- HH48	AAGCCACGCAAGGCTTTGGAGGTGACCTGGGGCCTCTGC GAAATTGAGACAATCATGAAT	660
WT- HH49	AAGCCACGCAAGGCTTTGGAGGTGACCTGGGGCCTCTGC GAAATTGAGACAATCATGAAT	660
R-HH5	AAGCCACGCAAGGCTTTGGAGGTGACCTGGGGCCTCTGC GAAATTGAGACAATCATGAAT	660
R-HH6	AAGCCACGCAAGGCTTTGGAGGTGACCTGGGGCCTCTGC GAAATTGAGACAATCATGAAT	660
R-HH8	AAGCCACGCAAGGCTTTGGAGGTGACCTGGGGCCTCTGC GAAATTGAGACAATCATGAAT	660
R-HH9	AAGCCACGCAAGGCTTTGGAGGTGACCTGGGGCCTCTGC GAAATTGAGACAATCATGAAT	660
R-HH10	AAGCCACGCAAGGCTTTGGAGGTGACCTGGGGCCTCTGC GAAATTGAGACAATCATGAAT	660
R-HH12	AAGCCACGCAAGGCTTTGGAGGTGACCTGGGGCCTCTGC GAAATTGAGACAATCATGAAT *****	660
LmxM.13.1530	ACCACAGCTGTGTTGCACACGAGCAAGCCAGACCCAGGGTTGCTGTGCTGGACGGGGCTG	720
WT- HH41	ACCACAGCTGTGTTGCACACGAGCAAGCCAGACCCAGGGTTGCTGTGCTGGACGGGGCTG	720
WT- HH42	ACCACAGCTGTGTTGCACACGAGCAAGCCAGACCCAGGGTTGCTGTGCTGGACGGGGCTG	720
WT- HH43	ACCACAGCTGTGTTGCACACGAGCAAGCCAGACCCAGGGTTGCTGTGCTGGACGGGGCTG	720
WT- HH44	ACCACAGCTGTGTTGCACACGAGCAAGCCAGACCCAGGGTTGCTGTGCTGGACGGGGCTG	720
WT- HH48	ACCACAGCTGTGTTGCACACGAGCAAGCCAGACCCAGGGTTGCTGTGCTGGACGGGGCTG	720
WT- HH49	ACCACAGCTGTGTTGCACACGAGCAAGCCAGACCCAGGGTTGCTGTGCTGGACGGGGCTG	720
R-HH5	ACCACAGCTGTGTTGCACACGAGCAAGCCAGACCCAGGGTTGCTGTGCTGGACGGGGCTG	720
R-HH6	ACCACAGCTGTGTTGCACACGAGCAAGCCAGACCCAGGGTTGCTGTGCTGGACGGGGCTG	720
R-HH8	ACCACAGCTGTGTTGCACACGAGCAAGCCAGACCCAGGGTTGCTGTGCTGGACGGGGCTG	720
R-HH9	ACCACAGCTGTGTTGCACACGAGCAAGCCAGACCCAGGGTTGCTGTGCTGGACGGGGCTG	720
R-HH10	ACCACAGCTGTGTTGCACACGAGCAAGCCAGACCCAGGGTTGCTGTGCTGGACGGGGCTG	720
R-HH12	ACCACAGCTGTGTTGCACACGAGCAAGCCAGACCCAGGGTTGCTGTGCTGGACGGGGCTG *****	720
LmxM.13.1530	TTGGAGATCAATGGCGAGGAGCACGCACTCTCGCTGGACCAAGTTCCCTGTATCGCGGCTGC	780
WT- HH41	TTGGAGATCAATGGCGAGGAGCACGCACTCTCGCTGGACCAAGTTCCCTGTATCGCGGCTGC	780
WT- HH42	TTGGAGATCAATGGCGAGGAGCACGCACTCTCGCTGGACCAAGTTCCCTGTATCGCGGCTGC	780
WT- HH43	TTGGAGATCAATGGCGAGGAGCACGCACTCTCGCTGGACCAAGTTCCCTGTATCGCGGCTGC	780
WT- HH44	TTGGAGATCAATGGCGAGGAGCACGCACTCTCGCTGGACCAAGTTCCCTGTATCGCGGCTGC	780
WT- HH48	TTGGAGATCAATGGCGAGGAGCACGCACTCTCGCTGGACCAAGTTCCCTGTATCGCGGCTGC	780
WT- HH49	TTGGAGATCAATGGCGAGGAGCACGCACTCTCGCTGGACCAAGTTCCCTGTATCGCGGCTGC	780
R-HH5	TTGGAGATCAATGGCGAGGAGCACGCACTCTCGCTGGACCAAGTTCCCTGTATCGCGGCTGC	780
R-HH6	TTGGAGATCAATGGCGAGGAGCACGCACTCTCGCTGGACCAAGTTCCCTGTATCGCGGCTGC	780
R-HH8	TTGGAGATCAATGGCGAGGAGCACGCACTCTCGCTGGACCAAGTTCCCTGTATCGCGGCTGC	780
R-HH9	TTGGAGATCAATGGCGAGGAGCACGCACTCTCGCTGGACCAAGTTCCCTGTATCGCGGCTGC	780
R-HH10	TTGGAGATCAATGGCGAGGAGCACGCACTCTCGCTGGACCAAGTTCCCTGTATCGCGGCTGC	780
R-HH12	TTGGAGATCAATGGCGAGGAGCACGCACTCTCGCTGGACCAAGTTCCCTGTATCGCGGCTGC *****	780
LmxM.13.1530	GTGTTACGCAACACCGACTGGGCGTGGGGCATGGTTGCCTACGCAGGTGTCGACACGAAG	840
WT- HH41	GTGTTACGCAACACCGACTGGGCGTGGGGCATGGTTGCCTACGCAGGTGTCGACACGAAG	840
WT- HH42	GTGTTACGCAACACCGACTGGGCGTGGGGCATGGTTGCCTACGCAGGTGTCGACACGAAG	840
WT- HH43	GTGTTACGCAACACCGACTGGGCGTGGGGCATGGTTGCCTACGCAGGTGTCGACACGAAG	840
WT- HH44	GTGTTACGCAACACCGACTGGGCGTGGGGCATGGTTGCCTACGCAGGTGTCGACACGAAG	840
WT- HH48	GTGTTACGCAACACCGACTGGGCGTGGGGCATGGTTGCCTACGCAGGTGTCGACACGAAG	840
WT- HH49	GTGTTACGCAACACCGACTGGGCGTGGGGCATGGTTGCCTACGCAGGTGTCGACACGAAG	840
R-HH5	GTGTTACGCAACACCGACTGGGCGTGGGGCATGGTTGCCTACGCAGGTGTCGACACGAAG	840
R-HH6	GTGTTACGCAACACCGACTGGGCGTGGGGCATGGTTGCCTACGCAGGTGTCGACACGAAG	840
R-HH8	GTGTTACGCAACACCGACTGGGCGTGGGGCATGGTTGCCTACGCAGGTGTCGACACGAAG	840
R-HH9	GTGTTACGCAACACCGACTGGGCGTGGGGCATGGTTGCCTACGCAGGTGTCGACACGAAG	840
R-HH10	GTGTTACGCAACACCGACTGGGCGTGGGGCATGGTTGCCTACGCAGGTGTCGACACGAAG	840

R-HH12 GTGTTACGCAACACGGACTGGGCGTGGGGCATGTTGCTACGCAGGTGTCGACACGAAG 840

LmxM.13.1530 CTGTTCCGAAACTTGAAGCCAAAACCGCCAAAAGTCGTGCAACCTCGACCGCAAGCTGAAC 900
 WT- HH41 CTGTTCCGAAACTTGAAGCCAAAACCGCCAAAAGTCGTGCAACCTCGACCGCAAGCTGAAC 900
 WT- HH42 CTGTTCCGAAACTTGAAGCCAAAACCGCCAAAAGTCGTGCAACCTCGACCGCAAGCTGAAC 900
 WT- HH43 CTGTTCCGAAACTTGAAGCCAAAACCGCCAAAAGTCGTGCAACCTCGACCGCAAGCTGAAC 900
 WT- HH44 CTGTTCCGAAACTTGAAGCCAAAACCGCCAAAAGTCGTGCAACCTCGACCGCAAGCTGAAC 900
 WT- HH48 CTGTTCCGAAACTTGAAGCCAAAACCGCCAAAAGTCGTGCAACCTCGACCGCAAGCTGAAC 900
 WT- HH49 CTGTTCCGAAACTTGAAGCCAAAACCGCCAAAAGTCGTGCAACCTCGACCGCAAGCTGAAC 900
 R-HH5 CTGTTCCGAAACTTGAAGCCAAAACCGCCAAAAGTCGTGCAACCTCGACCGCAAGCTGAAC 900
 R-HH6 CTGTTCCGAAACTTGAAGCCAAAACCGCCAAAAGTCGTGCAACCTCGACCGCAAGCTGAAC 900
 R-HH8 CTGTTCCGAAACTTGAAGCCAAAACCGCCAAAAGTCGTGCAACCTCGACCGCAAGCTGAAC 900
 R-HH9 CTGTTCCGAAACTTGAAGCCAAAACCGCCAAAAGTCGTGCAACCTCGACCGCAAGCTGAAC 900
 R-HH10 CTGTTCCGAAACTTGAAGCCAAAACCGCCAAAAGTCGTGCAACCTCGACCGCAAGCTGAAC 900
 R-HH12 CTGTTCCGAAACTTGAAGCCAAAACCGCCAAAAGTCGTGCAACCTCGACCGCAAGCTGAAC 900

LmxM.13.1530 TACTTTATCATAGCC 915
 WT- HH41 TACTTTATCATAGCC 915
 WT- HH42 TACTTTATCATAGCC 915
 WT- HH43 TACTTTATCATAGCC 915
 WT- HH44 TACTTTATCATAGCC 915
 WT- HH48 TACTTTATCATAGCC 915
 WT- HH49 TACTTTATCATAGCC 915
 R-HH5 TACTTTATCATAGCC 915
 R-HH6 TACTTTATCATAGCC 915
 R-HH8 TACTTTATCATAGCC 915
 R-HH9 TACTTTATCATAGCC 915
 R-HH10 TACTTTATCATAGCC 915
 R-HH12 TACTTTATCATAGCC 915

Fragment 2 (1013bp)

LmxM.13.1530 C CCAGAACATAACGCTGTGGGGGTACCGTTACTTGAGCTATTTTCATTTTGCTGAGCTAC 1080
 WT-HH19 CCAGAACATAACGCTGTGGGGGTACCGTTACTTGAGCTATTTTCATTTTGCTGAGCTAC 1080
 WT-HH21 CCAGAACATAACGCTGTGGGGGTACCGTTACTTGAGCTATTTTCATTTTGCTGAGCTAC 1080
 WT-HH22 CCAGAACATAACGCTGTGGGGGTACCGTTACTTGAGCTATTTTCATTTTGCTGAGCTAC 1080
 WT-HH23 CCAGAACATAACGCTGTGGGGGTACCGTTACTTGAGCTATTTTCATTTTGCTGAGCTAC 1080
 WT-HH24 CCAGAACATAACGCTGTGGGGGTACCGTTACTTGAGCTATTTTCATTTTGCTGAGCTAC 1080
 WT-HH25 CCAGAACATAACGCTGTGGGGGTACCGTTACTTGAGCTATTTTCATTTTGCTGAGCTAC 1080
 R-HH28 CCAGAACATAACGCTGTGGGGGTACCGTTACTTGAGCTATTTTCATTTTGCTGAGCTAC 1080
 R-HH29 CCAGAACATAACGCTGTGGGGGTACCGTTACTTGAGCTATTTTCATTTTGCTGAGCTAC 1080
 R-HH31 CCAGAACATAACGCTGTGGGGGTACCGTTACTTGAGCTATTTTCATTTTGCTGAGCTAC 1080
 R-HH32 CCAGAACATAACGCTGTGGGGGTACCGTTACTTGAGCTATTTTCATTTTGCTGAGCTAC 1080
 R-HH33 CCAGAACATAACGCTGTGGGGGTACCGTTACTTGAGCTATTTTCATTTTGCTGAGCTAC 1080
 R-HH34 CCAGAACATAACGCTGTGGGGGTACCGTTACTTGAGCTATTTTCATTTTGCTGAGCTAC 1080

LmxM.13.1530 TGCGTGCCCATCTCGCTGTTTCGTCACGATTGAGTTGTGCAAGGTGATCCAGGCGCAGTGG 1140
 WT-HH19 TGCGTGCCCATCTCGCTGTTTCGTCACGATTGAGTTGTGCAAGGTGATCCAGGCGCAGTGG 1140
 WT-HH21 TGCGTGCCCATCTCGCTGTTTCGTCACGATTGAGTTGTGCAAGGTGATCCAGGCGCAGTGG 1140
 WT-HH22 TGCGTGCCCATCTCGCTGTTTCGTCACGATTGAGTTGTGCAAGGTGATCCAGGCGCAGTGG 1140
 WT-HH23 TGCGTGCCCATCTCGCTGTTTCGTCACGATTGAGTTGTGCAAGGTGATCCAGGCGCAGTGG 1140
 WT-HH24 TGCGTGCCCATCTCGCTGTTTCGTCACGATTGAGTTGTGCAAGGTGATCCAGGCGCAGTGG 1140
 WT-HH25 TGCGTGCCCATCTCGCTGTTTCGTCACGATTGAGTTGTGCAAGGTGATCCAGGCGCAGTGG 1140
 R-HH28 TGCGTGCCCATCTCGCTGTTTCGTCACGATTGAGTTGTGCAAGGTGATCCAGGCGCAGTGG 1140
 R-HH29 TGCGTGCCCATCTCGCTGTTTCGTCACGATTGAGTTGTGCAAGGTGATCCAGGCGCAGTGG 1140
 R-HH31 TGCGTGCCCATCTCGCTGTTTCGTCACGATTGAGTTGTGCAAGGTGATCCAGGCGCAGTGG 1140
 R-HH32 TGCGTGCCCATCTCGCTGTTTCGTCACGATTGAGTTGTGCAAGGTGATCCAGGCGCAGTGG 1140
 R-HH33 TGCGTGCCCATCTCGCTGTTTCGTCACGATTGAGTTGTGCAAGGTGATCCAGGCGCAGTGG 1140
 R-HH34 TGCGTGCCCATCTCGCTGTTTCGTCACGATTGAGTTGTGCAAGGTGATCCAGGCGCAGTGG 1140

LmxM.13.1530 ATGCGGATGGACTGCCTCATGATGGAGTACATGAACAACCGCTGGCGGCAGTCCAGCCG 1200
 WT-HH19 ATGCGGATGGACTGCCTCATGATGGAGTACATGAACAACCGCTGGCGGCAGTCCAGCCG 1200
 WT-HH21 ATGCGGATGGACTGCCTCATGATGGAGTACATGAACAACCGCTGGCGGCAGTCCAGCCG 1200
 WT-HH22 ATGCGGATGGACTGCCTCATGATGGAGTACATGAACAACCGCTGGCGGCAGTCCAGCCG 1200
 WT-HH23 ATGCGGATGGACTGCCTCATGATGGAGTACATGAACAACCGCTGGCGGCAGTCCAGCCG 1200
 WT-HH24 ATGCGGATGGACTGCCTCATGATGGAGTACATGAACAACCGCTGGCGGCAGTCCAGCCG 1200
 WT-HH25 ATGCGGATGGACTGCCTCATGATGGAGTACATGAACAACCGCTGGCGGCAGTCCAGCCG 1200

R-HH33	CAGGAACACATAGAAAAGTGTGACATCCCTCTGACAGAGATGTCCTCGTCGGGGCTCCGC	1800
R-HH34	CAGGAACACATAGAAAAGTGTGACATCCCTCTGACAGAGATGTCCTCGTCGGGGCTCCGC	1800

LmxM.13.1530	ACACTGCTGGTGTGCGCCAAGGACATCACACGCCGCCAGTTTCGACCTGTGGTACGAGAAG	1860
WT-HH19	ACACTGCTGGTGTGCGCCAAGGACATCACACGCCGCCAGTTTCGACCTGTGGTACGAGAAG	1860
WT-HH21	ACACTGCTGGTGTGCGCCAAGGACATCACACGCCGCCAGTTTCGACCTGTGGTACGAGAAG	1860
WT-HH22	ACACTGCTGGTGTGCGCCAAGGACATCACACGCCGCCAGTTTCGACCTGTGGTACGAGAAG	1860
WT-HH23	ACACTGCTGGTGTGCGCCAAGGACATCACACGCCGCCAGTTTCGACCTGTGGTACGAGAAG	1860
WT-HH24	ACACTGCTGGTGTGCGCCAAGGACATCACACGCCGCCAGTTTCGACCTGTGGTACGAGAAG	1860
WT-HH25	ACACTGCTGGTGTGCGCCAAGGACATCACACGCCGCCAGTTTCGACCTGTGGTACGAGAAG	1860
R-HH28	ACACTGCTGGTGTGCGCCAAGGACATCACACGCCGCCAGTTTCGACCTGTGGTACGAGAAG	1860
R-HH29	ACACTGCTGGTGTGCGCCAAGGACATCACACGCCGCCAGTTTCGACCTGTGGTACGAGAAG	1860
R-HH31	ACACTGCTGGTGTGCGCCAAGGACATCACACGCCGCCAGTTTCGACCTGTGGTACGAGAAG	1860
R-HH32	ACACTGCTGGTGTGCGCCAAGGACATCACACGCCGCCAGTTTCGACCTGTGGTACGAGAAG	1860
R-HH33	ACACTGCTGGTGTGCGCCAAGGACATCACACGCCGCCAGTTTCGACCTGTGGTACGAGAAG	1860
R-HH34	ACACTGCTGGTGTGCGCCAAGGACATCACACGCCGCCAGTTTCGACCTGTGGTACGAGAAG	1860

LmxM.13.1530	TTCGTCGAGGTCGGCAAGTCTCTGCAGAACCGCAGCTCCAAGATTGATAAAGTCTGCCTTA	1920
WT-HH19	TTCGTCGAGGTCGGCAAGTCTCTGCAGAACCGCAGCTCCAAGATTGATAAAGTCTGCCTTA	1920
WT-HH21	TTCGTCGAGGTCGGCAAGTCTCTGCAGAACCGCAGCTCCAAGATTGATAAAGTCTGCCTTA	1920
WT-HH22	TTCGTCGAGGTCGGCAAGTCTCTGCAGAACCGCAGCTCCAAGATTGATAAAGTCTGCCTTA	1920
WT-HH23	TTCGTCGAGGTCGGCAAGTCTCTGCAGAACCGCAGCTCCAAGATTGATAAAGTCTGCCTTA	1920
WT-HH24	TTCGTCGAGGTCGGCAAGTCTCTGCAGAACCGCAGCTCCAAGATTGATAAAGTCTGCCTTA	1920
WT-HH25	TTCGTCGAGGTCGGCAAGTCTCTGCAGAACCGCAGCTCCAAGATTGATAAAGTCTGCCTTA	1920
R-HH28	TTCGTCGAGGTCGGCAAGTCTCTGCAGAACCGCAGCTCCAAGATTGATAAAGTCTGCCTTA	1920
R-HH29	TTCGTCGAGGTCGGCAAGTCTCTGCAGAACCGCAGCTCCAAGATTGATAAAGTCTGCCTTA	1920
R-HH31	TTCGTCGAGGTCGGCAAGTCTCTGCAGAACCGCAGCTCCAAGATTGATAAAGTCTGCCTTA	1920
R-HH32	TTCGTCGAGGTCGGCAAGTCTCTGCAGAACCGCAGCTCCAAGATTGATAAAGTCTGCCTTA	1920
R-HH33	TTCGTCGAGGTCGGCAAGTCTCTGCAGAACCGCAGCTCCAAGATTGATAAAGTCTGCCTTA	1920
R-HH34	TTCGTCGAGGTCGGCAAGTCTCTGCAGAACCGCAGCTCCAAGATTGATAAAGTCTGCCTTA	1920

LmxM.13.1530	GAGATGGAGCAAGACATGCGACTCGTCGGCGCCACCGCCATCGAGGACAAGCTGCAAGAC	1980
WT-HH19	GAGATGGAGCAAGACATGCGACTCGTCGGCGCCACCGCCATCGAGGACAAGCTGCAAGAC	1980
WT-HH21	GAGATGGAGCAAGACATGCGACTCGTCGGCGCCACCGCCATCGAGGACAAGCTGCAAGAC	1980
WT-HH22	GAGATGGAGCAAGACATGCGACTCGTCGGCGCCACCGCCATCGAGGACAAGCTGCAAGAC	1980
WT-HH23	GAGATGGAGCAAGACATGCGACTCGTCGGCGCCACCGCCATCGAGGACAAGCTGCAAGAC	1980
WT-HH24	GAGATGGAGCAAGACATGCGACTCGTCGGCGCCACCGCCATCGAGGACAAGCTGCAAGAC	1980
WT-HH25	GAGATGGAGCAAGACATGCGACTCGTCGGCGCCACCGCCATCGAGGACAAGCTGCAAGAC	1980
R-HH28	GAGATGGAGCAAGACATGCGACTCGTCGGCGCCACCGCCATCGAGGACAAGCTGCAAGAC	1980
R-HH29	GAGATGGAGCAAGACATGCGACTCGTCGGCGCCACCGCCATCGAGGACAAGCTGCAAGAC	1980
R-HH31	GAGATGGAGCAAGACATGCGACTCGTCGGCGCCACCGCCATCGAGGACAAGCTGCAAGAC	1980
R-HH32	GAGATGGAGCAAGACATGCGACTCGTCGGCGCCACCGCCATCGAGGACAAGCTGCAAGAC	1980
R-HH33	GAGATGGAGCAAGACATGCGACTCGTCGGCGCCACCGCCATCGAGGACAAGCTGCAAGAC	1980
R-HH34	GAGATGGAGCAAGACATGCGACTCGTCGGCGCCACCGCCATCGAGGACAAGCTGCAAGAC	1980

LmxM.13.1530	GAGGTGCCTGAGACACTGTCGTTTTTCTTGAACGCCGGTGTGATCATTGGATGC	2035
WT-HH19	GAGGTGCCTGAGACACTGTCGTTTTTCTTGAACGCCGGTGTGATCATTGGATGC	2035
WT-HH21	GAGGTGCCTGAGACACTGTCGTTTTTCTTGAACGCCGGTGTGATCATTGGATGC	2035
WT-HH22	GAGGTGCCTGAGACACTGTCGTTTTTCTTGAACGCCGGTGTGATCATTGGATGC	2035
WT-HH23	GAGGTGCCTGAGACACTGTCGTTTTTCTTGAACGCCGGTGTGATCATTGGATGC	2035
WT-HH24	GAGGTGCCTGAGACACTGTCGTTTTTCTTGAACGCCGGTGTGATCATTGGATGC	2035
WT-HH25	GAGGTGCCTGAGACACTGTCGTTTTTCTTGAACGCCGGTGTGATCATTGGATGC	2035
R-HH28	GAGGTGCCTGAGACACTGTCGTTTTTCTTGAACGCCGGTGTGATCATTGGATGC	2035
R-HH29	GAGGTGCCTGAGACACTGTCGTTTTTCTTGAACGCCGGTGTGATCATTGGATGC	2035
R-HH31	GAGGTGCCTGAGACACTGTCGTTTTTCTTGAACGCCGGTGTGATCATTGGATGC	2035
R-HH32	GAGGTGCCTGAGACACTGTCGTTTTTCTTGAACGCCGGTGTGATCATTGGATGC	2035
R-HH33	GAGGTGCCTGAGACACTGTCGTTTTTCTTGAACGCCGGTGTGATCATTGGATGC	2035
R-HH34	GAGGTGCCTGAGACACTGTCGTTTTTCTTGAACGCCGGTGTGATCATTGGATGC	2035

Fragment 3 (741bp)

LmxM.13.1530	AAGGAGCGGCCTGCACCTTGGTCATCGACGGCCCGGGGCTGAACATCTCGATGGAGCAT	2280
WT-HH77	AAGGAGCGGCCTGCACCTTGGTCATCGACGGCCCGGGGCTGAACATCTCGATGGAGCAT	2280
WT-HH79	AAGGAGCGGCCTGCACCTTGGTCATCGACGGCCCGGGGCTGAACATCTCGATGGAGCAT	2280
WT-HH80	AAGGAGCGGCCTGCACCTTGGTCATCGACGGCCCGGGGCTGAACATCTCGATGGAGCAT	2280
WT-HH81	AAGGAGCGGCCTGCACCTTGGTCATCGACGGCCCGGGGCTGAACATCTCGATGGAGCAT	2280
WT-HH82	AAGGAGCGGCCTGCACCTTGGTCATCGACGGCCCGGGGCTGAACATCTCGATGGAGCAT	2280
WT-HH83	AAGGAGCGGCCTGCACCTTGGTCATCGACGGCCCGGGGCTGAACATCTCGATGGAGCAT	2280

R-HH60	AAGGAGCGGCGTGCACCTTGGTCATCGACGGCCCGGGCTGAACATCTCGATGGAGCAT	2280
R-HH61	AAGGAGCGGCGTGCACCTTGGTCATCGACGGCCCGGGCTGAACATCTCGATGGAGCAT	2280
R-HH63	AAGGAGCGGCGTGCACCTTGGTCATCGACGGCCCGGGCTGAACATCTCGATGGAGCAT	2280
R-HH64	AAGGAGCGGCGTGCACCTTGGTCATCGACGGCCCGGGCTGAACATCTCGATGGAGCAT	2280
R-HH65	AAGGAGCGGCGTGCACCTTGGTCATCGACGGCCCGGGCTGAACATCTCGATGGAGCAT	2280
R-HH67	AAGGAGCGGCGTGCACCTTGGTCATCGACGGCCCGGGCTGAACATCTCGATGGAGCAT	2280

LmxM.13.1530	TACTTTAACCGAGTTCCCTGCGCATCTCCCATCAGTTAAACTCCGCCGTCTGCTGTCGTCTC	2340
WT-HH77	TACTTTAACCGAGTTCCCTGCGCATCTCCCATCAGTTAAACTCCGCCGTCTGCTGTCGTCTC	2340
WT-HH79	TACTTTAACCGAGTTCCCTGCGCATCTCCCATCAGTTAAACTCCGCCGTCTGCTGTCGTCTC	2340
WT-HH80	TACTTTAACCGAGTTCCCTGCGCATCTCCCATCAGTTAAACTCCGCCGTCTGCTGTCGTCTC	2340
WT-HH81	TACTTTAACCGAGTTCCCTGCGCATCTCCCATCAGTTAAACTCCGCCGTCTGCTGTCGTCTC	2340
WT-HH82	TACTTTAACCGAGTTCCCTGCGCATCTCCCATCAGTTAAACTCCGCCGTCTGCTGTCGTCTC	2340
WT-HH83	TACTTTAACCGAGTTCCCTGCGCATCTCCCATCAGTTAAACTCCGCCGTCTGCTGTCGTCTC	2340
R-HH60	TACTTTAACCGAGTTCCCTGCGCATCTCCCATCAGTTAAACTCCGCCGTCTGCTGTCGTCTC	2340
R-HH61	TACTTTAACCGAGTTCCCTGCGCATCTCCCATCAGTTAAACTCCGCCGTCTGCTGTCGTCTC	2340
R-HH63	TACTTTAACCGAGTTCCCTGCGCATCTCCCATCAGTTAAACTCCGCCGTCTGCTGTCGTCTC	2340
R-HH64	TACTTTAACCGAGTTCCCTGCGCATCTCCCATCAGTTAAACTCCGCCGTCTGCTGTCGTCTC	2340
R-HH65	TACTTTAACCGAGTTCCCTGCGCATCTCCCATCAGTTAAACTCCGCCGTCTGCTGTCGTCTC	2340
R-HH67	TACTTTAACCGAGTTCCCTGCGCATCTCCCATCAGTTAAACTCCGCCGTCTGCTGTCGTCTC	2340

LmxM.13.1530	ACGCCGATCCAGAAGGCAAGCGTCGTTTCGCATGTTCCAGAAGTCAACCGGTAAGACAGCG	2400
WT-HH77	ACGCCGATCCAGAAGGCAAGCGTCGTTTCGCATGTTCCAGAAGTCAACCGGTAAGACAGCG	2400
WT-HH79	ACGCCGATCCAGAAGGCAAGCGTCGTTTCGCATGTTCCAGAAGTCAACCGGTAAGACAGCG	2400
WT-HH80	ACGCCGATCCAGAAGGCAAGCGTCGTTTCGCATGTTCCAGAAGTCAACCGGTAAGACAGCG	2400
WT-HH81	ACGCCGATCCAGAAGGCAAGCGTCGTTTCGCATGTTCCAGAAGTCAACCGGTAAGACAGCG	2400
WT-HH82	ACGCCGATCCAGAAGGCAAGCGTCGTTTCGCATGTTCCAGAAGTCAACCGGTAAGACAGCG	2400
WT-HH83	ACGCCGATCCAGAAGGCAAGCGTCGTTTCGCATGTTCCAGAAGTCAACCGGTAAGACAGCG	2400
R-HH60	ACGCCGATCCAGAAGGCAAGCGTCGTTTCGCATGTTCCAGAAGTCAACCGGTAAGACAGCG	2400
R-HH61	ACGCCGATCCAGAAGGCAAGCGTCGTTTCGCATGTTCCAGAAGTCAACCGGTAAGACAGCG	2400
R-HH63	ACGCCGATCCAGAAGGCAAGCGTCGTTTCGCATGTTCCAGAAGTCAACCGGTAAGACAGCG	2400
R-HH64	ACGCCGATCCAGAAGGCAAGCGTCGTTTCGCATGTTCCAGAAGTCAACCGGTAAGACAGCG	2400
R-HH65	ACGCCGATCCAGAAGGCAAGCGTCGTTTCGCATGTTCCAGAAGTCAACCGGTAAGACAGCG	2400
R-HH67	ACGCCGATCCAGAAGGCAAGCGTCGTTTCGCATGTTCCAGAAGTCAACCGGTAAGACAGCG	2400

LmxM.13.1530	CTGGCCATCGGTGACGGCGCCAACGACGTGTCCATGATCCGGGAGGGACGTGTGGGCGTG	2460
WT-HH77	CTGGCCATCGGTGACGGCGCCAACGACGTGTCCATGATCCGGGAGGGACGTGTGGGCGTG	2460
WT-HH79	CTGGCCATCGGTGACGGCGCCAACGACGTGTCCATGATCCGGGAGGGACGTGTGGGCGTG	2460
WT-HH80	CTGGCCATCGGTGACGGCGCCAACGACGTGTCCATGATCCGGGAGGGACGTGTGGGCGTG	2460
WT-HH81	CTGGCCATCGGTGACGGCGCCAACGACGTGTCCATGATCCGGGAGGGACGTGTGGGCGTG	2460
WT-HH82	CTGGCCATCGGTGACGGCGCCAACGACGTGTCCATGATCCGGGAGGGACGTGTGGGCGTG	2460
WT-HH83	CTGGCCATCGGTGACGGCGCCAACGACGTGTCCATGATCCGGGAGGGACGTGTGGGCGTG	2460
R-HH60	CTGGCCATCGGTGACGGCGCCAACGACGTGTCCATGATCCGGGAGGGACGTGTGGGCGTG	2460
R-HH61	CTGGCCATCGGTGACGGCGCCAACGACGTGTCCATGATCCGGGAGGGACGTGTGGGCGTG	2460
R-HH63	CTGGCCATCGGTGACGGCGCCAACGACGTGTCCATGATCCGGGAGGGACGTGTGGGCGTG	2460
R-HH64	CTGGCCATCGGTGACGGCGCCAACGACGTGTCCATGATCCGGGAGGGACGTGTGGGCGTG	2460
R-HH65	CTGGCCATCGGTGACGGCGCCAACGACGTGTCCATGATCCGGGAGGGACGTGTGGGCGTG	2460
R-HH67	CTGGCCATCGGTGACGGCGCCAACGACGTGTCCATGATCCGGGAGGGACGTGTGGGCGTG	2460

LmxM.13.1530	GGCATTATTGGGCTGGAAGGTGCACATGCCGCCCTCGCCGCCGACTACGCGATTCCCGGG	2520
WT-HH77	GGCATTATTGGGCTGGAAGGTGCACATGCCGCCCTCGCCGCCGACTACGCGATTCCCGGG	2520
WT-HH79	GGCATTATTGGGCTGGAAGGTGCACATGCCGCCCTCGCCGCCGACTACGCGATTCCCGGG	2520
WT-HH80	GGCATTATTGGGCTGGAAGGTGCACATGCCGCCCTCGCCGCCGACTACGCGATTCCCGGG	2520
WT-HH81	GGCATTATTGGGCTGGAAGGTGCACATGCCGCCCTCGCCGCCGACTACGCGATTCCCGGG	2520
WT-HH82	GGCATTATTGGGCTGGAAGGTGCACATGCCGCCCTCGCCGCCGACTACGCGATTCCCGGG	2520
WT-HH83	GGCATTATTGGGCTGGAAGGTGCACATGCCGCCCTCGCCGCCGACTACGCGATTCCCGGG	2520
R-HH60	GGCATTATTGGGCTGGAAGGTGCACATGCCGCCCTCGCCGCCGACTACGCGATTCCCGGG	2520
R-HH61	GGCATTATTGGGCTGGAAGGTGCACATGCCGCCCTCGCCGCCGACTACGCGATTCCCGGG	2520
R-HH63	GGCATTATTGGGCTGGAAGGTGCACATGCCGCCCTCGCCGCCGACTACGCGATTCCCGGG	2520
R-HH64	GGCATTATTGGGCTGGAAGGTGCACATGCCGCCCTCGCCGCCGACTACGCGATTCCCGGG	2520
R-HH65	GGCATTATTGGGCTGGAAGGTGCACATGCCGCCCTCGCCGCCGACTACGCGATTCCCGGG	2520
R-HH67	GGCATTATTGGGCTGGAAGGTGCACATGCCGCCCTCGCCGCCGACTACGCGATTCCCGGG	2520

LmxM.13.1530	TTCAAACACCTGCGCCGCCTGTGCGCGGTGCATGGGCGCTACTCGCTCTTCCGAAACGCC	2580
WT-HH77	TTCAAACACCTGCGCCGCCTGTGCGCGGTGCATGGGCGCTACTCGCTCTTCCGAAACGCC	2580
WT-HH79	TTCAAACACCTGCGCCGCCTGTGCGCGGTGCATGGGCGCTACTCGCTCTTCCGAAACGCC	2580
WT-HH80	TTCAAACACCTGCGCCGCCTGTGCGCGGTGCATGGGCGCTACTCGCTCTTCCGAAACGCC	2580
WT-HH81	TTCAAACACCTGCGCCGCCTGTGCGCGGTGCATGGGCGCTACTCGCTCTTCCGAAACGCC	2580
WT-HH82	TTCAAACACCTGCGCCGCCTGTGCGCGGTGCATGGGCGCTACTCGCTCTTCCGAAACGCC	2580
WT-HH83	TTCAAACACCTGCGCCGCCTGTGCGCGGTGCATGGGCGCTACTCGCTCTTCCGAAACGCC	2580
R-HH60	TTCAAACACCTGCGCCGCCTGTGCGCGGTGCATGGGCGCTACTCGCTCTTCCGAAACGCC	2580

R-HH61	TTCAAACACCTGCGCCGCTGTGCGCGGTGCATGGGCGCTACTCGCTCTCCGAAACGCC	2580
R-HH63	TTCAAACACCTGCGCCGCTGTGCGCGGTGCATGGGCGCTACTCGCTCTCCGAAACGCC	2580
R-HH64	TTCAAACACCTGCGCCGCTGTGCGCGGTGCATGGGCGCTACTCGCTCTCCGAAACGCC	2580
R-HH65	TTCAAACACCTGCGCCGCTGTGCGCGGTGCATGGGCGCTACTCGCTCTCCGAAACGCC	2580
R-HH67	TTCAAACACCTGCGCCGCTGTGCGCGGTGCATGGGCGCTACTCGCTCTCCGAAACGCC	2580

LmxM.13.1530	AGCTGCATTCTGGTTAGCTTCCACAAGAACATCACCGTGTCCGGTGGTGCAGTTCATCTTT	2640
WT-HH77	AGCTGCATTCTGGTTAGCTTCCACAAGAACATCACCGTGTCCGGTGGTGCAGTTCATCTTT	2640
WT-HH79	AGCTGCATTCTGGTTAGCTTCCACAAGAACATCACCGTGTCCGGTGGTGCAGTTCATCTTT	2640
WT-HH80	AGCTGCATTCTGGTTAGCTTCCACAAGAACATCACCGTGTCCGGTGGTGCAGTTCATCTTT	2640
WT-HH81	AGCTGCATTCTGGTTAGCTTCCACAAGAACATCACCGTGTCCGGTGGTGCAGTTCATCTTT	2640
WT-HH82	AGCTGCATTCTGGTTAGCTTCCACAAGAACATCACCGTGTCCGGTGGTGCAGTTCATCTTT	2640
WT-HH83	AGCTGCATTCTGGTTAGCTTCCACAAGAACATCACCGTGTCCGGTGGTGCAGTTCATCTTT	2640
R-HH60	AGCTGCATTCTGGTTAGCTTCCACAAGAACATCACCGTGTCCGGTGGTGCAGTTCATCTTT	2640
R-HH61	AGCTGCATTCTGGTTAGCTTCCACAAGAACATCACCGTGTCCGGTGGTGCAGTTCATCTTT	2640
R-HH63	AGCTGCATTCTGGTTAGCTTCCACAAGAACATCACCGTGTCCGGTGGTGCAGTTCATCTTT	2640
R-HH64	AGCTGCATTCTGGTTAGCTTCCACAAGAACATCACCGTGTCCGGTGGTGCAGTTCATCTTT	2640
R-HH65	AGCTGCATTCTGGTTAGCTTCCACAAGAACATCACCGTGTCCGGTGGTGCAGTTCATCTTT	2640
R-HH67	AGCTGCATTCTGGTTAGCTTCCACAAGAACATCACCGTGTCCGGTGGTGCAGTTCATCTTT	2640

LmxM.13.1530	GCCTTCTACGTCGGCTTCTCGGGGCTAACACTCTTTGATGGGTGGATGCTGACCTTCTAC	2700
WT-HH77	GCCTTCTACGTCGGCTTCTCGGGGCTAACACTCTTTGATGGGTGGATGCTGACCTTCTAC	2700
WT-HH79	GCCTTCTACGTCGGCTTCTCGGGGCTAACACTCTTTGATGGGTGGATGCTGACCTTCTAC	2700
WT-HH80	GCCTTCTACGTCGGCTTCTCGGGGCTAACACTCTTTGATGGGTGGATGCTGACCTTCTAC	2700
WT-HH81	GCCTTCTACGTCGGCTTCTCGGGGCTAACACTCTTTGATGGGTGGATGCTGACCTTCTAC	2700
WT-HH82	GCCTTCTACGTCGGCTTCTCGGGGCTAACACTCTTTGATGGGTGGATGCTGACCTTCTAC	2700
WT-HH83	GCCTTCTACGTCGGCTTCTCGGGGCTAACACTCTTTGATGGGTGGATGCTGACCTTCTAC	2700
R-HH60	GCCTTCTACGTCGGCTTCTCGGGGCTAACACTCTTTGATGGGTGGATGCTGACCTTCTAC	2700
R-HH61	GCCTTCTACGTCGGCTTCTCGGGGCTAACACTCTTTGATGGGTGGATGCTGACCTTCTAC	2700
R-HH63	GCCTTCTACGTCGGCTTCTCGGGGCTAACACTCTTTGATGGGTGGATGCTGACCTTCTAC	2700
R-HH64	GCCTTCTACGTCGGCTTCTCGGGGCTAACACTCTTTGATGGGTGGATGCTGACCTTCTAC	2700
R-HH65	GCCTTCTACGTCGGCTTCTCGGGGCTAACACTCTTTGATGGGTGGATGCTGACCTTCTAC	2700
R-HH67	GCCTTCTACGTCGGCTTCTCGGGGCTAACACTCTTTGATGGGTGGATGCTGACCTTCTAC	2700

LmxM.13.1530	AACGTCTGATGACAAGTGTCCCGCCCTTCTTCATAGGCATATTCGATAAAGACCTCCCC	2760
WT-HH77	AACGTCTGATGACAAGTGTCCCGCCCTTCTTCATAGGCATATTCGATAAAGACCTCCCC	2760
WT-HH79	AACGTCTGATGACAAGTGTCCCGCCCTTCTTCATAGGCATATTCGATAAAGACCTCCCC	2760
WT-HH80	AACGTCTGATGACAAGTGTCCCGCCCTTCTTCATAGGCATATTCGATAAAGACCTCCCC	2760
WT-HH81	AACGTCTGATGACAAGTGTCCCGCCCTTCTTCATAGGCATATTCGATAAAGACCTCCCC	2760
WT-HH82	AACGTCTGATGACAAGTGTCCCGCCCTTCTTCATAGGCATATTCGATAAAGACCTCCCC	2760
WT-HH83	AACGTCTGATGACAAGTGTCCCGCCCTTCTTCATAGGCATATTCGATAAAGACCTCCCC	2760
R-HH60	AACGTCTGATGACAAGTGTCCCGCCCTTCTTCATAGGCATATTCGATAAAGACCTCCCC	2760
R-HH61	AACGTCTGATGACAAGTGTCCCGCCCTTCTTCATAGGCATATTCGATAAAGACCTCCCC	2760
R-HH63	AACGTCTGATGACAAGTGTCCCGCCCTTCTTCATAGGCATATTCGATAAAGACCTCCCC	2760
R-HH64	AACGTCTGATGACAAGTGTCCCGCCCTTCTTCATAGGCATATTCGATAAAGACCTCCCC	2760
R-HH65	AACGTCTGATGACAAGTGTCCCGCCCTTCTTCATAGGCATATTCGATAAAGACCTCCCC	2760
R-HH67	AACGTCTGATGACAAGTGTCCCGCCCTTCTTCATAGGCATATTCGATAAAGACCTCCCC	2760

LmxM.13.1530	GAAGAGGCCCTGCTGGAGCGGCCGAAGCTGTACACACCGTTGTCGCATGGCGAGTACTTT	2820
WT-HH77	GAAGAGGCCCTGCTGGAGCAGCCGAAGCTGTACACACCGTTGTCGCATGGCGAGTACTTT	2820
WT-HH79	GAAGAGGCCCTGCTGGAGCGGCCGAAGCTGTACACACCGTTGTCGCATGGCGAGTACTTT	2820
WT-HH80	GAAGAGGCCCTGCTGGAGCGGCCGAAGCTGTACACACCGTTGTCGCATGGCGAGTACTTT	2820
WT-HH81	GAAGAGGCCCTGCTGGAGCGGCCGAAGCTGTACACACCGTTGTCGCATGGCGAGTACTTT	2820
WT-HH82	GAAGAGGCCCTGCTGGAGCGGCCGAAGCTGTACACACCGTTGTCGCATGGCGAGTACTTT	2820
WT-HH83	GAAGAGGCCCTGCTGGAGCGGCCGAAGCTGTACACACCGTTGTCGCATGGCGAGTACTTT	2820
R-HH60	GAAGAGGCCCTGCTGGAGCGGCCGAAGCTGTACACACCGTTGTCGCATGGCGAGTACTTT	2820
R-HH61	GAAGAGGCCCTGCTGGAGCGGCCGAAGCTGTACACACCGTTGTCGCATGGCGAGTACTTT	2820
R-HH63	GAAGAGGCCCTGCTGGAGCGGCCGAAGCTGTACACACCGTTGTCGCATGGCGAGTACTTT	2820
R-HH64	GAAGAGGCCCTGCTGGAGCGGCCGAAGCTGTACACACCGTTGTCGCATGGCGAGTACTTT	2820
R-HH65	GAAGAGGCCCTGCTGGAGCGGCCGAAGCTGTACACACCGTTGTCGCATGGCGAGTACTTT	2820
R-HH67	GAAGAGGCCCTGCTGGAGCGGCCGAAGCTGTACACACCGTTGTCGCATGGCGAGTACTTT	2820

LmxM.13.1530	AACGTGACGACGCTTCTGCGGTGGTTCGCCGAATCACTAATAACAGCATTGATTCTCTTC	2880
WT-HH77	AACGTGACGACGCTTCTGCGGTGGTTCGCCGAATCACTAATAACAGCATTGATTCTCTTC	2880
WT-HH79	AACGTGACGACGCTTCTGCGGTGGTTCGCCGAATCACTAATAACAGCATTGATTCTCTTC	2880
WT-HH80	AACGTGACGACGCTTCTGCGGTGGTTCGCCGAATCACTAATAACAGCATTGATTCTCTTC	2880
WT-HH81	AACGTGACGACGCTTCTGCGGTGGTTCGCCGAATCACTAATAACAGCATTGATTCTCTTC	2880
WT-HH82	AACGTGACGACGCTTCTGCGGTGGTTCGCCGAATCACTAATAACAGCATTGATTCTCTTC	2880
WT-HH83	AACGTGACGACGCTTCTGCGGTGGTTCGCCGAATCACTAATAACAGCATTGATTCTCTTC	2880
R-HH60	AACGTGACGACGCTTCTGCGGTGGTTCGCCGAATCACTAATAACAGCATTGATTCTCTTC	2880
R-HH61	AACGTGACGACGCTTCTGCGGTGGTTCGCCGAATCACTAATAACAGCATTGATTCTCTTC	2880

R-HH63	AACGTGACGACGCTTCTGCGGTGGTTCGCCGAATCACTAATAACAGCATTGATTCTCTTC	2880
R-HH64	AACGTGACGACGCTTCTGCGGTGGTTCGCCGAATCACTAATAACAGCATTGATTCTCTTC	2880
R-HH65	AACGTGACGACGCTTCTGCGGTGGTTCGCCGAATCACTAATAACAGCATTGATTCTCTTC	2880
R-HH67	AACGTGACGACGCTTCTGCGGTGGTTCGCCGAATCACTAATAACAGCATTGATTCTCTTC	2880

LmxM.13.1530	TACGCTGCTTATCCGACATTGGTCCATCAAGACGGTCCCATCAACGCTACACTGGCGCT	2940
WT-HH77	TACGCTGCTTATCCGACATTGGTCCATCAAGACGGTCCCATCAACGCTACACTGGCGCT	2940
WT-HH79	TACGCTGCTTATCCGACATTGGTCCATCAAGACGGTCCCATCAACGCTACACTGGCGCT	2940
WT-HH80	TACGCTGCTTATCCGACATTGGTCCATCAAGACGGTCCCATCAACGCTACACTGGCGCT	2940
WT-HH81	TACGCTGCTTATCCGACATTGGTCCATCAAGACGGTCCCATCAACGCTACACTGGCGCT	2940
WT-HH82	TACGCTGCTTATCCGACATTGGTCCATCAAGACGGTCCCATCAACGCTACACTGGCGCT	2940
WT-HH83	TACGCTGCTTATCCGACATTGGTCCATCAAGACGGTCCCATCAACGCTACACTGGCGCT	2940
R-HH60	TACGCTGCTTATCCGACATTGGTCCATCAAGACGGTCCCATCAACGCTACACTGGCGCT	2940
R-HH61	TACGCTGCTTATCCGACATTGGTCCATCAAGACGGTCCCATCAACGCTACACTGGCGCT	2940
R-HH63	TACGCTGCTTATCCGACATTGGTCCATCAAGACGGTCCCATCAACGCTACACTGGCGCT	2940
R-HH64	TACGCTGCTTATCCGACATTGGTCCATCAAGACGGTCCCATCAACGCTACACTGGCGCT	2940
R-HH65	TACGCTGCTTATCCGACATTGGTCCATCAAGACGGTCCCATCAACGCTACACTGGCGCT	2940
R-HH67	TACGCTGCTTATCCGACATTGGTCCATCAAGACGGTCCCATCAACGCTACACTGGCGCT	2940

LmxM.13.1530	GAGACCGGCACGCTCGTGTTCAGCG	3964
WT-HH77	GAGACCGGCACGCTCGTGTTCAGCG	3964
WT-HH79	GAGACCGGCACGCTCGTGTTCAGCG	3964
WT-HH80	GAGACCGGCACGCTCGTGTTCAGCG	3964
WT-HH81	GAGACCGGCACGCTCGTGTTCAGCG	3964
WT-HH82	GAGACCGGCACGCTCGTGTTCAGCG	3964
WT-HH83	GAGACCGGCACGCTCGTGTTCAGCG	3964
R-HH60	GAGACCGGCACGCTCGTGTTCAGCG	3964
R-HH61	GAGACCGGCACGCTCGTGTTCAGCG	3964
R-HH63	GAGACCGGCACGCTCGTGTTCAGCG	3964
R-HH64	GAGACCGGCACGCTCGTGTTCAGCG	3964
R-HH65	GAGACCGGCACGCTCGTGTTCAGCG	3964
R-HH67	GAGACCGGCACGCTCGTGTTCAGCG	3964

Appendix 3 (Chapter 4)

Multiple amino acid sequences sequence alignment for each fragment of LmMT gene. 12 clones

for each fragment of LmMT sequenced compared LmxM.13.1530. The WT-prefix is for the pre-selection wildtype and the R-prefix for 700022-selected parasites. The HH code uniquely identifies the PCR clone sequenced.

Fragment 1

LmxM.13.1530	PLSFVLLVAII 120
WT-HH41	PLSFVLLVAII 120
WT-HH42	PLSFVLLVAII 120
WT-HH43	PLSFVLLVAII 120
WT-HH44	PLSFVLLVAII 120
WT-HH48	PLSFVLLVAII 120
WT-HH49	PLSFVLLVAII 120
WT-HH5	PLSFVLLVAII 120
WT-HH6	PLSFVLLVAII 120
WT-HH8	PLSFVLLVAII 120

WT-HH9	PLSFVLLVAII 120	
WT-HH10	PLSFVLLVAII 120	
WT-HH12	PLSFVLLVAII 120	

LmxM.13.1530	KEAVEDIKRHRADNRANSVLTQVMRKGLKLVSVHSKDIHPGDVVRIKNSEEVHADVVMLSS	180
WT-HH41	KEAVEDIKRHRADNRANSVLTQVMRKGLKLVSVHSKDIHPGDVVRIKNSEEVHADVVMLSS	180
WT-HH42	KEAVEDIKRHRADNRANSVLTQVMRKGLKLVSVHSKDIHPGDVVRIKNSEEVHADVVMLSS	180
WT-HH43	KEAVEDIKRHRADNRANSVLTQVMRKGLKLVSVHSKDIHPGDVVRIKNSEEVHADVVMLSS	180
WT-HH44	KEAVEDIKRHRADNRANSVLTQVMRKGLKLVSVHSKDIHPGDVVRIKNSEEVHADVVMLSS	180
WT-HH48	KEAVEDIKRHRADNRANSVLTQVMRKGLKLVSVHSKDIHPGDVVRIKNSEEVHADVVMLSS	180
WT-HH49	KEAVEDIKRHRADNRANSVLTQVMRKGLKLVSVHSKDIHPGDVVRIKNSEEVHADVVMLSS	180
WT-HH5	KEAVEDIKRHRADNRANSVLTQVMRKGLKLVSVHSKDIHPGDVVRIKNSEEVHADVVMLSS	180
WT-HH6	KEAVEDIKRHRADNRANSVLTQVMRKGLKLVSVHSKDIHPGDVVRIKNSEEVHADVVMLSS	180
WT-HH8	KEAVEDIKRHRADNRANSVLTQVMRKGLKLVSVHSKDIHPGDVVRIKNSEEVHADVVMLSS	180
WT-HH9	KEAVEDIKRHRADNRANSVLTQVMRKGLKLVSVHSKDIHPGDVVRIKNSEEVHADVVMLSS	180
WT-HH10	KEAVEDIKRHRADNRANSVLTQVMRKGLKLVSVHSKDIHPGDVVRIKNSEEVHADVVMLSS	180
WT-HH12	KEAVEDIKRHRADNRANSVLTQVMRKGLKLVSVHSKDIHPGDVVRIKNSEEVHADVVMLSS	180

LmxM.13.1530	SLEEGQAFIDTCNLDGESNLKPRKALEVTWGLCEIETIMNTTAVLHTSKPDPGLLSWTGL	240
WT-HH41	SLEEGQAFIDTCNLDGESNLKPRKALEVTWGLCEIETIMNTTAVLHTSKPDPGLLSWTGL	240
WT-HH42	SLEEGQAFIDTCNLDGESNLKPRKALEVTWGLCEIETIMNTTAVLHTSKPDPGLLSWTGL	240
WT-HH43	SLEEGQAFIDTCNLDGESNLKPRKALEVTWGLCEIETIMNTTAVLHTSKPDPGLLSWTGL	240
WT-HH44	SLEEGQAFIDTCNLDGESNLKPRKALEVTWGLCEIETIMNTTAVLHTSKPDPGLLSWTGL	240
WT-HH48	SLEEGQAFIDTCNLDGESNLKPRKALEVTWGLCEIETIMNTTAVLHTSKPDPGLLSWTGL	240
WT-HH49	SLEEGQAFIDTCNLDGESNLKPRKALEVTWGLCEIETIMNTTAVLHTSKPDPGLLSWTGL	240
WT-HH5	SLEEGQAFIDTCNLDGESNLKPRKALEVTWGLCEIETIMNTTAVLHTSKPDPGLLSWTGL	240
WT-HH6	SLEEGQAFIDTCNLDGESNLKPRKALEVTWGLCEIETIMNTTAVLHTSKPDPGLLSWTGL	240
WT-HH8	SLEEGQAFIDTCNLDGESNLKPRKALEVTWGLCEIETIMNTTAVLHTSKPDPGLLSWTGL	240
WT-HH9	SLEEGQAFIDTCNLDGESNLKPRKALEVTWGLCEIETIMNTTAVLHTSKPDPGLLSWTGL	240
WT-HH10	SLEEGQAFIDTCNLDGESNLKPRKALEVTWGLCEIETIMNTTAVLHTSKPDPGLLSWTGL	240
WT-HH12	SLEEGQAFIDTCNLDGESNLKPRKALEVTWGLCEIETIMNTTAVLHTSKPDPGLLSWTGL	240

LmxM.13.1530	LEINGEEHALSLDQFLYRGCVLRNTDWAAGMVAYAGVDTKLFRLNPKPKPKSSNLDRKLN	300
WT-HH41	LEINGEEHALSLDQFLYRGCVLRNTDWAAGMVAYAGVDTKLFRLNPKPKPKSSNLDRKLN	300
WT-HH42	LEINGEEHALSLDQFLYRGCVLRNTDWAAGMVAYAGVDTKLFRLNPKPKPKSSNLDRKLN	300
WT-HH43	LEINGEEHALSLDQFLYRGCVLRNTDWAAGMVAYAGVDTKLFRLNPKPKPKSSNLDRKLN	300
WT-HH44	LEINGEEHALSLDQFLYRGCVLRNTDWAAGMVAYAGVDTKLFRLNPKPKPKSSNLDRKLN	300
WT-HH48	LEINGEEHALSLDQFLYRGCVLRNTDWAAGMVAYAGVDTKLFRLNPKPKPKSSNLDRKLN	300
WT-HH49	LEINGEEHALSLDQFLYRGCVLRNTDWAAGMVAYAGVDTKLFRLNPKPKPKSSNLDRKLN	300
WT-HH5	LEINGEEHALSLDQFLYRGCVLRNTDWAAGMVAYAGVDTKLFRLNPKPKPKSSNLDRKLN	300
WT-HH6	LEINGEEHALSLDQFLYRGCVLRNTDWAAGMVAYAGVDTKLFRLNPKPKPKSSNLDRKLN	300
WT-HH8	LEINGEEHALSLDQFLYRGCVLRNTDWAAGMVAYAGVDTKLFRLNPKPKPKSSNLDRKLN	300
WT-HH9	LEINGEEHALSLDQFLYRGCVLRNTDWAAGMVAYAGVDTKLFRLNPKPKPKSSNLDRKLN	300

WT-HH10	LEINGEEHALSLDQFLYRGCVLRNTDWAAGMVAYAGVDTKLFRLKPKPKSSNLDRKLN	300
WT-HH12	LEINGEEHALSLDQFLYRGCVLRNTDWAAGMVAYAGVDTKLFRLKPKPKSSNLDRKLN	300

LmxM.13.1530	YFIIAIL	307
WT-HH41	YFIIAIL	307
WT-HH42	YFIIAIL	307
WT-HH43	YFIIAIL	307
WT-HH44	YFIIAIL	307
WT-HH48	YFIIAIL	307
WT-HH49	YFIIAIL	307
WT-HH5	YFIIAIL	307
WT-HH6	YFIIAIL	307
WT-HH8	YFIIAIL	307
WT-HH9	YFIIAIL	307
WT-HH10	YFIIAIL	307
WT-HH12	YFIIAIL	307

Fragment 2

LmxM.13.1530	RQNITLWGYRYSYFILLSY	360
WT-HH19	RQNITLWGYRYSYFILLSY	360
WT-HH21	RQNITLWGYRYSYFILLSY	360
WT-HH22	RQNITLWGYRYSYFILLSY	360
WT-HH23	RQNITLWGYRYSYFILLSY	360
WT-HH24	RQNITLWGYRYSYFILLSY	360
WT-HH25	RQNITLWGYRYSYFILLSY	360
R-HH28	RQNITLWGYRYSYFILLSY	360
R-HH29	RQNITLWGYRYSYFILLSY	360
R-HH31	RQNITLWGYRYSYFILLSY	360
R-HH32	RQNITLWGYRYSYFILLSY	360
R-HH33	RQNITLWGYRYSYFILLSY	360
R-HH34	RQNITLWGYRYSYFILLSY	360

LmxM.13.1530	CVPISLFVVTIELCKVIAQWMRMDCLMMEYMNNRWRHCQPNTSNLNEQLAMVRFIFSDKT	420
WT-HH19	CVPISLFVVTIELCKVIAQWMRMDCLMMEYMNNRWRHCQPNTSNLNEQLAMVRFIFSDKT	420
WT-HH21	CVPISLFVVTIELCKVIAQWMRMDCLMMEYMNNRWRHCQPNTSNLNEQLAMVRFIFSDKT	420
WT-HH22	CVPISLFVVTIELCKVIAQWMRMDCLMMEYMNNRWRHCQPNTSNLNEQLAMVRFIFSDKT	420
WT-HH23	CVPISLFVVTIELCKVIAQWMRMDCLMMEYMNNRWRHCQPNTSNLNEQLAMVRFIFSDKT	420
WT-HH24	CVPISLFVVTIELCKVIAQWMRMDCLMMEYMNNRWRHCQPNTSNLNEQLAMVRFIFSDKT	420
WT-HH25	CVPISLFVVTIELCKVIAQWMRMDCLMMEYMNNRWRHCQPNTSNLNEQLAMVRFIFSDKT	420
R-HH28	CVPISLFVVTIELCKVIAQWMRMDCLMMEYMNNRWRHCQPNTSNLNEQLAMVRFIFSDKT	420
R-HH29	CVPISLFVVTIELCKVIAQWMRMDCLMMEYMNNRWRHCQPNTSNLNEQLAMVRFIFSDKT	420
R-HH31	CVPISLFVVTIELCKVIAQWMRMDCLMMEYMNNRWRHCQPNTSNLNEQLAMVRFIFSDKT	420
R-HH32	CVPISLFVVTIELCKVIAQWMRMDCLMMEYMNNRWRHCQPNTSNLNEQLAMVRFIFSDKT	420

R-HH33	CVPISLFVTTIELCKVIAQAWMRMDCLMMEYMNNRWRHCQPNTSNLNEQLAMVRFIFSDKT	420
R-HH34	CVPISLFVTTIELCKVIAQAWMRMDCLMMEYMNNRWRHCQPNTSNLNEQLAMVRFIFSDKT	420

LmxM.13.1530	GTLTENVMKFKQGDALGIPIEADSLDKCIVQLRKEAESKRLGPLEYFLALALCNTVQPF	480
WT-HH19	GTLTENVMKFKQGDALGIPIEADSLDKCIVQLRKEAESKRLGPLEYFLALALCNTVQPF	480
WT-HH21	GTLTENVMKFKQGDALGIPIEADSLDKCIVQLRKEAESKRLGPLEYFLALALCNTVQPF	480
WT-HH22	GTLTENVMKFKQGDALGIPIEADSLDKCIVQLRKEAESKRLGPLEYFLALALCNTVQPF	480
WT-HH23	GTLTENVMKFKQGDALGIPIEADSLDKCIVQLRKEAESKRLGPLEYFLALALCNTVQPF	480
WT-HH24	GTLTENVMKFKQGDALGIPIEADSLDKCIVQLRKEAESKRLGPLEYFLALALCNTVQPF	480
WT-HH25	GTLTENVMKFKQGDALGIPIEADSLDKCIVQLRKEAESKRLGPLEYFLALALCNTVQPF	480
R-HH28	GTLTENVMKFKQGDALGIPIEADSLDKCIVQLRKEAESKRLGPLEYFLALALCNTVQPF	480
R-HH29	GTLTENVMKFKQGDALGIPIEADSLDKCIVQLRKEAESKRLGPLEYFLALALCNTVQPF	480
R-HH31	GTLTENVMKFKQGDALGIPIEADSLDKCIVQLRKEAESKRLGPLEYFLALALCNTVQPF	480
R-HH32	GTLTENVMKFKQGDALGIPIEADSLDKCIVQLRKEAESKRLGPLEYFLALALCNTVQPF	480
R-HH33	GTLTENVMKFKQGDALGIPIEADSLDKCIVQLRKEAESKRLGPLEYFLALALCNTVQPF	480
R-HH34	GTLTENVMKFKQGDALGIPIEADSLDKCIVQLRKEAESKRLGPLEYFLALALCNTVQPF	480

LmxM.13.1530	KDDTDGLSVIYEGSSPDEVALVETAAAVGYRLINRRTTKSITLLLQNDTRKVNILATLEF	540
WT-HH19	KDDTDGLSVIYEGSSPDEVALVETAAAVGYRLINRRTTKSITLLLQNDTRKVNILATLEF	540
WT-HH21	KDDTDGLSVIYEGSSPDEVALVETAAAVGYRLINRRTTKSITLLLQNDTRKVNILATLEF	540
WT-HH22	KDDTDGLSVIYEGSSPDEVALVETAAAVGYRLINRRTTKSITLLLQNDTRKVNILATLEF	540
WT-HH23	KDDTDGLSVIYEGSSPDEVALVETAAAVGYRLINRRTTKSITLLLQNDTRKVNILATLEF	540
WT-HH24	KDDTDGLSVIYEGSSPDEVALVETAAAVGYRLINRRTTKSITLLLQNDTRKVNILATLEF	540
WT-HH25	KDDTDGLSVIYEGSSPDEVALVETAAAVGYRLINRRTTKSITLLLQNDTRKVNILATLEF	540
R-HH28	KDDTDGLSVIYEGSSPDEVALVETAAAVGYRLINRRTTKSITLLLQNDTRKVNILATLEF	540
R-HH29	KDDTDGLSVIYEGSSPDEVALVETAAAVGYRLINRRTTKSITLLLQNDTRKVNILATLEF	540
R-HH31	KDDTDGLSVIYEGSSPDEVALVETAAAVGYRLINRRTTKSITLLLQNDTRKVNILATLEF	540
R-HH32	KDDTDGLSVIYEGSSPDEVALVETAAAVGYRLINRRTTKSITLLLQNDTRKVNILATLEF	540
R-HH33	KDDTDGLSVIYEGSSPDEVALVETAAAVGYRLINRRTTKSITLLLQNDTRKVNILATLEF	540
R-HH34	KDDTDGLSVIYEGSSPDEVALVETAAAVGYRLINRRTTKSITLLLQNDTRKVNILATLEF	540

LmxM.13.1530	TPDRKMMSIIVEDSDKQIMLYNKGADSFIRPQLSRAPDVQEHIESVDIPLTEMSSSGLR	600
WT-HH19	TPDRKMMSIIVEDSDKQIMLYNKGADSFIRPQLSRAPDVQEHIESVDIPLTEMSSSGLR	600
WT-HH21	TPDRKMMSIIVEDSDKQIMLYNKGADSFIRPQLSRAPDVQEHIESVDIPLTEMSSSGLR	600
WT-HH22	TPDRKMMSIIVEDSDKQIMLYNKGADSFIRPQLSRAPDVQEHIESVDIPLTEMSSSGLR	600
WT-HH23	TPDRKMMSIIVEDSDKQIMLYNKGADSFIRPQLSRAPDVQEHIESVDIPLTEMSSSGLR	600
WT-HH24	TPDRKMMSIIVEDSDKQIMLYNKGADSFIRPQLSRAPDVQEHIESVDIPLTEMSSSGLR	600
WT-HH25	TPDRKMMSIIVEDSDKQIMLYNKGADSFIRPQLSRAPDVQEHIESVDIPLTEMSSSGLR	600
R-HH28	TPDRKMMSIIVEDSDKQIMLYNKGADSFIRPQLSRAPDVQEHIESVDIPLTEMSSSGLR	600
R-HH29	TPDRKMMSIIVEDSDKQIMLYNKGADSFIRPQLSRAPDVQEHIESVDIPLTEMSSSGLR	600
R-HH31	TPDRKMMSIIVEDSDKQIMLYNKGADSFIRPQLSRAPDVQEHIESVDIPLTEMSSSGLR	600
R-HH32	TPDRKMMSIIVEDSDKQIMLYNKGADSFIRPQLSRAPDVQEHIESVDIPLTEMSSSGLR	600
R-HH33	TPDRKMMSIIVEDSDKQIMLYNKGADSFIRPQLSRAPDVQEHIESVDIPLTEMSSSGLR	600

R-HH34	TPDRKMMSIIVEDSDTKQIMLYNKGADSFIRPQLSRAPDVQEHIESVDIPLTEMSSSGLR	600

LmxM.13.1530	TLLVCAKDITRRQFDLWYEKFEVEVGKSLQNRSSKIDKVCLEMEQDMRLVGATAIEDKLQD	660
WT-HH19	TLLVCAKDITRRQFDLWYEKFEVEVGKSLQNRSSKIDKVCLEMEQDMRLVGATAIEDKLQD	660
WT-HH21	TLLVCAKDITRRQFDLWYEKFEVEVGKSLQNRSSKIDKVCLEMEQDMRLVGATAIEDKLQD	660
WT-HH22	TLLVCAKDITRRQFDLWYEKFEVEVGKSLQNRSSKIDKVCLEMEQDMRLVGATAIEDKLQD	660
WT-HH23	TLLVCAKDITRRQFDLWYEKFEVEVGKSLQNRSSKIDKVCLEMEQDMRLVGATAIEDKLQD	660
WT-HH24	TLLVCAKDITRRQFDLWYEKFEVEVGKSLQNRSSKIDKVCLEMEQDMRLVGATAIEDKLQD	660
WT-HH25	TLLVCAKDITRRQFDLWYEKFEVEVGKSLQNRSSKIDKVCLEMEQDMRLVGATAIEDKLQD	660
R-HH28	TLLVCAKDITRRQFDLWYEKFEVEVGKSLQNRSSKIDKVCLEMEQDMRLVGATAIEDKLQD	660
R-HH29	TLLVCAKDITRRQFDLWYEKFEVEVGKSLQNRSSKIDKVCLEMEQDMRLVGATAIEDKLQD	660
R-HH31	TLLVCAKDITRRQFDLWYEKFEVEVGKSLQNRSSKIDKVCLEMEQDMRLVGATAIEDKLQD	660
R-HH32	TLLVCAKDITRRQFDLWYEKFEVEVGKSLQNRSSKIDKVCLEMEQDMRLVGATAIEDKLQD	660
R-HH33	TLLVCAKDITRRQFDLWYEKFEVEVGKSLQNRSSKIDKVCLEMEQDMRLVGATAIEDKLQD	660
R-HH34	TLLVCAKDITRRQFDLWYEKFEVEVGKSLQNRSSKIDKVCLEMEQDMRLVGATAIEDKLQD	660

LmxM.13.1530	EVPETLSFFLNAGVIIWMLT	680
WT-HH19	EVPETLSFFLNAGVIIWMLT	680
WT-HH21	EVPETLSFFLNAGVIIWMLT	680
WT-HH22	EVPETLSFFLNAGVIIWMLT	680
WT-HH23	EVPETLSFFLNAGVIIWMLT	680
WT-HH24	EVPETLSFFLNAGVIIWMLT	680
WT-HH25	EVPETLSFFLNAGVIIWMLT	680
R-HH28	EVPETLSFFLNAGVIIWMLT	680
R-HH29	EVPETLSFFLNAGVIIWMLT	680
R-HH31	EVPETLSFFLNAGVIIWMLT	680
R-HH32	EVPETLSFFLNAGVIIWMLT	680
R-HH33	EVPETLSFFLNAGVIIWMLT	680
R-HH34	EVPETLSFFLNAGVIIWMLT	680

Fragment 3

LmxM.13.1530	KERRCTLVIDGPGLNISMEHYFNQFLRISHQLNSAVCCRL	780
WT-HH77	KERRCTLVIDGPGLNISMEHYFNQFLRISHQLNSAVCCRL	780
WT-HH79	KERRCTLVIDGPGLNISMEHYFNQFLRISHQLNSAVCCRL	780
WT-HH80	KERRCTLVIDGPGLNISMEHYFNQFLRISHQLNSAVCCRL	780
WT-HH81	KERRCTLVIDGPGLNISMEHYFNQFLRISHQLNSAVCCRL	780
WT-HH82	KERRCTLVIDGPGLNISMEHYFNQFLRISHQLNSAVCCRL	780
WT-HH83	KERRCTLVIDGPGLNISMEHYFNQFLRISHQLNSAVCCRL	780
R-HH60	KERRCTLVIDGPGLNISMEHYFNQFLRISHQLNSAVCCRL	780
R-HH61	KERRCTLVIDGPGLNISMEHYFNQFLRISHQLNSAVCCRL	780
R-HH63	KERRCTLVIDGPGLNISMEHYFNQFLRISHQLNSAVCCRL	780
R-HH64	KERRCTLVIDGPGLNISMEHYFNQFLRISHQLNSAVCCRL	780
R-HH65	KERRCTLVIDGPGLNISMEHYFNQFLRISHQLNSAVCCRL	780

R-HH67	KERRCTLVIDGPGLNISMEHYFNQFLRISHQLNSAVCCRL 780 *****	
LmxM.13.1530	TPIQKASVVRMFQKSTGKTALAIGDGANDVSMIREGRVGVGIIGLEGHAHAALAADYAI PR	840
WT-HH77	TPIQKASVVRMFQKSTGKTALAIGDGANDVSMIREGRVGVGIIGLEGHAHAALAADYAI PR	840
WT-HH79	TPIQ R ASVVRMFQKSTGKTALAIGDGANDVSMIREGRVGVGIIGLEGHAHAALAADYAI PR	840
WT-HH80	TPIQKASVVRMFQKSTGKTALAIGDGANDVSMIREGRVGVGIIGLEGHAHAALAADYAI PR	840
WT-HH81	TPIQKASVVRMFQKSTGKTALAIGDGANDVSMIREGRVGVGIIGLEGHAHAALAADYAI PR	840
WT-HH82	TPIQKASVVRMFQKSTGKTALAIGDGANDVSMIREGRVGVGIIGLEGHAHAALAADYAI PR	840
WT-HH83	TPIQKASVVRMFQKSTGKTALAIGDGANDVSMIREGRVGVGIIGLEGHAHAALAADYAI PR	840
R-HH60	TPIQKASVVRMFQKSTGKTALAIGDGANDVSMIREGRVGVGIIGLEGHAHAALAADYAI PR	840
R-HH61	TPIQKASVVRMFQKSTGKTALAIGDGANDVSMIREGRVGVGIIGLEGHAHAALAADYAI PR	840
R-HH63	TPIQKASVVRMFQKSTGKTALAIGDGANDVSMIREGRVGVGIIGLEGHAHAALAADYAI PR	840
R-HH64	TPIQKASVVRMFQKSTGKTALAIGDGANDVSMIREGRVGVGIIGLEGHAHAALAADYAI PR	840
R-HH65	TPIQKASVVRMFQKSTGKTALAIGDGANDVSMIREGRVGVGIIGLEGHAHAALAADYAI PR	840
R-HH67	TPIQKASVVRMFQKSTGKTALAIGDGANDVSMIREGRVGVGIIGLEGHAHAALAADYAI PR **** *****	840
LmxM.13.1530	FKHLRRLCAVHGGRYSLFRNASCILVSFHKNITVSVVQFIFAFYVGFSGLTFLFDGWMLTFY	900
WT-HH77	FKHLRRLCAVHGGRYSLFRNASCILVSFHKNITVSVVQFIFAFYVGFSGLTFLFDGWMLTFY	900
WT-HH79	FKHLRRLCAVHGGRYSLFRNASCILVSFHKNITVSVVQFIF L AFYVGFSGLTFLFDGWMLTFY	900
WT-HH80	FKHLRRLCAVHGGRYSLFRNASCILVSFHKNITVSVVQFIFAFYVGFSGLTFLFDGWMLTFY	900
WT-HH81	FKHLRRLCAVHGGRYSLFRNASCILVSFHKNITVSVVQFIFAFYVGFSGLTFLFDGWMLTFY	900
WT-HH82	FKHLRRLCAVHGGRYSLFRNASCILVSFHKNITVSVVQFIFAFYVGFSGLTFLFDGWMLTFY	900
WT-HH83	FKHLRRLCAVHGGRYSLFRNASCILVSFHKNITVSVVQFIFAFYVGFSGLTFLFDGWMLTFY	900
R-HH60	FKHLRRLCAVHGGRYSLFRNASCILVSFHKNITVSVVQFIFAFYVGFSGLTFLFDGWMLTFY	900
R-HH61	FKHLRRLCAVHGGRYSLFRNASCILVSFHKNITVSVVQFIFAFYVGFSGLTFLFDGWMLTFY	900
R-HH63	FKHLRRLCAVHGGRYSLFRNASCILVSFHKNITVSVVQFIFAFYVGFSGLTFLFDGWMLTFY	900
R-HH64	FKHLRRLCAVHGGRYSLFRNASCILVSFHKNITVSVVQFIFAFYVGFSGLTFLFDGWMLTFY	900
R-HH65	FKHLRRLCAVHGGRYSLFRNASCILVSFHKNITVSVVQFIFAFYVGFSGLTFLFDGWMLTFY	900
R-HH67	FKHLRRLCAVHGGRYSLFRNASCILVSFHKNITVSVVQFIFAFYVGFSGLTFLFDGWMLTFY *****	900
LmxM.13.1530	NVLMTSVPPFFIGIFDKDLPEEALLERPKLYTPLSHGEYFNVTLLRWFAESLITALILF	960
WT-HH77	NVLMTSVPPFFIGIFDKDLPEEALLE Q KLYTPLSHGEYFNVTLLRWFAESLITALILF	960
WT-HH79	NVLMTSVPPFFIGIFDKDLPEEALLERPKLYTPLSHGEYFNVTLLRWFAESLITALILF	960
WT-HH80	NVLMTSVPPFFIGIFDKDLPEEALLERPKLYTPLSHGEYFNVTLLRWFAESLITALILF	960
WT-HH81	NVLMTSVPPFFIGIFDKDLPEEALLERPKLYTPLSHGEYFNVTLLRWFAESLITALILF	960
WT-HH82	NVLMTSVPPFFIGIFDKDLPEEALLERPKLYTPLSHGEYFNVTLLRWFAESLITALILF	960
WT-HH83	NVLMTSVPPFFIGIFDKDLPEEALLERPKLYTPLSHGEYFNVTLLRWFAESLITALILF	960
R-HH60	NVLMTSVPPFFIGIFDKDLPEEALLERPKLYTPLSHGEYFNVTLLRWFAESLITALILF	960
R-HH61	NVLMTSVPPFFIGIFDKDLPEEALLERPKLYTPLSHGEYFNVTLLRWFAESLITALILF	960
R-HH63	NVLMTSVPPFFIGIFDKDLPEEALLERPKLYTPLSHGEYFNVTLLRWFAESLITALILF	960
R-HH64	NVLMTSVPPFFIGIFDKDLPEEALLERPKLYTPLSHGEYFNVTLLRWFAESLITALILF	960
R-HH65	NVLMTSVPPFFIGIFDKDLPEEALLERPKLYTPLSHGEYFNVTLLRWFAESLITALILF	960
R-HH67	NVLMTSVPPFFIGIFDKDLPEEALLERPKLYTPLSHGEYFNVTLLRWFAESLITALILF	960

LmxM.13.1530	YAAYP TLVHQD GSHQRYTGAETGTLVFSG	989
WT-HH77	YAAYP TLVHQD GSHQRYTGAETGTLVFSG	989
WT-HH79	YAAYP TLVHQD GSHQRYTGAETGTLVFSG	989
WT-HH80	YAAYP TLVHQD GSHQRYTGAETGTLVFSG	989
WT-HH81	YAAYP TLVHQD GSHQRYTGAETGTLVFSG	989
WT-HH82	YAAYP TLVHQD GSHQRYTGAETGTLVFSG	989
WT-HH83	YAAYP TLVHQD GSHQRYTGAETGTLVFSG	989
R-HH60	YAAYP TLVHQD GSHQRYTGAETGTLVFSG	989
R-HH61	YAAYP TLVHQD GSHQRYTGAETGTLVFSG	989
R-HH63	YAAYP TLVHQD GSHQRYTGAETGTLVFSG	989
R-HH64	YAAYP TLVHQD GSHQRYTGAETGTLVFSG	989
R-HH65	YAAYP TLVHQD GSHQRYTGAETGTLVFSG	989
R-HH67	YAAYP TLVHQD GSHQRYTGAETGTLVFSG	989

Appendix 3 (Chapter 4)

Multiple sequence alignment for each fragment of LmROS3 gene. 9 clones for each fragment of LmROS3 sequenced compared LmxM.31.0510. The WT-prefix is for the pre-selection wildtype and the R-prefix for 700022-selected parasites. The HH code uniquely identifies the PCR clone sequenced

LmxM.31.0510	ATGGCGTCTCTACCCCAAAGCCACATTTGAAAAACCGCGTTGAGCAGCAGCAGCTGCCG	60
WT-HH21	ATGGCGTCTCTACCCCAAAGCCACATTTGAAAAACCGCGTTGAGCAGCAGCAGCTGCCG	60
WT-HH22	ATGGCGTCTCTACCCCAAAGCCACATTTGAAAAACCGCGTTGAGCAGCAGCAGCTGCCG	60
WT-HH24	ATGGCGTCTCTACCCCAAAGCCACATTTGAAAAACCGCGTTGAGCAGCAGCAGCTGCCG	60
WT-HH25	ATGGCGTCTCTACCCCAAAGCCACATTTGAAAAACCGCGTTGAGCAGCAGCAGCTGCCG	60
WT-HH27	ATGGCGTCTCTACCCCAAAGCCACATTTGAAAAACCGCGTTGAGCAGCAGCAGCTGCCG	60
WT-HH30	ATGGCGTCTCTACCCCAAAGCCACATTTGAAAAACCGCGTTGAGCAGCAGCAGCTGCCG	60
WT-HH31	ATGGCGTCTCTACCCCAAAGCCACATTTGAAAAACCGCGTTGAGCAGCAGCAGCTGCCG	60
WT-HH32	ATGGCGTCTCTACCCCAAAGCCACATTTGAAAAACCGCGTTGAGCAGCAGCAGCTGCCG	60
WT-HH34	ATGGCGTCTCTACCCCAAAGCCACATTTGAAAAACCGCGTTGAGCAGCAGCAGCTGCCG	60
R-HH18	ATGGCGTCTCTACCCCAAAGCCACATTTGAAAAACCGCGTTGAGCAGCAGCAGCTGCCG	60
R-HH63	ATGGCGTCTCTACCCCAAAGCCACATTTGAAAAACCGCGTTGAGCAGCAGCAGCTGCCG	60
R-HH64	ATGGCGTCTCTACCCCAAAGCCACATTTGAAAAACCGCGTTGAGCAGCAGCAGCTGCCG	60
R-HH65	ATGGCGTCTCTACCCCAAAGCCACATTTGAAAAACCGCGTTGAGCAGCAGCAGCTGCCG	60
R-HH67	ATGGCGTCTCTACCCCAAAGCCACATTTGAAAAACCGCGTTGAGCAGCAGCAGCTGCCG	60
R-HH68	ATGGCGTCTCTACCCCAAAGCCACATTTGAAAAACCGCGTTGAGCAGCAGCAGCTGCCG	60
R-HH69	ATGGCGTCTCTACCCCAAAGCCACATTTGAAAAACCGCGTTGAGCAGCAGCAGCTGCCG	60
R-HH70	ATGGCGTCTCTACCCCAAAGCCACATTTGAAAAACCGCGTTGAGCAGCAGCAGCTGCCG	60
R-HH71	ATGGCGTCTCTACCCCAAAGCCACATTTGAAAAACCGCGTTGAGCAGCAGCAGCTGCCG	60

LmxM.31.0510	CACGTC TTTGTT CCTCATTCGCGCGTGTCTGTTTCTGTTGTCTTTTTTATTCTGGCAATT	120
WT-HH21	CACGTC TTTGTT CCTCATTCGCGCGTGTCTGTTTCTGTTGTCTTTTTTATTCTGGCAATT	120
WT-HH22	CACGTC TTTGTT CCTCATTCGCGCGTGTCTGTTTCTGTTGTCTTTTTTATTCTGGCAATT	120
WT-HH24	CACGTC TTTGTT CCTCATTCGCGCGTGTCTGTTTCTGTTGTCTTTTTTATTCTGGCAATT	120
WT-HH25	CACGTC TTTGTT CCTCATTCGCGCGTGTCTGTTTCTGTTGTCTTTTTTATTCTGGCAATT	120
WT-HH27	CACGTC TTTGTT CCTCATTCGCGCGTGTCTGTTTCTGTTGTCTTTTTTATTCTGGCAATT	120
WT-HH30	CACGTC TTTGTT CCTCATTCGCGCGTGTCTGTTTCTGTTGTCTTTTTTATTCTGGCAATT	120

R-HH70	GAGATCACGGAGCAATACCCGACTGCGCCGTACGGATCGCAGAAGTTTGTGCAACTCGAG	960
R-HH71	GAGATCACGGAGCAATACCCGACTGCGCCGTACGGATCGCAGAAGTTTGTGCAACTCGAG	960
	* ****	
LmxM.31.0510	ACCCGATCATGGATCGGGGGTAGAAGCCATGTTCTCGGCTCCCTGCTGATAATCATGGGT	1020
WT-HH21	ACCCGATCATGGATCGGGGGTAGAAGCCATGTTCTCGGCTCCCTGCTGATAATCATGGGT	1020
R-HH22	ACCCGATCATGGATCGGGGGTAGAAGCCATGTTCTCGGCTCCCTGCTGATAATCATGGGT	1020
WT-HH24	ACCCGATCATGGATCGGGGGTAGAAGCCATGTTCTCGGCTCCCTGCTGATAATCATGGGT	1020
WT-HH25	ACCCGATCATGGATCGGGGGTAGAAGCCATGTTCTCGGCTCCCTGCTGATAATCATGGGT	1020
WT-HH27	ACCCGATCATGGATCGGGGGTAGAAGCCATGTTCTCGGCTCCCTGCTGATAATCATGGGT	1020
WT-HH30	ACCCGATCATGGATCGGGGGTAGAAGCCATGTTCTCGGCTCCCTGCTGATAATCATGGGT	1020
WT-HH31	ACCCGATCATGGATCGGGGGTAGAAGCCATGTTCTCGGCTCCCTGCTGATAATCATGGGT	1020
WT-HH32	ACCCGATCATGGATCGGGGGTAGAAGCCATGTTCTCGGCTCCCTGCTGATAATCATGGGT	1020
WT-HH34	ACCCGATCATGGATCGGGGGTAGAAGCCATGTTCTCGGCTCCCTGCTGATAATCATGGGT	1020
R-HH18	ACCCGATCATGGATCGGGGGTAGAAGCCATGTTCTCGGCTCCCTGCTGATAATCATGGGT	1020
R-HH63	ACCCGATCATGGATCGGGGGTAGAAGCCATGTTCTCGGCTCCCTGCTGATAATCATGGGT	1020
R-HH64	ACCCGATCATGGATCGGGGGTAGAAGCCATGTTCTCGGCTCCCTGCTGATAATCATGGGT	1020
R-HH65	ACCCGATCATGGATCGGGGGTAGAAGCCATGTTCTCGGCTCCCTGCTGATAATCATGGGT	1020
R-HH67	ACCCGATCATGGATCGGGGGTAGAAGCCATGTTCTCGGCTCCCTGCTGATAATCATGGGT	1020
R-HH68	ACCCGATCATGGATCGGGGGTAGAAGCCATGTTCTCGGCTCCCTGCTGATAATCATGGGT	1020
R-HH69	ACCCGATCATGGATCGGGGGTAGAAGCCATGTTCTCGGCTCCCTGCTGATAATCATGGGT	1020
R-HH70	ACCCGATCATGGATCGGGGGTAGAAGCCATGTTCTCGGCTCCCTGCTGATAATCATGGGT	1020
R-HH71	ACCCGATCATGGATCGGGGGTAGAAGCCATGTTCTCGGCTCCCTGCTGATAATCATGGGT	1020
	* ****	
LmxM.31.0510	GGTACGGCCCTTATCATGGCAGTGACACTTCTTTCCGGTGAAGTGCTTGATCAGGCCAGGG	1080
WT-HH21	GGTACGGCCCTTATCATGGCAGTGACACTTCTTTCCGGTGAAGTGCTTGATCAGGCCAGGG	1080
WT-HH22	GGTACGGCCCTTATCATGGCAGTGACACTTCTTTCCGGTGAAGTGCTTGATCAGGCCAGGG	1080
WT-HH24	GGTACGGCCCTTATCATGGCAGTGACACTTCTTTCCGGTGAAGTGCTTGATCAGGCCAGGG	1080
WT-HH25	GGTACGGCCCTTATCATGGCAGTGACACTTCTTTCCGGTGAAGTGCTTGATCAGGCCAGGG	1080
WT-HH27	GGTACGGCCCTTATCATGGCAGTGACACTTCTTTCCGGTGAAGTGCTTGATCAGGCCAGGG	1080
WT-HH30	GGTACGGCCCTTATCATGGCAGTGACACTTCTTTCCGGTGAAGTGCTTGATCAGGCCAGGG	1080
WT-HH31	GGTACGGCCCTTATCATGGCAGTGACACTTCTTTCCGGTGAAGTGCTTGATCAGGCCAGGG	1080
WT-HH32	GGTACGGCCCTTATCATGGCAGTGACACTTCTTTCCGGTGAAGTGCTTGATCAGGCCAGGG	1080
WT-HH34	GGTACGGCCCTTATCATGGCAGTGACACTTCTTTCCGGTGAAGTGCTTGATCAGGCCAGGG	1080
R-HH18	GGTACGGCCCTTATCATGGCAGTGACACTTCTTTCCGGTGAAGTGCTTGATCAGGCCAGGG	1080
R-HH63	GGTACGGCCCTTATCATGGCAGTGACACTTCTTTCCGGTGAAGTGCTTGATCAGGCCAGGG	1080
R-HH64	GGTACGGCCCTTATCATGGCAGTGACACTTCTTTCCGGTGAAGTGCTTGATCAGGCCAGGG	1080
R-HH65	GGTACGGCCCTTATCATGGCAGTGACACTTCTTTCCGGTGAAGTGCTTGATCAGGCCAGGG	1080
R-HH67	GGTACGGCCCTTATCATGGCAGTGACACTTCTTTCCGGTGAAGTGCTTGATCAGGCCAGGG	1080
R-HH68	GGTACGGCCCTTATCATGGCAGTGACACTTCTTTCCGGTGAAGTGCTTGATCAGGCCAGGG	1080
R-HH69	GGTACGGCCCTTATCATGGCAGTGACACTTCTTTCCGGTGAAGTGCTTGATCAGGCCAGGG	1080
R-HH70	GGTACGGCCCTTATCATGGCAGTGACACTTCTTTCCGGTGAAGTGCTTGATCAGGCCAGGG	1080
R-HH71	GGTACGGCCCTTATCATGGCAGTGACACTTCTTTCCGGTGAAGTGCTTGATCAGGCCAGGG	1080
	* ****	
LmxM.31.0510	TATACAGAGTAG	1092
WT-HH21	TATACAGAGTAG	1092
WT-HH22	TATACAGAGTAG	1092
WT-HH24	TATACAGAGTAG	1092
WT-HH25	TATACAGAGTAG	1092
WT-HH27	TATACAGAGTAG	1092
WT-HH30	TATACAGAGTAG	1092
WT-HH31	TATACAGAGTAG	1092
WT-HH32	TATACAGAGTAG	1092
WT-HH34	TATACAGAGTAG	1092
R-HH18	TATACAGAGTAG	1092
R-HH63	TATACAGAGTAG	1092
R-HH64	TATACAGAGTAG	1092
R-HH65	TATACAGAGTAG	1092
R-HH67	TATACAGAGTAG	1092
R-HH68	TATACAGAGTAG	1092
R-HH69	TATACAGAGTAG	1092
R-HH70	TATACAGAGTAG	1092
R-HH71	TATACAGAGTAG	1092
	* ****	

Appendix 5 (Chapter 4)

Multiple amino acid sequences sequence alignment for each fragment of LmROS3 gene. 9

clones for each fragment of LmROS3 sequenced compared LmxM.31.0510. The WT-prefix is for the pre-selection wildtype and the R-prefix for 70022-selected parasites. The HH code uniquely identifies the PCR clone sequenced.

LmxM.31.0510	MASLPPKPHLKNRVEQQQLPHVFVPHSPLSVSVVFFILAILAIPIGVVVIVTGDRTTRLD	60
WT-HH21	MASLPPKPHLKNRVEQQQLPHVFVPHSPLSVSVVFFILAILAIPIGVVVIVTGDRTTRLD	60
WT-HH22	MASLPPKPHLKNRVEQQQLPHVFVPHSPLSVSVVFFILAILAIPIGVVVIVTGDRTTRLD	60
WT-HH24	MASLPPKPHLKNRVEQQQLPHVFVPHSPLSVSVVFFILAILAIPIGVVVIVTGDRTTRLD	60
WT-HH25	MASLPPKPHLKNRVEQQQLPHVFVPHSPLSVSVVFFILAILAIPIGVVVIVTGDRTTRLD	60
WT-HH27	MASLPPKPHLKNRVEQQQLPHVFVPHSPLSVSVVFFILAILAIPIGVVVIVTGDRTTRLD	60
WT-HH30	MASLPPKPHLKNRVEQQQLPHVFVPHSPLSVSVVFFILAILAIPIGVVVIVTGDRTTRLD	60
WT-HH31	MASLPPKPHLKNRVEQQQLPHVFVPHSPLSVSVVFFILAILAIPIGVVVIVTGDRTTRLD	60
WT-HH32	MASLPPKPHLKNRVEQQQLPHVFVPHSPLSVSVVFFILAILAIPIGVVVIVTGDRTTRLD	60
WT-HH34	MASLPPKPHLKNRVEQQQLPHVFVPHSPLSVSVVFFILAILAIPIGVVVIVTGDRTTRLD	60
R-HH18	MASLPPKPHLKNRVEQQQLPHVFVPHSPLSVSVVFFILAILAIPIGVVVIVTGDRTTRLD	60
R-HH63	MASLPPKPHLKNRVEQQQLPHVFVPHSPLSVSVVFFILAILAIPIGVVVIVTGDRTTRLD	60
R-HH64	MASLPPKPHLKNRVEQQQLPHVFVPHSPLSVSVVFFILAILAIPIGVVVIVTGDRTTRLD	60
R-HH65	MASLPPKPHLKNRVEQQQLPHVFVPHSPLSVSVVFFILAILAIPIGVVVIVTGDRTTRLD	60
R-HH67	MASLPPKPHLKNRVEQQQLPHVFVPHSPLSVSVVFFILAILAIPIGVVVIVTGDRTTRLD	60
R-HH68	MASLPPKPHLKNRVEQQQLPHVFVPHSPLSVSVVFFILAILAIPIGVVVIVTGDRTTRLD	60
R-HH69	MASLPPKPHLKNRVEQQQLPHVFVPHSPLSVSVVFFILAILAIPIGVVVIVTGDRTTRLD	60
R-HH70	MASLPPKPHLKNRVEQQQLPHVFVPHSPLSVSVVFFILAILAIPIGVVVIVTGDRTTRLD	60
R-HH71	MASLPPKPHLKNRVEQQQLPHVFVPHSPLSVSVVFFILAILAIPIGVVVIVTGDRTTRLD	60

LmxM.31.0510	FRYDHINNYKFAMGAAGEHAVNFPFNDTTYSSGVKTLVMFSLSQSLTAPVHLQYRLRPF	120
WT-HH21	FRYDHINNYKFAMGAAGEHAVNFPFNDTTYSSGVKTLVMFSLSQSLTAPVHLQYRLRPF	120
WT-HH22	FRYDHINNYKFAMGAAGEHAVNFPFNDTTYSSGVKTLVMFSLSQSLTAPVHLQYRLRPF	120
WT-HH24	FRYDHINNYKFAMGAAGEHAVNFPFNDTTYSSGVKTLVMFSLSQSLTAPVHLQYRLRPF	120
WT-HH25	FRYDHINNYKFAMGAAGEHAVNFPFNDTTYSSGVKTLVMFSLSQSLTAPVHLQYRLRPF	120
WT-HH27	FRYDHINNYKFAMGAAGEHAVNFPFNDTTYSSGVKTLVMFSLSQSLTAPVHLQYRLRPF	120
WT-HH30	FRYDHINNYKFAMGAAGEHAVNFPFNDTTYSSGVKTLVMFSLSQSLTAPVHLQYRLRPF	120
WT-HH31	FRYDHINNYKFAMGAAGEHAVNFPFNDTTYSSGVKTLVMFSLSQSLTAPVHLQYRLRPF	120
WT-HH32	FRYDHINNYKFAMGAAGEHAVNFPFNDTTYSSGVKTLVMFSLSQSLTAPVHLQYRLRPF	120
WT-HH34	FRYDHINNYKFAMGAAGEHAVNFPFNDTTYSSGVKTLVMFSLSQSLTAPVHLQYRLRPF	120
R-HH18	FRYDHINNYKFAMGAAGEHAVNFPFNDTTYSSGVKTLVMFSLSQSLTAPVHLQYRLRPF	120
R-HH63	FRYDHINNYKFAMGAAGEHAVNFPFNDTTYSSGVKTLVMFSLSQSLTAPVHLQYRLRPF	120
R-HH64	FRYDHINNYKFAMGAAGEHAVNFPFNDTTYSSGVKTLVMFSLSQSLTAPVHLQYRLRPF	120
R-HH65	FRYDHINNYKFAMGAAGEHAVNFPFNDTTYSSGVKTLVMFSLSQSLTAPVHLQYRLRPF	120
R-HH67	FRYDHINNYKFAMGAAGEHAVNFPFNDTTYSSGVKTLVMFSLSQSLTAPVHLQYRLRPF	120
R-HH68	FRYDHINNYKFAMGAAGEHAVNFPFNDTTYSSGVKTLVMFSLSQSLTAPVHLQYRLRPF	120
R-HH69	FRYDHINNYKFAMGAAGEHAVNFPFNDTTYSSGVKTLVMFSLSQSLTAPVHLQYRLRPF	120
R-HH70	FRYDHINNYKFAMGAAGEHAVNFPFNDTTYSSGVKTLVMFSLSQSLTAPVHLQYRLRPF	120
R-HH71	FRYDHINNYKFAMGAAGEHAVNFPFNDTTYSSGVKTLVMFSLSQSLTAPVHLQYRLRPF	120

LmxM.31.0510	QNYRYFTASVDYAQLSGRASVISKSCAPFRFPGEAAGIIVPGYYPGAYPWAIFNDSIS	180
WT-HH21	QNYRYFTASVDYAQLSGRASVISKSCAPFRFPGEAAGIIVPGYYPGAYPWAIFNDSIS	180
WT-HH22	QNYRYFTASVDYAQLSGRASVISKSCAPFRFPGEAAGIIVPGYYPGAYPWAIFNDSIS	180
WT-HH24	QNYRYFTASVDYAQLSGRASVISKSCAPFRFPGEAAGIIVPGYYPGAYPWAIFNDSIS	180
WT-HH25	QNYRYFTASVDYAQLSGRASVISKSCAPFRFPGEAAGIIVPGYYPGAYPWAIFNDSIS	180
WT-HH27	QNYRYFTASVDYAQLSGRASVISKSCAPFRFPGEAAGIIVPGYYPGAYPWAIFNDSIS	180
WT-HH30	QNYRYFTASVDYAQLSGRASVISKSCAPFRFPGEAAGIIVPGYYPGAYPWAIFNDSIS	180
WT-HH31	QNYRYFTASVDYAQLSGRASVISKSCAPFRFPGEAAGIIVPGYYPGAYPWAIFNDSIS	180
WT-HH32	QNYRYFTASVDYAQLSGRASVISKSCAPFRFPGEAAGIIVPGYYPGAYPWAIFNDSIS	180
WT-HH34	QNYRYFTASVDYAQLSGRASVISKSCAPFRFPGEAAGIIVPGYYPGAYPWAIFNDSIS	180
R-HH18	QNYRYFTASVDYAQLSGRASVISKSCAPFRFPGEAAGIIVPGYYPGAYPWAIFNDSIS	180
R-HH63	QNYRYFTASVDYAQLSGRASVISKSCAPFRFPGEAAGIIVPGYYPGAYPWAIFNDSIS	180
R-HH64	QNYRYFTASVDYAQLSGRASVISKSCAPFRFPGEAAGIIVPGYYPGAYPWAIFNDSIS	180
R-HH65	QNYRYFTASVDYAQLSGRASVISKSCAPFRFPGEAAGIIVPGYYPGAYPWAIFNDSIS	180
R-HH67	QNYRYFTASVDYAQLSGRASVISKSCAPFRFPGEAAGIIVPGYYPGAYPWAIFNDSIS	180
R-HH68	QNYRYFTASVDYAQLSGRASVISKSCAPFRFPGEAAGIIVPGYYPGAYPWAIFNDSIS	180
R-HH69	QNYRYFTASVDYAQLSGRASVISKSCAPFRFPGEAAGIIVPGYYPGAYPWAIFNDSIS	180

R-HH70	QNYRYFTASVDYAQLSGRASVISKSCAPFRFPGEAAGIIVPGYINPCGAYPWAI FNDSIS	180
R-HH71	QNYRYFTASVDYAQLSGRASVISKSCAPFRFPGEAAGIIVPGYINPCGAYPWAI FNDSIS *****	180
LmxM.31.0510	LYRMDGTLICDGGAF TVDGRSLLADNKC VKSGI ARKSDV KERFKPPRLIPGN GPMWSGGG	240
WT-HH21	LYRMDGTLICDGGAF TVDGRSLLADNKC VKSGI ARKSDV KERFKPPRLIPGN GPMWSGGG	240
WT-HH22	LYRMDGTLICDGGAF TVDGRSLLADNKC VKSGI ARKSDV KERFKPPRLIPGN GPMWSGGG	240
WT-HH24	LYRMDGTLICDGGAF TVDGRSLLADNKC VKSGI ARKSDV KERFKPPRLIPGN GPMWSGGG	240
WT-HH25	LYRMDGTLICDGGAF TVDGRSLLADNKC VKSGI ARKSDV KERFKPPRLIPGN GPMWSGGG	240
WT-HH27	LYRMDGTLICDGGAF TVDGRSLLADNKC VKSGI ARKSDV KERFKPPRLIPGN GPMWSGGG	240
WT-HH30	LYRMDGTLICDGGAF TVDGRSLLADNKC VKSGI ARKSDV KERFKPPRLIPGN GPMWSGGG	240
WT-HH31	LYRMDGTLICDGGAF TVDGRSLLADNKC VKSGI ARKSDV KERFKPPRLIPGN GPMWSGGG	240
WT-HH32	LYRMDGTLICDGGAF TVDGRSLLADNKC VKSGI ARKSDV KERFKPPRLIPGN GPMWSGGG	240
WT-HH34	LYRMDGTLICDGGAF TVDGRSLLADNKC VKSGI ARKSDV KERFKPPRLIPGN GPMWSGGG	240
R-HH18	LYRMDGTLICDGGAF TVDGRSLLADNKC VKSGI ARKSDV KERFKPPRLIPGN GPMWSGGG	240
R-HH63	LYRMDGTLICDGGAF TVDGRSLLADNKC VKSGI ARKSDV KERFKPPRLIPGN GPMWSGGG	240
R-HH64	LYRMDGTLICDGGAF TVDGRSLLADNKC VKSGI ARKSDV KERFKPPRLIPGN GPMWSGGG	240
R-HH65	LYRMDGTLICDGGAF TVDGRSLLADNKC VKSGI ARKSDV KERFKPPRLIPGN GPMWSGGG	240
R-HH67	LYRMDGTLICDGGAF TVDGRSLLADNKC VKSGI ARKSDV KERFKPPRLIPGN GPMWSGGG	240
R-HH68	LYRMDGTLICDGGAF TVDGRSLLADNKC VKSGI ARKSDV KERFKPPRLIPGN GPMWSGGG	240
R-HH69	LYRMDGTLICDGGAF TVDGRSLLADNKC VKSGI ARKSDV KERFKPPRLIPGN GPMWSGGG	240
R-HH70	LYRMDGTLICDGGAF TVDGRSLLADNKC VKSGI ARKSDV KERFKPPRLIPGN GPMWSGGG	240
R-HH71	LYRMDGTLICDGGAF TVDGRSLLADNKC VKSGI ARKSDV KERFKPPRLIPGN GPMWSGGG *****	240
LmxM.31.0510	DKSATDPYLKEGYYYQEPGHKIPFN VDEDLIVWLDPSFTSDVTKNYRILNV DLPAGDYFF	300
WT-HH21	DKSATDPYLKEGYYYQEPGHKIPFN VDEDLIVWLDPSFTSDVTKNYRILNV DLPAGDYFF	300
WT-HH22	DKSATDPYLKEGYYYQEPGHKIPFN VDEDLIVWLDPSFTSDVTKNYRILNV DLPAGDYFF	300
WT-HH24	DKSATDPYLKEGYYYQEPGHKIPFN VDEDLIVWLDPSFTSDVTKNYRILNV DLPAGDYFF	300
WT-HH25	DKSATDPYLKEGYYYQEPGHKIPFN VDEDLIVWLDPSFTSDVTKNYRILNV DLPAGDYFF	300
WT-HH27	DKSATDPYLKEGYYYQEPGHKIPFN VDEDLIVWLDPSFTSDVTKNYRILNV DLPAGDYFF	300
WT-HH30	DKSATDPYLKEGYYYQEPGHKIPFN VDEDLIVWLDPSFTSDVTKNYRILNV DLPAGDYFF	300
WT-HH31	DKSATDPYLKEGYYYQEPGHKIPFN VDEDLIVWLDPSFTSDVTKNYRILNV DLPAGDYFF	300
WT-HH32	DKSATDPYLKEGYYYQEPGHKIPFN VDEDLIVWLDPSFTSDVTKNYRILNV DLPAGDYFF	300
WT-HH34	DKSATDPYLKEGYYYQEPGHKIPFN VDEDLIVWLDPSFTSDVTKNYRILNV DLPAGDYFF	300
R-HH18	DKSATDPYLKEGYYYQEPGHKIPFN VDEDLIVWLDPSFTSDVTKNYRILNV DLPAGDYFF	300
R-HH63	DKSATDPYLKEGYYYQEPGHKIPFN VDEDLIVWLDPSFTSDVTKNYRILNV DLPAGDYFF	300
R-HH64	DKSATDPYLKEGYYYQEPGHKIPFN VDEDLIVWLDPSFTSDVTKNYRILNV DLPAGDYFF	300
R-HH65	DKSATDPYLKEGYYYQEPGHKIPFN VDEDLIVWLDPSFTSDVTKNYRILNV DLPAGDYFF	300
R-HH67	DKSATDPYLKEGYYYQEPGHKIPFN VDEDLIVWLDPSFTSDVTKNYRILNV DLPAGDYFF	300
R-HH68	DKSATDPYLKEGYYYQEPGHKIPFN VDEDLIVWLDPSFTSDVTKNYRILNV DLPAGDYFF	300
R-HH69	DKSATDPYLKEGYYYQEPGHKIPFN VDEDLIVWLDPSFTSDVTKNYRILNV DLPAGDYFF	300
R-HH70	DKSATDPYLKEGYYYQEPGHKIPFN VDEDLIVWLDPSFTSDVTKNYRILNV DLPAGDYFF	300
R-HH71	DKSATDPYLKEGYYYQEPGHKIPFN VDEDLIVWLDPSFTSDVTKNYRILNV DLPAGDYFF *****	300
LmxM.31.0510	EITEQYPTAPYGSQKFVQLETRSWIGGRSHVLGSLLIIMGGTALIMAVTLLSVKCLIRPG	360
WT-HH21	EITEQYPTAPYGSQKFVQLETRSWIGGRSHVLGSLLIIMGGTALIMAVTLLSVKCLIRPG	360
WT-HH22	EITEQYPTAPYGSQKFVQLETRSWIGGRSHVLGSLLIIMGGTALIMAVTLLSVKCLIRPG	360
WT-HH24	EITEQYPTAPYGSQKFVQLETRSWIGGRSHVLGSLLIIMGGTALIMAVTLLSVKCLIRPG	360
WT-HH25	EITEQYPTAPYGSQKFVQLETRSWIGGRSHVLGSLLIIMGGTALIMAVTLLSVKCLIRPG	360
WT-HH27	EITEQYPTAPYGSQKFVQLETRSWIGGRSHVLGSLLIIMGGTALIMAVTLLSVKCLIRPG	360
WT-HH30	EITEQYPTAPYGSQKFVQLETRSWIGGRSHVLGSLLIIMGGTALIMAVTLLSVKCLIRPG	360
WT-HH31	EITEQYPTAPYGSQKFVQLETRSWIGGRSHVLGSLLIIMGGTALIMAVTLLSVKCLIRPG	360
WT-HH32	EITEQYPTAPYGSQKFVQLETRSWIGGRSHVLGSLLIIMGGTALIMAVTLLSVKCLIRPG	360
WT-HH34	EITEQYPTAPYGSQKFVQLETRSWIGGRSHVLGSLLIIMGGTALIMAVTLLSVKCLIRPG	360
R-HH18	EITEQYPTAPYGSQKFVQLETRSWIGGRSHVLGSLLIIMGGTALIMAVTLLSVKCLIRPG	360
R-HH63	EITEQYPTAPYGSQKFVQLETRSWIGGRSHVLGSLLIIMGGTALIMAVTLLSVKCLIRPG	360
R-HH64	EITEQYPTAPYGSQKFVQLETRSWIGGRSHVLGSLLIIMGGTALIMAVTLLSVKCLIRPG	360
R-HH65	EITEQYPTAPYGSQKFVQLETRSWIGGRSHVLGSLLIIMGGTALIMAVTLLSVKCLIRPG	360
R-HH67	EITEQYPTAPYGSQKFVQLETRSWIGGRSHVLGSLLIIMGGTALIMAVTLLSVKCLIRPG	360
R-HH68	EITEQYPTAPYGSQKFVQLETRSWIGGRSHVLGSLLIIMGGTALIMAVTLLSVKCLIRPG	360
R-HH69	EITEQYPTAPYGSQKFVQLETRSWIGGRSHVLGSLLIIMGGTALIMAVTLLSVKCLIRPG	360
R-HH70	EITEQYPTAPYGSQKFVQLETRSWIGGRSHVLGSLLIIMGGTALIMAVTLLSVKCLIRPG	360
R-HH71	EITEQYPTAPYGSQKFVQLETRSWIGGRSHVLGSLLIIMGGTALIMAVTLLSVKCLIRPG *****	360
LmxM.31.0510	YTE	363
WT-HH21	YTE	363
WT-HH22	YTE	363
WT-HH24	YTE	363
WT-HH25	YTE	363
WT-HH27	YTE	363
WT-HH30	YTE	363
WT-HH31	YTE	363
WT-HH32	YTE	363

WT-HH34	YTE	363
R-HH18	YTE	363
R-HH63	YTE	363
R-HH64	YTE	363
R-HH65	YTE	363
R-HH67	YTE	363
R-HH68	YTE	363
R-HH69	YTE	363
R-HH70	YTE	363
R-HH71	YTE	363

Appendix 6 (Chapter 5)

Relative bioluminescence (%) following the MMV Pathogen Box screen at 10 μ M and 2 μ M, against axenic amastigotes expressing NanoLuc-PEST.

COMPOUND ID	DISEASE SET	COMMON NAME	RELATIVE BIOLUMINESCENCE (%)	
			10 μ M	2 μ M
MMV690102	KINETOPLASTIDS		-1.34	-5.29
MMV595321	KINETOPLASTIDS		-3.1	-4.54
MMV687251	TUBERCULOSIS		-0.24	-4.37
MMV688262	TUBERCULOSIS	DELAMANID	-2.71	-4.37
MMV688978	REFERENCE COMPOUNDS	AURANOFIN	-2.2	-2.6
MMV019189	MALARIA		-1.42	-1.73
MMV688763	SCHISTOSOMIASIS		-0.71	-1.63
MMV652003	KINETOPLASTIDS		-1.54	-1.53
MMV002817	ONCHOCERCIASIS	IODOQUINOL	-1.46	-1.49
MMV676477	TUBERCULOSIS		-0.92	-0.98
MMV676558	TUBERCULOSIS		-0.77	-0.86
MMV011903	MALARIA		-1.14	-0.43
MMV689480	REFERENCE COMPOUNDS	BUPARVAQUONE	0.15	-0.24
MMV676501	TUBERCULOSIS		-0.69	-0.04
MMV102872	TUBERCULOSIS		-0.65	0.33
MMV676412	TUBERCULOSIS		-0.09	0.46
MMV676388	TUBERCULOSIS		0.16	0.56
MMV687807	TUBERCULOSIS		0.53	0.88
MMV003152	REFERENCE COMPOUNDS	MEBENDAZOLE	-0.49	0.9
MMV676476	TUBERCULOSIS		-0.27	1.36

MMV688776	KINETOPLASTIDS		1.7	1.9
MMV272144	TUBERCULOSIS		0.19	2.64
MMV153413	TUBERCULOSIS		0.97	4.5
MMV688467	KINETOPLASTIDS		2.46	6.98
MMV099637	KINETOPLASTIDS		1.6	7.25
MMV676162	KINETOPLASTIDS		-0.97	7.36
MMV001499	REFERENCE COMPOUNDS	NIFURTIMOX	-2.17	7.65
MMV090930	TUBERCULOSIS		-0.77	11.16
MMV021013	TUBERCULOSIS		1.47	11.73
MMV676512	TUBERCULOSIS		-0.58	15.66
MMV688372	KINETOPLASTIDS		6.87	17.89
MMV688942	KINETOPLASTIDS	BITERTANOL	15.45	20.98
MMV689244	KINETOPLASTIDS		0.66	23.97
MMV028694	MALARIA		3.77	24.99
MMV688943	KINETOPLASTIDS	DIFENOCONAZOL	8.96	26.19
MMV688755	TUBERCULOSIS		0.45	26.38
MMV393995	TUBERCULOSIS		3	27.43
MMV688774	REFERENCE COMPOUNDS	POSACONAZOLE	-1.25	31.32
MMV658988	KINETOPLASTIDS		-2.26	32.93
MMV688853	CRYPTOSPORIDIOSIS		42.96	34.19
MMV689243	KINETOPLASTIDS		8.5	34.53
MMV689437	KINETOPLASTIDS		1.17	37.21
MMV676409	TUBERCULOSIS		12.84	37.25
MMV103079 9	MALARIA		-5.56	37.62
MMV688761	SCHISTOSOMIASIS		-1.44	39.52
MMV671636	ONCHOCERCIASIS		3.97	40.19
MMV688514	KINETOPLASTIDS		34.58	40.8
MMV687800	REFERENCE COMPOUNDS	CLOFAZIMINE	37.9	41.07
MMV676270	MALARIA		18	41.26
MMV687762	KINETOPLASTIDS		31.4	41.49
MMV688990	REFERENCE COMPOUNDS	MIL	11.5	43.04
MMV010576	MALARIA		21.84	44.69
MMV016838	MALARIA		13.69	44.83
MMV020320	MALARIA		0.21	47.21
MMV637229	TRICHURIASIS	CLEMASTINE	11.15	47.31
MMV688775	REFERENCE COMPOUNDS	RIFAMPICIN	2.74	47.59
MMV461553	TUBERCULOSIS		-0.44	48.03
MMV687703	TUBERCULOSIS		76.96	48.25
MMV676411	TUBERCULOSIS		-0.81	48.75
MMV687180	TUBERCULOSIS		1.44	49.23
MMV676384	TUBERCULOSIS		59.9	51.03
MMV675995	ONCHOCERCIASIS		31.11	51.88

MMV687813	TUBERCULOSIS		58.34	52.93
MMV003270	HOOKWORM	ZOXAZOLAMINE	57.93	53.16
MMV676589	TUBERCULOSIS		15.64	54.08
MMV689028	KINETOPLASTIDS		72.62	54.14
MMV676406	TUBERCULOSIS		35.79	54.35
MMV687775	LYMPHATIC FILARIASIS		7.4	54.77
MMV676539	TUBERCULOSIS		62.48	54.78
MMV000023	REFERENCE COMPOUNDS	PRIMAQUINE	76.84	55.01
MMV611037	TUBERCULOSIS		44.6	55.3
MMV690028	KINETOPLASTIDS		1.5	55.46
MMV667494	MALARIA		61.89	55.75
MMV688313	SCHISTOSOMIASIS		18.47	55.91
MMV020512	MALARIA		56.11	56.59
MMV687138	TUBERCULOSIS		48.25	56.61
MMV676520	TUBERCULOSIS		68.82	56.86
MMV026313	MALARIA		66.48	56.9
MMV687776	LYMPHATIC FILARIASIS		-1.15	57.43
MMV007638	MALARIA		52.58	57.66
MMV023985	MALARIA		46.63	57.95
MMV102880 6	MALARIA		-0.6	58.01
MMV689000	REFERENCE COMPOUNDS	AMPHOTERICIN B	48.35	58.31
MMV688283	KINETOPLASTIDS		101.72	58.4
MMV688270	SCHISTOSOMIASIS		51.88	58.63
MMV688471	TOXOPLASMOSIS		49.33	59.14
MMV690103	KINETOPLASTIDS		0.48	59.86
MMV101998 9	MALARIA		45.92	59.9
MMV676524	TUBERCULOSIS		65.52	60
MMV676492	LYMPHATIC FILARIASIS		23.83	60.28
MMV688122	TUBERCULOSIS		16.72	61.39
MMV023370	MALARIA		54.43	62.35
MMV021057	MALARIA	AZOXYSTROBIN	55.66	62.63
MMV688415	KINETOPLASTIDS		31.88	63.04
MMV675996	ONCHOCERCIASIS		25.83	63.13
MMV688555	TUBERCULOSIS		83.23	63.56
MMV020165	MALARIA		61.89	63.67
MMV687254	TUBERCULOSIS		-0.07	63.72
MMV006372	MALARIA		81.31	63.77
MMV688846	TUBERCULOSIS		60.58	63.77
MMV688938	TUBERCULOSIS		76.8	63.8
MMV688273	KINETOPLASTIDS		0.09	63.86
MMV676395	TUBERCULOSIS		0.76	63.89

MMV004168	KINETOPLASTIDS		52.89	64.14
MMV062221	MALARIA		7.64	64.16
MMV560185	MALARIA		94.77	64.27
MMV688798	KINETOPLASTIDS		62.11	64.37
MMV688845	TUBERCULOSIS		67.13	64.6
MMV024443	MALARIA		32.6	64.75
MMV002529	REFERENCE COMPOUNDS	PRAZIQUANTEL	93.76	64.85
MMV200748	TUBERCULOSIS		61.91	64.99
MMV688543	DENGUE		39.32	65.1
MMV687243	TUBERCULOSIS		78.5	65.34
MMV019721	MALARIA		69.43	65.53
MMV085210	MALARIA		73.33	65.83
MMV687749	TUBERCULOSIS		56.67	66.01
MMV687812	TUBERCULOSIS		77.79	66.08
MMV688352	DENGUE		8.52	66.17
MMV675993	CRYPTOSPORIDIOSIS		27.37	66.21
MMV688550	KINETOPLASTIDS		56.13	66.32
MMV1110498	WOLBACHIA LF		77.35	66.34
MMV676389	TUBERCULOSIS		71.87	67.21
MMV689029	KINETOPLASTIDS		57.59	67.41
MMV687700	TUBERCULOSIS		61.64	67.55
MMV688754	KINETOPLASTIDS	TRIFLOXYSTROBIN	-1.92	67.57
MMV020623	MALARIA		86.96	68.14
MMV668727	ONCHOCERCIASIS		78.89	68.46
MMV687273	TUBERCULOSIS		81.32	68.48
MMV688934	KINETOPLASTIDS	TOLFENPYRAD	68.13	68.55
MMV689255	CRYPTOSPORIDIOSIS	D-ERITADENINE	73.04	68.65
MMV024937	MALARIA		69.28	68.74
MMV021375	MALARIA		58.94	68.9
MMV019742	MALARIA		102.67	69.14
MMV676260	MALARIA		85.22	69.43
MMV687765	TUBERCULOSIS		74.28	69.43
MMV010764	MALARIA		31.69	69.5
MMV000063	REFERENCE COMPOUNDS	SITAMAQUINE	73.62	69.63
MMV001625	REFERENCE COMPOUNDS	α -DIFLUOROMETHYLORNITHINE	81.23	69.72
MMV019807	MALARIA		111.93	69.92
MMV688771	SCHISTOSOMIASIS		37.89	70.08
MMV084603	MALARIA		61.1	70.21
MMV688509	TOXOPLASMOSIS		27.84	70.28
MMV019551	MALARIA		42.2	70.29
MMV407834	MALARIA		63.07	70.36
MMV688279	KINETOPLASTIDS		75.33	70.45
MMV676588	TUBERCULOSIS		69.13	70.58

<i>MMV392832</i>	MALARIA		51.5	70.6
<i>MMV1088520</i>	MALARIA		-3.27	70.72
<i>MMV010545</i>	MALARIA		68.48	70.73
<i>MMV495543</i>	TUBERCULOSIS		27.02	70.9
<i>MMV688552</i>	SCHISTOSOMIASIS		47.85	71
<i>MMV688991</i>	REFERENCE COMPOUNDS	NITAZOXANIDE	0.38	71.09
<i>MMV688557</i>	TUBERCULOSIS		58.46	71.96
<i>MMV000062</i>	REFERENCE COMPOUNDS	PENTAMIDINE	96.76	72.21
<i>MMV688274</i>	KINETOPLASTIDS		7.31	72.23
<i>MMV553002</i>	TUBERCULOSIS		58.91	72.57
<i>MMV045105</i>	KINETOPLASTIDS		44.11	73.02
<i>MMV688889</i>	TUBERCULOSIS		59.03	73.23
<i>MMV687172</i>	TUBERCULOSIS		54.36	73.27
<i>MMV688852</i>	TOXOPLASMOSIS		34.77	73.28
<i>MMV688762</i>	SCHISTOSOMIASIS		84.34	73.33
<i>MMV659004</i>	KINETOPLASTIDS		-1.44	73.83
<i>MMV676382</i>	SCHISTOSOMIASIS		64.75	73.92
<i>MMV228911</i>	TUBERCULOSIS		11.53	73.96
<i>MMV676050</i>	CRYPTOSPORIDIOSIS		42.99	74.33
<i>MMV022236</i>	MALARIA		94.61	74.51
<i>MMV688793</i>	KINETOPLASTIDS		52.13	74.59
<i>MMV084864</i>	MALARIA		55.81	74.64
<i>MMV024829</i>	MALARIA		69.82	74.8
<i>MMV688703</i>	TOXOPLASMOSIS		81.84	74.84
<i>MMV675994</i>	CRYPTOSPORIDIOSIS		81.16	74.96
<i>MMV687188</i>	TUBERCULOSIS		98.1	75.17
<i>MMV688939</i>	TUBERCULOSIS		51.85	75.51
<i>MMV688891</i>	TUBERCULOSIS		64.36	75.74
<i>MMV161996</i>	TUBERCULOSIS		98.9	75.91
<i>MMV688768</i>	SCHISTOSOMIASIS		-1.33	75.96
<i>MMV661713</i>	TUBERCULOSIS		83.31	76.01
<i>MMV688417</i>	TOXOPLASMOSIS		-0.98	76.07
<i>MMV688416</i>	DENGUE		66.54	76.11
<i>MMV026356</i>	MALARIA		65.05	76.21
<i>MMV688980</i>	MALARIA		48.08	76.34
<i>MMV023969</i>	TUBERCULOSIS		74.16	76.39
<i>MMV687747</i>	TUBERCULOSIS		30.38	76.47
<i>MMV687729</i>	TUBERCULOSIS		62.67	76.47
<i>MMV676881</i>	MALARIA		54	76.51
<i>MMV687803</i>	REFERENCE COMPOUNDS	LINEZOLID	111.44	76.55
<i>MMV202553</i>	KINETOPLASTIDS		77.09	76.92
<i>MMV688797</i>	KINETOPLASTIDS		71.92	76.99
<i>MMV676528</i>	MALARIA		57.74	77.13

MMV1236379	KINETOPLASTIDS		52.39	77.18
MMV689709	KINETOPLASTIDS		68.1	77.39
MMV688844	TUBERCULOSIS		91.56	77.54
MMV689061	KINETOPLASTIDS		95.91	77.6
MMV688474	KINETOPLASTIDS		76.43	77.71
MMV676377	TUBERCULOSIS		74.59	78.14
MMV676182	CRYPTOSPORIDIOSIS		53.64	78.18
MMV688941	TUBERCULOSIS		74.74	78.23
MMV688888	TUBERCULOSIS		89.99	78.28
MMV011511	MALARIA		88.55	78.49
MMV688548	TOXOPLASMOSIS		77.2	78.88
MMV676008	KINETOPLASTIDS		-1.15	79
MMV688795	KINETOPLASTIDS		86.7	79.12
MMV676445	TUBERCULOSIS		77.96	79.21
MMV687796	REFERENCE COMPOUNDS	AMIKACIN	58.25	79.34
MMV032967	MALARIA		75.35	79.58
MMV023860	MALARIA		74.37	79.77
MMV676461	TUBERCULOSIS		54.88	79.84
MMV676599	CRYPTOSPORIDIOSIS		31.83	80.19
MMV030734	MALARIA		87.08	80.21
MMV023949	MALARIA		52.45	80.37
MMV688936	TUBERCULOSIS		77.21	80.4
MMV023227	MALARIA		64.23	80.48
MMV688364	TOXOPLASMOSIS		58.45	80.73
MMV676605	MALARIA		84.63	81.06
MMV676604	KINETOPLASTIDS		33.57	81.35
MMV676379	TUBERCULOSIS		79.42	81.42
MMV687699	TUBERCULOSIS		62.05	81.42
MMV188296	KINETOPLASTIDS		106.72	81.46
MMV687248	TUBERCULOSIS		88.99	81.54
MMV688766	SCHISTOSOMIASIS		-2.36	82.4
MMV1198433	SCHISTOSOMIASIS		91.16	82.52
MMV688958	KINETOPLASTIDS		101.3	82.55
MMV687798	REFERENCE COMPOUNDS	LEVOFLOXACIN (OFLOXACIN)	74.5	83.03
MMV676603	TUBERCULOSIS		75.26	83.14
MMV008439	MALARIA		126.81	83.2
MMV688704	TOXOPLASMOSIS		53.57	83.23
MMV1037162	MALARIA		85.96	83.26
MMV676584	TUBERCULOSIS		89.36	83.3
MMV676439	TUBERCULOSIS		95.86	83.45
MMV688472	TOXOPLASMOSIS		74.96	83.48
MMV016136	MALARIA		91.85	83.56
MMV006741	MALARIA		113.49	83.56
MMV009135	MALARIA		73.86	83.57

<i>MMV202458</i>	TUBERCULOSIS		79.97	83.71
<i>MMV676186</i>	KINETOPLASTIDS		21.54	83.95
<i>MMV102920</i> 3	MALARIA		52.7	83.99
<i>MMV023388</i>	MALARIA		76.22	84.1
<i>MMV676474</i>	TUBERCULOSIS		88.48	84.28
<i>MMV676380</i>	MALARIA		97.79	84.54
<i>MMV676350</i>	MALARIA		104.94	84.72
<i>MMV688921</i>	DENGUE		105.56	84.76
<i>MMV011765</i>	MALARIA		45.24	84.8
<i>MMV676536</i>	SCHISTOSOMIASIS		103.25	84.93
<i>MMV019790</i>	MALARIA		56.75	85.04
<i>MMV007625</i>	MALARIA		76.47	85.1
<i>MMV688124</i>	TUBERCULOSIS		56.21	85.13
<i>MMV688360</i>	KINETOPLASTIDS		58.5	85.35
<i>MMV023953</i>	MALARIA		83.96	85.42
<i>MMV676269</i>	MALARIA		76.17	85.78
<i>MMV687730</i>	TUBERCULOSIS		52.52	85.81
<i>MMV688547</i>	KINETOPLASTIDS		128.07	85.85
<i>MMV676597</i>	TUBERCULOSIS		73.07	85.91
<i>MMV024406</i>	MALARIA		93.72	85.94
<i>MMV687706</i>	KINETOPLASTIDS		75.35	85.99
<i>MMV063404</i>	TUBERCULOSIS		79.51	86.21
<i>MMV047015</i>	TUBERCULOSIS		82.9	86.47
<i>MMV688125</i>	TUBERCULOSIS		100.33	86.53
<i>MMV024035</i>	MALARIA		79.61	86.6
<i>MMV676470</i>	TUBERCULOSIS		79.72	87.35
<i>MMV020591</i>	MALARIA		94.51	87.56
<i>MMV007471</i>	MALARIA		69.68	87.8
<i>MMV688327</i>	TUBERCULOSIS	RADEZOLID	125.56	87.81
<i>MMV022478</i>	MALARIA		5.54	88.45
<i>MMV688796</i>	KINETOPLASTIDS		91.91	88.65
<i>MMV002816</i>	REFERENCE COMPOUNDS	DIETHYLCARBAMAZINE	62.54	88.75
<i>MMV688756</i>	TUBERCULOSIS	SUTEZOLID	64.54	88.9
<i>MMV021660</i>	TUBERCULOSIS		56.67	89.16
<i>MMV676444</i>	TUBERCULOSIS		81.76	89.21
<i>MMV019087</i>	MALARIA		89.32	89.61
<i>MMV024195</i>	MALARIA		76.61	89.61
<i>MMV020152</i>	MALARIA		108.81	89.71
<i>MMV020391</i>	MALARIA		17.09	89.71
<i>MMV001561</i>	KINETOPLASTIDS	FLUOXETINE	52.43	90.42
<i>MMV688553</i>	TUBERCULOSIS		98.31	90.94
<i>MMV676401</i>	TUBERCULOSIS		75.18	91.23
<i>MMV688178</i>	SCHISTOSOMIASIS		94.95	91.24
<i>MMV026550</i>	MALARIA		87.66	91.5
<i>MMV676602</i>	KINETOPLASTIDS		77.62	91.95

MMV676509	TUBERCULOSIS		59.65	92.05
MMV688854	CRYPTOSPORIDIOSIS		66.13	92.07
MMV024397	MALARIA		86.39	92.24
MMV393144	MALARIA		81.97	92.24
MMV676449	TUBERCULOSIS		88.05	92.26
MMV026490	MALARIA		60.31	92.31
MMV687189	TUBERCULOSIS		81.16	92.36
MMV675998	KINETOPLASTIDS		65.21	92.81
MMV020120	MALARIA		99.97	92.92
MMV676358	MALARIA		64.12	93
MMV085071	MALARIA		82.11	93.07
MMV000014	REFERENCE COMPOUNDS		109.49	93.41
MMV676478	TUBERCULOSIS		56.18	93.56
MMV658993	KINETOPLASTIDS		64.93	93.82
MMV688994	REFERENCE COMPOUNDS	STREPTOMYCIN	84.34	94.02
MMV026020	MALARIA		94.82	94.58
MMV689758	REFERENCE COMPOUNDS	BEDAQUILINE	45.41	94.89
MMV000011	REFERENCE COMPOUNDS	DOXYCYCLINE	94.68	94.97
MMV688362	KINETOPLASTIDS		90.68	95.5
MMV688371	KINETOPLASTIDS		61.94	95.57
MMV000907	MALARIA		78.62	95.69
MMV659010	KINETOPLASTIDS		88.01	95.95
MMV688955	TOXOPLASMOSIS		96.76	95.96
MMV688361	KINETOPLASTIDS		78.94	96.04
MMV020670	MALARIA		97.66	96.09
MMV663250	MALARIA		69.77	96.52
MMV688470	TOXOPLASMOSIS		53.17	96.68
MMV690027	KINETOPLASTIDS		33.47	96.72
MMV676480	ONCHOCERCIASIS		61.83	96.73
MMV006901	MALARIA		107.15	96.82
MMV019993	MALARIA		70.73	96.83
MMV687794	MALARIA		72.05	97.3
MMV032995	MALARIA		90.22	97.31
MMV020517	MALARIA		63.1	97.7
MMV146306	TUBERCULOSIS		40.43	97.77
MMV676554	TUBERCULOSIS		103.74	97.83
MMV688330	TOXOPLASMOSIS		79.07	97.96
MMV687146	TUBERCULOSIS		84.77	98.04
MMV085499	MALARIA		54.27	98.08
MMV688508	TUBERCULOSIS		65.29	98.16
MMV012074	TUBERCULOSIS		123.86	98.27
MMV688180	KINETOPLASTIDS		81.67	98.32
MMV687801	REFERENCE COMPOUNDS	ETHAMBUTOL	126.55	98.57

<i>MMV006833</i>	MALARIA		81.43	98.68
<i>MMV020081</i>	MALARIA		73.47	98.78
<i>MMV688271</i>	KINETOPLASTIDS		56.1	98.92
<i>MMV024101</i>	MALARIA		49.51	98.92
<i>MMV688407</i>	KINETOPLASTIDS		50.94	99.2
<i>MMV676063</i>	ONCHOCERCIASIS		66.65	99.42
<i>MMV689060</i>	KINETOPLASTIDS		112.63	99.56
<i>MMV022029</i>	MALARIA		101.7	99.81
<i>MMV085230</i>	MALARIA		105.91	100.02
<i>MMV675968</i>	CRYPTOSPORIDIOSIS		86.04	100.09
<i>MMV676877</i>	MALARIA		116.3	100.77
<i>MMV000858</i>	MALARIA		108.52	100.91
<i>MMV676159</i>	KINETOPLASTIDS		98.27	101.47
<i>MMV688350</i>	DENGUE		91.24	101.75
<i>MMV020710</i>	MALARIA		128.98	102.08
<i>MMV011229</i>	MALARIA		84.66	102.18
<i>MMV676571</i>	TUBERCULOSIS		85.94	102.29
<i>MMV007133</i>	MALARIA		71.2	102.77
<i>MMV023183</i>	MALARIA		84.53	103.26
<i>MMV020289</i>	MALARIA		71.21	103.5
<i>MMV024114</i>	MALARIA		69.99	103.63
<i>MMV676526</i>	TUBERCULOSIS		46.48	103.78
<i>MMV687246</i>	MALARIA		82.04	103.95
<i>MMV688469</i>	TOXOPLASMOSIS		53.28	103.98
<i>MMV676555</i>	TUBERCULOSIS		90.53	104.08
<i>MMV676048</i>	KINETOPLASTIDS		53.9	104.27
<i>MMV637953</i>	REFERENCE COMPOUNDS	SURAMIN	116.61	104.52
<i>MMV675969</i>	ONCHOCERCIASIS		77.56	104.76
<i>MMV407539</i>	WOLBACHIA LF		70.84	104.77
<i>MMV676431</i>	TUBERCULOSIS		65.31	104.86
<i>MMV688345</i>	TOXOPLASMOSIS		69.94	105.25
<i>MMV011691</i>	MALARIA		73.17	105.27
<i>MMV053220</i>	TUBERCULOSIS		82.56	105.3
<i>MMV676064</i>	ONCHOCERCIASIS		123.9	105.34
<i>MMV688411</i>	TOXOPLASMOSIS		65.85	105.51
<i>MMV688179</i>	KINETOPLASTIDS		54.5	105.96
<i>MMV687239</i>	TUBERCULOSIS		118.8	106.04
<i>MMV019234</i>	MALARIA		39.61	106.08
<i>MMV009054</i>	MALARIA		100.62	106.08
<i>MMV676053</i>	CRYPTOSPORIDIOSIS		78.76	106.26
<i>MMV676472</i>	TUBERCULOSIS		93.04	106.46
<i>MMV023233</i>	MALARIA		120.49	106.85
<i>MMV676468</i>	TUBERCULOSIS		84.33	106.85
<i>MMV687170</i>	TUBERCULOSIS		104.36	107.56
<i>MMV006239</i>	MALARIA		108.03	107.64
<i>MMV676191</i>	CRYPTOSPORIDIOSIS		94.76	107.96

MMV020136	MALARIA		122.06	108.03
MMV688466	TUBERCULOSIS		117.26	108.11
MMV676161	KINETOPLASTIDS		116.07	108.65
MMV020520	MALARIA		127.42	108.71
MMV020982	MALARIA		93.07	109.38
MMV024311	TUBERCULOSIS		88.36	109.56
MMV001059	MALARIA		96.75	109.79
MMV688773	REFERENCE COMPOUNDS	BENZNIDAZOLE	132.2	110.17
MMV031011	MALARIA		84.55	110.57
MMV676600	KINETOPLASTIDS		114.36	110.66
MMV634140	MALARIA		73.96	112.61
MMV007920	MALARIA		88.96	112.76
MMV687696	TUBERCULOSIS		57.87	113.56
MMV007803	MALARIA		107.95	113.68
MMV688410	KINETOPLASTIDS		63.15	114.6
MMV069458	TUBERCULOSIS		112.41	115.05
MMV676398	WOLBACHIA LF		84.49	115.47
MMV026468	MALARIA		104.46	116.14
MMV675997	KINETOPLASTIDS		97.48	116.18
MMV020537	MALARIA		146.04	116.22
MMV676204	ONCHOCERCIASIS		99.37	116.49
MMV020291	MALARIA		111.14	117.25
MMV688554	TUBERCULOSIS		66.57	117.68
MMV020321	MALARIA		131.13	118.65
MMV676442	MALARIA		113.29	118.75
MMV676057	KINETOPLASTIDS		36.52	119.16
MMV054312	TUBERCULOSIS		116.16	120.77
MMV020388	MALARIA		143.84	121.02
MMV019838	MALARIA		86.78	125.18
MMV676386	TUBERCULOSIS		120.21	127.03
MMV001493	ONCHOCERCIASIS	ISRADIPINE	89.57	129.79
MMV687145	TUBERCULOSIS		130.77	132.61
MMV676383	TUBERCULOSIS		127.92	136.33